



JANSKY & BAILEY ENGINEERING DEPARTMENT

AD 660318

TROPICAL PROPAGATION RESEARCH

Final Report

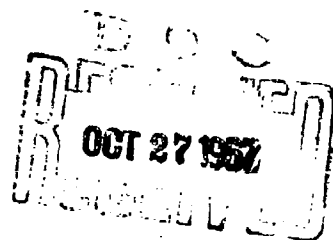
Volume I

**Prepared for
U.S. ARMY ELECTRONICS COMMAND
Fort Monmouth, New Jersey**

**Signal Corps Contract
DA 36-039 SC 90889**

**Sponsored by
ADVANCED RESEARCH PROJECTS AGENCY
Office of Secretary of Defense
ARPA ORDER 371**

Reproduced by the
CLEARINGHOUSE
for Federal Scientific & Technical
Information Springfield Va. 22151



ATLANTIC  RESEARCH

Distribution of this Document is Unlimited

506

TROPICAL PROPAGATION RESEARCH
FINAL REPORT VOLUME I

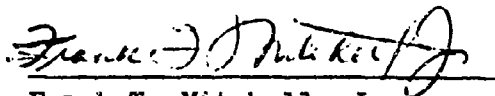
Jansky & Bailey
Engineering Department
of
Atlantic Research Corporation
Alexandria, Virginia

Prepared for
U. S. ARMY ELECTRONICS COMMAND

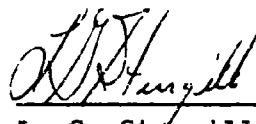
Sponsored by
ADVANCED RESEARCH PROJECTS AGENCY
Office of Secretary of Defense
ARPA Order 371

Program Code Number: 2860
Contract Number: DA 36-039 SC-90889

Approved by



Frank T. Mitchell, Jr.
Department Director



L. G. Sturgill
Project Director

Distribution of this Document is Unlimited.

ABSTRACT

This Final Report, Volume I, presents the results obtained from the first phase of an extensive experimental and theoretical research program on radio wave propagation in the environment of a tropical, thickly vegetated jungle. Although aimed primarily at the problems encountered by ground based, tactical radio communications systems, the measured data and the results derived therefrom are general enough to have applications in the field of electromagnetic surveillance and intrusion detection.

The experimental work during this first phase has been carried out in Thailand in a geographical area classified as a wet-dry, or monsoon, tropical region. The vegetation in the main test area has a density of about 130 tons per acre and is considered to be typical of many jungle regions throughout Southeast Asia. The propagation tests and analyses contained in this report cover the frequency range of 100 kc/s to 10 Gc/s for propagation distances extending from 25 feet to 30 miles and antenna heights from about 7 to 80 feet above ground. Except at the lowest frequencies, all tests were conducted at both horizontal and vertical polarizations. Most of the data is presented in graphs of basic transmission loss plotted against horizontal distance, terrain characteristic, antenna height, transmission polarization or frequency. Also covered are the results of special measurements in the 1 to 10-Gc/s frequency range, the data from which is applicable to problems with line-of-sight systems operating over vegetated terrain

and with short range radar systems propagating horizontally through vegetation. The large quantity of measured data demonstrates the complex effects upon path loss of irregular topography combined with dense tropical vegetation.

The findings of the program to date, which have been drawn from the data analysis, are summarized into a number of tentative conclusions which may be applied to many types of problems involving radio propagation in tropically vegetated regions.

PREFACE

The radio propagation research program which constitutes the subject of this report is one of several communications research programs sponsored by the Advanced Research Projects Agency (ARPA), of the Department of Defense, as a part of its Project SEACORE (SEACORE being a loose acronym for Southeast Asia Communications Research). This research program is under the contractual and technical direction of the United States Army Electronics Command (USAECOM), Fort Monmouth, New Jersey. The over-all purpose of this particular investigation, in coordination with other SEACORE research projects, is to obtain information that will enable presently available radio equipment to be more efficiently used, and that will assist in the design and development of new equipments to provide improved short range tactical communications in jungle areas in Southeast Asia, as well as in other areas with similar environments.

The objectives of this program are such that it involves experimental and theoretical efforts, both of which are rather extensive in scope as well as activity. The experimental part of the program is carried out in Thailand through the guidance and support of the Joint Thai - U. S. Military Research and Development Center (MRDC). Dedicated in late 1963, the activities of MRDC have grown to encompass a wide variety of research and development efforts in the application of science and technology to military operations. The results of some of its work can be applied to commercial operations as well. The activities of MRDC span scientific disciplines ranging from physics to botany.

A fundamentally important aspect of this radio propagation research program is that data obtained from the field measurements is representative of the environmental conditions that would be encountered in real tactical operations in actual jungle areas. Since the data must reflect the influence upon radio propagation of the effects of dense tropical vegetation (jungle), tropical climate, and topography of various degrees of roughness, it was therefore essential to the program objectives that these environmental factors be as carefully recorded, studied, and evaluated as the propagation data obtained from the propagation measurements. To achieve the various experimental objectives of the field measurements, it was necessary to locate a jungle area having certain essential characteristics. The area had to be about 30 miles square to provide the necessary distance ranges. It had to be covered by dense jungle growth that was penetrable by means of a system of roads, cart tracks, and foot trails and was situated over terrain with appropriate variations in its topographic features. Also, the location of the area had to be amenable to the logistic support necessary to carry out the measurement activities.

By its nature, such an experimental program is a complex operation in respect to both the technology it involves, as well as the logistics required to support it. It could not have been carried out in Thailand without the cooperation and assistance of several organizations and individuals there. Particular acknowledgment is due MRDC, which includes ARPA's Research and Development Field Unit - Thailand (RDFU-T), for the constant cooperation and assistance this organization has provided to this project. Also, in the early phases of the work of Thailand, when the

country was being surveyed to find a proper location for the field tests, the assistance of several officers in the Joint U. S. Military Advisory Group (JUSMAG) was invaluable. In addition to providing the much needed map information, JUSMAG personnel were very helpful in furnishing a comprehensive synopsis of the operational communications problems that were being encountered in Southeast Asia at that time. Thanks are due, also, to the Thai Forestry Department for its cooperation and assistance, especially during the survey and site construction work in the Thai National Forest area south of Pak Chong.

It would be impossible to list all of the individuals in Thailand who have helped this project along in one way or another. Such a list would number well over a hundred. Among these people, special thanks are extended to Prapat Chandaket, Captain, Royal Thai Navy, and Sukdichai Nivatmaraka, Captain, Royal Thai Air Force, of MRDC, both of whom have been associated with the program from the beginning and have been a constant source of help.

Finally, the assistance of several individuals in the U. S. Government, who have contributed significantly to the guidance of this program in the scientific and technologic sense, is gratefully acknowledged. Many of the basic ideas and aims of this program have been obtained through numerous discussions with Colonel Harry E. Tabor, Lt. Col. James L. Jones, and Lt. Col. Thomas W. Doeppner, of ARPA; and Mr. Robert A. Kulinyi and Mr. Howard L. Kitts, of USAECOM, Fort Monmouth, New Jersey.

THIS PAGE INTENTIONALLY BLANK

CONTENTS

	<u>Page</u>
ABSTRACT	i
PREFACE	iii
LIST OF ILLUSTRATIONS	xi
LIST OF TABLES	xxv
1. INTRODUCTION	1
2. GENERAL DISCUSSION	5
3. SUMMARY OF DATA ANALYSIS	15
3.1 Propagation Loss as a Function of Distance in the Presence of Vegetation	16
3.2 Propagation Loss as a Function of Antenna Height in the Presence of Vegetation	19
3.3 Propagation Loss as a Function of Frequency in the Presence of Vegetation	20
3.4 Propagation Loss as a Function of Polarization in the Presence of Vegetation	21
3.5 Propagation Loss as a Function of Terrain in the Presence of Vegetation	21
3.6 Propagation Loss as a Function of Climate in the Presence of Vegetation	22
3.7 Propagation Loss as a Function of Ionospheric Conditions in the Presence of Vegetation	22
4. TEST SITE DESCRIPTION.	23
4.1 Brief History	23
4.2 Environment	27
4.2.1 Climate	27
4.2.2 Vegetation	27
4.3 Description of Base Site	31
4.4 Test Procedures	31
5. ANALYSIS OF THE DATA	37
5.1 Summary of Propagation Data Over Foliated, Uneven Terrain	46
5.1.1 0.1 to 30-Mile Fixed Point Path Loss Measurements	47
5.1.2 Propagation Loss for Short, Foliated Paths	88
5.1.3 Variability of Path Loss with Distance	102

CONTENTS, Continued

	<u>Page</u>
5.2 Propagation Loss as a Function of Antenna Height in the Presence of Foliage	112
5.2.1 Height-Gain for Separation Distances of 2 to 30 Miles	117
5.2.2 Height Gain for Separation Distances of 0.2 to 1.0 Mile	128
5.2.3 Propagation Path Loss as a Function of Terrain Height	141
5.2.4 Height Variation	146
5.3 Propagation Path Loss as a Function of Frequency	155
5.4 Polarization	163
5.4.1 Polarization Comparison	164
5.4.2 Depolarization	171
5.4.3 Antenna Orientation	176
5.5 Propagation Loss as Influenced by Terrain in a Foliated Environment	178
5.5.1 Modified Egli Model	187
5.5.2 General Statistical Model	190
5.5.3 NBS Terrain Model	196
5.5.4 Simplified Terrain Model Results	201
5.5.4.1 Modified LaGrone Model	205
5.5.4.2 Equivalent Knife-Edge Model	217
5.6 Climatological Data	218
5.7 Radio Noise Measurements	228
5.7.1 General Background	228
5.7.2 Measuring Device Limitations	231
5.7.3 Results of Noise Measurements	233
5.8 Ionospheric Measurements	236
5.8.1 Test Measurements	237
5.8.2 Test Results	240
5.9 10 Gc/s Measurements	256
5.9.1 Line-of-Sight Test Series	257
5.9.1.1 Theoretical Knife-edge Diffraction	257
5.9.1.2 Diffraction Loss Measurements	261
5.9.1.3 Diffraction Test Results	264
5.9.1.4 Diurnal Fading Tests	271
5.9.2 In-Foliage Measurements	275
5.9.2.1 Test Area Environment	276
5.9.2.1.1 Area A Description	276
5.9.2.1.2 Area B Description	295
5.9.2.2 Parameters Influencing Median Foliage Attenuation	297
5.9.2.2.1 Frequency	302
5.9.2.2.2 Polarization	303
5.9.2.2.3 Path Length	304
5.9.2.2.4 Foliage Density	305
5.9.2.2.5 Type of Vegetation	306
5.9.2.2.6 Antenna Beamwidth	307
5.9.2.3 "Fine Grain" Field Variations	308

CONTENTS, Continued

	<u>Page</u>
5.9.2.3.1 Time Variability	309
5.9.2.3.2 Small Sector Variability	318
5.9.2.4 Test Setup and Data Reduction Methods for Foliage Attenuation Measurements	319
5.9.2.5 Results of Foliage Attenuation Tests	347
5.9.2.6 24-Hour In-Foliage Measurements	350
5.9.2.7 Antenna Pattern Measurements	351
5.9.2.7.1 Test Setup and Procedure	354
5.9.2.7.2 Test Results	365
5.9.2.7.3 General Conclusions	365
5.9.2.8 Treetop Mode Study	375
5.9.3 Refractivity Measurements	377
5.9.3.1 Measurement Setup	379
5.9.3.2 Measurement Accuracy	380
5.9.3.3 Refractivity Analysis	398
5.9.3.4 Conclusions of the Refractivity Analysis	398
6. INSTRUMENTATION, EQUIPMENT, AND TECHNIQUES	401
6.1 Transmitters	402
6.1.1 100 Gc/s to 400 Mc/s Test Transmitters	403
6.1.2 400 Mc/s to 10 Gc/s Test Transmitters	404
6.2 Transmitter Calibration	404
6.2.1 RF Power Measurements (0.1 to 25 Mc/s)	405
6.2.2 Power Meters (25 to 400 Mc/s)	406
6.2.3 Power Measurements (0.4 to 10 Gc/s)	407
6.2.4 Equipment Calibration	409
6.3 Transmitting Antennas	411
6.3.1 Transmitting Antennas (0.1 to 2.0 Mc/s)	412
6.3.2 Transmitting Antennas (2.0 - 12.0 Mc/s)	419
6.3.3 Transmitting Antennas (12 to 400 Mc/s)	425
6.3.4 Transmitting and Receiving Antennas (0.4 to 10 Gc/s)	434
6.4 Transmitting Antenna Calibration	437
6.4.1 Transmission Path Loss and Antenna Calibra- tion Equations (0.1 to 400 Mc/s)	437
6.4.2 Transmission Loss Equation (0.4 to 10 Gc/s)	443
6.5 Field Strength Meters	446
6.5.1 Meters	447
6.5.2 Measuring Antennas	449
6.5.3 Calibration	452
6.6 Special Equipment	454
6.6.1 Portable Mast	454
6.6.2 10-Gc/s Antenna Towers and Positioners	464
6.6.3 Recorder Chart Drives	468
6.6.4 Recorders	472

CONTENTS, Continued

Page

REFERENCES 475

DOCUMENT CONTROL DATA - R&D, DD Form 1473

DISTRIBUTION LIST

LIST OF ILLUSTRATIONS

<u>Figure</u>		<u>Page</u>
2.1	Various Test Frequencies for Jungle Propagation Measurements	10
4.1	Map of Thailand Showing Test Area	24
4.2	Map of Total Pak Chong Test Area	26
4.3	Installation of Air Conditioned Transmitter Shelter	32
4.4	Test Compound Plan	33
4.5	Aerial View of Test Site	34
5.1	Path Loss Summary for Low Antennas $L_b = F_{A,B}(f, \text{Low}, V, d, \text{Low})$	51
5.2	Path Loss Summary for Low Antennas $L_b = F_{A,B}(f, \text{Low}, H, d, \text{Low})$	52
5.3	Path Loss Summary for High Antennas $L_b = F_{A,B}(f, 80, V, d, 79)$	53
5.4	Path Loss Summary for High Antennas $L_b = F_{A,B}(f, 80, H, d, 79)$	54
5.5	Measured Path Loss $L_b = F_{A,B}(0.1, 80, V, d, 17)$	55
5.6	Measured Path Loss $L_b = F_{A,B}(0.3, 80, V, d, 17)$	56
5.7	Measured Path Loss $L_b = F_{A,B}(0.88, 80, V, d, 17)$	57
5.8	FCC Ground Wave Propagation Curves and Pak Chong Measured Data $L_b = F_{A,B}(0.88, 80, V, d, 17)$	58
5.9	Measured Path Loss $L_b = F_{A,B}(2, 80, V, d, 17)$	59
5.10	Measured Path Loss $L_b = F_{A,B}(6, 40, V, d, 17)$	60

ILLUSTRATIONS continued

<u>Figure</u>		<u>Page</u>
5.11	Measured Path Loss $L_b = F_{A,B}(12, 20, V, d, 17)$	61
5.12	Measured Path Loss $L_b = F_{A,B}(25, 10, V, d, 11)$	62
5.13	Measured Path Loss $L_b = F_{A,B}(50, 13, V, d, 11)$	63
5.14	Measured Path Loss $L_b = F_{A,B}(100, 13, V, d, 11)$	64
5.15	Measured Path Loss $L_b = F_{A,B}(250, 13, V, d, 11)$	65
5.16	Measured Path Loss $L_b = F_{A,B}(400, 13, V, d, 11)$	66
5.17	Measured Path Loss $L_b = F_{A,B}(2, 40, H, d, 17)$	67
5.18	Measured Path Loss $L_b = F_{A,B}(6, 40, H, d, 17)$	68
5.19	Measured Path Loss $L_b = F_{A,B}(12, 40, H, d, 17)$	69
5.20	Measured Path Loss $L_b = F_{A,B}(25, 13, H, d, 11)$	70
5.21	Measured Path Loss $L_b = F_{A,B}(50, 13, H, d, 11)$	71
5.22	Measured Path Loss $L_b = F_{A,B}(100, 13, H, d, 11)$	72
5.23	Measured Path Loss $L_b = F_{A,B}(250, 13, H, d, 11)$	73
5.24	Measured Path Loss $L_b = F_{A,B}(400, 13, H, d, 11)$	74
5.25	Measured Path Loss $L_b = F_{A,B}(2, 80, V, d, 79)$	75

ILLUSTRATIONS continued

<u>Figure</u>		<u>Page</u>
5.26	Measured Path Loss $L_b = F_{A,B} (50, 80, V, d, 79)$	76
5.27	Measured Path Loss $L_b = F_{A,B} (100, 80, V, d, 79)$	77
5.28	Measured Path Loss $L_b = F_{A,B} (250, 80, V, d, 79)$	78
5.29	Measured Path Loss $L_b = F_{A,B} (400, 80, V, d, 79)$	79
5.30	Measured Path Loss $L_b = F_{A,B} (2, 80, H, d, 79)$	80
5.31	Measured Path Loss $L_b = F_{A,B} (6, 80, H, d, 79)$	81
5.32	Measured Path Loss $L_b = F_{A,B} (12, 80, H, d, 79)$	82
5.33	Measured Path Loss $L_b = F_{A,B} (25, 80, H, d, 79)$	83
5.34	Measured Path Loss $L_b = F_{A,B} (50, 80, H, d, 79)$	84
5.35	Measured Path Loss $L_b = F_{A,B} (100, 80, H, d, 79)$	85
5.36	Measured Path Loss $L_b = F_{A,B} (250, 80, H, d, 79)$	86
5.37	Measured Path Loss $L_b = F_{A,B} (400, 80, H, d, 79)$	87
5.38	Comparison of Theoretical Model with Measured Data $L_b = F_{A,B} (100, 13, V, d, 6)$	91
5.39	Comparison of Theoretical Model with Measured Data $L_b = F_{A,B} (400, 13, V, d, 6)$	92

ILLUSTRATIONS continued

<u>Figure</u>		<u>Page</u>
5.40	Comparison of Exponential and Logarithmic Models with Measured Data $L_b = F_{A,B} (100, 13, V, d, 6)$	95
5.41	Comparison of Theoretical Model with Measured Data $L_b = F_{A,B} (25, 10, V, d, 6)$	98
5.42	Comparison of Theoretical Model with Measured Data $L_b = F_{A,B} (100, 13, H, d, 6)$	100
5.43	Theoretical and Measured Short Range Path Loss $L_b = F_{A,B} (400, 13, H, d, 6)$	101
5.44	Example of Vehicular Raw Data $F_A (25.5, 40, V, d, 1.0-1.2, 7)$	103
5.45	Example of Vehicular Raw Data $F_A (250, 80, V, 0.8-1.0, 7)$	104
5.46	Example of High Resolution Vehicular Raw Data $F_B (100, 40, H, 0.8, 7)$	106
5.47	Average Half-Cycle Widths.	108
5.48	Typical Distribution for Half-Cycle Widths (100 Mc/s, Vertical Polarization) .	109
5.49	Average Peak-to-Null Ratio	110
5.50	Typical Distribution for Peak-to-Null Ratio (100 Mc/s, Horizontal Polarization)	111
5.51	Summary of Height Gain Profiles $L_b = F_{A,B} (25, 40, H, d, H_T)$	114
5.52	Summary of Height Gain Profiles $L_b = F_{A,B} (100, 40, H, d, H_T)$	116

ILLUSTRATIONS continued

<u>Figure</u>		<u>Page</u>
5.53	Average Height Gain for Vertical Polarization at 25 Mc/s	120
5.54	Average Height Gain for Horizontal Polarization at 25 Mc/s	122
5.55	Average Height Gain for Vertical Polarization at 100 Mc/s.	123
5.56	Average Height Gain for Horizontal Polarization at 100 Mc/s.	124
5.57	Average and Measured Height Gain. $L_b = F_A(100, H_t, V, 2.0, H_r)$	125
5.58	Average and Measured Height Gain $L_b = F_A(100, H_t, V, 3.0, H_r)$	126
5.59	Average and Measured Height Gain $L_b = F_A(100, H_t, V, 4.0, H_r)$	127
5.60	Height Gain Profile $L_b = F_{A,B}(25, 10, V, d, H_r)$	131
5.61	Height Gain Profile $L_b = F_{A,B}(50, 13, V, d, H_r)$	132
5.62	Height Gain Profile $L_b = F_{A,B}(100, 13, V, d, H_r)$	133
5.63	Height Gain Profile $L_b = F_{A,B}(250, 13, V, d, H_r)$	134
5.64	Height Gain Profile $L_b = F_{A,B}(400, 13, V, d, H_r)$	135
5.65	Height Gain Profile $L_b = F_{A,B}(25, 13, H, d, H_r)$	136
5.66	Height Gain Profile $L_b = F_{A,B}(50, 13, H, d, H_r)$	137

ILLUSTRATIONS continued

<u>Figure</u>		<u>Page</u>
5.67	Height Gain Profile $L_b = F_{A,B} (100, 13, H, d, H_r)$	138
5.68	Height Gain Profile $L_b = F_{A,B} (250, 13, H, d, H_r)$	139
5.69	Height Gain Profile $L_b = F_{A,B} (400, 13, H, d, H_r)$	140
5.70	Measured Fixed Point Path Loss Data $L_b = F_{A,B} (250, 80, H, d, 80)$	142
5.71	Measured Fixed Point Path Loss Data $L_b = F_{A,B} (50, 80, H, d, 80)$	144
5.72	Sector B Terrain Profile Showing Pak Chong Distribution of Tree Heights. . .	145
5.73	Sample Data Recording $L_b = F_A (25, 40, V, .2, 76)$	148
5.74	Sample Data Recording $L_b = F_A (400, 40, V, .2, 76)$	149
5.75	Sample Polar Plot $F_A (25, 40, V, .2, H_r)$	150
5.76	Sample Polar Plot $F_A (50, 40, V, .2, H_r)$	151
5.77	Sample Polar Plot $F_A (100, 40, V, .2, H_r)$	152
5.78	Sample Polar Plot $F_A (250, 40, V, .2, H_r)$	153
5.79	Sample Polar Plot $F_A (400, 40, V, .2, H_r)$	154
5.80	Summary of Path Loss vs. Frequency $L_b = F_{A,B} (f, H_t, V, 1.0, H_r)$	158

ILLUSTRATIONS continued

<u>Figure</u>		<u>Page</u>
5.81	Summary of Path Loss Vs. Frequency $L_b = F_{A,B} (f, H_t, H, 1.0, H_r)$	159
5.82	Polarization Margin Vs. Frequency	170
5.83	Horizontal Polarization Advantage Vs. Antenna Height.	172
5.84	Horizontal Polarization Advantage Vs. Height.	173
5.85	Radial Points and Field Points in Sector A. .	179
5.86	Radial Points and Field Points in Sector B. .	181
5.87	Sector A Short Range Terrain Profile.	182
5.88	Sector B Short Range Terrain Profile.	183
5.89	Terrain Profiles for Field Points in Sector A	185
5.90	Terrain Profiles for Field Points in Sector B	186
5.91	Southwesterly View from Base Site	188
5.92	Deviation of Measured Values from General Statistical Model for 50 Mc/s Horizontal Polarization.	197
5.93	Comparison Between Measured Results and NBS Model Including G (H) Functions $L_b = F_A (25.5, 80, V, d, 80)$	199
5.94	Best Fit to Measured Results $L_b = F_A (25, 80, V, d, 80)$	200
5.95	Best Fit 10 dB Below Measured Results $L_b = F_A (25, 80, V, d, 80)$	202
5.96	Comparison of Measured and Predicted Path Losses $L_b = F_B (100, 80, H\&V, d, 80)$	206

ILLUSTRATIONS continued

<u>Figure</u>		<u>Page</u>
5.97	Comparison of Measured and Predicted Path Losses $L_p = F_B$ (50, 80, H&V, d, 80)	207
5.98	Comparison of Measured and Predicted Path Losses $L_p = F_B$ (25, 80, H&V, d, 80)	208
5.99	Terrain Profile Showing Major Obstacles for FPA-5.	213
5.100	Terrain Profile Showing Major Obstacles for FPA-6.	214
5.101	Terrain Profile Showing Major Obstacles for FPA-8.	215
5.102	Terrain Profile Showing Major Obstacles for FPA-7.	216
5.103	Rainfall Measurement Points.	220
5.104	Climatological Data.	223
5.105	Combined Median Noise Levels for Nov., Dec., and Jan. For Horizontal Polarization	234
5.106	Combined Median Noise Levels for Nov., Dec., and Jan. For Vertical Polarization .	235
5.107	Ionospheric Test Transmitting and Receiving Sites.	239
5.108	Raw Data from Ionospheric Tests	241
5.109	Measured Field Strength Vs. Time of Day - FPB-10	242
5.110	Measured Field Strength Vs. Time of Day - FPB-6	243
5.111	Measured Field Strength Vs. Time of Day - FPB-10	244

ILLUSTRATIONS continued

<u>Figure</u>		<u>Page</u>
5.112	Measured Field Strength Vs. Time of Day - FPB-6	245
5.113	Measured Field Strength Vs. Time of Day - FPB-6	246
5.114	Measured Field Strength Vs. Time of Day - FPB-6	247
5.115	Measured Field Strength Vs. Time of Day - FPB-6	248
5.116	Measured Field Strength Vs. Time of Day - FPB-6	249
5.117	Measured Field Strength Vs. Time of Day - FPB-6	250
5.118	Critical Frequency Versus Time of Day for 29 January 1966	252
5.119	A(v) and $\phi(v)$ Vs. v for Perfect Knife Edge	260
5.120	Line-of-Sight Profile for Area A.	263
5.121	Receiving Setup for Line-of-Sight Tests . . .	265
5.122	Receiving Setup for Line-of-Sight Tests . . .	265
5.123	Measured Knife-Edge Loss at 550 Mc/s	266
5.124	Measured Knife-Edge Loss at 1.0 Gc/s	267
5.125	Measured Knife-Edge Loss at 2.5 Gc/s	268
5.126	Measured Knife-Edge Loss at 5.0 Gc/s	269
5.127	Measured Knife-Edge Loss at 10.0 Gc/s	270
5.128	Diurnal Variation of L_b at 550 Mc/s	272
5.129	Diurnal Variation of L_b at 1.0 Gc/s	273

ILLUSTRATIONS continued

<u>Figure</u>		<u>Page</u>
5.130	Diurnal Variation of L_p at 10 Gc/s	274
5.131	Transmission Path Layout for Area A	278
5.132	Typical Foliage in Area A	279
5.133	Tree Plot for T-R ₁ Path, Area A	281
5.134	Tree Plot for T-R ₂ Path, Area A	282
5.135	Tree Plot for T-R ₂ Path, Area A	283
5.136	Tree Plot for T-R ₃ Path, Area A	284
5.137	Tree Plot for T-R ₃ Path, Area A	285
5.138	Tree Plot for T-R ₃ Path, Area A	286
5.139	Cumulative Distribution of Tree Heights for T-R ₁ Path	288
5.140	Cumulative Distribution of Tree Heights for T-R ₂ Path	289
5.141	Cumulative Distribution of Tree Heights for T-R ₃ Path	290
5.142	Cumulative Distribution of Tree Diameter for T-R ₁ Path	291
5.143	Cumulative Distribution of Tree Diameter for T-R ₂ Path	292
5.144	Cumulative Distribution of Tree Diameter for T-R ₃ Path	293
5.145	Transmission Path Layout for Area B	296
5.146a	Typical Views of Bamboo in Area B	298
5.146b	Typical Views of Bamboo in Area B	299
5.147	Tree Plot of Area B	300
5.148	Strip Chart Recording of Wind and Signal . . .	311

ILLUSTRATIONS continued

<u>Figure</u>		<u>Page</u>
5.149	Strip Chart Recording of Wind and Signal . . .	312
5.150	Strip Chart Recording of Wind and Signal . . .	313
5.151	Strip Chart Recording of Wind and Signal . . .	314
5.152	Typical Wind-Signal Correlation	315
5.153	Typical Wind-Signal Correlation	316
5.154	Typical View of Receiver Tower Located in Vegetation	321
5.155	Rate of Attenuation, α , Vs. Antenna Height Frequency = 2.5 Gc/s	329
5.156	Rate of Attenuation, α , Vs. Antenna Height Frequency = 5 Gc/s	330
5.157	Rate of Attenuation, α , Vs. Antenna Height Frequency = 10 Gc/s	331
5.158	Rate of Attenuation, α , Vs. Frequency H_t = 6 feet	333
5.159	Rate of Attenuation, α , Vs. Frequency H_t = 9 feet	334
5.160	Rate of Attenuation, α , Vs. Frequency H_t = 15 feet	335
5.161	Rate of Attenuation, α , Vs. Frequency H_t = 21 feet	336
5.162	Rate of Attenuation, α , Vs. Frequency H_t = 33 feet	337
5.163	Rate of Attenuation, α , Vs. Frequency H_t = 45 feet	338
5.164	Rate of Attenuation, α , Vs. Frequency H_t = 9 and 21 feet	340
5.165	Composite Attenuation Curves for Areas A and B	341

ILLUSTRATIONS continued

<u>Figure</u>		<u>Page</u>
5.166	Comparison of Thailand Data with Other Measurements	342
5.167	LaGrone Function and Measured α Vs. Frequency	344
5.168	LaGrone Function and Measured α Vs. Frequency	345
5.169	LaGrone Function and Measured α Vs. Frequency	346
5.170	All Three Transmission Paths Normalized at 2.5 Gc/s	348
5.171	Typical Strip Chart Recording of Antenna Pattern	353
5.172	Dish Patterns Showing Effect of Changing Beamwidth of Auxiliary Antenna	356
5.173	Foliage Effect on Large Aperture Antenna . . .	358
5.174	In-Foliage and In-Clearing Patterns of Horn Antenna	359
5.175	In-Foliage Pattern of Widebeam Horn	361
5.176	In-Foliage Pattern of Narrow Beam Horn	362
5.177	In-Foliage Pattern of Widebeam Dish	363
5.178	In-Foliage Pattern of Widebeam Horn	364
5.179	Test Setup for Treetop Mode Study	367
5.180	Antenna Patterns Showing Treetop Mode	369
5.181	Antenna Patterns Showing Treetop Mode	370
5.182	Antenna Patterns Showing Treetop Mode	371
5.183	Antenna Patterns Showing Treetop Mode	372
5.184	Antenna Patterns Showing Treetop Mode	373
5.185	Diurnal Variation of Refractivity Profile (1-2 August 1965)	383

ILLUSTRATIONS continued

<u>Figure</u>		<u>Page</u>
5.186	Diurnal Variation of Refractivity Profile (30-31 July 1965)	384
5.187	Diurnal Variation of In-Foliage Refractivity for July 25-26, 1965	386
5.188	Diurnal Variation of In-Foliage Refractivity for July 26-27, 1965	387
5.189	Diurnal Variation of Out-of-Foliage Refractivity for August 21-22, 1965	388
5.190	Diurnal Variation of Out-of-Foliage Refractivity for October 7-8, 1965	389
5.191	Diurnal Variation of Out-of-Foliage Refractivity for September 21-22, 1965 . . .	390
5.192	24-Hour Refractivity Gradients Taken In- Foliage During July 1965	391
5.193	24-Hour Refractivity Gradients Taken In- Foliage During Latter July and August, 1965	392
5.194	24-Hour Refractivity Gradients Taken Out-of- Foliage During September 1965	393
5.195	24-Hour Refractivity Gradients Taken Out-of- Foliage During October 1965	394
5.196	Monthly Refractivity Gradients Taken Out-of-Foliage	395
5.197	Comparison of Tri-Monthly Measured Gradient with NBS Model	397
6.1	Antenna Locations for 0.100-400 Mc/s Measurements	414
6.2	Cage Antenna (0.1 to 2.0 Mc/s)	416
6.3a	0.880 Mc/s Matching Network	417
6.3b	0.100 and 0.300 Mc/s Matching Network	417

ILLUSTRATIONS continued

<u>Figure</u>		<u>Page</u>
6.4	Cage Antenna Ground Radial Layout	418
6.5	Whip Antenna for 12-Mc/s Operation	420
6.6	Modified BC-939 Antenna Matching Unit for 2 and 6-Mc/s Monopoles	421
6.7	Ground Plane for 2, 6, 12, and 25-Mc/s Monopoles	422
6.8	Horizontal Dipole Antenna for 2, 6, and 12 Mc/s	424
6.9	2, 6, and 12-Mc/s Tuner and Balun	425
6.10	25-Mc/s Vertical Dipole Transmitting Antenna .	426
6.11	Vertical Dipole Antenna 50 to 100 Mc/s Range .	428
6.12	Vertical Dipole Antenna 225 to 400 Mc/s Range	429
6.13	25-Mc/s Horizontal Dipole Transmitting Antenna	431
6.14	Adjustable Horizontal Dipole Antenna 50 to 100-Mc/s Range	432
6.15	Military Antenna 225 to 400-Mc/s Range	433
6.16	Vehicular Antenna for Horizontal Polarization Tests at 250 and 400 Mc/s	451
6.17	Mast Tubes in Their Carrying Case	458
6.18	Mast-Joining Sleeves	459
6.19	Tripod and All Working Accessories	460
6.20	Guyed Mast	462
6.21	Insulated Mast Base Plate	463
6.22	Transmitter Tower	467
6.23	Antenna Positioner System	467
6.24	Fifth Wheel Assembly	469
6.25	Internal and External Views of Drive Take-Off Mounted Above the Tower Tripod	471

LIST OF TABLES

	<u>Page</u>
4.1 Physical Characteristics of the Pak Chong Forest	29
5.1 0.1 Mile Path Loss for 80-Foot Antennas	89
5.2 Attenuation Constants for Theoretical Model . .	99
5.3 Height Ranges Used in Height-Gain Study	113
5.4 TP-Point Separation Distances	115
5.5 Estimates of Relative Height Gain	119
5.6 Height Gains for Short and Long Paths	129
5.7 Tabulation of Field Strength Variations $F_A(f, H_t, V, 1.0, H_r)$	156
5.8 Tabulation of Field Strength Variations $F_A(f, H_t, V, 0.2, H_r)$	157
5.9 L_b at One Mile, Vertical Polarization	162
5.10 Polarization Comparison for Frequencies ≥ 25 Mc/s	166
5.11 Polarization Comparison for Frequencies < 25 Mc/s	167
5.12 Polarization Comparison for Low Receiver Heights	168
5.13 Cross Polarization Measurement Program	175
5.14 Rough Earth Statistics	189
5.15 Height Gain Functions for General Statistical Model	191
5.16 Average Difference Between Measured Data and General Statistical Model	193
5.17 Number of Samples Used to Derive Results Shown in Table 5.16	194
5.18 Standard Deviation of Difference Between Measured Data and General Statistical Model	195

TABLES continued

	<u>Page</u>
5.19 Constants for Modified LaGrone Model	210
5.20 Cumulative Monthly Rainfall	221
5.21 Number of Samples Used in Wet-Dry Comparison . .	225
5.22 Median Wet-Dry Path Loss Difference	226
5.23 Conditions and Equipment in Ionospheric Tests .	238
5.24 Comparison Between Skywave and Horizontally Polarized Groundwave	255
5.25 Distribution of Tree Size	287
5.26 Tree Characteristics in Area A Test Paths . . .	294
5.27 Average Wind Effects	318
5.28 Antenna Beamwidths in 10 Gc/s Program	322
5.29 Comparison of Treetop and Line-of-Sight Losses .	376
6.1 Basic Program Transmitters	403
6.2 10 Gc/s Program Transmitters	404
6.3 Transmitting Antennas for Basic and 10-Gc/s Programs	413
6.4 10 Gc/s Program Antenna Specifications	435
6.5 Antenna Characteristics, 10-Gc/s Program	436

1. INTRODUCTION

Final Report Volume I contains the results obtained from the first phase of an extensive experimental and theoretical program on radio propagation in a tropical jungle environment. The purpose of this program is to obtain basic propagation data and related information, both to determine the most efficient use of presently available radio equipment and to assist in the design and development of new equipment for short range tactical communications in such environments. While this program is aimed primarily at the problems encountered in ground based, tactical radio communications systems, the measured data and the results deduced therefrom are general enough to also be applicable to many problems in the fields of electromagnetic surveillance and intrusion detection.

The first phase of this program involves a series of propagation measurements in a tropical forested area in central Thailand. In terms of its climate and the character of its vegetation, this area is characterized as a wet-dry, or monsoon, type of tropical forest. In order to correlate the measured radio propagation data with the natural characteristics of the environment that exert an influence upon radio propagation, the environmental characteristics have been measured in a variety of ways. The total compilation of the radio propagation and environmental data from this first phase of measurements is, therefore, representative of radio wave behavior in one type of tropical, vegetated environment that is common to much of Southeast Asia, as well as other regions of the world.

The second phase of field measurements, which is now under way, is being carried out in a tropical rain forest area in southern Thailand, near the towns of Songkhla and Satun. Here, the annual rainfall is much greater than in central Thailand, and the quantity of vegetation per unit of land area is almost three times as great as in the Pak Chong area, where the first phase measurements have been made. Careful environmental measurements are also included in the second phase experiments. Ultimately, through analysis of these data, simplified techniques will be developed through which the performance of tactical radio systems can be assessed and predicted in any type of tropical environment.

This report is comprised of six sections. The next section is a general discussion of radio propagation in tropical, vegetated environments. Following this is Section 3, which presents a summary of the results obtained from the first phase of the Thailand measurements. Anyone familiar with the previous semiannual reports of this program will realize that a tremendous amount of measured data has been collected and analyzed. Therefore, it is the purpose of Section 3 to summarize only those results that have emerged from the analysis with some degree of distinctiveness, and which may be immediately useful to those who are engaged in tropical propagation problems.

The next section, Section 4, presents a general description of the test area in terms of its geography and environmental characteristics. It will be seen that the test area was especially selected to be representative of a typical jungle area in Southeast Asia in which tactical operations are commonly conducted.

Section 5, titled Data Analysis, is the largest portion of this report. This section presents the results of the analysis of the field measurements in terms of path loss as a function of several variables and parameters. First, the behavior of path loss as a function of distance is presented. Next, the behavior of path loss as the transmitting and receiving antennas are elevated to various heights above the ground is presented. Then, the manner in which path loss in a vegetated environment depends upon the frequency is discussed. This section also includes a discussion of the effects of polarization, terrain, climate, and atmospheric and ionospheric noise upon path loss. The final part of this section discusses the results obtained from the 550 to 10,000-Mc/s measurements.

Finally, in Section 6, the field instrumentation equipment and measurement techniques are discussed. The essential equipment used in the field measurements, as well as the means by which equipment calibration was maintained, is covered. This section also includes a brief description of the various transmitting antennas and of the methods used to calculate transmission path loss.

THIS PAGE INTENTIONALLY BLANK

2. GENERAL DISCUSSION

The natural environment of typical jungle areas often introduces severe radio communication problems in the form of dense vegetation, high levels of radio frequency noise, and rugged topography, all of which seriously reduce the range performance of ground based radio sets. These problems exert a more pronounced influence upon small unit tactical operations in such areas because the mobile character of these operations obliges the use of small size, portable, and relatively low powered radio systems. Yet the ability to communicate within areas having these environmental constraints - at will, rapidly, reliably, and continuously - is an essential prerequisite to successful tactical operations in such areas. Thus, the ultimate effect of these operational and environmental constraints on radio communications is either to limit the range at which tactical operations may be successful, or to reduce the reliability of communications performance if the range of operations is extended beyond the limits of its radio systems. The fundamental problem in regard to this situation is the inability to predict these limits when the set of environmental constraints, taken as a whole, varies significantly from one area to another.

Because the attributes of the environment, such as the terrain roughness or the spatial distribution of the vegetation, are of a statistical character, the limits they impose upon the range performance of radio communications systems are also of a statistical character. Strictly speaking, the environmental attributes associated with any pair of transmitters and receivers are unique to their

locations; and, if either location is changed, the attributes will change. There are, therefore, random parameters, or variables, to be associated with movement, or mobility of the radio terminals. The nature of the problem is such that the influence of these parameters upon the range performance of the radio sets cannot be predicted by purely theoretical means. This is especially true when the propagation path includes a tropical jungle growth. While the science of radio antennas and propagation has provided several excellent mathematical models with which the propagation loss between the transmitter and the receiver can be predicted, and which can be partially applied to the problems at hand, none of these models permits the inclusion of all of the factors involved in a real environment. Nor, at the present time, does there exist a complete mensurative system with which to relate all of the environmental factors, such as topographic roughness, or vegetation parameters, to the prediction of propagation loss for a given path length. And, even if such a system existed, there still would be lacking the knowledge of how these environmental factors vary from one type of tropical area to another.

The ability to predict the course of events and the outcome, within an acceptable level of confidence, is one of the major essentials in the planning and execution of military operations. All of the factors that will affect the progress of the operations must be foreseen and assessed. Because radio systems provide the command and control of these operations, the ability to predict the performance of tactical radio systems, in relation to the effects of the real environment in different types of geographical areas,

is just as important as the other factors of the operations. The techniques for predicting such communications performance are also highly important to the problems involved in improving the performance of presently available radio equipment, and in designing and developing new equipment for use in the future.

The ultimate objective of this propagation research program is to develop the models and techniques necessary to provide this predictive ability. From the foregoing discussion it can be perceived that the approach to this objective must necessarily be concerned with two distinctly different domains of radio propagation phenomena and environmental characteristics, with the relationships between them, and with the significant ways in which these relationships differ from place to place. The approach, therefore, has to be empirical in concept, its authority depending upon the collection of experimental propagation data from actual tropical environments that are realistically typical of those encountered by tactical operations.

The area in Thailand in which the first phase of the experimental measurements has been carried out was selected with the above philosophy in mind. It is a rectangular forested area, about 30 miles on a side, having climate and terrain characteristics very similar to those encountered in military operations in other parts of Southeast Asia. Almost all of the area is covered with jungle growth that is classified as broad-leaved evergreen tropical forest with a two-story canopy.^{1,2} There is an average of 362 trees per acre, with a median tree height

of about ten meters. The topography of the area varies from flat to mountainous, depending on the length and direction of a given terrain profile within the area. Within a world-wide geographical classification system, which is based upon the climatic conditions that prevail in a given region, the test area is classified as a wet-dry tropical region, having an annual rainfall of about 63 inches with a definite dry season of four to six months. The important point is that all of the above factors are parts of a set of characteristics, or attributes, of the natural environment in the test area, by which it is uniquely distinguished from that of other areas. They may be considered as a set of components whose magnitudes are different from one type of area to another. From the point of view of world geography, climate is the most basic and important component of this set. Landforms, soils, hydrology, and vegetation all feel the impact of its authority. Climate, soil, and surface features play roles in influencing the type, abundance, and variety of vegetation, and there is an especially close correlation between zones of climate and zones of vegetation. But, while jungle vegetation is the primary concern of this research program, it must take into account all the other environmental factors which influence radio propagation in a given jungle area. Only by doing this can the propagation models resulting from the experimental data be structured so that they can be transferred to other geographical regions.

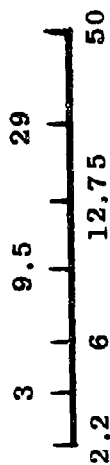
The adverse attenuation effects of tropical vegetation upon ground based radio transmissions have been known qualitatively for quite some time. These effects were

noticeably encountered during World War II operations in the South Pacific theatre. Following this, the first quantitative studies were conducted by Herbstreit and Crichlow in Panama in 1943.³ Later, Dr. Whale conducted similar studies in a tropical forested region in New Guinea.⁴ These two studies, taken together, included the test frequencies of 2, 2.2, 3, 6, 9.5, 12.75, 29, 49, 50, and 99 Mc/s, and demonstrated some of the attenuation effects out to a range of about a mile from the transmitters. Following these investigations, no directly applicable work was done until the last few years when events in Southeast Asia brought this problem to the forefront again.

In order that the propagation data collected from the test area in Thailand might be compared with the data collected from the experiments in Panama and New Guinea, the Thailand test frequencies were carefully selected in relation to the frequencies given above. The relationship of these three sets of test frequencies is shown in Figure 2.1. In this way, this program continues to build up a base of experimental data on the subject of tropical jungle propagation that is consistent with respect to test frequencies so that the propagation data from the different geographical areas may be compared on the basis of the same test frequencies.

The fundamental propagation characteristics that are determined from the experimental measurements in the test area are quantities known as radio path loss. Measurements are made with a calibrated transmitter and a calibrated receiver (more commonly known as a field strength meter). In these measurements, all of the transmitters were located

Whale - 1945
(New Guinea)



Herbstreit & Crichlow - 1943
(Panama)

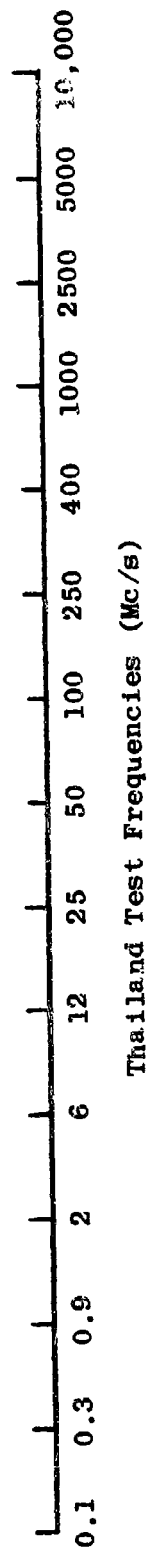


Figure 2.1 Various Test Frequencies for Jungle Propagation Measurements

at a single location in the test area, called the base site. The field strength meter constituted the moveable, or mobile, terminal in the system of measurement activities. By moving the field strength meter out along the trails in the area, measurements of path loss as a function of range and antenna height above ground were accumulated for each test frequency and transmitting antenna polarization. The distances range from 25 feet to 30 miles, and the antenna heights vary from 7 to 80 feet above the ground. As a general rule, the antennas were surrounded by jungle vegetation for all of the measurements.

In view of its importance to this program, it is appropriate to review here some of the basic considerations involved in the concept of radio path loss. The power radiated from the antenna of any transmitting device is ordinarily spread over a relatively large area. As a result, the power available at the antenna of the receiving device is only a small fraction of the radiated power. The transmission loss in decibels is defined as

$$L = 10 \log \frac{P_t}{P_r} \quad (1)$$

where

P_t = power radiated by the transmitting antenna

P_r = power available from an equivalent loss-free antenna in the same units as P_t

The "basic transmission loss," L_b , is defined as
 $L_b = L + G_p$, or

$$L_b = 10 \log P_t - 10 \log P_r + G_p \quad (2)$$

where

G_p = path antenna directive in dB

For isotropic antennas in free space, $G_p = 0$ and equation 2 becomes

$$L_b = 10 \log \left(\frac{4\pi d}{\lambda} \right)^2 \quad (3)$$

Basic transmission loss is simply the system loss to be expected in the actual situation if isotropic antennas are substituted for the real transmitting and receiving antennas. However, since isotropic antennas cannot be created in actuality, it is never possible to entirely separate the quantity, L_b , from the antenna directive gain, G_p . Thus, an experimental measurement of L_b cannot be obtained directly and will always depend upon the accuracy with which the measurement of antenna gains, including cable losses, can be taken into account.

The experimental measurements reported herein all involve carefully controlled calibration procedures and techniques to keep the possibility of this kind of error as low as practical. These procedures are discussed in detail in Section 6 of this report, but a fundamental principle that was employed in almost all of the measurements needs to be mentioned here. Noting equation 2, it can be seen that transmission loss, L , (neglecting antenna losses), is the quantity actually measured. The system accuracy therefore

depends on the accuracy with which P_t , P_r , and G_p can be calibrated. Recognizing that a calibration of P_t and P_r can be more accurately obtained than of G_p , and that the difference between P_t and P_r is generally in the order of tens of decibels, or more, the antennas used for the measurements were purposely selected to have directive gains as low as practical for the situation involved. For this reason, the measurement antennas were generally classic monopoles, or half-wave dipoles for which theoretically calculated performance is known to agree quite closely with actual performance. This has the effect in equation 2 of keeping the quantity G_p very low in comparison to the quantity $(10 \log P_t - 10 \log P_r)$. Throughout the analysis of the experimental data obtained on this program there has been abundant evidence that the choice of this principle of approach to the measurements was a wise one.

THIS PAGE INTENTIONALLY BLANK

3. SUMMARY OF DATA ANALYSIS

The intent of this section is to compactly summarize the principal results of the data analysis from Phase I of the Tropical Propagation Research Program. It should be considered that these results have been drawn from a series of analyses of a very large propagation data base involving many experimental variables. The data covers all the 100 kc/s to 10 Gc/s measurements made in the vicinity of Pak Chong, Thailand, and all the 550 Mc/s to 10 Gc/s measurements made near Sattahip, Thailand. These results may be regarded in the nature of hypotheses, some of which are strongly supported by the experimental evidence, whereas others have not been as conclusively supported as would be desired. The latter sort are, therefore, advanced on a much more tentative basis.

This set of hypotheses has evolved out of analyzing the existing data base from many different points of view. In this way, a large number of separately distinct results, or hypotheses, has emerged. In some cases, the result, or hypothesis, should be viewed more as a conclusion applicable to a single set of data reflecting a specific situation. In other words, the results probably have a more general application to propagation in heavily vegetated areas. However, the reader should be cautioned against hasty acceptance of these results without a full appreciation of the corresponding details in the section of the report on data analysis.

Further work in the next phase of this program will be required to properly condense and generalize the hypotheses presented here. As this second phase of this program progresses, it is likely that some hypotheses will be extended

or modified, others dropped, and some new ones added. It is particularly expected that the second phase of field measurements within the taller and denser tropical vegetation in southern Thailand will lead to a further refinement of many existing results, as well as a better understanding of the phenomena suggested by them.

3.1 Propagation Loss as a Function of Distance in the Presence of Vegetation

- (1) If the quantitative effect of vegetation is regarded as the difference between the measured path loss over a short vegetated path and the calculated path loss without vegetation, then the measured data suggests that the effect of the vegetation upon path loss is independent of the horizontal distance beyond a nominal distance of about 0.1 mile and greater. This result appears to apply in the frequency range of 100 kc/s to 400 Mc/s, and suggests that the principal mode of propagation in a vegetated area is along the treetop-air boundary (lateral wave propagation).
- (2) The vegetative effect referred to above is less for horizontally transmitted polarization than it is for vertically transmitted polarization, particularly in the lower HF region. This difference disappears somewhere between 400 Mc/s and 1000 Mc/s, where the received wave appears to be depolarized. This behavior suggests that propagation within the vegetation above 400 Mc/s acts in a manner characteristic of scattered and multiple diffraction propagation.
- (3) When there is no vegetation within the induction field region of the antenna, the vegetation appears to have no measurable effect upon the antenna

impedance factors. In fact, none of the data at 1 Mc/s and above demonstrates any effect upon the antenna impedance, although the induction field presumably did extend into the vegetation to some extent. However, below 1 Mc/s the effects of the vegetation upon the antenna appear to involve interactions between the antenna and elements of the vegetation within the complex induction field of the antenna. As yet, the work has not provided meaningful quantitative results to associate with these effects.

- (4) For vertically transmitted polarization, at frequencies of less than 1 Mc/s and at distances beyond the induction field of the antenna, the presence of vegetation apparently has no discernable effect upon propagation loss other than a possible slight effect upon the apparent ground constant. This result is based on the measurements made for vertical polarization, using frequencies below 1 Mc/s at separation distances greater than 3 wavelengths. Under these circumstances, average path loss as a function of distance tends to follow the loss expected for the normal surface wave mode. For distances less than 3 wavelengths, path loss increases with increasing distance at a rate less than $20 \log d$.
- (5) From 1 Mc/s to 12 Mc/s, using vertically polarized transmissions at low antenna heights, average path loss increases as $40 \log d$, which is characteristic of the theoretical surface wave in the absence of vegetation. However, there is an additional constant amount of loss apparently due to the exit and entry of the lateral wave through the vegetation surrounding the antennas. This loss component varies from 0 dB at 1 Mc/s to 19 dB at 2 Mc/s, and then continues to increase gradually to 24 dB at 25 Mc/s.
- (6) From 1 Mc/s to 12 Mc/s, using horizontally polarized transmission and low

transmitting and receiving antenna heights, average path loss increases as $40 \log d$, which is characteristic of the theoretical surface wave in the absence of foliage. However, the path loss measured in the presence of vegetation appears to be less than that which would be expected from theoretical calculations for horizontal polarization path loss in the absence of vegetation. This result is not intended to imply that path loss for horizontal polarization is less than it is for vertical polarization; rather, it indicates measured horizontal polarization loss is less than what would be theoretically expected.

- (7) Regardless of polarization, the measured data suggests that both a "through-the-vegetation" mode and a "treetop" mode exist at distances near to the transmitting antenna for frequencies from 50 to 400 Mc/s. It appears that, at distances less than about 0.2 mile, the "through-the-vegetation" mode dominates and that, at distances greater than about 0.2 mile, the "treetop" mode dominates. The "through-the-vegetation" mode is characterized by a $20 \log d$ increase in loss plus an exponential attenuation term. The treetop mode is characterized by an average $40 \log d$ increase in loss.
- (8) Although the average increase in propagation loss with distance is $40 \log d$, the terrain profile has a strong effect on path loss for the UHF-VHF frequencies resulting in a large standard deviation about the expected value.
- (9) At low antenna heights the received field strength fluctuates relatively rapidly with changes in distance. This pseudocyclic spatial variation is characterized by an average half-cycle width of 0.37 wavelength for frequencies between 25 and 400 Mc/s for either transmitted polarization. This variation is further characterized by an average

amplitude which varies from 10 dB at 25 Mc/s to 15 dB at 400 Mc/s for vertical polarization and from 4 dB at 25 Mc/s to 12 dB at 400 Mc/s for horizontal polarization.

- (10) As antenna height is increased, the rapid spatial variation referred to above tends to decrease.

3.2 Propagation Loss as a Function of Antenna Height in the Presence of Foliage

- (1) There appears to be no height gain for vertical polarization below 12 Mc/s for heights up to 80 feet above ground. There is only a slight height gain for vertical polarization at 12 Mc/s.
- (2) The following height gain averages apply to 1 mile or greater transmission paths over rough, foliated terrain.

<u>Freq.</u> <u>(Mc/s)</u>	<u>Pol.</u>	<u>Height</u> <u>Range</u> <u>(feet)</u>	<u>Advantage (dB)</u> <u>in Changing One</u> <u>Antenna Height</u> <u>from 10' to 80'</u>
25	V	10-80	18
50	V	10-80	18
100	V	10-80	14
25	H	10-80	14
50	H	10-80	11
100	H	10-80	14

- (3) The following height gain averages apply to transmission paths of less than 1 mile over smooth, vegetated terrain.

<u>Freq. (Mc/s)</u>	<u>Pol.</u>	<u>Height Range (feet)</u>	<u>Advantage (dB) in Changing One Antenna Height from 10' to 80'</u>
25	V	10-20	0
25	V	20-80	13
50	V	10-20	0
50	V	20-80	18
100-400	V	10-20	0
100-400	V	20-80	24
25	H	10-80	18
50	H	10-80	14
100	H	10-30	0
100	H	30-80	20
250-400	H	10-20	0
250-400	H	20-80	24

3.3

Propagation Loss as a Function of Frequency in the Presence of Vegetation

- (1) For frequencies below 1 Mc/s, the frequency dependence of path loss appears to follow the Norton surface wave function for a smooth earth surface without vegetation.
- (2) At frequencies above 2 Mc/s, using vertical polarization and low antenna heights, measured path loss increases as $40 \log f$.
- (3) For horizontal polarization and 80-foot antennas, propagation loss appears to increase as $10 \log f$ between 2 and 25 Mc/s and as $20 \log f$ between 25 and 400 Mc/s.
- (4) For horizontal polarization and 40-foot-high antennas, measured propagation loss increases as $10 \log f$ between 2 and

25 Mc/s and as $40 \log f$ between 25 and 400 Mc/s.

- (5) At 25 to 400 Mc/s, for horizontal polarization and low antenna heights (13 feet), propagation loss increases as $40 \log f$.

3.4 Propagation Loss as a Function of Polarization in the Presence of Vegetation

- (1) Propagation losses are lower for horizontal polarization than for vertical polarization by as much as 20 dB at 25 Mc/s and low antenna heights. The difference between horizontal and vertical polarization decreases to zero as frequency increases to about 400 Mc/s and as antenna heights are increased to about 80 feet.
- (2) Under vegetated (jungle) conditions, the received wave appears to always be significantly depolarized relative to the polarization of the transmitting antenna. For vertically polarized transmission, the received horizontal component tends to be as large as the vertical component. For horizontally polarized transmission, the received vertical component tends to be 10-20 dB less than the horizontal component. At about 400 Mc/s the depolarization appears to be complete, and there is no average difference between the received horizontal and vertical components.

3.5 Propagation Loss as a Function of Terrain in the Presence of Vegetation

- (1) For frequencies above 25 Mc/s over rough terrain, propagation loss is on the order of 10-20 dB greater in a vegetated environment than would be expected without vegetation. Average path loss increases

as $40 \log d$ and average height gain is as described in Section 3.2. The variation in path loss is large and is comparable to Egli's rough terrain statistic.

- (2) There is no significant statistical difference between the data collected in Sector A and Sector B of the test area for distances of 2 miles and greater, although the topography of the two sectors appears to differ in roughness.

3.6 Propagation Loss as a Function of Climate in the Presence of Vegetation

- (1) There is no significant statistical difference between the data collected in the wet and dry seasons in tropical vegetations.

3.7 Propagation Loss as a Function of Ionospheric Conditions in the Presence of Vegetation

- (1) There are significant periods of each day during which short range communications can be carried out via the ionospheric mode (sky wave) using low HF frequencies. These periods are generally predictable by standard techniques.
- (2) For short ranges (1-20 miles), ionospheric path loss is not significantly influenced by separation distance.
- (3) Atmospheric noise levels appear to be the same for antennas which are submerged in vegetation and antennas which are elevated above the vegetation.

4. TEST SITE DESCRIPTION

This report marks the completion of the measurements at the Pak Chong and Sattahip test sites. During the two and one half years, from December 1964 to June 1966, that this phase of the program has been in operation, a very large quantity of data has been obtained from the propagation and environmental measurements in the test areas; data that ultimately will be used to develop the prediction techniques which are the objective of this program. Since the philosophy behind the creation and operation of the test areas has been so instrumental in acquiring the data base, it is felt that a comprehensive description of these areas will lead to a clearer understanding of the data so far accumulated.

4.1 Brief History

One of the primary goals of the Tropical Propagation Research Program was to conduct the tests in an environment having the features of tropical regions commonly encountered by tactical operations in Southeast Asia. In initiating the program effort, Company and military personnel cooperated in searching Thailand for an area about 30 miles square, uniformly covered with jungle vegetation and having a varied terrain. From map studies, aerial reconnaissance missions and a jeep survey came the selection of a jungle region in central Thailand near the village of Pak Chong. The test area is shown as Area A on the map in Figure 4.1.

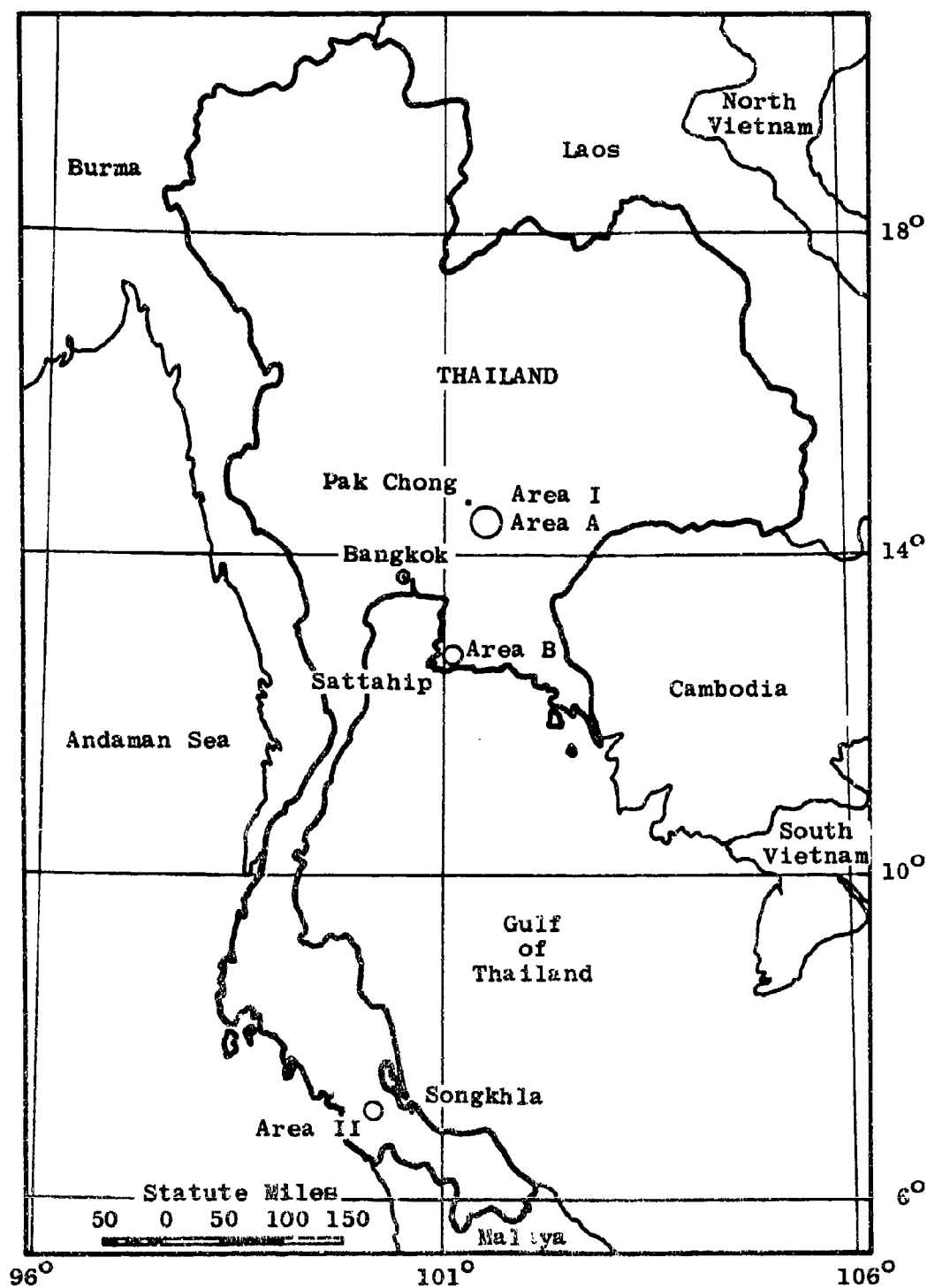
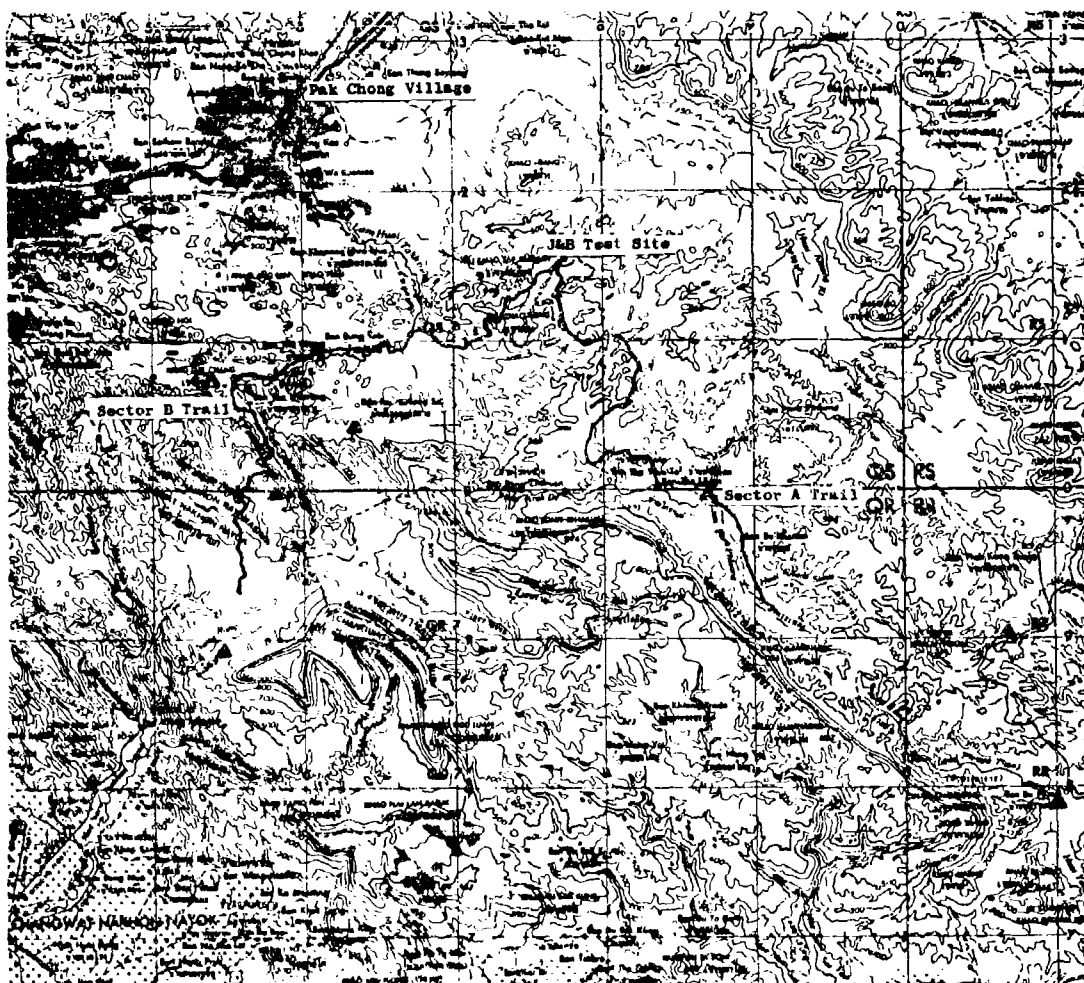


Figure 4.1 Locations of Thailand Test Areas

Figure 4.2, a map of the measurement area itself, shows the main features of the terrain and the locations of the test site and the two trail systems along which measurements were made. The exact coordinates of the test site are $14^{\circ}35'42''$ North and $101^{\circ}34'18''$ East. Although it was only 17 miles by vehicular trail to the village of Pak Chong, which is on a main highway, site logistics by ground were very difficult, particularly during the rainy season.

The initial test plan included propagation tests only in the 100 kc/s to 400 Mc/s range. In 1964 the program was extended to include tests in the microwave frequency range from 550 Mc/s to 10 Gc/s. The purpose behind these microwave measurements was to obtain some basic information about the effects of jungle foliage on detection and surveillance systems. Additional equipment and personnel were sent to the Pak Chong camp to make these tests. Near the camp two microwave transmitting and receiving systems were set up; one to measure diffraction loss over a single, well defined obstacle, the other to measure propagation attenuation directly through the vegetation. Where the test paths in the vegetation were laid out in Area A of the jungle, near the Pak Chong base site, each tree greater than 2 inches diameter at breast height was accurately measured for size and location. About 200 miles south, near the coastal town of Sattahip, also shown in Figure 4.1, a similarly sized area was likewise minutely inventoried and used to make identical attenuation measurements for purposes of comparison. At the Sattahip site, called Area B, the vegetation was characterized by many bamboo clumps and was of much different



5 0 5 10 15
Statute Miles

▲ Helicopter Receiving Sites
Contour lines are in meters.

Figure 4.2 Map of Total Pak Chong Test Area

character than the jungle foliage at Pak Chong. The results of the two tree surveys are in Section 5.9.2.1. Since the test area at Sattahip was located near a town, no base camp was established. Instead, field personnel stayed at nearby lodgings and commuted to the test area.

4.2 Environment

Environmental studies of the Pak Chong area have encompassed its terrain, vegetation, and climate. Certain of these studies have been done in a very exact and detailed way so that they may be statistically correlated with path loss data. These studies are presented in the pertinent chapters of the data analysis section. This section discusses the more general environmental studies.

4.2.1 Climate

The climate at Pak Chong consists of a wet season extending from April to November. During that time the foliage grows considerably, and the ground is always wet. From November to March the ground is generally dry, and growth ceases, though the foliage remains green. Yearly rainfall is around 60 inches, and daytime temperatures average 80 degrees Fahrenheit.

4.2.2 Vegetation

One of the important objectives of this program is to study and understand the quantitative relationships

between the physical aspects of tropical vegetation and the influence of the vegetation upon radio propagation phenomena. Consequently, the subject of the physical characteristics of the vegetation in the Pak Chong test area has received a great deal of attention. Several different surveys have been conducted, but the most definitive work has been done by the Joint Thai-U.S. Military Research and Development Center, supported by a forestry team from the Royal Thai Forestry Department. Their results have been published in two reports.^{1,2}

Climate is the most basic element of the environment. Landforms, soils, hydrology and vegetation all feel the impact of its authority. Climate, soils, and surface features all play roles in influencing the type, abundance, and variety of vegetation. There is an especially close correlation between the zones of climate and zones of vegetation.

The climate of Pak Chong produces a leafy semi-evergreen type of forest, with heavy undergrowth, which can be penetrated on foot with a modest amount of path cutting. The forest is typically dry and has a two-storied canopy. Logging operations ten years ago have modified the forest, and most of the area is now covered with second growth. The following table, which has been obtained from the several surveys and studies, summarizes some of the important physical data associated with the Pak Chong test area.

Table 4.1

Physical Characteristics of the Pak Chong Forest

<u>Characteristic</u>	<u>Unit</u>	<u>Quantity</u>
Rainfall	Annually	63
Total Trees	Per Acre	362
Height Class		
6-16 Meters	Per Acre	290
17-29 Meters	Per Acre	62
30-50 Meters	Per Acre	10
Median Tree Height	Meters	10
Biomass	Tons/Acre	130
Median Tree Diam.	cm.	10
Mean Distance to Nearest Neighbor	Meters	1.3

Because "biomass" is a measure of the total weight of vegetation on a given area of ground, it is anticipated that it will prove to be a useful parameter in the problems of relating vegetation characteristics to propagation predictions. Also, this parameter appears to be potentially useful as a quantitative means of classifying different types of forest growth in correlation with the annual rainfall in the area. In this respect it is worthy of note that the biomass of the test area in Songkhla, where the second phase of this program is now in progress, is about 300 tons/acre, and the rainfall there is about 100 inches annually. Of course, the different history of the two areas must be taken into account, and the area near Songkhla has never been logged. But, it is not likely that normal logging operations would remove some 170 tons per acre from the Songkhla area, and

there would still remain a significant difference in biomass between the two areas if they were compared on the same historical basis.

The biomass of the Pak Chong area has been previously given in Semiannual Report Number 7 as 1276 tons per acre. The calculation of this figure made use of some empirical data obtained from Puerto Rico quite some time ago. However, based on some data recently collected by Dr. Leonard Wood and his Environmental Sciences Division of MRDC, Thailand, this figure is now known to be wrong by a factor of approximately ten.⁷ It is not practical to review the Puerto Rico data and find the reason for the initial error.

Based on the data collected by Dr. Wood, in Thailand, he gives the following empirical equation to estimate the green weight of a tree.

$$W = 0.05(D^2H)$$

where

W = weight in kilograms

D = diameter breast height in centimeters

H = total height in meters

The error of this estimate may be expressed as follows: If W_t is the true weight of a tree, then it is virtually certain that

$$1/2 W \leq W_t \leq 2W$$

The above relations were determined by cutting down some thirty trees of different sizes and species, and weighing them, including the leaf and stem material.

4.3 Description of Base Site

The Pak Chong base site was designed to best meet the operational requirements of the test program. A complex of modular buildings, designed by the Company, was built by Thai contractors. To best cope with the rain, heat, and insects which abound in this region, the buildings were raised off the ground, connected by boardwalks, fitted with louvered walls, and completely screened in.

The transmitting equipment arrived at the site preinstalled in air-conditioned shelters, shown in Figure 4.3, which were placed along a boardwalk. The base itself was cleared and surrounded by a wire mesh fence. Four diesel electric generators supplied power. A helicopter landing pad, garage facilities, an infirmary, and quarters for the Thai support personnel made up the other functional units of the camp. Figures 4.4 and 4.5 show how the buildings were laid out and how they appeared. During periods of the most intense activity, as many as 60 people worked out of this base.

4.4 Test Procedures

Apart from the 10 Gc/s program and tests very near the base site involving hand carried antennas, all the other path loss data came from measurements made along the two



Figure 4.3 Installation of Air Conditioned
Transmitter Shelter

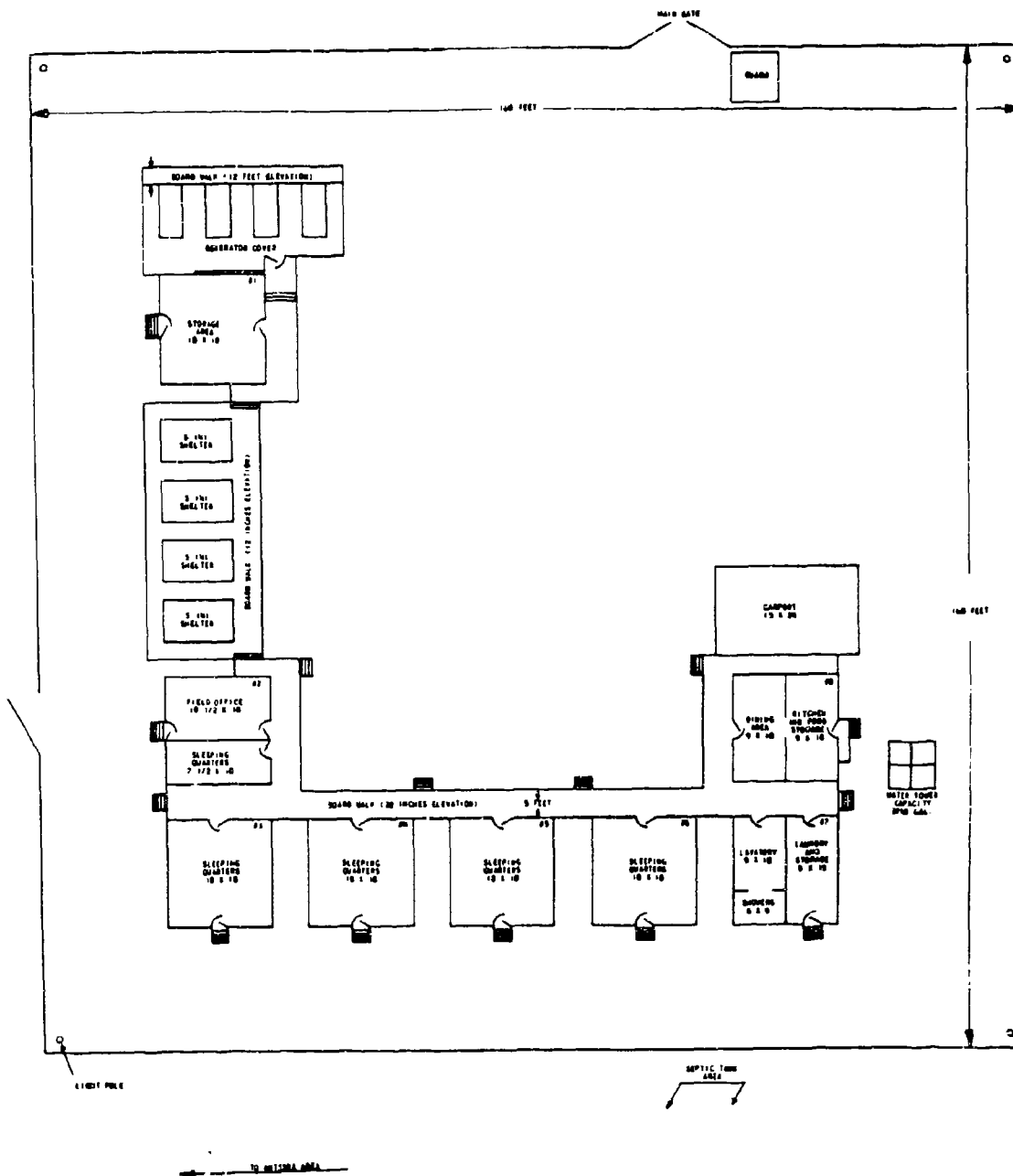


Figure 4.4. Test Compound Plan.



Figure 4.5 Aerial View of Test Site

trails, shown in Figure 4.2, that led out from the base camp. Though both trails are about 20 miles long, the southeasterly trail in Sector A is shorter and less mountainous than the southwesterly trail in Sector B.

In conducting these measurements, the usual procedure was to send out a Nissan Patrol vehicle carrying the receiving equipment and a 3/4-ton truck with the antennas, mast, and other support equipment for the fixed-point tests on one of the trails. Since these tests went on during the wet and dry seasons, the trails occasionally became impassible for these vehicles, and Rolligon vehicles were used in their stead.

Insofar as possible, the vehicles and equipment returned to the base at night. However, at the furthest trail points it was not possible to do so. After the receiving equipment had been set up at some fixed point site, the standard procedure was to cover as many of the different frequencies, antenna heights, and polarization combinations as possible in order to avoid the considerable time delay involved in moving the receiving equipment to another site. Generally only one set of vehicles was sent out on the trail at one time. In traveling to the measuring points, Nissan Patrol vehicles carried a strip chart recorder and a roof antenna, along with the receiving equipment needed to make a continuous recording of field strength for a single frequency. For the group of distant fixed point sites at ranges near to thirty miles, which were inaccessible by vehicle, helicopters transported the equipment.

THIS PAGE INTENTIONALLY BLANK

5. ANALYSIS OF THE DATA

The experimental test program in Thailand has collected a very large quantity of propagation data for a wide variety of transmission paths. It has also accumulated a great deal of data on those elements of the physical environment in the test areas that influence radio propagation. The methods by which the different experimental measurements were carried out are fully detailed in the formal Field Tests Plans^{8,9} and preceding Semiannual Reports, and they are summarized elsewhere in this report. However, the important point to be emphasized here is that this field data exists in a number of formats, each format depending on the peculiarities of the experiment from which the data was obtained. Graphic chart recorders, with special modifications to the drive systems, were used wherever possible. But a considerable amount of the remaining data had to be collected in the form of manually tabulated field notes.

Initially it was planned to carry out a stage of preliminary data reduction and analysis in Thailand with the intention of reducing the raw field data to graphic plots of such basic quantities as radio path loss as a function of distance or antenna height, etc. But it soon became evident that it was not practical to include this step in the field operations, for the rate of accumulation of the experimental data was too great and the computational effort required to convert the data from the units of measure associated with the field equipment to units of path loss was too tedious to be handled by the field personnel. Instead, the quantity of data involved made it

necessary to use electronic computers and other machine methods to convert and analyze the field data efficiently. Therefore, all of the data was sent to the Principal Laboratories where computers and other appropriate machine methods were available for the data reduction and analysis.

The data reduction and analysis effort on this program, which begins with the receipt of the data at the Principal Laboratories, thus encompasses two main steps, or stages, which are somewhat distinct from each other in the purposes they serve.

The first stage, which may be thought of as data reduction, is concerned with cataloging the data so that it can be stored and quickly retrieved as needed. It also involves doing the computations necessary to convert the field data to formats and units of measure more suitable for the analysis and interpretation which follow this stage.

This first stage of the analysis effort created a second generation of data which has turned out to be of much more immediate importance than was at first realized. There are many government and industrial laboratories working on a variety of radio system problems that involve the influence of a tropical, vegetated terrain on radio path loss. Until this program was underway, not much experimental data representative of actual environmental conditions was available with which to attack such problems. It was therefore desirable to distribute this second generation of data as widely and promptly as possible to these laboratories. This was done under the Government's auspices, through a relatively wide distribution of the Semiannual

Reports in which almost all of this data obtained to date has been presented. It is known that this step has already provided useful guidance to several projects concerned with the problems mentioned above. This data has been presented in units of measure that can be easily applied in a quantitative sense to a variety of radio propagation problems.

The second stage of the data handling process puts the data through an operation that is closer to the proper meaning of the word "analysis" than is the first stage of cataloging and converting. As Webster defines "analysis," it is a separating or breaking up of any whole into its parts so as to find out the nature, proportion, function, or relationship of the components, and, furthermore, it includes a statement of the results of this process. This definition can be aptly applied to the procedures and purposes of the second stage of the data analysis effort on this program. Here the behavior of the measured data as a function of the experimental variables, or parameters, is studied. The nature and degree of the relationships between path loss and the variables and parameters evident in the data are determined. Where a strongly dependent relationship is found to exist, a causal relationship is implied. For example beyond some minimum distance, the measured data has indicated that the difference between the measured path loss between two antennas immersed in the vegetation and the calculated path loss without the vegetation is statistically independent of the distance of separation. Strictly speaking, this finding is derived from the spatial domain of experimental variables, and it implies that whatever causal relationships are operating in this case are localized in the near regions around the antennas.

The finding, in itself, gives only a faint set of clues about the actual physical causes of this phenomenon and further experiments and analysis are necessary to fully understand the nature of the situation from a physical point of view. It is, of course, just such an understanding that is necessary to the ultimate objectives of this program, which, besides an understanding of the causes of path loss, also include the development of a generalized model for the prediction of radio path loss characteristics in any tropical environment.

The main purpose of this section of the report is to present a comprehensive summary of the propagation data that has been collected in Thailand so far. The data has been obtained from three series of experiments: (1) experiments in the 100 kc/s to 400 Mc/s range in the Khao Yai, or Pak Chong, area; (2) experiments in the 550 Mc/s to 10,000 Mc/s range in the Khao Yai, or Pak Chong, area; (3) experiments in the 550 Mc/s to 10,000 Mc/s range in an area near Sattahip that is dominated by bamboo growth. With respect to the second and third series of measurements the Khac Yai area is designated as Area A and the Sattahip area is designated as Area B.

An effort has been made to present the data in a carefully organized and systematic way. The order in which it is presented in this section corresponds approximately to the degree of influence of the experimental variables upon path loss. For example, among all of the experimental variables the magnitude of path loss depends most significantly upon the transmission range or distance. Therefore, the data which illustrates the distance dependence of path

loss in the 100 kc/s to 400 Mc/s range is presented first. However, the complete order of the data presentation can perhaps be best illustrated by means of the following matrix which was used to organize this report.

	Fre- quency	Trans- mitting Antenna Height	Trans- mitting Polariz- ation	Dis- tance	Receiv- ing Antenna Height
Vegetation	3	2	4	1	2
Topography			5		
Climate			6		
Ambient Radio Noise	7&8				7&8

In this matrix the headings of the columns correspond to the experimental test variables. In a broader sense these experimental variables correspond to the system variables that are ultimately associated with the design and operational features of most ground-based tactical radio systems. For the present purposes, however, the column headings should be thought of simply as the experimental variables that were subject to control in the course of the field measurements.

The rows of the matrix are identified with the important elements or attributes of the natural environment

that generally must be taken into account in radio propagation problems. When any one or more of these elements are measured in some way, they become test parameters. For example, the biomass of an area is a vegetative parameter and the annual rainfall is a climatic parameter. It is difficult to distinguish rigorously between the meaning of a variable and the meaning of a parameter, and these two terms are often used interchangeably. But in the problem at hand it is desirable to distinguish between the experimental variables on the one hand and the environmental parameters on the other, because the quantities associated with the environmental parameters are not subject to the control of the investigator, whereas the experimental variables appearing in the column headings can be controlled. From the viewpoint of a system's philosophy, these parameters represent the independent elements of the system because they act upon and influence the system performance rather than being subject to the influence of the system.

With the variables and parameters set out as explained above, the individual locations of the above matrix then may be considered to represent either a set of data or a set of functions that express radio path loss as a function of the corresponding column variable and row parameter. For example, the matrix location marked 1 identifies the data plots, or functions, that present path loss as a function of distance with some numerical aspect of tropical vegetation as a parameter. As indicated in a preceding paragraph, this location is given the number 1 because path loss depends more strongly on distance than on any other variable or parameter. The first part of this section of the report is therefore devoted to a summary of the data illustrating the distance dependence of path loss.

Continuing with the order shown in the matrix, the second part of this section deals with the dependence of path loss on the transmitting antenna height, H_t , and receiving antenna height, H_r , when the antennas are immersed in tropical vegetation. Throughout this discussion it should be remembered that all of the 100 kc/s to 400 Mc/s measurements have been conducted in the Khao Yai test area in which the vegetation is considered to be homogeneous with respect to tree density, biomass, and other vegetative parameters. The vegetative parameters are, therefore, regarded as constants throughout these experiments. To introduce variation into these parameters, it would be necessary to conduct the experiments in a different geographical location, having a significantly different set of vegetative parameters.

Next, the frequency dependence of path loss in a tropical, vegetated environment is presented. Here, the frequency range of 100 Kc/s to 400 Mc/s is covered with the thought that the primary application of this data is to ground communications systems. The data on the frequency dependence of path loss in the 550 Mc/s to 10,000 Mc/s range is presented in a later part of Section 5.

The fourth part of Section 5 deals with the influence of the transmitting antenna polarization on path loss in the tropical vegetated region near Pak Chong. Again, the frequency range of concern here is below 400 Mc/s; the effects of antenna polarization in the 550 Mc/s to 10,000 Mc/s range are treated in a later part of Section 5.

In the fifth sub-section, the effects of rough terrain upon the Pak Chong path loss measurements are discussed. The experimental results of these tests have been compared with a number of existing propagation models which do not account for the effects of vegetation. The purpose of this comparison is to analyze the nature and magnitude of the effects of the vegetated rough terrain. In the frequency range of 50 to 400 Mc/s, the best fitting over-all comparison to date has been obtained with a propagation model suggested by Mr. John Egli in 1957,⁶ modified for tropical vegetated terrain. Other models also are examined, including the models developed at the National Bureau of Standards,¹⁰ now ESSA, and a model proposed by A. H. LaGrone.¹¹

Sub-section 5.6 covers the climatological data that was obtained from the test areas in the course of the measurement operations. The collected data covers the period from January 1964 to July 1966 and includes measurements of daily rainfall, barometric pressure, wet-bulb temperature, and dry-bulb temperature. The essential purpose of this data is to permit various correlations between the measured values of path loss and the climatic conditions that existed in the test areas at the time of these measurements. This data also serves the important purpose of accurately documenting the climate of the test areas in quantitative measures.

The following two sub-sections deal with the data obtained from the measurements of radio noise in the Pak Chong test areas. Sub-section 5.7 covers noise measurements made with the same field strength meters that were

used for the path loss measurements. These measurements were intended to serve the following three purposes: (1) to correct the path loss field strength readings at certain test frequencies when the field strength level began to approach the noise level, (2) to examine the possibility that the presence of the vegetation might affect the radio noise level as a function of receiver antenna height in the vegetation, (3) to characterize the noise environment of the Pak Chong test areas in relation to other areas where similar measurements have been made, or may be made in the future. Noise measurements from the point of view of ionospheric propagation are discussed in sub-section 5.8.

Sub-section 5.9, the last part of Section 5, is an integrated summary of the measurements made in the 550 to 10,000 Mc/s range. Since the experimental techniques used in this frequency range were somewhat different from those employed in the measurements below 400 Mc/s, it was thought that the results could be presented better separately, rather than by merging them in the order of presentation applied to the preceding 100 kc/s to 400 Mc/s results. This last sub-section also presents the results of measurements of radio refractive index profiles, both in and out of the foliage.

Throughout the nine subsections described above, there are numerous graphs of basic path loss plotted against a particular variable. All of these graphs also have a number of parameters. To systematize and shorten the listing of the main variables and parameters, an identifying formula is included with each path loss figure. The general expression of the identifying formula is

$$L_b = F_T (f, H_t, P, d, H_r)$$

The formula structure says that basic path loss, " L_b ," is a function "F" of the six quantities shown. The subscript "T" indicates the trail or trails on which the measurements were made, "f" is frequency in Mc/s, " H_t " is transmitting antenna height in feet, "P" is polarization, "d" is transmission distance in feet or miles, and " H_r " is receiving antenna height in feet.

Where these quantities appear as shown above, they represent the variable in a figure or a parameter with more than one value. Fixed parameters are indicated by numerical values in the identifying formula. For example, the identifier in Figure 5.3 is " $L_b = F_{A,B} (f, 80, V, d, 79)$." " $F_{A,B}$ " tells that Figure 5.3 reflects measurements made on trails A and B, "f" indicates that frequency is a variable parameter, "80" is the transmitting antenna height in feet, "V" represents vertical polarization, "d" is the abscissa variable, and "79" is the receiving antenna height in feet.

In some figures the identifying formula appears without " L_b ." This means that some quantity other than basic path loss is shown on the figure. The quantity that is being shown will be identified on the figure and explained in the pertinent part of the text.

5.1 Summary of Propagation Data Over Foliated, Uneven Terrain

The fixed point field strength measurements made at Pak Chong have produced some 27,000 data samples. Additional data is contained in the continuous strip recordings

of field strength. These sets of data comprise a data base which spans the frequency range 0.1 to 400 Mc/s and includes measurements for separation distances as small as 50 feet and as great as 30 miles. This large data base has served as a major tool in unscrambling the dependence of radio propagation on tropical environments. That part of the data base which shows the distance dependence of the propagation path loss is discussed in this section.

5.1.1 0.1 to 30-Mile Fixed Point Path Loss Measurements

The first four figures of this section (Figures 5.1 through 5.4) provide a summary of the average propagation path loss to be expected in a foliated area of the type found in the vicinity of Pak Chong. Figure 5.1 summarizes the fixed point data for vertical polarization with the lowest antenna heights which were used at each frequency. The curves shown on Figure 5.1 represent smooth curves drawn through the fixed point data. All applicable data was used in deriving the curves shown in this and the other figures within Section 5.1.1.

Figures 5.5 through 5.7 and Figures 5.9 through 5.16 show the spread of the measured data about each of the smooth curves in Figure 5.1. As shown in Figure 5.5, path loss increases as $20 \log d$, for a vertically polarized signal at 100 kc/s, in the distance range from 0.1 to 20 miles. This is equivalent to an inverse distance loss. Figures 5.6 and 5.7 show that for 300 kc/s and 880 kc/s path loss increases at a rate less than inverse distance out to about 0.5 mile, and then at a rate greater than

inverse distance for distances beyond 0.5 mile. The rate of increase in loss with distance at 300 kc/s and 880 kc/s is comparable to ground wave propagation with a low conductivity, for example, 0.5 mhos/meter. Figure 5.8 demonstrates this similarity at 880 kc/s by means of a comparison between the range of measured data at Pak Chong and the FCC ground wave curves for 880 kc/s.¹² The FCC data shown in Figure 5.8 has been converted to units of basic transmission loss. Figures 5.9 through 5.12 show that the smooth curves fit the measured data well for frequencies between 2.0 and 25 Mc/s. The propagation loss for a theoretical surface wave is on the order of 20 dB lower than the losses measured in Pak Chong. However, as distance is increased for the measured data, the rate of increase in propagation loss is comparable to the rate of increase expected for the theoretical surface wave.

Figures 5.13 through 5.16 show that, for the VHF-UHF range, a straight logarithmic line no longer fits the measured data nearly as well as it does at the lower frequencies. However, at these frequencies other important effects are coming into play. Three factors to be noted are as follows:

1. Existing data indicates that two modes of propagation exist, i.e., a "through-the-foliage" mode and a "treetop diffraction" mode. The "through-the-foliage" mode is the dominant one out to separation distance of approximately 0.2 mile, at which point the "treetop-diffraction" mode begins to dominate. These two modes and the transition region between them are discussed in Section 5.1.2.

2. The terrain profile has a strong impact upon propagation path loss. While the terrain profiles are treated in Section 5.5, it should be noted here that the relatively constant propagation loss over separation distances of 0.45, 0.7 and 1.0 mile can be explained on the basis of a "treetop diffraction" mode and the particular terrain profile which exists for these separation distances.
3. The system sensitivity limits the range of field strengths which can be measured. This factor is reflected in the reduced spread of the measured data at the most distant field points where measurements were made. At these distant field points, only those field strengths above the system sensitivity are recorded, thus giving the impression of a reduced rate of increase in propagation path loss with distance. This effect can be seen at separation distances in the range of 0.45 to 1.0 mile in Figure 5.16, showing 400 Mc/s data.

The smooth curve approximation to measured data in the 50 to 400 Mc/s range is based upon a theoretical model applicable to the 0.005 to 1.0 mile distance range. The model, discussed in Section 5.1.2, accounts for both the "through-the-foliage" mode and the "treetop diffraction" mode. Where the "treetop diffraction" mode predominates, the model predicts a straight line with a slope of 40 dB per decade.

Figure 5.2 is a summary of the smooth fixed point data for horizontal polarization and low antenna heights. The curves for 2, 6, and 12 Mc/s are derived from measured data for a transmitting antenna height of 40 feet, the lowest height used for horizontal polarization in this

frequency range. The curves for frequencies in the range 25 to 400 Mc/s are based upon measured data for a transmitting antenna height of 13 feet.

All of the smooth curves on Figure 5.2 are straight lines with slopes of 40 dB per decade. The spread of the measured data about these curves is shown on Figures 5.17 through 5.24. At 2 and 6 Mc/s the smooth curves are an excellent approximation to the measured data. At 12 Mc/s, Figure 5.19, the effects of terrain are perceptible at 0.7 and 2.0 miles, and the terrain effects become more pronounced at 25 Mc/s, Figure 5.20. For frequencies of 50 to 400 Mc/s, the theoretical model discussed in Section 5.5 was used to determine the smooth-curve fit to the measured data. This model characterizes the data in excellent fashion at 50 and 100 Mc/s, Figures 5.21 and 5.22. However, in order to interpret the comparison between the smooth curves and the measured data at 250 and 400 Mc/s, Figures 5.23 and 5.24, the three factors previously mentioned in connection with vertically polarized low antenna height data must be considered, namely the effects of terrain, the propagation mode and the system sensitivity.

Figures 5.3 and 5.4 show the summary of smoothed fixed point data for high antenna heights, vertical and horizontal polarization, respectively. The smooth curve approximations to the measured data in all cases are straight lines with slopes of 40 dB per decade. The spread of the measured data about the smooth curves presented in Figures 5.3 and 5.4 is shown in Figures 5.25 to 5.29 and Figures 5.30 to 5.37, respectively.

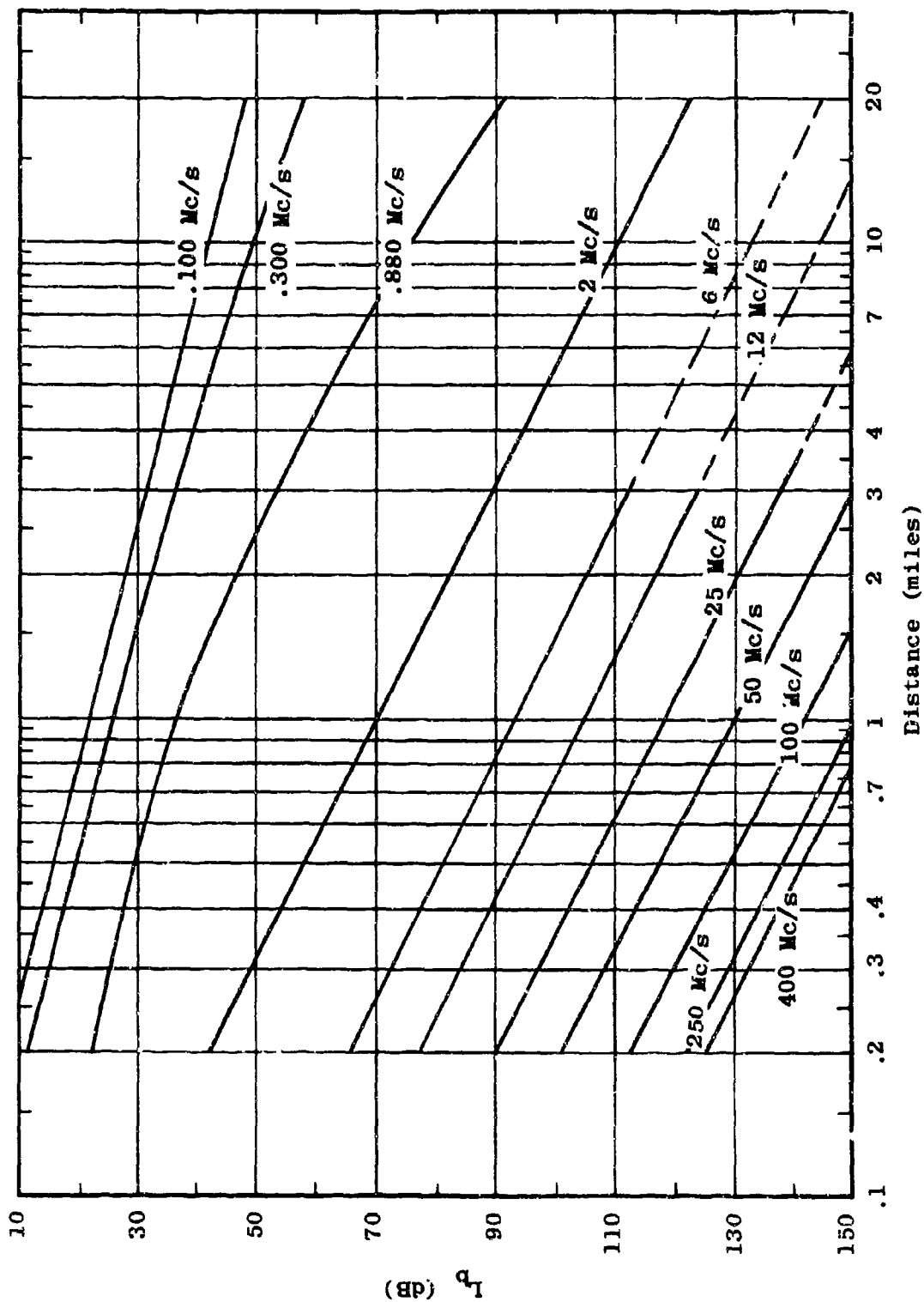


Figure 5.1 Path Loss Summary for Low Antennas *See Figs. 5.5-5.16
 $L_b = F_{A,B}(f, \text{Low}^*, V, d, \text{Low}^*)$
 for exact heights.

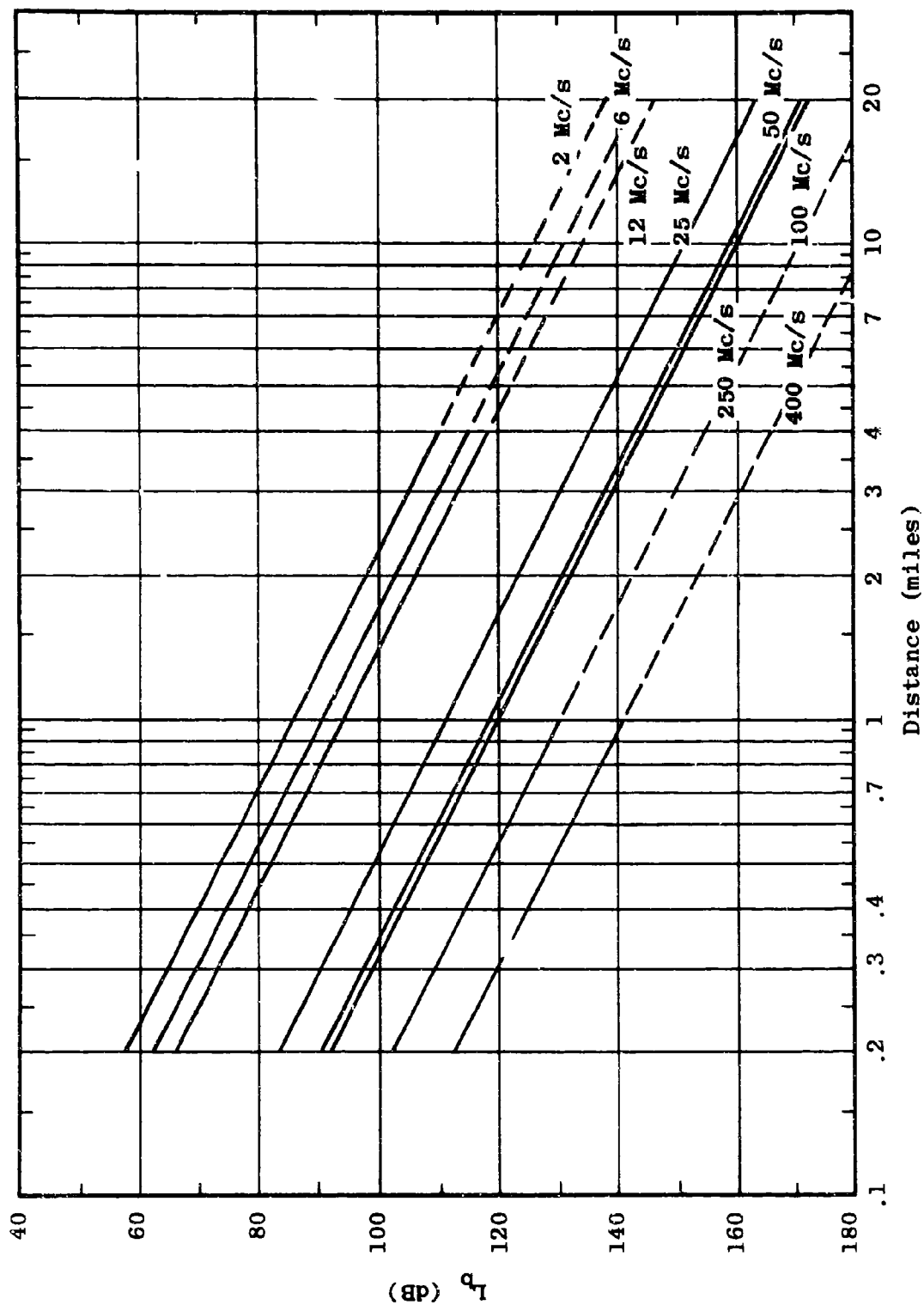


Figure 5.2 Path Loss Summary for Low Antennas *See Figs. 5.17-5.24
 $L_b = F_{A,B}(f, \text{Low}^*, H, d, \text{Low}^*)$ for exact heights.

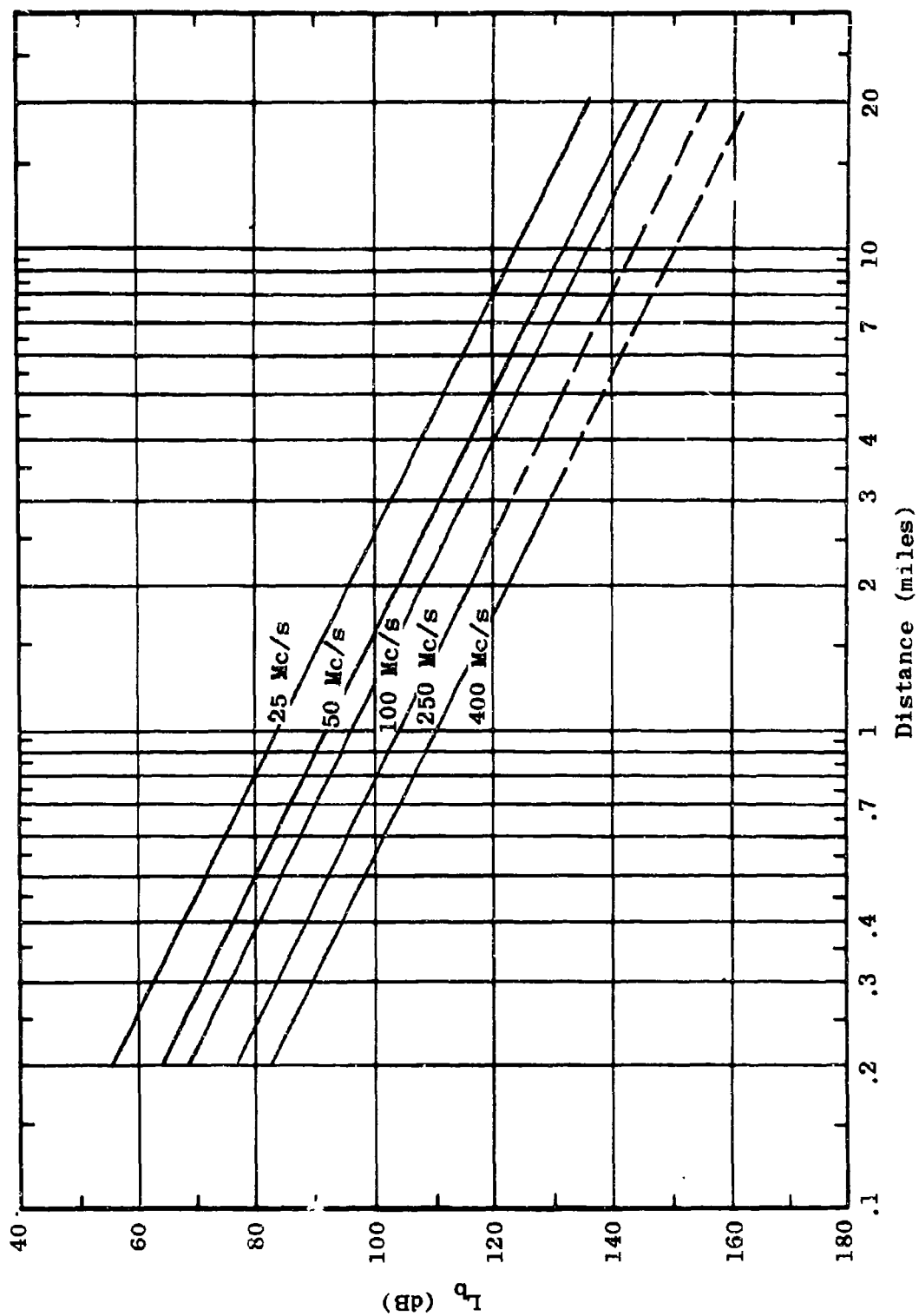


Figure 5.3 Path Loss Summary for High Antennas
 $L_b = F_{A,B}(f, 80, V, d, 79)$

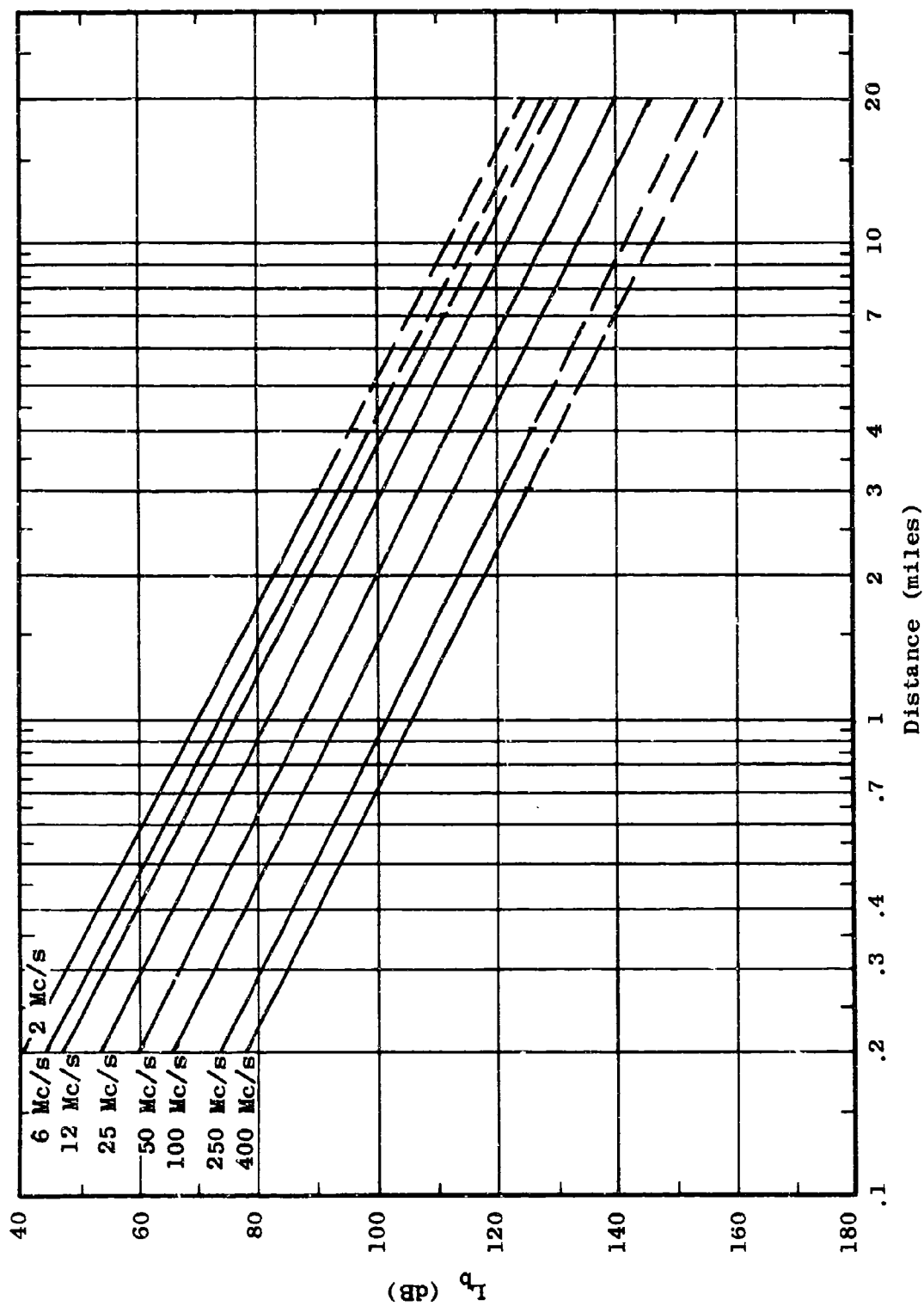


Figure 5.4 Path Loss Summary for High Antennas
 $L_b = F_{A,B}(f, 80, H, d, 79)$

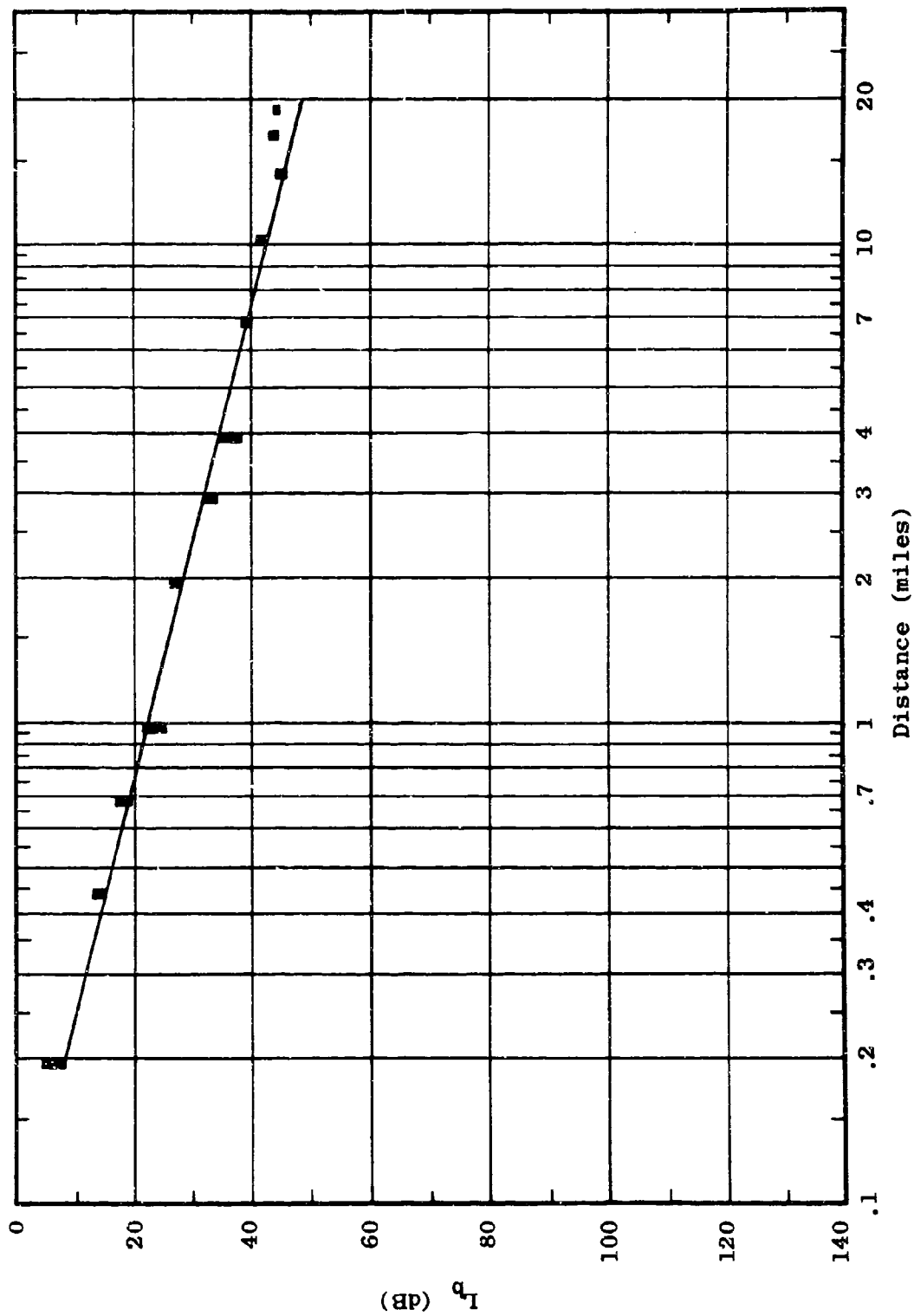


Figure 5.5 Measured Path Loss
 $L_b = F_{A,B}(0.1, 80, V, d, 17)$

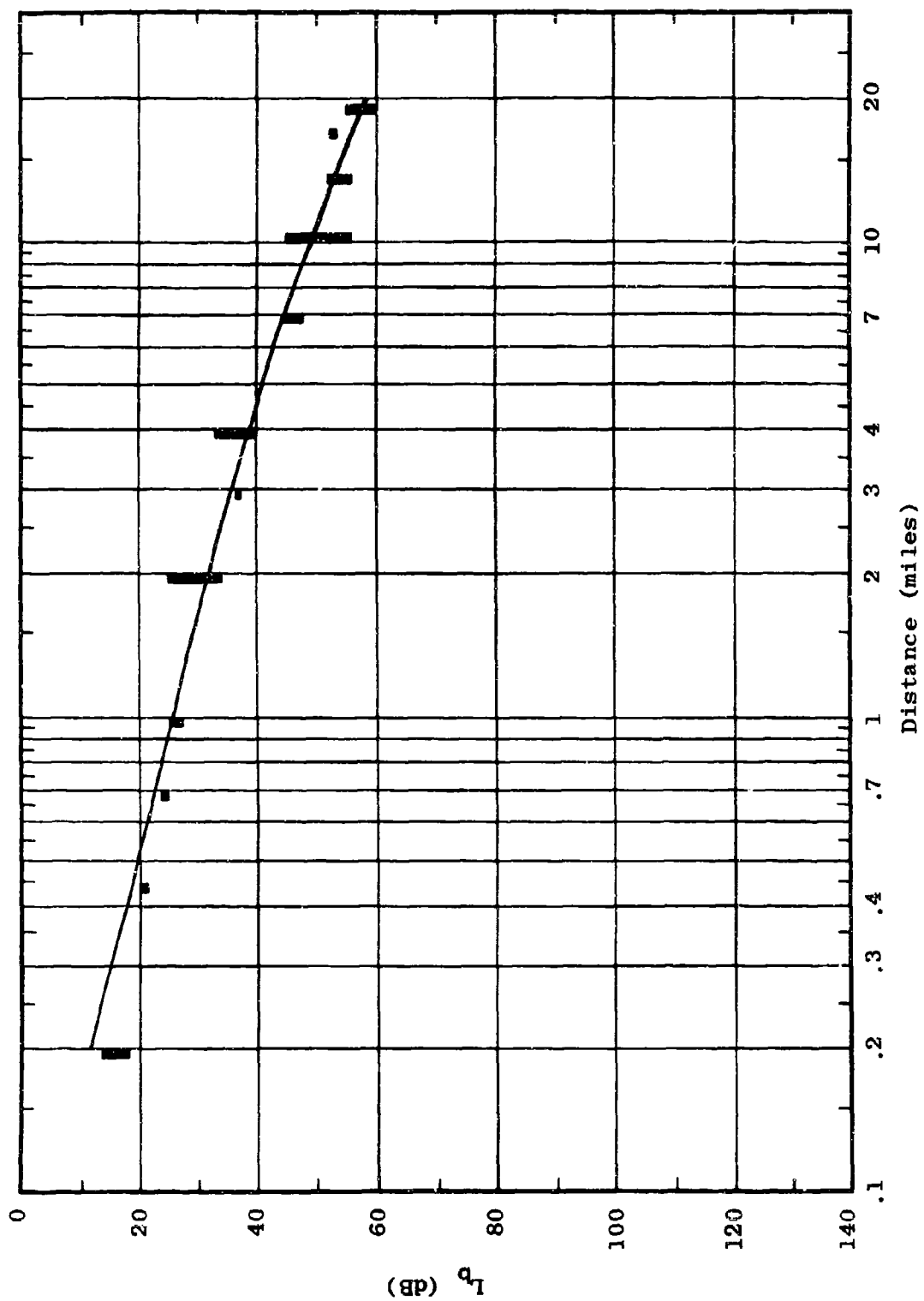


Figure 5.6 Measured Path Loss
 $L_p = F_{A,B}(0.3, 80, v, d, 17)$

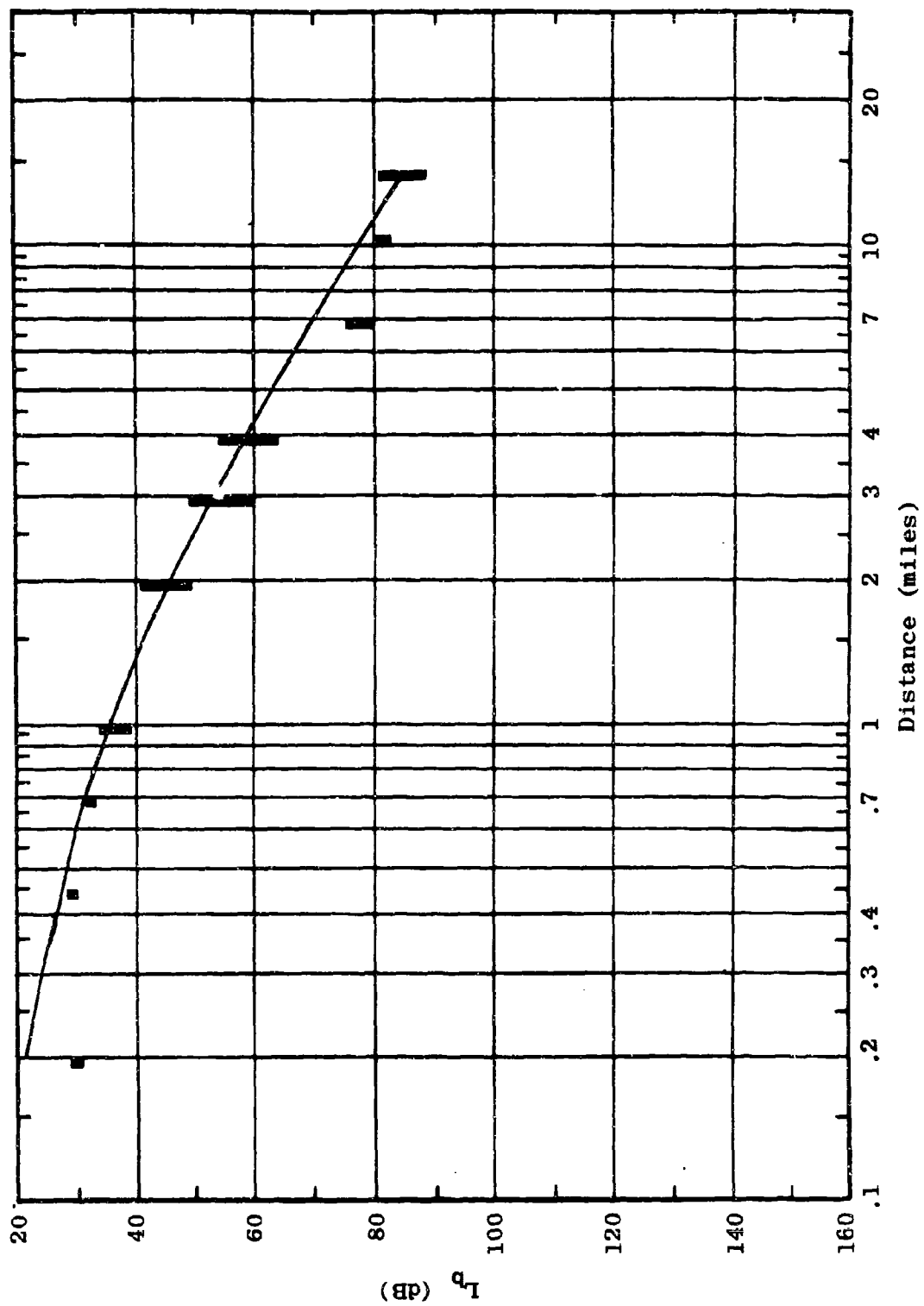


Figure 5.7 Measured Path Loss
 $L_b = F_{A,B}(0.88, 80, V, d, 17)$

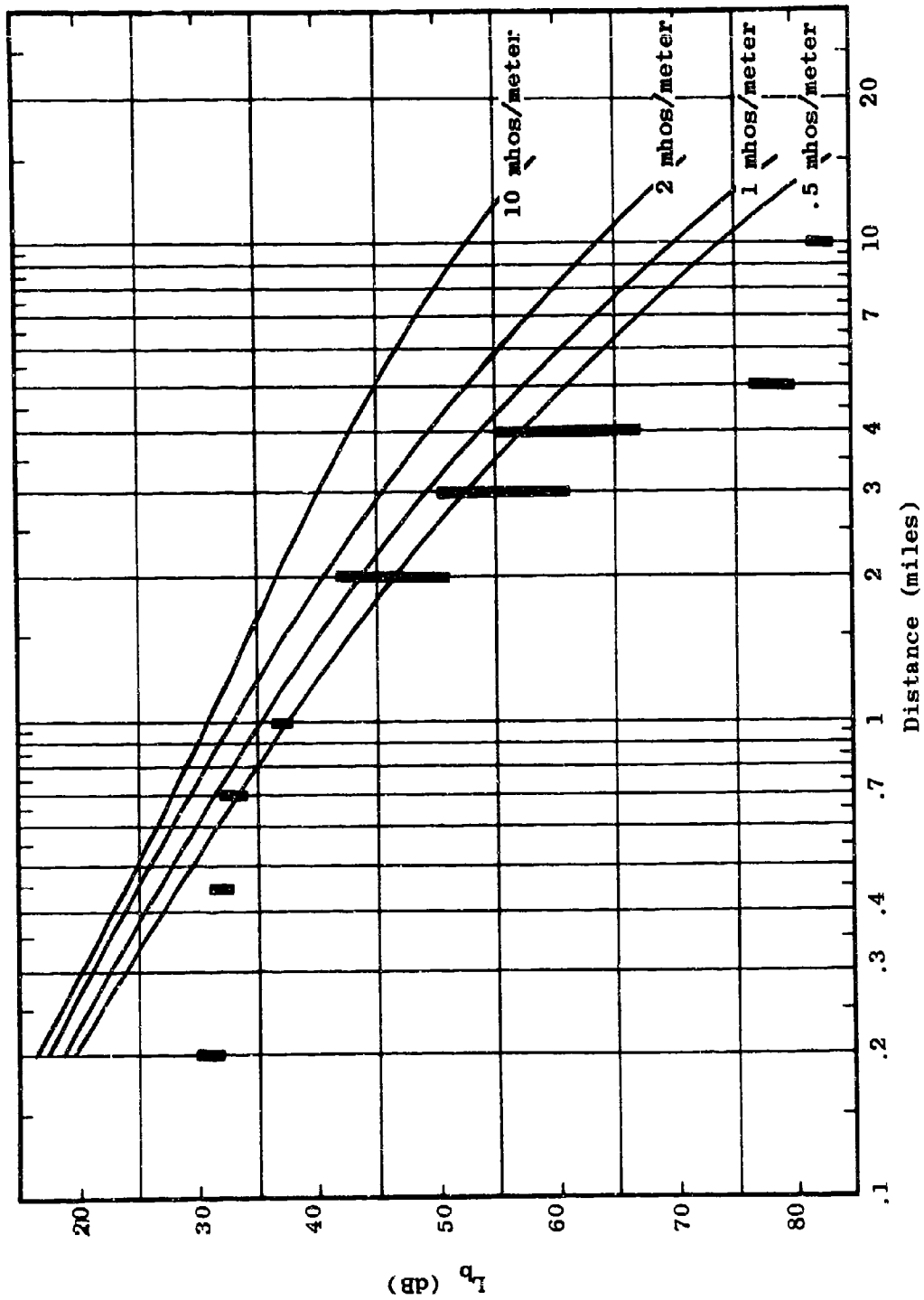


Figure 5.8 FCC Ground Wave Propagation Curves and Pak Chong Measured Data
 $L_b = F_{A,B}(0.88, 80, V, d, 17)$

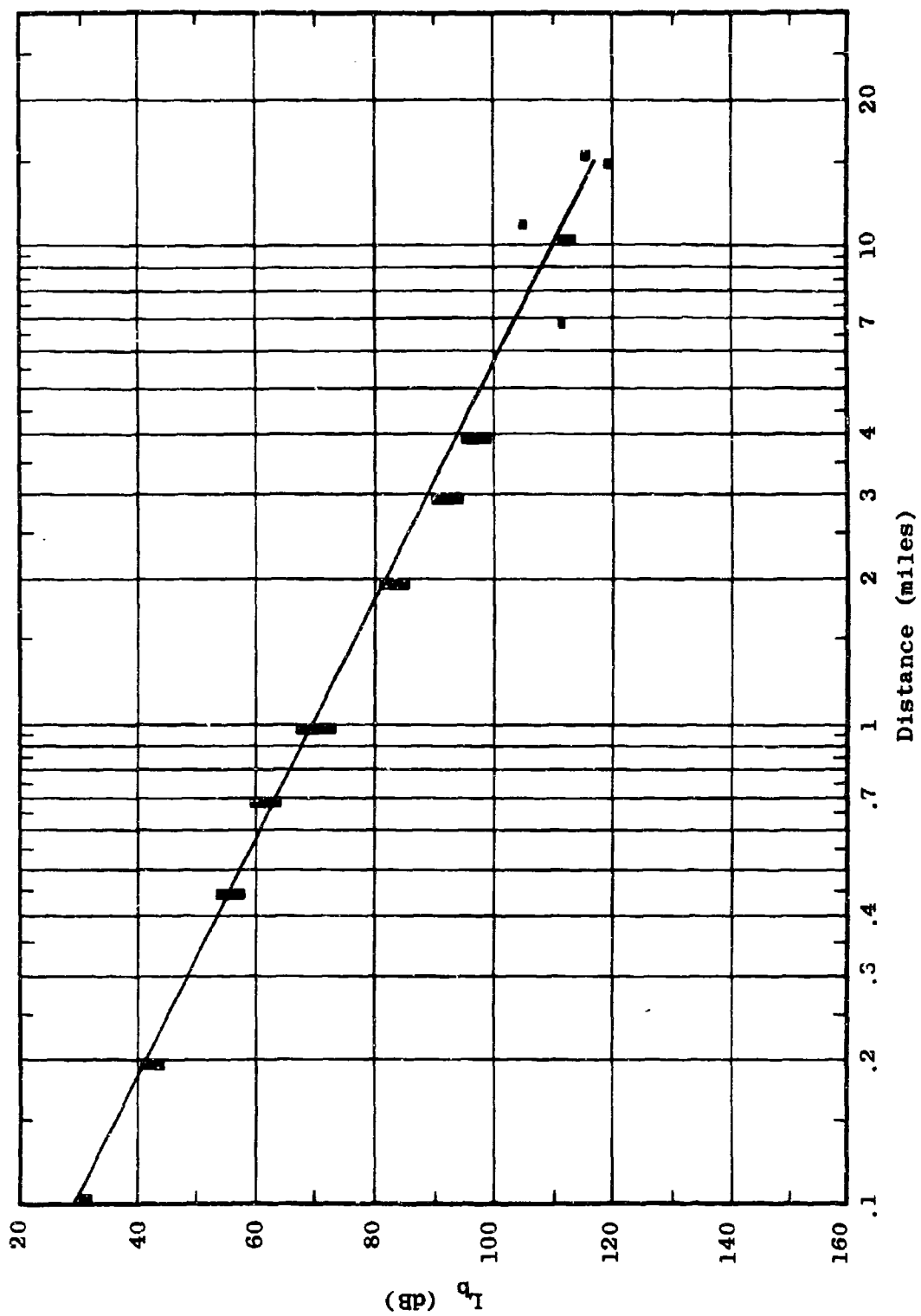


Figure 5.9 Measured Path Loss
 $L_b = F_{A,B}(2, 80, V, d, 17)$

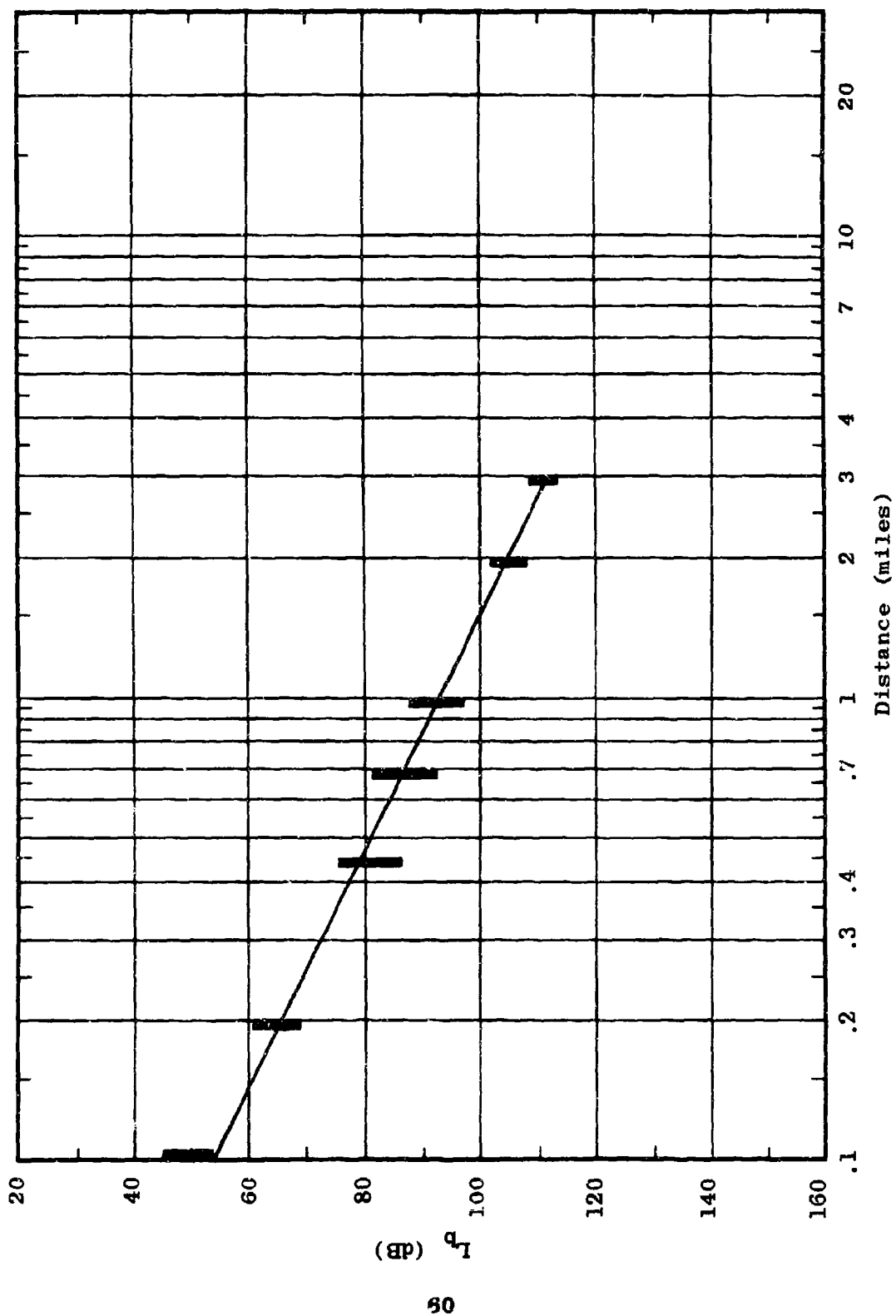


Figure 5.10 Measured Path Loss
 $L_p = F_{A,B}(6, 40, V, d, 17)$

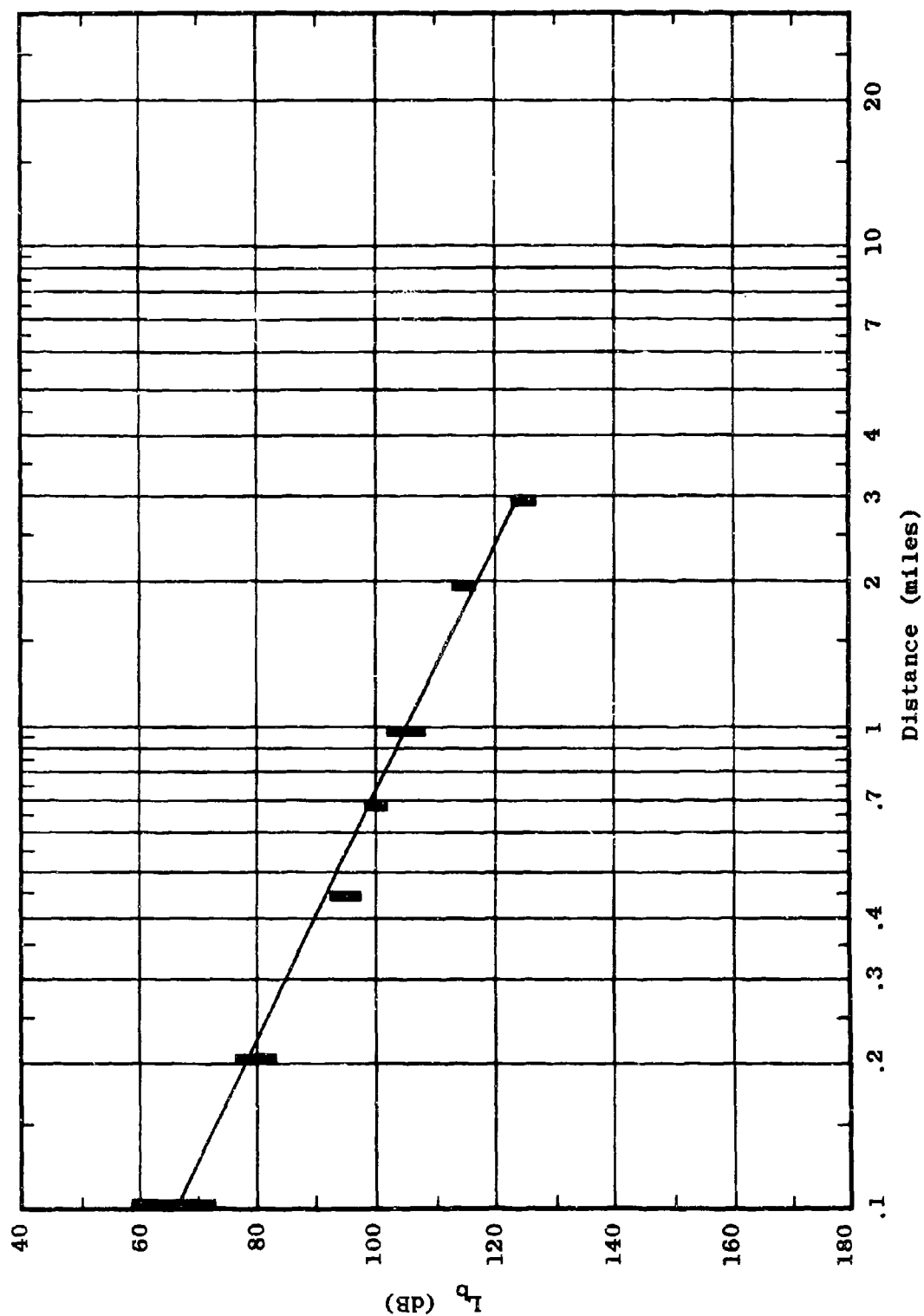


Figure 5.11 Measured Path Loss
 $L_b = F_{A,B}(12, 20, V, d, 17)$

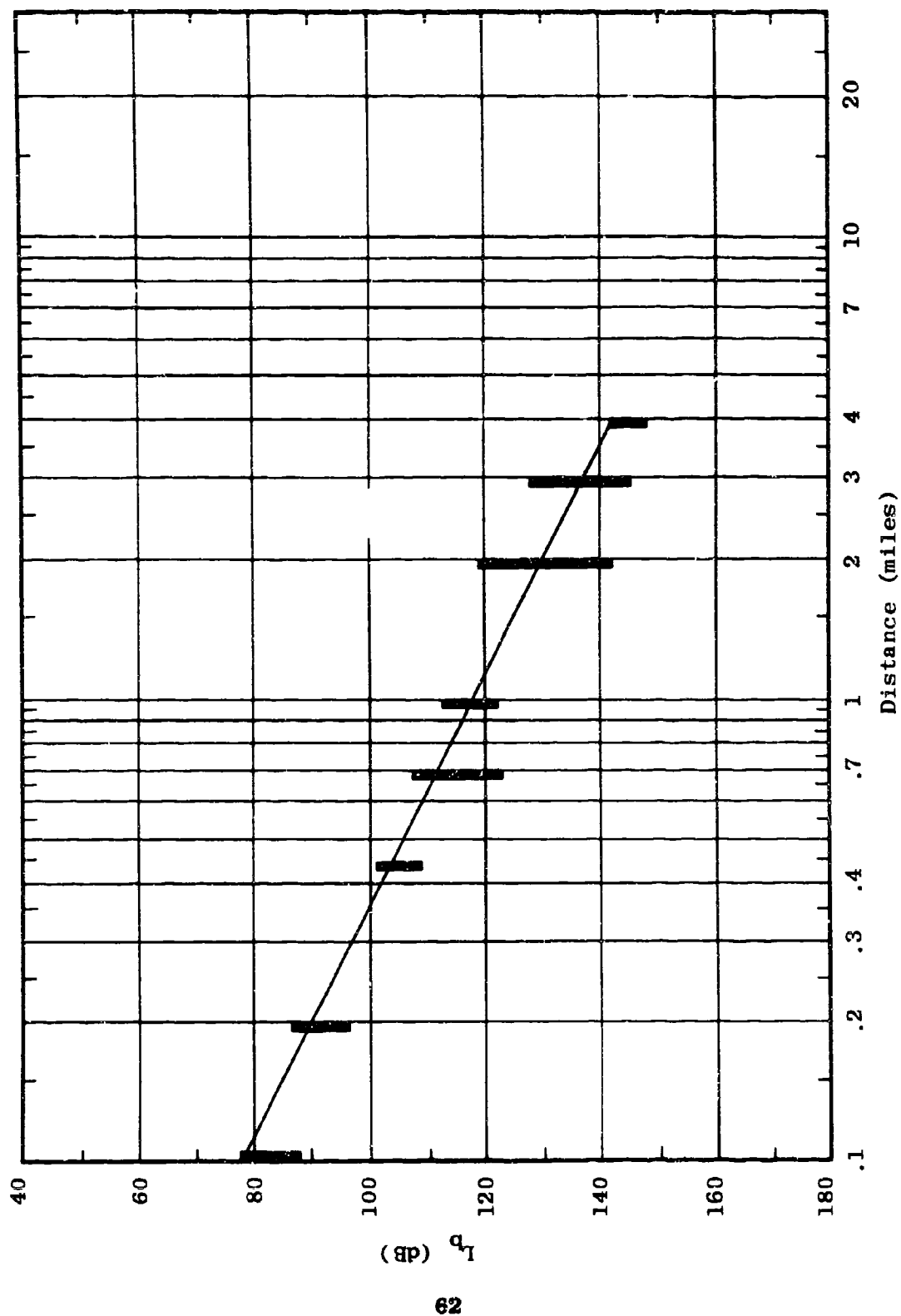


Figure 5.12 Measured Path Loss
 $L_p = F_{A,B}(25, 10, V, d, 11)$

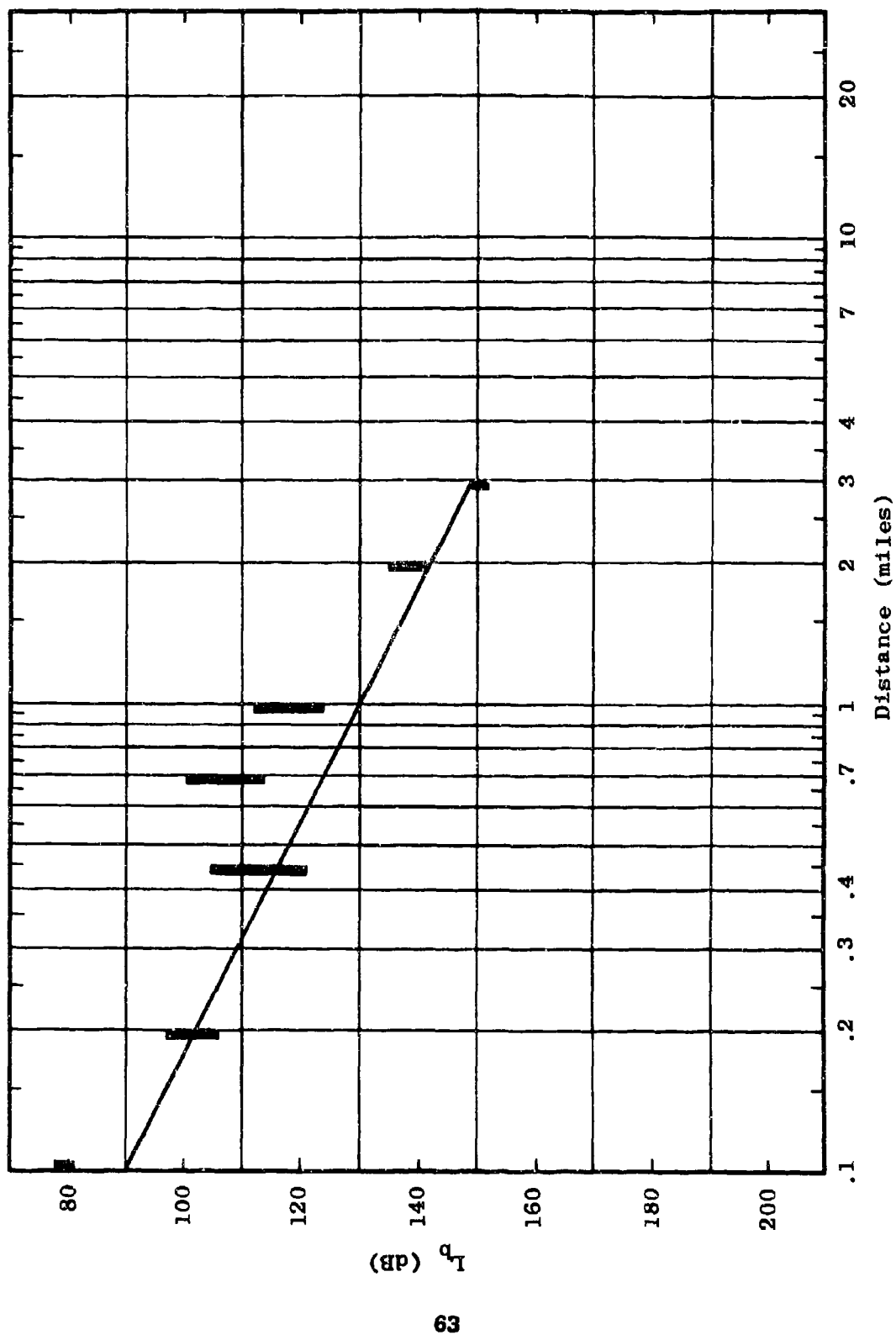


Figure 5.13 Measured Path Loss
 $L_p = F_{A,B}(50, 13, V, d, 11)$

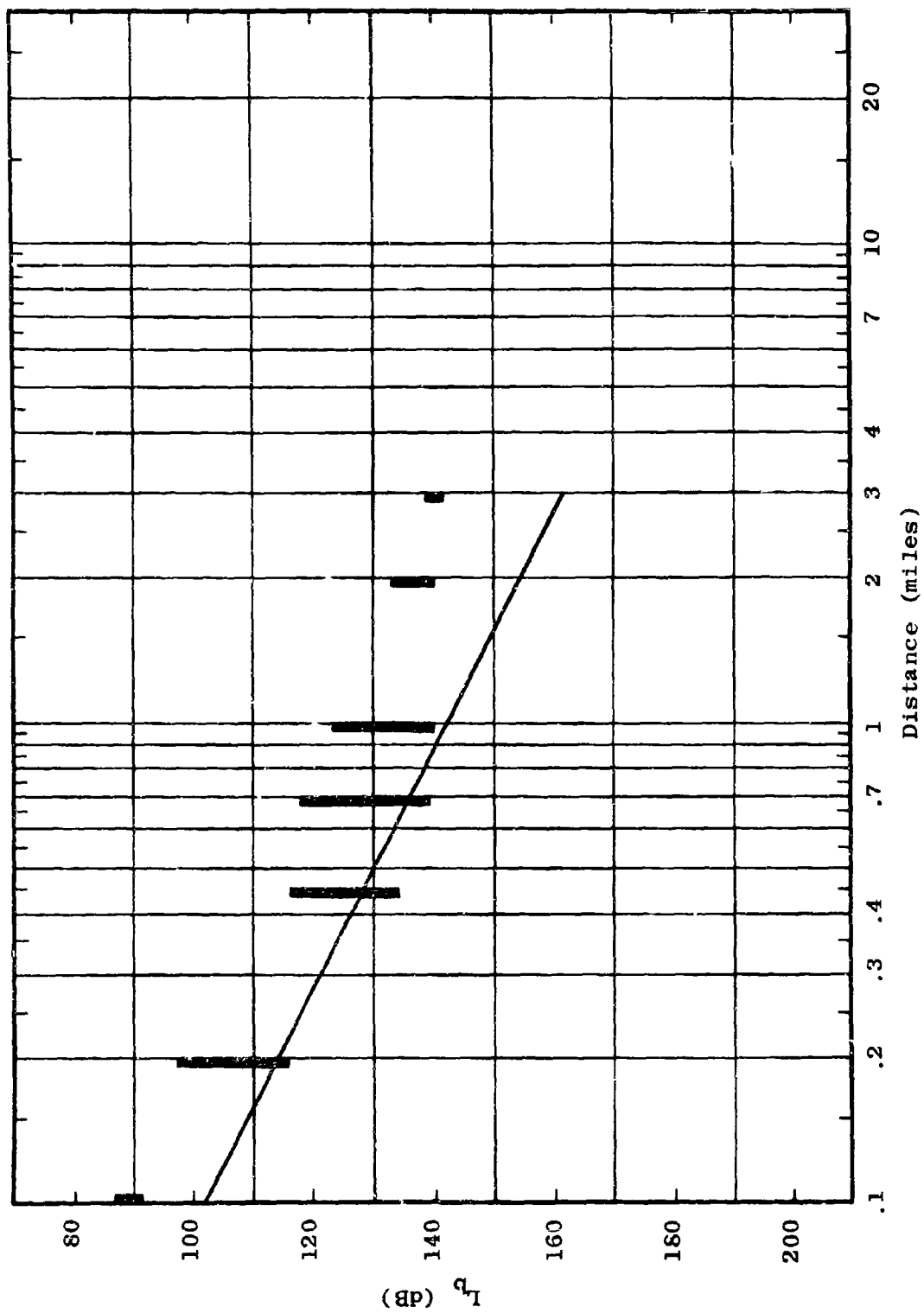


Figure 5.14 Measured Path Loss
 $L_p = F_{A,B}(100, 13, v, d, 11)$

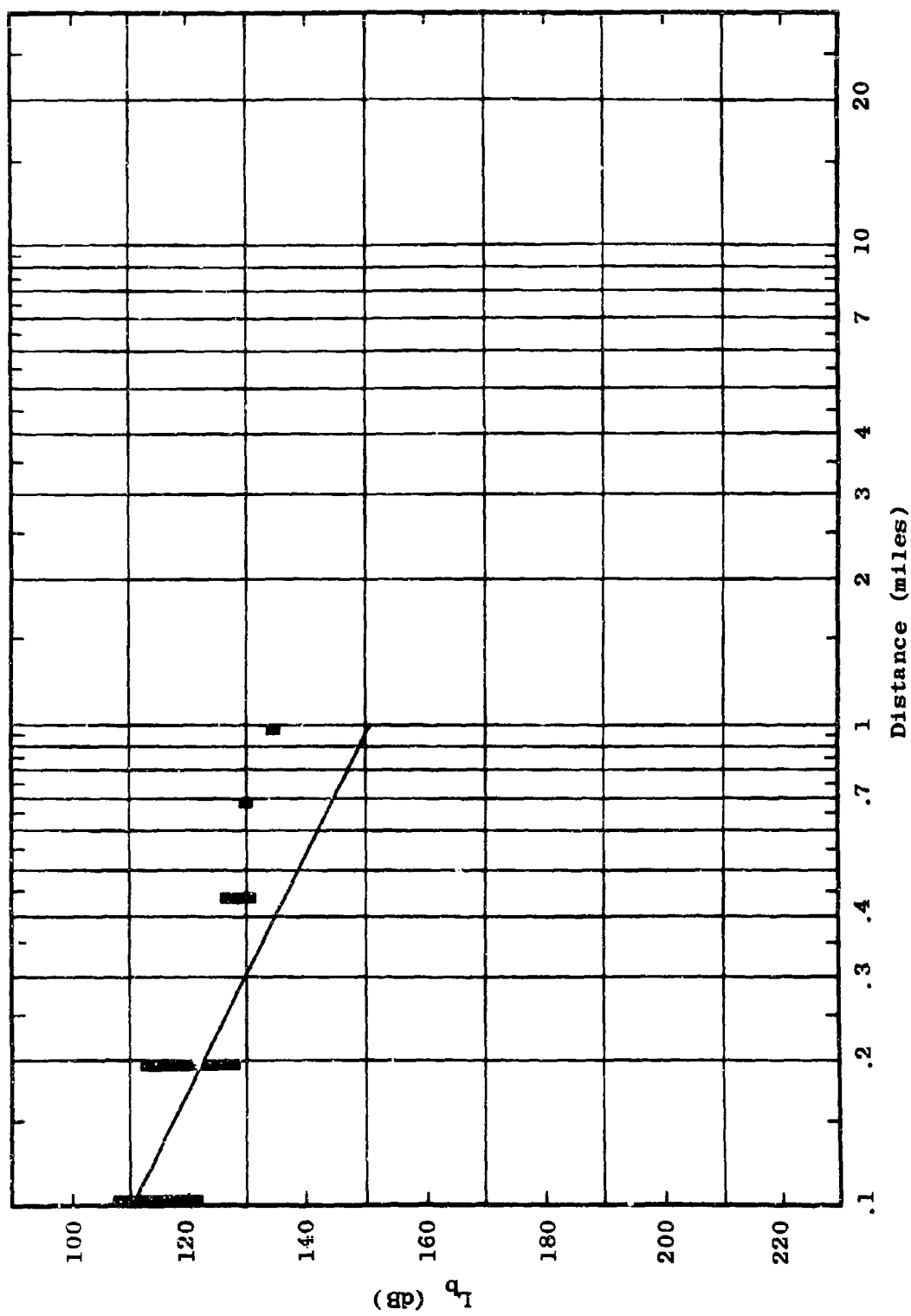


Figure 5.15 Measured Path Loss
 $L_b = F_{A,B}(250, 13, V, d, 11)$

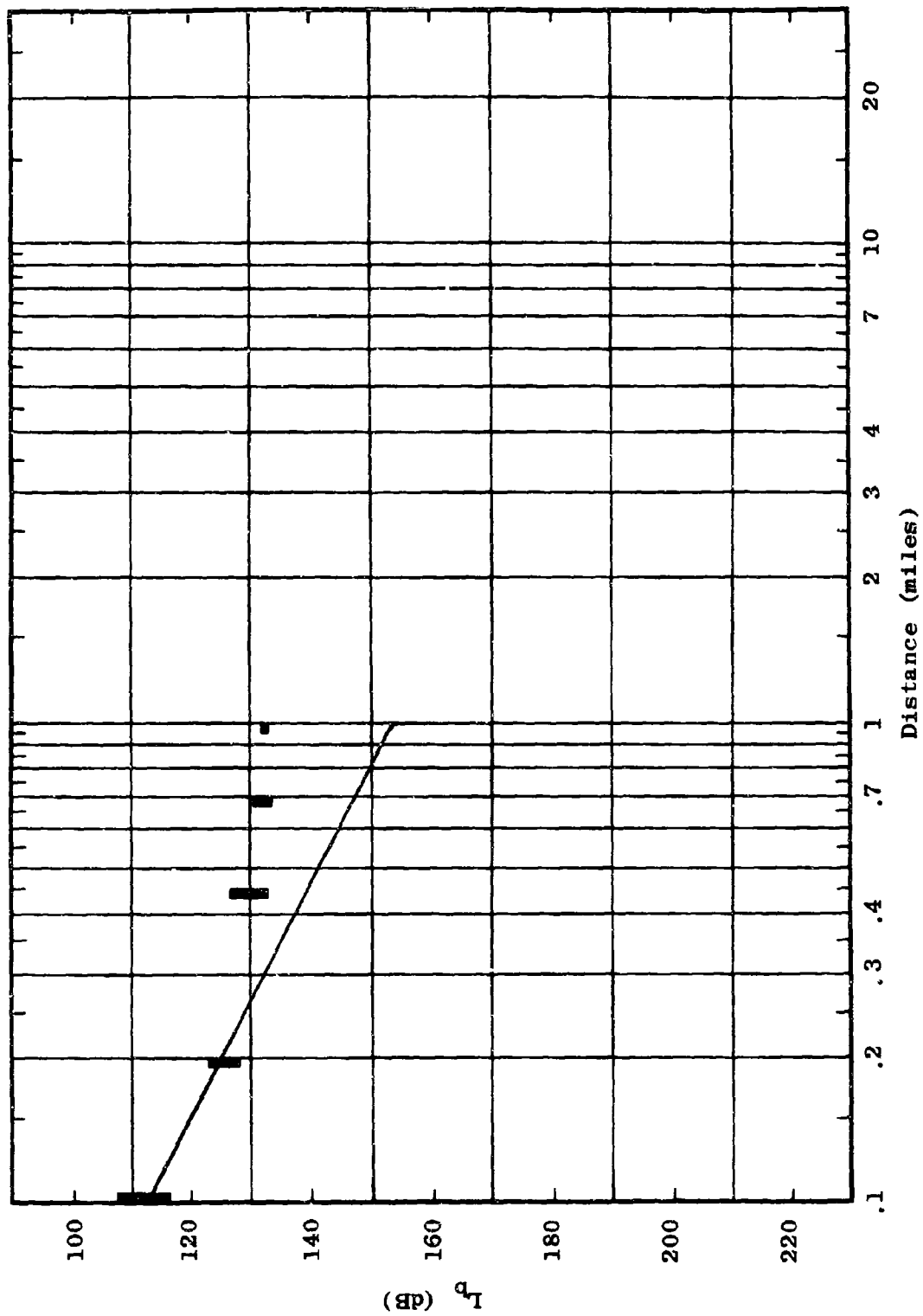


Figure 5.16 Measured Path Loss
 $L_b = F_{A,B}(400, 13, V, d, 11)$

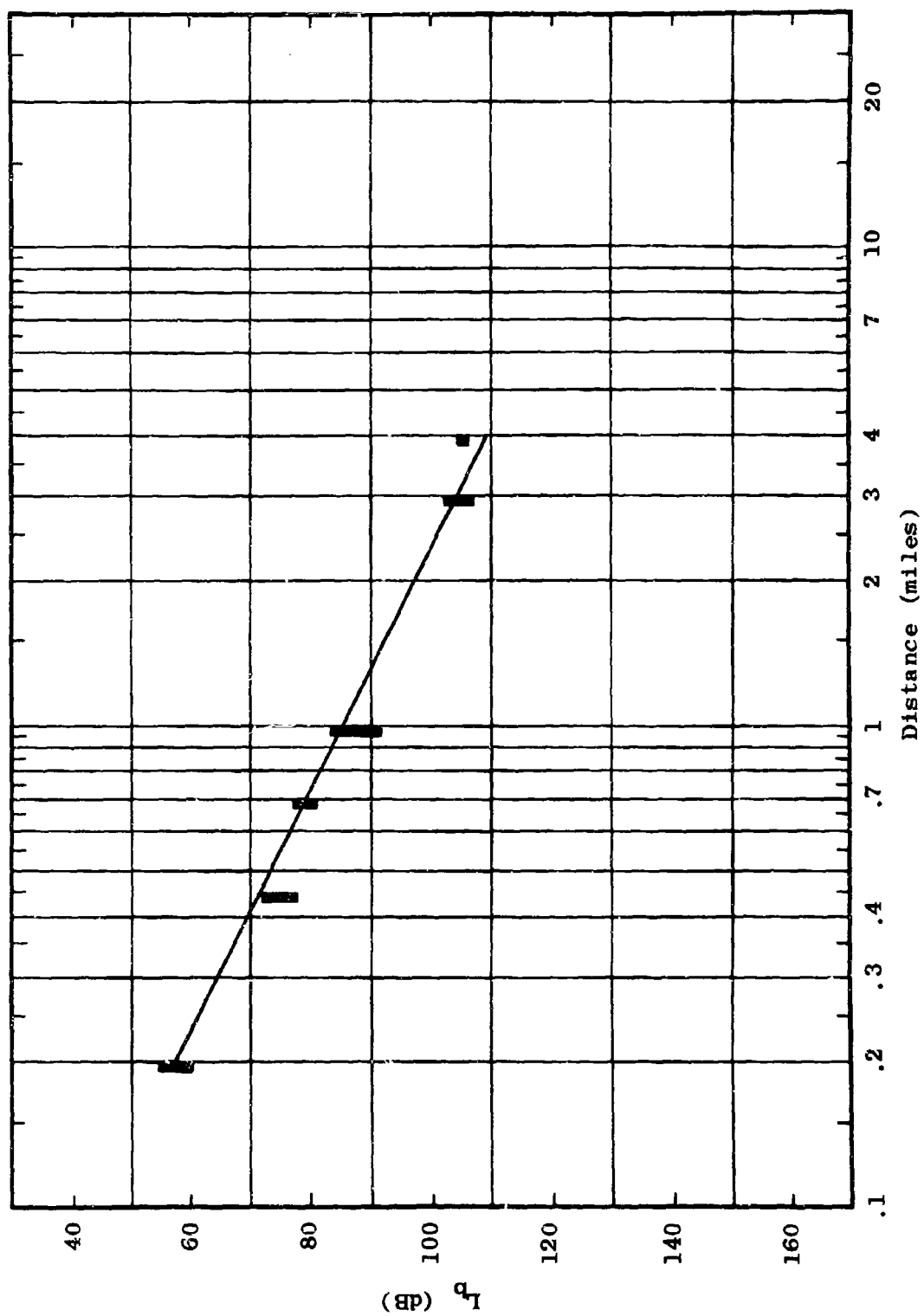


Figure 5.17 Measured Path Loss
 $L_b = F_{A,B}(2, 40, H, d, 17)$

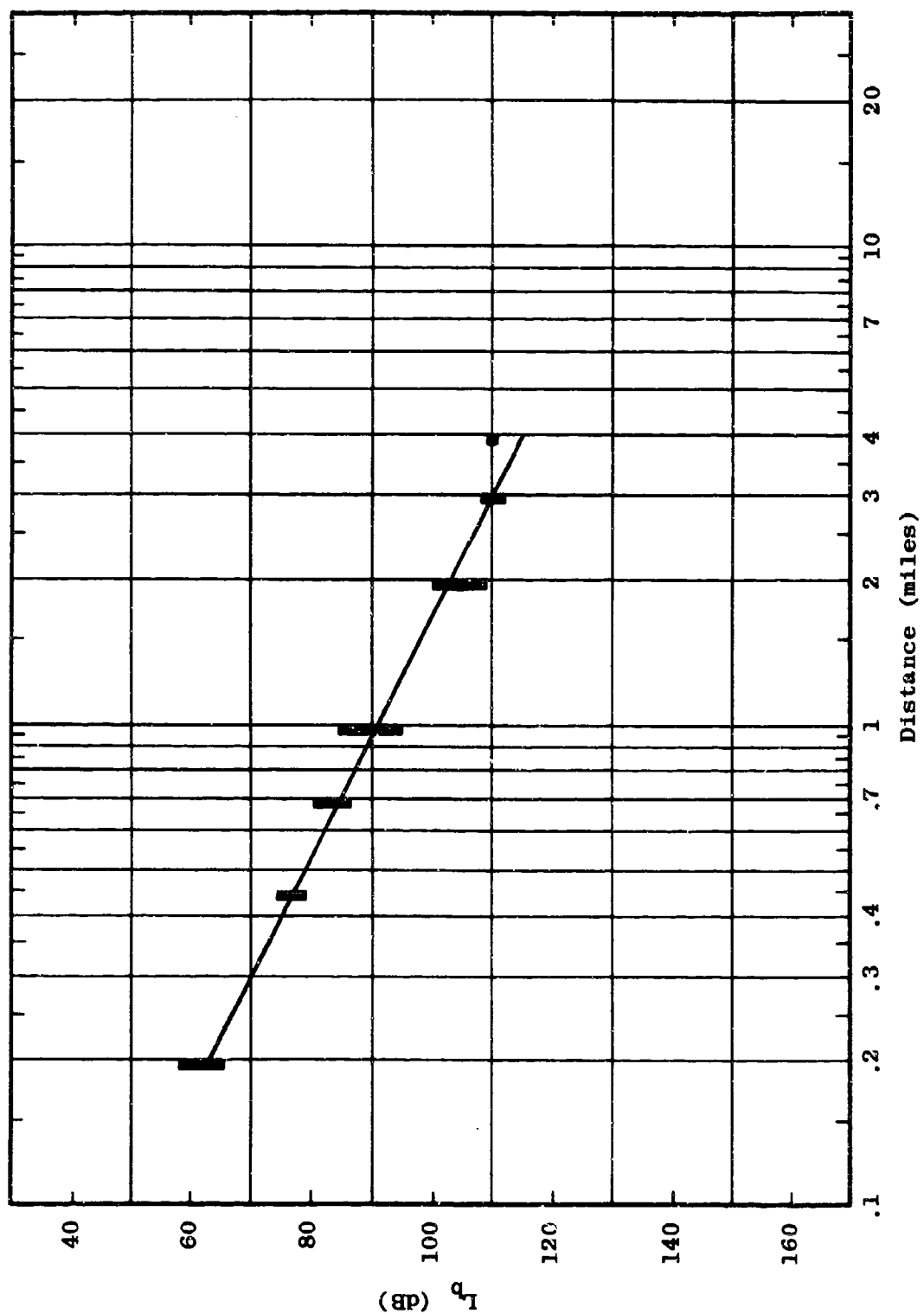


Figure 5.18 Measured Path Loss
 $L_b = F_{A,B}(6, 40, H, d, 17)$

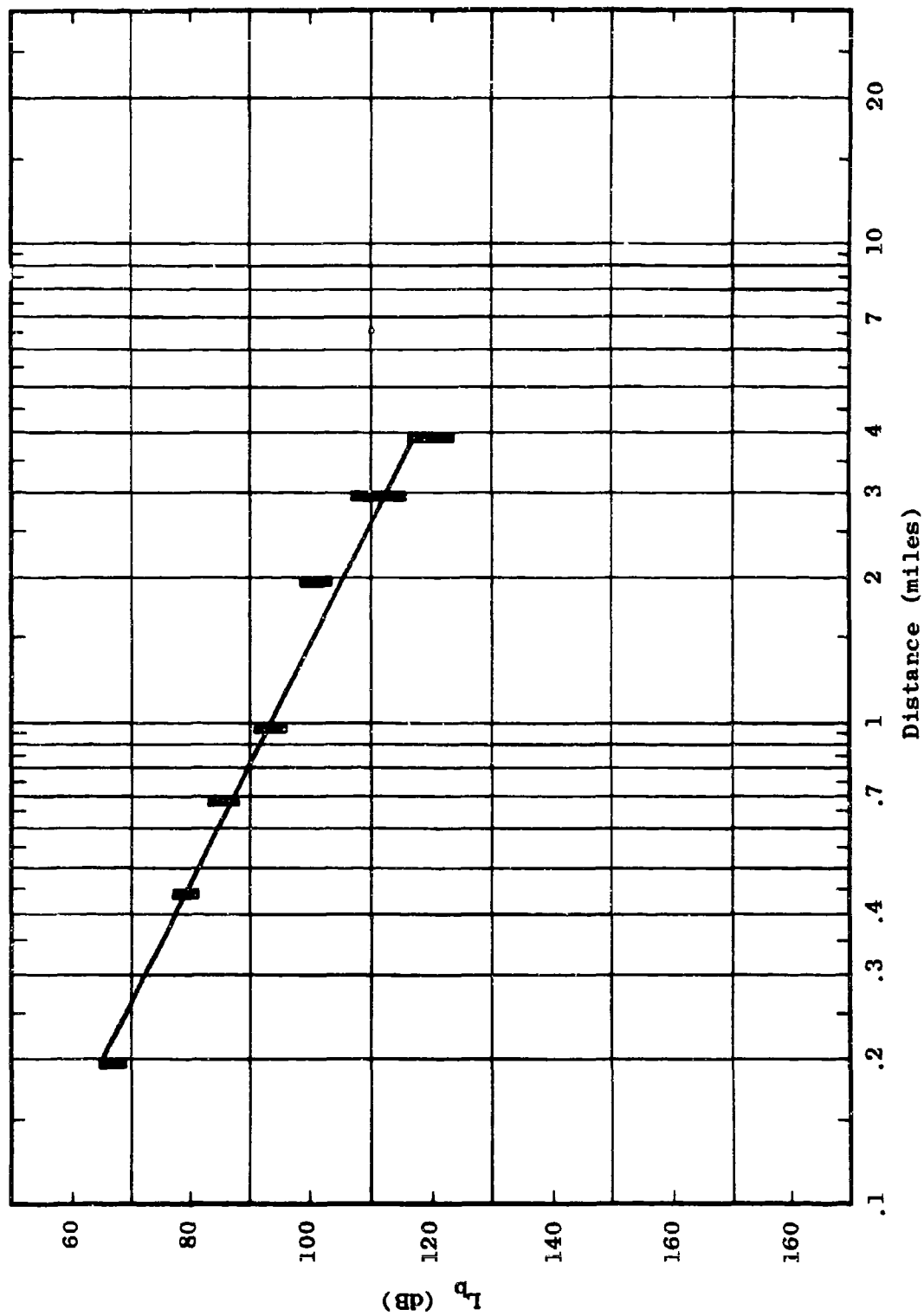


Figure 5.19 Measured Path Loss
 $L_b = F_{A,B}(12, 40, H, d, 17)$

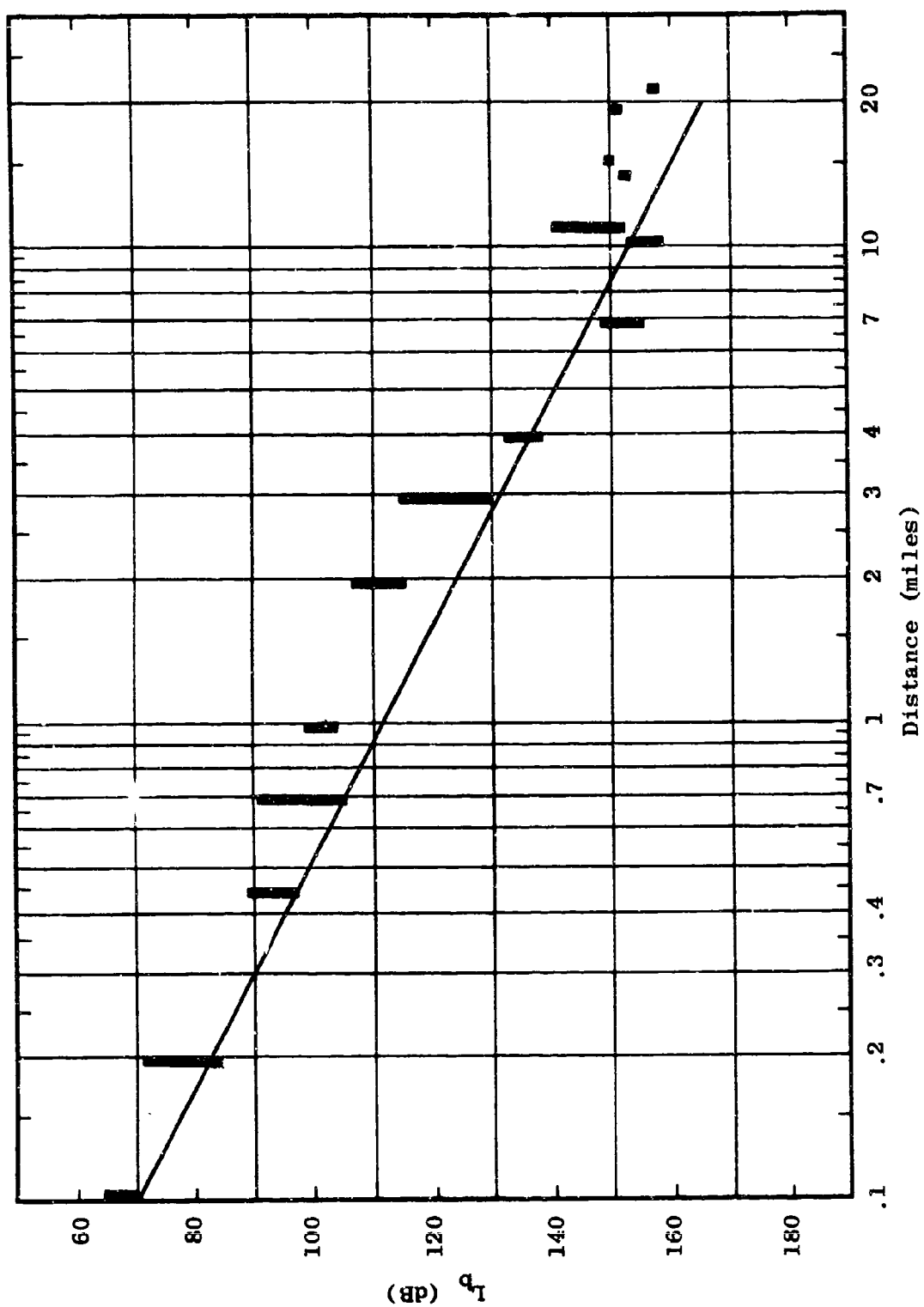


Figure 5.20 Measured Path Loss
 $L_p = F_A, B(25, 13, H, d, 11)$

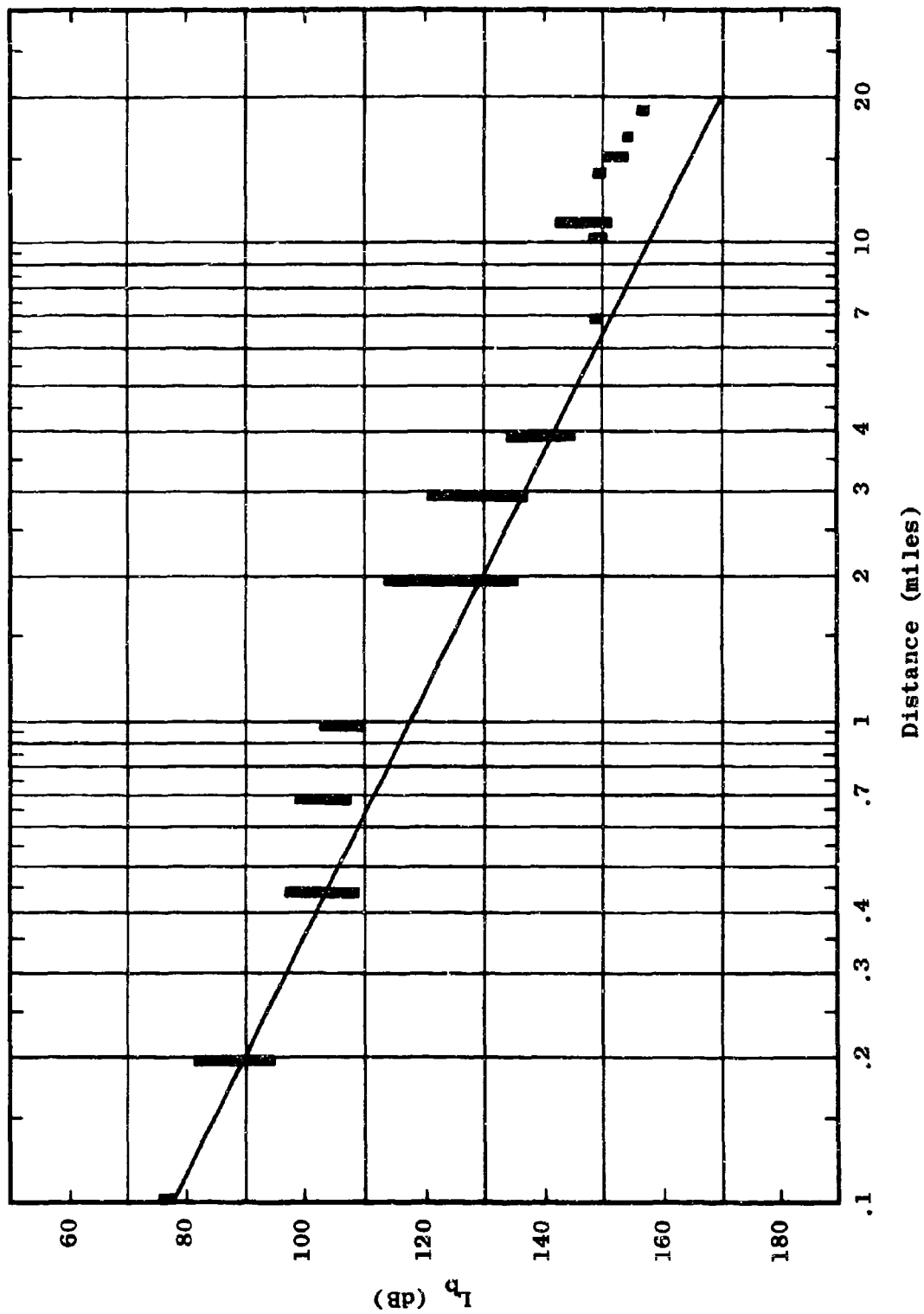


Figure 5.21 Measured Path Loss
 $L_p = F_{A,B}(50, 13, H, d, 11)$

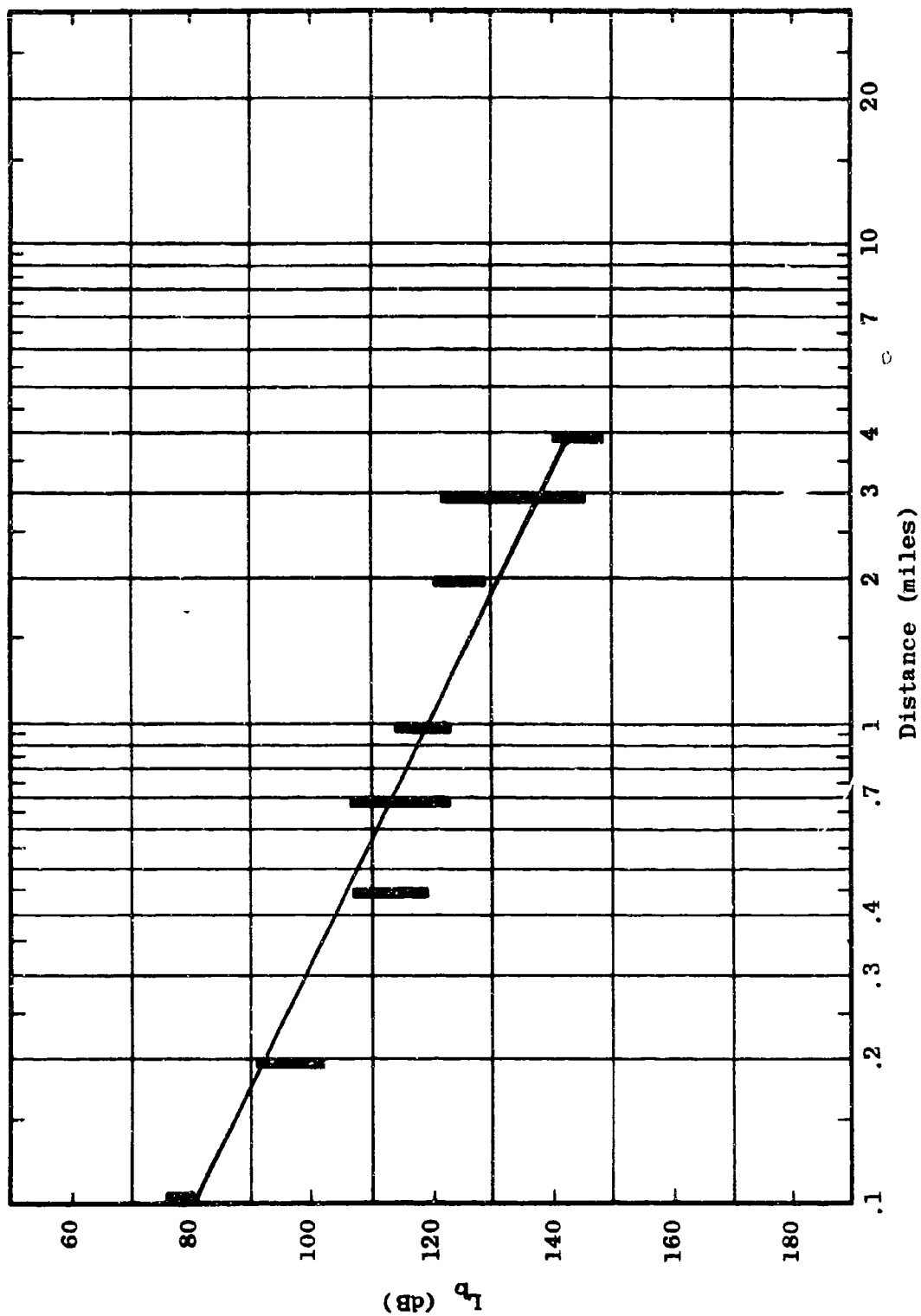


Figure 5.22 Measured Path Loss
 $L_b = F_{A,B}(100, 13, H, d, 11)$

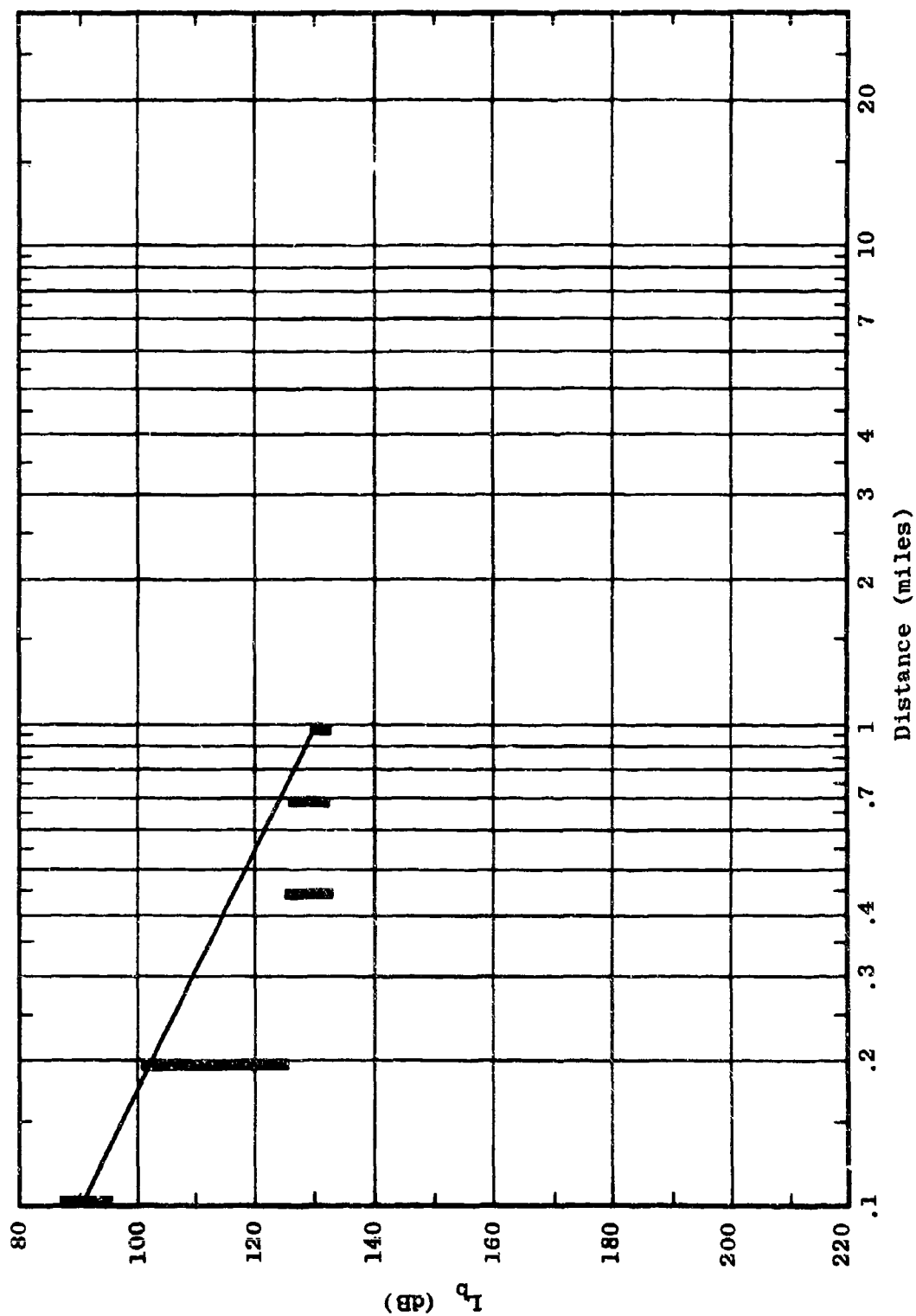


Figure 5.23 Measured Path Loss
 $L_b = F_{A,P}(250, 13, H, d, 11)$

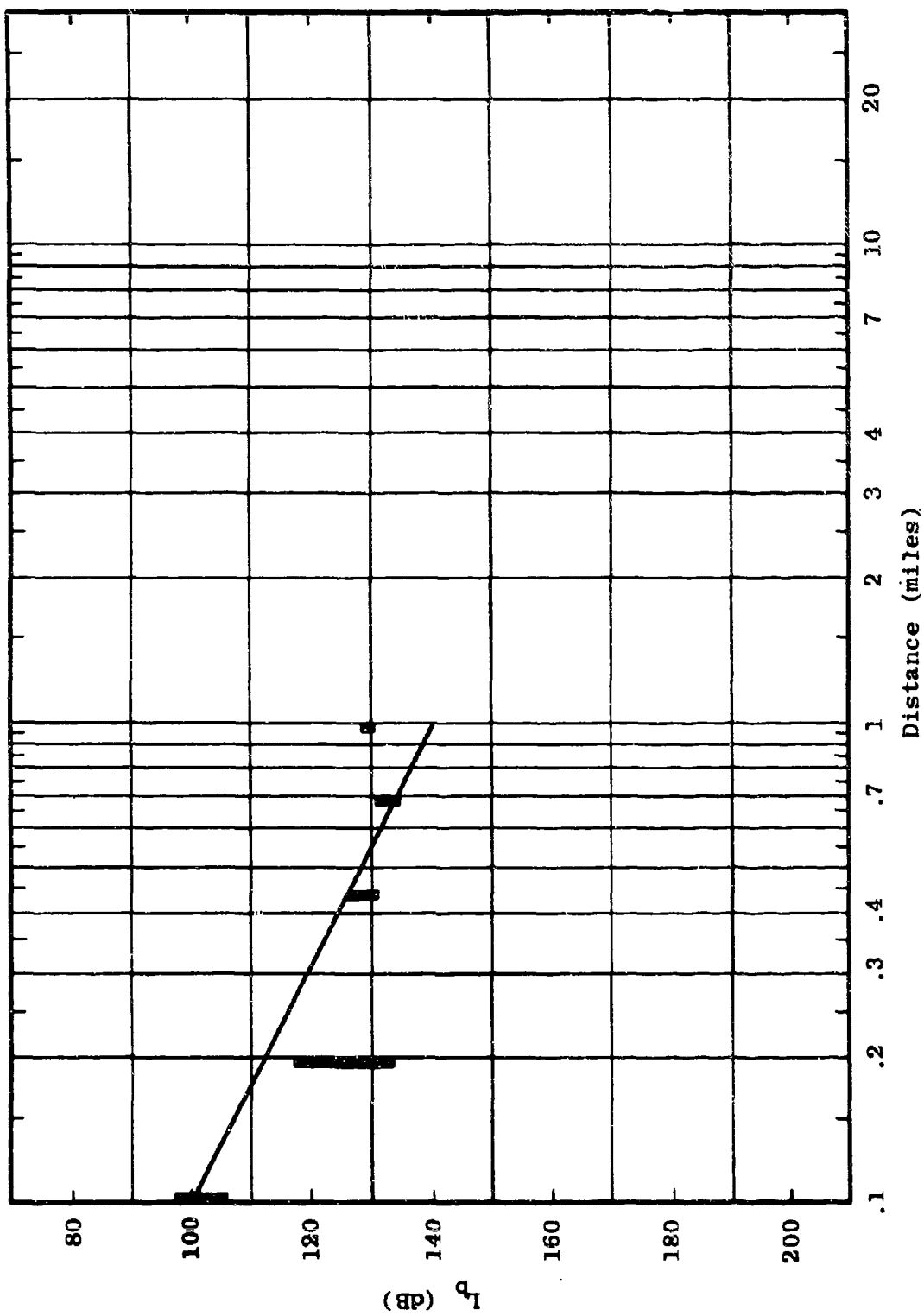


Figure 5.24 Measured Path Loss
 $L_p = F_{A,B}(400, 13, H, d, 11)$

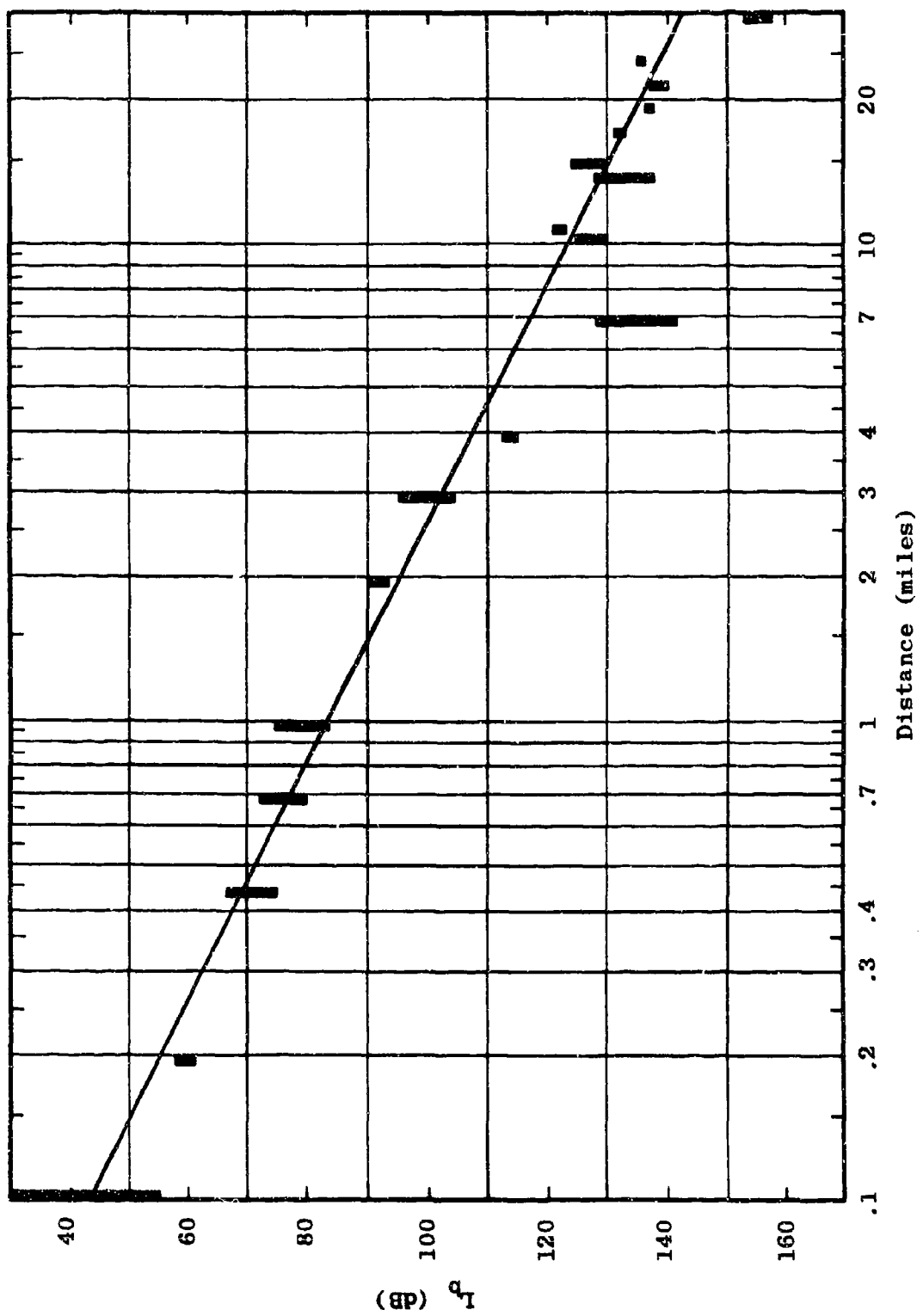


Figure 5.25 Measured Path Loss
 $L_b = F_{A,B}(25, 80, V, d, 79)$

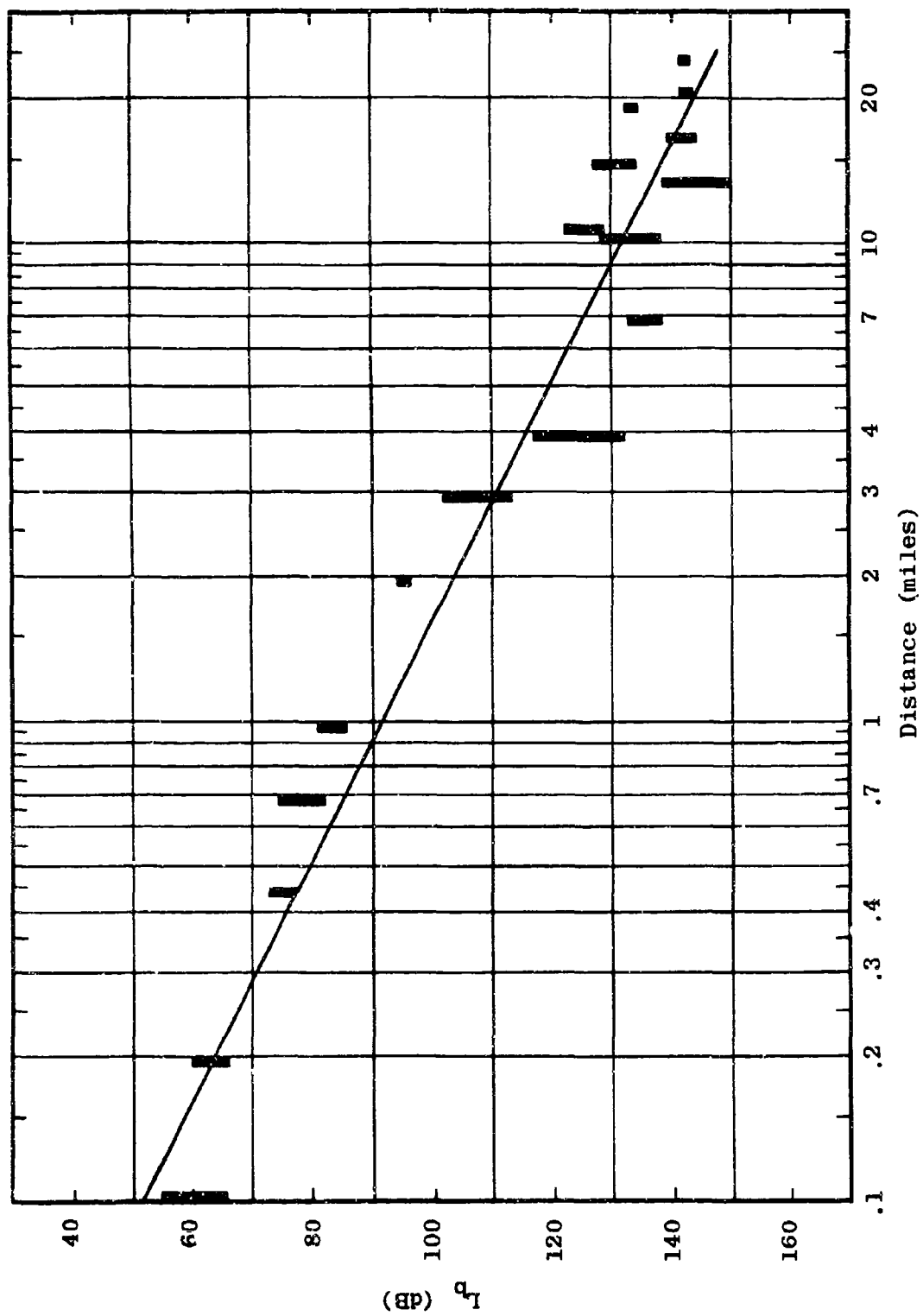


Figure 5.26 Measured Path Loss
 $L_b = F_{A,B}(50, 80, V, d, 79)$

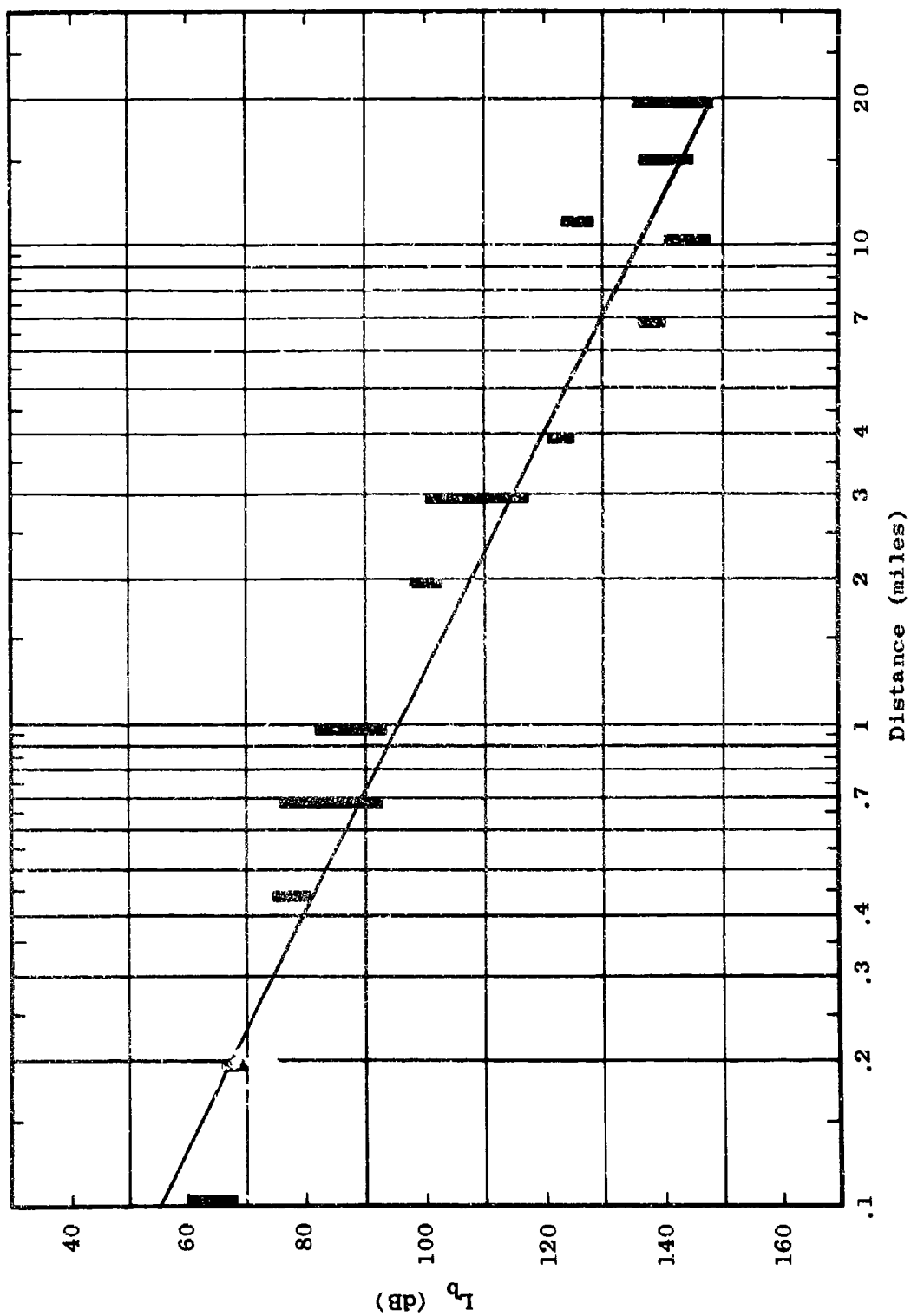


Figure 5.27 Measured Path Loss
 $L_p = F_{A,B}(100, 80, V, d, 79)$

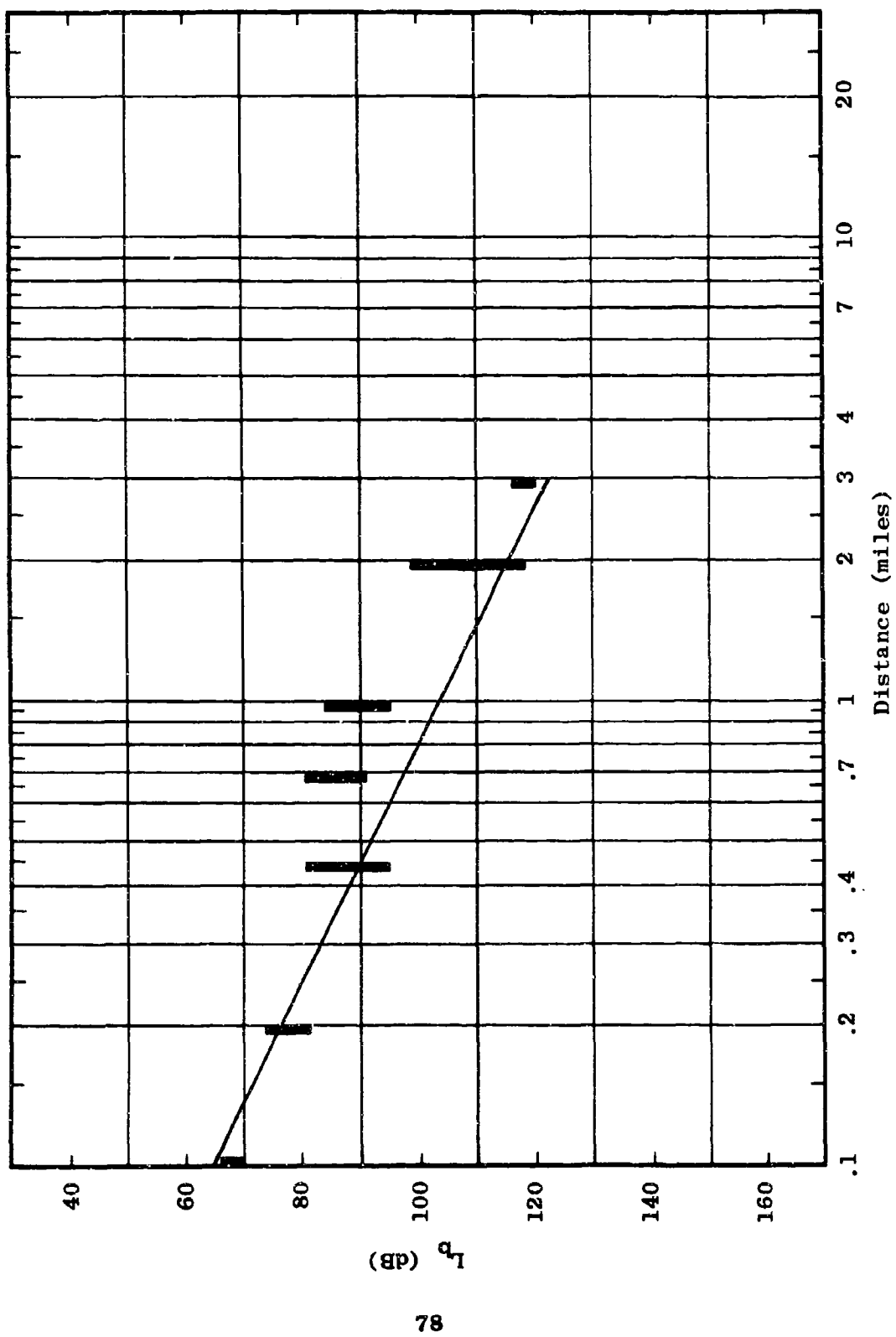


Figure 5.28 Measured Path Loss
 $L_b = F_{A,B}(250, 80, V, d, 79)$

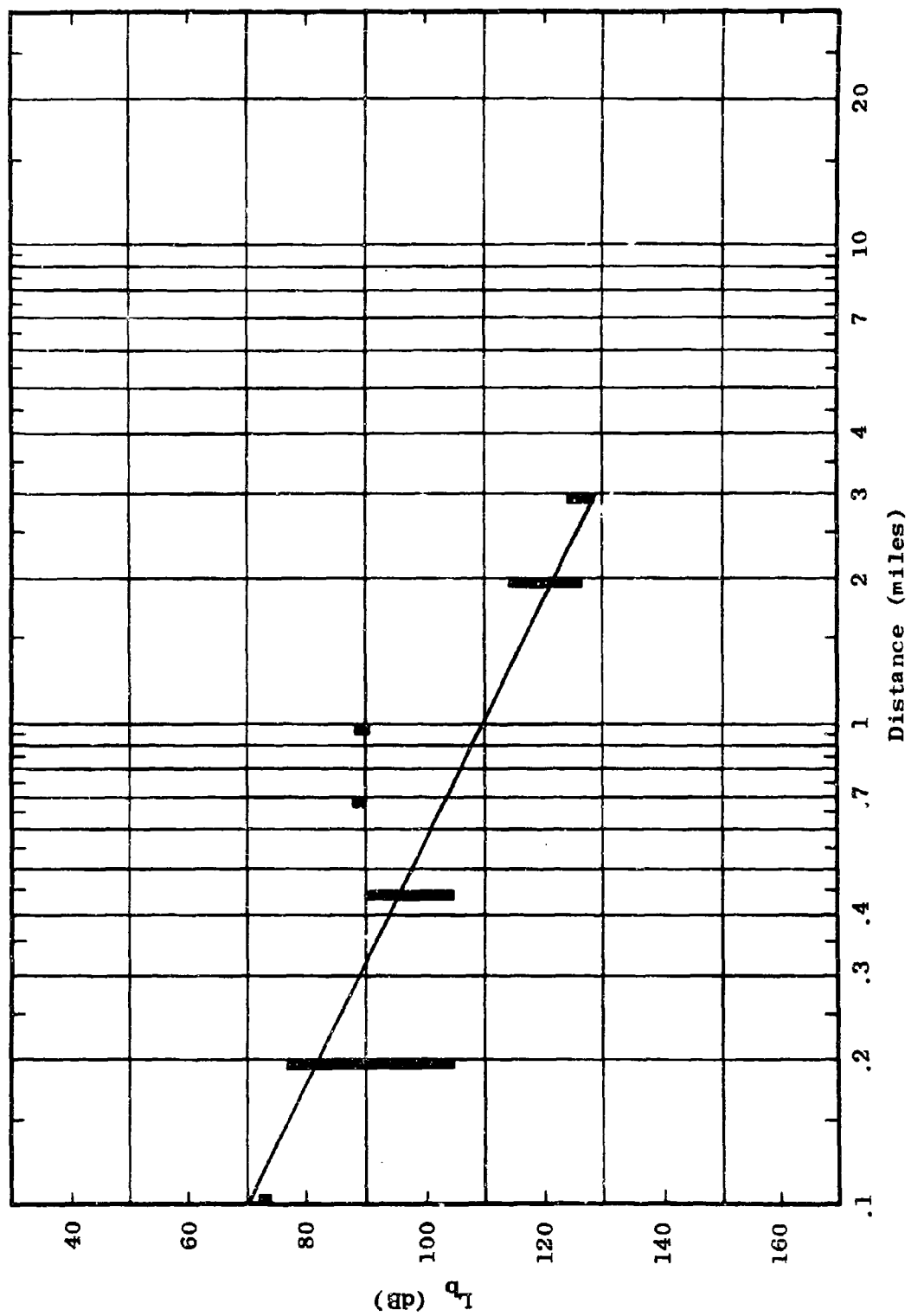


Figure 5.29 Measured Path Loss
 $L_b = F_{A,B}(400, 80, V, d, 79)$

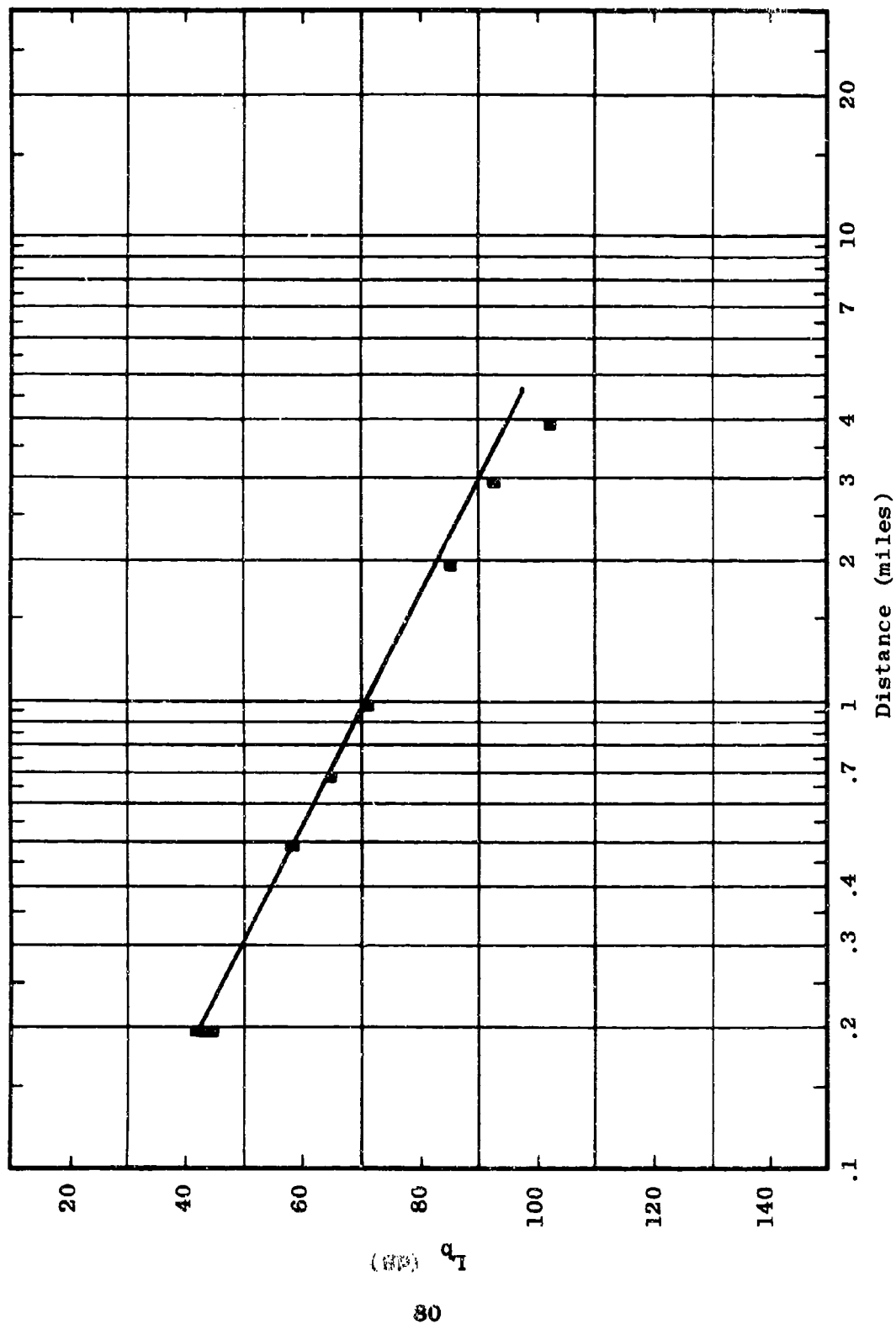


Figure 5.30 Measured Path Loss
 $L_b = F_{A,B}(2, 80, H, d, 79)$

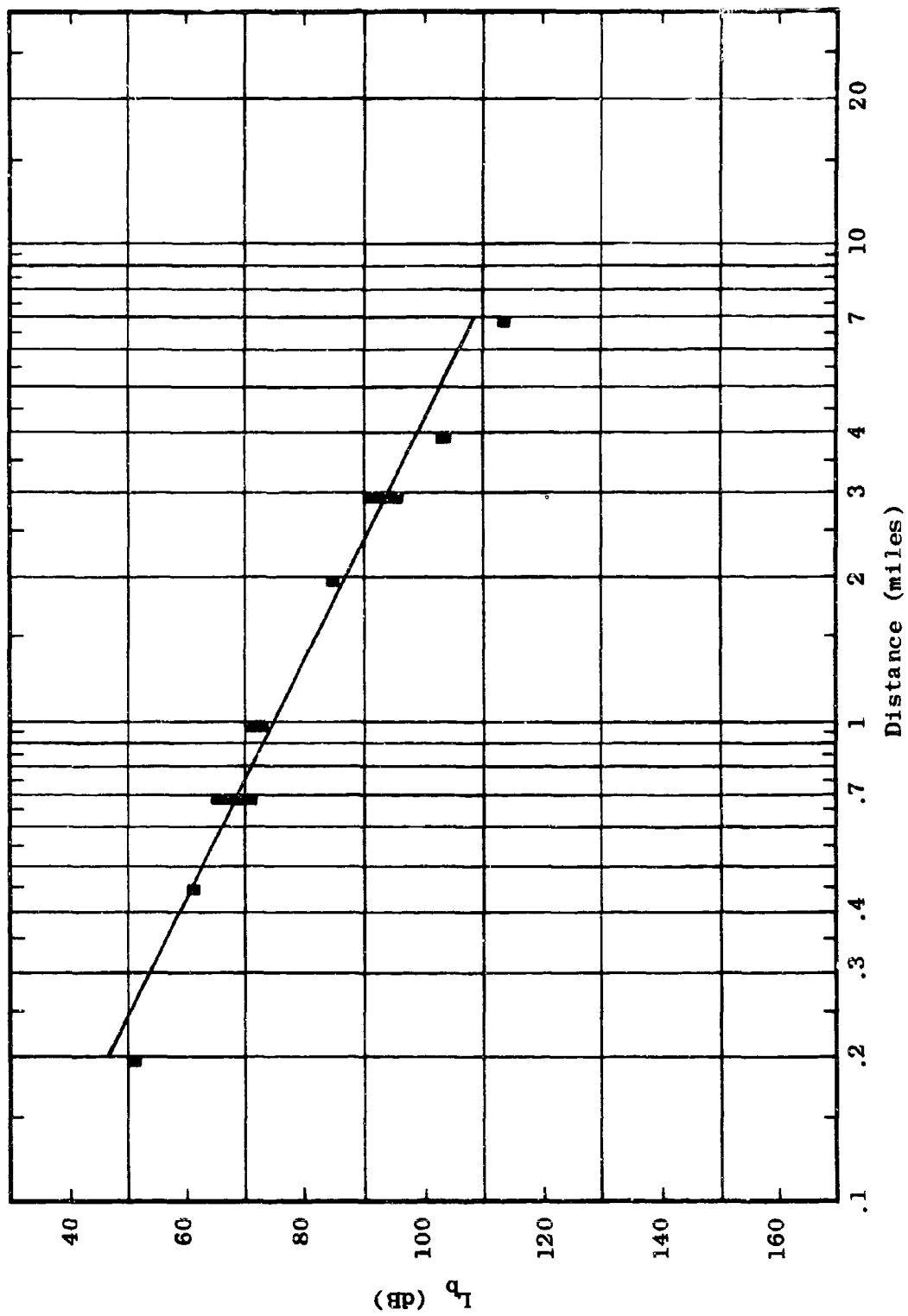


Figure 5.31 Measured Path Loss
 $L_p = F_{A,B}(6, 80, H, d, 79)$

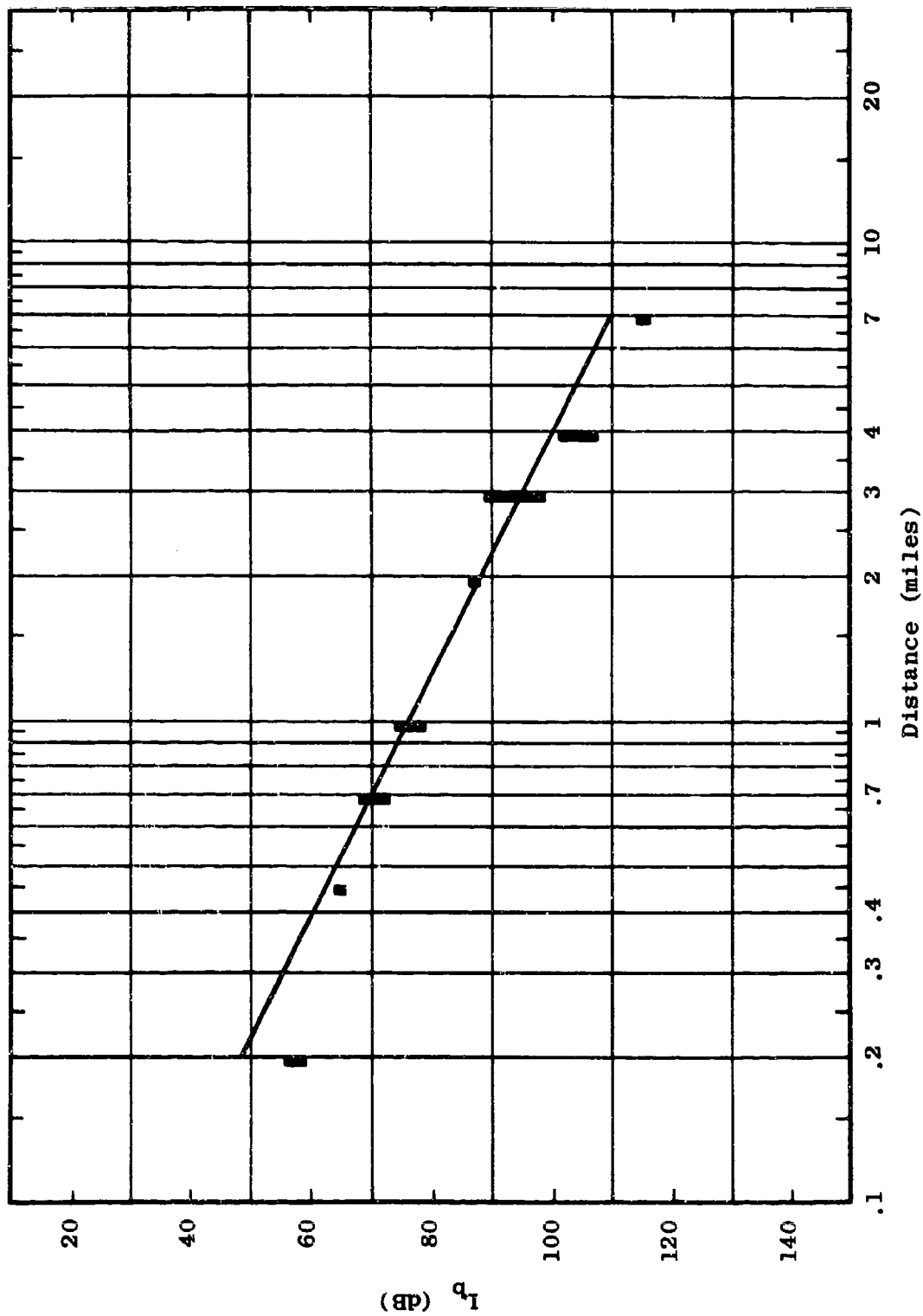


Figure 5.32 Measured Path Loss
 $L_p = F_{A,B}(12, 80, H, d, 79)$

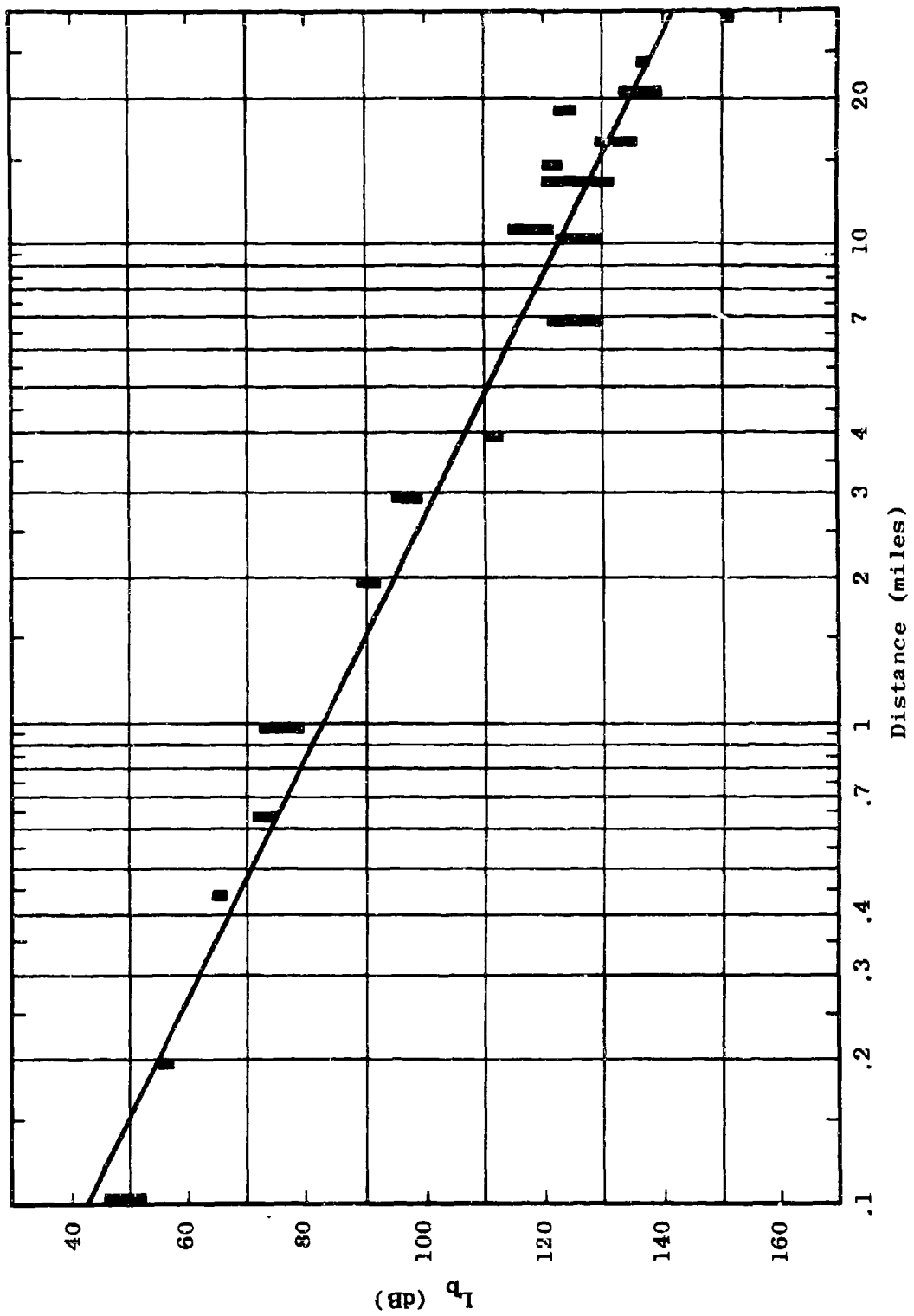


Figure 5.33 Measured Path Loss
 $L_0 = F_{A,B}(25, 80, H, d, 79)$

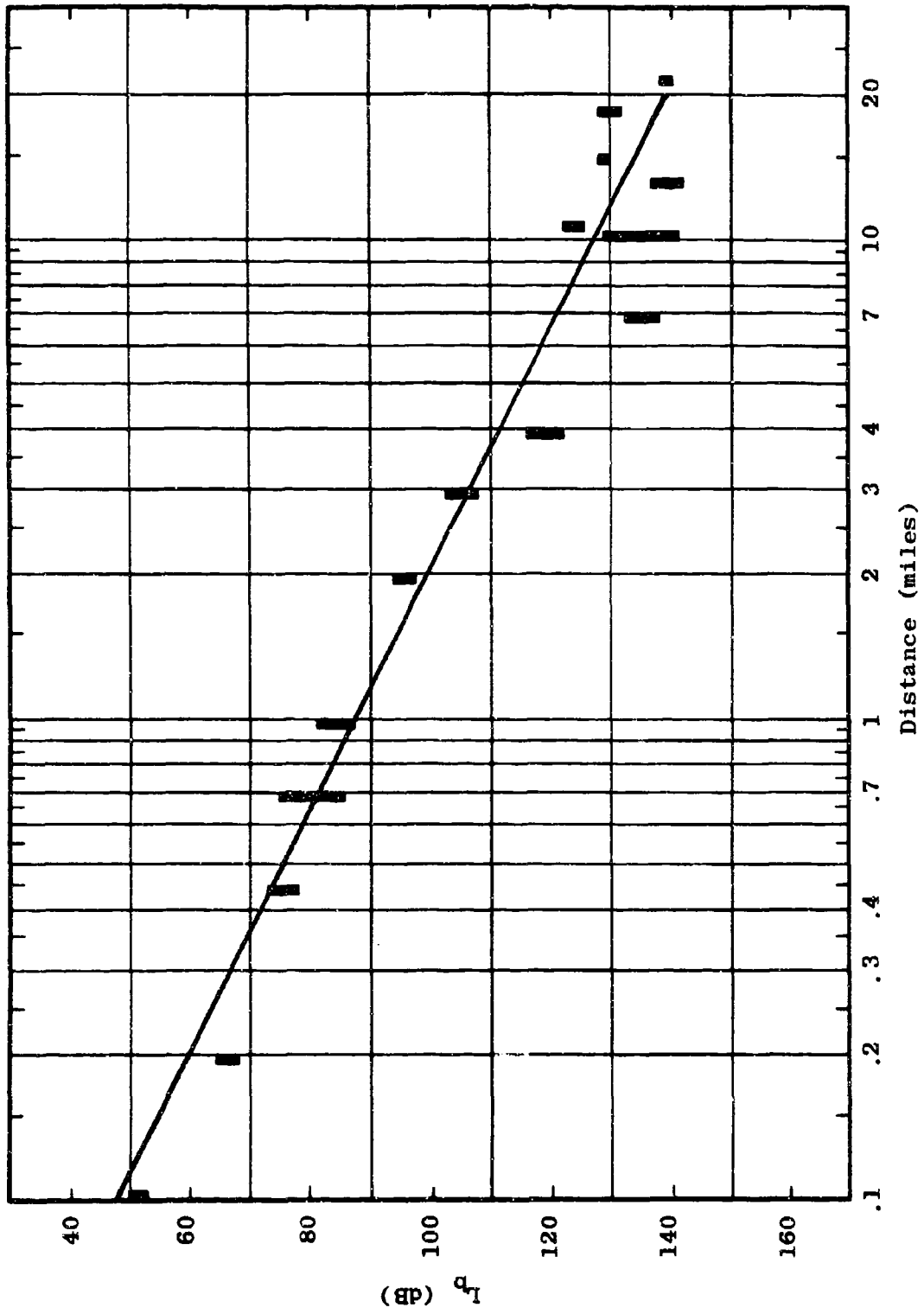


Figure 5.34 Measured Path Loss
 $L_p = F_{A,B}(50, 80, H, d, 79)$

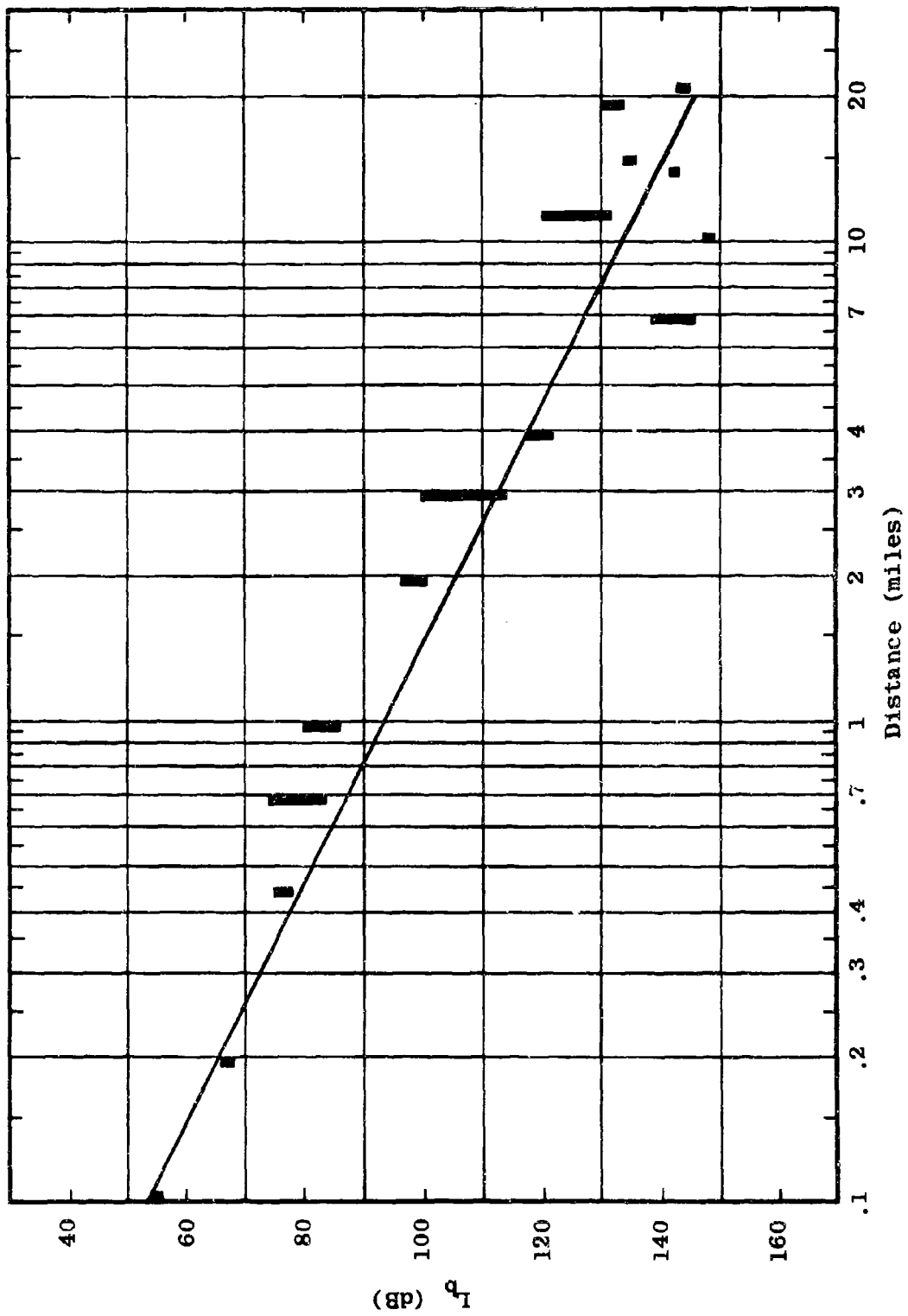


Figure 5.35 Measured Path Loss
 $L_b = F_{A,B}(100, 80, H, d, 79)$

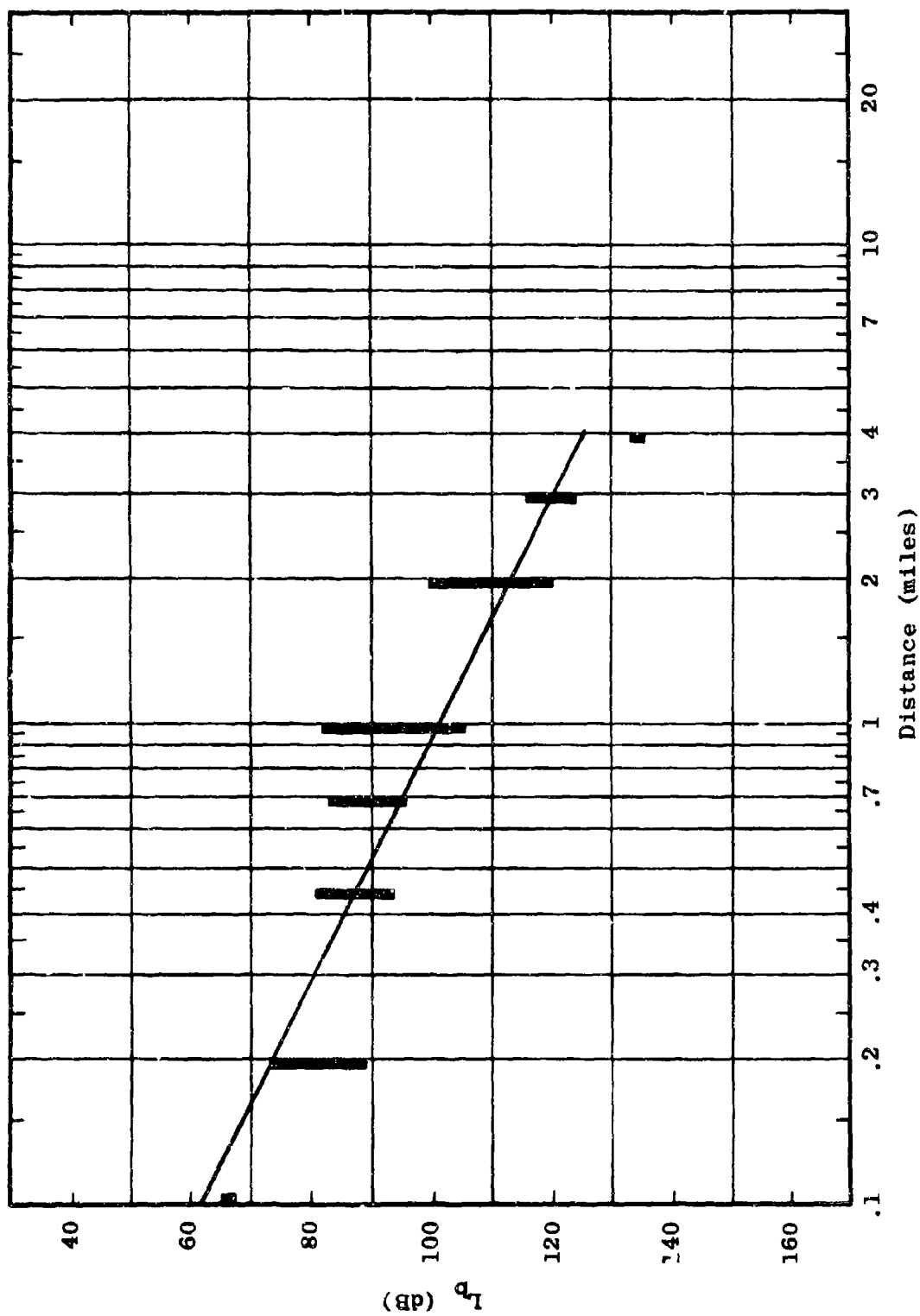


Figure 5.36 Measured Path Loss
 $L_p = F_{A,B}(250, 80, H, d, 79)$

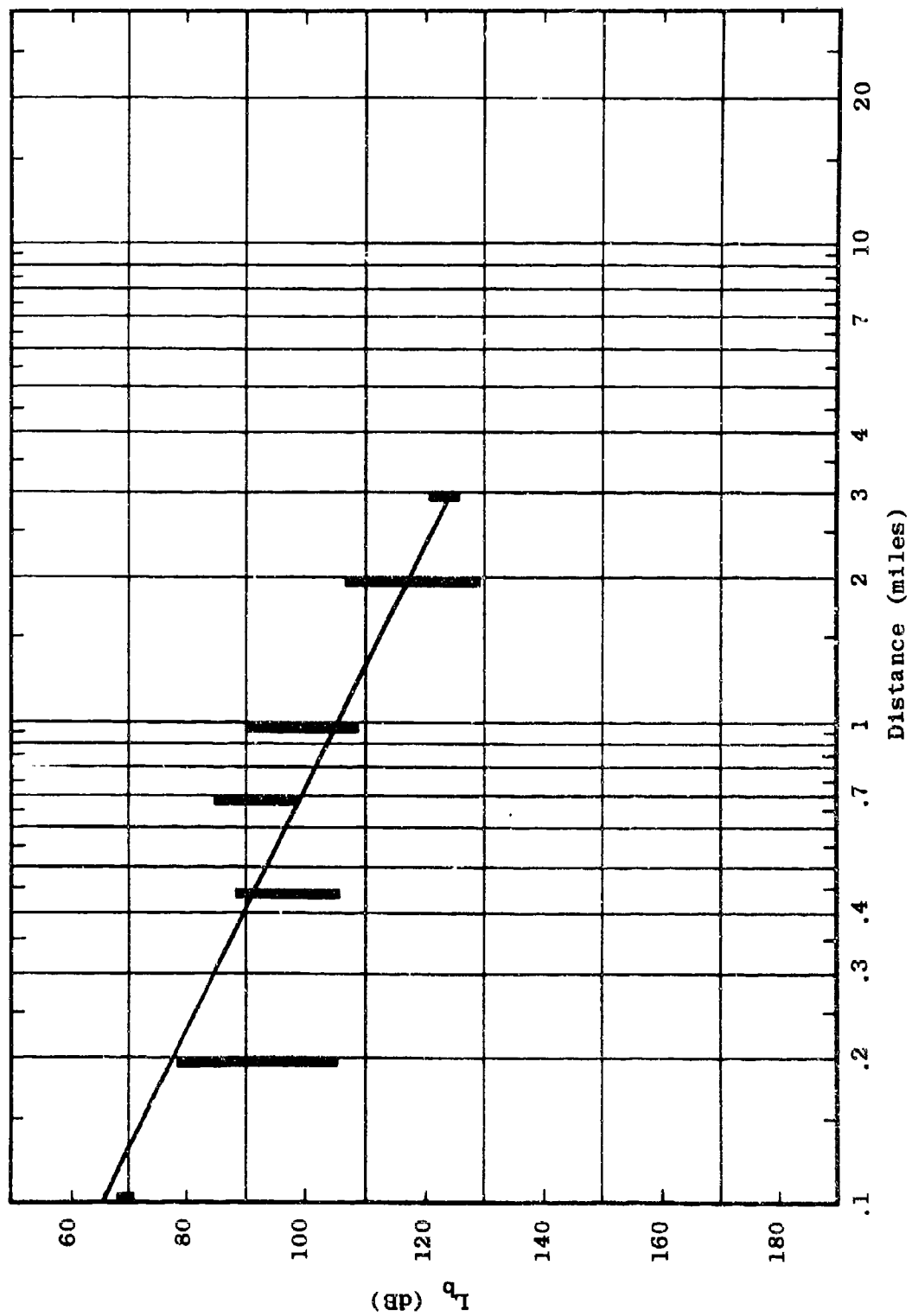


Figure 5.37 Measured Path Loss
 $L_b = F_{A,B}(400, 80, H, d, 79)$

When both the transmitting and receiving antennas are elevated to 80 feet, the antennas are nearly out of the foliage. Thus, the "through-the-foliage" mode is never really in force. Instead, free-space propagation is the controlling propagation mode for the initial separation distance of 0.1 mile. In general, the agreement between measured data and the smoothed curves is better for horizontal polarization than for vertical polarization. Table 5.1 compares theoretical free-space loss with the measured loss at Pak Chong for 80-foot transmitting and receiving antennas placed 0.1 mile apart.

5.1.2 Propagation Loss for Short, Foliated Paths

This section discusses propagation path loss data collected for separation distances from 25 feet to 1 mile and for frequencies spanning 25 to 400 Mc/s. Data for both vertical and horizontal polarizations is covered.

When antennas are immersed in foliage one theoretically expects that their radiated energy would propagate through the foliage and be attenuated in an exponential manner, i.e., by a given number of dB per meter. Data analyses presented in Semiannual Reports Numbers 6 and 7 indicated, however, that none of the measured data taken at separation distances of 0.2 mile and beyond gave any indication of a "through-the-foliage" mode of propagation. The measured path loss data indicated only a "treetop" mode of propagation for which path loss increased at about the rate of 40 times the logarithm of distance. Thus, the conclusion was that if a "through-the-foliage" mode of

Table 5.1
0.1 MILE PATH LOSS FOR 80-FOOT ANTENNAS

<u>Frequency (Mc/s)</u>	<u>Polarization</u>	<u>Median Measured Path Loss (dB)</u>	<u>Theoretical Free Space Path Loss (dB)</u>
25	V	48	45
50	V	57	51
100	V	60	56
250	V	68	64
400	V	73	68
25	H	50	45
50	H	50	51
100	H	55	56
250	H	66	64
400	H	70	68

propagation existed, then this mode was attenuated so rapidly as to be insignificant when compared to the "treetop" mode existing at 0.2 mile and beyond. With this idea in mind, additional path loss data was collected closer to the transmitting antenna in order to explore the possibility of a transition region between the "through-the-foliage" and the "treetop" modes of propagation. Toward this end, standard fixed-point measurements have been made at two additional field points, 0.05 and 0.1 mile from the transmitting antenna. In addition, discrete measurements have been made every fifty feet, starting at a point 25 feet (.005 mile) from the transmitting antenna and extending out to one mile. The descriptive term "walking measurements" is attached to this data, since the data was taken with a hand carried portable field strength meter.

The "walking data" was collected for a transmitting antenna height of 13 feet for frequencies in the range 25 to 400 Mc/s, using both vertical and horizontal polarizations. The measurements were taken so as to provide a reading of the maximum and minimum field strengths over a small area centered at each nominal separation distance.

Figures 5.38 and 5.39 summarize the measured data for vertically polarized signals at 100 Mc/s and 400 Mc/s, respectively. The data presented in these figures is for separation distances in the range 0.005 to 1.0 mile. Both "walking data" and fixed point data are shown on these graphs. The solid vertical bars represent the total range (Sectors A and B) of measured fixed point data for a transmitting antenna height of 13 feet and a receiving antenna height of 11 feet. The fixed point data ranges on

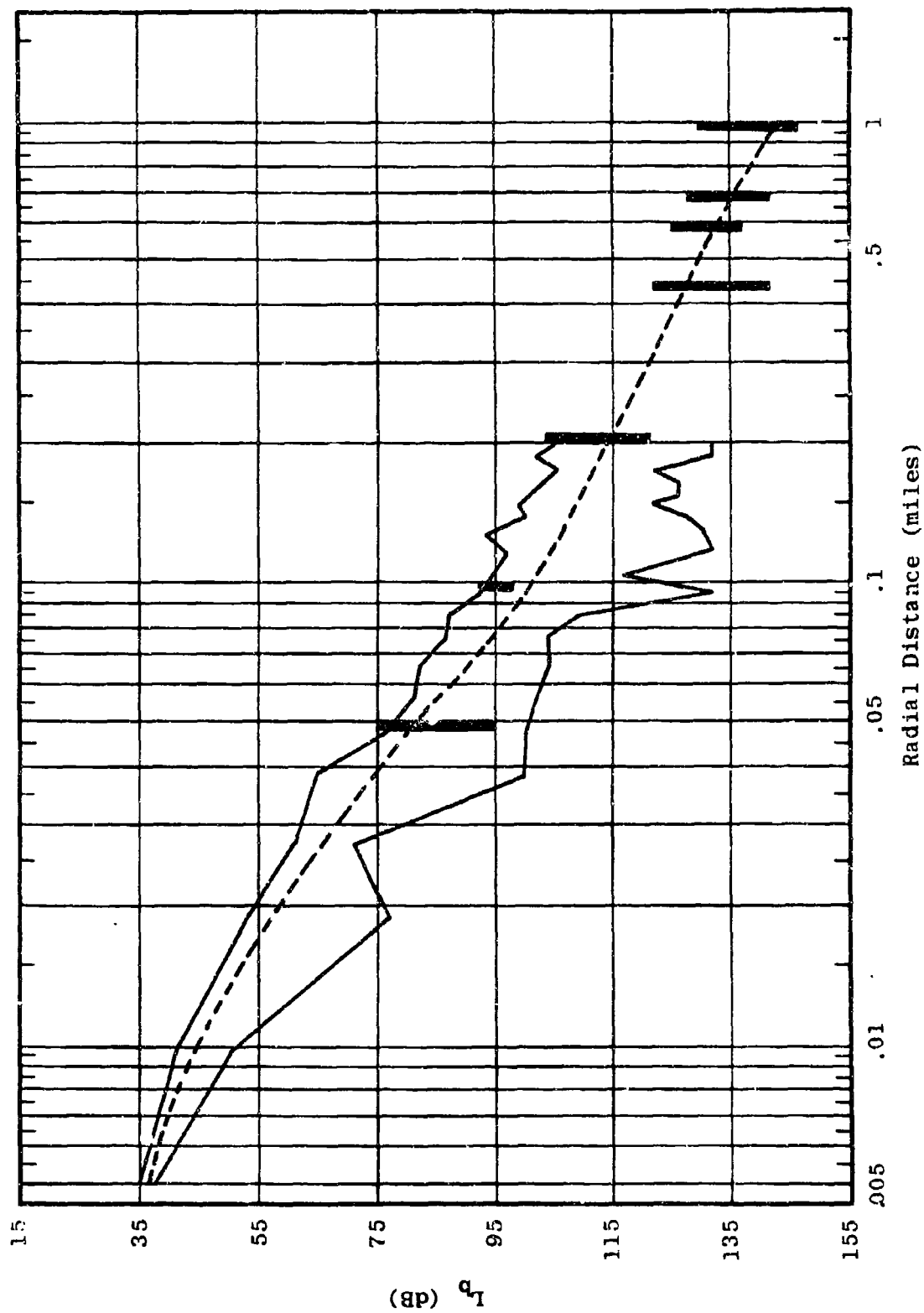


Figure 5.38 Comparison of Theoretical Model with Measured Data
 $L_b = F_{A,B}(100, 13, V, d, 6)$

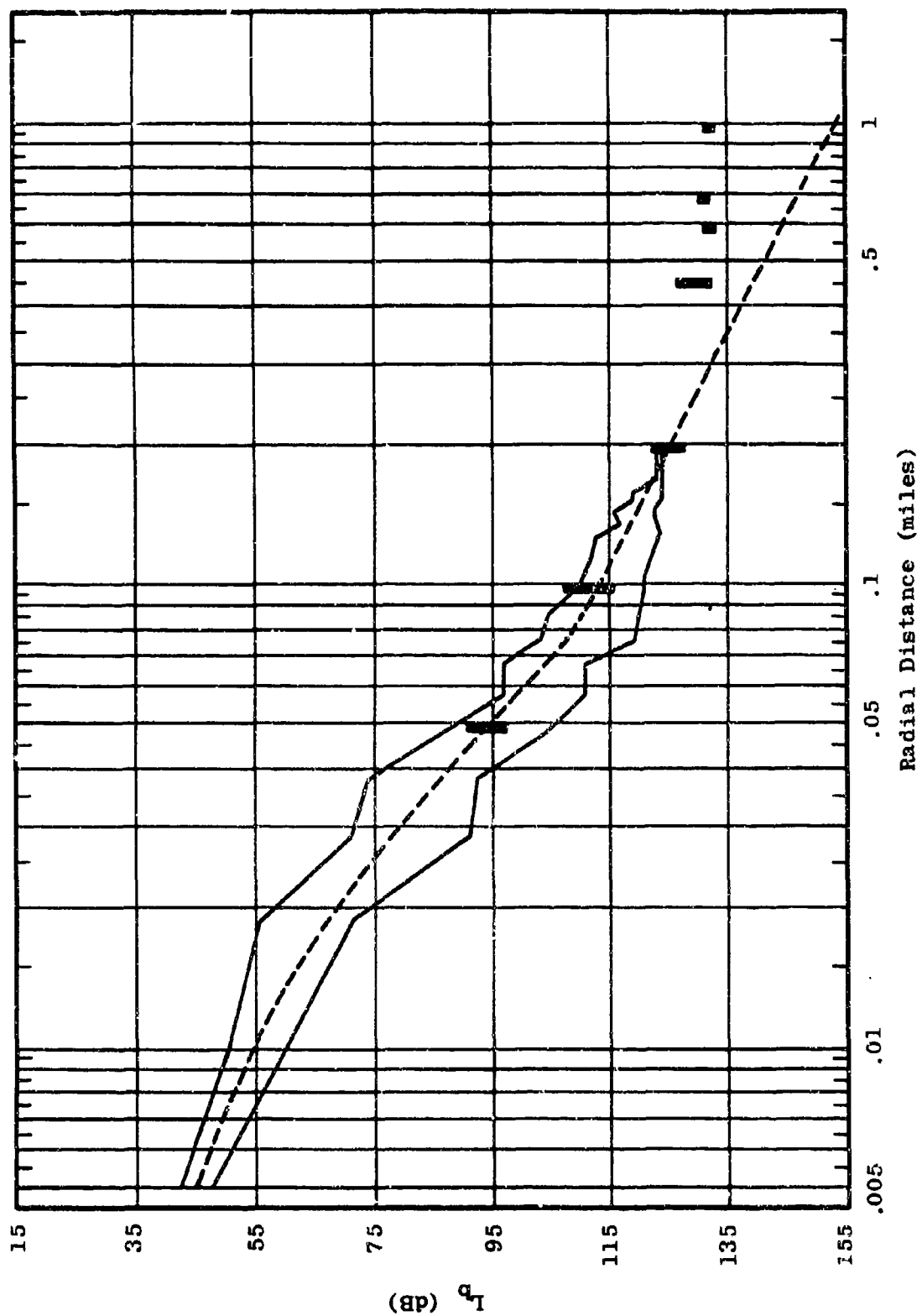


Figure 5.39 Comparison of Theoretical Model with Measured Data
 $L_b = F_{A,B}(400, 13, V, d, 6)$

Figures 5.38 and 5.39 have been adjusted by six dB to account for the expected difference in path loss caused by going from 6 foot to 11 foot high antennas. The adjustment was made so that the "walking data," measured at a receiving height of 6 feet, and the fixed point data measured at 11 feet could be compared at roughly equivalent heights. The two irregular curves shown on each figure define the maximum and minimum losses determined from the "walking measurements."

In addition to the measured data, a dashed curve has been plotted on each figure. The dashed curve is a plot of a theoretical model which describes an exponential increase in path loss for the initial separation distances, and a 40 dB per decade increase for distances beyond about 0.2 mile. The theoretical basic transmission loss, L , is given by equation (1)

$$L = 36.57 + 20 \log f - 20 \log \left[\frac{Ae^{-1609 \alpha d}}{d} + \frac{B}{d^2} \right] \quad (1)$$

where

- L = predicted basic transmission loss (dB)
- f = propagation frequency expressed in megacycles per second
- A, B = constants determined from the measured data
- α = constant describing the rate of attenuation through the foliage in dB per meter
- d = separation distance in miles

To understand the basis for proposing a model of the above form, consider the measured data for vertical

polarization at 100 Mc/s, Figure 5.40. As shown in the figure, the measured data indicates an exponential type of increase in path loss for separation distances in the 0.005-0.05 mile range and a possible 40 dB per decade increase in the 0.1-1.0 mile range. The transition between the exponential and logarithmic increase in loss appears to occur in the region of 0.05-0.1 mile. Figure 5.40 shows measured data compared against the two primary components of the theoretical models. In this figure the following loss function, denoted as L_1 , is plotted from 0.005-0.1 mile.

$$L_1 = 36.57 + 20 \log f - 20 \log \left[\frac{Ae^{-1609 \alpha d}}{d} \right] \quad (2)$$

where

$$A = 0.615$$

$$\alpha = 0.045 \text{ dB per meter}$$

L_1 represents the exponential component of the theoretical model. For the distance range 0.1-1.0 mile the following loss function denoted as L_2 is plotted.

$$L_2 = 36.57 + 20 \log f - 20 \log \left[\frac{B}{d^2} \right] \quad (3)$$

where

$$B = 0.000529$$

The dashed curve shown on Figure 5.40 represents a composite of L_1 and L_2 and is simply a graph of basic transmission loss versus distance using equation 1 with the following parameter values.

$$A = 0.615$$

$$\alpha = 0.045$$

$$B = 0.000529$$

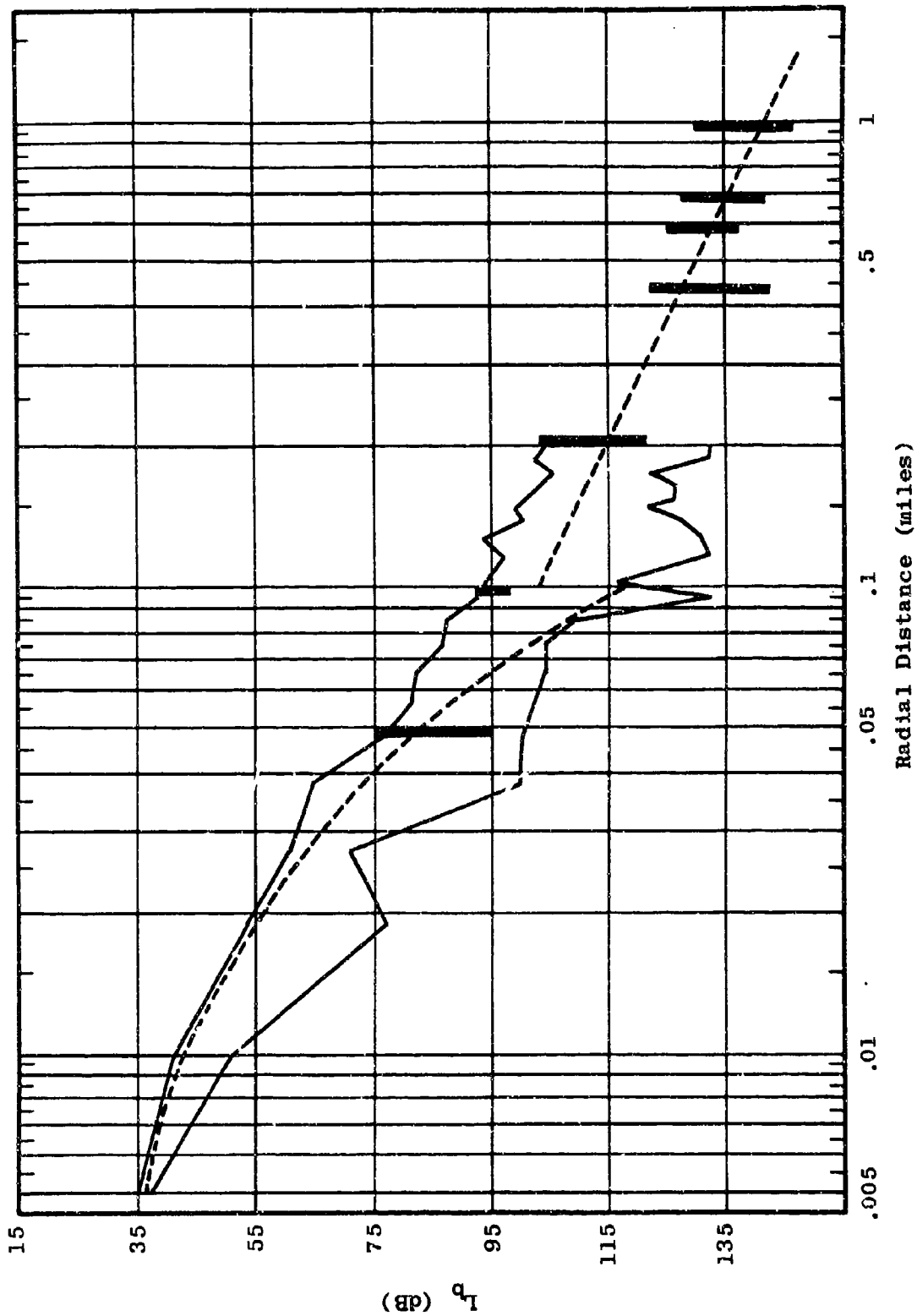


Figure 5.40 Comparison of Exponential and Logarithmic Models with Measured Data
 $L_b = F_{A,B}(100, 13, V, d, 6)$

The constants A and B were chosen by forcing equation 1 to pass through selected values of path loss at separation distances of 0.005 and 0.1 mile respectively. The theoretical curves plotted in Figure 5.38 and 5.39 show the results of attempting to describe the median measured path loss envelope while at the same time confining the theoretical curve within the envelope of measured data.

At 400 Mc/s, Figure 5.39, and to some extent at 100 Mc/s, Figure 5.38, the measured path loss data shows a tendency to flatten out over the range from 0.5 to 1.0 mile. There is some disagreement between theoretical and measured results in the region from 0.5 to 1.0 mile where the measured path loss does not appear to increase with distance. This tendency is brought about in part by the terrain profile and in part by high propagation losses encountered at 400 Mc/s. As discussed in detail in Section 5.2.3, the terrain profile for Sector B begins to rise in the range from 0.5 to 1.0 mile, allowing the receiving antenna to intercept energy which has been propagated along a path which is well above treetop level for a substantial portion of the path.

The flattening effect at 100 Mc/s is much more pronounced at 400 Mc/s, for here there is the added problem of system sensitivity. The measuring system used at this frequency does not respond to a signal which has suffered a propagation loss of more than 134 dB. As can be seen in Figure 5.39, only the signal peaks having less than 134 dB loss appear in the distance range from 0.5 to 1.0 mile.

Figure 5.41 shows the measured data for 25 Mc/s and vertical polarization. As shown in the figure, there is no real indication of an exponential increase in path loss with increasing distance at this frequency. The measured path losses do, however, increase at a rate of 40 times the logarithm of distance. The measured data at 50 Mc/s shows similar tendencies. Thus, the theoretical model fit to the measured data at 25 and 50 Mc/s assumes the constant A in equation 1 to be zero.

Table 5.2 lists the constants α , A and B used in equation 1 for both polarizations in the frequency range 25-400 Mc/s. For both polarizations at 25 Mc/s and 50 Mc/s, the constant A in equation 1 was set equal to zero. The attenuation constants selected in Table 5.2 for α , A and B are not the only ones which fit the measured data. A large number of theoretical curves were evaluated on the digital computer for various choices of the constants, α , A and B. For the moment, the curves selected seem to best describe the measured data while at the same time employing reasonable and logical values for the three parameters in Equation 1.

Figures 5.42 and 5.43 show the comparison between the theoretical model of Equation 1 and the measured data for horizontal polarization at frequencies of 100 Mc/s and 400 Mc/s respectively.

In summary the measured data strongly indicates a "through-the-foliage" propagation mode for separation distances between 0.005 and .05 mile at frequencies of 100, 250 and 400 Mc/s. At 25 and 50 Mc/s for both polarizations,

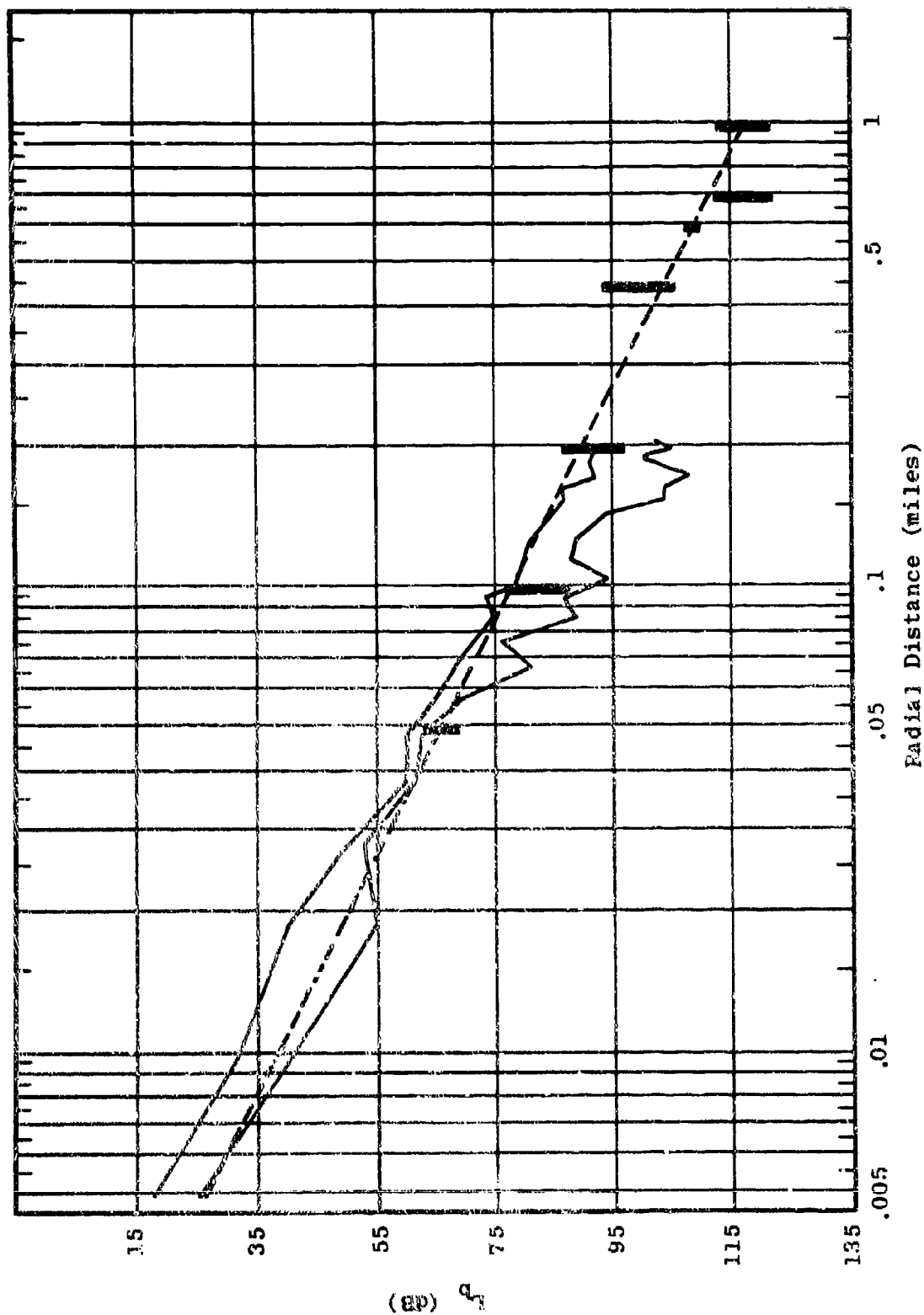


Figure 5.41 Comparison of Theoretical Model with Measured Data
 $L_D = F_{A,B}(25, 10, V, d, 6)$

Table 5.2

ATTENUATION CONSTANTS FOR THEORETICAL MODEL

<u>Frequency</u> <u>(Mc/s)</u>	<u>Polarization</u>	<u>α</u> <u>dB/meter</u>	<u>A</u>	<u>B</u>
25	V	-	0	0.00212
50	V	-	0	0.00106
100	V	0.045	0.615	0.000529
250	V	0.050	0.759	0.000443
400	V	0.055	1.02	0.000523
25	H	-	0	0.00424
50	H	-	0	0.00424
100	H	0.020	0.472	0.00551
250	H	0.025	0.774	0.000588
400	H	0.035	1.11	0.000598

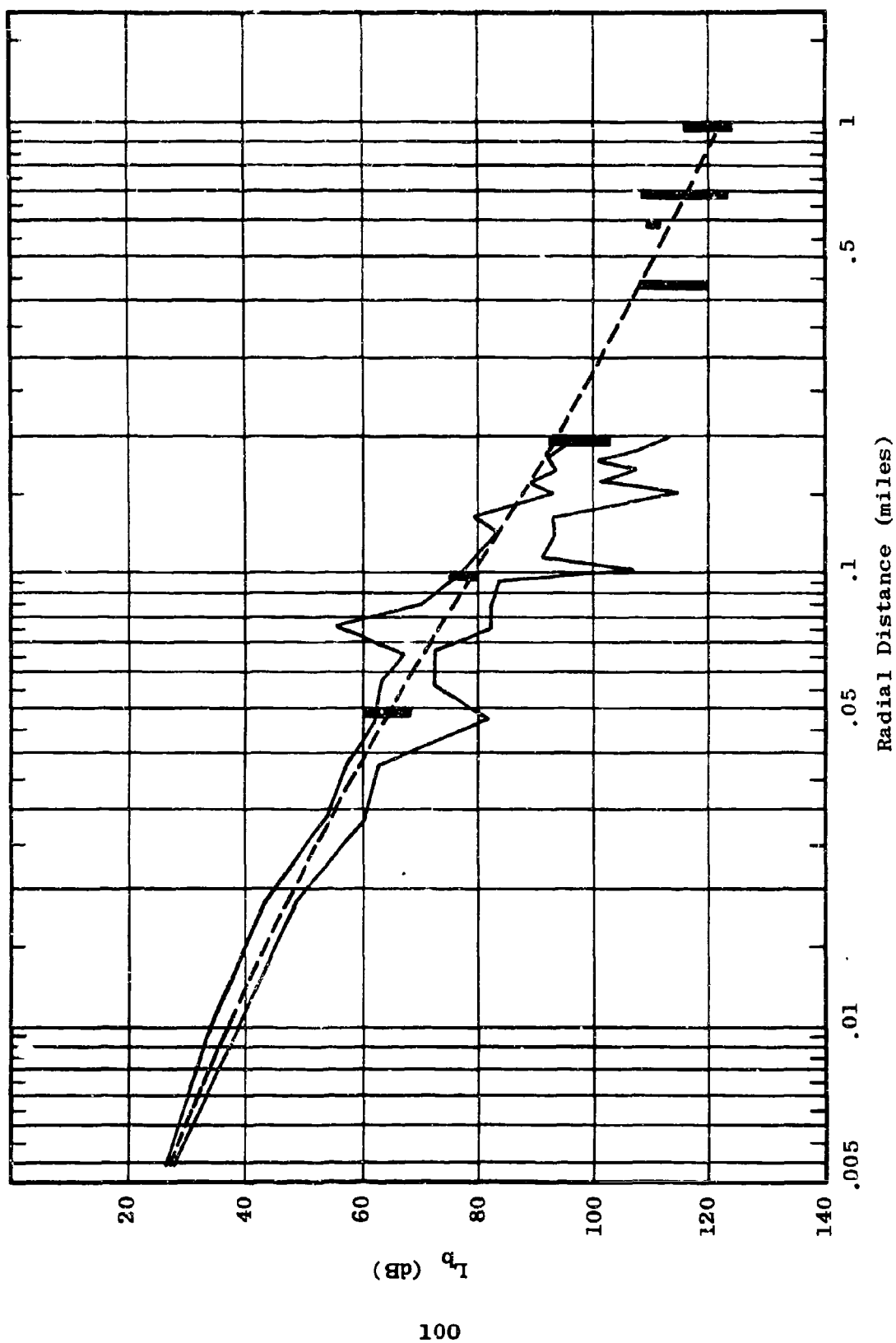


Figure 5.42 Comparison of Theoretical Model with Measured Data
 $L_b = F_{A,B}(100, 13, H, d, 6)$

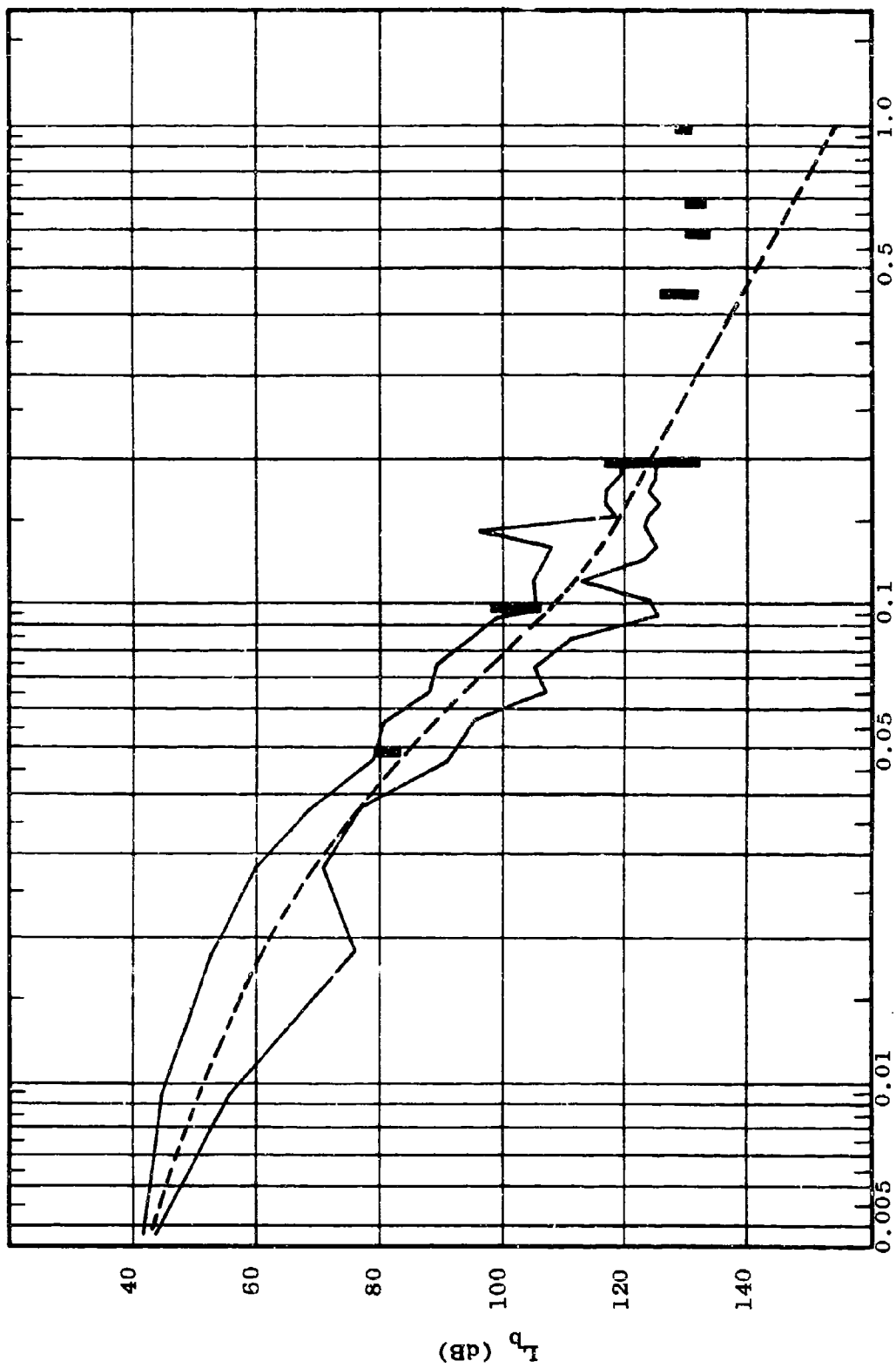


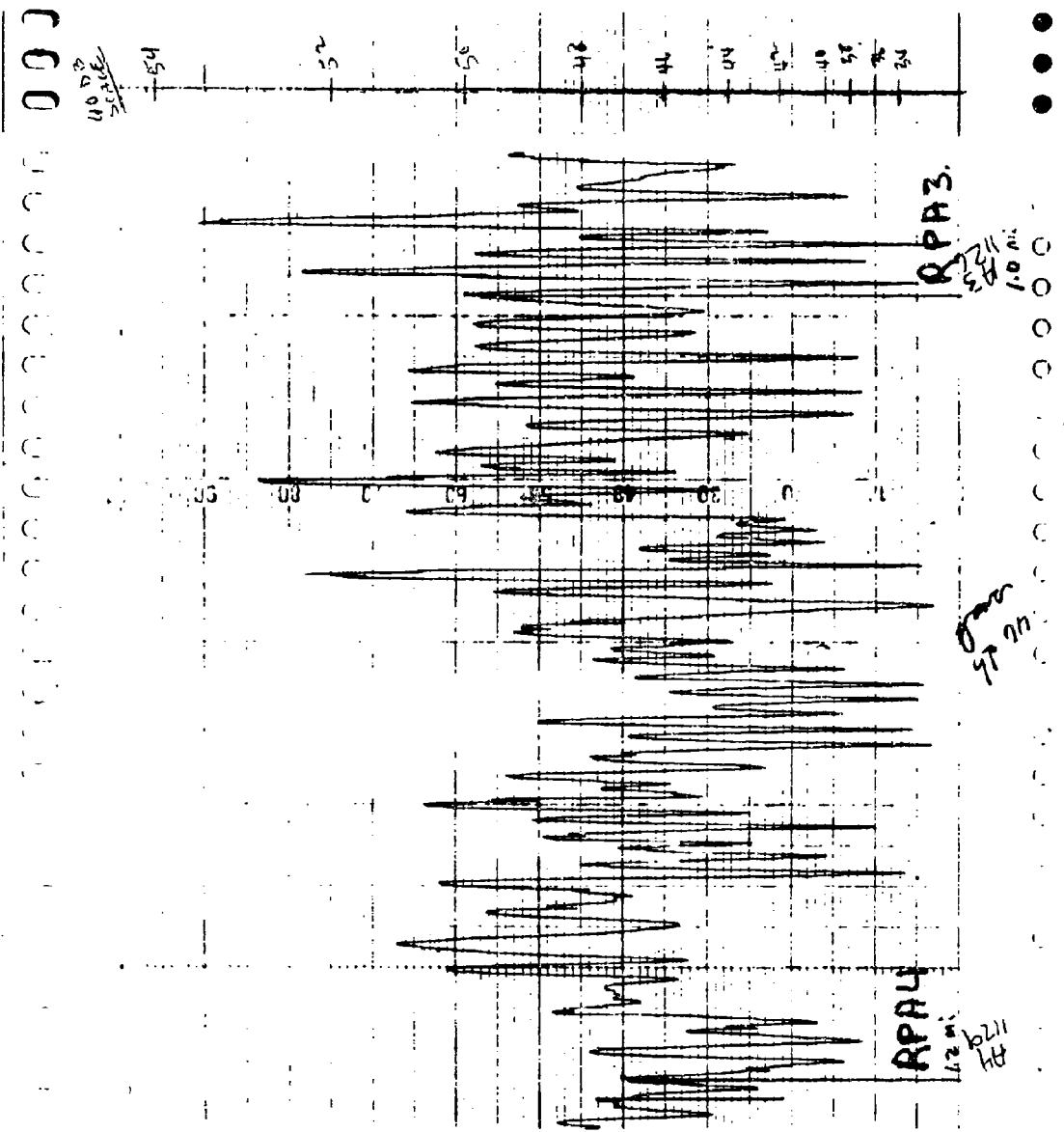
Figure 5.43 Theoretical and Measured Short Range Path Loss
 $L_b = F_{A,B}(400, 13, H, d, 6)$

the exponential increase in path loss is not so apparent. Instead, the path loss at these two frequencies closely follows a consistent 40 dB per decade increase over the entire distance range of 0.005 to 1.0 mile. This consistency indicates a single mode of propagation for these two frequencies at all distances less than one mile. Since the measured data shows a significant decrease in path loss when the antenna is raised, it is improbable that the mode here is a simple surface wave, such as described by Norton.¹³

5.1.3 Variability of Path Loss with Distance

Continuous vehicular recordings of field strength versus distance have been made to provide a detailed insight into the spatial variability of transmission loss at low receiving antenna heights within the foliage. Figure 5.44 is a typical field-strength recording, taken at 25 Mc/s. The trails along which the vehicle moves are calibrated in terms of radial distance from the transmitter at 0.2-mile intervals for distances from 0.2 mile to 3 miles and at .5-mile intervals thereafter. Each time the vehicle passes one of these calibration points, the strip recording is marked. The trails are never exact radials, and thus the actual distance represented on any strip chart is always somewhat greater than the indicated radial distance. The sample shown in Figure 5.44 has distance markings at 1 mile and 1.2 miles. The actual dB calibration scale is shown at the right of Figure 5.44.

Figure 5.45 provides a similar example of data taken at 250 Mc/s. The rate with which the data varies



5978

Figure 5.44 Example of Vehicular Raw Data
 $F_A(25.5, 40, V, 1.0-1.2, 7)$

5981

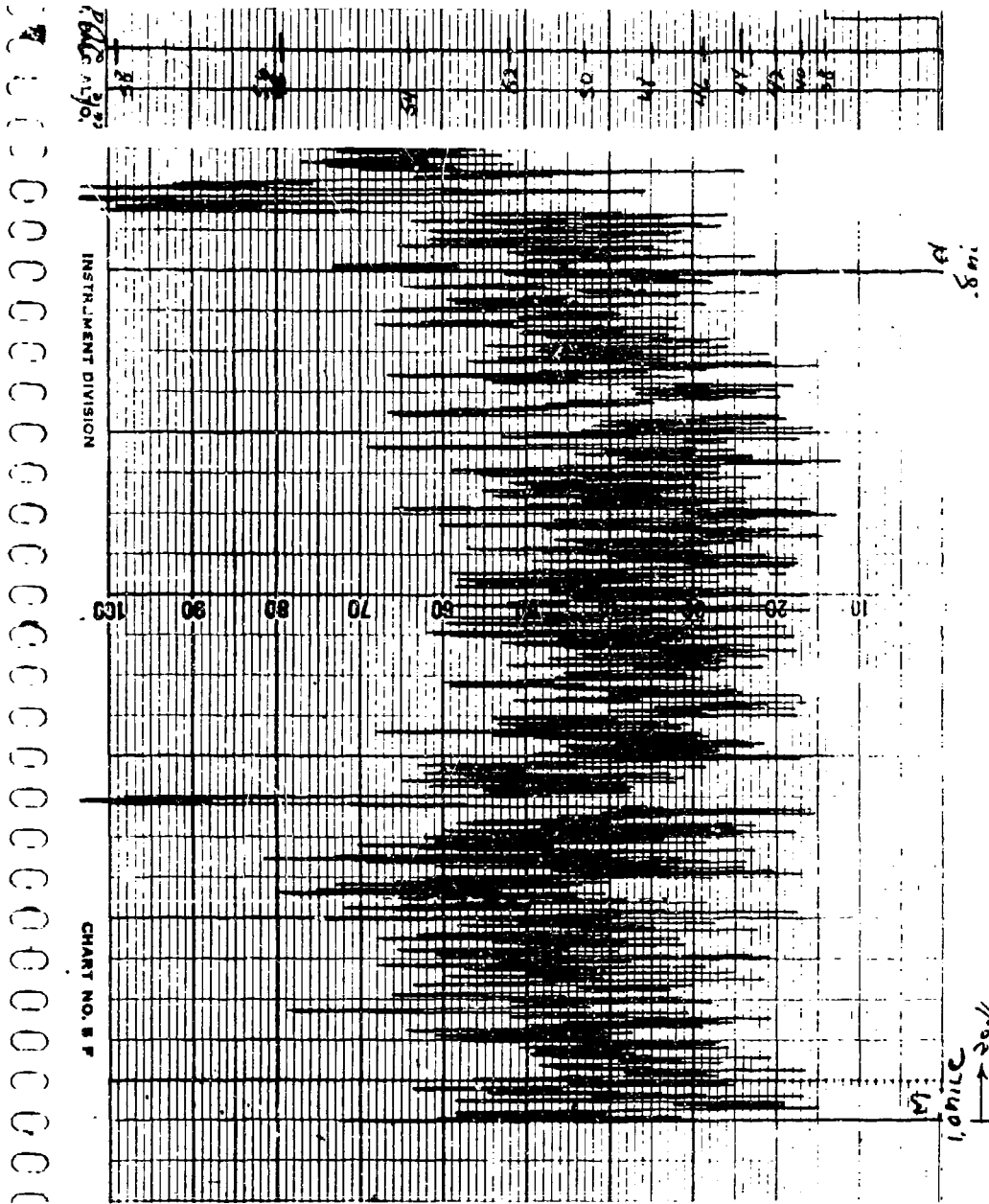


Figure 5.45 Example of Vehicular Raw Data
F_A (250, 80, V, 0.8-1.0, 7)

increases as radio frequency is increased. Below 25 Mc/s the frequency of data variation is relatively low as distance changes. However, at 250 and 400 Mc/s the data variation is extremely rapid, as Figure 5.45 indicates.

A number of vehicular strip recordings have been taken with about ten times the distance resolution shown in Figures 5.44 and 5.45. An example of a portion of one of these higher resolution strip recordings is shown in Figure 5.46. The expanded distance scale allows a more accurate analysis of the fine grain field variations.

The field strength variations with distance have two distinct components. One is the very obvious, rapid fluctuation in signal level as distance is varied. The other is a longer-term fluctuation, one cycle of which can be seen in Figure 5.45. This longer-term variation is similar to that which is generally associated with propagation over rough terrain in the absence of foliage. The more rapid variation is typical of that which is generally encountered near or within foliage and among tall buildings or other manmade structures.

The rapid variation can be conveniently thought of as a cyclic variation for which the peak-to-null ratio of each half cycle and the width of each half cycle are random variables. The half-cycle width is defined as the number of feet one must travel along the ground to go from a signal null to a signal peak or vice versa.

A careful analysis of some of the high-resolution vehicular strip recordings has shown that on the average

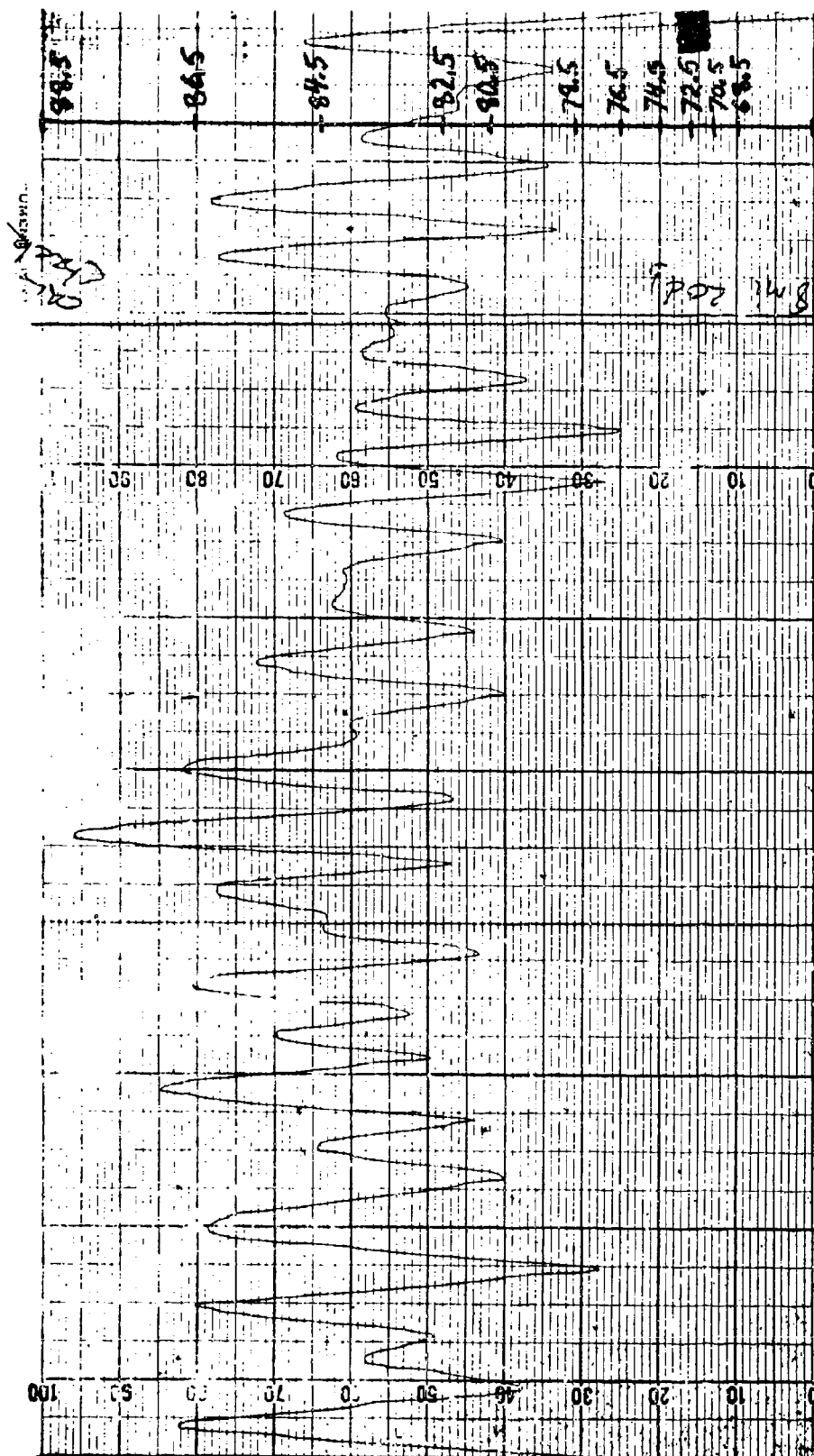


Figure 5.46 Example of High Resolution Vehicular Raw Data
 $F_B(100, 40, H, 0.8, 7)$

the half-cycle widths tend to be .37 wave lengths regardless of frequency for frequencies between 25 and 400 Mc/s. Figure 5.47 shows the half-cycle widths in feet for frequencies from 25 to 400 Mc/s. The solid line represents a width of .37 wave lengths. The solid black points represent averages taken for vertical polarization at each of the test frequencies. The point denoted by an open circle represents an average taken for horizontal polarization at 100 Mc/s.

The results shown on Figure 5.47 indicate, for example, that if space diversity were to be considered, separation distances in excess of 30 feet would be required at 25 Mc/s but that very short separation distances could be utilized at the higher frequencies.

The half-cycle widths shown in Figure 5.47 represent average values from a random population. A typical distribution for half-cycle widths at 100 Mc/s, vertical polarization is shown in Figure 5.48.

An estimate of the average peak-to-null ratio for a half cycle of the rapid variation is shown as a function of frequency in Figure 5.49. The ratio is greater for vertical polarization than horizontal and the ratio increases as frequency is increased. However, the rate of increase appears to be slightly greater for horizontal polarization than for vertical. A typical distribution of peak-to-null ratios for 100 Mc/s, horizontal polarization is shown in Figure 5.50.

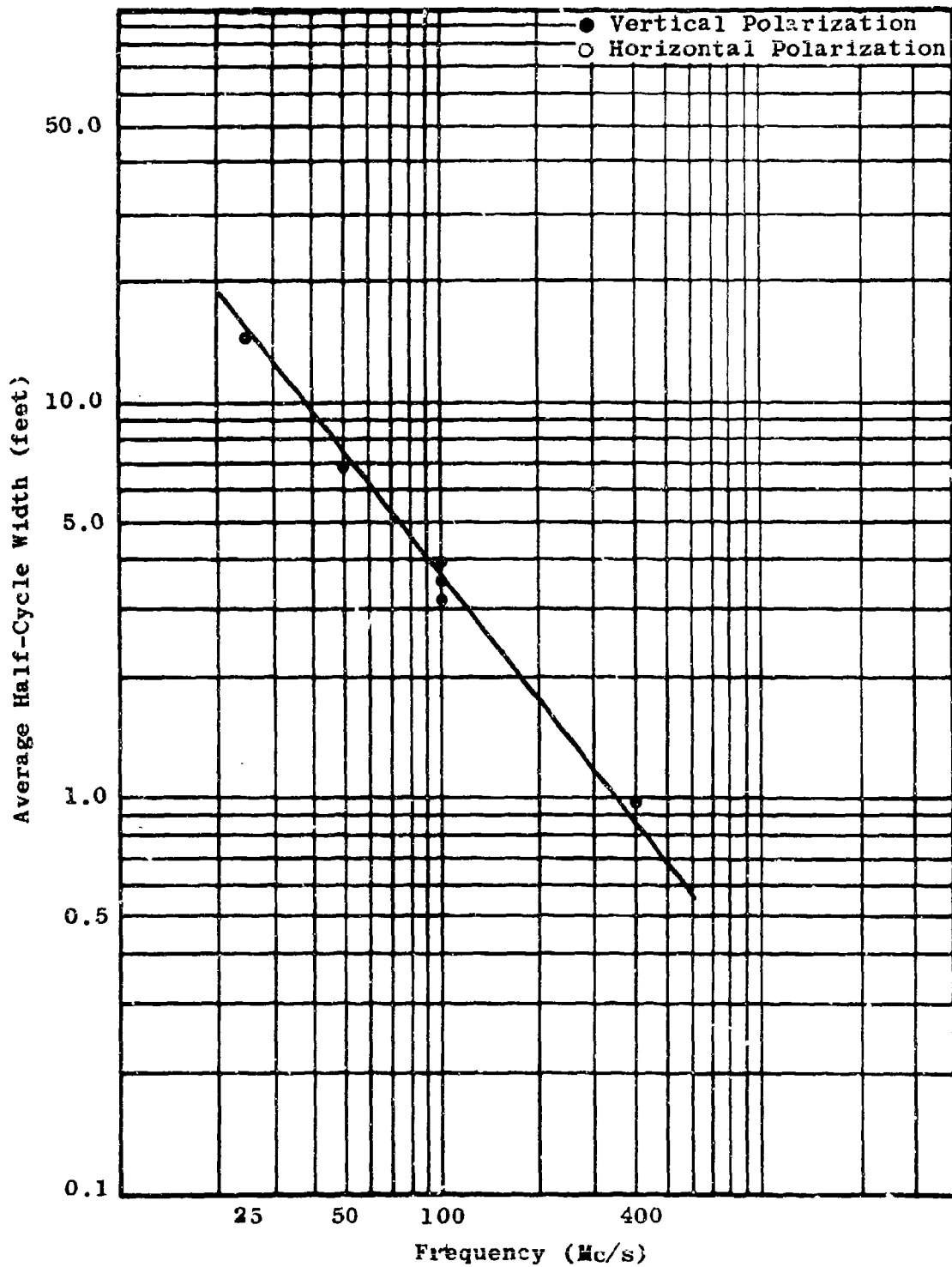


Figure 5.47 Average Half-Cycle Widths

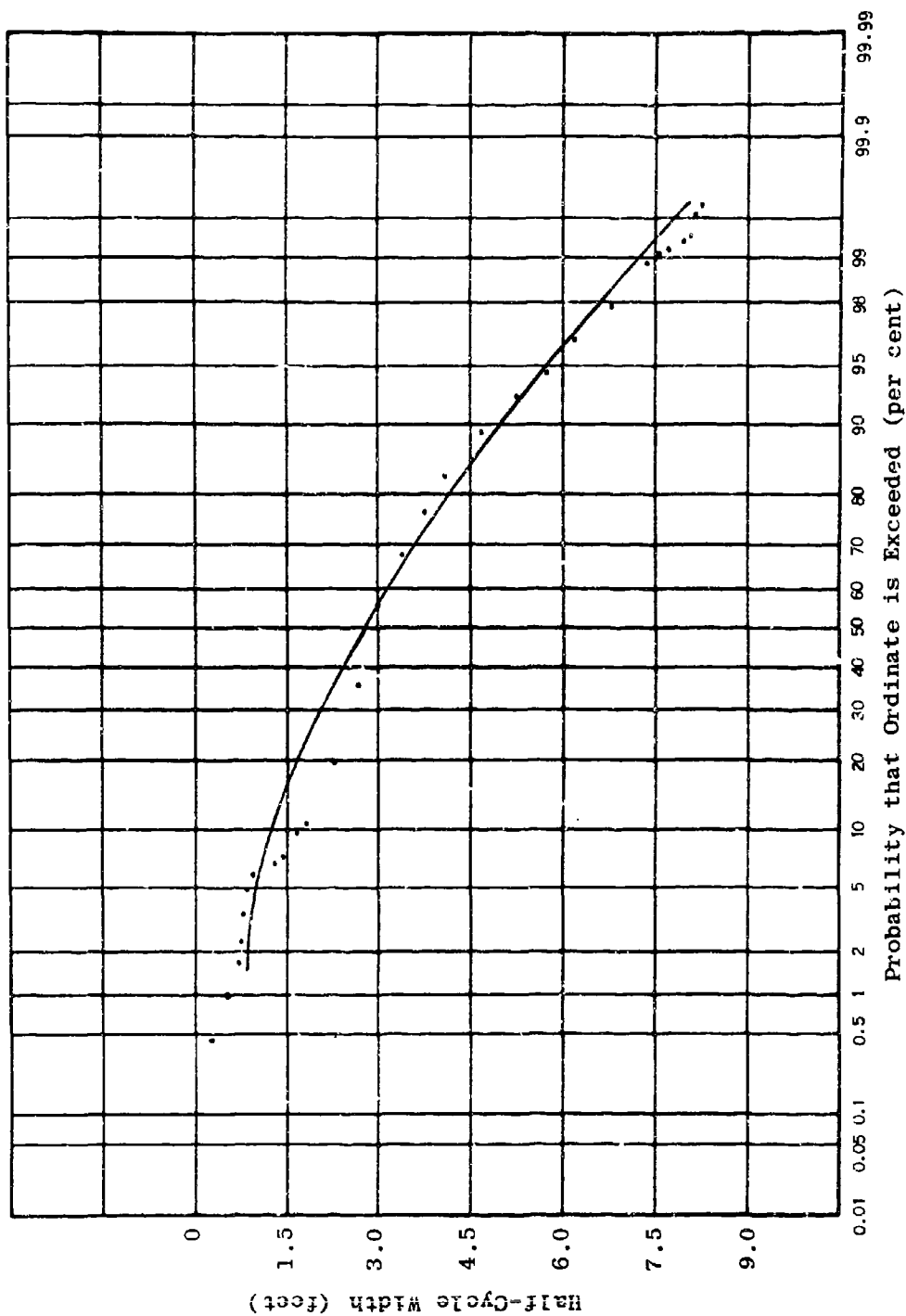


Figure 5.48 Typical Distribution for Half-Cycle Widths
(100 Mc/s, Vertical Polarization)

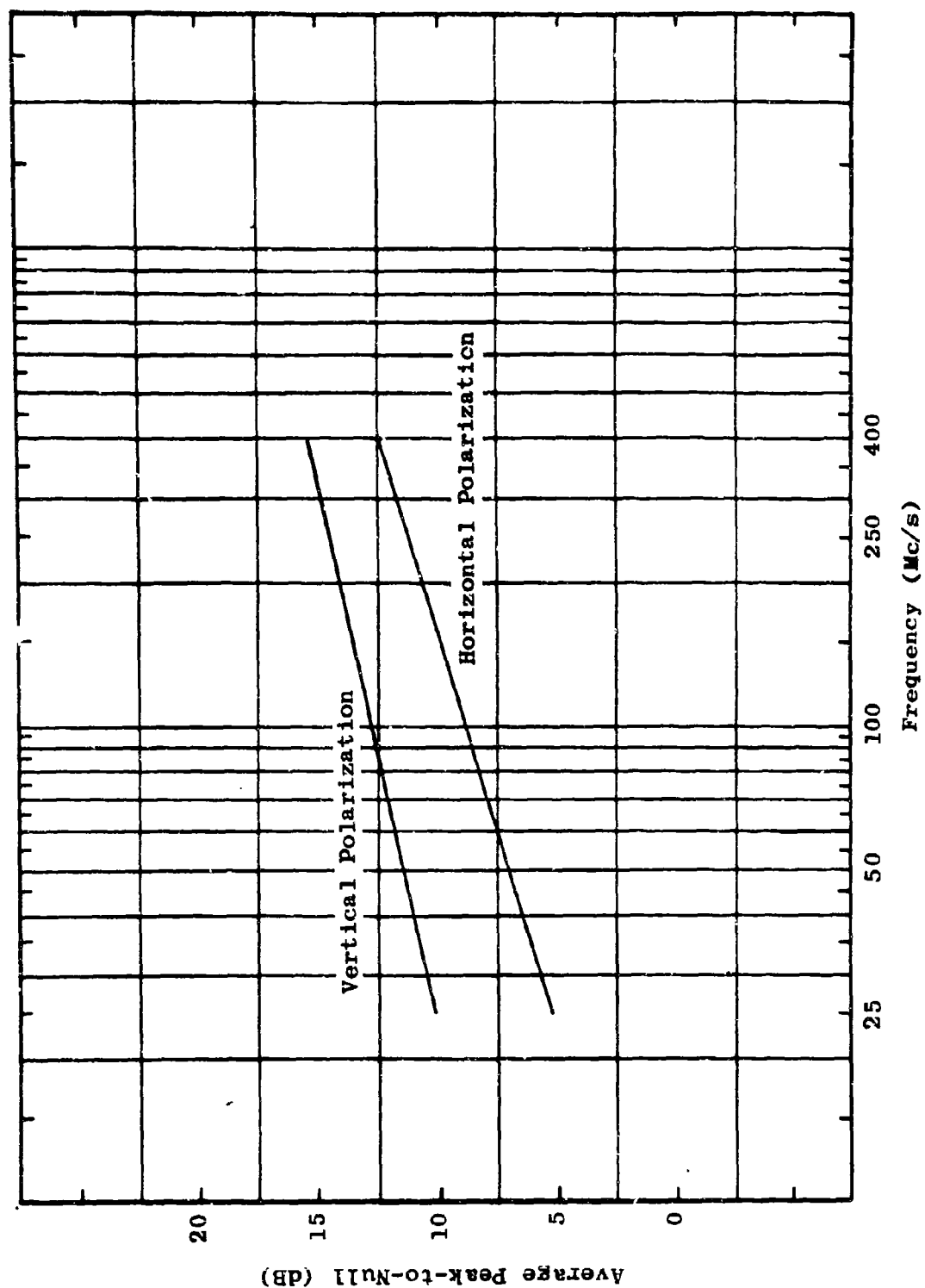


Figure 5.49 Average Peak-to-Null Ratio

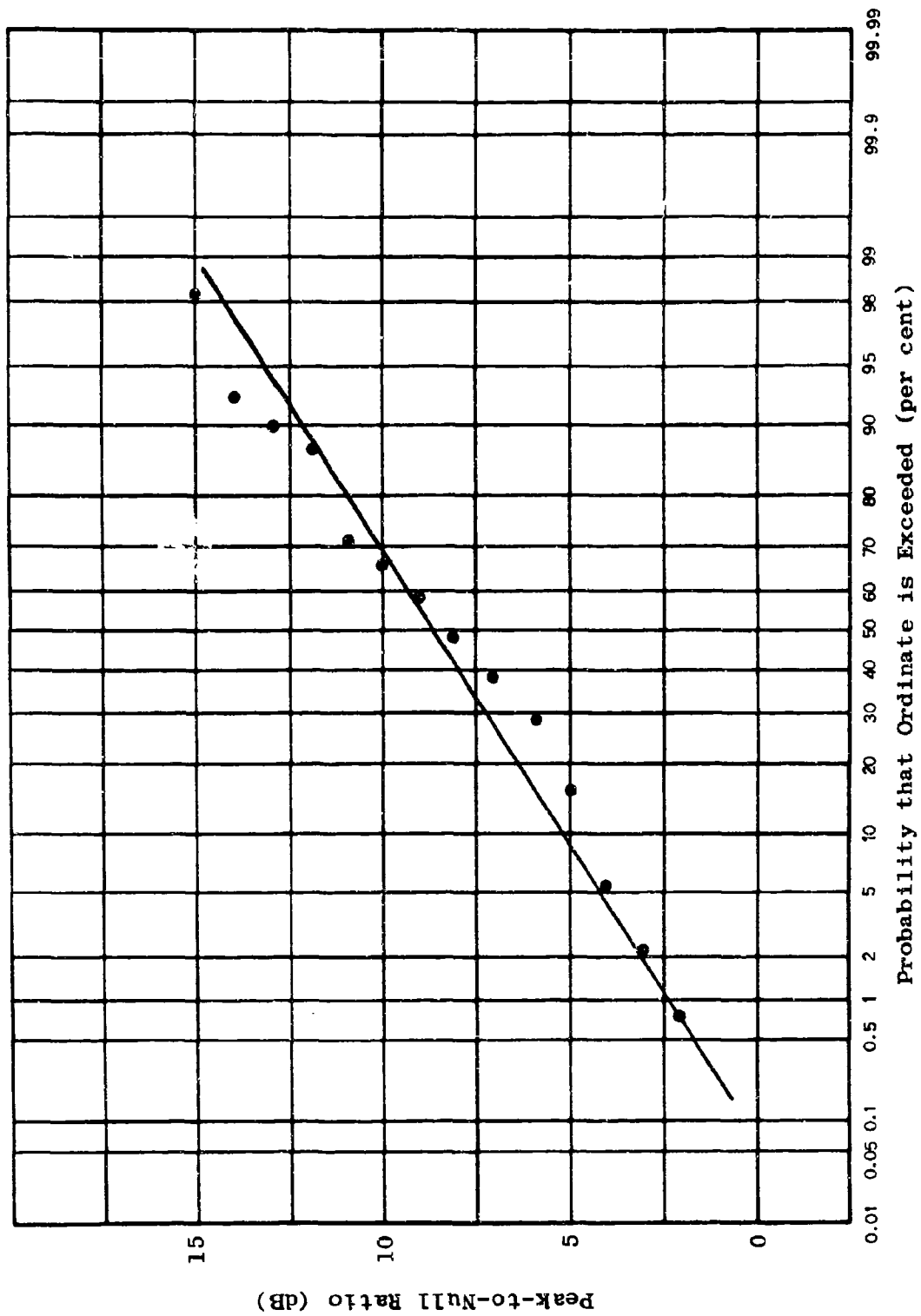


Figure 5.50 Typical Distribution for Peak-to-Null Ratio
(100 Mc/s, Horizontal Polarization)

5.2 Propagation Loss as a Function of Antenna Height in the Presence of Foliage

The Pak Chong data base contains a large number of vertical path loss profiles. These profiles, taken at fixed points within the jungle, provide a continuous record of loss versus receiving antenna heights ranging from 11 feet to 80 feet. In almost all cases, the vertical profiles of propagation path loss show path loss decreasing with increasing antenna height. This phenomenon is referred to as "height gain." From an operational point of view, it is important to know how the over-all system gain may be improved by elevating one or more of the terminals. In addition, for modeling purposes, one of the surest ways to test the validity of a model is to study how well it predicts changes in path loss caused by different antenna heights.

The continuous records of path loss as a function of antenna height are statistically reduced to a set of median values of measured field strength corresponding to different segments of antenna height segments. Table 5.3 shows the receiving antenna height segments which were used and the nominal receiver height assigned to each height segment. The measurements which were made at 11 feet are fixed measurements and hence do not have an associated height range.

Figure 5.51 is a summary of all the height gain profiles taken at 25 Mc/s with horizontal polarization and a transmitting antenna height of 40 feet. The curves included in Figure 5.51 have been selected to provide a representative cross section of results for antenna

Table 5.3
HEIGHT RANGES USED IN HEIGHT-GAIN STUDY

Nominal Height (ft)	Height Range Over Which Median Field Strength was Determined (ft)
11	11.0
20	17.5 - 23.0
26	23.0 - 28.5
31	28.5 - 34.0
37	34.0 - 39.5
42	39.5 - 45.0
48	45.0 - 50.5
53	50.5 - 56.0
59	56.0 - 61.0
64	61.0 - 66.0
69	66.0 - 71.0
73	71.0 - 76.0
79	76.0 - 81.5

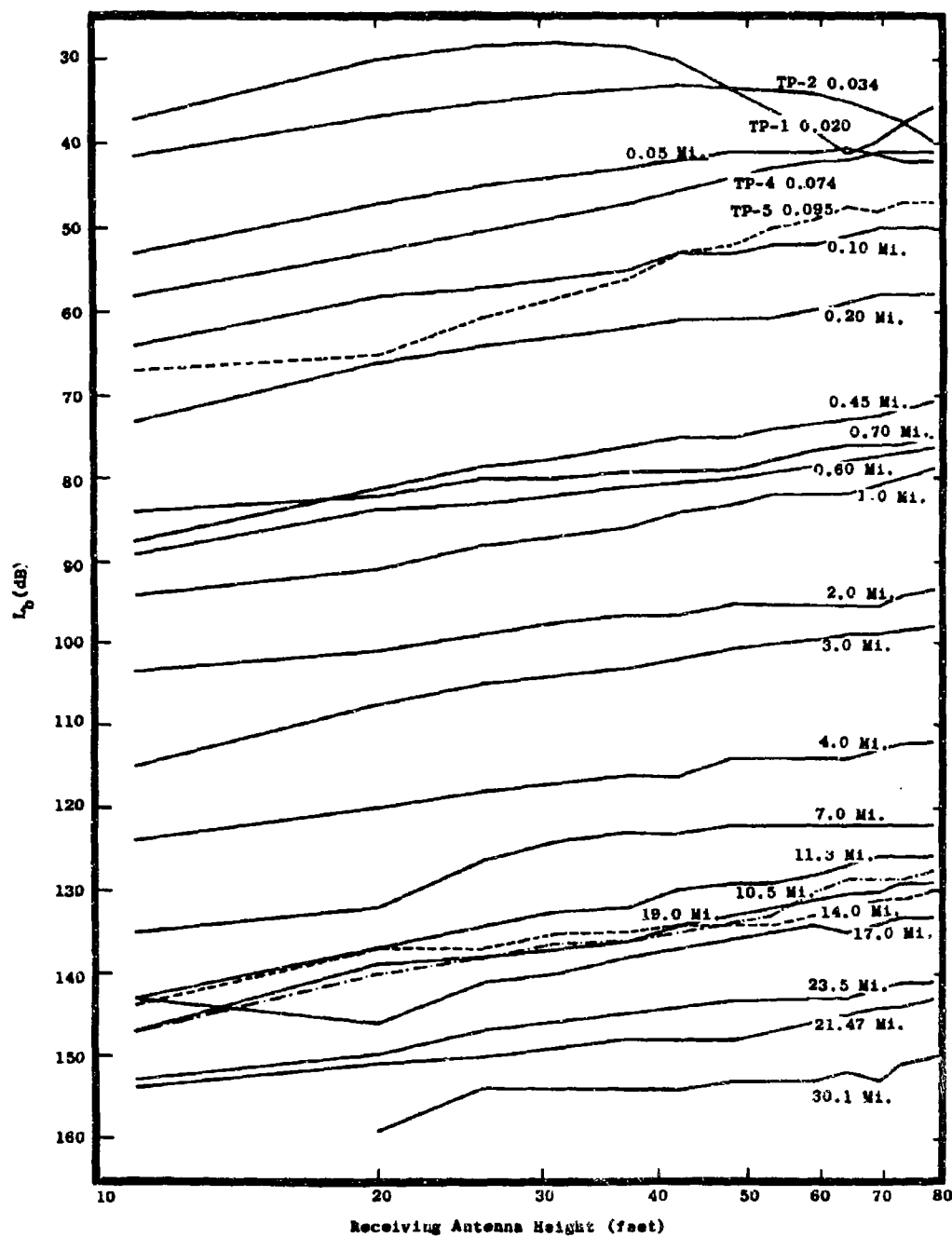


Figure 5.51 Summary of Height-Gain Profiles
 $L_b = F_{A,B}(25, 40, H, d, H_r)$

separations varying from .02 to 30 miles. All height-gain curves, except those marked with TP numbers, were taken at the standard fixed measuring points at the distances indicated. The curves labeled TP-1 and TP-2 correspond to special measurement points located within the base compound clearing where there was no foliage between the transmitting and receiving antennas. The curves labeled TP-4 and TP-5 correspond to special measurement points located within the jungle foliage, just beyond the base compound clearing. Table 5.4 lists the TP points and their distance separation from the transmitting antenna. The edge of the foliage is 0.038 miles from the transmitting antenna.

Table 5.4
TP-POINT SEPARATION DISTANCES

<u>TEST POINTS</u>	<u>SEPARATION DISTANCE (miles)</u>
TP-1	0.020
TP-2	0.034
TP-3	0.057
TP-4	0.074
TP-5	0.095

Figure 5.52 provides a similar set of height-gain examples for 100 Mc/s with horizontal polarization and a transmitting antenna height of 40 feet. These curves provide a composite view of the way in which height variations change with distance. The interaction between

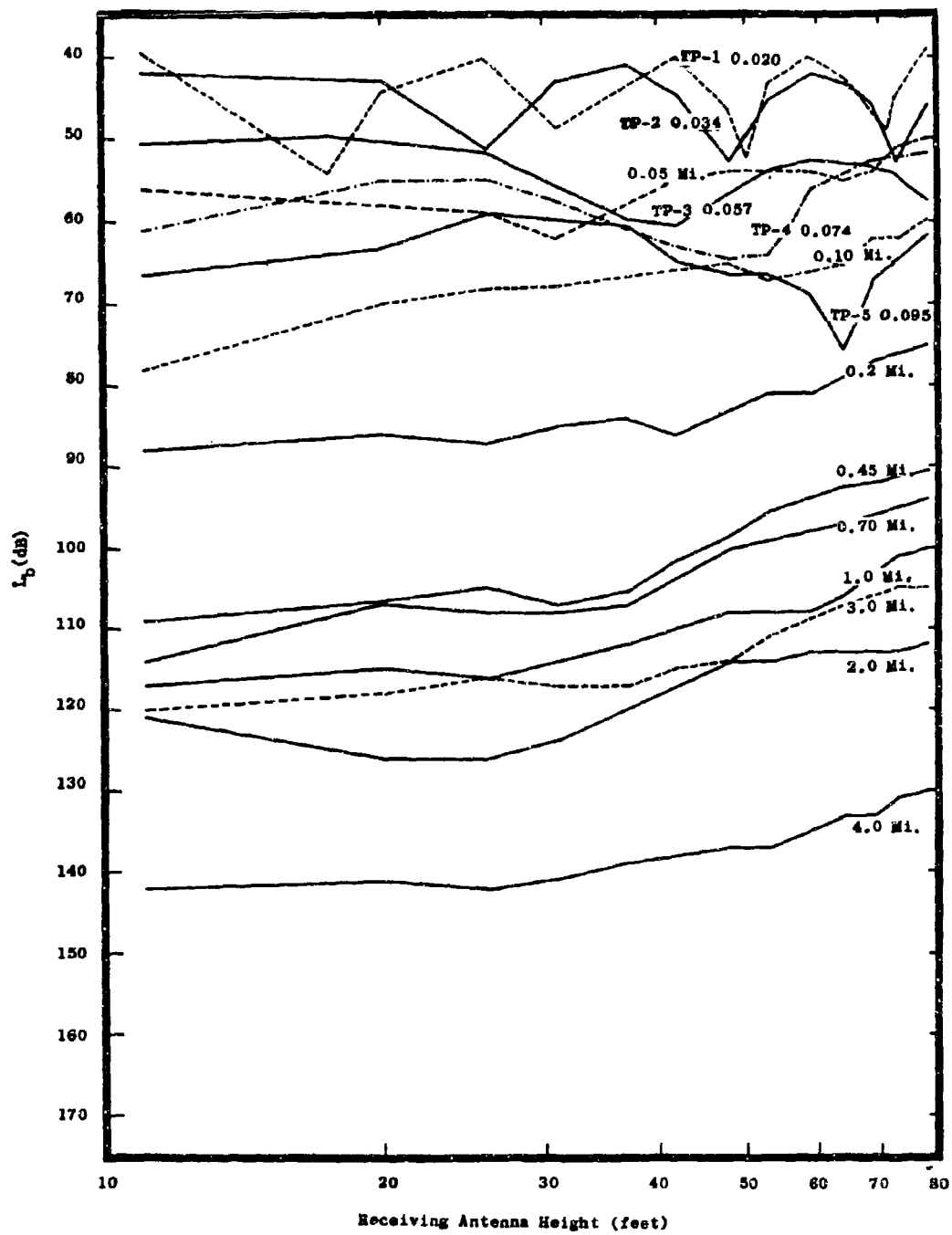


Figure 5.52 Summary of Height-Gain Profiles
 $L_b = F_{A,B}(100, 40, H, d, H_r)$

a direct and ground reflected ray is very much in evidence at the two measurement points within the clearing. This interaction is also present to a lesser degree at measurement points within the nearby foliage. The height-gain curves for distances of 0.2 mile and beyond should be viewed in conjunction with the terrain profiles given in Figures 5.89 and 5.90 which show the major terrain features between each measuring point and the transmitting antenna.

5.2.1 Height Gain for Separation Distances of 2 to 30 Miles

The vertical path loss profiles vary considerably from field point to field point. The intent of this and the following section is to provide an over-all summary of the average measured height gain as determined from the complete Pak Chong data base. The height gains presented in this section are given in terms of the relative change in path loss as antenna height is varied from 10 to 80 feet.

The various propagation paths encountered at Pak Chong fall into two distinct classes. The first consists of paths over rugged terrain which are one mile or more in length. The second consists of paths which are less than one mile in length and span non-rugged terrain. This section is devoted to height gain along the first type, the longer and more rugged terrain paths. The next section discusses height gain along the shorter, non-rugged paths. The height gain discussions in these two sections are confined to the frequency range from 25 to 400 Mc/s.

Table 5.5 contains expressions relating the average decrease in path loss to increases in antenna height when propagation paths extend more than one mile over rugged terrain. The expressions are normalized to an antenna height of ten feet. As shown in Table 5.5, there are apparently two basic types of height gain for separation distances in the range 2 to 30 miles. For vertical polarization and frequencies of 25 and 50 Mc/s, the path loss decreases with increasing antenna height at twenty times the logarithm of antenna height, normalized to a height of ten feet. At frequencies of 100, 250 and 400 Mc/s, path loss on the average decreases linearly with increasing antenna height at a rate of 2 dB per ten feet. For horizontal polarization, the vertical path loss profile varies logarithmically with antenna height at 25, 50, 250 and 400 Mc/s and linearly at 100 Mc/s.

The height-gain averages presented in Table 5.5 were obtained by considering all fixed point data in the indicated distance range. A distance factor of 40 times the logarithm of distance was subtracted from each of the measured data points. Data points from both sectors at all distances greater than one mile were then averaged for each combination of polarization, frequency, transmitting antenna height and nominal receiving antenna height. The resulting averages for each transmitting antenna height (13 feet, 40 feet and 80 feet) were then normalized to a transmitting antenna height of 13 feet. The normalizing factor used was derived from the median height gain displayed by the corresponding receiving antenna height-gain averages. The data points shown on Figure 5.53 are examples of the normalized averages for the three trans-

Table 5.5
ESTIMATES OF RELATIVE HEIGHT GAIN

<u>Polarization</u>	<u>Frequency (Mc/s)</u>	<u>Normalized Height Gain (dB)</u>	
		<u>10</u>	<u>h 80 feet</u>
V	25	20 log	$\frac{h}{10}$
V	50	20 log	$\frac{h}{10}$
V	100	0.2h - 2	
V	250	0.2h - 2	
V	400	0.2h - 2	
H	25	15 log	$\frac{h}{10}$
H	50	12 log	$\frac{h}{10}$
H	100	0.2h - 2	
H	250	23 log	$\frac{h}{10}$
H	400	23 log	$\frac{h}{10}$

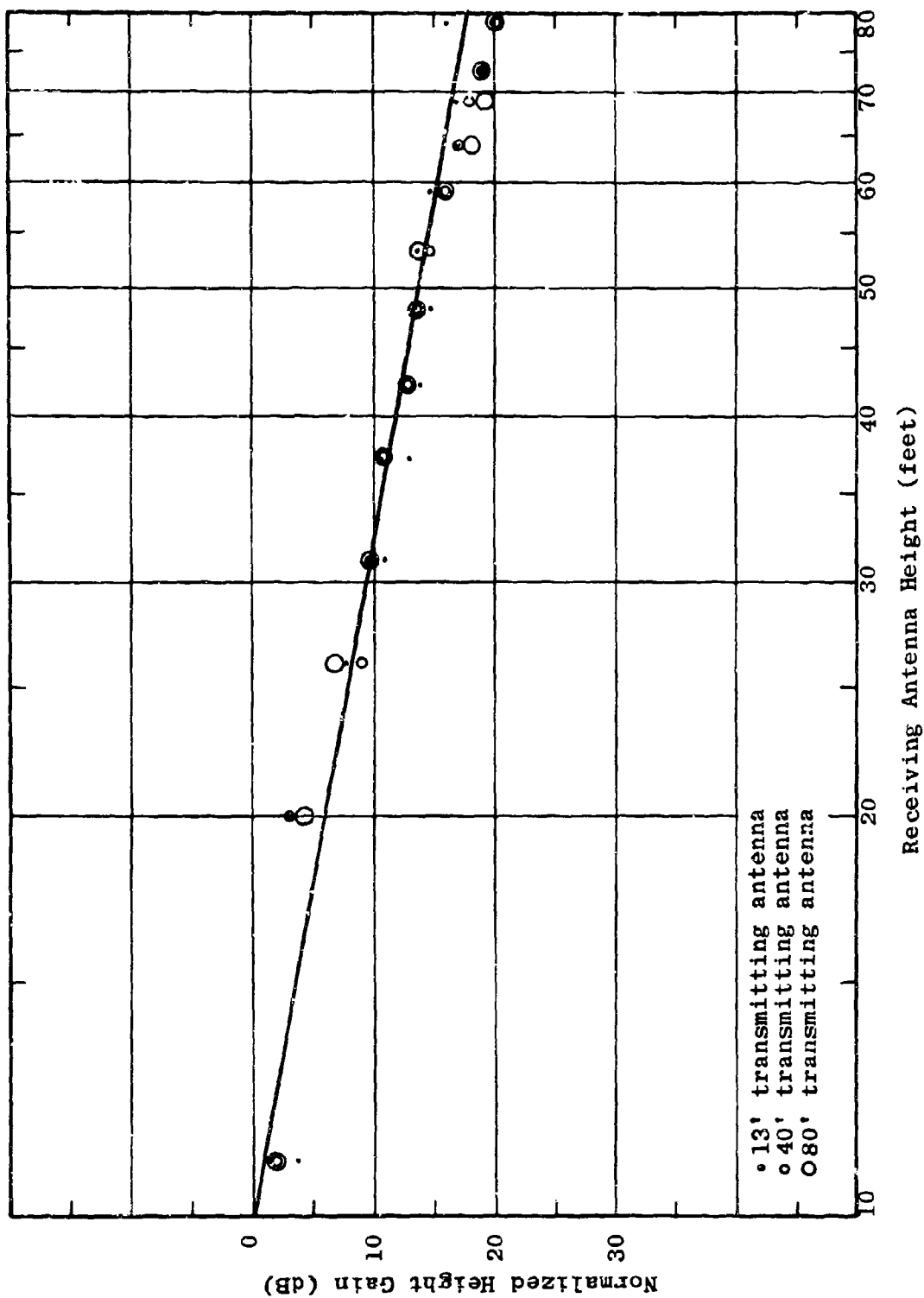


Figure 5.53 Average Height Gain for Vertical Polarization at 25 Mc/s

mitting antenna heights which were obtained for 25 Mc/s with vertical polarization. The solid curve shown in the figure is a plot of the average height gain function listed in Table 5.5 for 25 Mc/s and vertical polarization.

Figures 5.54, 5.55 and 5.56 are, respectively, similar plots for horizontal polarization at 25 Mc/s and vertical and horizontal polarizations at 100 Mc/s.

These curves demonstrate that the smooth functions given in Table 5.5 follow the averages well and that the average height gain at the receiving point is independent of the height of the transmitting antenna within the foliage. The analysis has also shown that the average transmitting height gain is similar to the average receiving antenna height gain.

The standard deviation of the measured data points about their respective averages ranged from 6 to 10 dB indicating that even though the average height gain is relatively smooth, individual height-gain curves can deviate significantly from the smoothed averages. The smooth height-gain average is compared with individual height gain profiles for 100 Mc/s with vertical polarization in Figures 5.57, 5.58 and 5.59. The three figures show the profiles taken at 2, 3 and 4 miles in Sector A. Representative measured height-gain curves for the three test transmitting antenna heights are plotted on each figure. The solid smooth curve at the top of each figure is the smoothed average height gain. These figures show that the individual height gain curves follow the average closely at 2 and 4 miles but deviate significantly from the average at 3 miles.

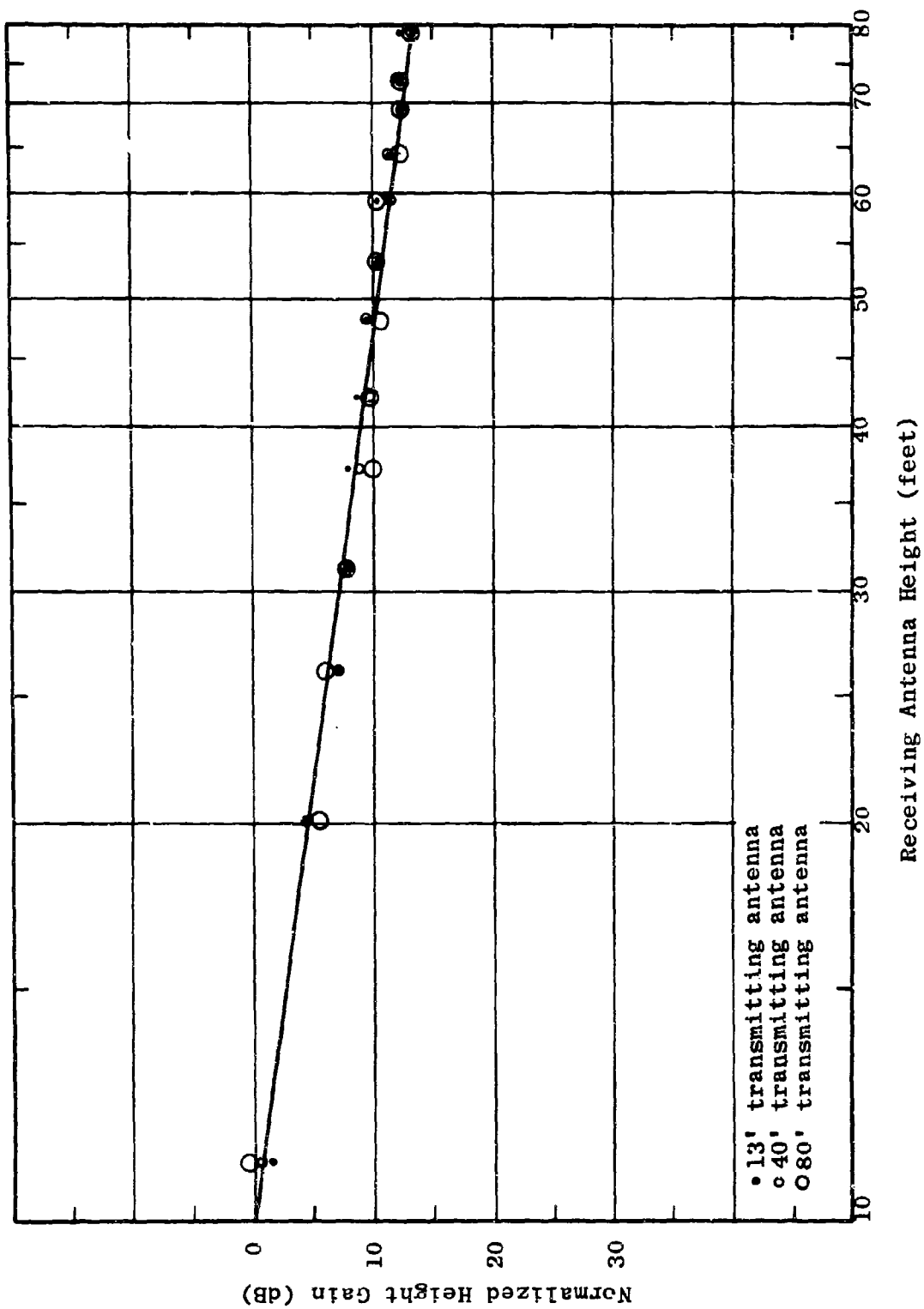


Figure 5.54 Average Height Gain for Horizontal Polarization at 25 Mc/s

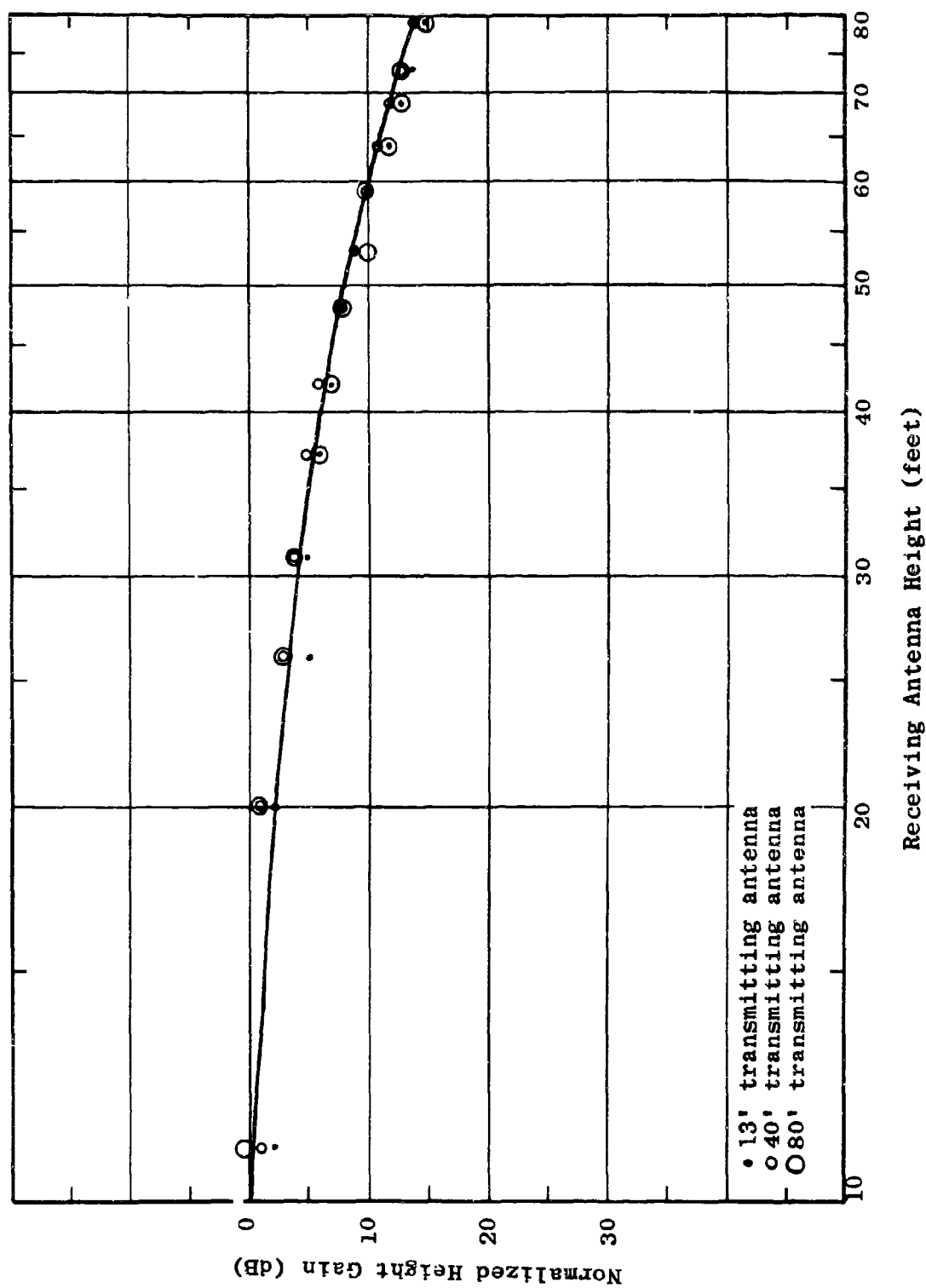


Figure 5.55 Average Height Gain for Vertical Polarization at 100 Mc/s

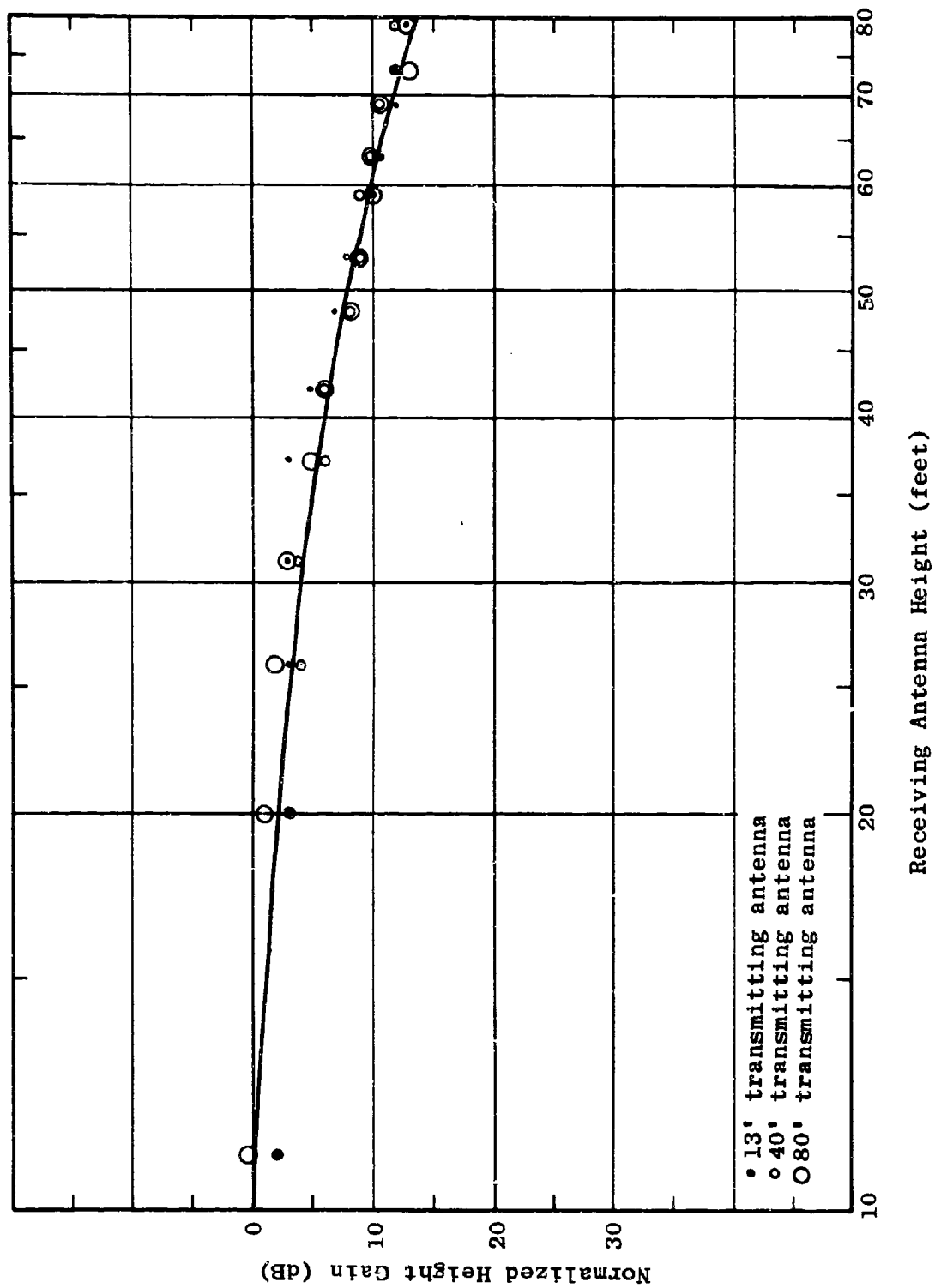


Figure 5.56 Average Height Gain for Horizontal Polarization at 100 Mc/s

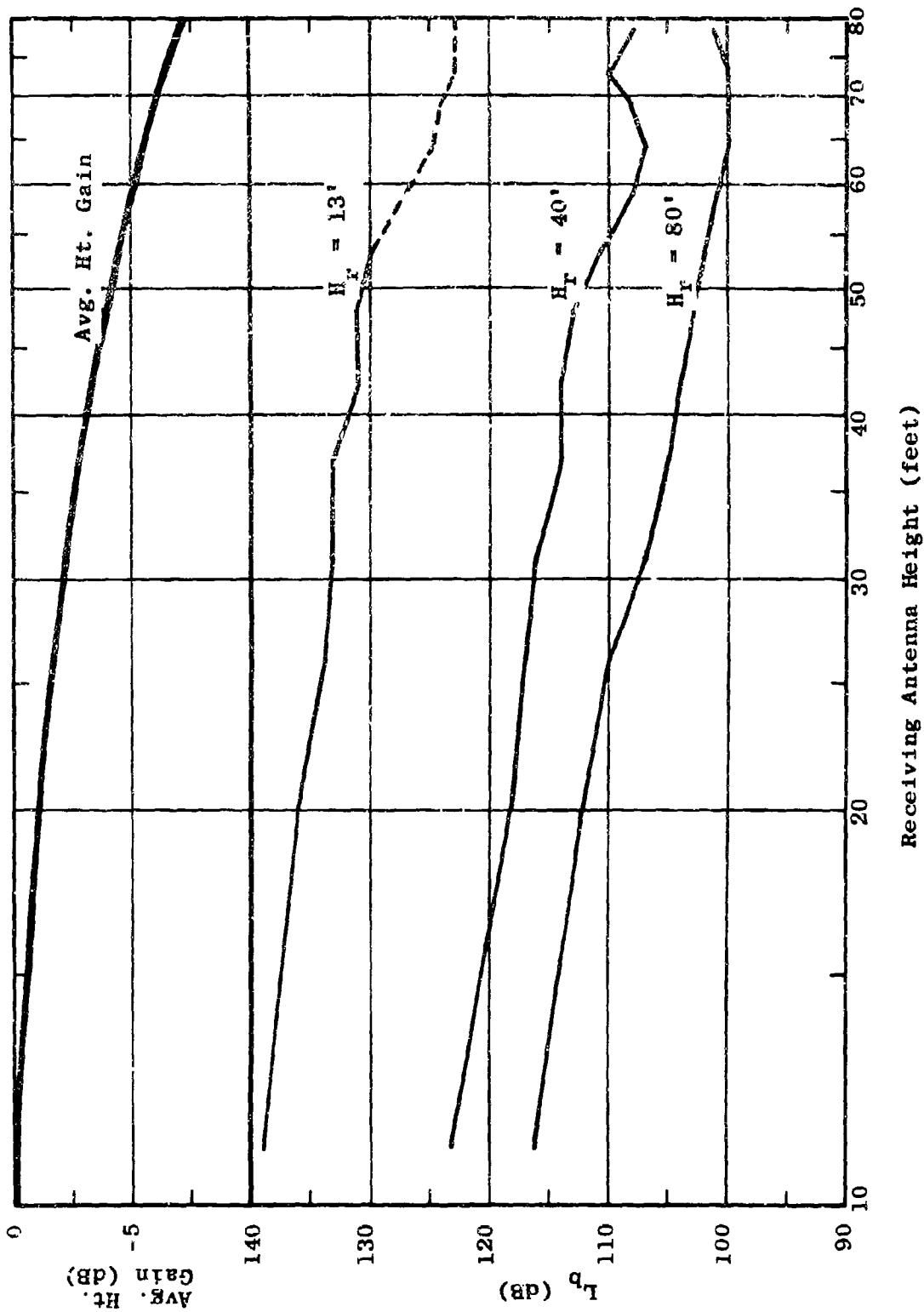


Figure 5.57 Average and Measured Height Gain
 $L_p = F_A(100, H_t, V, 2.0, H_t)$

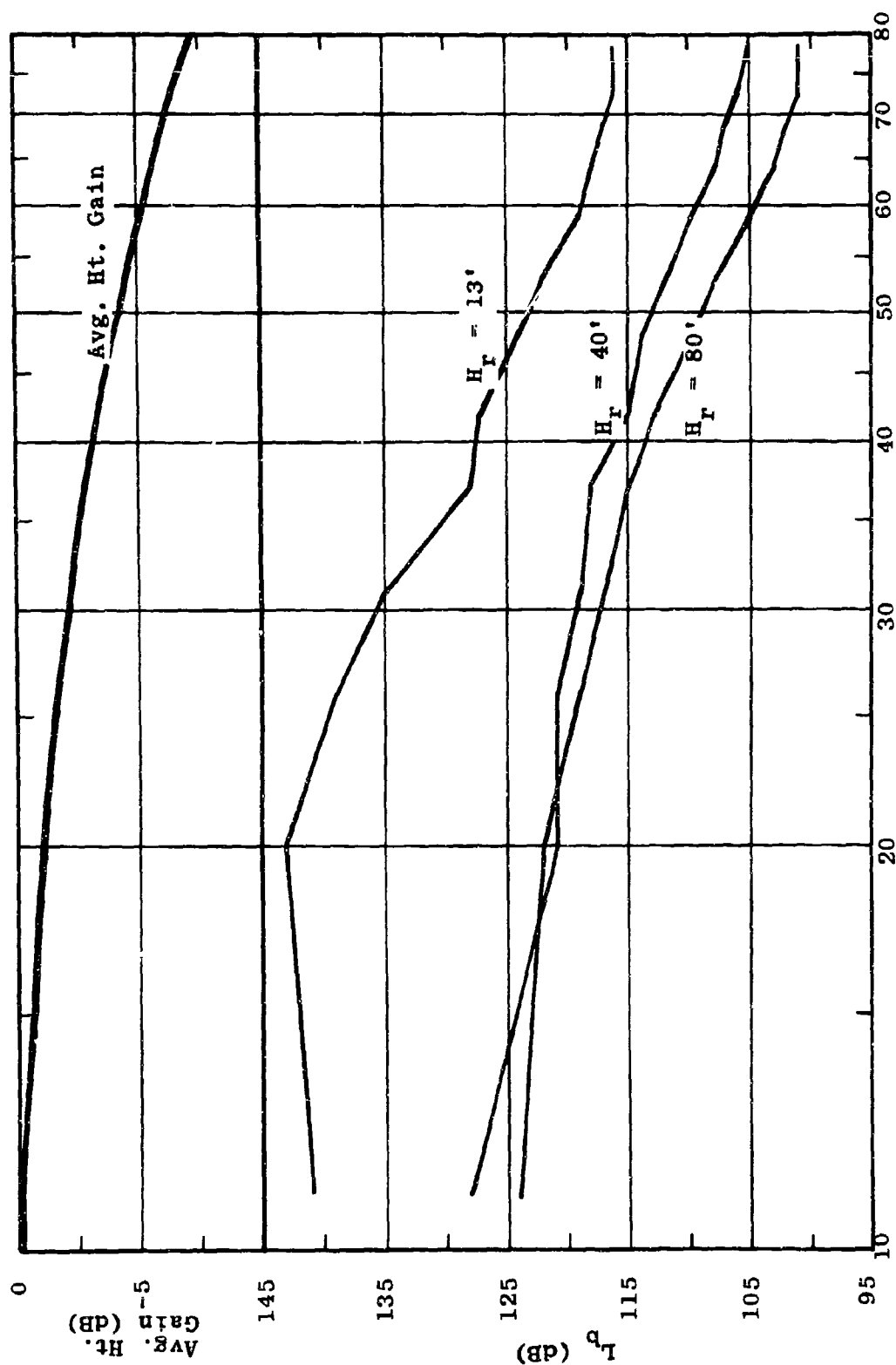


Figure 5.58 Average and Measured Height Gain
 $L_p = F_A(100, H_t, V, 3.0, H_r)$

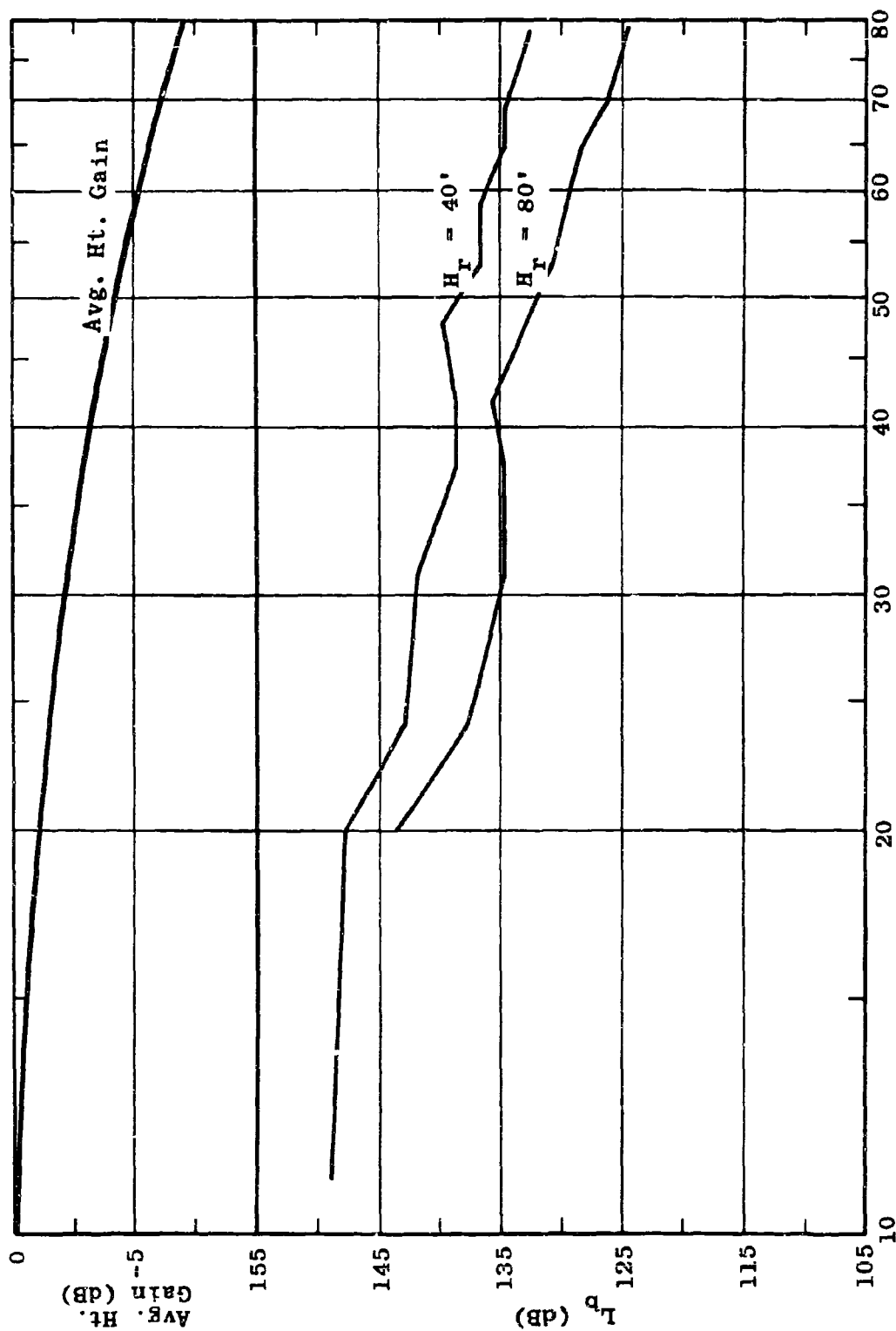


Figure 5.59 Average and Measured Height Gain
 $L_b = F_A(100, H_t, V, 4.0, H_t)$

5.2.2 Height Gain for Separation Distances of 0.2 to 1.0 Mile

This section presents a summary of the vertical path loss profiles for separation distances less than one mile. Within this distance range the terrain is sufficiently smooth to produce unobstructed line-of-sight paths between the antennas in the absence of foliage.

Normalized estimates of the average height gain expected over short paths and flat foliated terrain are presented in Table 5.6. The estimates in Table 5.6 are for both polarizations and for test frequencies in the range 25 to 400 Mc/s. The estimates are derived from measured fixed point data at a transmitting height of 13 feet. For these separation distances, it was found that the relative estimates of height gain are independent of the transmitting antenna height, as was the case with the longer paths discussed in Section 5.2.1.

By way of comparison, the fourth column in Table 5.6 repeats the relative height gain estimates presented in Section 5.2.1 for long propagation paths. Columns 5 and 6 list the total height gain expected over a height range 10-80 feet as predicted by the relative estimates given in Columns 3 and 4, respectively.

The height gain estimates for flat terrain over distances less than one mile are in general higher than those for the longer, rugged paths. Three particulars should be noted about the height gain estimates for these short, smooth, foliated paths.

Table 5.6
HEIGHT GAINS FOR SHORT AND LONG PATHS

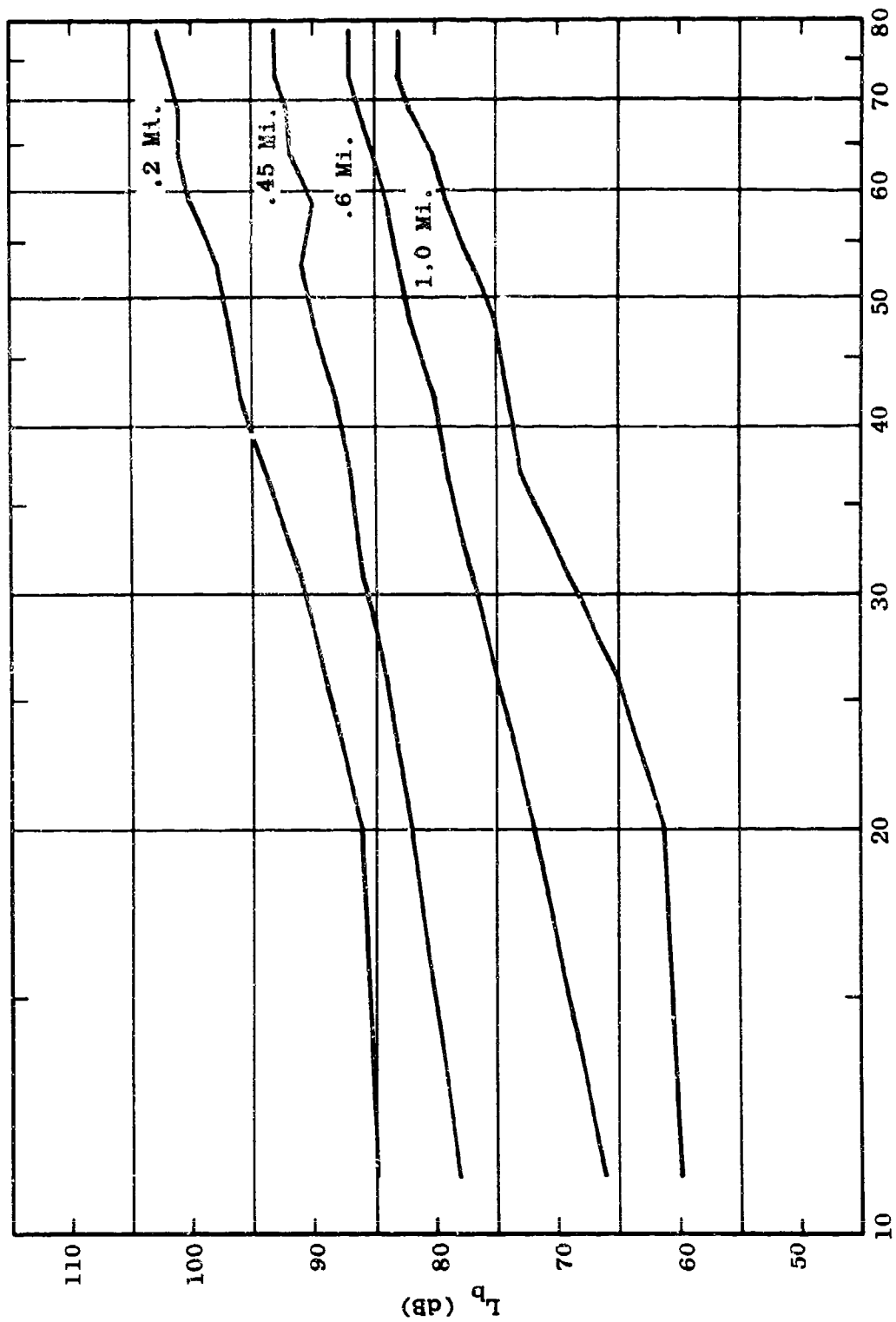
Polarization	Frequency (Mc/s)	Normalized Height Gain Function (dB) 10 to 80 feet			Total Estimated Height Gain From 10 to 80 feet (dB)	
		0.2 to 1.0 miles	2 to 30 miles		0.2 to 1.0 miles	2 to 30 miles
V	25	$20 \log \frac{h}{10}$ *	$20 \log \frac{h}{10}$		13*	18
V	50	$0.3h - 3*$	$20 \log \frac{h}{10}$		18*	18
V	100	$0.4h - 4*$	$0.2h - 2$		24*	14
V	250	$0.4h - 4*$	$0.2h - 2$		24*	14
V	400	$0.4h - 4*$	$0.2h - 2$		24*	14
H	25	$20 \log \frac{h}{10}$	$15 \log \frac{h}{10}$		18	14
H	50	$15 \log \frac{h}{10}$	$12 \log \frac{h}{10}$		14	11
H	100	$0.4h - 4+$	$0.2h - 2$		20+	14
H	250	$0.4h - 4*$	$23 \log \frac{h}{10}$		24*	21
H	400	$0.4h - 4*$	$23 \log \frac{h}{10}$		24*	21

* No height gain from 10' - 20', estimates apply to height range 20' - 80'.

+ No height gain from 10' - 30', estimates apply to height range 30' - 80'.

1. There is a greater tendency toward linear height gain for the short, smooth paths than for the long, rugged paths.
2. The vertical path loss profiles in general show little or no change in loss over the height range, 10-20 feet. However, over the height range 20-80 feet, path loss decreases much more rapidly with increasing antenna height for the short paths than for the longer paths.
3. For the short, smooth paths, the estimated height gain is the same whether vertical or horizontal polarization is used, with the exception of the estimates at 50 Mc/s. This similarity between the height gain estimates for vertical and horizontal polarizations does not hold true for the longer, more rugged paths.

Figures 5.60 through 5.64 are typical examples of the measured height gain profiles from which the estimates in Table 5.6 are derived. The figures show measured profiles for vertical polarization at frequencies of 25, 50, 100, 250, and 400 Mc/s, respectively. Each graph presents curves of measured height gain for distances in the range 0.2-1.0 mile and for a transmitting antenna height of 13 feet. Figures 5.65 through 5.69 contain the same information for horizontal polarization.



Receiving Antenna Height (feet)

Figure 5.60 Height Gain Profile

$L_b = F_{A,B}(25, 10, V, d, H_r)$

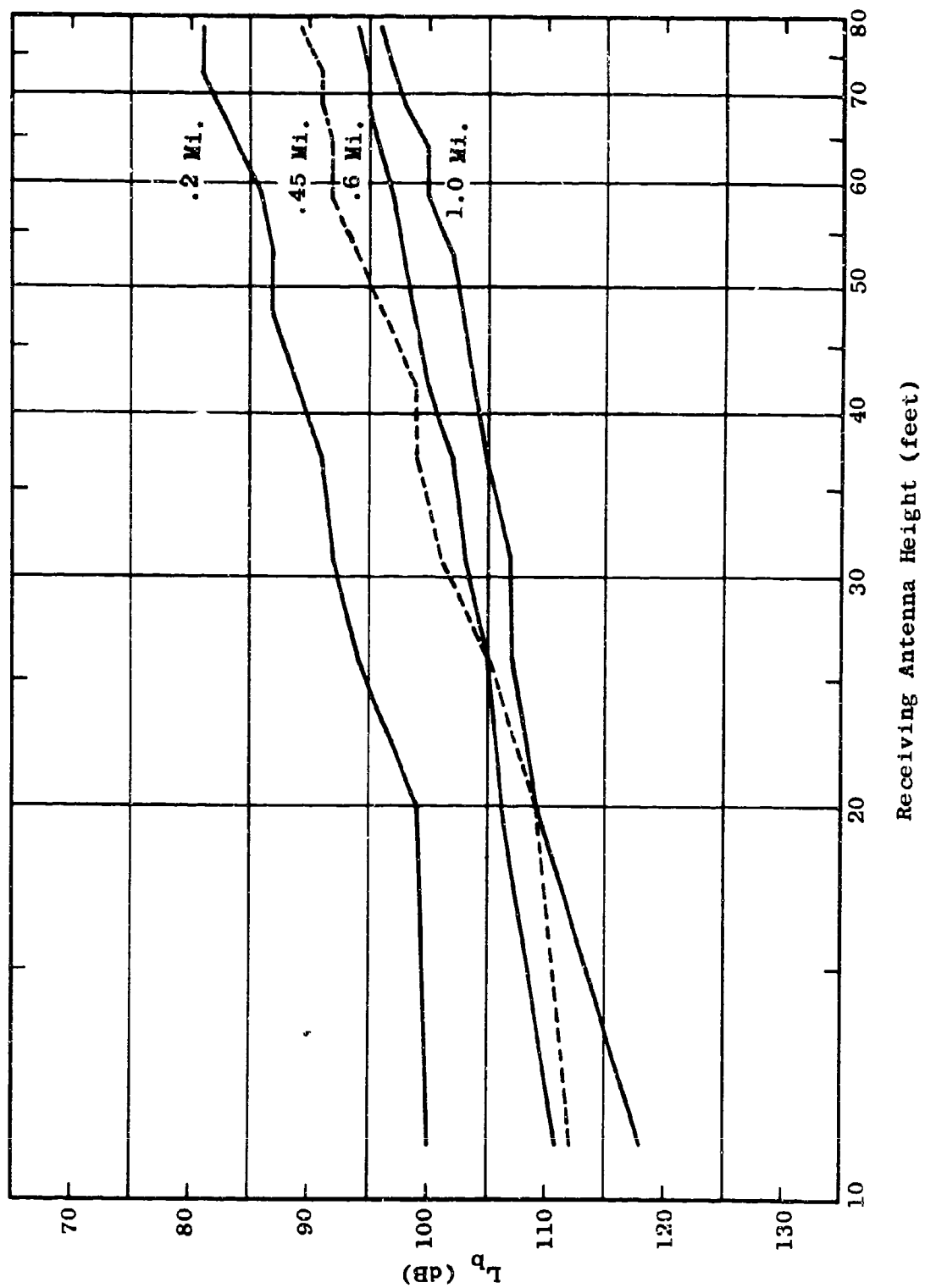
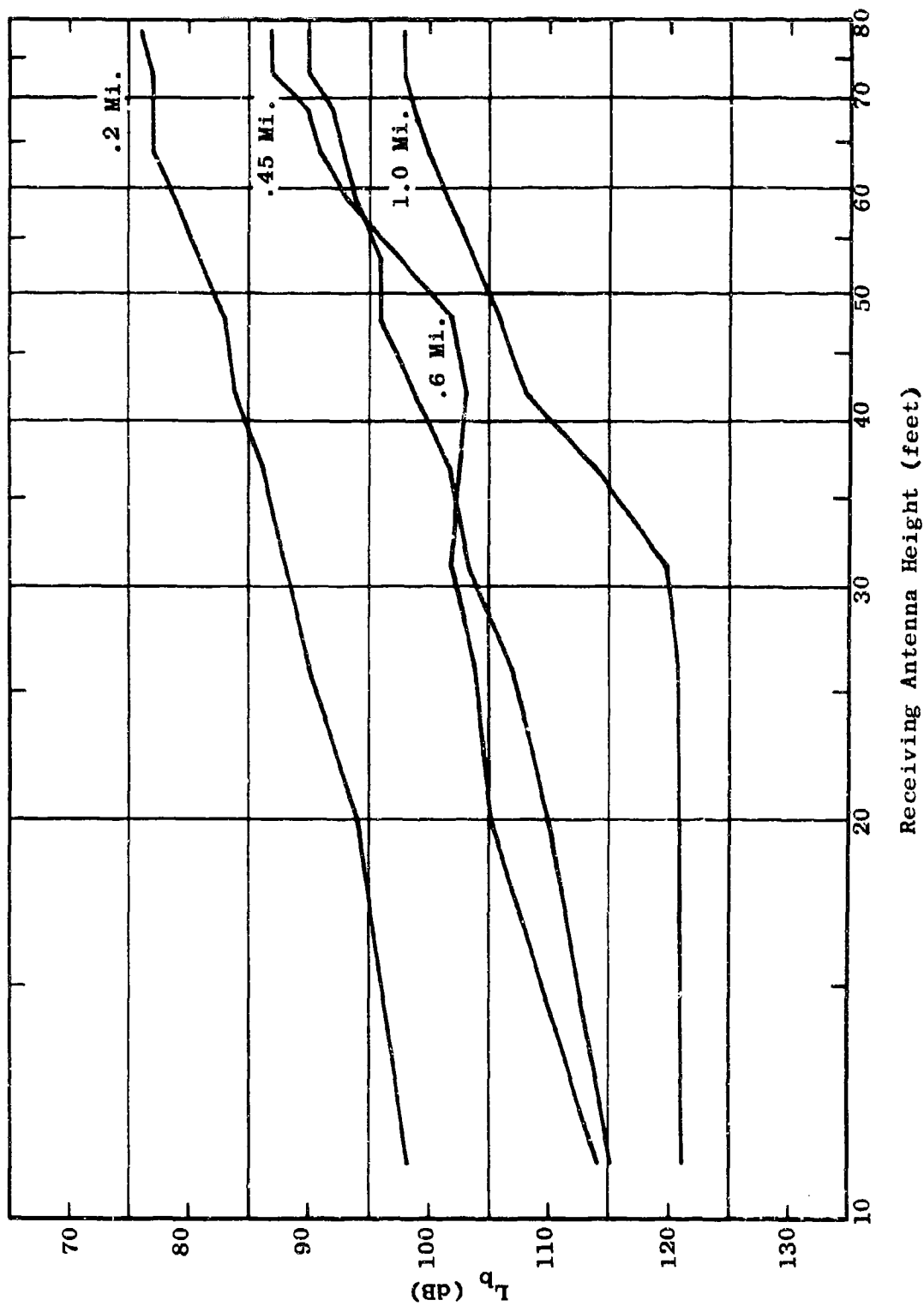


Figure 5.61 Height Gain Profile
 $L_b = F_{A,B}(50, 13, V, d, H_r)$



Receiving Antenna Height (feet)

Figure 5.62 Height Gain Profile
 $L_b = F_{A,B}(100, 13, V, d, H_r)$

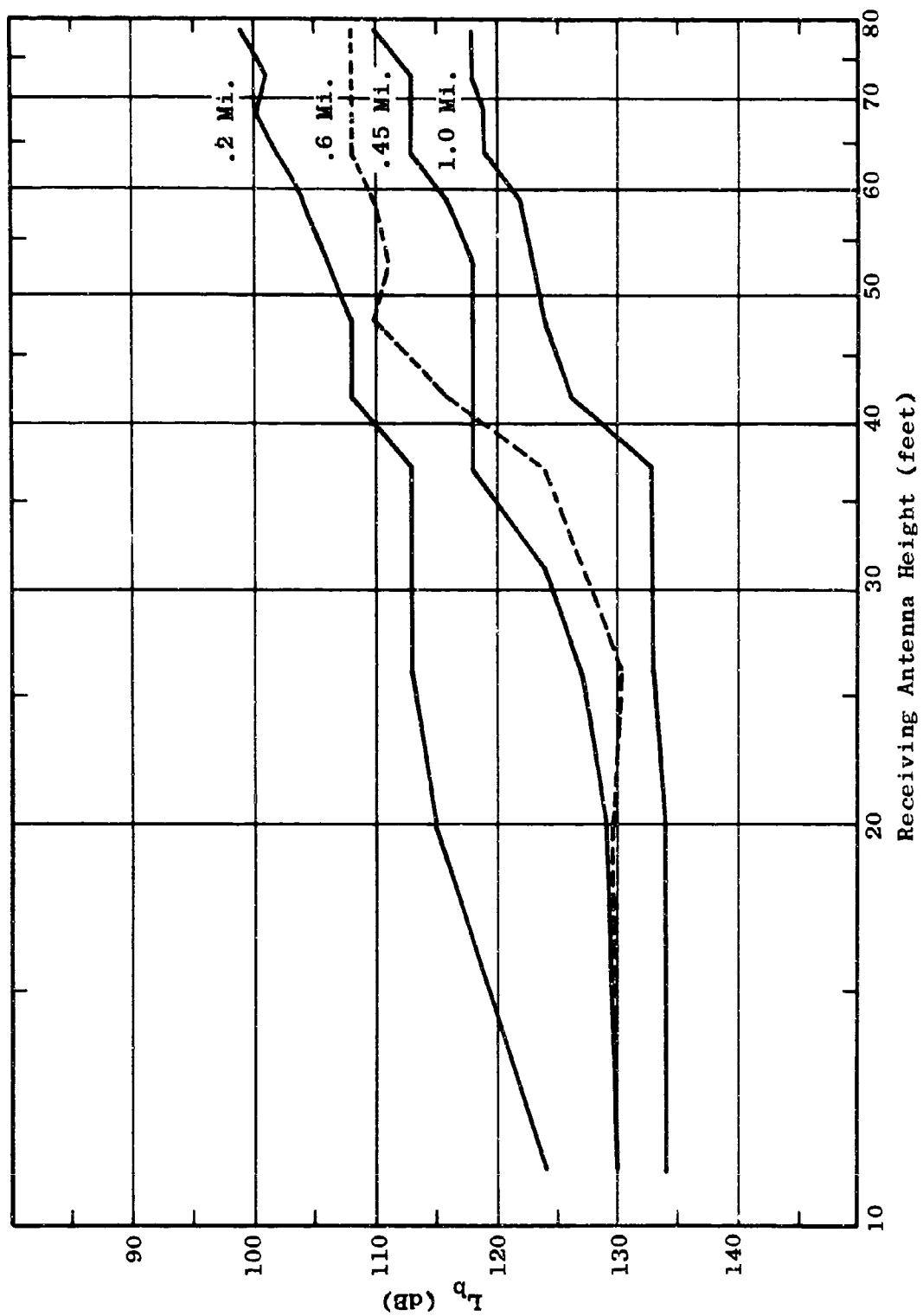


Figure 5.63 Height Gain Profile
 $L_b = F_{A,B}(250, 13, V, d, H_r)$

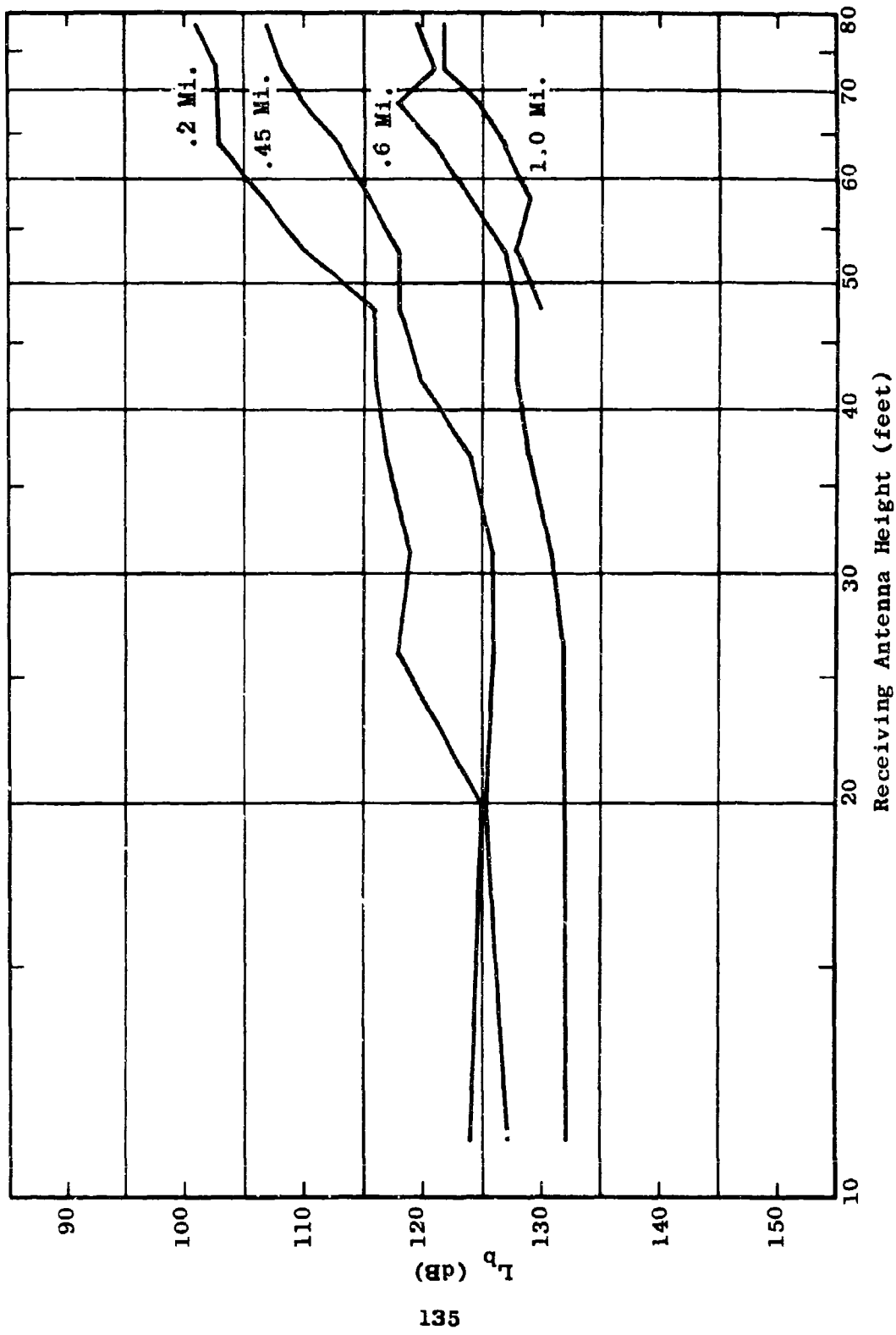


Figure 5.64 Height Gain Profile
 $L_p = F_A, B(400, 13, V, d, H_r)$

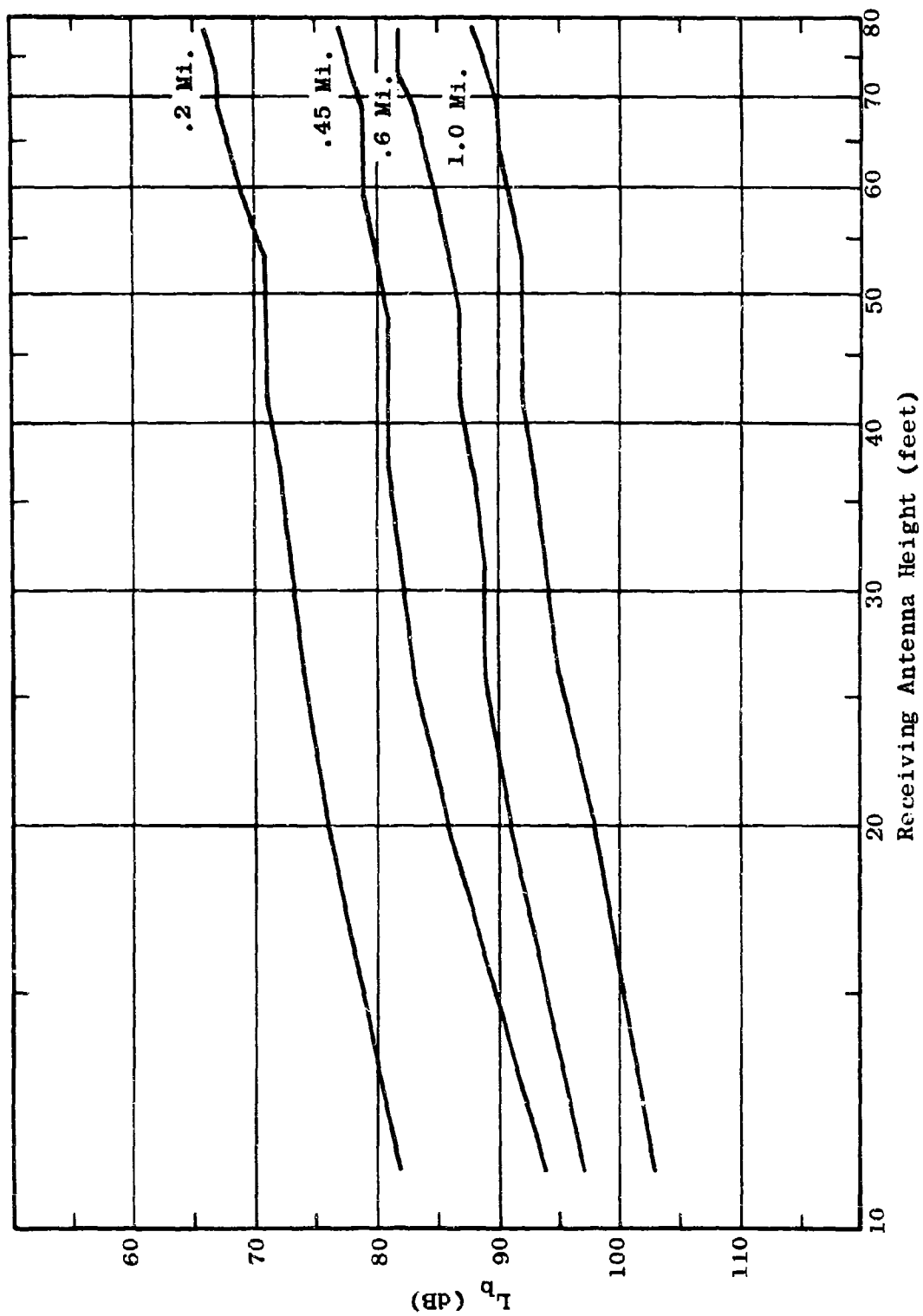


Figure 5.65 Height Gain Profile
 $L_p = F_{A,B}(25, 13, H, d, H_r)$

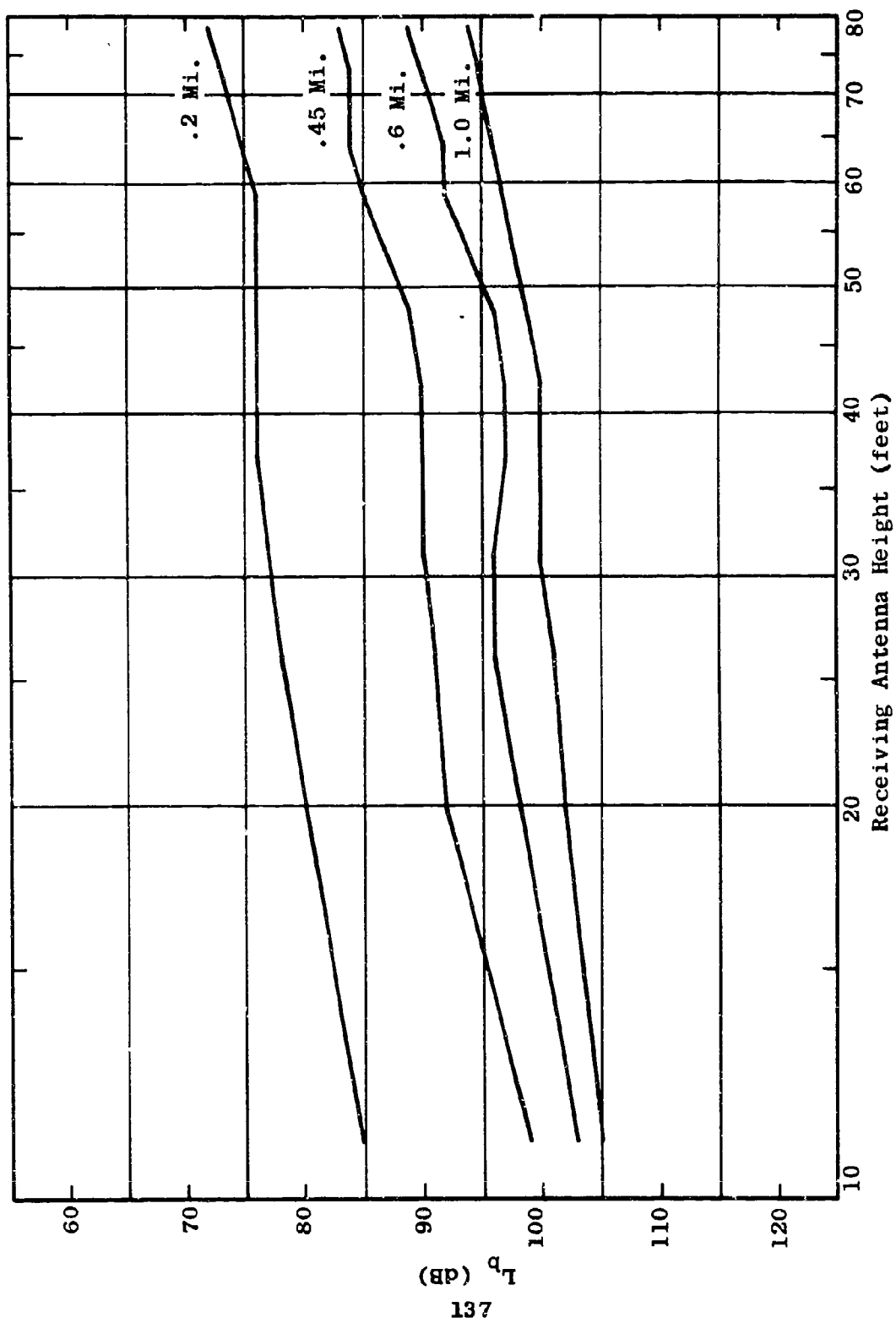


Figure 5.66 Height Gain Profile
 $L_p = F_{A,B}(50, 13, H, d, H_r)$

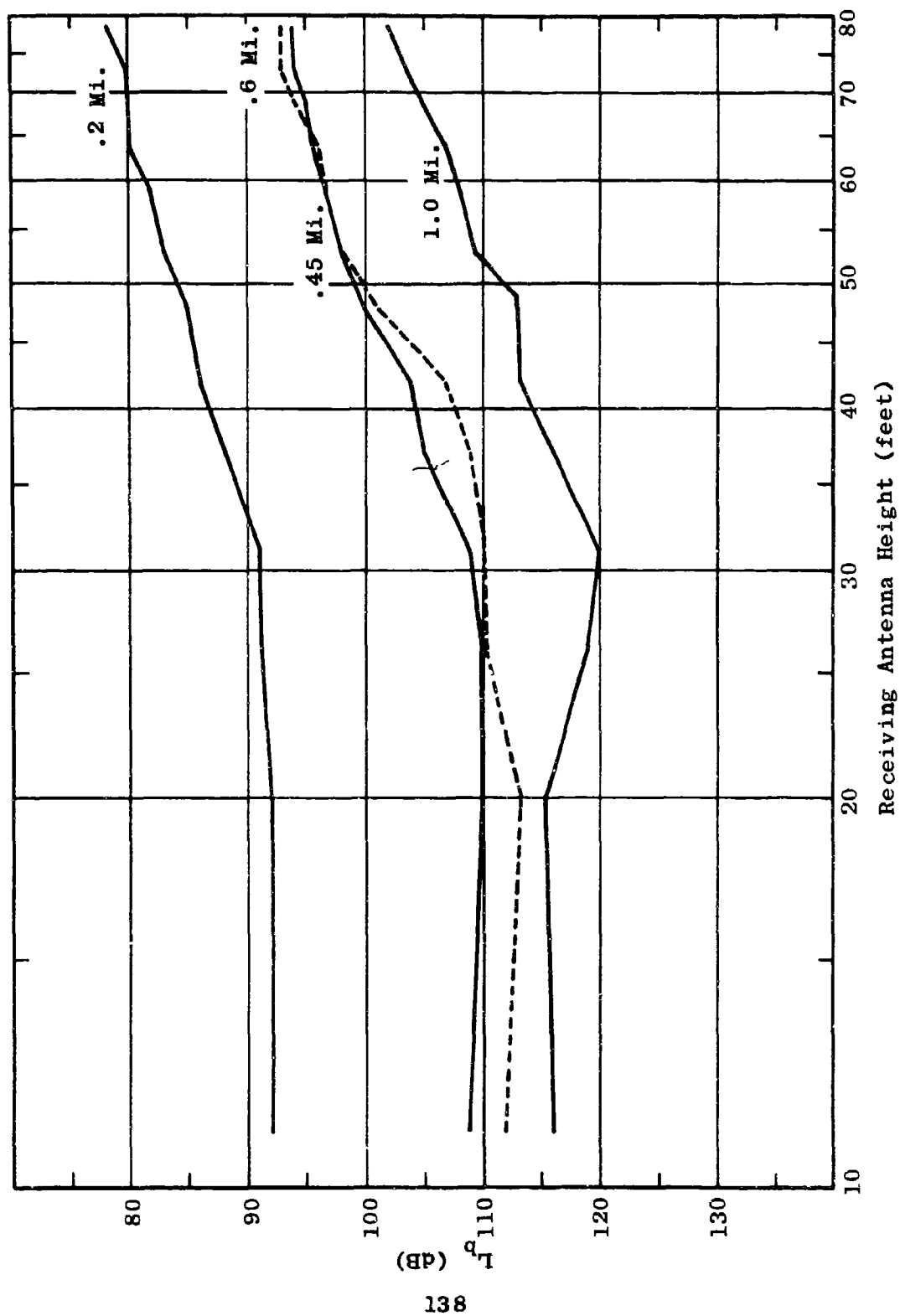


Figure 5.67 Height Gain Profile
 $L_p = F_{A,B}(100, 13, H, d, H_r)$

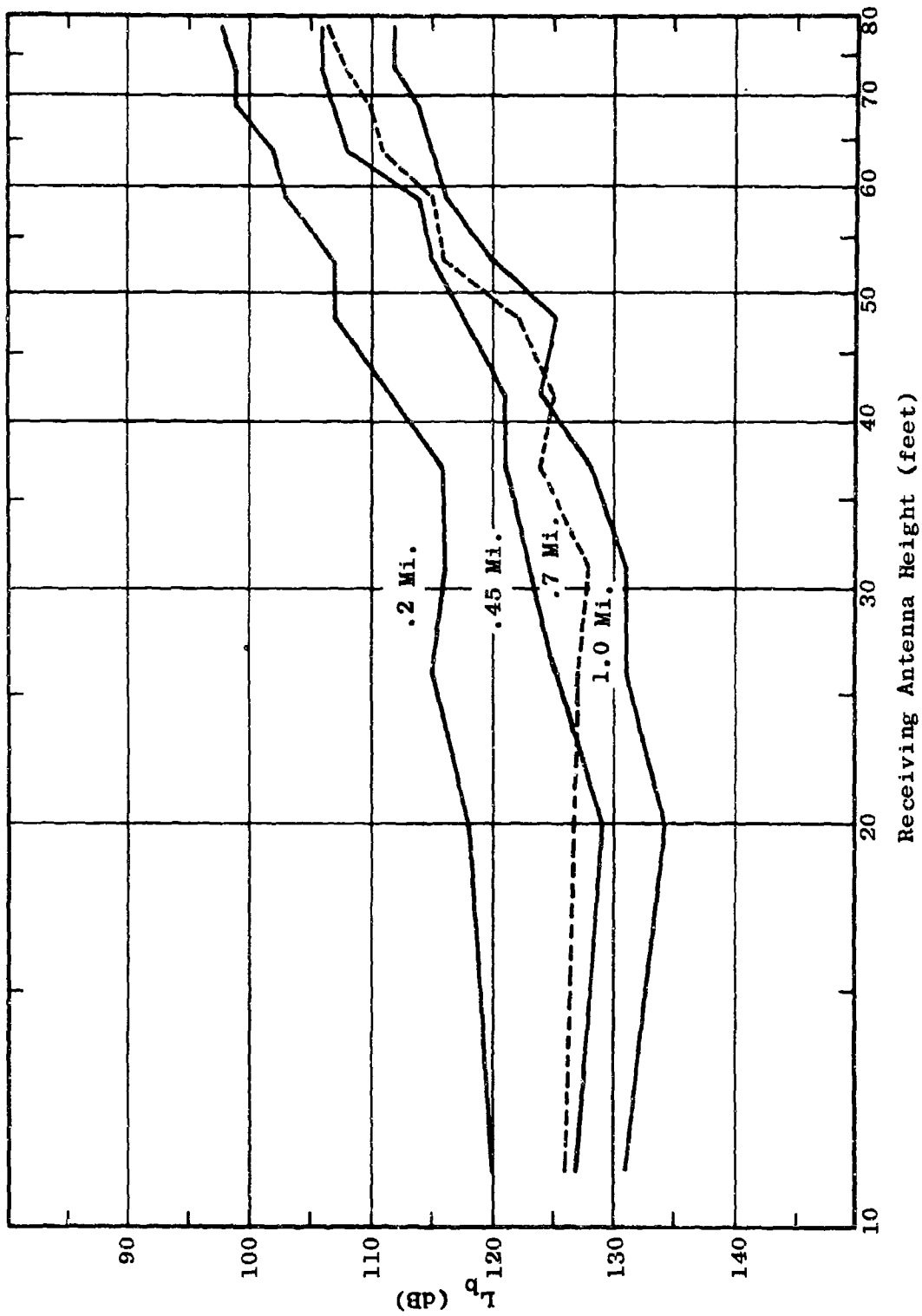


Figure 5.68 Height Gain Profile
 $L_p = F_{A,B}(250, 13, H, d, H_r)$

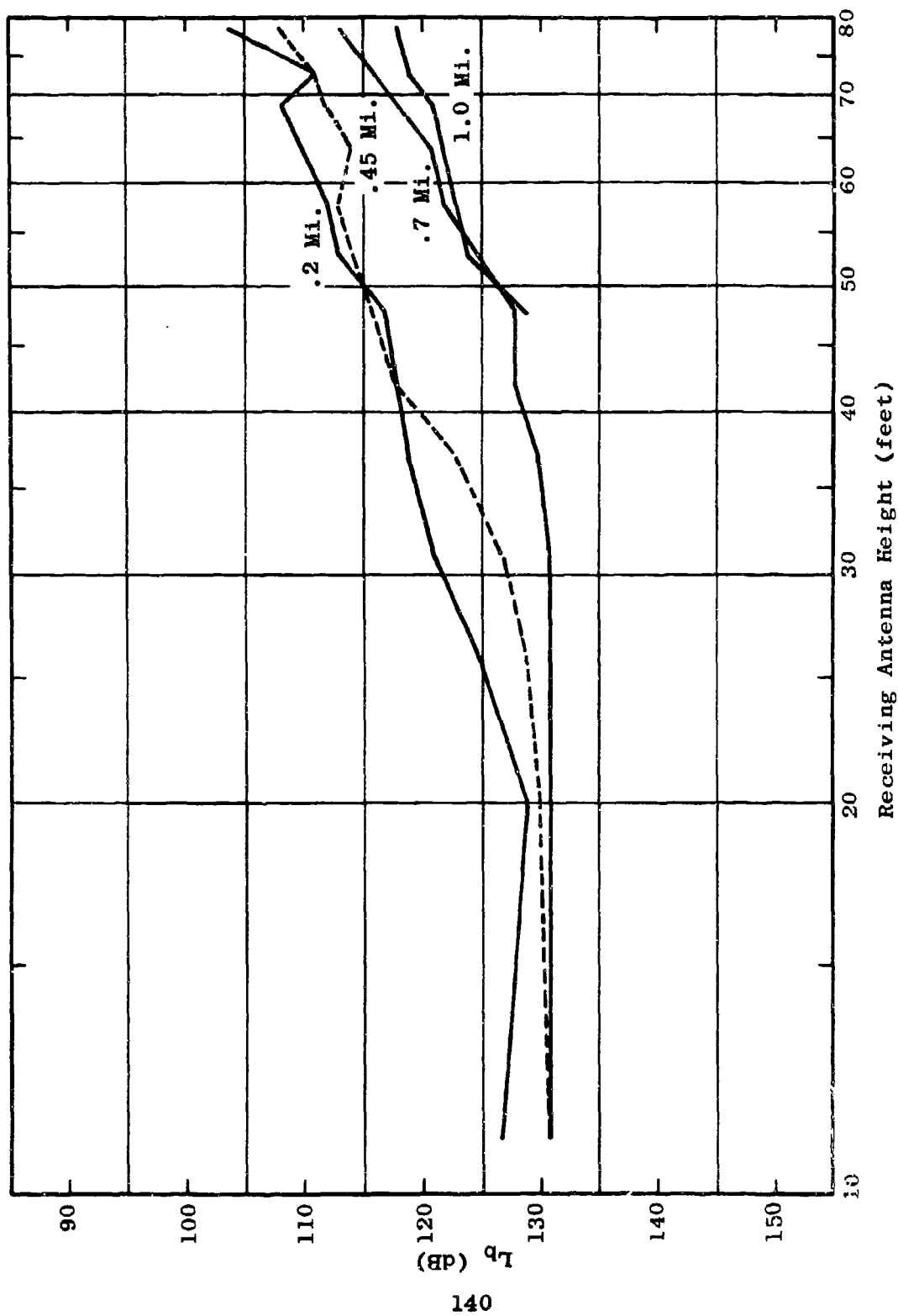


Figure 5.69 Height Gain Profile
 $L_b = F_{A,B}(400, 13, H, d, H_r)$

5.2.3 Propagation Path Loss as a Function of Terrain Height

The measured fixed point path loss data taken in Sector B within one mile of the transmitting antenna shows a marked tendency to flatten out for distances in the range 0.5-1.0 mile. That is, the measured path loss in many cases does not increase with increasing distance, and in some cases even decreases. To uncover the cause of this anomaly, the terrain profiles of both sectors were accurately measured with a precision altimeter. The profiles were determined from the transmitting antenna out to the field point at one mile. Figures 5.87 and 5.88 show the terrain profiles out to one mile for Sectors A and B. For Sector A, the terrain falls off gradually by 80 feet out to one mile. For Sector B, however, the terrain is flat for the first 0.2 mile, then falls off 40 feet in the next 0.2 mile and then continues to rise out to one mile. The elevation at one mile is approximately 50 feet above the elevation of the transmitting antenna site.

Figure 5.70 illustrates the advantage provided by the elevated terrain in Sector B. The vertical solid bars on this figure represent the total range of the measured fixed point data in Sector B. The dashed bars represent the range of measured data from Sector A. Figure 5.70 is derived from data for horizontal polarization, antenna heights of 80 feet and a frequency of 250 Mc/s.

Figure 5.70 also shows that path loss tends to be approximately the same for Sectors A and B for distance separations of 0.2 and 0.45 miles. The variation in data also tends to be wide for these distances. However,

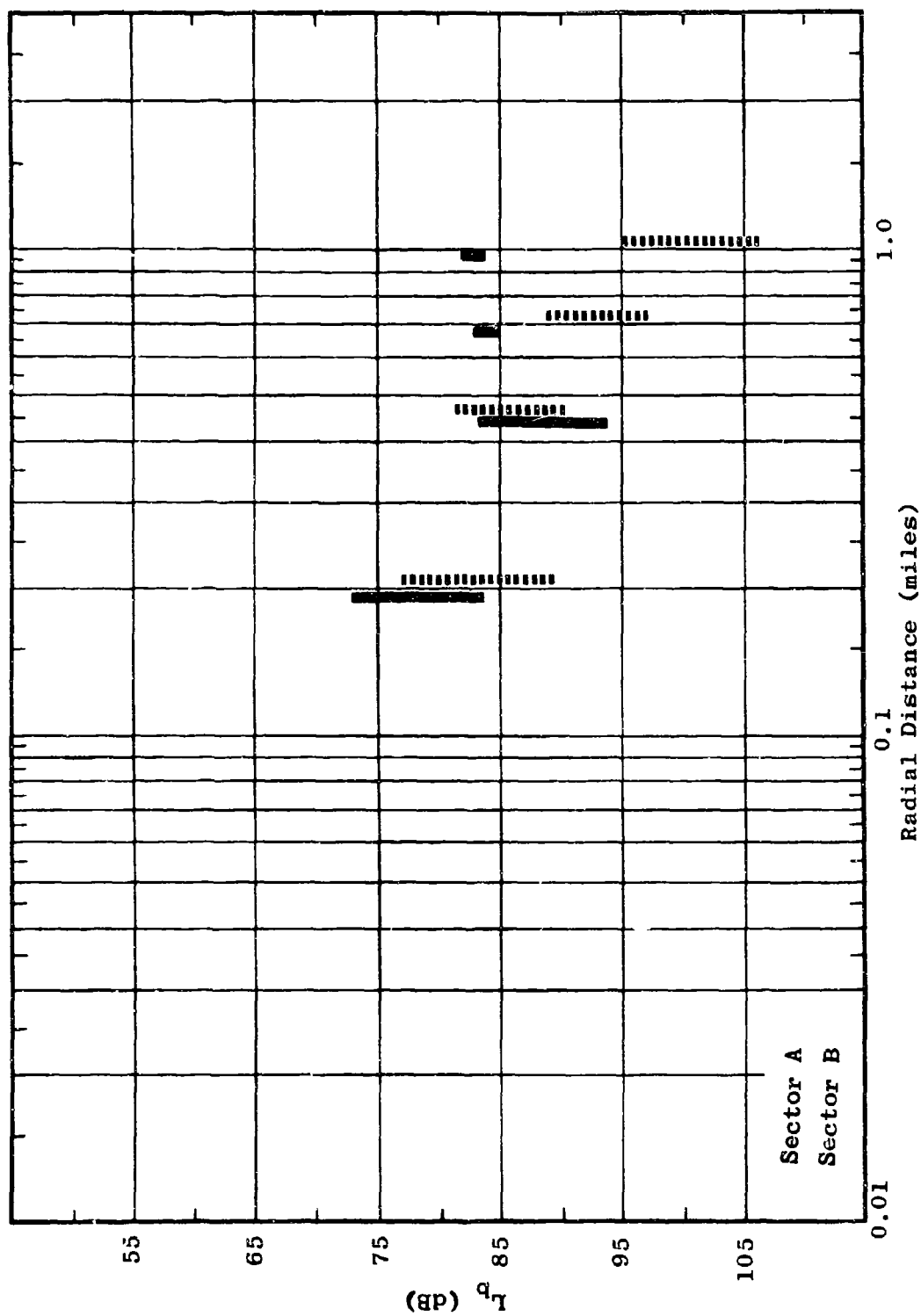


Figure 5.70 Measured Fixed Point Path Loss Data
 $L_b = F_{A,B}(250, 80, H, d, 80)$

at 0.7 and 1.0 mile, the path loss variability and over-all magnitude decrease significantly for Sector B, demonstrating the advantages of slightly elevated terrain.

Figure 5.71 shows a similar example for 50 Mc/s, a significantly longer wave length at which the effect is similar but much less pronounced.

Figure 5.72 illustrates the vertical distribution of foliage in the Pak Chong area. The Sector B terrain profile and a distribution of vertical lines are plotted in the figure. The vertical lines represent trees and have a height distribution representing the distribution of tree heights found in the Pak Chong area. The shortest vertical lines represent the median tree height. The longer lines represent the 70 percent, 90 percent, and 99 percent tree heights, respectively. The longest vertical line reflects those trees above the 99 percent height. The Pak Chong distribution of tree heights was originally presented in Semiannual Report Number 6. Also plotted in Figure 5.72 are four dashed lines which represent line-of-sight paths from a transmitting antenna at 80 foot elevation, to a receiving antenna at the same height. Each dashed line terminates at one of the four field points located at 0.2, 0.45, 0.7 and 1.0 mile from the transmitter.

As shown in Figure 5.72, the density of foliage in the line-of-sight paths to the field points is about the same for the two points at 0.2 and 0.45 mile. However, the line-of-sight foliage density then decreases for the 0.7 mile field point and decreases even more for the field point at 1.0 mile.

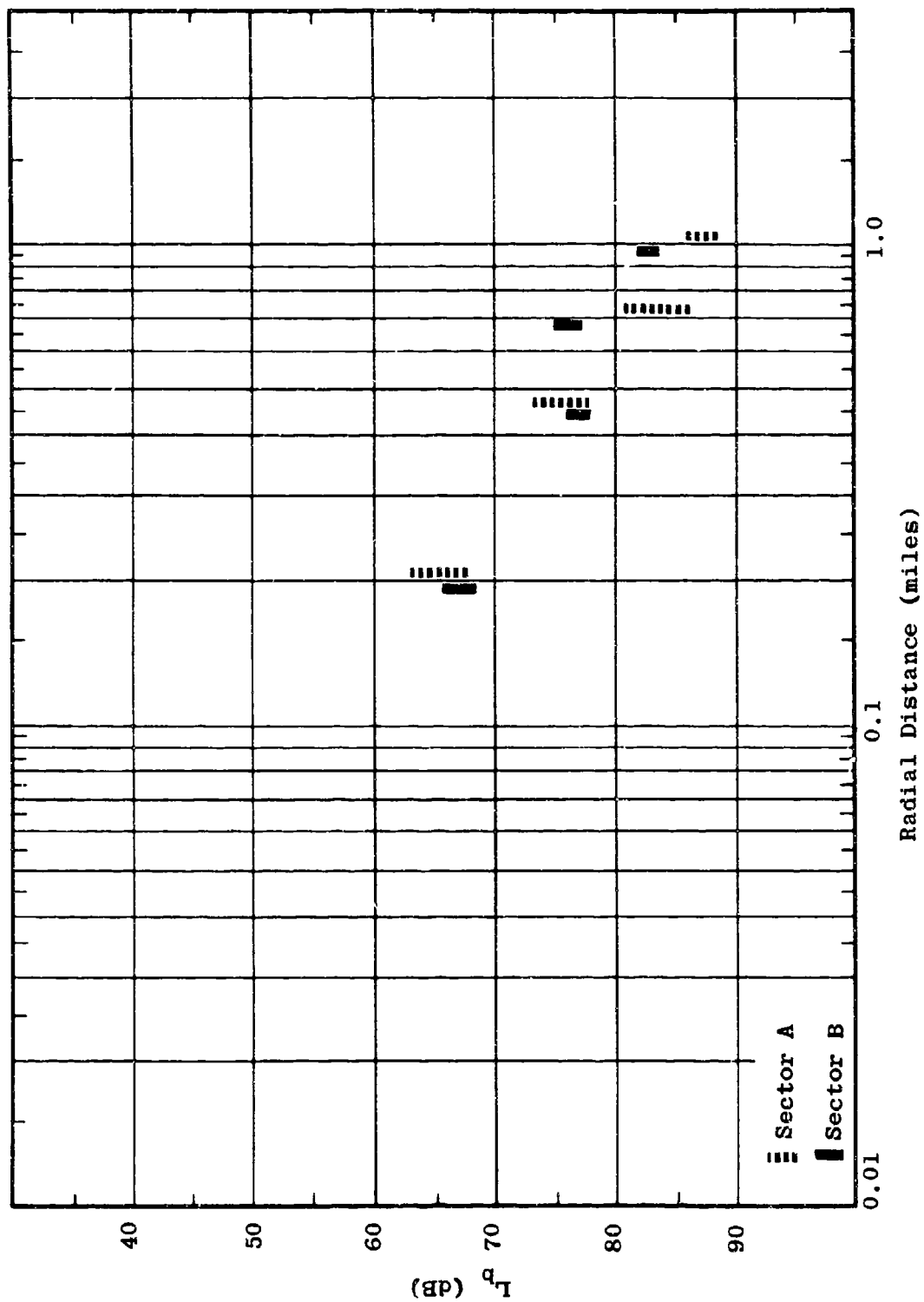


Figure 5.71 Measured Fixed Point Path Loss Data
 $L_b = F_{A,B}(50, 80, H, d, 80)$

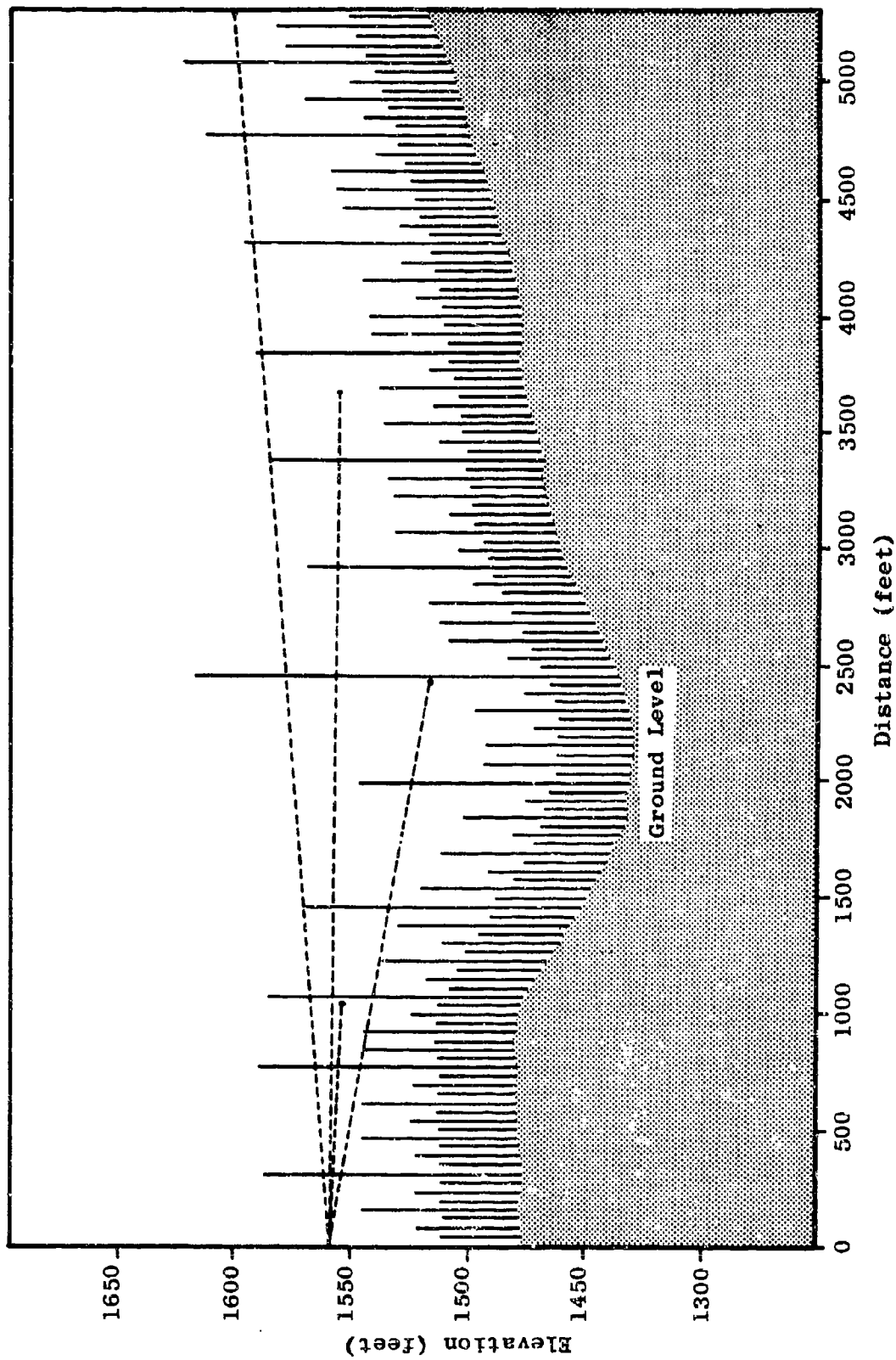


Figure 5.72 Sector B Terrain Profile Showing
Pak Chong Distribution of Tree Heights

5.2.4 Height Variation

A knowledge of the fine-grain changes in propagation loss with small changes in antenna height, distance and time is essential to an understanding of the propagation mechanism for tactical communications.

The continuous recordings of field strength vs height are normally analyzed by dividing the 11 to 80 foot height range of the antennas into 5-foot long increments. Then the median field strength is determined within each of these 5-foot height increments. A maximum variation of about 6 dB from this median has been noted within any height interval. A variation of 2 dB or less from the median within an interval is typical. The fine-grain variability of received field with height tends to be greatest for low antenna heights, i.e., when the antennas are deeply immersed in the foliage. In addition, the variability tends to be higher at higher frequencies. The time variability of recorded field strength over periods of approximately a minute has been very small, usually on the order of a fraction of a decibel. This indicates that the fine-grain variation in any particular height-gain profile is a function of position and not of time.

In addition to the vertical field strength profiles, a series of "boom measurements" was conducted to characterize the field variability when slight changes in receiving antenna positions are made. The boom measurements were carried out in the following manner. A receiving tower, which could be adjusted in height, was electrically turned by an antenna rotor. An 8-foot counterweighted

boom was placed at the top of the tower so that when an antenna was mounted at one end of the boom it described a circle with a radius of 4 feet as the tower rotated. A minimum of metallic parts was used to assure, insofar as possible, an unaffected receiving pattern.

An electrical antenna drive provided uniform tower rotation which in turn allowed good angular resolution on the strip chart recordings. Figures 5.73 and 5.74 provide examples of the actual strip chart recordings which were taken during the boom measurement series. Vertical polarized dipoles were used to provide azimuthally omnidirectional antenna patterns. Thus the observed variation is associated with small changes in path length or antenna position with respect to nearby foliage, rather than the azimuthal pattern of the antenna. On the right of Figure 5.73 is a calibration, in the center, a time recording, and on the left, a recording of field strength as the antenna boom is rotated. Figure 5.73 was taken at 25 Mc/s and demonstrates that there is no variation at this frequency as the antenna follows a circle with a 4-foot radius.

Figure 5.74 shows a calibration in the center which applies to the rotational recording on the left. The recording at the right of Figure 5.74 is a duplicate of the recording on the left with rotation in the opposite direction and a different scale factor.

The strip recordings provide the data from which a series of polar plots such as those shown in Figures 5.75 through 5.79 is graphed. These figures show the variation in received field strength, labeled "FS" on the figures,

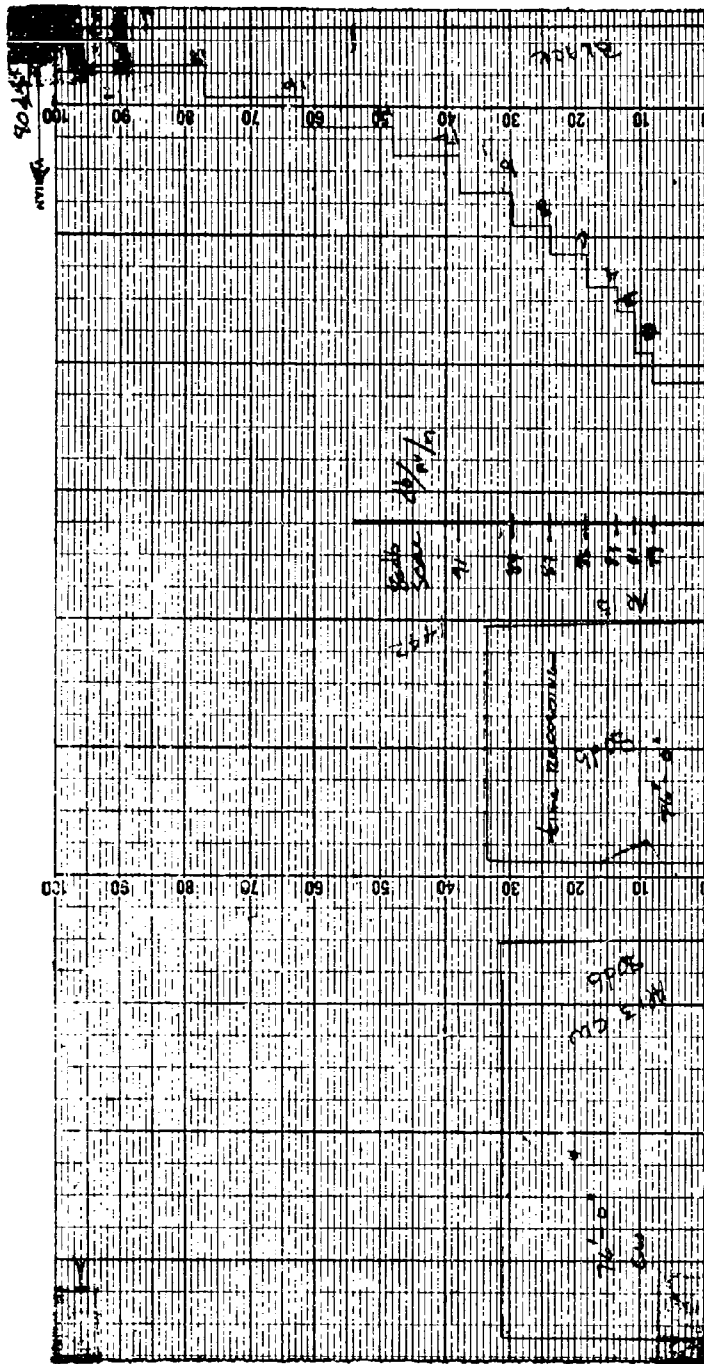


Figure 5.73 Sample Data Recording
 $L_b = F_A(25, 40, V, .2, 76)$

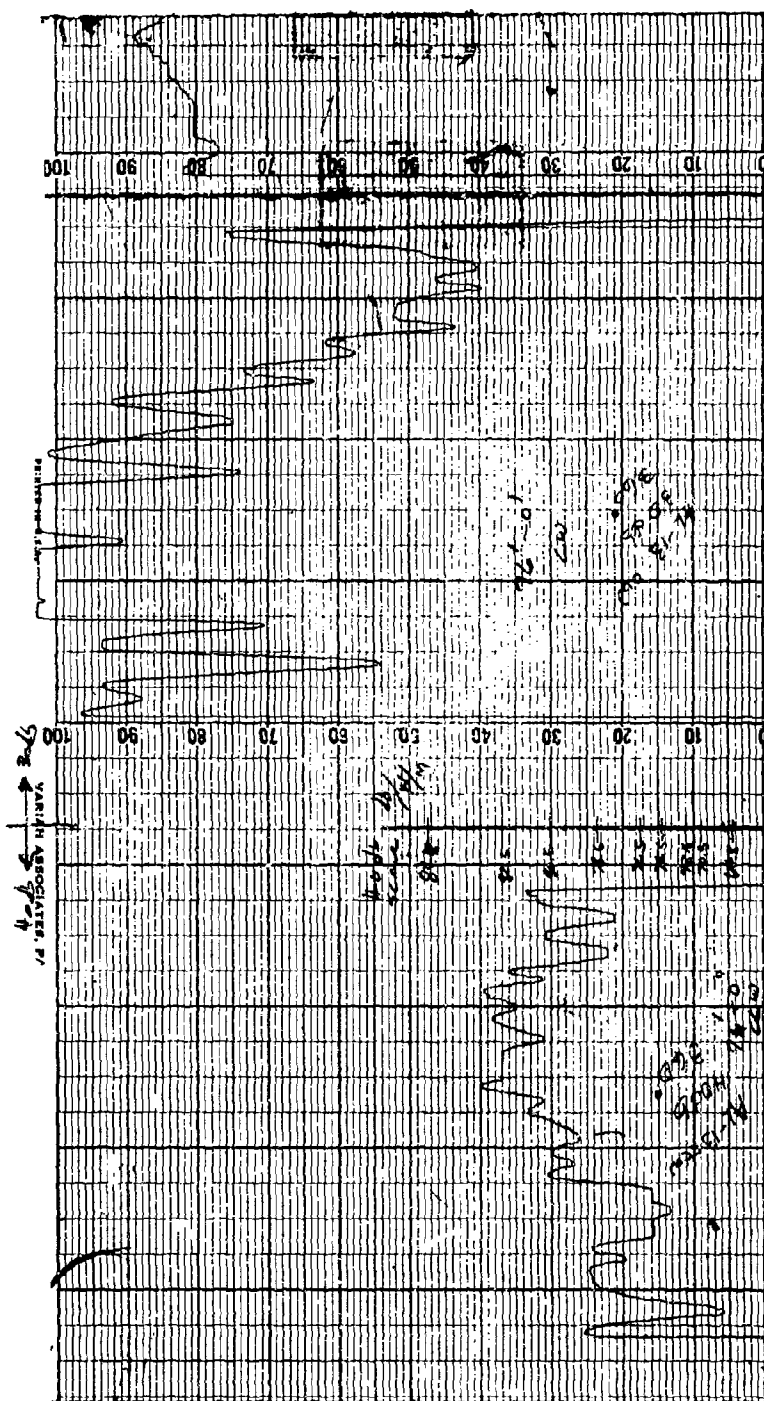


Figure 5.74 Sample Data Recording
 $L_b - F_A(400, 40, V, .2, 76)$

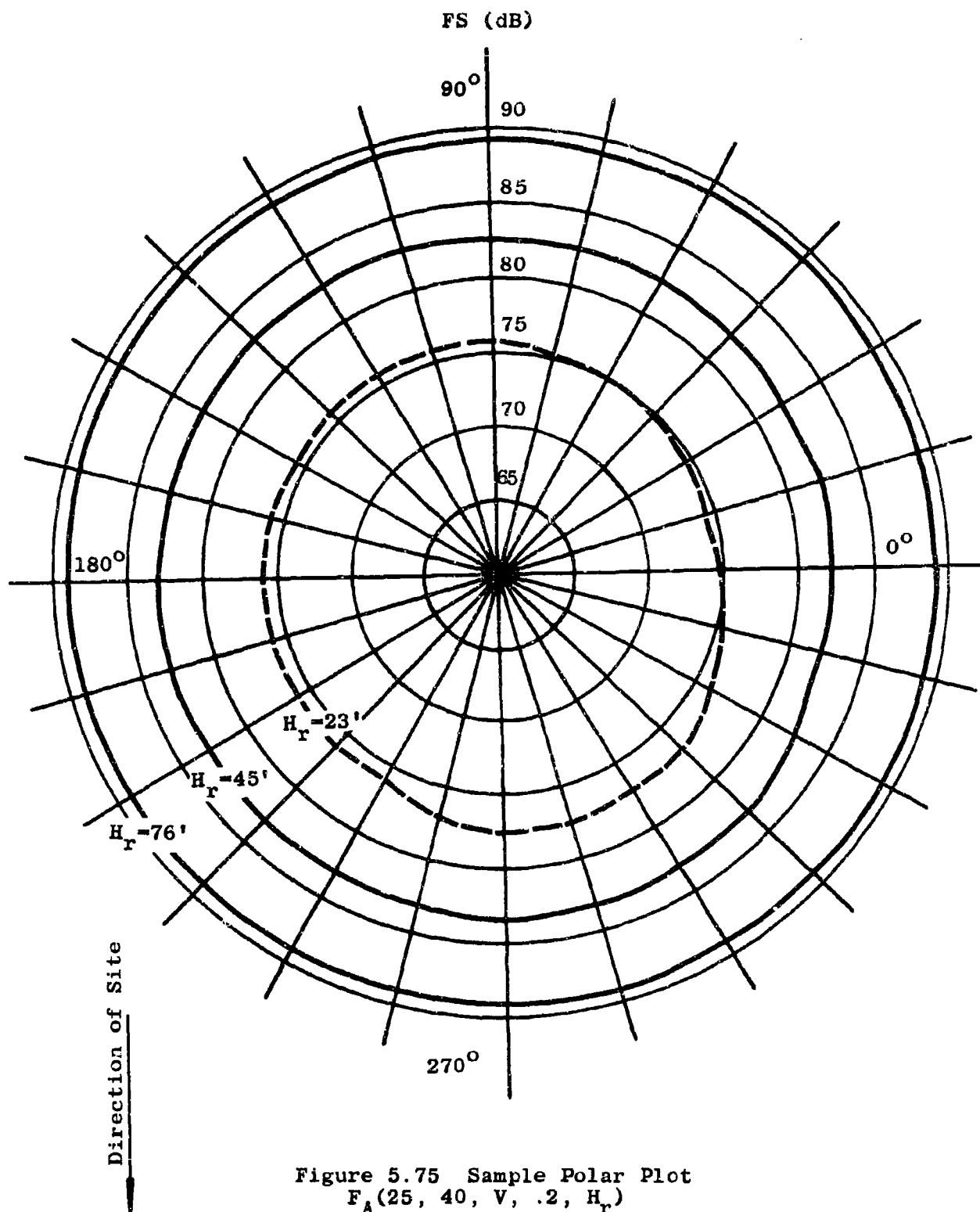


Figure 5.75 Sample Polar Plot
 $F_A(25, 40, V, .2, H_r)$

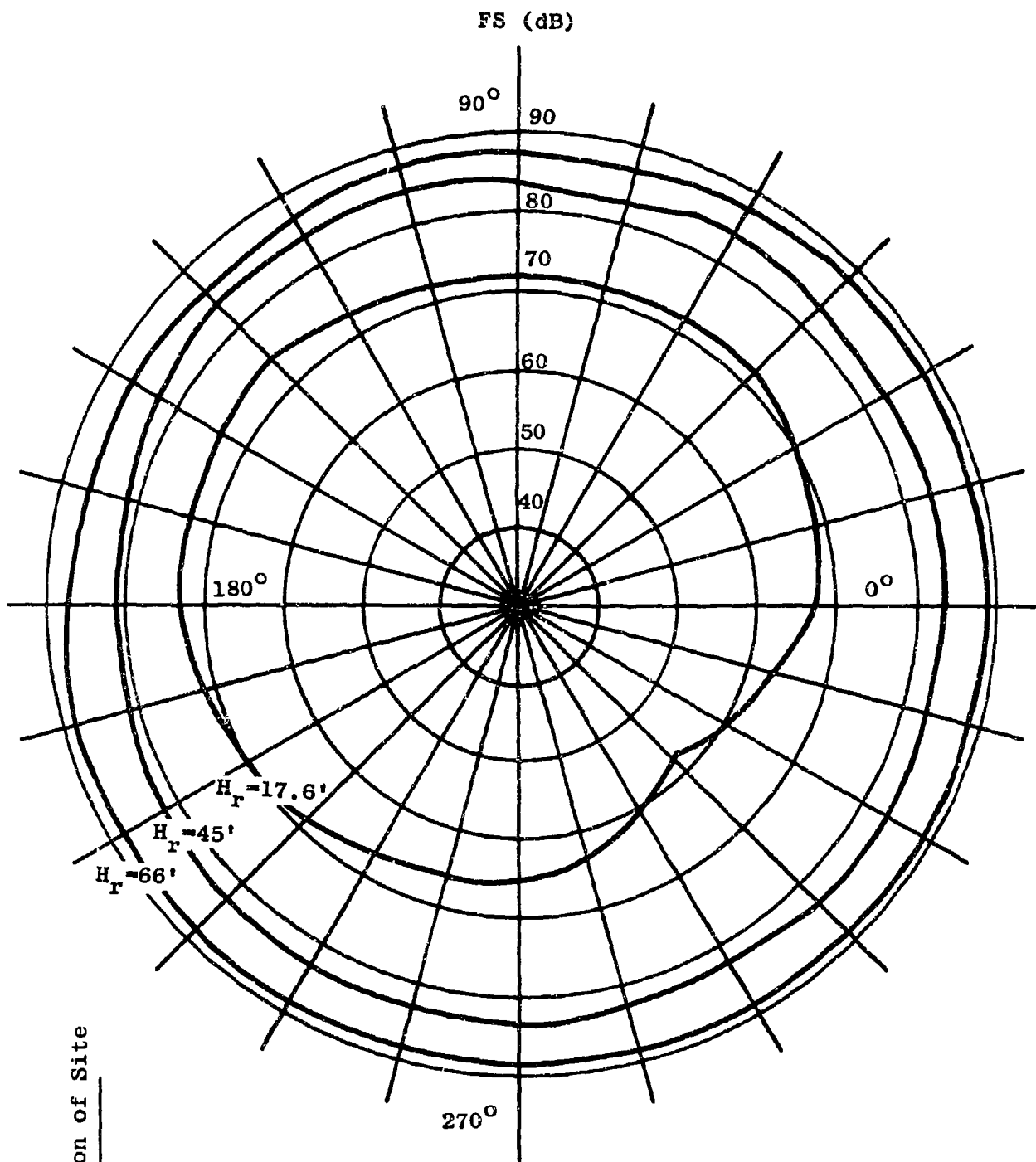


Figure 5.76 Sample Polar Plot
 $F_A(50, 40, V, .2, H_r)$

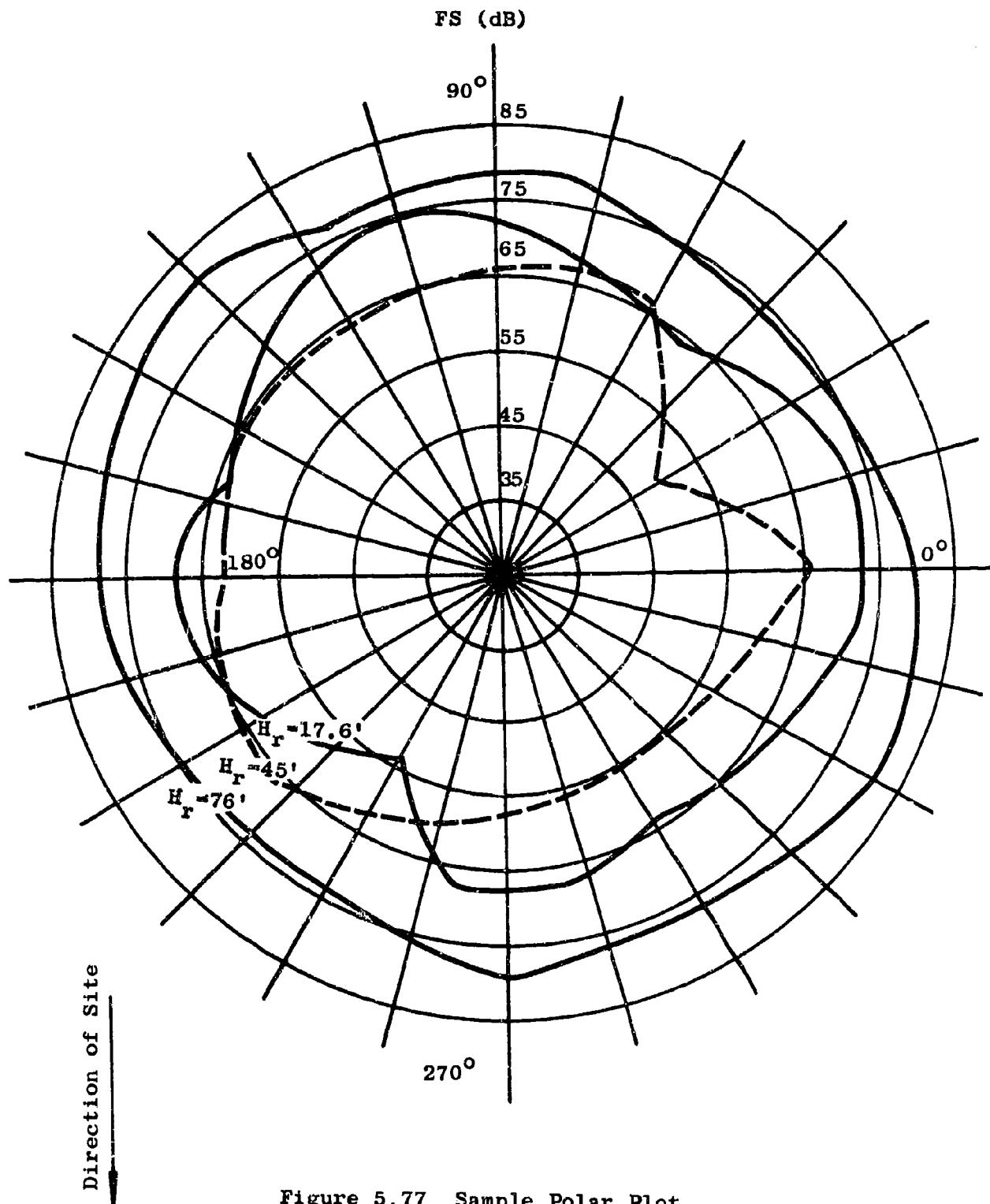


Figure 5.77 Sample Polar Plot
 $F_A(100, 40, V, .2, H_r)$

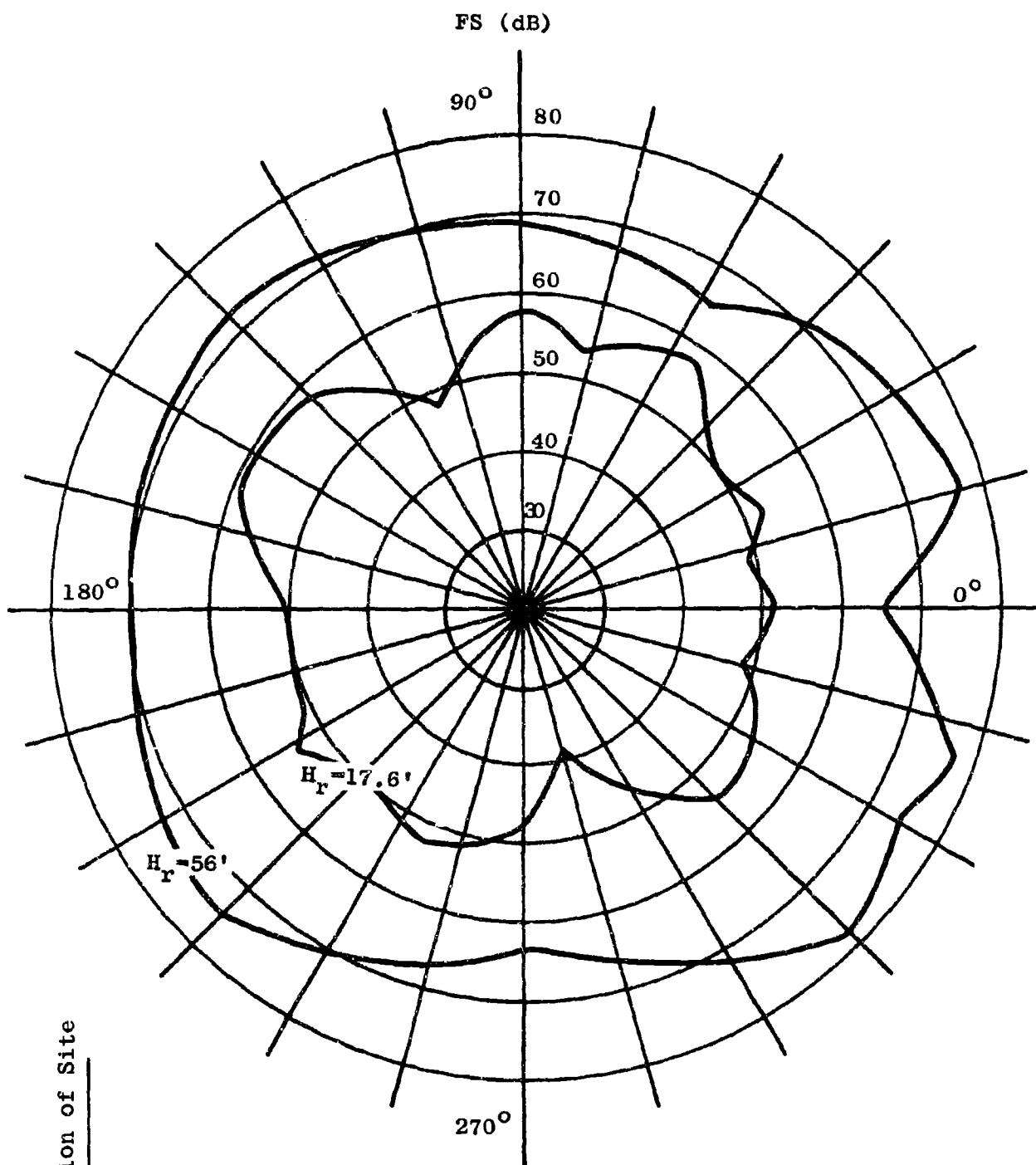


Figure 5.78 Sample Polar Plot
 $F_A(250, 40, V, .2, H_r)$

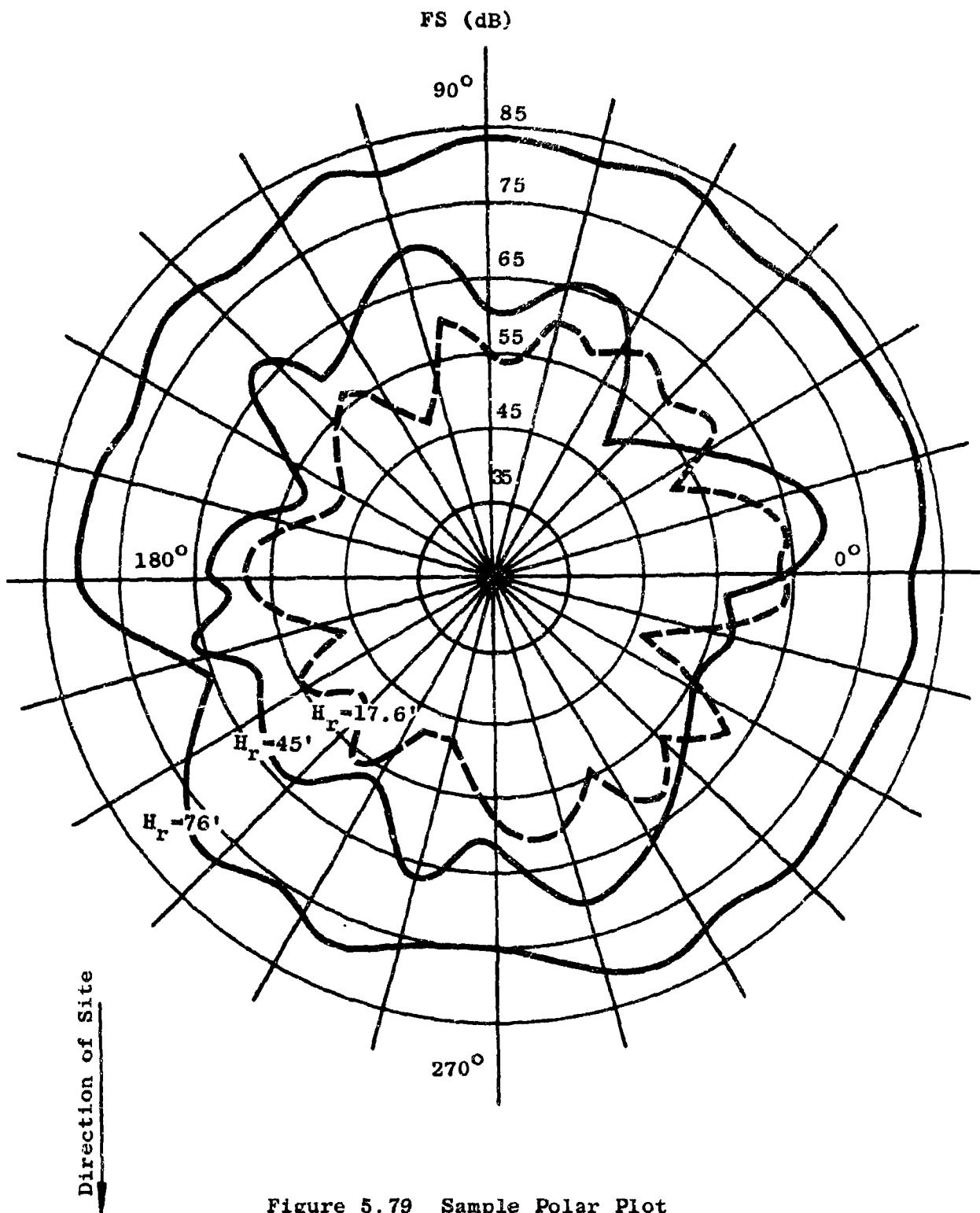


Figure 5.79 Sample Polar Plot
 $F_A(400, 40, V, .2, H_r)$

as the receiving antenna changes position. Each figure applies to one frequency and has plots for three antenna heights.

It can be seen from these polar plots that the received field variations increase with frequency. Also, as each of the individual plots on the same sheet is examined, it can be seen that when the antenna height is lowered, the signal strength becomes lower but subject to greater variations.

A tabulation of the data taken at FPA-1, a 1.0 mile distance, using vertically polarized antennas is presented in Table 5.7. From the data in this table, it becomes readily apparent that signal variations increase significantly with increasing frequency, and, to a somewhat lesser extent, with decreasing antenna height. Changes in receiving antenna height seem to have a slightly greater effect on signal variation at the receiver than a corresponding change in transmitting antenna height. Table 5.8 shows data leading to similar conclusions at FPA-4, a distance of 0.2 mile.

5.3 Propagation Path Loss as a Function of Frequency

A summary of the dependence of propagation path loss upon frequency is displayed graphically in Figures 5.80 and 5.81. Three curves are plotted in each figure, the first representing a transmitting and receiving antenna height of 80 feet, which is essentially out of the foliage, the second representing a height of 40 feet, which is

Table 5.7

TABULATION OF FIELD STRENGTH VARIATIONS
 $F_A(f, H_t, V, 1.0, H_r)$

Freq. (Mc/s)	H_r (ft)	$H_t = 80 \text{ ft.}$			$H_t = 40 \text{ ft.}$			$H_t = 13 \text{ ft.}$		
		Variation (dB)	Diff. (dB)		Variation (dB)	Diff. (dB)		Variation (dB)	Diff. (dB)	
25	80	-	-		-	-		-	-	
	40	62-64	2		56-58	2		44-48	4	
	23	55-58	3		50-54	4		39-43	4	
50	80	-	-		-	-		-	-	
	40	64-66	2		42-56	14		40-47	7	
	17	54-58	4		36-50	14		24-38	14	
100	80	-	-		58-70	12		-	-	
	40	50-67	17		27-49	22		46-56	10	
	17	40-58	18		26-39	13		30-48	18	
250	80	-	-		-	-		-	-	
	40	46-64	18		44-58	14		-	-	
	17	40-60	20		40-50	10		-	-	
400	80	-	-		-	-		-	-	
	40	50-66	16		44-53	9		-	-	
	17	45-58	13		43-46	3		-	-	

Table 5.8

TABULATION OF FIELD STRENGTH VARIATIONS
 $F_A(f, H_t, V, 0.2, H_r)$

Freq. (Mc/s)	H_r (ft)	$H_t = 80 \text{ ft}$			$H_t = 40 \text{ ft}$			$H_t = 13 \text{ ft}$		
		Variation (dB)	Diff. (dB)		Variation (dB)	Diff. (dB)		Variation (dB)	Diff. (dB)	
25	80	88-91	2		89-89	0		77-78	1	
	40	83-86	3		82-84	2		70-72	2	
	23	77-81	4		74-78	4		61-65	4	
50	80	94-97	3		86-89	3		78-82	4	
	40	89-91	2		82-84	2		68-73	5	
	23	66-81	15		66-77	11		52-64	12	
100	80	90-95	5		73-82	9		66-81	15	
	40	75-89	14		60-75	15		54-72	18	
	17	49-72	23		48-67	19		37-63	26	
250	80	89-95	6		69-80	11		60-73	13	
	40	66-83	17		55-75	20		40-64	24	
	17	60-75	15		41-62	21		36-54	18	
400	80	87-91	4		66-83	17		60-75	15	
	40	64-80	16		53-71	18		43-61	18	
	17	50-71	21		45-64	19		41-53	12	

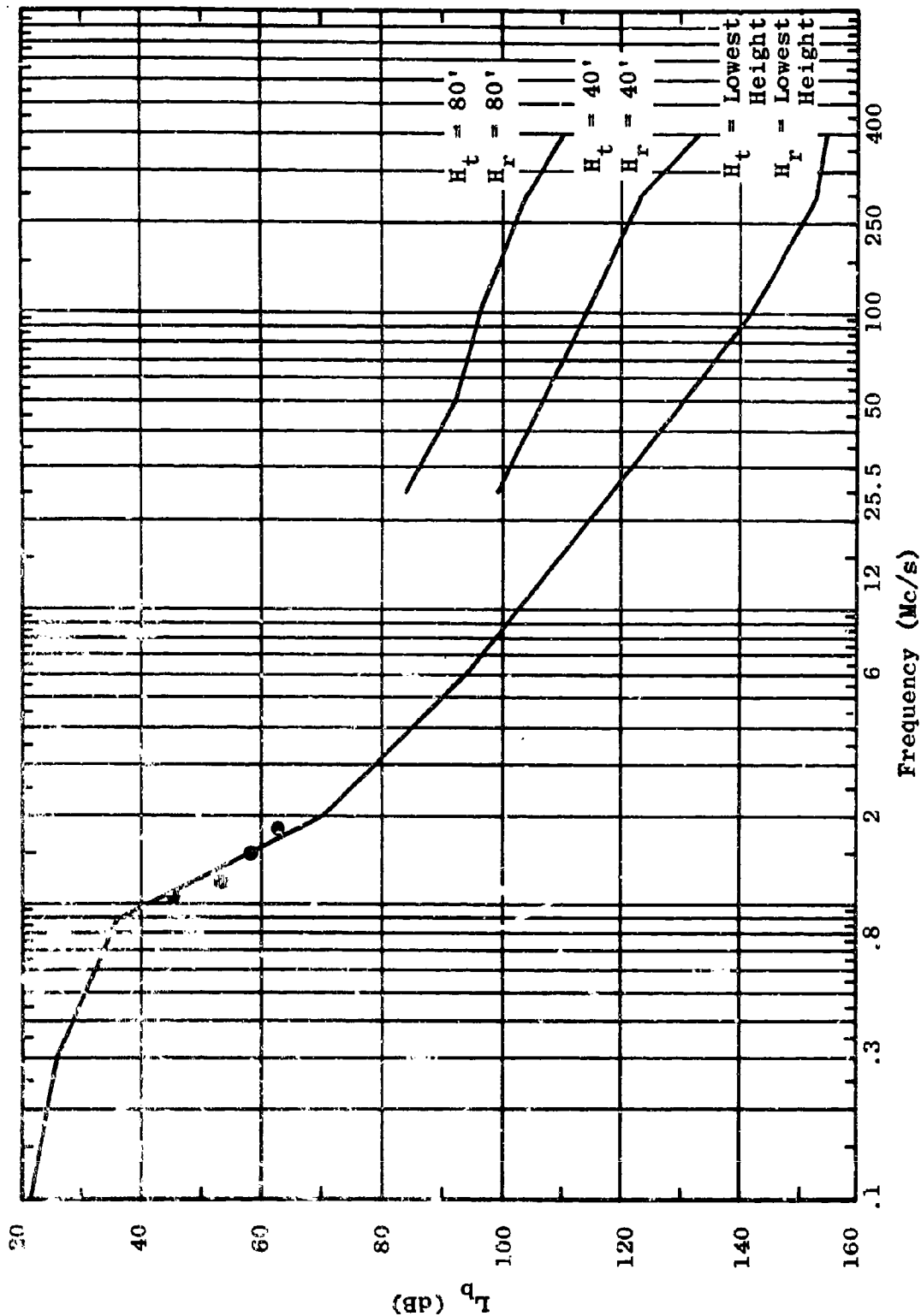


Figure 5.80 Summary of Path Loss vs. Frequency
 $L_b = F_{A,B}(f, H_t, V, 1.0, H_r)$

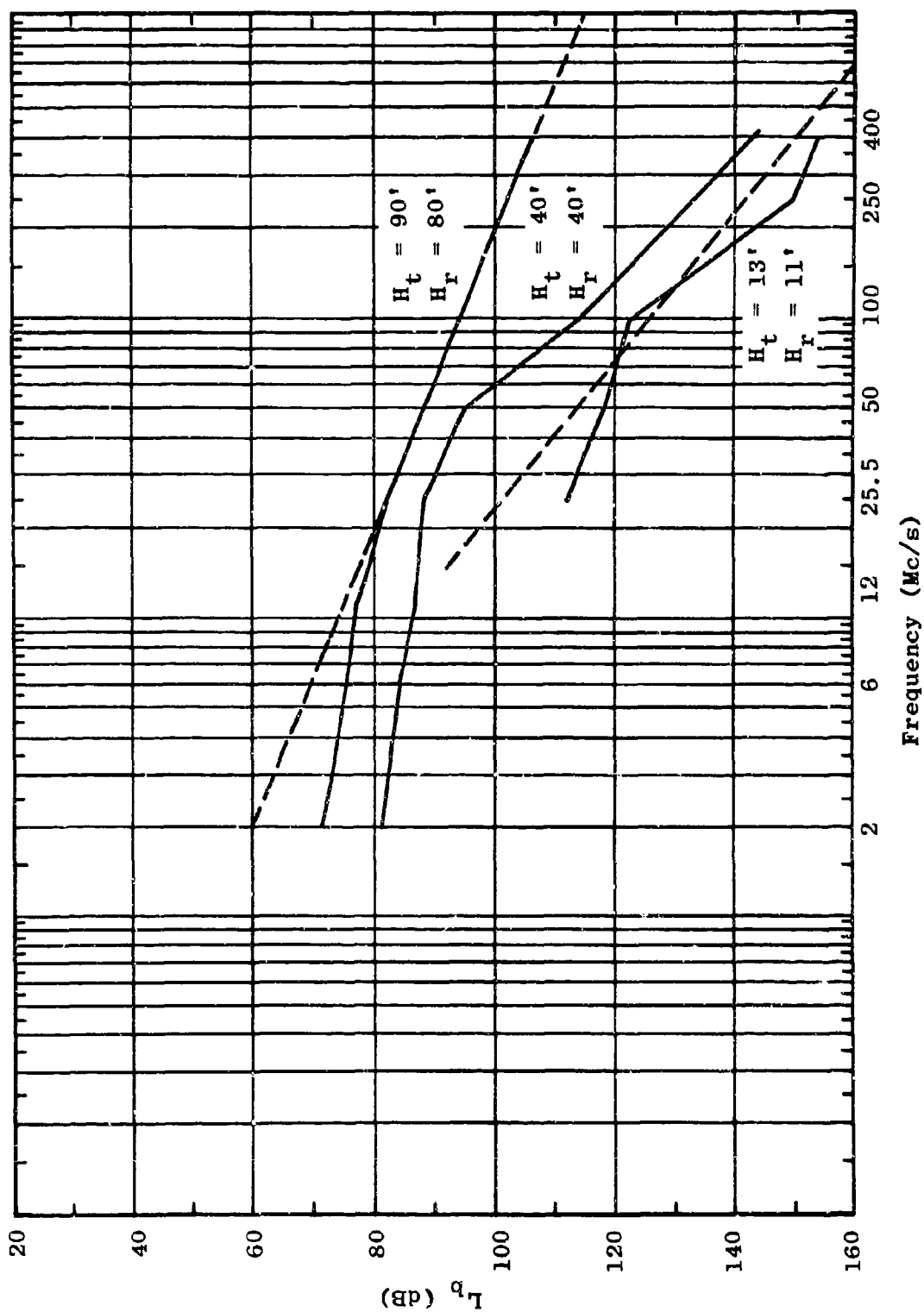


Figure 5.81 Summary of Path Loss vs. Frequency
 $L_p = F_{A,B}(f, H_t, H, 1.0, H_r)$

slightly above the median treetop height, and the third representing low antenna heights, for which both antennas are well immersed in the foliage. For vertical polarization, Figure 5.80, ground-based antennas were used in the frequency range 0.100-12 Mc/s as well as at 25 Mc/s for the lowest transmitting antenna height. For this reason, the curves for antennas elevated to 40 and 80 feet do not extend over the frequency range 0.100-12 Mc/s. In the case of horizontal polarization $\lambda/2$ dipole antennas were used at all of the horizontal polarization test frequencies. However, the lowest transmitting antenna height used at 2, 6 and 12 Mc/s was 40 feet.

The curves shown on the figures were derived from smooth estimates of propagation path loss versus distance. All of the curves in both Figures 5.80 and 5.81 are plotted for a separation distance of one mile.

For vertical polarization, Figure 5.80, path loss appears to depend logarithmically upon frequency for frequencies above 0.880 Mc/s. The logarithmic dependence, however, varies from twenty times the logarithm of frequency, in Mc/s, for antennas elevated to 80 feet, to 40 times the logarithm of frequency for low antenna heights.

As Figure 5.80 indicates, measurements have been made at a distance of 1 mile for vertical polarizations at frequencies of 1.0, 1.3, 1.5 and 1.7 Mc/s in addition to the regular measurements at .100, .300, .880, 2, 6, 12, 25, 50, 100, 250 and 400 Mc/s. Preliminary analyses reported in Semiannual Report Number 7 indicated a sharp discontinuity

in results between .880 and 2 Mc/s. The transmitting antenna used at .880 Mc/s was a ground-based vertical radiator with capacitive top loading and a wire radial ground system located several hundred feet from the foliage. The transmitting antenna used at 2 Mc/s was a ground-based vertical whip tuned with a BC 939B tuning unit. The fact that both the type of transmitting antenna and its position with respect to foliage changed at a point of apparent discontinuity led to the hypothesis that there was either a significant and unaccounted for difference between the two antennas or, more likely, that there was a significant antenna-to-foliage coupling effect. The whip antenna tuned with a BC 939B tuning unit was used at .880 Mc/s to explore the possibility of unaccounted for differences between the top loaded antenna normally used at .880 Mc/s and below, and the whip antenna normally used at 2 Mc/s and above. Path loss results based on measurements one mile from the base camp at .880 Mc/s were identical for the two antennas. This result provides strong evidence that there is no unaccounted-for difference between the transmitting antenna used at .880 Mc/s and the transmitting antenna used at 2 Mc/s.

In another series of special tests, measurements were made at 1 mile, using the HF vertical antenna located alternately at the HF pad within the foliage and then at the LF pad several hundred feet from the foliage. The results are shown in Table 5.9 for receiving loop antenna heights of 17 feet and 80 feet.

Table 5.9

 L_b AT ONE MILE, VERTICAL POLARIZATION

Fre- quency (Mc/s)	Receiving Antenna Height (feet)	Antenna at LF Pad Outside Foliage (L_b in dB)	Antenna at HF Pad Inside Foliage (L_b in dB)	Difference (dB)
2	17	67	68	1
2	80	68	70	2
6	17	86	92	6
6	80	82	89	7
12	17	99	106	7
12	80	88	94	6

These results plus the supplemental points measured between .880 and 2 Mc/s indicate that the steep increase in path loss in this region is not due to differences in the transmitting antenna's proximity to foliage.

Table 5.9 indicates that there is about 2 dB more loss for the antenna closer to the foliage at 2 Mc/s and about 6 dB more loss for the antenna closer to the foliage at 6 and 12 Mc/s.

The data shown in Figure 5.80 at .880 Mc/s represents a measuring point which is 4.7 wavelengths from the transmitter whereas at .300 Mc/s the separation drops to

1.6 wavelengths. This indicates that the break in the curve at the low frequency end could be influenced by the induction field of the transmitting antenna.

The dependence of path loss upon frequency for horizontal polarization, Figure 5.81, is somewhat different from the dependence observed for vertical polarization. For horizontal polarization and frequencies below 25 Mc/s, path loss varies as eight times the logarithm of frequency, the dependence appearing to be independent of antenna height. For frequencies above 25 Mc/s with horizontal polarization the dependence appears to range from 20 times the logarithm of frequency in Mc/s for antennas elevated above the foliage to something greater than 40 times the logarithm of frequency in Mc/s for low antenna heights.

5.4 Polarization

Based on the analysis of a large cross section of data gathered in the Pak Chong area, a reduction in loss can usually be realized by utilizing horizontal rather than vertical polarization. Under certain conditions the loss reduction may be as much as 20 dB, but for other conditions the advantage may be only slight or even in favor of vertical polarization. It was further found that the scattering effect of the jungle foliage gives rise to a significant depolarized component of the transmitted signal and also changes the antenna direction for maximum energy transfer from what it is under free-space conditions.

5.4.1 Polarization Comparison

This section contains the major findings of a polarization analysis and a discussion of the transmission setups that provide the maximum horizontal loss reduction.

The analysis consisted of a direct comparison of the basic transmission loss observed with vertically polarized antennas to the corresponding loss observed with horizontal antennas at the same terminal points. The data base consisted of standard fixed point field measurements taken in Sectors A and B in both the wet and dry seasons, and special "walking" measurements taken between 250 feet and 1000 feet from the transmitter. The standard field point measurements extended from about 0.05 to 10.5 miles and represented many tests made beyond the horizon or over terrain obstacles. The "walking" measurements were taken over areas which would have allowed line-of-sight transmission paths if there were no foliage.

The frequencies examined ranged from 2 to 400 Mc/s. In the 25-400 Mc/s range the transmitting antennas were half-wave dipoles, and the same antenna was used for both vertical and horizontal polarizations. In the 2 to 12 Mc/s range the transmitting antennas consisted of ground based monopoles for vertical polarization and half-wave dipoles for horizontal polarization.

The receiving antenna was a half-wave dipole for frequencies above 25 Mc/s and a loop for frequencies of 25 Mc/s and lower.

The receiving antenna heights ranged from about 13 to 80 feet in the fixed point measurements and from ground level to 6 feet in the "walking" measurements.

The analysis results are summarized in Tables 5.10, 5.11 and 5.12. The values listed in these tables are simply the number of dB by which vertical losses exceeded horizontal losses. Positive values indicate that horizontal polarization is favored while negative signs signify an advantage with vertical polarization.

Consider first Table 5.10. This table gives the fixed point data comparison for frequencies of 25 Mc/s and above. Scanning the table horizontally shows how the "difference-loss" varies with distance, and scanning in the vertical direction shows the "difference-loss" as a function of antenna height. In this case the receiving and transmitting antennas were always at the same height. Three heights are shown: (1) 13 feet, both antennas deeply immersed in foliage, (2) 40 feet, both antennas at average treetop elevation, and (3) 80 feet, both antennas elevated well above most of the surrounding trees.

The predominance of positive values in Table 5.10 reveals at a glance the desirability of horizontal polarization in nearly all of the cases covered.

At a given antenna height and frequency, the "difference-loss" does not appear to be functionally related to distance, but, by observing the "difference-loss" at a given distance as the antenna height is raised, a definite trend is noted. For frequencies up to about 250 Mc/s, horizontal

Table 5.10

POLARIZATION COMPARISON FOR FREQUENCIES ≥ 25 MC/s

Freq. (MC/s)	Ht & Ht (ft)	L _b (vertical)-L _b (horizontal) at Indicated Distance (dB)											Average for all Distances
		0.05 mi.	0.1 mi.	0.2 mi.	0.45 mi.	0.7 mi.	1.0 mi.	2.0 mi.	3.0 mi.	4.0 mi.	7.0 mi.	10.5 mi.	
25	13	4	18	14	12	15	18	17	19	10	-	-	14
	40	2	5	9	7	7	10	7	9	11	14	5	7
	80	-4	-2	4	8	4	3	0	4	5	9	9	3
50	13	19	5	16	13	7	12	19	21	-	-	-	14
	40	6	10	7	5	3	0	0	7	4	5	2	4
	80	0	7	-3	-1	-4	-4	0	7	1	1	2	0
100	13	17	12	16	9	18	11	12	4	-	-	-	12
	40	5	0	1	5	1	0	-2	-6	-1	-	-	0
	80	2	5	2	4	11	10	0	7	1	-3	-2	3
250	13	11	17	0	3	0	3	-	-	-	-	-	5
	40	6	-3	-6	-2	4	4	0	2	-	-	-	0
	80	0	2	2	1	-5	-10	4	2	-	-	-	-0
400	13	11	10	-3	2	0	4	-	-	-	-	-	4
	40	4	-5	-8	-1	-2	0	2	-	-	-	-	-1
	80	0	3	0	1	-2	-7	0	3	-	-	-	-0

Table 5.11

POLARIZATION COMPARISON FOR FREQUENCIES < 25 Mc/s

Freq. (Mc/s)	H _t (Horiz.)	H _t (Vert.)	(ft)	L _p (vertical) - L _p (horizontal) at Indicated Distance (dB)								Average for all Distances
				0.2 mi.	0.45 mi.	0.7 mi.	1.0 mi.	2.0 mi.	3.0 mi.	4.0 mi.		
2	40 ft. Dipole	80 ft. Monopole	40	-9	-15	-13	-9	-11	-8	-7	-10	
	80 ft. Dipole	80 ft. Monopole	80	0	-5	-4	-1	-3	-2	-6	-3	
6	40 ft. Dipole	40 ft. Monopole	40	6	8	8	10	11	10	0	7	
	40 ft. Dipole	20 ft. Monopole	40	15	18	17	16	15	19	17	16	
12	80 ft. Dipole	20 ft. Monopole	80	12	17	16	18	15	19	18	16	

Table 5.12

POLARIZATION COMPARISON FOR LOW RECEIVER HEIGHTS

Freq. (Mc/s)	H_t (ft)	H_r (ft)	L_b (vertical) - L_b (horizontal) at Indicated Distance (dB)				Average for all Distances
			250'	500'	750'	1000'	
50	13	Gnd.	3	2	1	3	2
		1	7	5	4	8	6
		2	12	7	7	9	9
		3	13	8	9	12	10
		4	13	6	11	12	11
		5	13	7	11	12	10
100	13	6	14	8	10	13	11
		Gnd.	1	4	0	1	2
		1	9	13	6	12	10
		2	12	14	8	14	12
		3	13	16	9	14	13
		4	-	-	-	-	-
250	13	5	21	19	13	20	18
		6	21	19	10	19	17
		Gnd.	-1	1	-1	-2	-1
		1	16	6	7	3	8
		2	13	10	5	5	8
		3	11	11	8	2	8
400	13	4	13	13	6	4	9
		5	15	13	3	3	9
		6	11	10	9	4	9
		Gnd.	8	1	0	-	3
		1	9	5	5	-	6
		2	10	6	8	-	8
168	13	3	7	0	12	-	6
		4	4	1	7	-	4
		5	-5	9	11	-	5
		6	-3	10	11	-	6

polarization is heavily favored at low antenna heights but, as the antennas are raised, the margin by which horizontal polarization is favored decreases and approaches zero at 80 feet.

The dB margin in favor of horizontal polarization is also observed to decrease with increasing frequency in Table 5.10. This can be more clearly seen in Figure 5.82. This graph was generated by averaging the loss-margin over all distances for each particular frequency and antenna height.

For frequencies of 2, 6 and 12 Mc/s, Table 5.11 gives the same type of information contained in Table 5.10. However, at the frequencies in this table, the transmitting antennas were not identical. For vertical polarization ground based whips were used. The loss measured with the vertical whip antennas is compared to the loss measured with horizontal half-wave dipoles, elevated to 40 or 80 feet.

Table 5.11 shows that at 6 and 12 Mc/s a substantial loss-margin in favor of horizontal polarization still exists. For these two cases the length of the whip is less than the average tree height. At 2 Mc/s, however, vertical polarization is favored. It should be noted here that the whip height is 80 feet at 2 Mc/s and so extends well above the average tree height. It is difficult to state whether a mode favoring vertical polarization is beginning to appear at 2 Mc/s or whether antenna height differences are responsible.

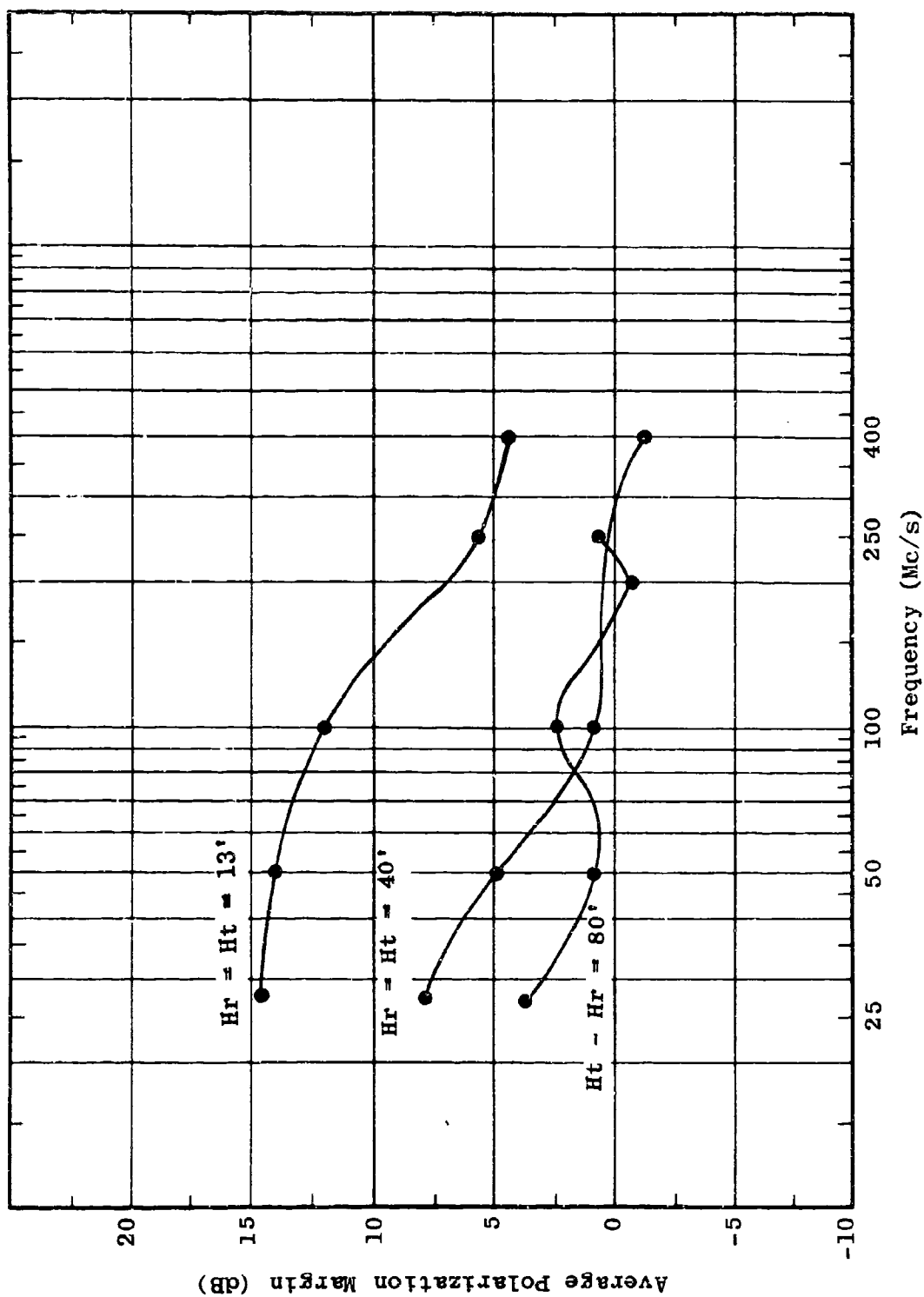


Figure 5.82 Polarization Margin Vs. Frequency

Table 5.12 is designed to show the polarization "difference-margin" for very low receiving heights and short range transmissions. The transmitting antennas were identical half-wave dipoles situated 13 feet above ground. The receiving antennas were also half-wave dipoles varying in height from ground level to about 6 feet. When oriented vertically, the receiver height above ground was measured to the tip of the element closest to ground.

Table 5.12 also displays significant differences in favor of horizontal polarization. However, the important observation to be made from this table is that the general tendency of the "difference-margin" is to decrease with a decrease in receiver height. The opposite trend was observed for the data presented in the previous tables for receiver heights greater than 13 feet.

Figures 5.83 and 5.84 illustrate this trend reversal as a function of receiving antenna height. The data above 13 feet in each case was taken at the same distance from the transmitter as the data taken in the 1 to 6-foot height range. These curves suggest that maximum polarization difference occurs for receiver heights around 10 to 20 feet and decreases if the antenna is moved either upward or downward.

5.4.2 Depolarization

For frequencies above about 25 Mc/s, the field measured in foliage varies significantly in amplitude over a small sector of a few wavelengths. The magnitude of

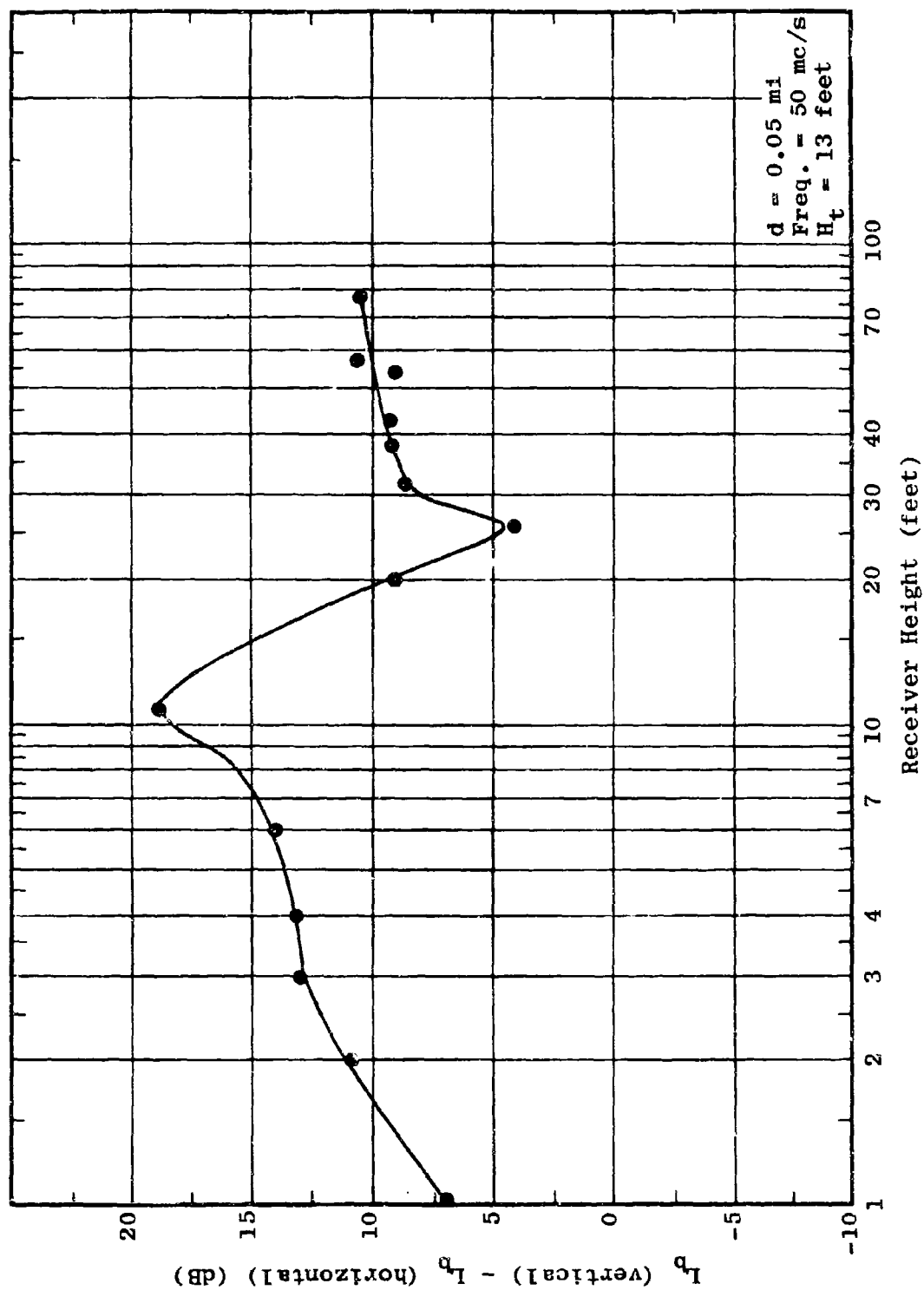


Figure 5.83 Horizontal Polarization Advantage Vs. Antenna Height

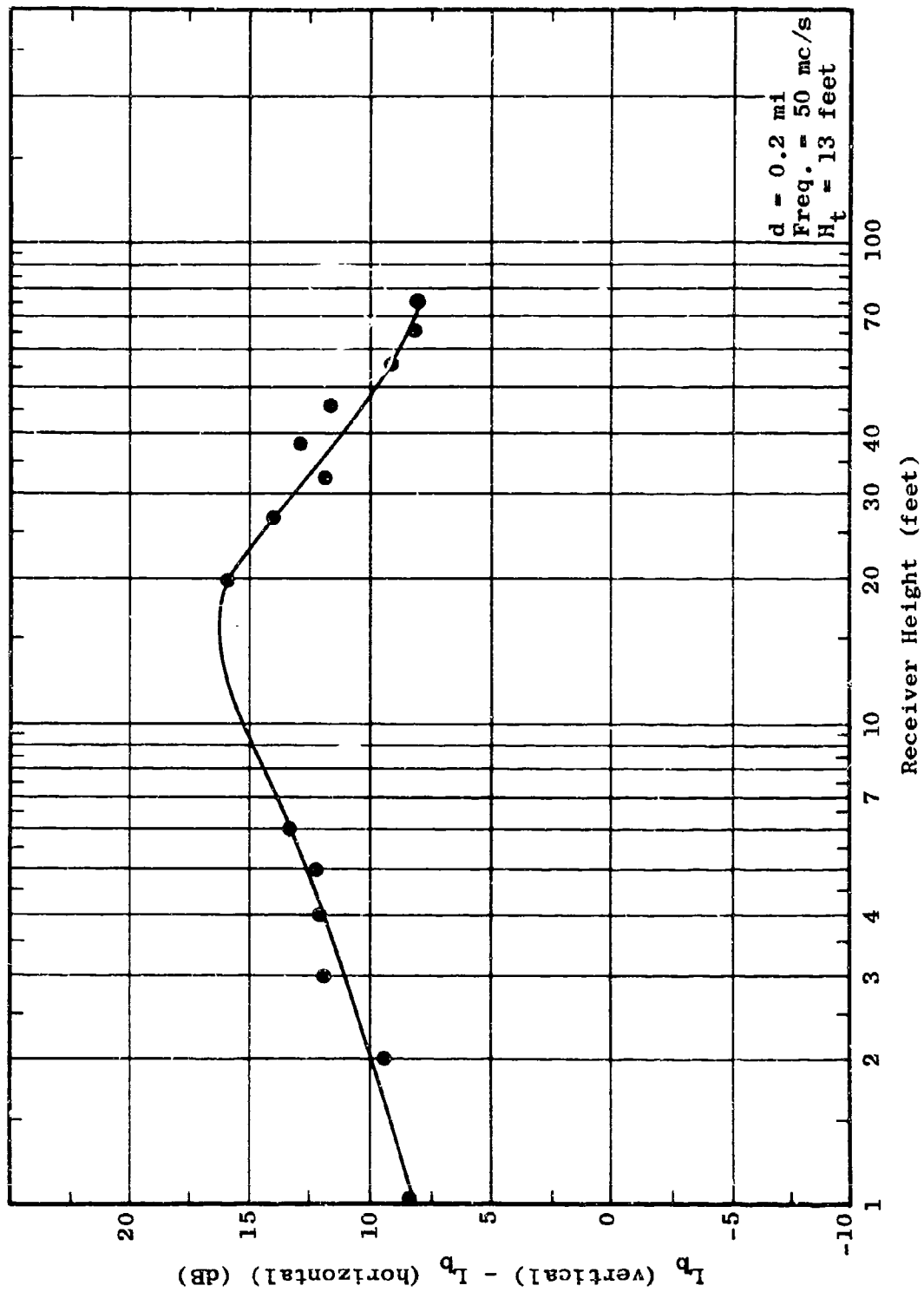


Figure 5.84 Horizontal Polarization Advantage Vs. Antenna Height

variation generally increases with frequency while the distance between peaks or nulls decreases. Such behavior of the field is characteristic within a scatter volume.

When appreciable scattering takes place, energy is lost from the original plane of polarization and appears in other planes. In order to determine the depolarization potential of the foliated environment, special cross-polarization measurements were performed at some of the in-foliage field points on Radial A.

The test consisted of first measuring the field strength in the plane of the transmitting antenna. Then, without physically displacing the receiving antenna, it was rotated to an orientation perpendicular to the plane of emission and the field transmitted from that plane was measured. To obtain representative readings for a certain location, this procedure was carried out at seven points over a small sector. The average values thus obtained were used to represent the two field components at a particular receiving height. The above procedure was performed at five in-foliage receiving elevations ranging from about 6 feet to 37 feet.

These tests were made with the transmitting antenna vertically polarized and were then repeated with it horizontally polarized. The test results are summarized in Table 5.13. The radiated power from the transmitter was the same for both polarizations, allowing a direct comparison of the received field strengths. The values in Table 5.13 are average field strengths obtained from the seven horizontal

Table 5.13

CROSS POLARIZATION MEASUREMENT PROGRAM

Dist. (mi)	Freq. (Mc/s)	H _t (ft)	XMTR Pol.	RCVR Pol.	Signal Level at Indicated Receiving Height (dB/μV/m)				
					6'	10.5'	16.5'	22'	27.5'
0.05	25	10' whip	V	V	88.5	93.5	92.5	93.5	93.5
		13' dipole	H	H	-	79.5	81.5	84.5	89.0
			H	H	-	94.5	97.5	100.5	102.5
			V	V	-	75.5	75.5	78.0	80.5
0.05	50	13' dipole	V	V	71.5	79.0	84.0	86.5	89.0
		13' dipole	H	H	80.5	81.5	82.5	86.5	90.0
			H	H	95.5	97.5	95.5	93.5	95.5
			V	V	77.0	83.0	87.5	86.5	85.5
0.05	100	13' dipole	V	V	85.0	85.0	88.0	88.5	87.0
		13' dipole	H	H	84.0	86.5	89.0	86.5	81.0
			H	H	102.0	105.5	108.0	107.0	107.5
			V	V	86.0	86.5	83.0	91.5	90.0
0.05	250	13' dipole	V	V	82.0	88.0	87.5	85.0	88.5
		13' dipole	H	H	83.5	84.0	83.0	82.0	80.5
			H	H	95.8	99.5	102.8	105.0	103.0
			V	V	85.0	86.0	86.5	85.5	86.5
0.05	400	13' dipole	V	V	71.2	70.5	78.8	74.8	77.2
		13' dipole	H	H	73.8	73.5	68.8	72.8	69.8
			H	H	81.1	84.1	80.8	84.5	82.5
			V	V	72.5	71.8	74.8	74.1	68.5

sample points spaced over a small sector at a particular receiver height. The significant observations to be made from this table are: (1) The depolarized component of a horizontal emission is about the same as the depolarized component of a vertical emission on an average basis. (2) For vertical emission, the depolarized component is often as large as the original vertical component. (3) For horizontal emission, the depolarized component is always about 10 to 20 dB less than the original horizontal component.

The above tests were made at a separation distance of 0.05 mile. Additional measurements made at 0.7 mile from the transmitter provide over-all results similar to those presented in Table 5.13.

5.4.3 Antenna Orientation

Special antenna performance measurements were carried out at 100 Mc/s. These measurements were designed to provide some knowledge of the vertical angle of arrival of energy received in foliage and the nature of the in-foliage scatter field. Unfortunately, due to practical limitations, the measurement results are not as conclusive as could be desired. However, worthwhile additional information was gained. The test setup and major implications derived from the measurements are discussed below.

In order to provide directivity, the dipoles normally used for transmitting and receiving at 100 Mc/s were replaced by seven-element Yagi-type antennas. Prior to in-foliage tests, the Yagi characteristics were carefully

evaluated through separate measurements made under conditions closely approximating free space. The "free-space" parameters measured were antenna gain, azimuth pattern and elevation pattern.

The vertical angle of arrival in foliage was measured by orienting both transmitting and receiving antennas in azimuth and elevation for maximum power transfer. The elevation angles thus obtained were compared with the free-space elevation alignments which produced maximum power transfer.

For nearly all receiver positions the optimum transmitter elevation angle was about 10 degrees above the optimum free-space angle. The optimum receiver elevation angle for all separation distances and receiver heights was around 10 to 20 degrees above the free-space angle. Had it been possible to utilize a more narrow beamwidth at the receiver end, it is expected that the angle of arrival would have varied with antenna height and possibly separation distance. However, the relatively wide beamwidth of the Yagi does not provide the resolution required to pinpoint the arrival angle with any degree of precision.

Nevertheless, the fact that both the transmitting and receiving antennas were always oriented upward for maximum power transfer strongly suggests that the dominant mode of propagation is via treetop diffraction at 100 Mc/s.

To gain insight into the relative level of the in-foliage scatter component, azimuth patterns taken in

"free space" were compared with in-foliage azimuth patterns taken at 13, 40 and 80 foot heights above the ground. The 80-foot pattern agreed very well with the "free space" pattern, and degradation increased as the receiving antenna was taken closer to ground level. Deep free-space nulls began to fill in more and more as antenna height was decreased. If the null filling is attributed totally to scattered energy, it appears that at 100 Mc/s, the scattered energy level is about 10 to 20 dB below the level of the major mode.

Between half power points the receiver pattern was virtually unchanged. This suggests that most directive antennas may be expected to perform normally between half power points when operated in foliage for frequencies below 100 Mc/s.

5.5 Propagation Loss as Influenced by Terrain in a Foliated Environment

A measurement area about 30 miles in extent has been established in the Pak Chong area. Propagation measurements are made by transmitting from a base camp and measuring received field strengths at various remote points within the foliage. Two measurement sectors have been established. The first, denoted as Sector A, extends in a southeasterly direction from the transmitting site. The trail which has been established through this sector is shown in Figure 5.85. Points along the trail, designated as A1 through A41 in Figure 5.85, have been calibrated in terms of radial distance from the transmitting site. Within 3 miles of the transmitting site, points at intervals of 0.2

mile have been surveyed and marked. Beyond 3 miles, points have been calibrated at 0.5 mile intervals. Certain calibrated points along the trail have been designated FP, or field points. Detailed height gain measurements are made at these FP locations. Continuous vehicular recordings of field strength are made at fixed antenna heights between FP locations.

Sector B, which runs in a southwesterly direction from the transmitter site, is shown in Figure 5.86. As shown in Figure 5.86, radial distance from the transmitter site has been calibrated within this sector in the same manner used in Sector A.

The word terrain as used here is defined to mean the deviation of the earth's surface from a smooth spherical earth. This definition does not account for foliage or man-made obstructions. The terrain profiles discussed in this section are radial profiles between a transmitting antenna location and a field point location. The influence of terrain upon propagation path loss and the propagation models which purport to predict this influence are discussed in this section and Section 5.2.3.

Basically, two types of terrain profiles were encountered in the Pak Chong measurement area: relatively flat, unobstructed profiles and rugged, obstructed profiles.

Figures 5.87 and 5.88 show the terrain profiles out to a separation distance of one mile for Sectors A and

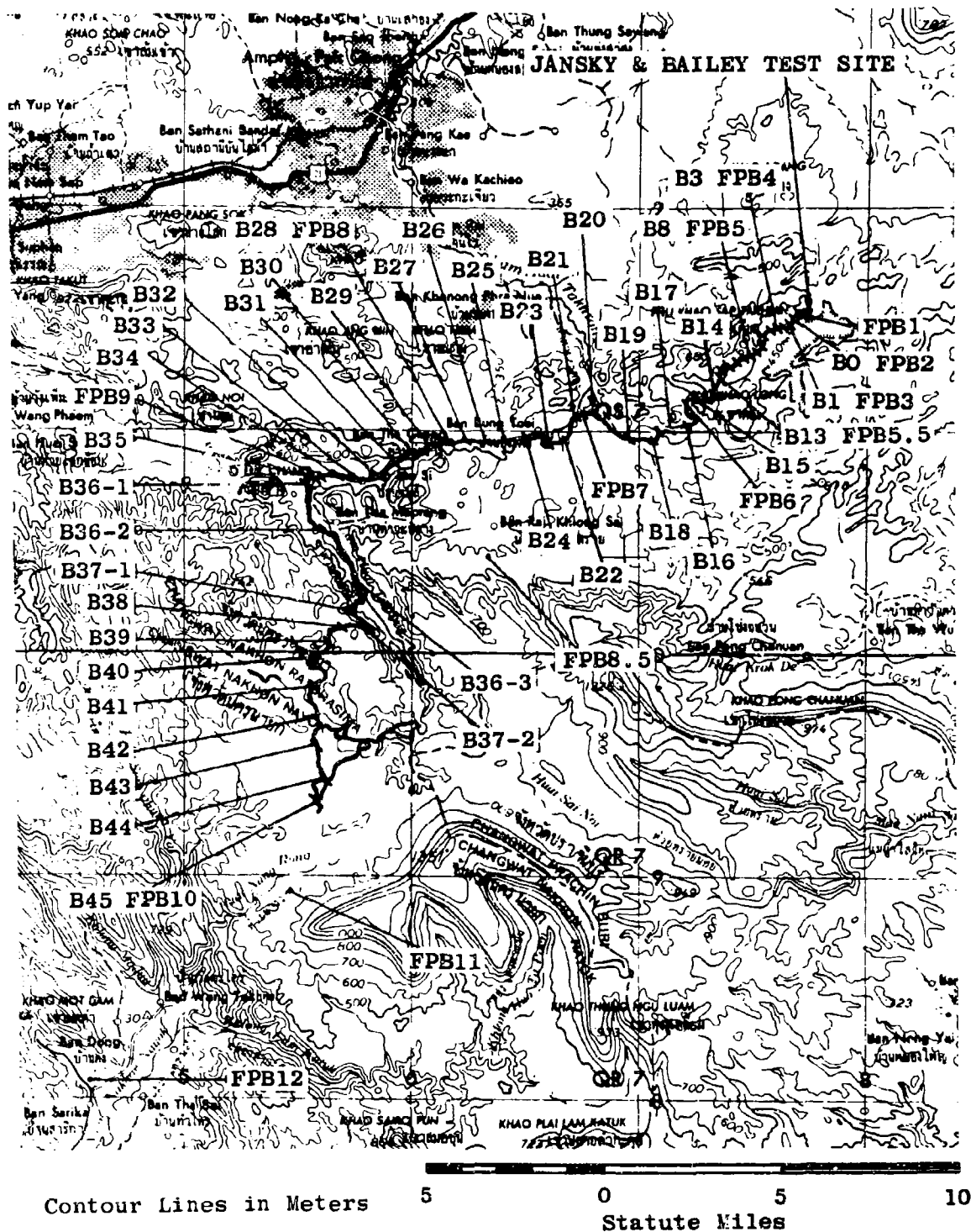


Figure 5.86 Radial Points and Field Points in Sector B

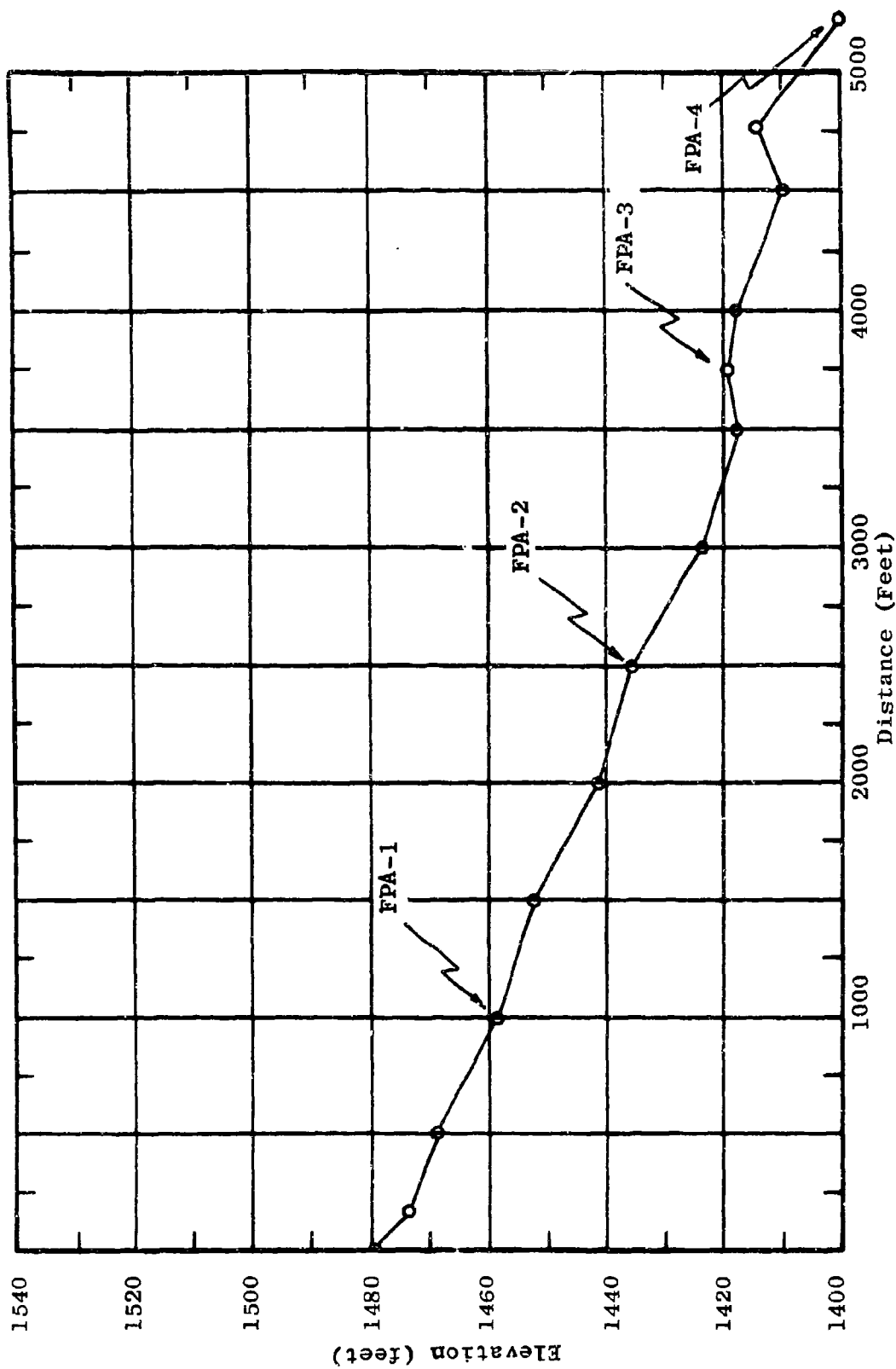


Figure 5.87 Sector A Short Range Terrain Profile

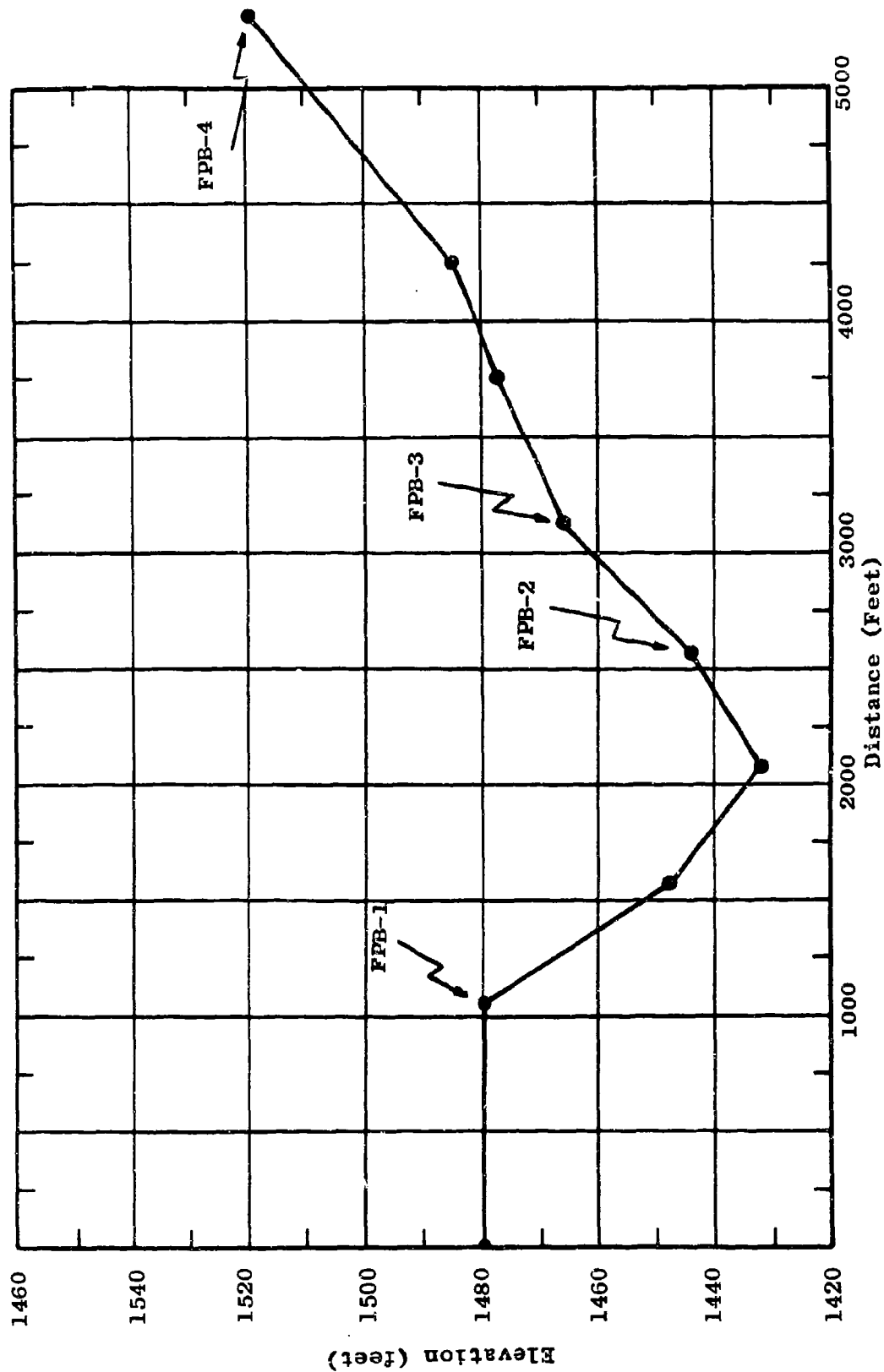


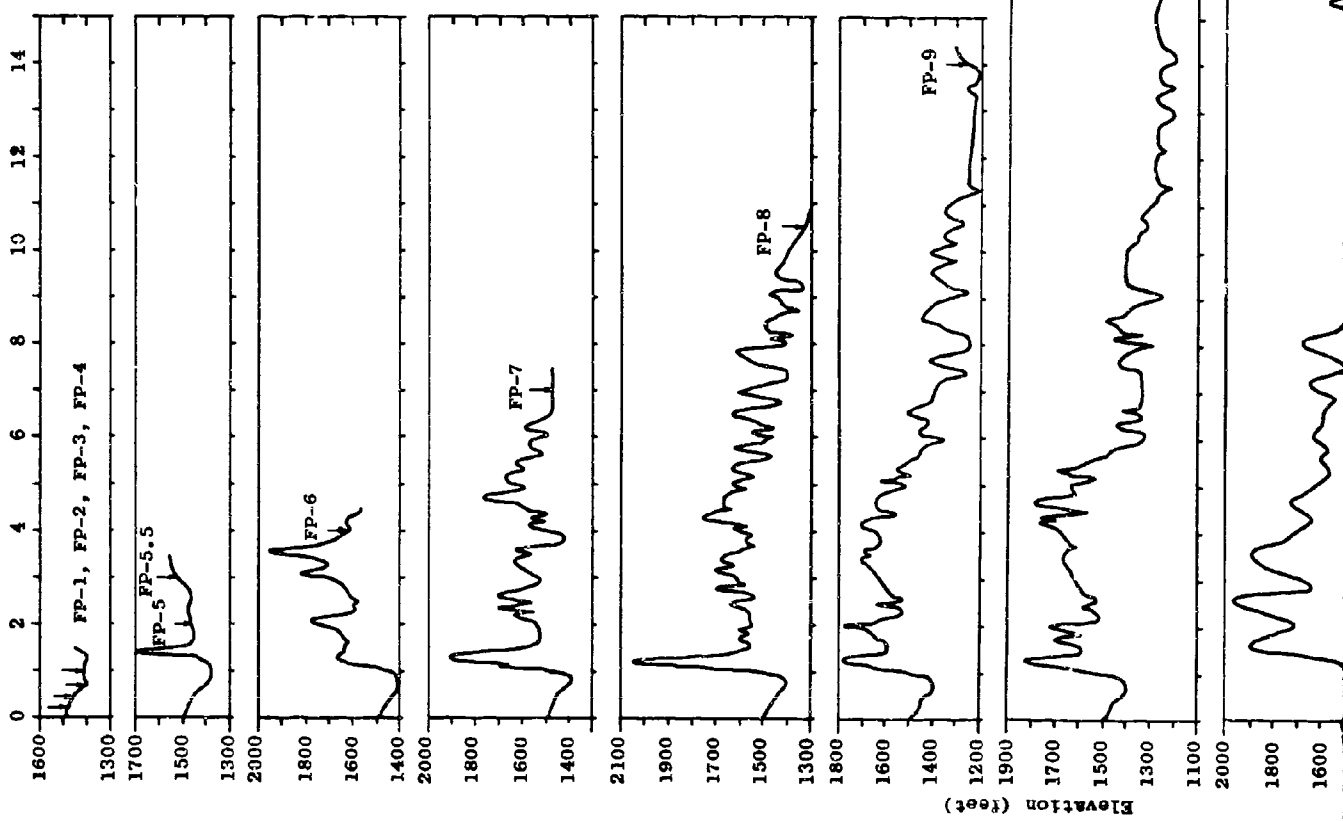
Figure 5.88 Sector B Short Range Terrain Profile

B, respectively. The first four fixed measurement points in each sector fall within 1 mile of the base camp, as shown in Figures 5.87 and 5.88. The profiles represented in these figures were measured with a precision altimeter. As shown in Figure 5.87, the Sector A profile has a continuous fall-off, totaling some 80 feet, from the transmitting antenna location out to one mile. The Sector B profile, Figure 5.88, is flat for the first 0.2 mile, then falls off approximately 50 feet in the next 0.2 mile, and finally continues to rise some 90 feet out to a separation distance of one mile. The impact of these smooth terrain variations upon measured field strength is discussed in Section 5.2.3.

Since the field points which lie beyond one mile do not generally fall on a straight line for either sector; the terrain profiles vary from field point to field point. Figure 5.89 shows all of the terrain profiles for Sector A. The profiles have the same vertical scale and are drawn so that the horizontal radial distance scales coincide. Each of the profiles has been corrected for the effects of atmospheric refraction and the curvature of the earth. The combined correction factor is d^3 , where d is the number of miles along the profile and the factor, d^3 , is the height correction in feet. This correction factor is based on an effective earth's radius of $4/3$.

As shown in Figure 5.89, each of the field points which lies beyond one mile is obstructed by a major terrain obstacle situated at a distance of approximately 1.5 miles. However, the Sector A terrain profiles are for the most

A



NOTE: Curves are corrected to an effective earth's radius factor $k = 4/3$

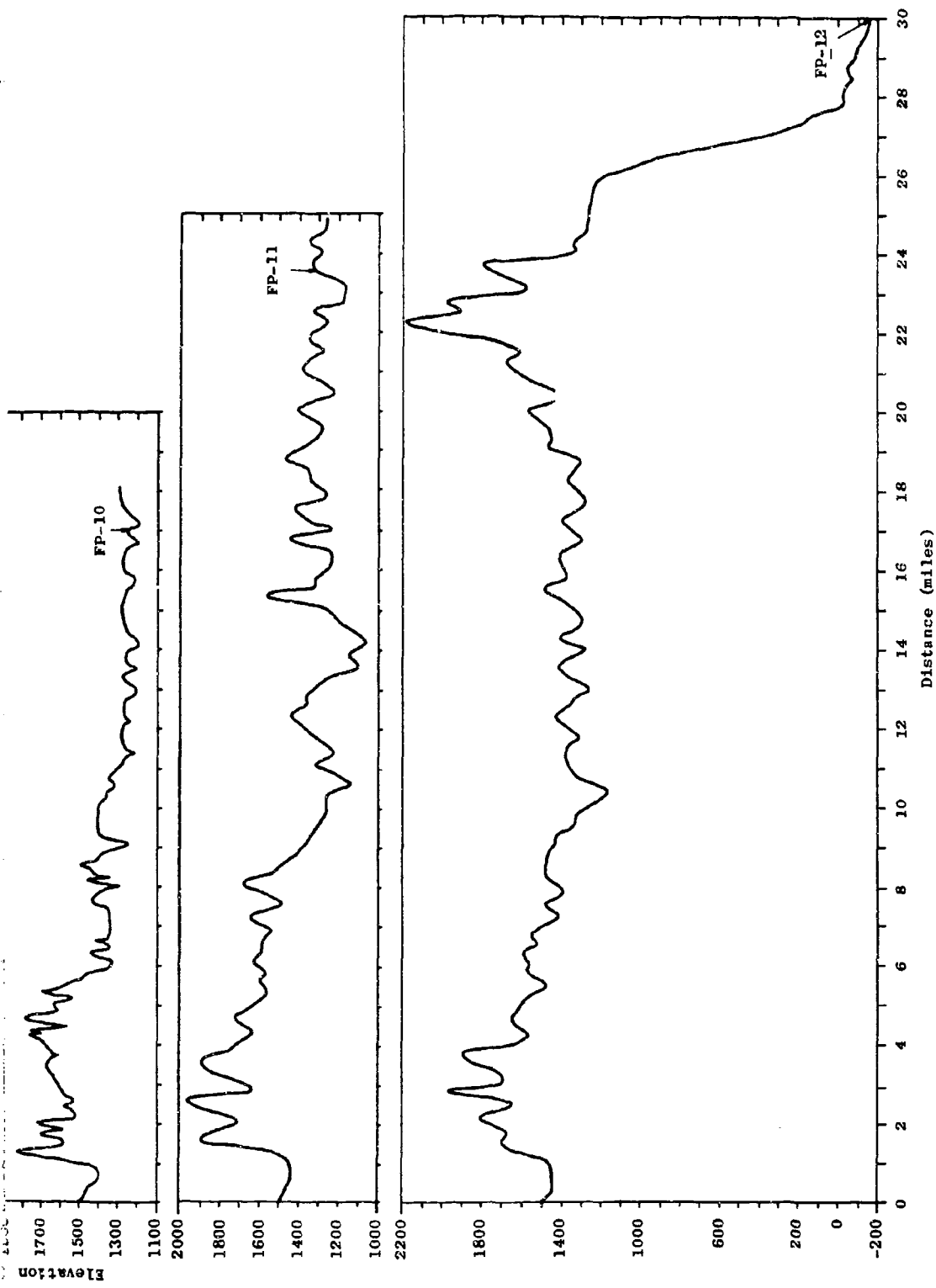
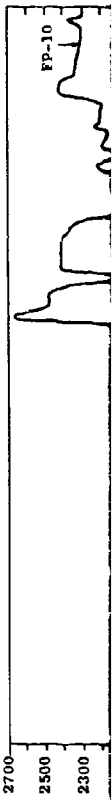
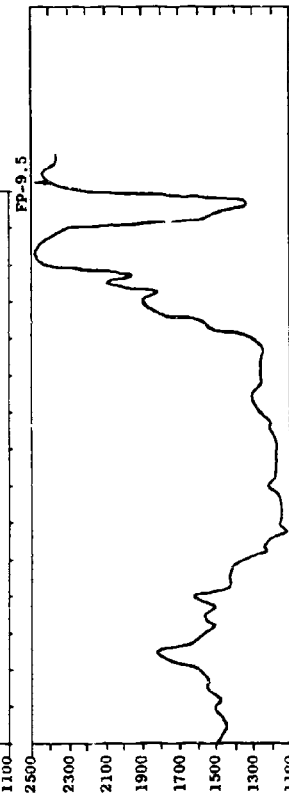
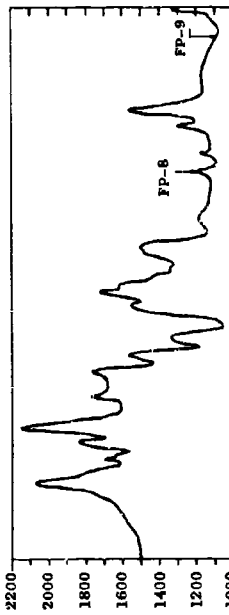
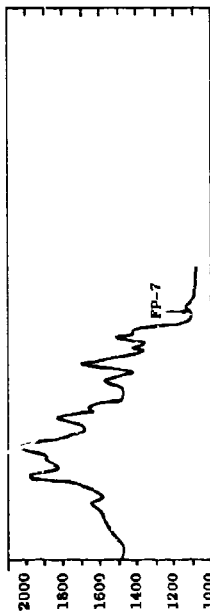
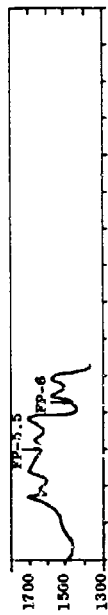


Figure 5.89 Terrain Profiles for
Field Points in Sector A



NOTE: Curves are corrected to an effective earth's radius factor $k = 4.3$.

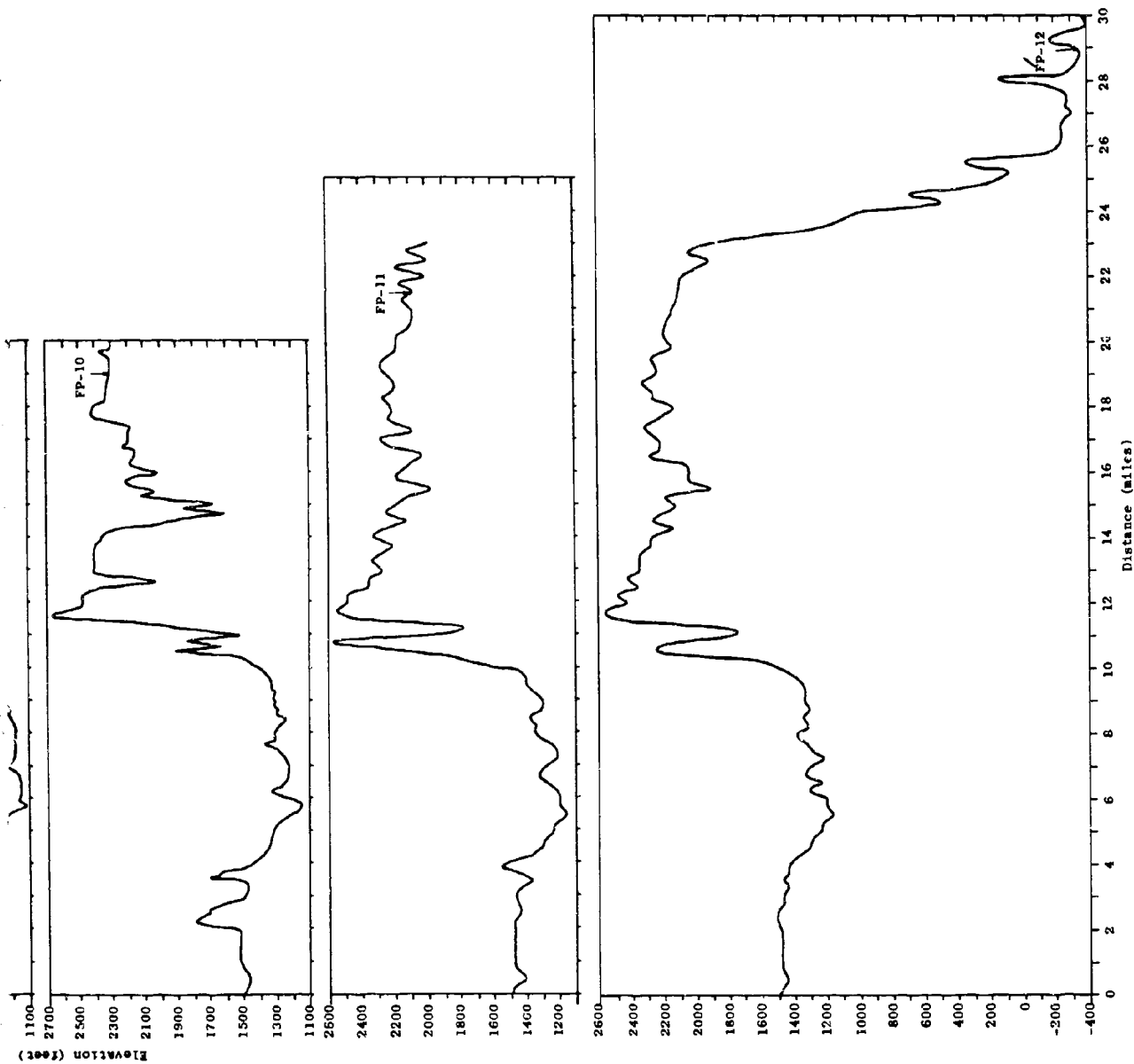


Figure 5.90 Terrain Profiles for
Field Points in Sector B

part less rugged than the profiles for Sector B, which are shown in Figure 5.90. The Sector B profiles, with the exception of those for FPB-11 and FPB-12, also show a large terrain obstruction. In this case, the obstruction is located about 2 miles from the transmitting antenna. Figure 5.91 is a photograph of this terrain obstacle taken from a helicopter near the test site. The Sector B profiles also reveal a large precipice obstructing the field points beyond 12 miles.

5.5.1 Modified Egli Model

To assess the effect of foliage, it is necessary to adopt a model which represents the propagation characteristics to be expected in the absence of foliage. Since the environment includes rough terrain as well as foliage, a propagation model which predicts terrain effects is required. A rather detailed analysis based on a model suggested by John Egli⁶ was presented in Semiannual Report Number 6. The model which predicts the median loss expected over rough terrain is given by equation (4).

$$L_b = 116.57 + 20 \log f + 40 \log d - 20 \log (H_t H_r) \quad (4)$$

where

L_b = median basic transmission loss in dB

f = frequency in megacycles per second

d = distance in miles

H_t, H_r = transmitting and receiving
antenna heights, respectively,
in feet.

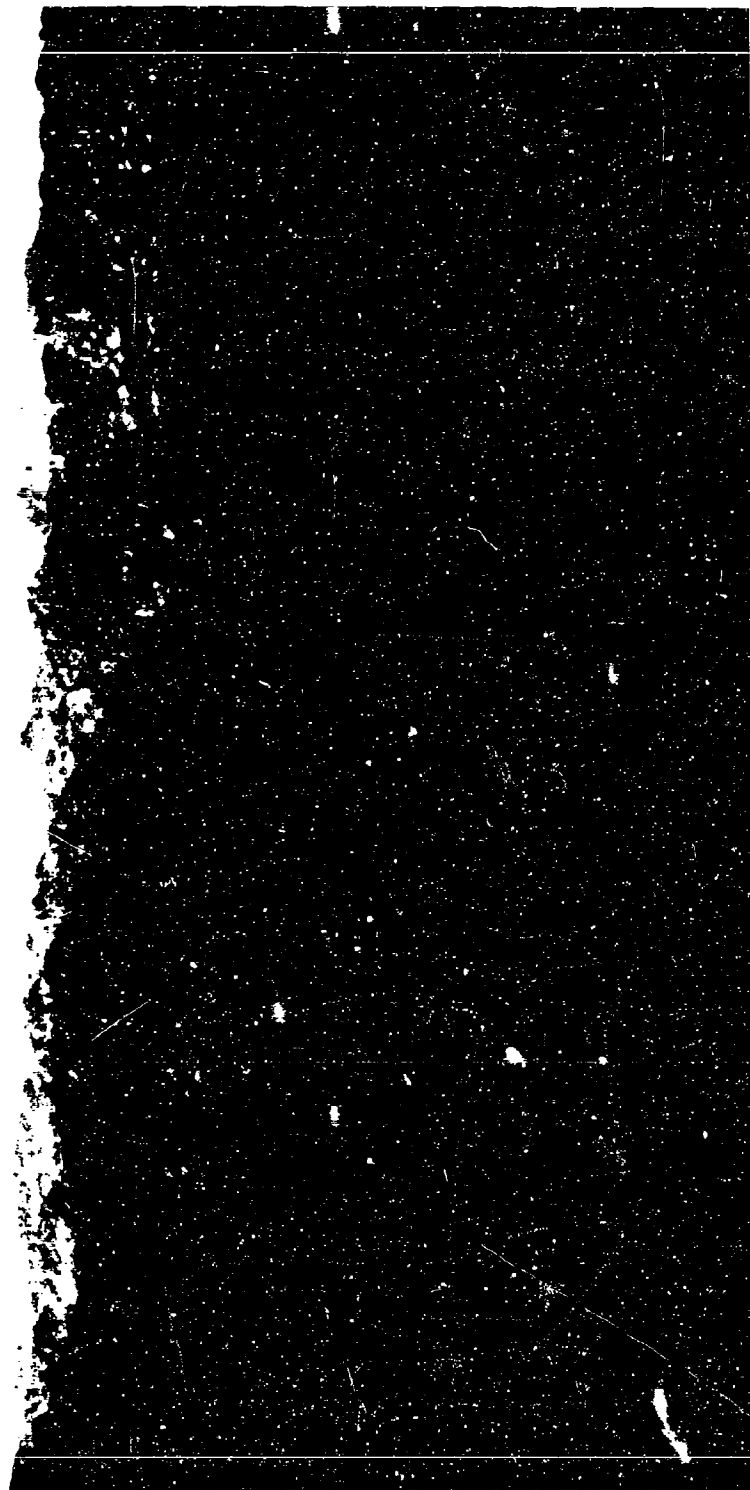


Figure 5.91 Southwesterly View from Base Site toward first Terrain Obstacle

The model also predicts a range of propagation loss which is normally distributed about the median value given by Equation 4. The standard deviation predicted by the model is given in Table 5.14.

Table 5.14
ROUGH EARTH STATISTICS

<u>Frequency (Mc/s)</u>	<u>Standard Deviation (dB)</u>	<u>10% to 90% Range (dB)</u>	<u>1% to 99% Range (dB)</u>
25	4.6*	12*	21*
50	6.1	16	28
100	7.7	20	35
250	9.2	24	42
400	10.7	28	49

*Extrapolated

The preliminary analysis reported in Semiannual Report Number 6 showed that the differences between Equation 4 and measured data appeared to be relatively simple and could be logically classed as a "foliage factor" so that the Egli model plus this foliage factor could be used to estimate propagation loss in foliage and terrain of the type to be found in Pak Chong. However, this preliminary analysis was based on a small percentage of the measured data now available. Subsequent analysis based on the entire data base has shown that the Egli model tends to fit measured data well in the distance dimension only and fails to fit

satisfactorily in the frequency and height dimensions. The analysis described in the next section provides a similar compact statistical summary of the Pak Chong data base.

5.5.2 General Statistical Model

The following analysis was pursued in an attempt to produce a meaningful statistical summary of the thousands of fixed point data samples which were taken at Pak Chong beyond 2 miles. This analysis is restricted to data at 2 miles and beyond so that the results may be classed as applicable to "rough" foliated terrain. The model used follows the Egli model except for the height function and is given by the following equation.

$$L_b = 116.57 + 20 \log f + 40 \log d - G(h) \quad (5)$$

where

L_b = median basic transmission loss
in dB

f = frequency in megacycles per second

d = distance in miles

$G(h)$ = an unknown function depending
upon antenna height and foliage

The only demand made upon the function $G(h)$ was that it be relatively simple. A detailed computer analysis of all measured data produced the results shown on Table 5.15. The quantities H_t and H_r represent the transmitting and receiving antenna heights above ground.

TABLE 5.15

HEIGHT GAIN FUNCTIONS
FOR GENERAL STATISTICAL MODEL

Vertical Polarization

$$25 \text{ Mc/s: } G(h) = -17 + 20 \log H_t H_r$$

$$50 \text{ Mc/s: } G(h) = -16 + 20 \log H_t H_r$$

$$100, 250, 400 \text{ Mc/s: } G(h) = 31 + 0.2(H_t + H_r)$$

Horizontal Polarization

$$25 \text{ Mc/s: } G(h) = 4 + 17.5 \log H_t + 15 \log H_r$$

$$50 \text{ Mc/s: } G(h) = 12.6 + 12 \log H_t H_r$$

$$100 \text{ Mc/s: } G(h) = 34 + 0.2(H_t + H_r)$$

$$250, 400 \text{ Mc/s: } G(h) = -19.4 + 23 \log H_t H_r$$

These relationships are restricted to height ranges from 10 to 80 feet. The model for vertical polarization at 25 and 50 Mc/s shows the $20 \log h$ height dependence typical of the Egli model. The models for horizontal polarization at 25 and 50 Mc/s differ in that different multipliers are used for the logarithmic height function. The height dependence becomes linear at 100 Mc/s for both polarizations.

The models shown at 250 and 400 Mc/s represent the best fit to the data available; but, unfortunately, limited data was available at low antenna heights for these frequencies at ranges of 2 miles and beyond. Therefore, no strong conclusions should be drawn from what is shown statistically for these frequencies.

Table 5.16 gives the average difference between measured data and the general statistical model introduced above. A zero entry in the table means that on the average the general statistical model matches measured data. A negative entry indicates that on the average the model overestimated the propagation loss. A positive entry indicates that on the average the model underestimated the propagation loss. As an example, consider the first entry in the top left-hand corner of Table 5.16. The entry is -3. This means that on the average for a frequency of 25 Mc/s, vertical polarization, a transmitting height of 10 feet and a receiving height of 11 feet, the general statistical model overestimated the measured propagation loss by 3 db. Table 5.17 presents a tabulation of the number of samples used to obtain each average shown in Table 5.16. Table 5.18 gives the standard deviations which correspond to the averages given in Table 5.16.

Table 5.16

AVERAGE DIFFERENCE BETWEEN
MEASURED DATA AND GENERAL STATISTICAL MODEL

Freq. (Mc/s)	Pol.	H _t (ft)	H _r (ft)													
			11	20	26	31	37	42	48	53	59	64	69	73	79	
25	V	10	-3	4	1	0	0	0	0	1	1	0	0	0	3	
	V	40	-2	3	0	0	0	0	0	0	0	-1	-1	-1	-1	
	V	80	-2	2	1	0	0	0	0	0	0	-1	-1	-1	-1	
50	V	13	-8	-6	-1	0	0	-1	-2	2	0	0	0	0	0	
	V	40	-1	1	0	0	0	1	1	1	1	1	0	0	0	
	V	80	-1	1	0	0	0	1	1	1	1	1	0	0	0	
100	V	13	1	1	0	0	0	0	0	0	0	2	1	1	2	
	V	40	-3	1	0	-1	-5	-4	0	0	-1	0	-2	0	-1	
	V	80	-2	-1	0	0	-1	-1	0	0	-1	-1	0	0	-2	
250	V	40	-5	1	1	1	-1	1	0	1	3	4	4	4	3	
		80	4	5	5	7	1	0	0	-2	-2	0	1	1	3	
25	H	13	-1	-1	-2	-2	-1	-1	-1	-1	-1	-1	-1	-1	-1	
	H	40	0	0	0	0	0	0	0	0	0	0	-1	0	-1	
	H	80	3	1	2	1	1	1	1	2	2	1	2	2	1	
50	H	13	-3	-2	-2	0	0	-1	0	1	0	0	0	-1	-1	
	H	40	1	2	3	1	1	1	1	1	1	1	1	1	1	
	H	80	-1	0	-1	-1	-1	-1	0	-1	-1	-1	-1	-1	-1	
100	H	13	-1	-1	-1	0	1	0	-2	-1	-2	-1	-2	-2	-1	
	H	40	0	4	5	2	2	-1	-3	-1	-1	0	1	1	2	
	H	80	-1	0	1	1	0	0	0	0	1	2	2	2	2	
250	H	40	-12	0	0	-2	0	-3	1	0	0	0	0	0	0	
	H	80	-6	0	0	2	2	1	-1	-1	-2	-2	-2	-2	-2	

Table 5.17
NUMBER OF SAMPLES USED
TO DERIVE RESULTS SHOWN IN TABLE 5.16

Freq. (Mc/s)	Pol.	H _t (ft)	H _r (ft)														
			11	20	26	31	37	42	48	53	59	64	69	73	79		
25	V	10	13	14	15	15	16	20	20	22	22	22	22	22	25		
		40	26	29	32	35	38	38	41	41	41	41	41	41	41		
		80	39	40	41	42	42	43	43	43	43	43	44	44	44		
50	V	13	6	9	9	10	12	14	15	18	19	19	21	21	22		
		40	17	23	26	27	28	28	29	31	34	35	36	37	38		
		80	24	30	34	35	39	40	42	42	42	42	42	43	43		
100	V	13	8	8	10	11	12	13	14	15	15	15	15	15	15		
		40	14	18	19	19	20	19	20	20	23	24	25	26	27		
		80	19	23	25	26	26	27	27	27	26	28	30	30	29		
250	V	13	0	0	1	1	1	2	2	4	3	3	4	4	2		
		40	3	5	6	7	9	10	10	11	10	11	11	13	13		
		80	6	9	9	9	9	9	10	10	10	11	11	11	10		
25	H	13	29	38	39	39	40	39	41	39	41	41	40	42	40		
		40	35	38	40	40	40	40	39	40	40	40	40	40	40		
		80	39	40	41	42	42	43	43	43	43	43	44	44	44		
50	H	13	26	31	29	33	33	33	35	36	36	38	39	39	39		
		40	26	37	36	35	37	38	40	42	42	41	42	43	44		
		80	34	42	43	43	43	44	44	44	44	44	44	44	44		
100	H	13	16	19	19	20	21	21	21	21	22	23	23	23	23		
		40	14	17	18	21	21	20	21	22	22	23	24	22	23		
		80	24	28	29	30	29	30	30	32	33	34	34	33	34		
250	H	40	3	4	5	5	8	9	11	11	11	11	11	12	12		
		80	9	8	11	13	12	12	12	13	13	13	15	15	15		

Table 5.18

STANDARD DEVIATION OF DIFFERENCE
BETWEEN MEASURED DATA AND GENERAL STATISTICAL MODEL

Freq. (Mc/s)	Pol.	H _t (ft)	H _r (ft)											
			11	20	26	31	37	42	48	53	59	64	69	73
25	V	10	7	6	6	5	5	6	6	7	7	7	6	7
	V	40	9	7	7	8	8	7	8	8	8	8	8	8
	V	80	9	8	7	7	8	8	7	8	8	9	9	8
50	V	13	7	5	5	6	8	8	8	7	7	7	7	7
	V	40	9	8	8	8	8	9	8	8	8	8	8	8
	V	80	8	8	8	8	9	9	8	8	8	8	7	7
100	V	13	6	3	5	7	8	8	7	8	8	7	7	7
	V	40	6	8	8	8	8	8	8	8	8	8	8	8
	V	80	7	8	7	8	9	9	9	9	9	8	8	8
250	V	40	4	2	4	3	4	4	6	5	4	5	5	5
	V	80	6	4	6	6	6	6	6	6	6	7	7	7
25	H	13	7	7	6	6	6	6	5	5	6	5	5	5
	H	40	6	6	6	6	6	6	6	6	6	6	6	5
	H	80	6	6	6	6	6	6	6	6	6	6	6	6
50	H	13	6	6	6	7	7	6	6	7	6	6	6	6
	H	40	6	6	6	6	6	6	6	6	6	6	6	6
	H	80	6	6	7	7	7	7	7	7	7	7	6	7
100	H	13	7	7	7	7	7	7	7	7	7	8	8	8
	H	40	9	10	10	10	10	10	10	10	10	10	11	11
	H	80	8	8	8	9	8	9	9	9	9	10	10	10
250	K	40	4	2	3	3	3	5	5	5	5	6	5	5
	H	80	6	6	4	7	7	7	7	7	8	8	7	7

The average differences shown in Table 5.16 indicate that the model fits well on the average for most antenna heights and frequencies. The generally larger values for 250 Mc/s are indicative of the limited data available at that frequency.

Figure 5.92 is an example which provides some insight concerning the over-all variation which is typical of the measured propagation data. The upper and lower horizontal lines bracket the 1 per cent to 99 per cent range to be expected using Egli's standard deviation given in Table 5.14. The vertical bars give the range of measured data at various distances after the general statistical model has been subtracted out. As the figure indicates, the range of measured data at any one distance is significantly smaller than the range predicted by Egli's standard deviation. However, when the differences between locations are considered, the over-all range of measured data is comparable to Egli's range. Although Figure 5.92 applies to horizontal polarization at 50 Mc/s, the data is representative of both polarizations for frequencies from 25 to 400 Mc/s.

5.5.3 NBS Terrain Model

The statistical models discussed in the previous sections treat propagation as it would appear averaged over many different types of rough terrain. Consideration has been given to more complex terrain models which are designed to predict at least the gross effects of major terrain obstacles. Single-obstacle analyses have been considered along with rough-earth analyses based on the four-arc method. 10,14

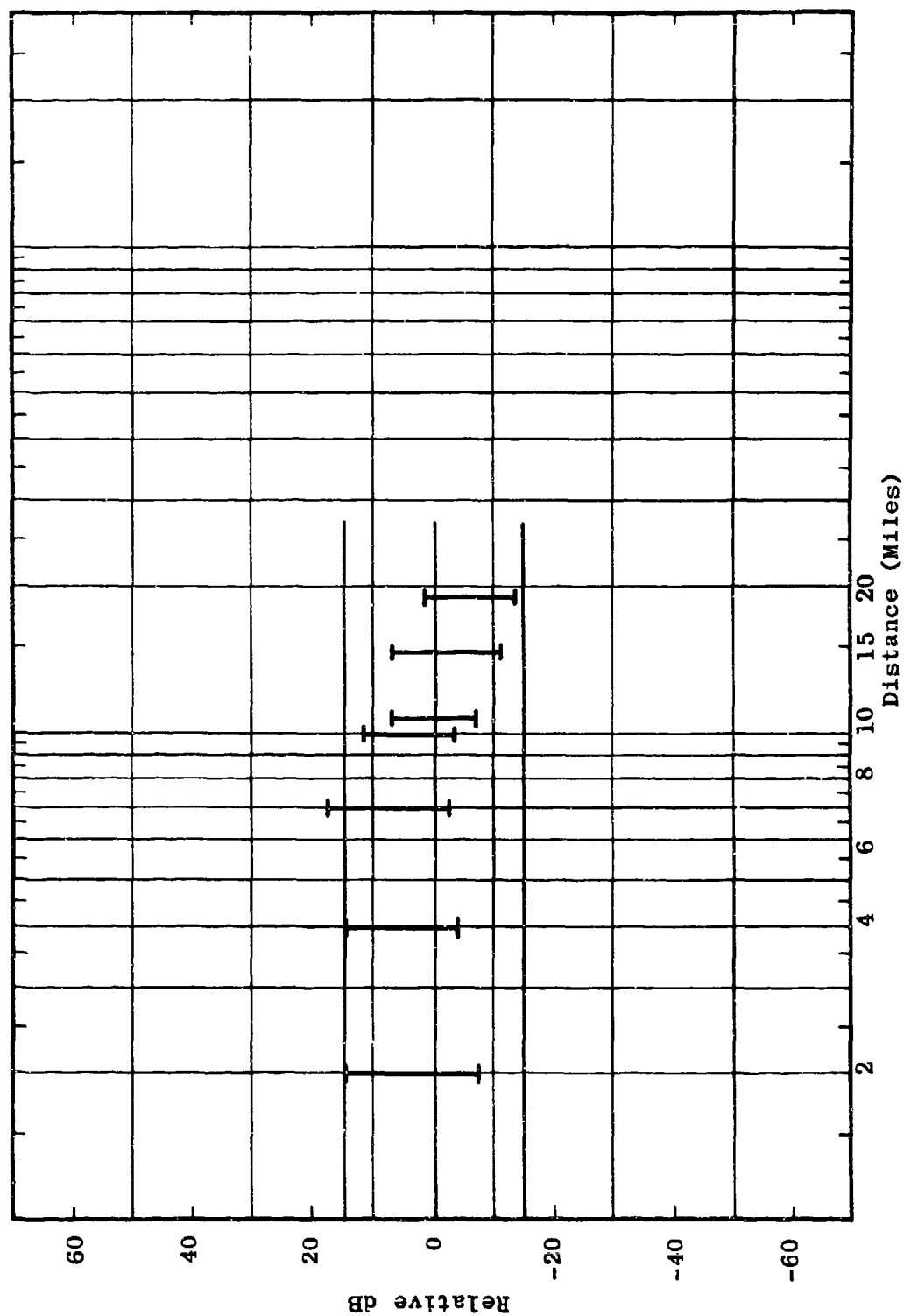


Figure 5.92 Deviation of Measured Values from General Statistical Model for 50 Mc/s Horizontal Polarization

Figure 5.93 compares measured data to the results of a detailed rough-terrain prediction. When a single obstacle would have occurred between the transmitting and receiving antennas in the absence of foliage, knife-edge diffraction theory was used. The points on Figure 5.93 which resulted from knife-edge calculations are marked with a K. When multiple obstacles would have existed in the absence of foliage, rough-earth calculations were used. These points are marked on Figure 5.93 with an R. The correspondence between measured and theoretical results was not good in general.

Height-gain functions, $G(H)$, were used to take into account the possibility of reflections over rough terrain between either of the antennas and their radio horizons. Due to a number of factors, there is some question as to when these factors apply and when they do not. In order to decide whether a detailed study of these functions might be rewarding, the following experiment was made. The rough-earth propagation calculations were repeated, and the $G(H)$ functions were used only in those cases for which their use provided a better fit to the measured data. The results of this experiment at 25 Mc/s are shown in Figure 5.94. The letter T beside a calculated point indicates that the $G(H)$ function was used at the transmitting end but not at the receiving end. For those calculated points marked with an R, the converse is true. For those points marked with both T and R, the $G(H)$ functions were used at both the transmitting and receiving ends. Those computed points for which the $G(H)$ functions were used at neither end are unmarked. As Figure 5.94 shows, the fit at 25 Mc/s is relatively good except for the point at 4 miles.

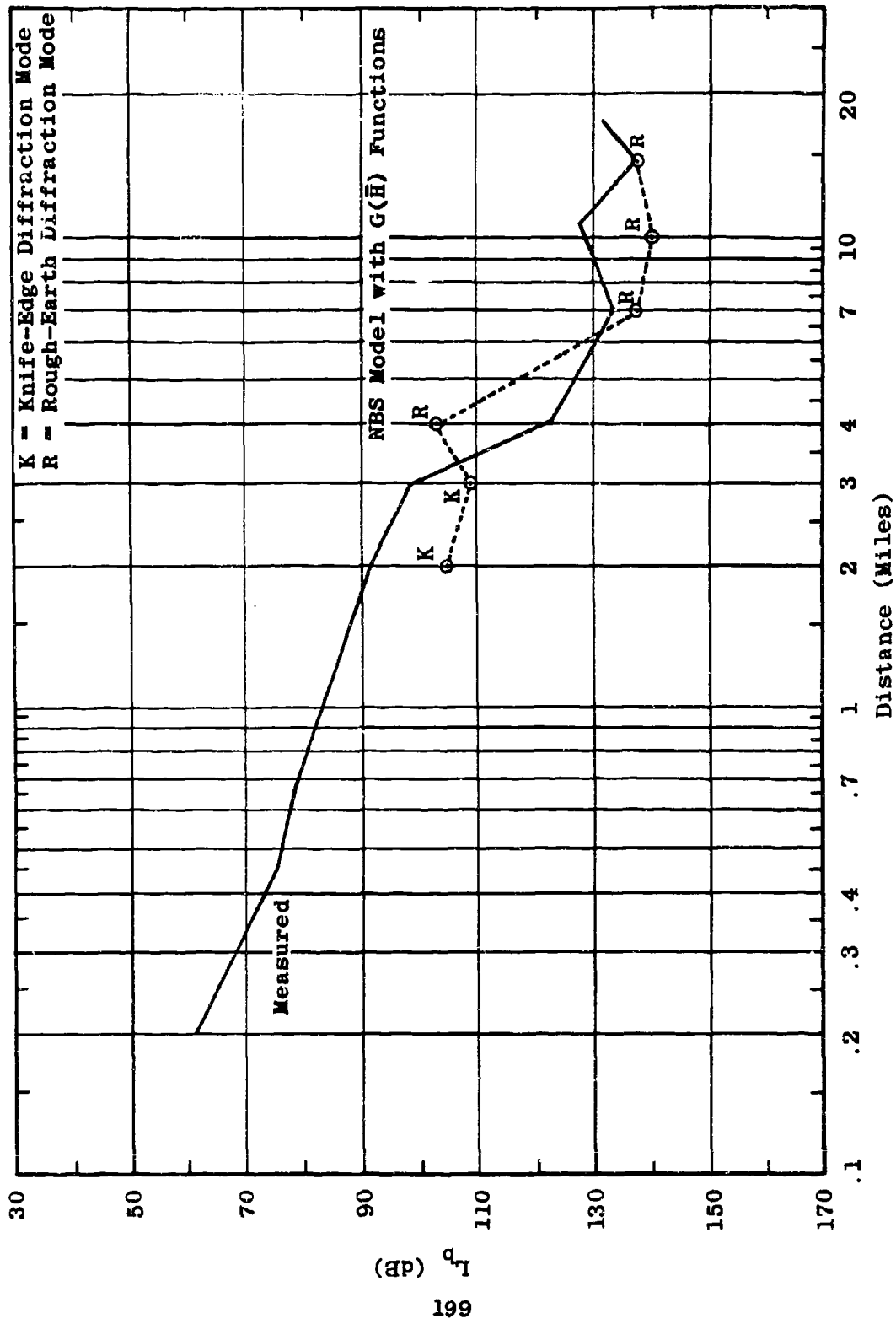


Figure 5.93 Comparison Between Measured Results and NBS Model Including $G(\bar{H})$ Functions
 $I_b = F_A(25, 80, V, d, 80)$

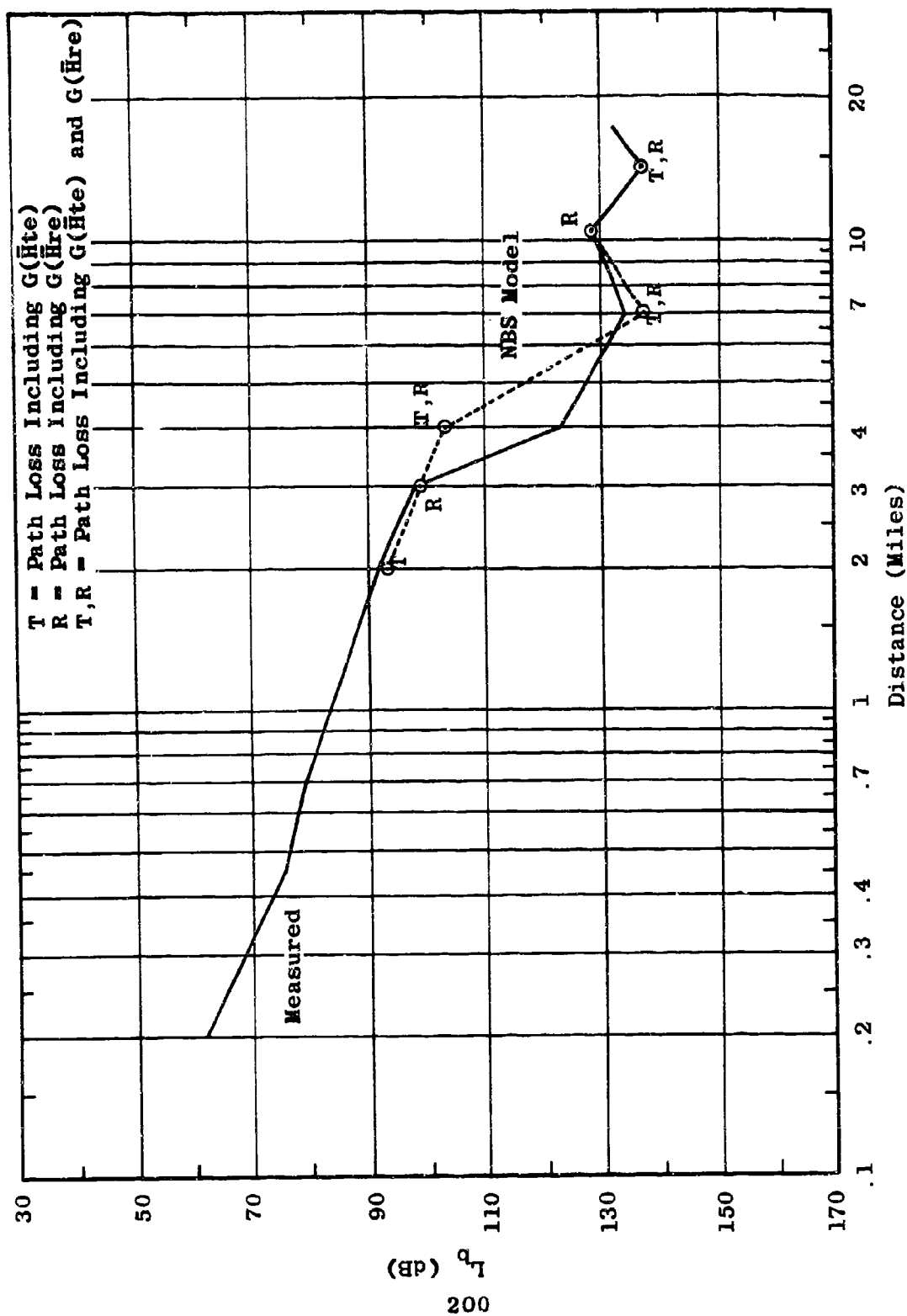


Figure 5.94 Best Fit to Measured Results
 $L_b - F_A(25, 80, V, d, 80)$

Since the measured data includes the presence of foliage and the theoretical calculation does not, it is reasonable to assume that the theoretical losses might differ from the measurements by some foliage effect. The attempt in Figure 5.94 was to fit the data with theory as closely as possible. However, hypothesizing a foliage effect, the experiment was repeated in an attempt to find the best theoretical function corresponding to a loss 10 dB below that which was measured. The result, which is shown in Figure 5.95 appears to be quite good. Although the results in general have not been exceptionally good, there is enough correlation to justify a continuation of this type of analysis.

5.5.4 Simplified Terrain Model Results

The applicability of two relatively simple terrain models has been explored in an attempt to separate the terrain and foliage effects which appear in the Pak Chong propagation data. These two models are referred to as the "Modified LaGrone Model" and the "Equivalent Knife Edge Model."

The requirement for better terrain models arises in part because of the relatively low transmitting and receiving antenna heights relative to the surrounding terrain and the relatively short separation distances which are characteristic of tactical communications.

When either terminal point is high, the number of diffracting objects between the transmitter and receiver is

likely to be small even for very mountainous terrain. When both terminal points are low, the number is likely to be large even for slightly irregular terrain.

For short and medium paths with one diffractor, simple knife-edge theory works very well when the Fresnel ellipse is unobstructed by terrain or foliage at the terminal points. It has also been shown that, for a given beyond-the-horizon path, the loss decreases substantially when the number of diffractors is decreased. Such paths are referred to as obstacle-gain paths since a gain is realized when one large diffracting ridge or mountain replaces numerous smaller diffractors that would have been present had the large ridge or mountain not existed.

The above facts indicate that the loss between two points over rough terrain depends strongly upon the number of diffractors or perturbers encountered. Moreover, it appears from observation of measured data that the rate of loss increases sharply when going from one to two and then three diffractors, but seems to saturate and remain fairly constant as additional diffractors are encountered. In the Pak Chong area at most fixed field points beyond about a mile from the transmitter, the number of diffractors between transmitter and receiver varies from one to four or five. The variation in path loss due to these obstacles is typically on the order of 10 to 20 dB.

Several simple models were examined for applicability in predicting the observed loss deviations for the individual profiles encountered. Of particular interest was a model¹⁵ developed by Alfred H. LaGrone based upon measured television signals propagated over rough terrain.

This model in its original form did not accurately predict the observed loss in Sectors A and B. Further study has led to the hypothesis that the failure of the model is related to the number of diffractions encountered, as discussed previously. The LaGrone model basically involves computing the signal deviation due to diffractors close to the receiver, and then superimposing these deviations upon a smooth earth function which is biased by an empirical constant.

The failure of this method to predict our observed losses is most likely caused by the particular values of the empirical constants originally proposed. It is hypothesized that the original constants apply to paths that contain more than three major diffractors and therefore should be modified when the number of major diffractors becomes less than about three or four.

Using LaGrone's basic method of computing terrain deviations, empirical constants applicable to one, two and three knife edges were derived from measured data taken on radial A. These constants were then used in conjunction with the LaGrone model to predict the basic transmission loss for Radial B. Predictions were made at 25, 50 and 100 Mc/s for Field Points 6 through 11. The agreement is good for 50 and 100 Mc/s and fairly good at 25 Mc/s. The constants were found to be frequency sensitive. The prediction at 25 Mc/s used constants derived for 50 Mc/s. Closer agreement might have been obtained had separate constants been used.

Since simple knife-edge theory was found to produce good results when one diffractor was involved, an equivalent knife-edge mode, using the empirical constants derived for the LaGrone model, was tested to see if multiple knife-edge effects could also be predicted. Surprisingly good agreement was obtained when predictions made on Radial B were compared with measured data.

The results of applying these two terrain models to the Pak Chong data of Radial B is shown in Figure 5.96 for 100 Mc/s, Figure 5.97 for 50 Mc/s and Figure 5.98 for 25 Mc/s. As these figures indicate, both models predict the path loss irregularities due to major terrain features quite well.

Both the equivalent knife-edge and modified LaGrone models are discussed in detail below.

5.5.4.1 Modified LaGrone Model

The original LaGrone model is expressed as follows:

$$L_b = L_b(\text{smooth earth}) + K_1 \left[(h_1)^{\frac{1}{2}} e^{-d_1} + (h_2)^{\frac{1}{2}} e^{-d_2} + \dots \right. \\ \left. \dots + (h_n)^{\frac{1}{2}} e^{-d_n} - (h_r)^{\frac{1}{2}} e^{-d_0} \right] + K_2 \quad (6)$$

where

K_1 and K_2 = frequency sensitive constants

$L_b(\text{smooth earth})$ = loss expected over a smooth earth

h_n = differential height between successive hills

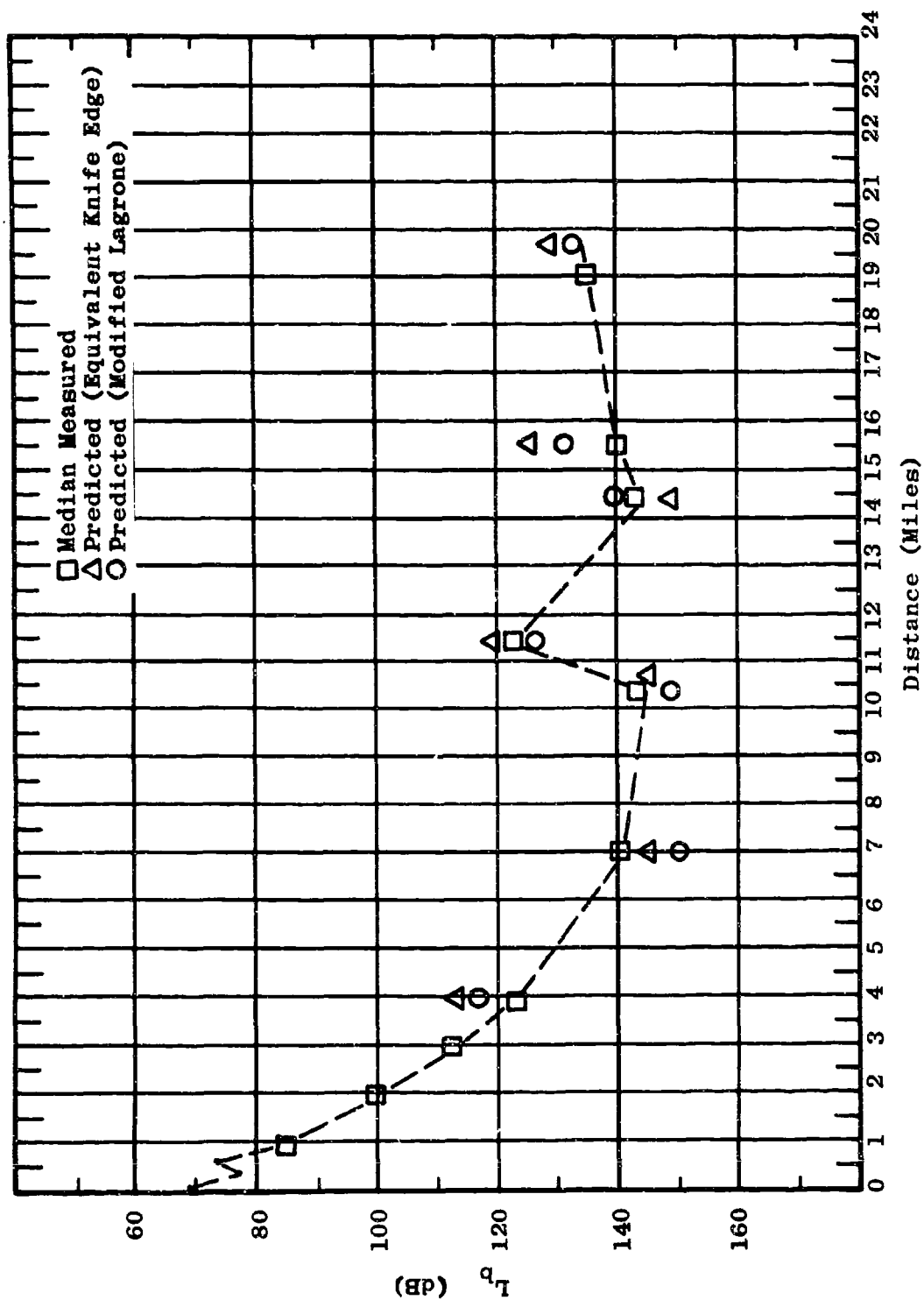


Figure 5.96 Comparison of Measured and Predicted Path Losses
 $L_p = F (100, 80, H\&V, d, 80)$

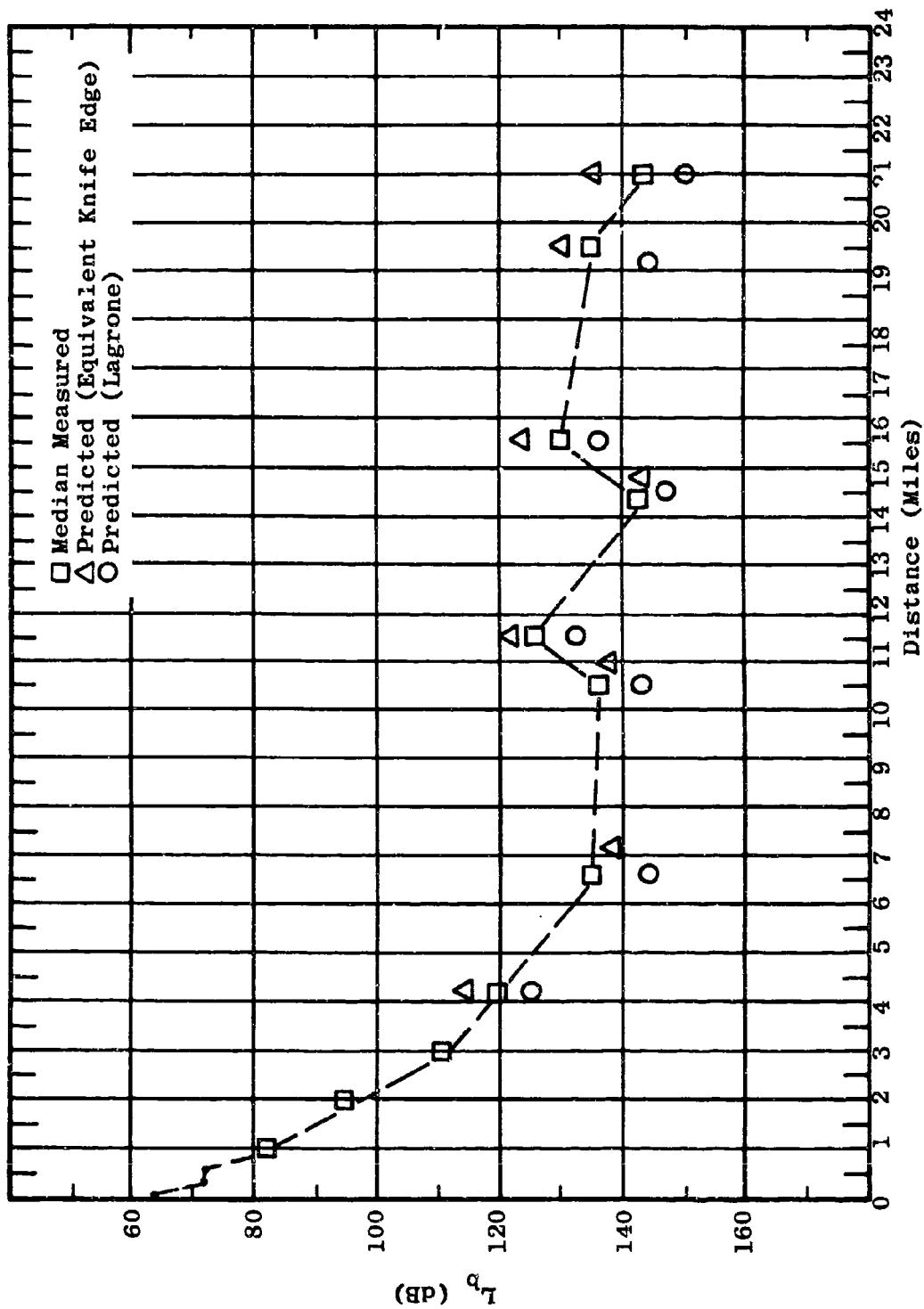


Figure 5.97 Comparison of Measured and Predicted Path Losses
 $L_b = F_B(50, 80, H\&V, d, 80)$

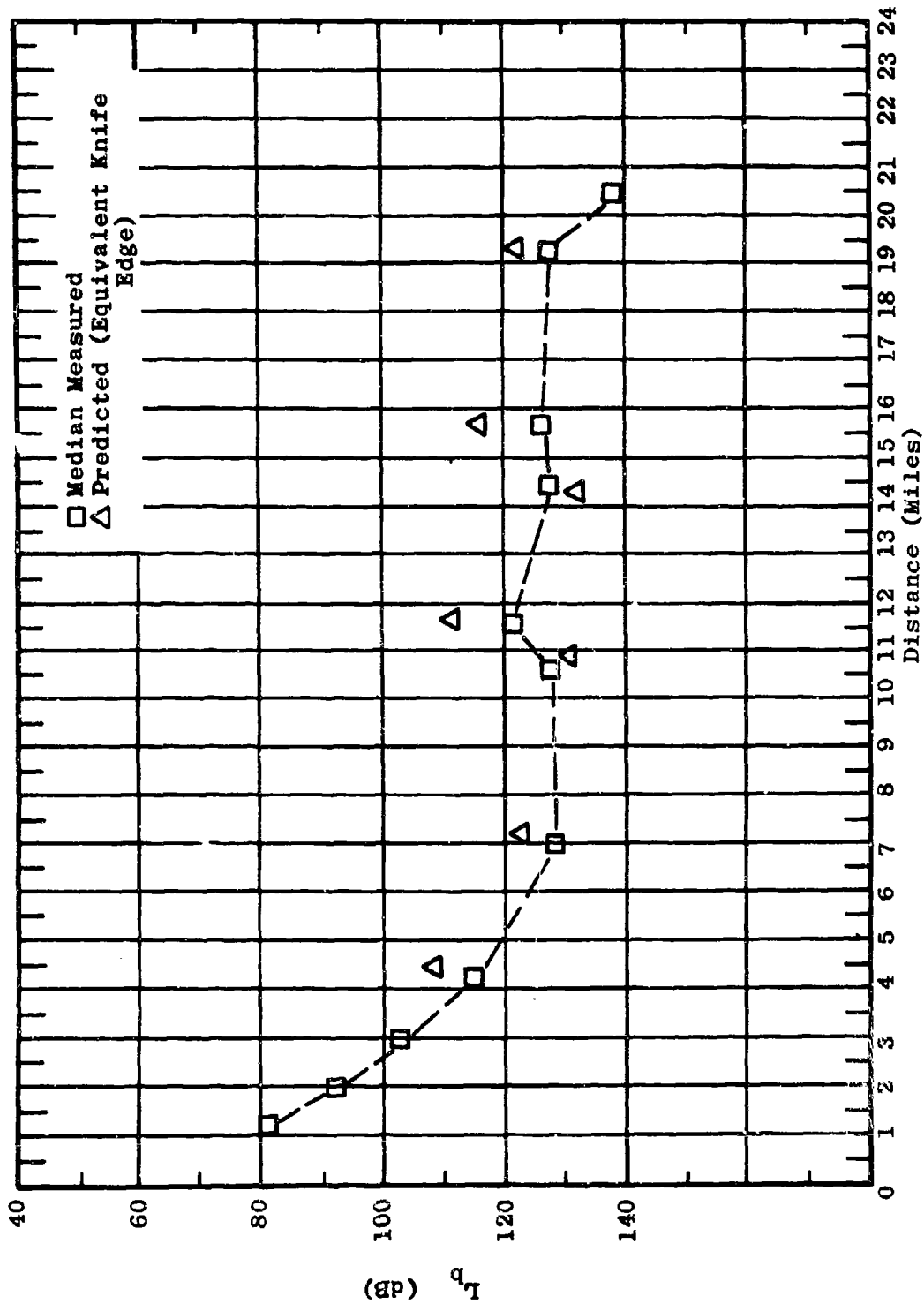


Figure 5.98 Comparison of Measured and Predicted Path Losses
 $L_p = F_B(25, 80, H\&V, d, 80)$

d_n = effective distance between
hill and receiver
 h_r = height of receiver relative to
first valley
 d_o = effective distance between
receiver and first valley

K_1 changes with frequency in order to explain the change in shadow loss with frequency. LaGrone uses $K_1 = 1.6$ for the VHF range. K_2 is the bias level by which the smooth-earth curve must be increased to coincide with the median loss over rough terrain. LaGrone uses $K_2 = 22$ dB for the VHF range. The exponential terms inside the brackets give the deviation of the field about the median. It is important to note that only the close-in gross terrain features to the receiver will contribute significantly to the deviation about the median. For the type of terrain in the Pak Chong area only features within about 2 miles of the receiver contribute to the deviation.

In the modified method, the constant K_1 is made to vary only with frequency whereas K_2 is made to vary with frequency and the number of diffractors encountered. Clearly LaGrone's constant of 22 dB will not work for a single knife edge and probably not for two knife edges. The values of K_1 and K_2 which were derived from the Radial A data are given in Table 5.19. For the frequencies that were used in fitting this model to the measured data, Table 5.19 shows that 25 and 50 Mc/s signals were both affected the same amount by terrain diffraction. However, the 100 Mc/s signal had a higher multiplicative factor, K_1 , but for the case of 2 diffractors, it has a lower bias value, K_2 . The method of evaluating these constants is described later.

Table 5.19

CONSTANTS FOR MODIFIED
LAGRONE MODEL

Fre- quency Mc/s	K_1	K ₂ (dB) For a Given No. of Diffractors		
		1	2	3 or more
25	1.0	0	17	25
50	1.0	0	17	25
100	1.6	0	10	25

The modified LaGrone model is used in the following manner.

1. Construct the gross terrain profile between transmitter and receiver (from topographical map)
2. Compute the deviation from median by the LaGrone method, i.e., all terms inside the brackets of LaGrone Model equation
3. Using a straight edge determine the number of diffractors. An object may be considered as a diffractor even though it does not touch an L.O.S. ray. (see drawing below)



Rough earth path with five diffractors

4. Compute the smooth earth loss using either the interference region, transhorizon region or beyond horizon regions.
5. Knowing the frequency and number of diffractors select K_1 and K_2 from the above table.
6. Insert the applicable numbers into the Modified LaGrone Equation, shown below. This equation holds for treeless terrain or antennas elevated above foliage.

$$L_b = L_b \text{ (smooth earth)} + K_1 \text{ deviation} + K_2 \quad (7)$$

The above equation gives the predicted loss via modified LaGrone method. This equation can also be used to predict the loss for a transmitter or receiver immersed in foliage, simply by adding the median height gain derived from measurements, that is,

$$L_b = L_b \text{ (smooth earth)} + K_1 \text{ deviation} + K_2 + \text{height gain function} \quad (8)$$

The constant, K_2 , that accounts for the actual number of diffractors in the path was empirically determined as follows. Observations of the topographical map for radials A and B revealed that the number of diffractors between the transmitter and the various field points varied from zero for close-in points to four or five for the further out points. Radial A offered the best selection of well defined obstacles between transmitter and receiving, so it was selected over Radial B. Only diffraction cases

were considered. The first paths considered were FPA5 and FPA5.5 with one diffractor. (See Figure 5.99.) Using LaGrone's expression without the constant, K_2 , the basic transmission loss was calculated at 100 Mc/s for the above cases. The calculated losses were subtracted from the corresponding measured losses for 80 foot antennas. This difference was then assigned to K_2 . For FPA5 and FPA5.5 this difference was essentially zero.

Next, field points on Radial A containing two major diffractors were examined. Only FPA6 has two obstacles. (See Figure 5.100.) Again, the LaGrone calculation without K_2 was made and subtracted from measured data for 80 foot antenna heights. This time about 10 dB of residual loss was obtained and assigned to K_2 . Next, paths with three major diffractors were examined. (See Figure 5.101.) Field points 7 and 8 were considered to be in this category. Notice that Figure 5.101 shows two obstacles touching the LOS rays for both cases. However, one or two other obstacles are very close to the LOS rays. These obstacles are probably in the first Fresnel ellipse and are questionable. The number of diffractors probably should be considered as three or more for these cases. The LaGrone computations were made and again subtracted from measurements for 80 foot antennas. This time a residual loss of about 25 dB was obtained and assigned to K_2 . Other field points on Radial A containing three or more diffractors, as shown in Figure 5.102, were examined and in each case a residual loss of about 25 dB was observed. This led to the speculation that a saturation effect takes place when more than three diffracting obstacles are there.

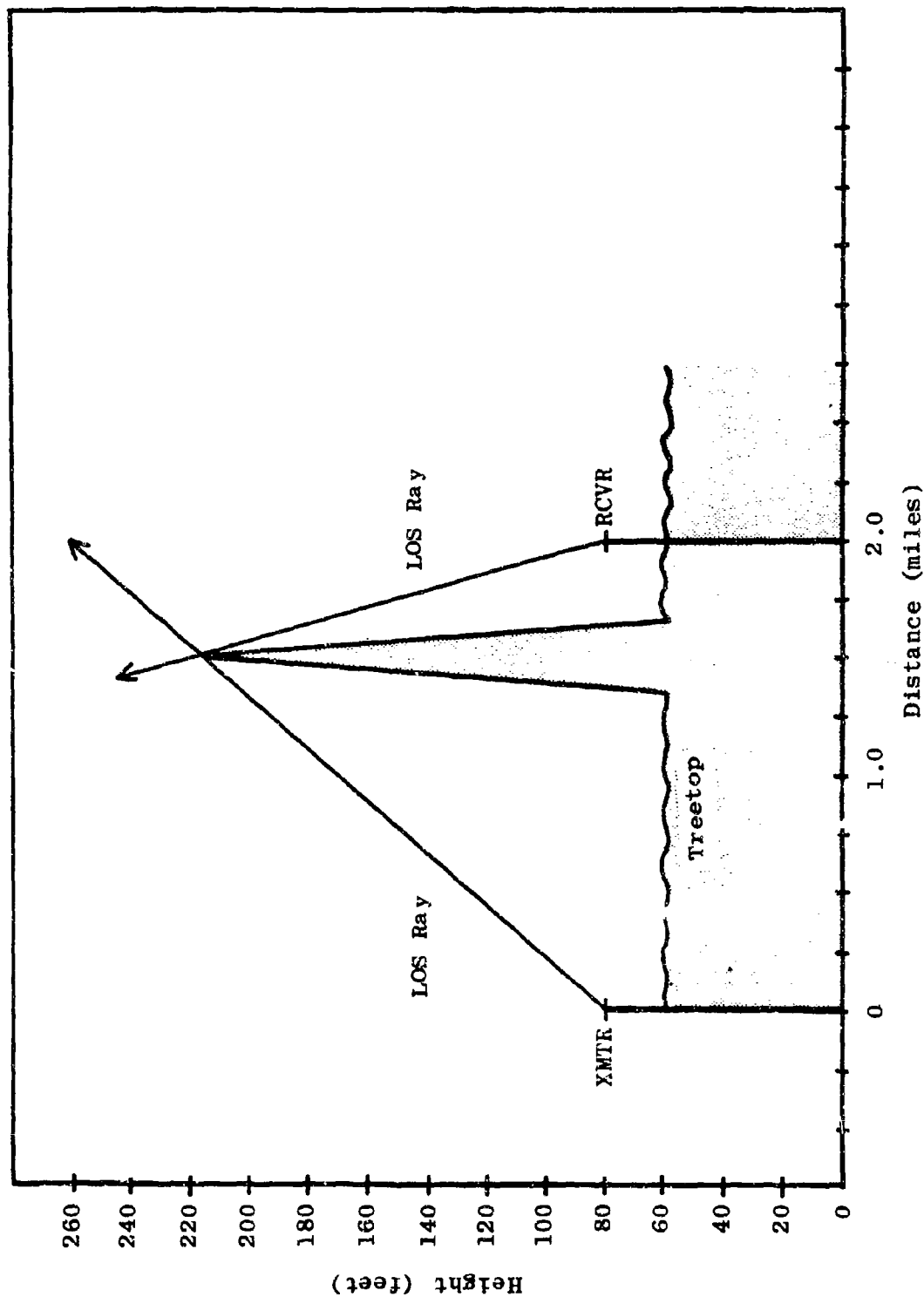


Figure 5.99 Terrain Profile Showing Major Obstacles for FPA-5

NOTE: FPA-5.5 Same as Above Except $d=3$ miles, $H=280$ feet

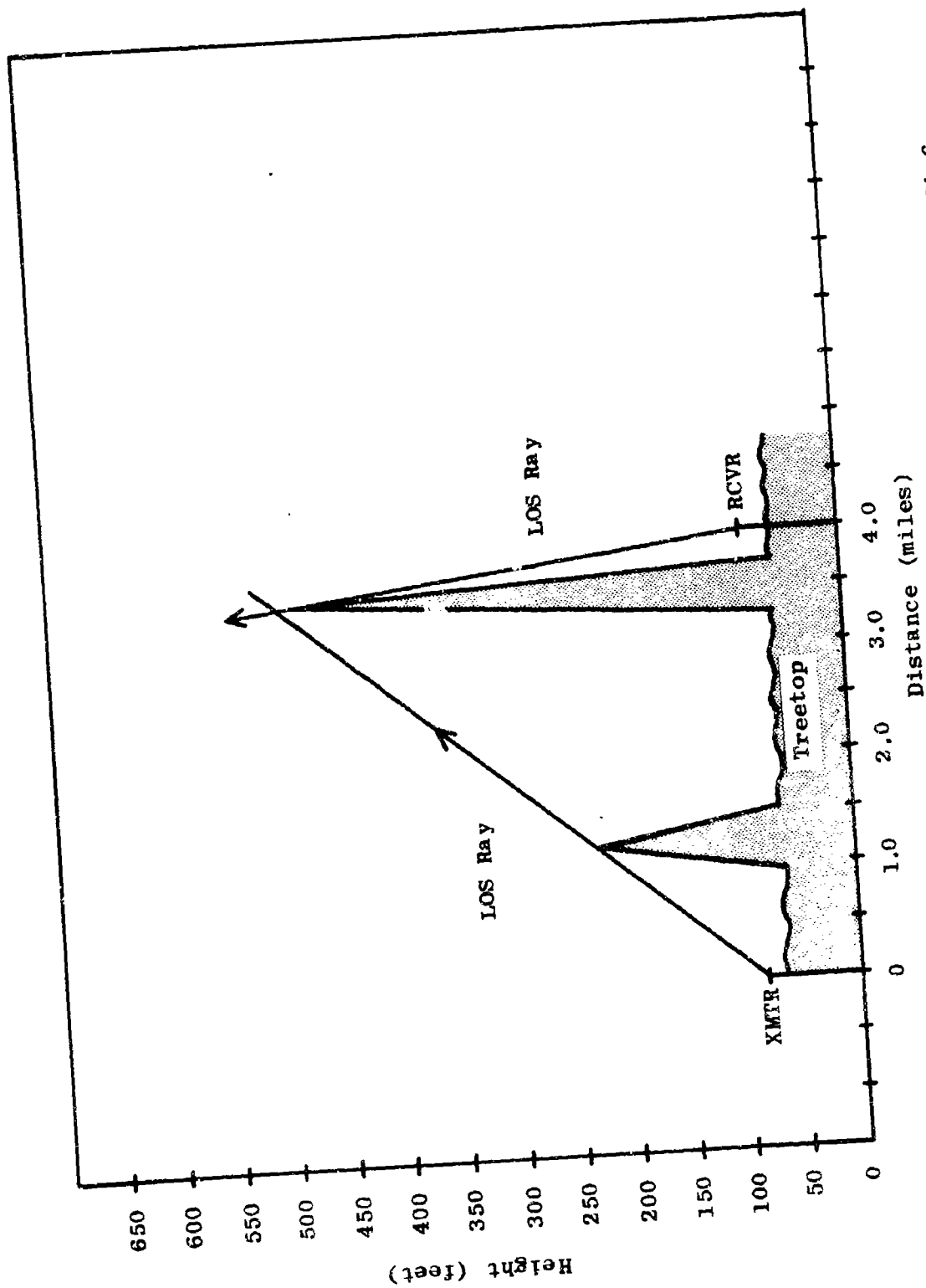


Figure 5.100 Terrain Profile Showing Major Obstacles for FPA-6

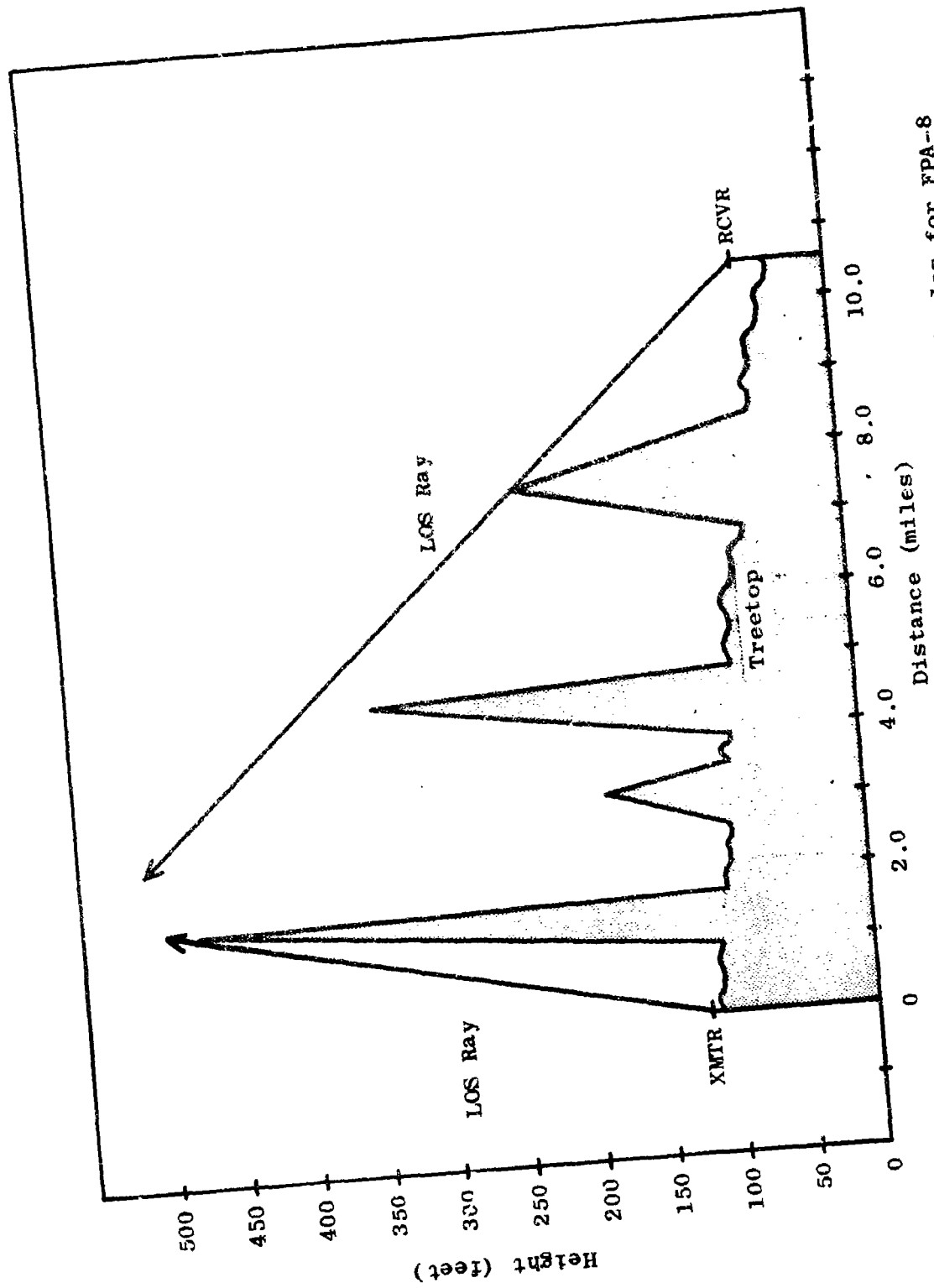


Figure 5.101 Terrain Profile Showing Major Obstacles for FPA-8

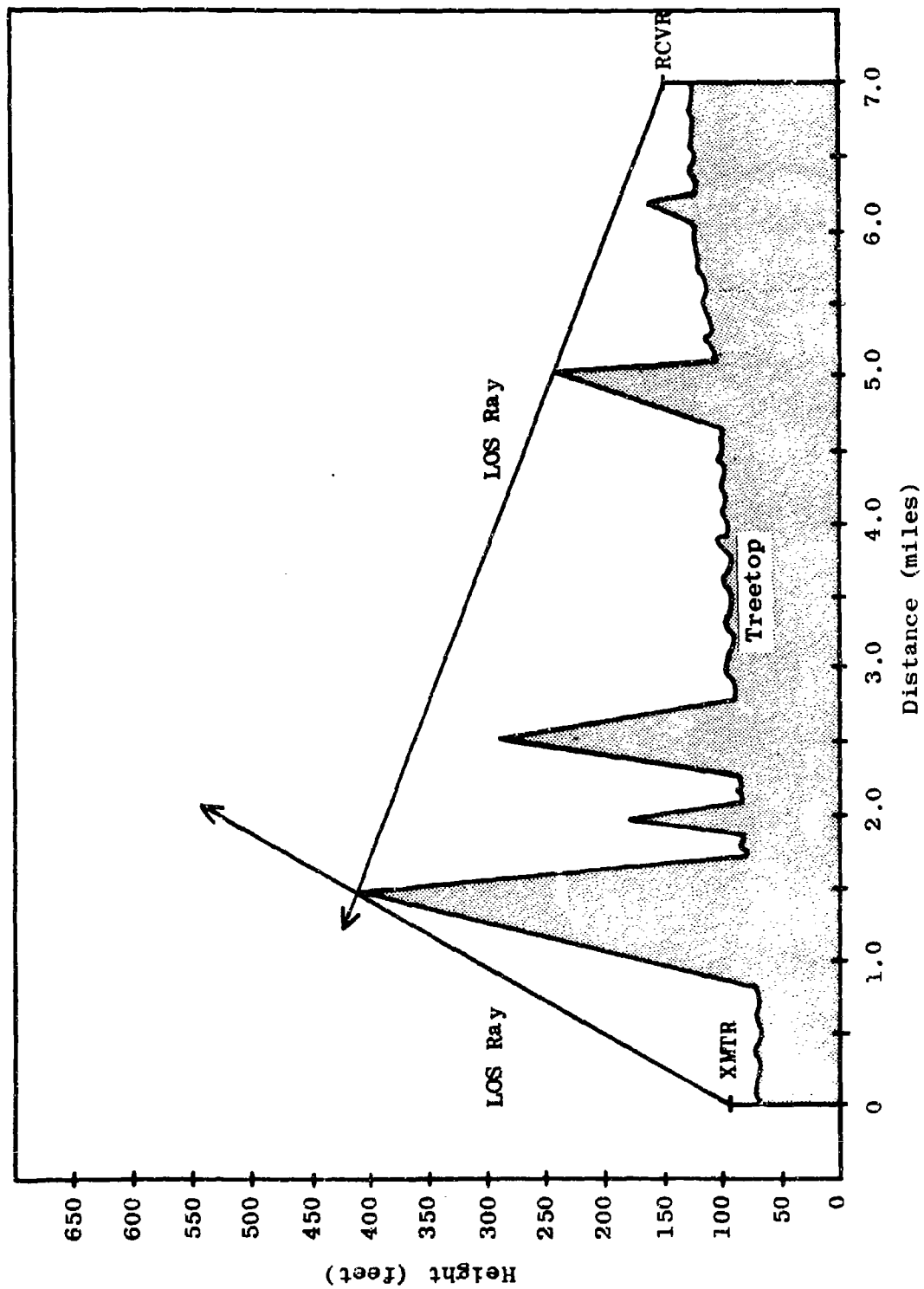
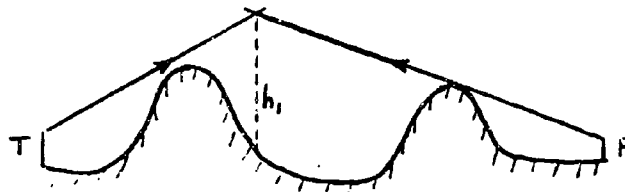


Figure 5.102 Terrain Profile Showing Major Obstacles for FPA-7

5.5.4.2 Equivalent Knife-Edge Model

The equivalent knife-edge method essentially involves the computation of knife-edge diffraction loss for a single equivalent diffractor and then adding the constants that account for multiple diffractors. An equivalent knife edge is created by the intersection of the two radio horizon rays as shown below.



Equivalent knife edge given by h_1

The equation expressing the total loss is then given by:¹⁵

$$L_b = L_b(fs) + A(v) + K_2 \text{ (for 80 foot antennas)} \quad (9)$$

where

$L_b(fs)$ = free space basic transmission loss

$A(v)$ = diffraction loss for equivalent knife edge

K_2 = empirical constant representing the true number of diffractors in the path (same as for LaGrone model)

When the loss is desired for a terminal point immersed in foliage the equation becomes:

$$L_b = L_b(fs) + A(v) + K_2 + \text{height gain function} \quad (10)$$

Where the height gain function gives the median value derived from measurements.

5.6 Climatological Data

The effects of climatic phenomena on radio propagation loss change with location and time. These effects are generally related to the influence of climate on the dielectric constant of the atmosphere in the propagation path and, more indirectly, to its influence on the electrical properties of the ground and vegetation in the path. Also, the degree of these effects will depend upon frequency, the separation distance, and the directivity of the antennas. Although the cause-effect relationships are well understood from a phenomenological view, it is generally not possible to reduce any given practical situation to a mathematically analytical state. Therefore, a study of the influence of the climate on radio path loss must first rely on the techniques of statistical correlation. In order to provide a base of climatic data for an examination of the various correlations between climatic conditions and path loss, climatological data has been taken on a daily basis since the beginning of the measurement program in Thailand.

Data on hand covers the period from February 1964 to July 1966 and represents four types of measurements:

(1) wet bulb temperature, (2) dry bulb temperature, (3) barometric pressure, and (4) rainfall. The temperature and pressure readings were made at the base camp three times daily. Rainfall samples were taken three times a day at the base site prior to March 1965, when automatic rain gauge recorders were installed at five different locations in the test area to provide continuous monitoring of the cumulative rainfall.

All rainfall sampling points are either in Sectors A or B, where the field strength measurements were taken. Figure 5.103 shows the general locations of the sampling points. The monthly cumulative rainfall at each of the measurement points is shown in Table 5.20. This table also shows the monthly average rainfall for Sector A and Sector B individually as well as the overall average for all five measurement points.

The unusually high rainfall recorded at FPB-10 deserves special notice. This recording point is on the north slope of a ridge of a mountain known as Khao Khieo. The mountain and its ridge are some 1200 meters above sea level, and the recording point is about 440 meters lower. Because the ridge system runs in a northeasterly direction, it effectively shelters the recording site from the prevailing due-east wind in this region. Thus, a low-pressure system can be expected to prevail over the recording point, promoting a high rainfall. The data from this point is also indicative of the wide variation in climatic data that is typical of regions with steep mountains and ridges.

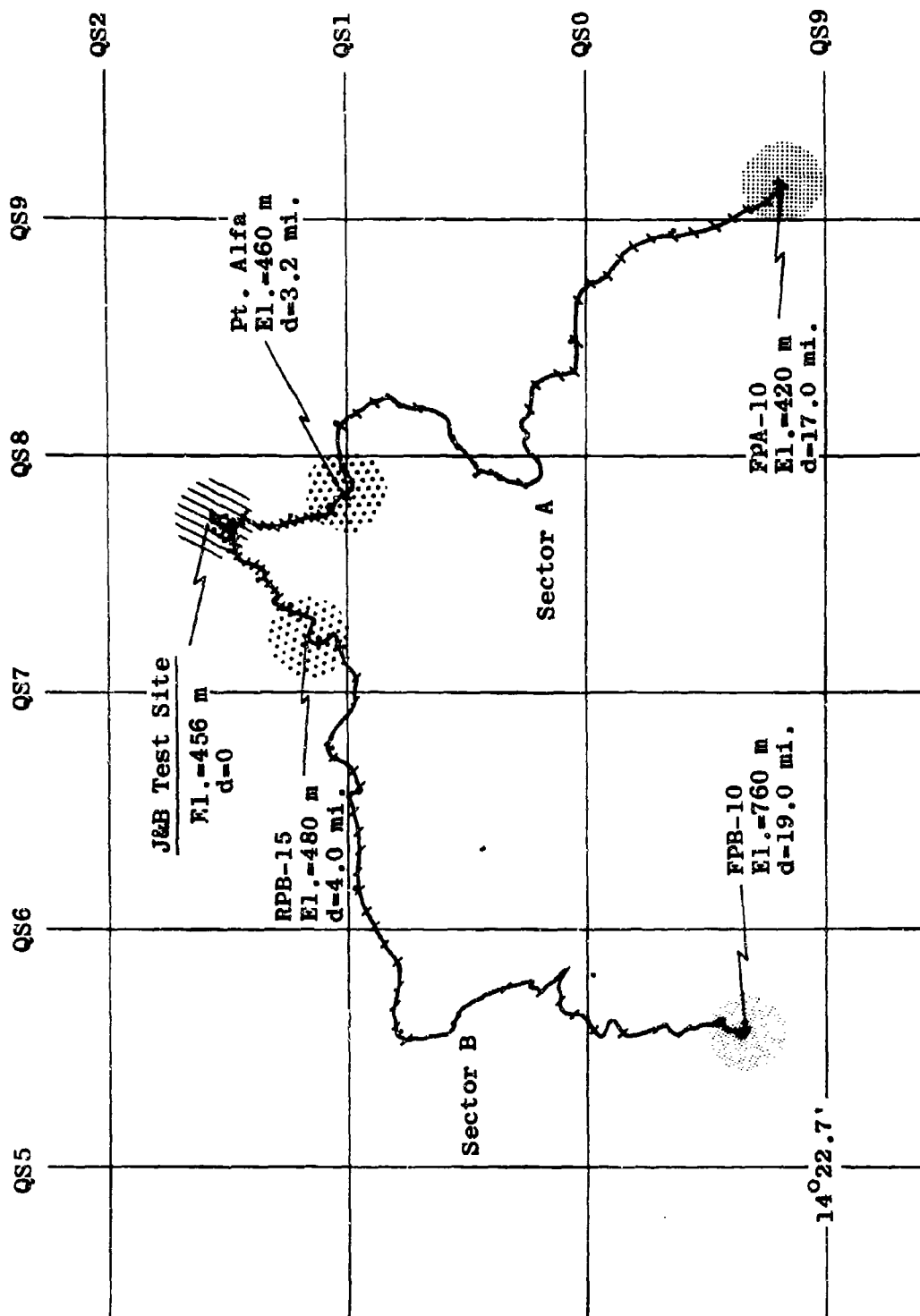


Figure 5.103 Rainfall Measurement Points

Table 5.20

CUMULATIVE MONTHLY RAINFALL (INCHES)

Year	Month	Base Site	Sector A		Sector B		Sector A Avg.	Sector B Avg.	Avg. All 5 Meas. Pts.
			Pt. Alpha	FPA-10	FPB-15	FPB-10			
1964	Feb	0.22							
1964	Mar	2.92							
1964	Apr	7.31							
1964	May	11.66							
1964	June	0.23							
1964	July	7.29							
1964	Aug	6.81							
1964	Sept	10.11							
1964	Oct	10.12							
1964	Nov	1.39							
1964	Dec	0.05							
1965	Jan	0.00							
1965	Feb	1.30							
1965	Mar	3.53							
1965	Apr	3.35							
1965	May	8.88							
1965	June	3.24							
1965	July	2.78							
1965	Aug	6.73							
1965	Sept	11.28							
1965	Oct	5.55							
1965	Nov	1.34							
1965	Dec	0							
1966	Jan	0							
1966	Feb	1.63							
1966	Mar	0.36							
1966	Apr	7.27							
1966	May	11.41							
1966	June	1.16							
1966	July	2.37							

--	--	--	--	--	--	--	--	--	--	--	--	--	--	--	--	--	--	--	--	--	--	--	--	--	--	--	--	--	--	--	--	--	--	--	--	--	--	--	--	--	--	--	--	--	--	--	--	--	--	--	--	--	--	--	--	--	--	--	--	--	--	--	--	--	--	--	--	--	--	--	--	--	--	--	--	--	--	--	--	--	--	--	--	--	--	--	--	--	--	--	--	--	--	--	--	--	--	--	--	--	--	--	--	--	--	--	--	--	--	--	--	--	--	--	--	--	--	--	--	--	--	--	--	--	--	--	--	--	--	--	--	--	--	--	--	--	--	--	--	--	--	--	--	--	--	--	--	--	--	--	--	--	--	--	--	--	--	--	--	--	--	--	--	--	--	--	--	--	--	--	--	--	--	--	--	--	--	--	--	--	--	--	--	--	--	--	--	--	--	--	--	--	--	--	--	--	--	--	--	--	--	--	--	--	--	--	--	--	--	--	--	--	--	--	--	--	--	--	--	--	--	--	--	--	--	--	--	--	--	--	--	--	--	--	--	--	--	--	--	--	--	--	--	--	--	--	--	--	--	--	--	--	--	--	--	--	--	--	--	--	--	--	--	--	--	--	--	--	--	--	--	--	--	--	--	--	--	--	--	--	--	--	--	--	--	--	--	--	--	--	--	--	--	--	--	--	--	--	--	--	--	--	--	--	--	--	--	--	--	--	--	--	--	--	--	--	--	--	--	--	--	--	--	--	--	--	--	--	--	--	--	--	--	--	--	--	--	--	--	--	--	--	--	--	--	--	--	--	--	--	--	--	--	--	--	--	--	--	--	--	--	--	--	--	--	--	--	--	--	--	--	--	--	--	--	--	--	--	--	--	--	--	--	--	--	--	--	--	--	--	--	--	--	--	--	--	--	--	--	--	--	--	--	--	--	--	--	--	--	--	--	--	--	--	--	--	--	--	--	--	--	--	--	--	--	--	--	--	--	--	--	--	--	--	--	--	--	--	--	--	--	--	--	--	--	--	--	--	--	--	--	--	--	--	--	--	--	--	--	--	--	--	--	--	--	--	--	--	--	--	--	--	--	--	--	--	--	--	--	--	--	--	--	--	--	--	--	--	--	--	--	--	--	--	--	--	--	--	--	--	--	--	--	--	--	--	--	--	--	--	--	--	--	--	--	--	--	--	--	--	--	--	--	--	--	--	--	--	--	--	--	--	--	--	--	--	--	--	--	--	--	--	--	--	--	--	--	--	--	--	--	--	--	--	--	--	--	--	--	--	--	--	--	--	--	--	--	--	--	--	--	--	--	--	--	--	--	--	--	--	--	--	--	--	--	--	--	--	--	--	--	--	--	--	--	--	--	--	--	--	--	--	--	--	--	--	--	--	--	--	--	--	--	--	--	--	--	--	--	--	--	--	--	--	--	--	--	--	--	--	--	--	--	--	--	--	--	--	--	--	--	--	--	--	--	--	--	--	--	--	--	--	--	--	--	--	--	--	--	--	--	--	--	--	--	--	--	--	--	--	--	--	--	--	--	--	--	--	--	--	--	--	--	--	--	--	--	--	--	--	--	--	--	--	--	--	--	--	--	--	--	--	--	--	--	--	--	--	--	--	--	--	--	--	--	--	--	--	--	--	--	--	--	--	--	--	--	--	--	--	--	--	--	--	--	--	--	--	--	--	--	--	--	--	--	--	--	--	--	--	--	--	--	--	--	--	--	--	--	--	--	--	--	--	--	--	--	--	--	--	--	--	--	--	--	--	--	--	--	--	--	--	--	--	--	--	--	--	--	--	--	--	--	--	--	--	--	--	--	--	--	--	--	--	--	--	--	--	--	--	--	--	--	--	--	--	--	--	--	--	--	--	--	--	--	--	--	--	--	--	--	--	--	--	--	--	--	--	--	--	--	--	--	--	--	--	--	--	--	--	--	--	--	--	--	--	--	--	--	--	--	--	--	--	--	--	--	--	--	--	--	--	--	--	--	--	--	--	--	--	--	--	--	--	--	--	--	--	--	--	--	--	--	--	--	--	--	--	--	--	--	--	--	--	--	--	--	--	--	--	--	--	--	--	--	--	--	--	--	--	--	--	--	--	--	--	--	--	--	--	--	--	--	--	--	--	--	--	--	--	--	--	--	--	--	--	--	--	--	--	--	--	--	--	--	--	--	--	--	--	--	--	--	--	--	--	--	--	--	--	--	--	--	--	--	--	--	--	--	--	--	--	--	--	--	--	--	--	--	--	--	--	--	--	--	--	--	--	--	--	--	--	--	--	--	--	--	--	--	--	--	--	--	--	--	--	--	--	--	--	--	--	--	--	--	--	--	--	--	--	--	--	--	--	--	--	--	--	--	--	--	--	--	--	--	--	--	--	--	--	--	--	--	--	--	--	--	--	--	--	--	--	--	--	--	--	--	--	--	--	--	--	--	--	--	--	--	--	--	--	--	--	--	--	--	--	--	--	--	--	--	--	--	--	--	--	--	--	--	--	--	--	--	--	--	--	--	--	--	--	--	--	--	--	--	--	--	--	--	--	--	--	--	--	--	--	--	--	--	--	--	--	--	--	--	--	--	--	--	--	--	--	--	--	--	--	--	--	--	--	--	--	--	--	--	--	--	--	--	--	--	--	--	--	--	--	--	--	--	--	--	--	--	--	--	--	--	--	--	--	--	--	--	--	--	--	--	--	--	--	--	--	--	--	--	--	--	--	--	--	--	--	--	--	--	--	--	--	--	--	--	--	--	--	--	--	--	--	--	--	--	--	--	--	--	--	--	--	--	--	--	--	--	--	--	--	--	--	--	--	--	--	--	--	--	--	--	--	--	--	--	--	--	--	--	--	--	--	--	--	--	--	--	--	--	--	--	--	--	--	--	--	--	--	--	--	--	--	--	--	--	--	--	--	--	--	--	--	--	--	--

Note: Unattended recording equipment not available during this period.

* Data accumulation began March 10, 1965.

Figure 5.104 presents a comparison of certain significant factors of interest. Only data collected at the base camp was used in this figure. The lower curve gives the monthly cumulative rainfall recorded at the base site, and the upper curves show monthly averages of the other parameters considered factors likely to affect path loss.

The parameter, k , is the effective earth's radius as derived from computed values of surface refractivity. Surface refractivity values, in turn, are derived from measurements of atmospheric pressure, wet bulb temperature and dry bulb temperature.

The climatological data presented in this report is intended to serve basically as a quantitative measure of the climatic parameters with which to study the correlation between variations in these parameters and measured radio path loss.

The weather cycles in the Pak Chong area are divided into two distinct seasons: a wet season which lasts from approximately May 15 until November 15, and a dry season which lasts from approximately November 15 to May 15. The wet season is characterized by frequent and intense rainfalls, by slightly heavier vegetation, and by the almost continual moistness of the ground. During the dry season, a significant amount of rain continues to fall, vegetation is not quite as heavy, and the ground tends to dry out.

Complete sets of propagation loss measurements have been made in each of the two seasons. It is of interest to compare propagation loss between these two seasons to

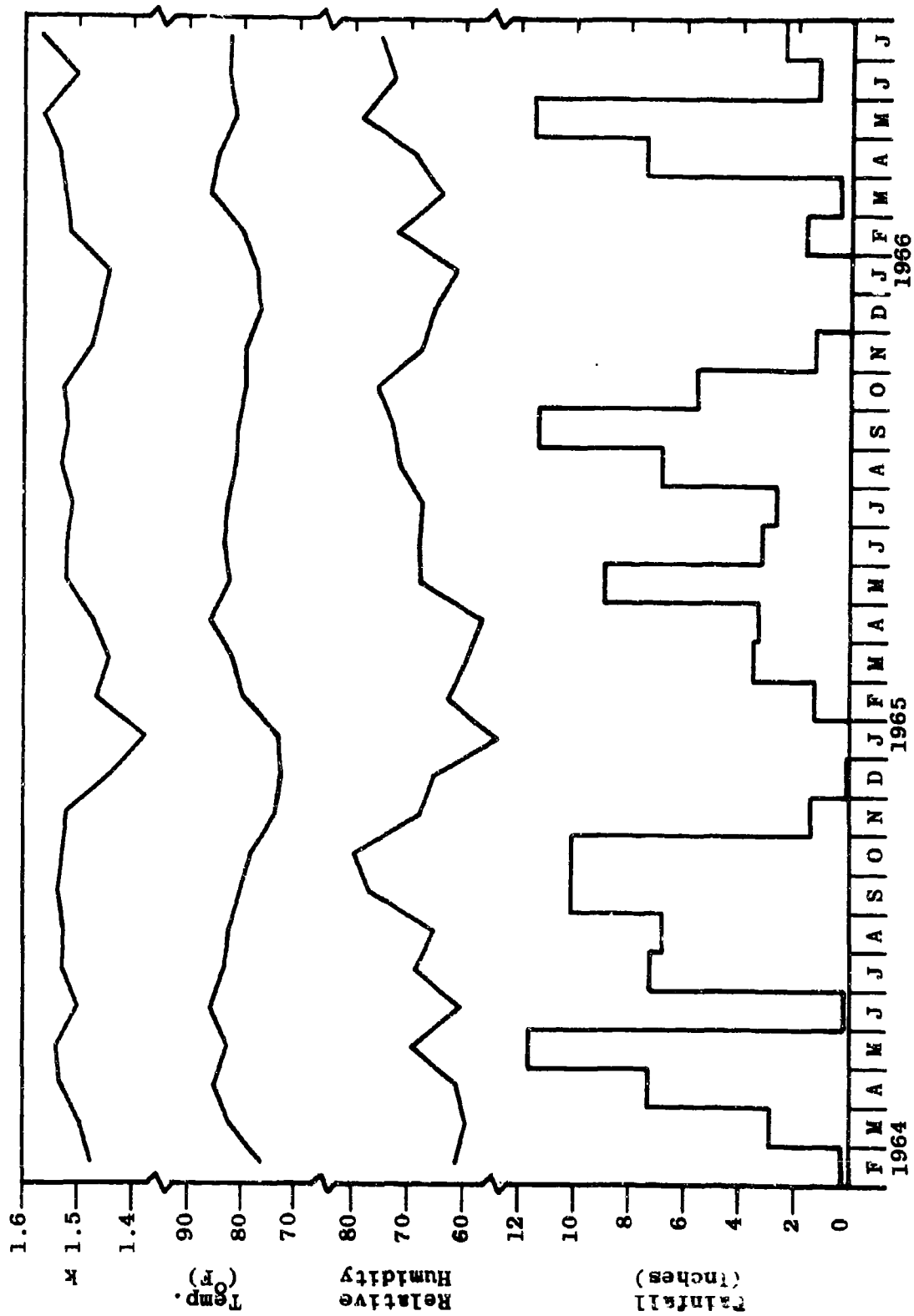


Figure 5.104 Climatological Data

determine if there is a significant difference. If there is a significant seasonal difference in propagation characteristics, it is important to learn if this difference is a function of frequency, antenna height, communication range, or polarization. To begin the study, the wet-dry propagation path-loss differences were tabulated. Intuitively, one would expect the path loss to be greater in the wet season than in the dry season. Therefore, the differences were taken so that greater wet-season losses would lead to positive differences, and greater dry-season losses would lead to negative differences.

The tabulated path-loss differences were then grouped in the following manner. Two distinct distance categories were established: short range and long range. The short-range category applies to all path distances from 0.2 mile to 1 mile. The long-range distance category includes all distances greater than 1 mile. The data was also grouped according to antenna heights: low, medium and high. The low antenna category includes all cases for which both antennas had heights of less than 26 feet. The medium antenna category includes all cases in which both antennas were between 26 and 59 feet. The high antenna category includes all cases for which both antennas were higher than 59 feet. All ground-based antennas, regardless of length, were considered to be low antennas. Additional categorizations by frequency and polarization were made. Table 5.21 gives the number of wet-dry difference samples which were available in each of the categories. In only a few cases were there no samples available. The median wet-dry difference in each of the categories is presented in Table 5.22.

Table 5.21
NUMBER OF SAMPLES USED IN WET-DRY COMPARISON

Freq. (Mc/s)	Antenna Height	Number of Samples			
		Short Range Vert.	Long Range Vert.	Short Range Horiz.	Long Range Horiz.
0.100	Low	52	52	-	-
0.300	Low	52	52	-	-
0.880	Low	65	39	-	-
2	Low	100	38	100	37
6	Low	100	25	88	60
12	Low	100	46	101	65
	Low	24	14	24	23
25	Medium	40	34	40	40
	High	40	40	40	40
	Low	12	6	21	21
50	Medium	40	36	40	38
	High	40	40	39	40
	Low	24	9	24	13
100	Medium	40	30	40	30
	High	40	35	40	40
	Low	18	0	11	0
250	Medium	40	12	40	9
	High	40	15	40	20
	Low	6	0	0	0
400	Medium	37	0	18	0
	High	40	18	40	15

Table 5.22
MEDIAN WET-DRY PATH LOSS DIFFERENCE

Freq. (Mc/s)	Antenna Height	Median Difference (dB)			
		Short Range Vert.	Long Range Vert.	Short Range Horiz.	Long Range Horiz.
0.100	Low	-1	0	-	-
0.300	Low	0	0	-	-
0.880	Low	-2	-1	-	-
2	Low	3	2	2	3
6	Low	3	1	0	2
12	Low	0	0	1	2
	Low	1	2	0	1
25	Medium	-2	-1	0	1
	High	-1	0	0	1
	Low	-2	0	2	0
50	Medium	0	0	2	0
	High	2	2	2	0
	Low	-1	3	-3	4
100	Medium	0	2	1	1
	High	-1	3	0	1
	Low	0	-	2	-
250	Medium	3	5	7	6
	High	0	2	2	1
	Low	3	-	4	-
400	Medium	-4	-	7	-
	High	1	1	4	2
Average Difference		0.1	1.2	1.8	1.7

The overall average difference is given at the bottom of Table 5.22. The overall median wet-dry difference varied from about -3 dB to about +7 dB. The overall averages were positive, but small, indicating that there is a slightly greater loss on the average during the wet season. The differences for vertical polarization tended to be slightly smaller than for horizontal polarization, particularly at higher frequencies. The wet-dry differences tend to increase with increasing frequency for horizontal polarization but appear to have no consistent variation with frequency for vertical polarization. The difference tends to be slightly higher for the long-range category for vertical polarization. For horizontal polarization, the short-range and long-range differences tend to be approximately the same.

Although the data shows that there is no distinctive difference between major seasonal cycles, there could still be some question about the influence of periods of relatively heavy rainfall on propagation loss. In order to gain an insight into the more immediate effects of rainfall, the following two correlations were attempted. First, the total rainfall in the 24-hour period immediately preceding each measurement was tabulated. Then, the differences in rainfall for the 24-hour period immediately preceding each measurement were correlated with the differences in path loss. This analysis showed that there was no correlation between these two parameters. A similar correlation was attempted using the total rainfall in the 7-day period immediately preceding each measurement. Again, there appeared to be no correlation between total weekly rainfall and propagation loss.

5.7 Radio Noise Measurements

The experimental program in Thailand includes measurements of radio noise in the vegetation of the test area, using the same equipment normally employed for making field strength measurements. These measurements were made at all test frequencies below 50 Mc/s and were intended to serve three purposes. First, the measurements were sometimes needed to correct the field strength readings at certain test frequencies when the field strength level began to approach the noise level. Second, the measurements were used to examine the possibility that the radio noise level might be a function of receiving antenna height in the vegetation. Third, the collection of noise data serves the ultimate purpose of characterizing the noise environment of the Thailand area in relation to other areas where similar measurements have been made, or may be made in the future.

Before presenting the results of the noise measurements, it is important to understand some of the basic complexities involved in accurately measuring atmospheric noise levels. The following sub-sections review some of the latest techniques used in analyzing the effects of atmospheric noise on radio transmission, and describe the equipment presently used to measure the desired noise parameters.

5.7.1 General Background

When communications equipment is operated at frequencies of less than about 50 Mc/s, atmospheric noise

determines the minimum allowable signal level for a given grade of service. For higher frequencies, thermal noise associated with the receiving equipment becomes the dictating factor.

The interference potential of atmospheric noise is a function not only of its average level, but also of its detailed characteristics. Due to the complex nature of the atmospheric noise wave-form, these characteristics are best described by a statistical process, such as the amplitude distribution function. This is simply a plot of instantaneous noise level vs. the probability (based on percent of time) that the level is exceeded.

Early investigators concluded that atmospheric noise behaved exactly as thermal noise, whose amplitude distribution function obeys the Rayleigh law. As a consequence, the interfering potential was thought to be fully assessed by specifying the RMS, average, and peak values of the noise pulses. However, recent work has established that the typical atmospheric noise wave form does not completely follow a Rayleigh distribution, but instead deviates and eventually becomes log-normal at the low probability end of the distribution. The Rayleigh distribution results from the fact that the low-amplitude portions of the components of the wave form are composed of random overlapping events, each containing a small portion of the total energy. As the levels increase in amplitude, less and less random overlapping occurs until the extreme low end of the amplitude distribution function is composed of widely spaced, discrete components.

The National Bureau of Standards, through the use of a measurement system capable of responding to and recording the instantaneous noise envelope, has accumulated numerous amplitude distributions at various locations throughout the world. The shape of the distribution was found not to change significantly from one location to another, although the RMS level varied over a wide range. This uniformity of shape of the distribution as a function of time and location has made it feasible to accurately predict the amplitude distribution when a few of the measured statistical parameters in the time domain are known. Special equipment, which has been designed to measure these statistical parameters, now operates on a continuous recording basis at selected points around the world. Present theoretical work being done at the National Bureau of Standards is directed toward methods of transforming the amplitude distribution function from the bandwidth of the measuring device to any desired bandwidth of interest.

The RMS, peak and average values of atmospheric noise, however, vary with bandwidth in a simple, predictable fashion. These relationships were experimentally determined and have been used for many years.

When the peak, average, and RMS voltages are plotted versus the bandwidth of the measuring equipment on a log-log graph, the plots are approximately straight lines of similar slopes. On an average, the slopes indicate that the peak, average, and RMS voltage levels all vary approximately as the square root of the bandwidth. Due to slight variations in the structure of atmospheric noise as a function of time and location, the slopes of the lines

will vary over a small range that depends on the particular sample. Thus, to convert noise level data from one bandwidth to another, it is only necessary to multiply the level by the square root of the ratio of bandwidths, and this procedure is used in this study.

Generally speaking, the variations in atmospheric noise levels within a given geographical region are much greater and more dynamic in the time and frequency domains than in the spatial domain. The methods of instrumentation to comprehensively study noise behavior must, therefore, be capable of sensing and recording widely separated and rapidly varying levels as a function of time. Also, an extended time span and a large amount of data are required for thorough analysis. In this regard, the Thailand noise measurements cannot be considered a comprehensive study of noise behavior. Rather, these measurements were designed to serve a limited set of specific objectives, as described previously in this section. However, the noise measurements thus far obtained do afford some insight into the behavior of radio noise in the test area, and the results of these measurements are discussed at the end of this section.

5.7.2 Measuring Device Limitations

Noise levels were measured using the Empire Devices NF-105 field strength meter with the detector circuitry operated in the "peak" mode. When operated in this mode, the "charge" time of the detector is shortened and the "discharge" time lengthened. This allows the detector to rapidly respond to increases of the noise wave form and

to be less sensitive to decreases of the wave form. Thus the detector tends to seek out and hold the peaks of the incoming noise. Detectors that operate in the manner just described work best when the pulse duration is at least as long as the "charge" time and the pulse repetition rate is much faster than the "discharge" time constant. If these conditions are met, the detector output can be expected to accurately respond to the noise peaks. However, when measuring atmospheric noise, the duration of the peaks is usually short, and the repetition rate usually varies over a wide range, especially in the presence of local discharge. Thus, the peak detector may or may not respond to the true peaks of the wave form. This uncertainty contributes to the disadvantage of using field strength meters to measure a varying complex wave form.

Although noise measurements are uncertain in an absolute sense when using a field strength meter, this method should provide a reliable way to compare measurements in a relative sense. For example, possible changes in noise level with antenna height should show up on a field strength meter. Also the change in noise level with frequency should likewise be reflected in field strength measurements.

When comparing noise measurements presented in this section with results obtained by other measurement devices, the equipment limitations previously discussed should be kept in mind. The field strength meter remains one of the common field devices for measuring noise levels, although more sophisticated equipment is used in specialized situations.

5.7.3 Results of Noise Measurements

Initial noise measurements carried out in foliage involved continuously recording noise as the receiving antenna was moved from 10 feet above ground to about 80 feet. Additional measurements were made as a function of time at a fixed antenna height. Comparison of the two types of data revealed that the "short term" time variation of the noise was about equal to the antenna height variation, indicating that time variations were masking possible height variations.

In an attempt to eliminate time variations the above measurement procedure was altered. Rather than continuously measuring noise as a function of antenna height only, three discrete antenna elevations were selected and the noise was sampled as a function of time at each of these preselected levels. The heights selected were roughly 10, 42 and 80 feet. The median value of noise at each antenna level was recorded as well as the total variation with time.

Samples were accumulated over a three-month period and the overall median value at each antenna height was determined. This data is shown plotted vs. frequency in Figure 5.105 for horizontal polarization. Vertical polarization is plotted in Figure 5.106. The threshold level of the measurement system is shown in each plot. This threshold level is simply the level below which atmospheric noise cannot be detected due to the presence of "set" noise and to the losses in the measuring antenna system. Shown plotted with the measured data are two curves representing

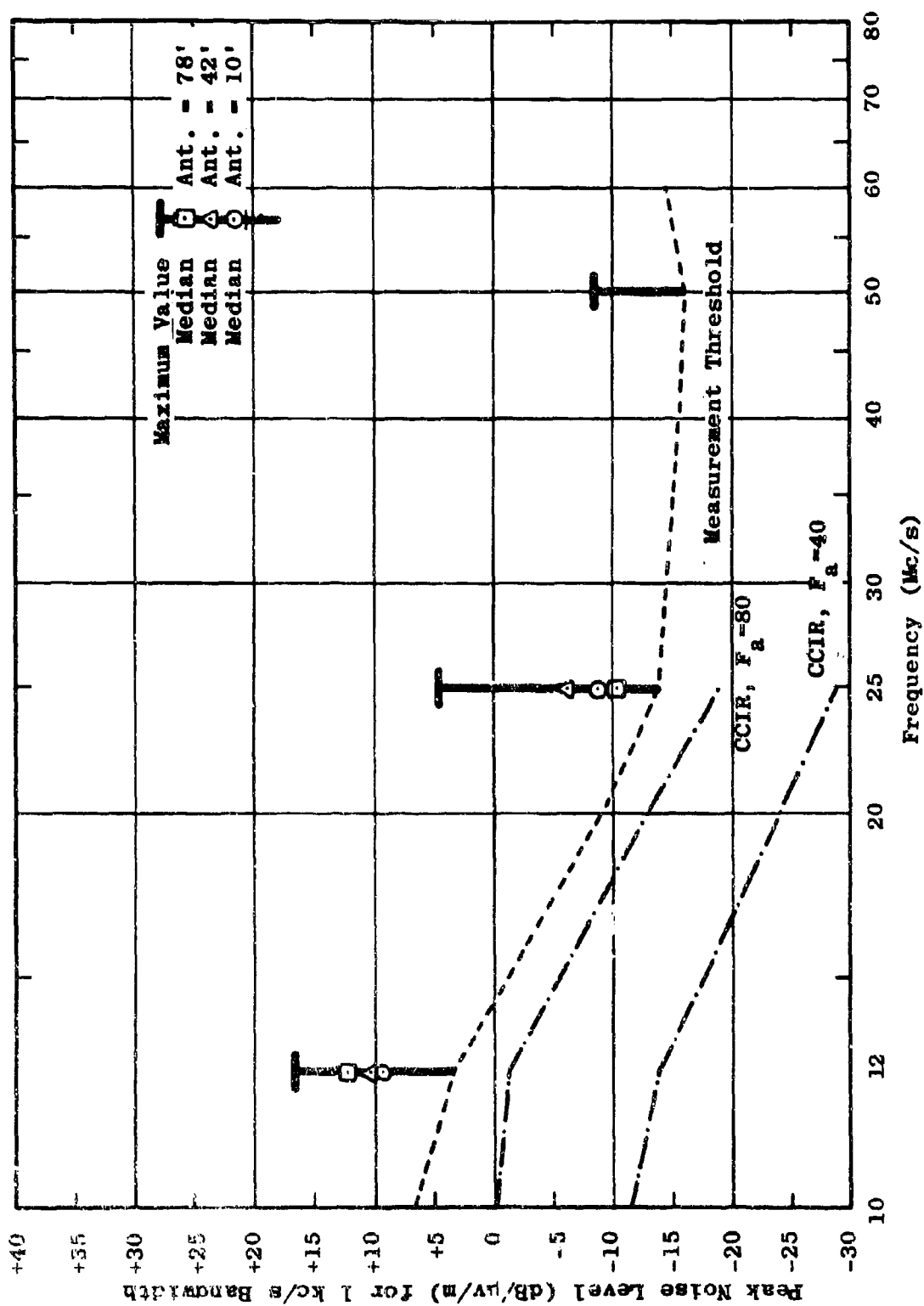


Figure 5.105 Combined Median Noise Levels for Nov., Dec., and Jan.
For Horizontal Polarization

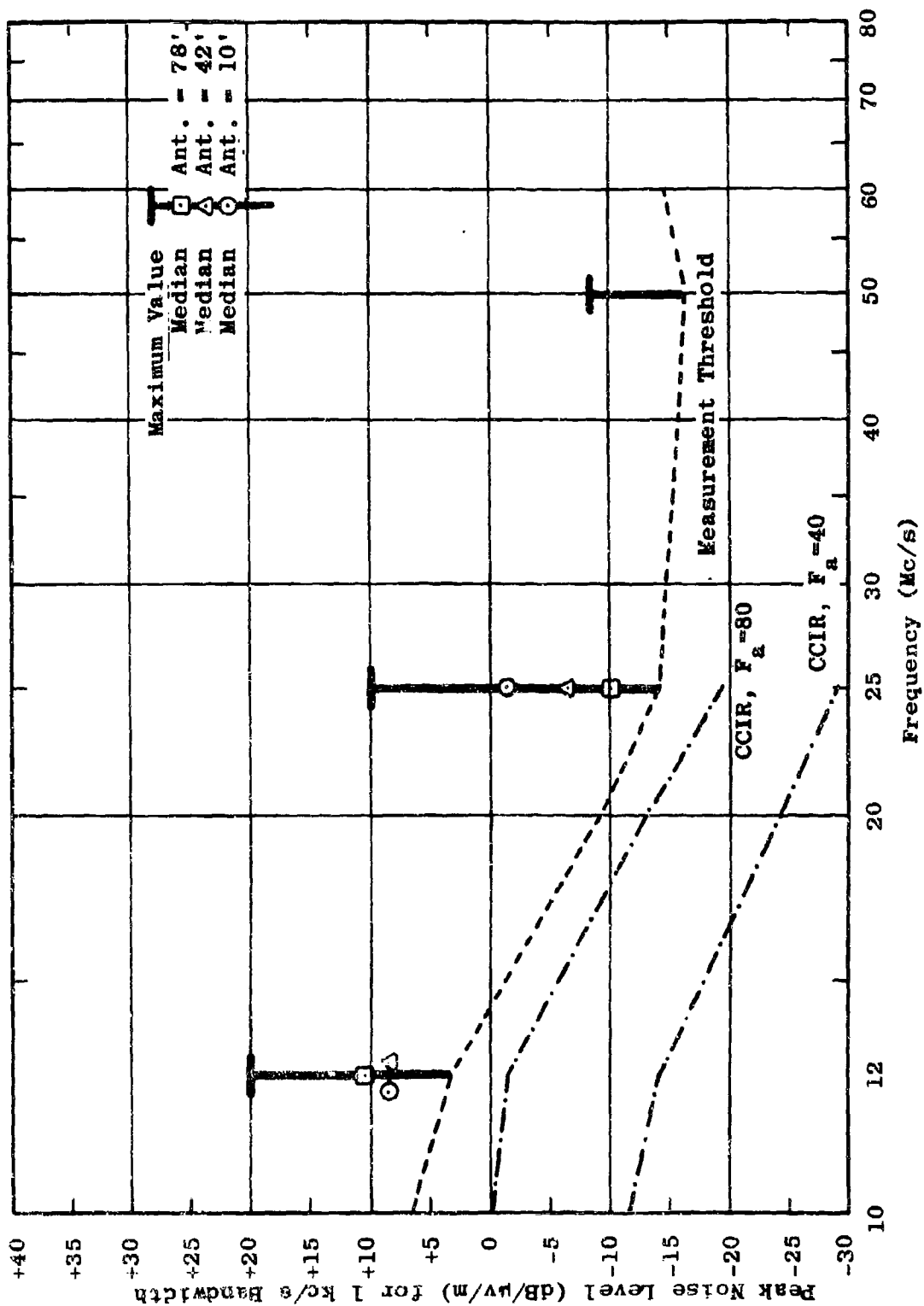


Figure 5.106 Combined Median Noise Levels for Nov., Dec., and Jan.
for Vertical Polarization

noise grades of 40 and 80 which are typical of the noise level variations in Southeast Asia.¹⁶

It should be noted that the noise grade curves represent RMS noise levels, while the measured data is more indicative of peak values. If a 10-dB difference is attributed to the ratio between peak and RMS, then the measured data would follow roughly the contour presented by a noise grade of 80.

5.8 Ionospheric Measurements

In the course of investigating the possible propagation modes within tropically foliated tactical environments, the ionospheric mode should not be overlooked. When considering if the ionospheric mode of propagation is useful for tactical communications, the question arises of whether or not the presence of foliage adds any unusual effects to the propagation mode. In particular, is the path loss significantly greater for submerged antennas than for elevated antennas, and, if the receiving antenna is submerged, does the foliage present significantly more loss to the noise arriving at oblique angles than to the signal arriving at nearly vertical angles? The ionospheric measurement results, discussed in the following paragraphs, tend to indicate that both the skywave signal and the noise are equally affected by the presence of foliage.

5.8.1 Test Measurements

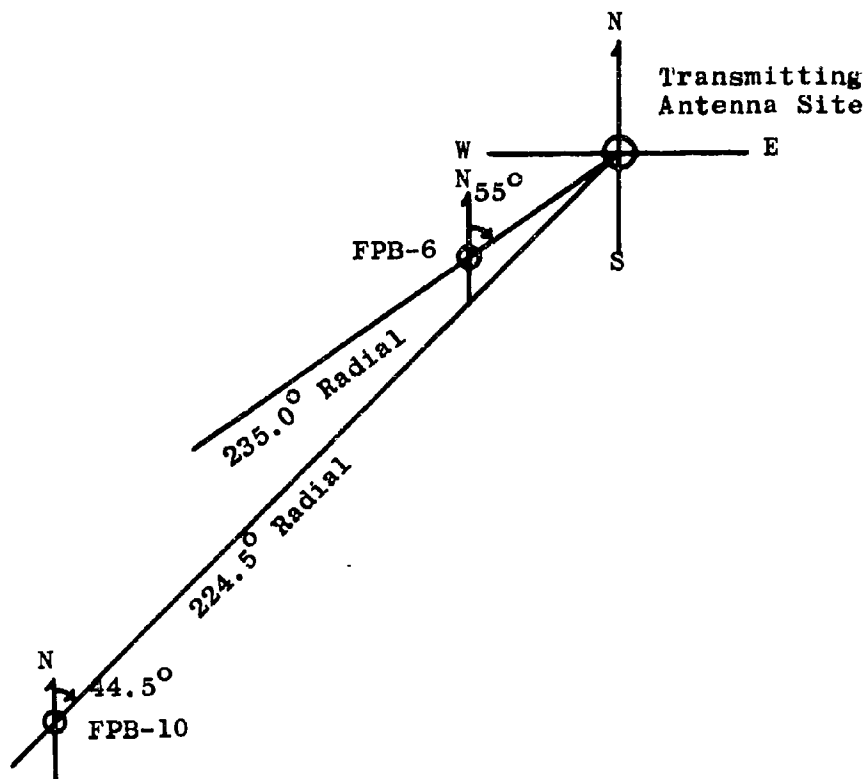
The ionospheric measurements consist of three sequences as shown in Table 5.23. The first sequence consists of three simultaneous 24-hour signal strength recordings taken at 6 Mc/s numbered IA, IB and IC. One recording was made 4.3 miles from the transmitter with a receiving loop elevated in foliage to a height of 7 feet. The other two recordings were taken at a distance of 19 miles from the transmitter with a receiving loop at 7 feet and a halfwave dipole at 21 feet. Each of the three receiving antennas was oriented so that it presented a null in the direction of the transmitter. Figure 5.107 shows the relative positions of the transmitter and the two receiving locations.

The second sequence consists of three simultaneous, 6 Mc/s signal strength recordings taken 4.3 miles from the transmitter. A 1-foot loop and two 3-foot loops were used to receive. The 3-foot loop was oriented in the north-south direction while the 1-foot loop was oriented in the east-west direction. These loops were 7 feet above ground. A second 3-foot loop, oriented in the north-south direction, was used at a receiving height of 60 feet.

The third sequence consists of three simultaneous, 2 Mc/s recordings of signal strength taken 4.3 miles from the transmitter. The receiving antenna arrangement for this third sequence was identical to that used for the second sequence.

Table 5.23
CONDITIONS AND EQUIPMENT IN IONOSPHERIC TESTS

Test No.	Freq. (Mc/s)	RCVR Loc.	XMTR Ant. Type	XMTR Ant. Height (ft)	RCVR Ant. Type	RCVR Ant. Height (ft)	RCVR Ant. Orientation	Test Date	Comments
IA	6	FPB-6	1/2 Dipole	40	3' Loop	7	Vert. Plane Null'd Toward XMTR	Jan. 25-26, 1966	
IB	6	FPE-10	1/2 Dipole	40	3' Loop	7	Vert. Plane Null'd Toward XMTR	Jan. 25-26, 1966	
IC	6	FPB-10	1/2 Dipole	40	1/2 Dipole	21	Vert. Plane Null'd Toward XMTR	Jan. 25-26, 1966	
IIA	6	FPB-6	1/2 Dipole	40	3' Loop	60	Vert. Plane N-S Direction	Jan. 27-28, 1966	Above trees
IIB	6	FPB-6	1/2 Dipole	40	3' Loop	7	Vert. Plane N-S Direction	Jan. 27-28, 1966	In heavy foliage
IIC	6	FPB-6	1/2 Dipole	40	1' Loop	7	Vert. Plane E-W Direction	Jan. 27-28, 1966	In heavy foliage
IIIA	2	FPB-6	1/2 Dipole	80	3' Loop	60	Vert. Plane N-S Direction	Jan. 29-30, 1966	Above trees
IIIB	2	FPB-6	1/2 Dipole	80	3' Loop	7	Vert. Plane N-S Direction	Jan. 29-30, 1966	In heavy foliage
IIIC	2	FPB-6	1/2 Dipole	80	1' Loop	7	Vert. Plane E-W Direction	Jan. 29-30, 1966	In heavy foliage



Scale: 1 inch = 4 miles

Figure 5.107 Ionospheric Test Transmitting and Receiving Sites

During each measurement sequence, 24-hour signal strength recordings were made. Periodically during the tests atmospheric noise and interfering signals were measured to gain signal-to-noise ratio information. Figure 5.108 shows a typical portion of one of the strip recordings. The example shown in Figure 5.108 is from test IIIA. That portion of the recording marked 01 to 06 represents a 5-minute noise sample. The remainder of the chart is a signal recording.

C-2 vertical incidence sounder negatives were obtained for the period of these tests to serve as corollary data.

5.8.2 Test Results

The results of the various test sequences are shown in Figures 5.109 through 5.117. The open circles represent average signal values and the black circles represent average noise values. For that portion of the plots during which the signal samples are nearly equal to the noise samples, all samples, black or white, actually represent noise levels.

For example, Figure 5.109 shows that a good signal, well above the noise, was present on January 26 from 1500 to about 2000. Then the signal either dropped out or the noise level came up so that the signal was indistinguishable from the noise until 0900 on January 27.

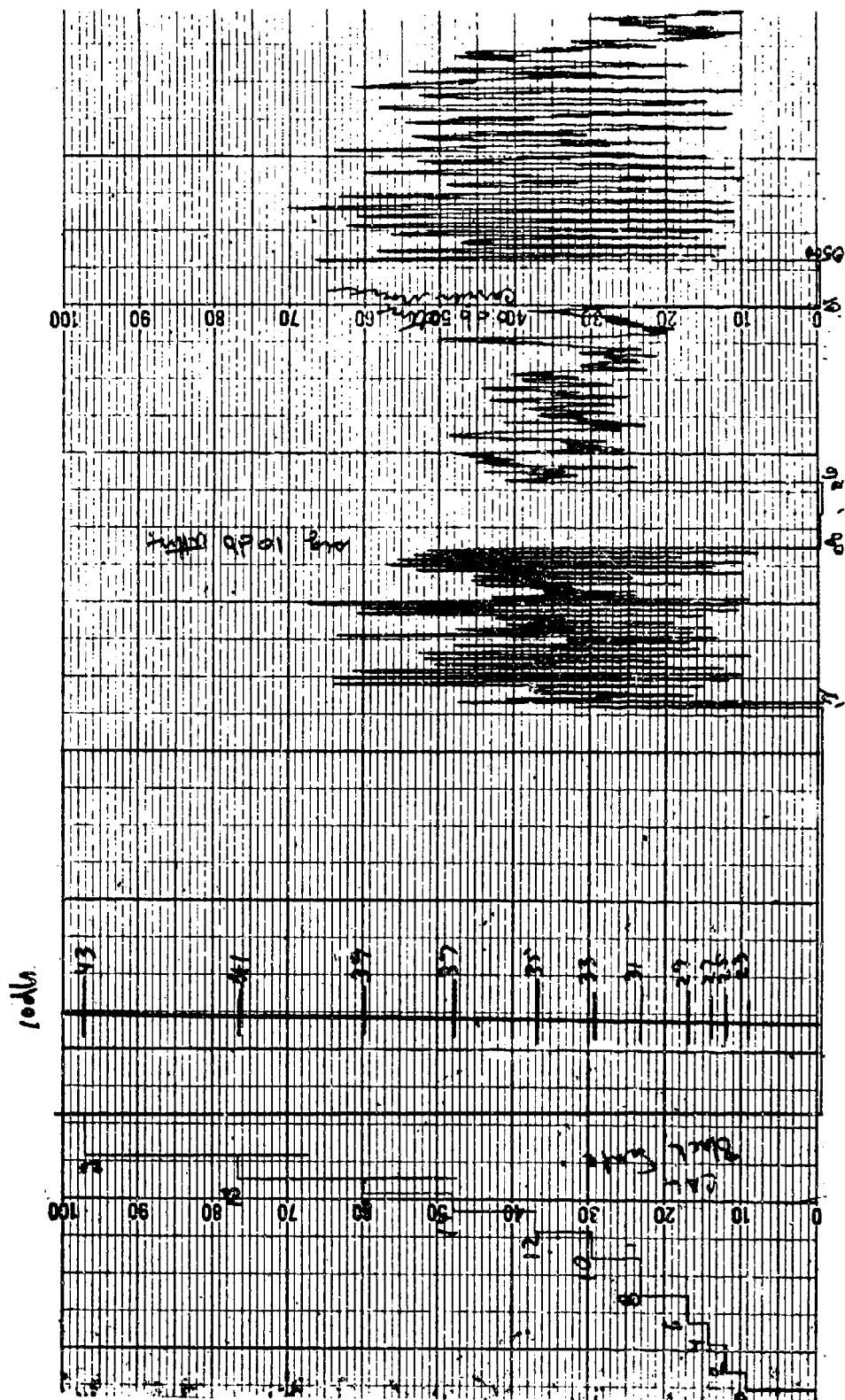


Figure 5.108 Raw Data from Ionospheric Tests

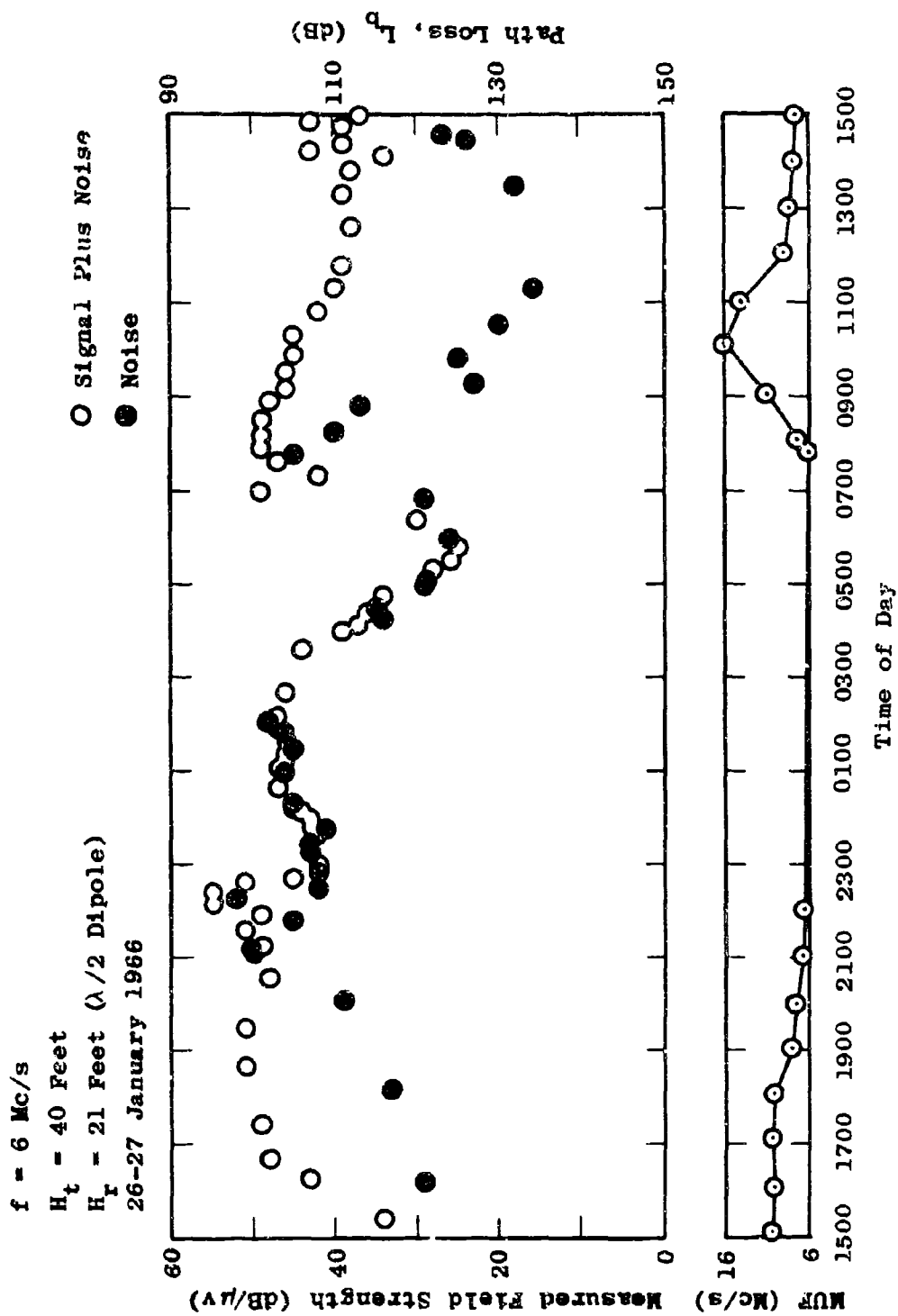


Figure 5.109 Measured Field Strength Versus Time of Day - FPB-10

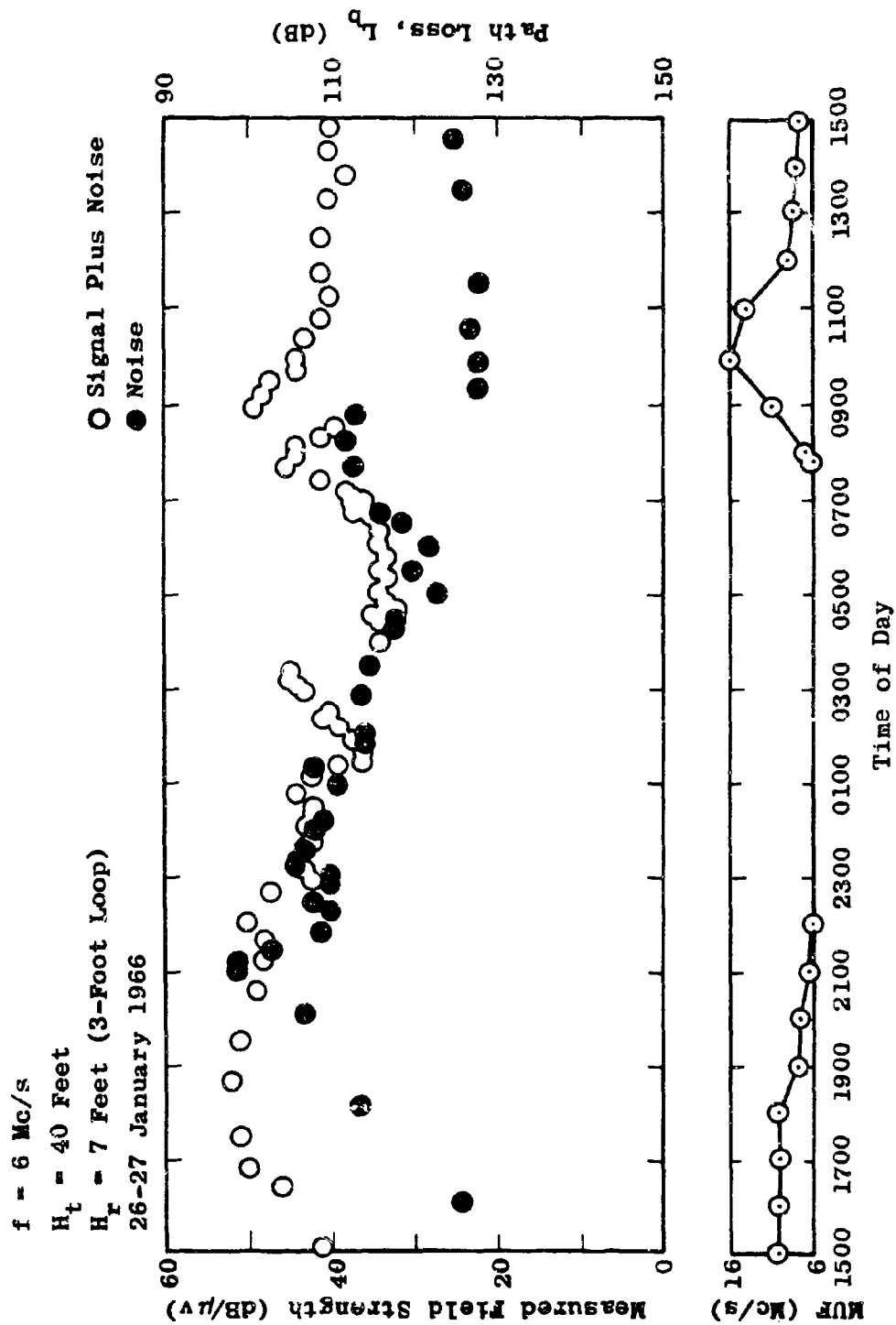


Figure 5.110 Measured Field Strength Versus Time of Day - FPB-6

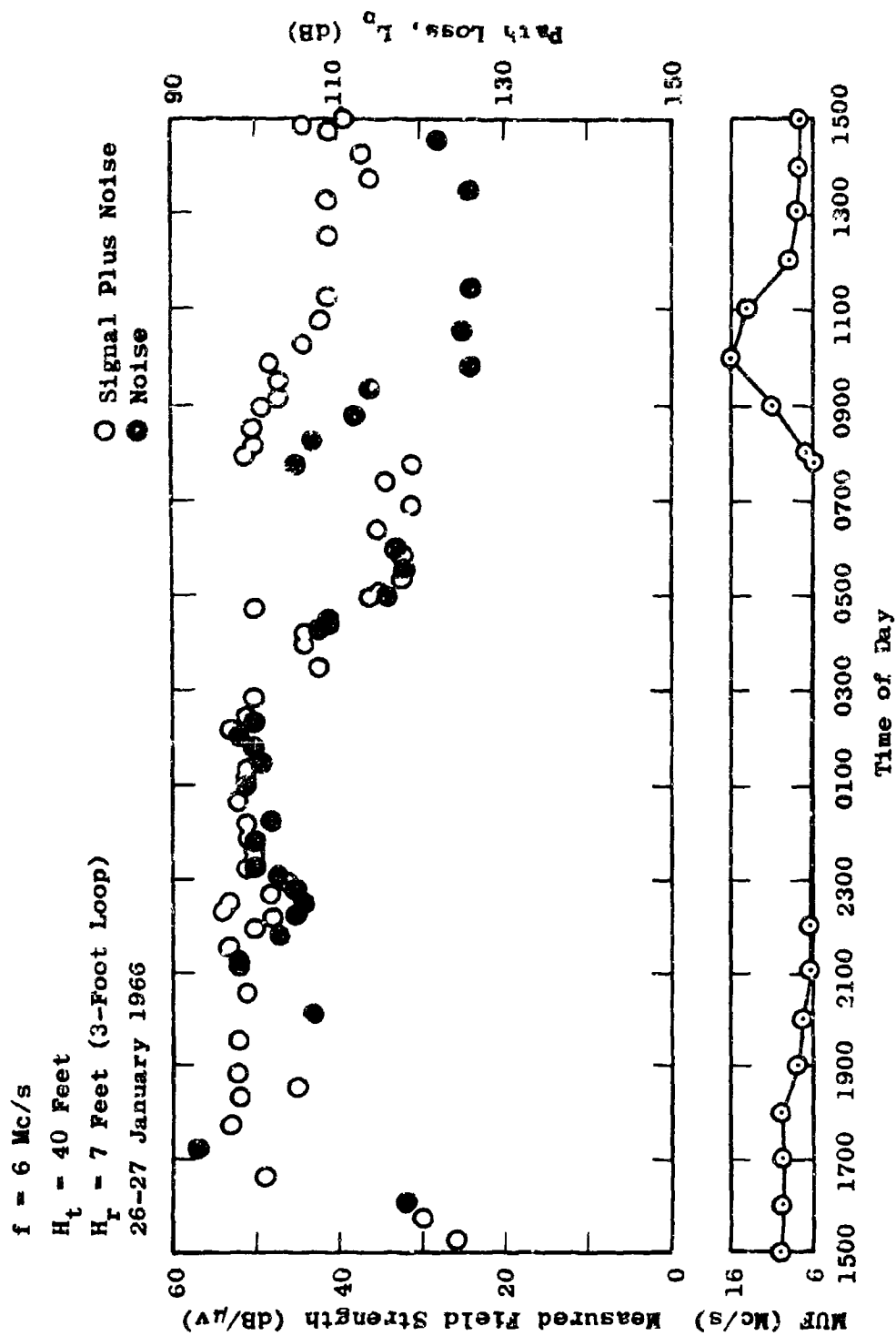


Figure 5.111 Measured Field Strength Versus Time of Day - FFB-10

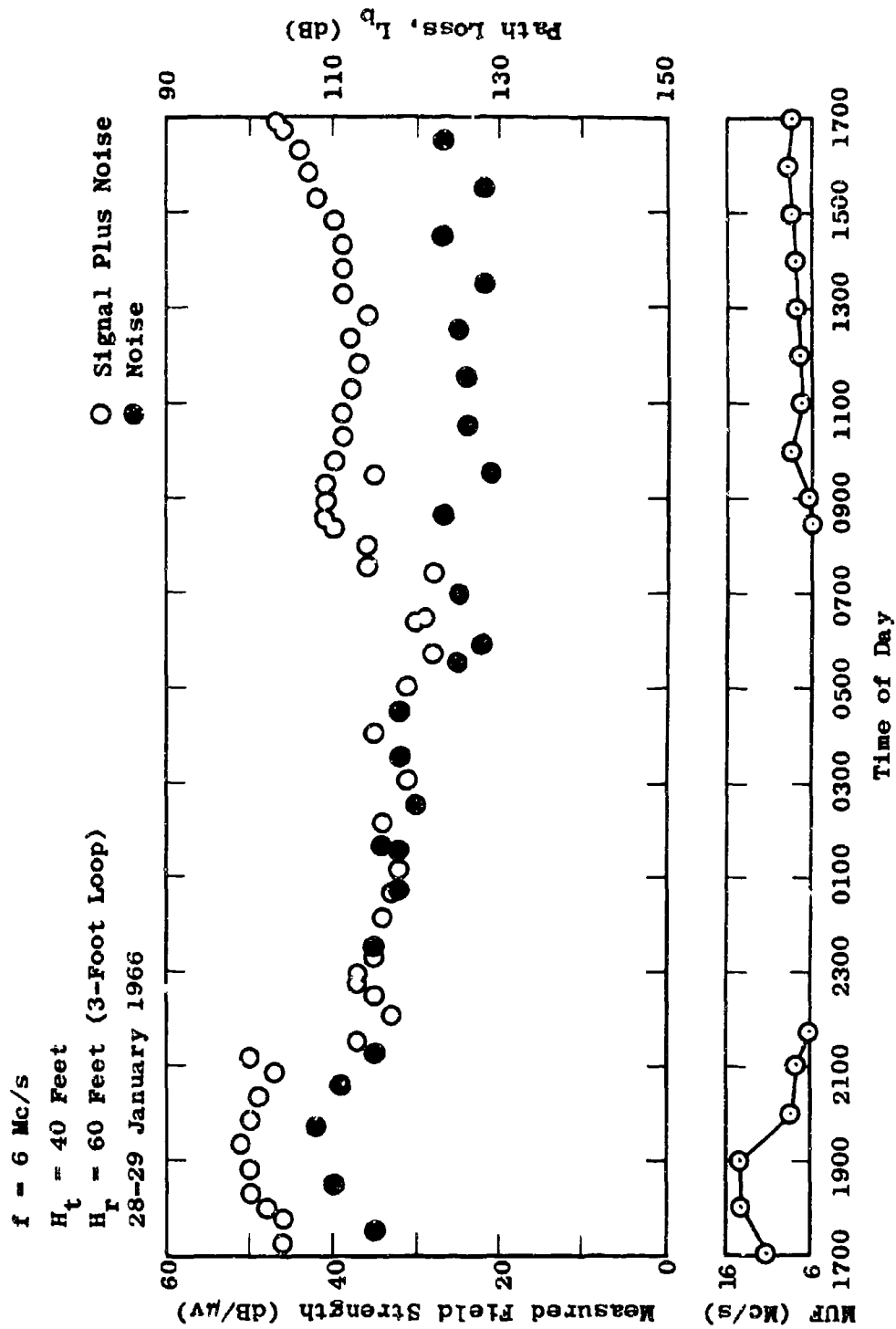


Figure 5.112 Measured Field Strength Versus Time of Day - FFB-6

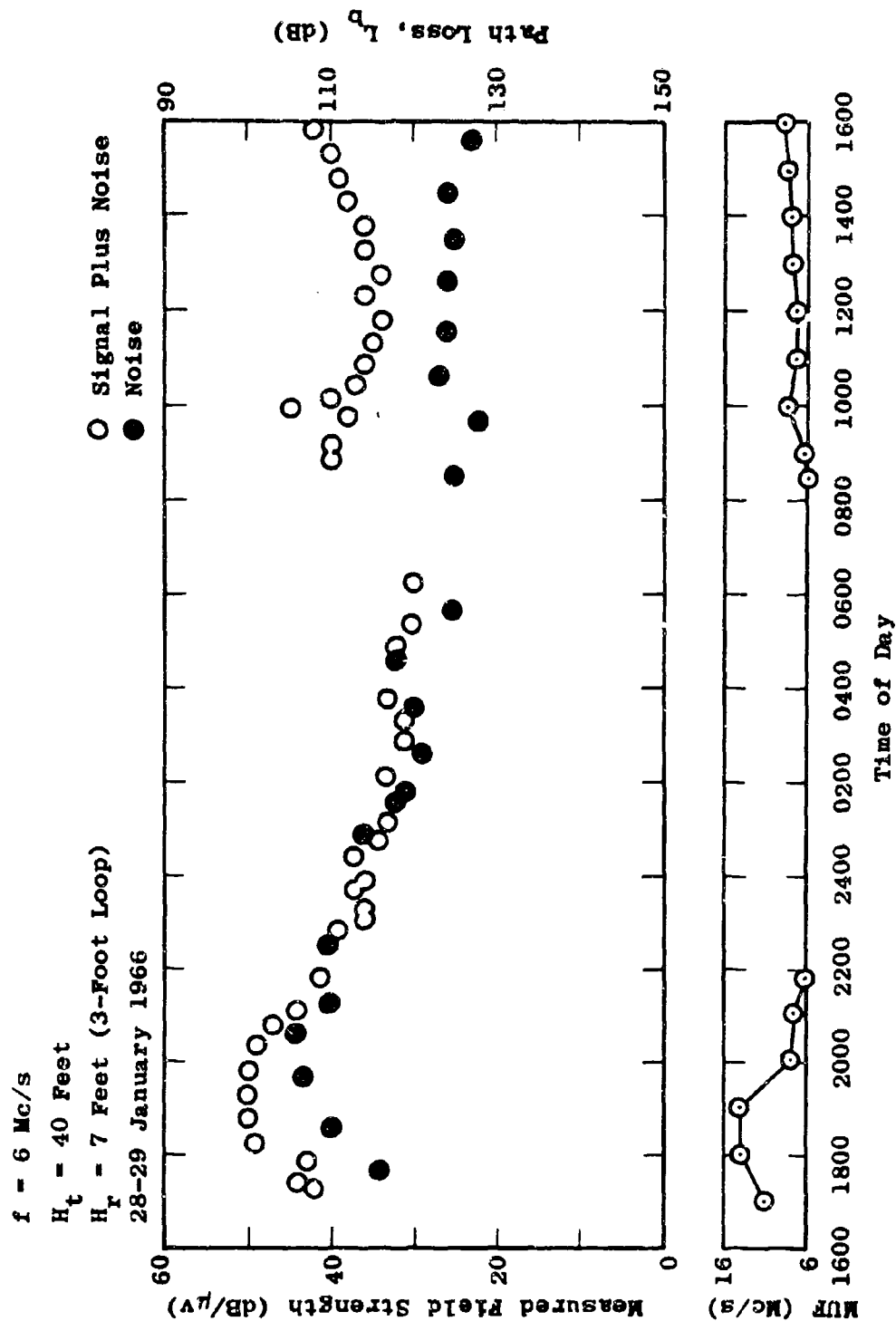


Figure 5.113 Measured Field Strength Versus Time of Day - FPB-6

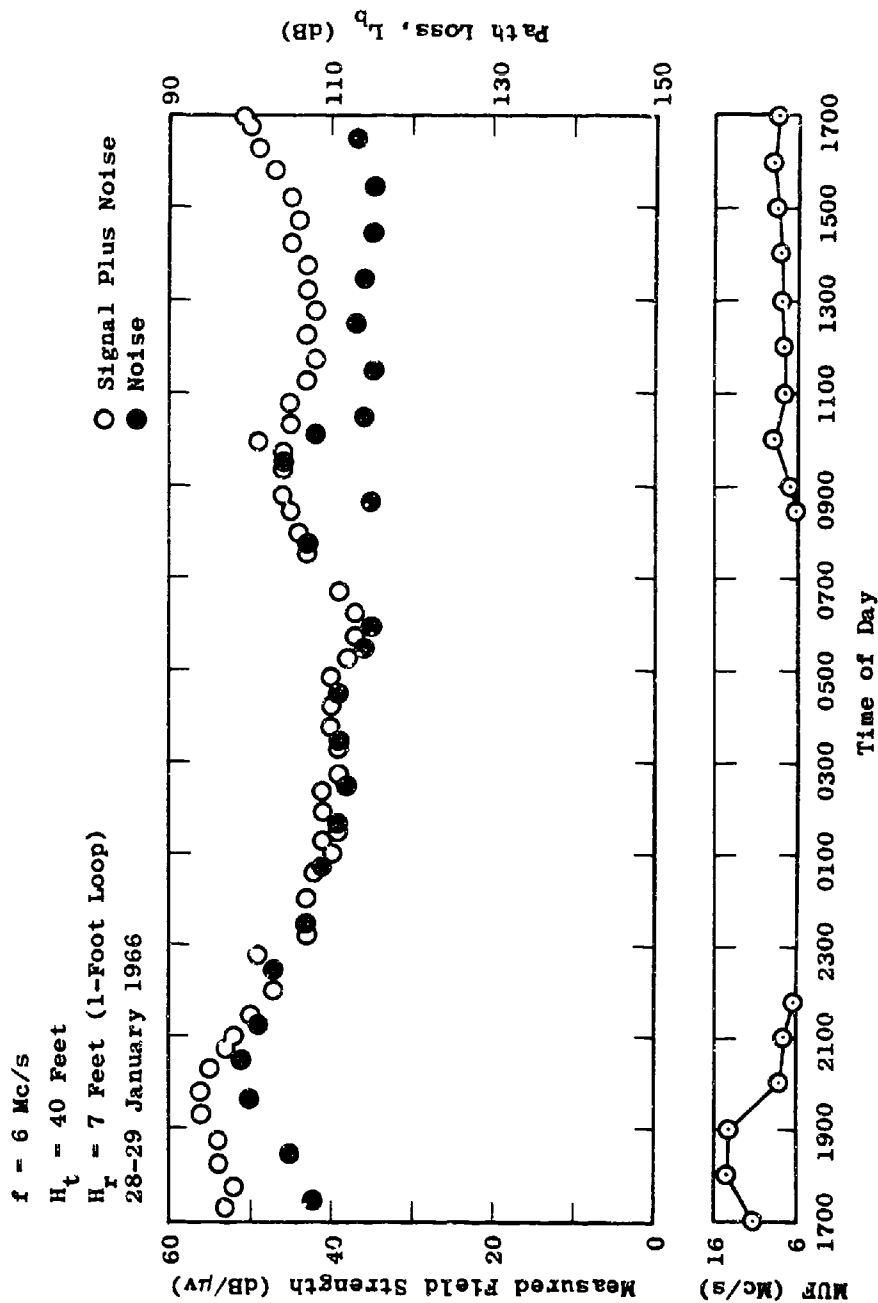


Figure 5.114 Measured Field Strength Versus Time of Day - FPB-6

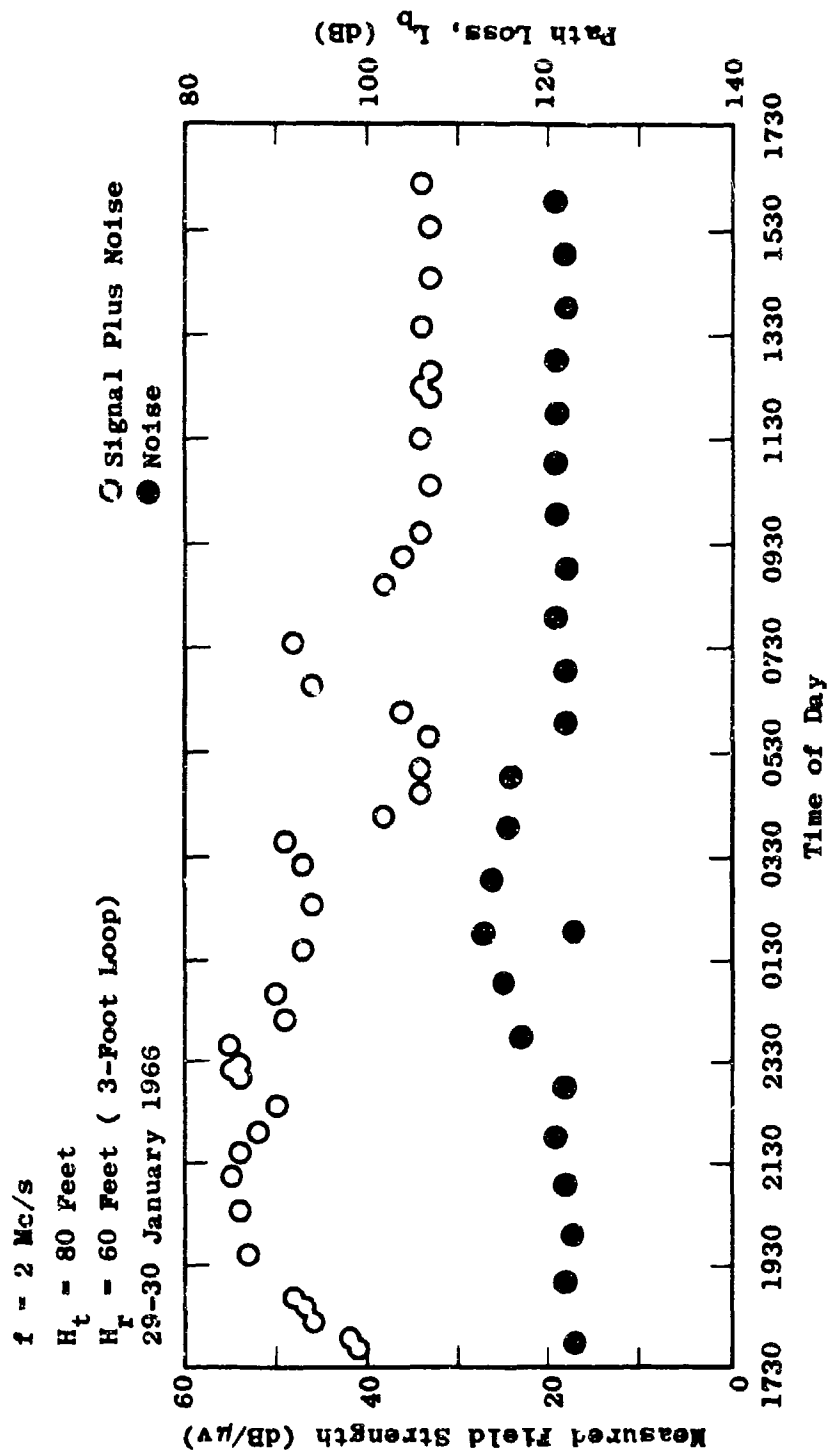


Figure 5.115 Measured Field Strength Versus Time of Day - FPB-6

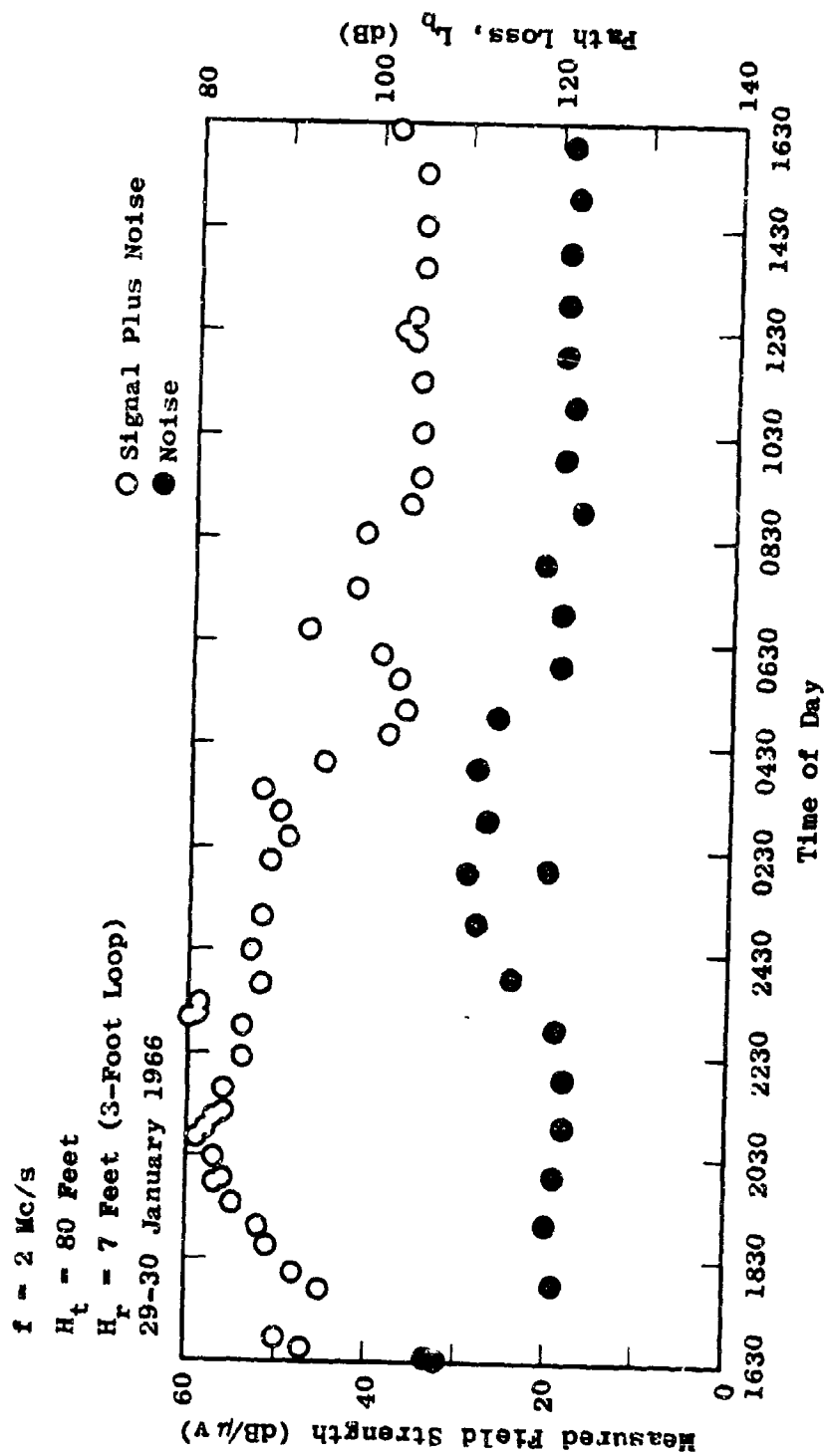


Figure 5.116 Measured Field Strength Versus Time of Day - FPB-6

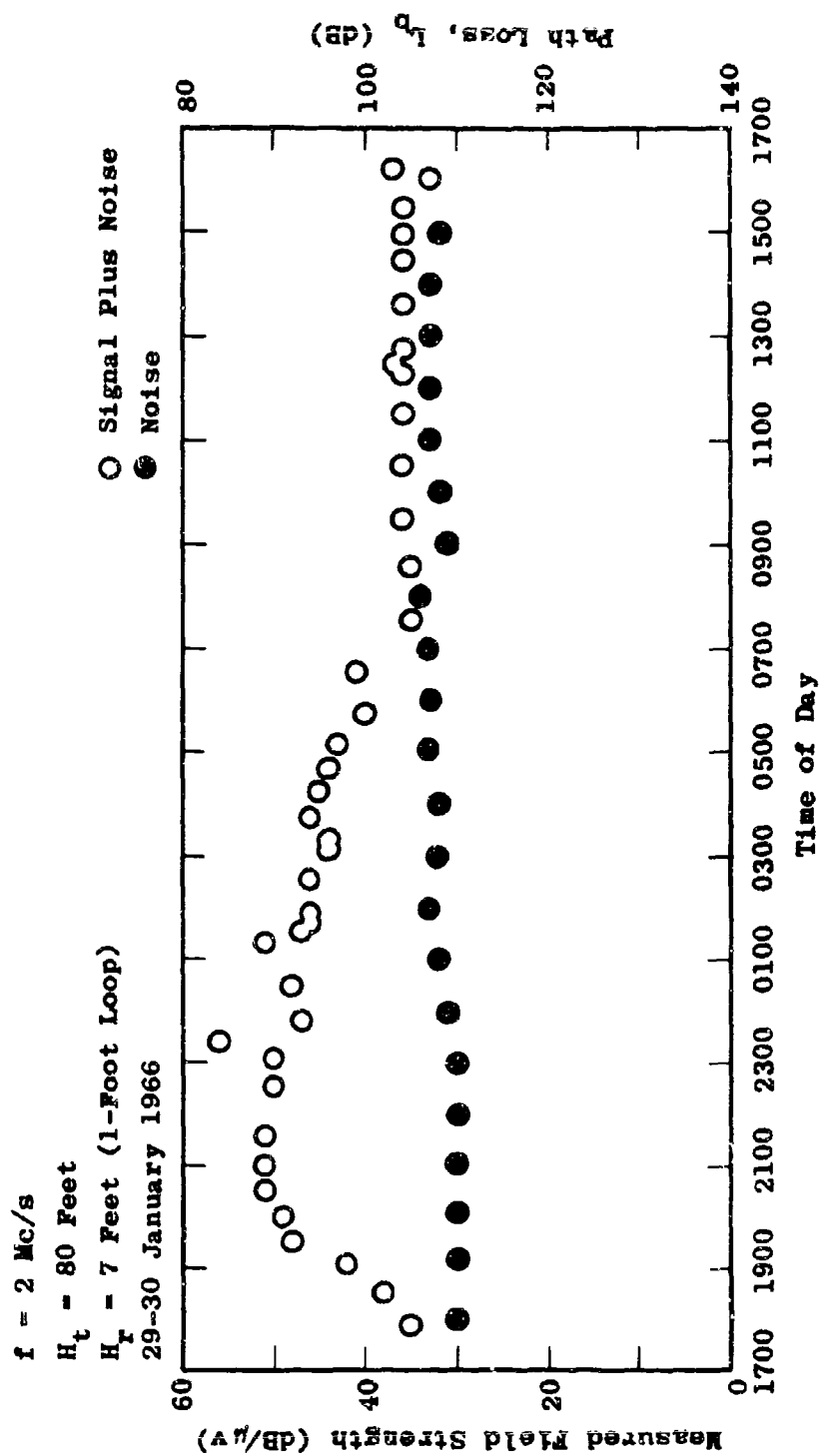


Figure 5.117 Measured Field Strength Versus Time of Day - FPB-6

The curve plotted along the bottom of the figure gives the MUF indicated by the ionograms. As Figure 5.109 shows, the MUF dropped below 6 Mc/s at 2200, and hence the signal dropped out completely at 2200 and did not appear again until 0800 the next day. The MUF has not been plotted on the 2 Mc/s results since this frequency was almost always below the MUF.

Figure 5.118 shows a typical result from the ionograms for January 29, 1966. A signal at 2 Mc/s is always below the MUF shown on Figure 5.118. However, 6 Mc/s is below the MUF only from 0800 to 2100. The MUF comes closest to 2 Mc/s at about 0600. The effect of this can be seen at 0600 on Figures 5.115, 5.116 and 5.117.

Turning now to the simultaneous measurements shown in Figures 5.109, 5.110 and 5.111, the following comparisons can be made. At the 7-foot receiving height there is no significant difference between signal levels or noise levels recorded at the two different distances, except between 2300 and 0500 hours. During this period, there is no signal present at either location and the noise level at the distant site is about 10 dB higher than the noise level at the nearer site.

In comparing the results at the two receiving antenna heights at FPB-10, no appreciable difference is seen between the received signal level at the two heights. However, the noise level is about 6 dB higher for the lower receiving antenna. The higher receiving antenna is a horizontal half-wave dipole and the lower antenna is a vertically oriented loop. The 6 dB difference most likely

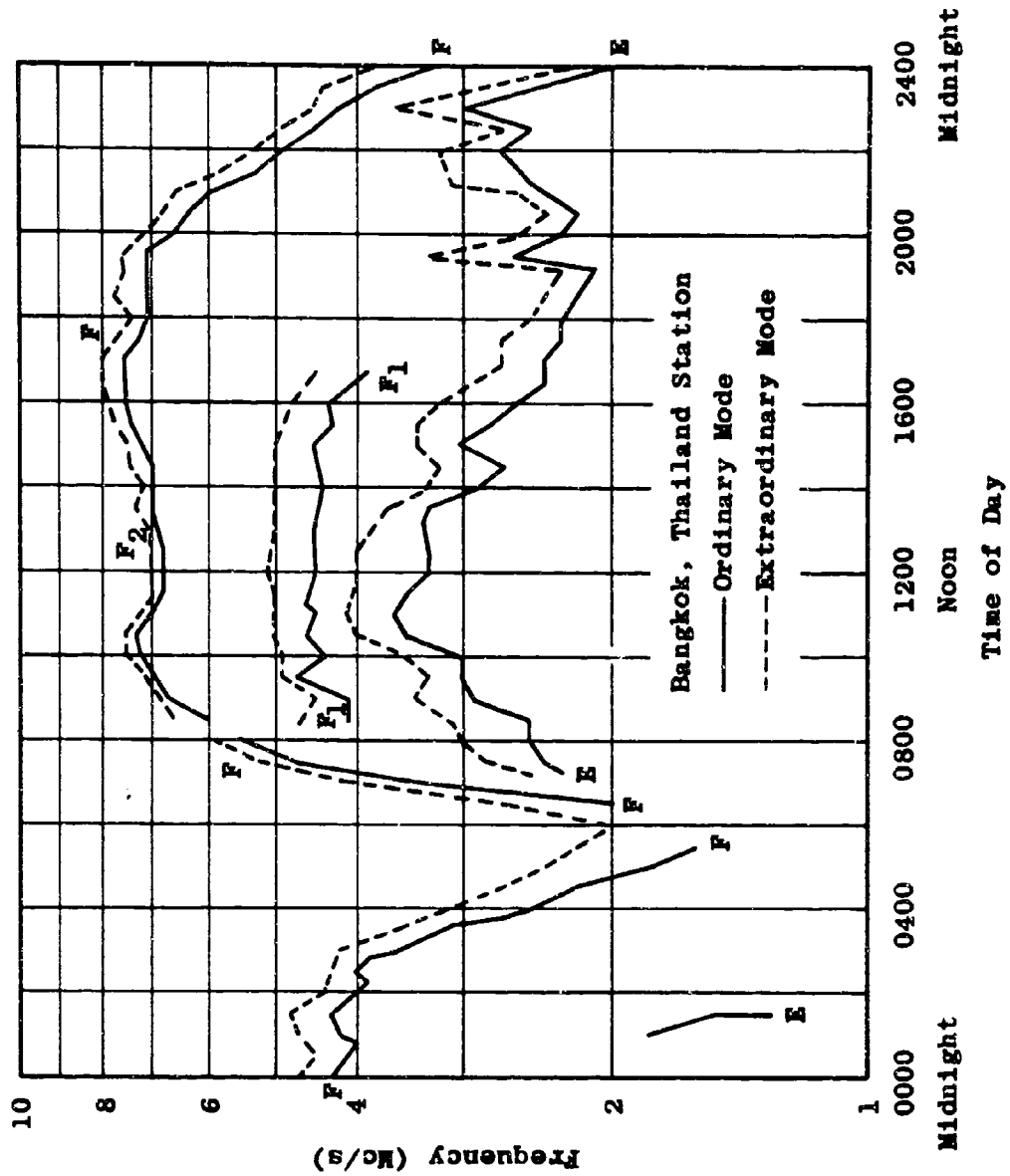


Figure 5.118 Critical Frequency Versus Time of Day for 29 January 1966

represents the difference in noise level for the two polarizations.

Turning now to the second measurement sequence, shown in Figures 5.112, 5.113 and 5.114, no difference in either noise or signal level can be detected at the two antenna heights for antennas oriented in the same plane. The lower antenna, at 7-feet, was immersed in heavy foliage. The higher antenna, at 60 feet, was above the surrounding trees. These results indicate that no significant differences in either noise or signal levels exist for antennas at 6 Mc/s which are immersed in the type of foliage found in the Pak Chong area.

The effects of antenna orientation can be examined by comparing Figure 5.113 with Figure 5.114. A 3-foot receiving loop oriented in the north-south direction was used for the data shown in Figure 5.113, while a 1-foot receiving loop oriented in the east-west direction was used for the data shown in Figure 5.114.

Extensive calibration tests have shown that the 1-foot loop and 3-foot loop differ by less than 1 dB when appropriate antenna factors are used. In comparing the Figures 5.113 and 5.114, it becomes apparent that both the 6 Mc/s signal and noise levels are on the order of 8 dB higher for the antenna which is oriented in the east-west direction.

A comparison of Figures 5.115, 5.116 and 5.117 reveals that the signal level is as much as 8 dB higher

at 2 Mc/s for the antenna which is oriented in the north-south direction. However, in this case no conclusions can be drawn concerning noise levels since the external noise levels, as received by the two loop antennas, were below the input sensitivity of the receiver except for the period from 24:00 to 6:00 on Figure 5.116. The minimum field which could be measured at 2 Mc/s was 20 dB/uv/m using the 3-foot loop, and 30 dB/uv/m using the 1-foot loop.

A comparison of Figures 5.115 and 5.116 reveals that at 2 Mc/s the signal received on the lower antenna was about 3 dB higher than the signal received on the higher antenna.

Table 5.24 compares the minimum observed skywave losses and the range of groundwave losses which were observed for horizontal polarization as a result of the fixed-point measurements. Table 5.24 lists the minimum skywave loss observed during each 24-hour period and the range of measured surface wave path losses. The range of measured path losses for FPB-10 is an extrapolation of data taken at closer field points, since the surface wave is below receiver sensitivity at 6 Mc/s at FPB-10.

In every case, the best skywave signal was stronger than the measured groundwave losses. However, the skywave signal does not retain its maximum value for very long each day and often the skywave signal only exists for a relatively short portion of the day. The last column in Table 5.25 lists the maximum amount by which the skywave was stronger than the groundwave. During the horizontal groundwave measurements the receiving loop was oriented so that there was a

Table 5.24
COMPARISON BETWEEN SKYWAVE AND HORIZONTALLY POLARIZED GROUNDWAVE

Test No.	Freq. (Mc/s)	H _t (ft)	H _r (ft)	Field Point	Minimum Skywave L _b (dB)	Measurer Range Groundwave L _b (dB)	Maximum Difference (dB)
IA	6	40	7	FPB-6	100	98-115	15
IB	6	40	7	FPB-6	100	98-115	15
IC	6	40	21	FPB-10	100	128-148	48
IIA	6	40	60	FPB-6	100	98-115	15
IIB	6	40	7	FPB-6	100	98-115	15
IIC	6	40	7	FPB-6	94	98-115	21
IIIA	2	80	60	FPB-6	85	95-110	25
IIIB	2	80	7	FPB-6	81	95-110	29
IIIC	2	80	7	FPB-6	90	95-110	20

null in the vertical direction. This null provided a 20-25 dB discrimination against skywave modes. This 20-25 dB discrimination was sufficient to eliminate skywave components in most, but not all, of the cases shown in Table 5.24.

During the groundwave measurements the test engineers were able to identify the presence of a skywave by its characteristic rapid time variation as opposed to the relatively stable nature of the groundwave signal. Measured groundwave data which appeared to be contaminated by a skywave was not included in the groundwave data base.

5.9 10 Gc/s Measurements

A number of propagation measurements have been made in the frequency range from 550 Mc/s to 10 Gc/s in addition to the extensive set of measurements performed below 500 Mc/s.

The measurements from 550 Mc/s to 10 Gc/s are called "10 Gc/s Measurements" and consist primarily of two basic types of measurement. One type is concerned with line-of-sight transmission over a foliated obstacle and the other involves the measurement of short-range transmission directly through the foliage. The line-of-sight measurements are applicable to point-to-point relay systems which operate over heavily vegetated paths while the through-the-foliage measurements are applicable to short-range microwave systems for which at least one terminal must operate within the foliage.

The following sections present experimental results from the 10 Gc/s measurement program along with associated environmental data.

5.9.1 Line-of-Sight Test Series

When the first Fresnel ellipse between the transmitting and receiving antennas is obstructed, transmission loss rises above its free space value. If the obstructing object is perfectly conducting and in the form of a knife-edge, the additional loss due to diffraction is accurately given by theoretical expressions. However, if the obstacle deviates in shape from a knife-edge and is heavily foliated in addition, the diffraction loss might be expected to be of greater magnitude than that predicted theoretically.

To determine how well existing theory predicts losses under these conditions, loss measurements were performed over a heavily foliated ridge in the Pak Chong area. In addition to the absolute loss measurements, variations in path loss over 24-hour periods were monitored to provide diurnal fading estimates.

The results of these tests are presented in this section along with a theoretical discussion of the diffraction loss for a perfect knife edge.

5.9.1.1 Theoretical Knife-edge Diffraction

For a perfect knife-edge path with Fresnel zone clearance between each antenna and the knife edge, the

theoretical basic transmission loss is given by

$$L_b = L_b(fs) + A(v) \quad (11)$$

where

$L_b(fs)$ = free-space basic transmission loss in dB

$A(v)$ = gain or loss due to diffraction over a perfect knife edge in dB

The function $A(v)$ is defined as

$$A(v) = \frac{E}{E_0} \quad (12)$$

where

E = measured field strength at a given point

E_0 = free-space field which would exist at the same point

$A(v)$ can be written in complex form as

$$A(v) = a + jb \quad (13)$$

where a and b can be written in terms of the Fresnel integral as

$$a = \frac{1}{\sqrt{2}} \int_v^\infty \cos \frac{\pi v^2}{2} dv \quad (14)$$

$$b = \frac{1}{\sqrt{2}} \int_v^\infty \sin \frac{\pi v^2}{2} dv \quad (15)$$

$$v = H \frac{2}{\lambda} \left[\frac{1}{r_1} + \frac{1}{r_2} \right]^{\frac{1}{2}} \quad (6)$$

where

H = height of obstacle

λ = wavelength

r_1 = distance between transmitter and obstacle

r_2 = distance between receiver and obstacle

(each of the above must have the same units).

The above integrals have been evaluated for a wide range of values of v , and the resultant curve is shown in Figure 5.119. From equation 12, it can be seen that when $A(v) = 0$ db, E is equal to E_0 , and free-space conditions exist. For increasing negative values of v , the received field oscillates about the free-space field in a damped fashion. In a physical sense, increasing v in the negative direction means raising the line-of-sight ray farther and farther above the obstacle in the propagation path. When the obstruction just touches the line-of-sight ray between antennas, $v = 0$. Positive values of v occur when the knife edge obstructs the line-of-sight ray. For these cases, the received field is always less than the free-space field. This region is sometimes referred to as the "shadow region," and the resultant loss is termed "shadow loss."

From equation 13, it is noted that $A(v)$ is a complex function whose magnitude and phase depend upon the value of v . Figure 5.119 gives the magnitude of $A(v)$ and

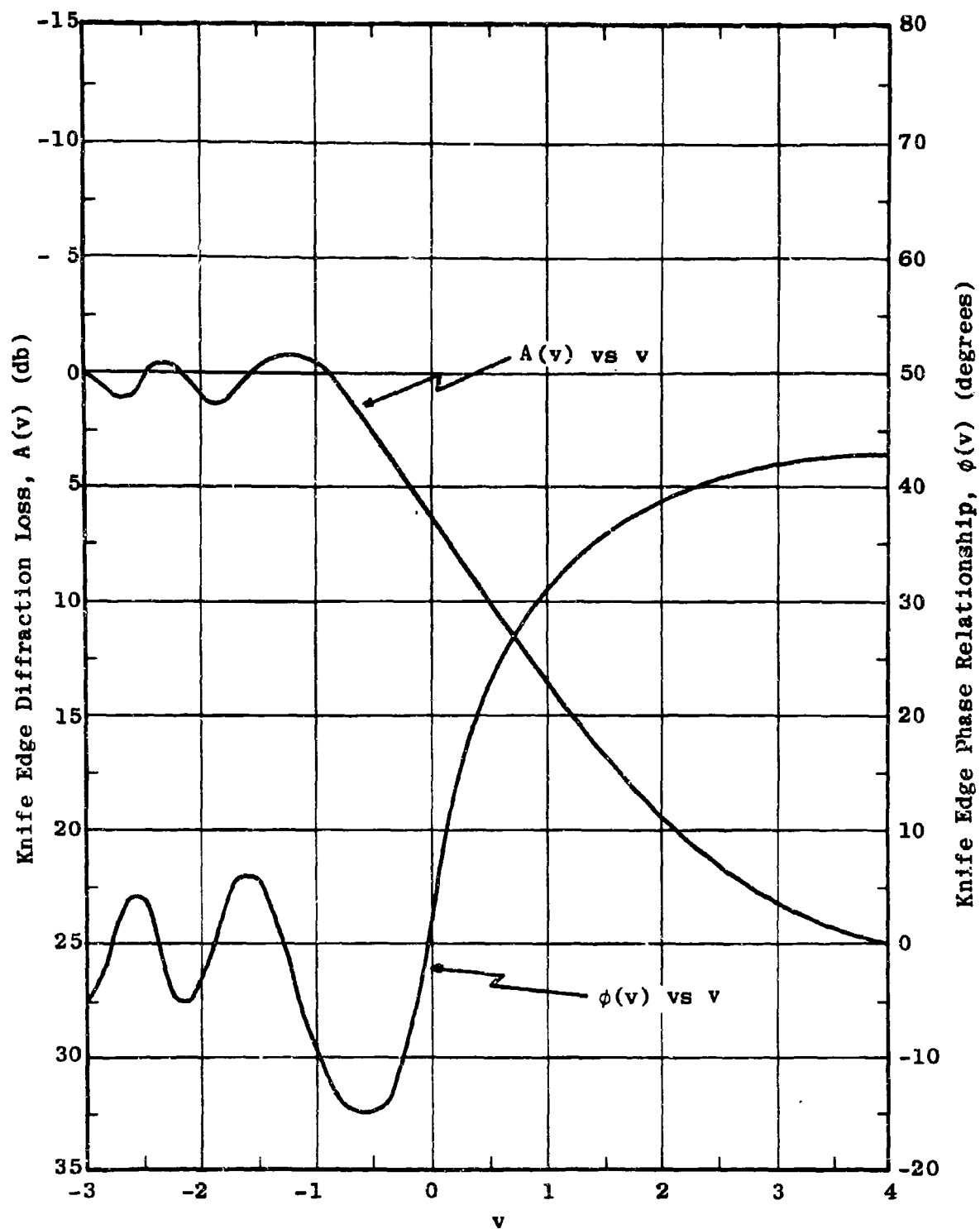


Figure 5.119 $A(v)$ and $\phi(v)$ vs v for Perfect Knife Edge

its phase relationship, $\phi(v)$. The phase, ϕ , becomes an important factor when computing the received field when ground reflections exist, but need not be considered for cases where ground reflections do not occur.

To permit easy computations of $A(v)$ with a digital computer, the following approximate expressions have been generated for various ranges of v .¹⁷

For $-1 \leq v \leq 0$

$$A(v) = 2.78 v^2 + 9.95 v + 6.17 \quad (17)$$

For $0 \leq v \leq 3$

$$A(v) = 6.08 - 0.005 v^4 + 0.159 v^3 - 1.7 v^2 + 9.3 v \quad (18)$$

For $v \geq 3$

$$A(v) = 12.953 + 20 \log v \quad (19)$$

5.9.1.2 Diffraction Loss Measurements

From Section 5.9.1.1, it is noted that the theoretical knife-edge loss function is given as $A(v)$ in dB. The parameter, v , is related to the geometrical relationship between the transmitter, receiver and intervening obstacle. In simplified form it is given by the following formula.

$$v = \sqrt{2} \frac{H_o}{R} \quad (20)$$

where

R = radius of first Fresnel ellipse
at the obstacle

H_o = physical distance between line-
of-sight ray and peak of obstacle

To adequately measure the $A(v)$ function, a range of values of v from about -2 to +4 should be considered. This range of v provides a loss range of about 25 dB. Figure 5.119 graphically displays the theoretical $A(v)$ function.

The above range of v values was obtained in the measurement setup by varying H_o in Equation 20. The physical arrangement used to do this is illustrated in the path profile presented in Figure 5.120. In this figure two transmitter sites and nine receiver locations are shown. By selecting various transmit-receive combinations, a range of H_o values and hence a range of v values were attained. It is important to note that all H_o values were determined by allowing the obstacle height to include the height of the trees. All of the transmit-receive combinations used were "shadowed" only by the trees on the main obstacle. Positive values of H_o denote obstruction of the line-of-sight ray while negative values of H_o denote line-of-sight clearance.

The transmitters and receivers were situated so that first Fresnel zone clearance from terrain and foliage existed at the terminal points of the path. Thus, the deviation of measured losses from free-space loss is assumed to be totally due to the foliated main obstacle. Photographs

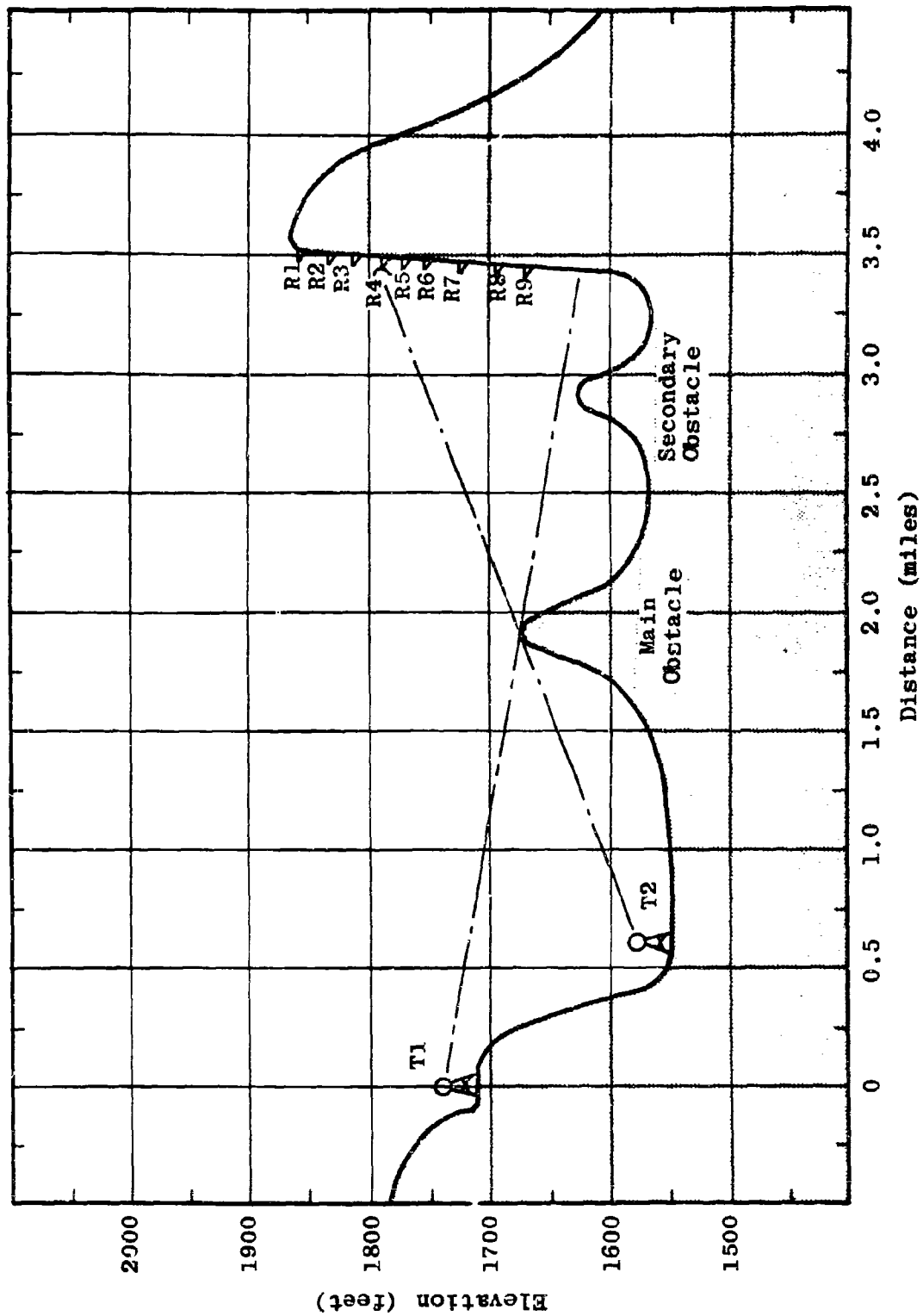


Figure 5.120 Line-of-Sight Profile for Area A

showing the receiving antenna setup and the degree of clearance from terrain and foliage at the receiver are in Figures 5.121 and 5.122.

5.9.1.3 Diffraction Test Results

In order to compare the measured losses with those for theoretical perfect knife-edge diffraction, the values of v corresponding to the various transmitter-receiver combinations were computed using the equation in Section 5.9.1.2. The measured diffraction loss $A(v)$ for a given value of v is simply the basic transmission loss derived from measurements less the normal free-space basic transmission loss.

The measured values of $A(v)$ are plotted as a function of v for the five test frequencies in Figures 5.123 through 5.127. Superimposed on these plots is the theoretical function of loss due to a perfect knife edge, as discussed in Section 5.9.1.1.

The significant observation to be made from Figures 5.123 through 5.127 is that there is close agreement between the theoretical perfect knife-edge loss and the measured diffraction loss. Since the obstacle used in the line-of-sight path deviated considerably from what would be considered a "perfect" knife edge, it is expected that there would have been even closer agreement if a "more perfect" obstacle has been used. Again the importance of considering the trees on the obstacle to be the diffracting edge should be noted. The close theoretical agreement seen in Figures 5.123 through 5.127 would not have resulted had the actual terrain



Figure 5.121 Receiving Setup for Line-of-Sight Tests



Figure 5.122 Receiving Setup for Line-of-Sight Tests

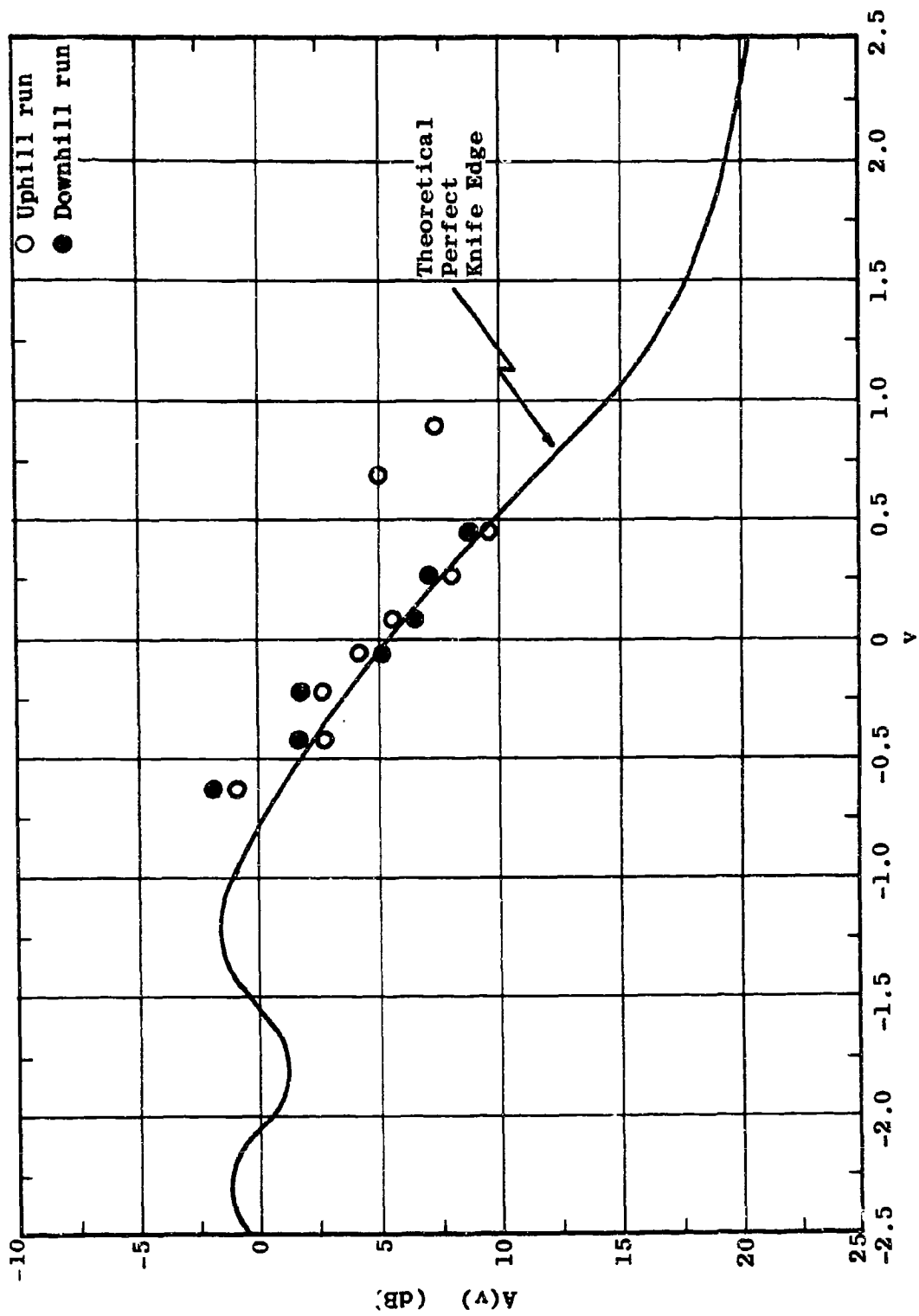


Figure 5.123 Measured Knife-Edge Loss at 550 Mc/s

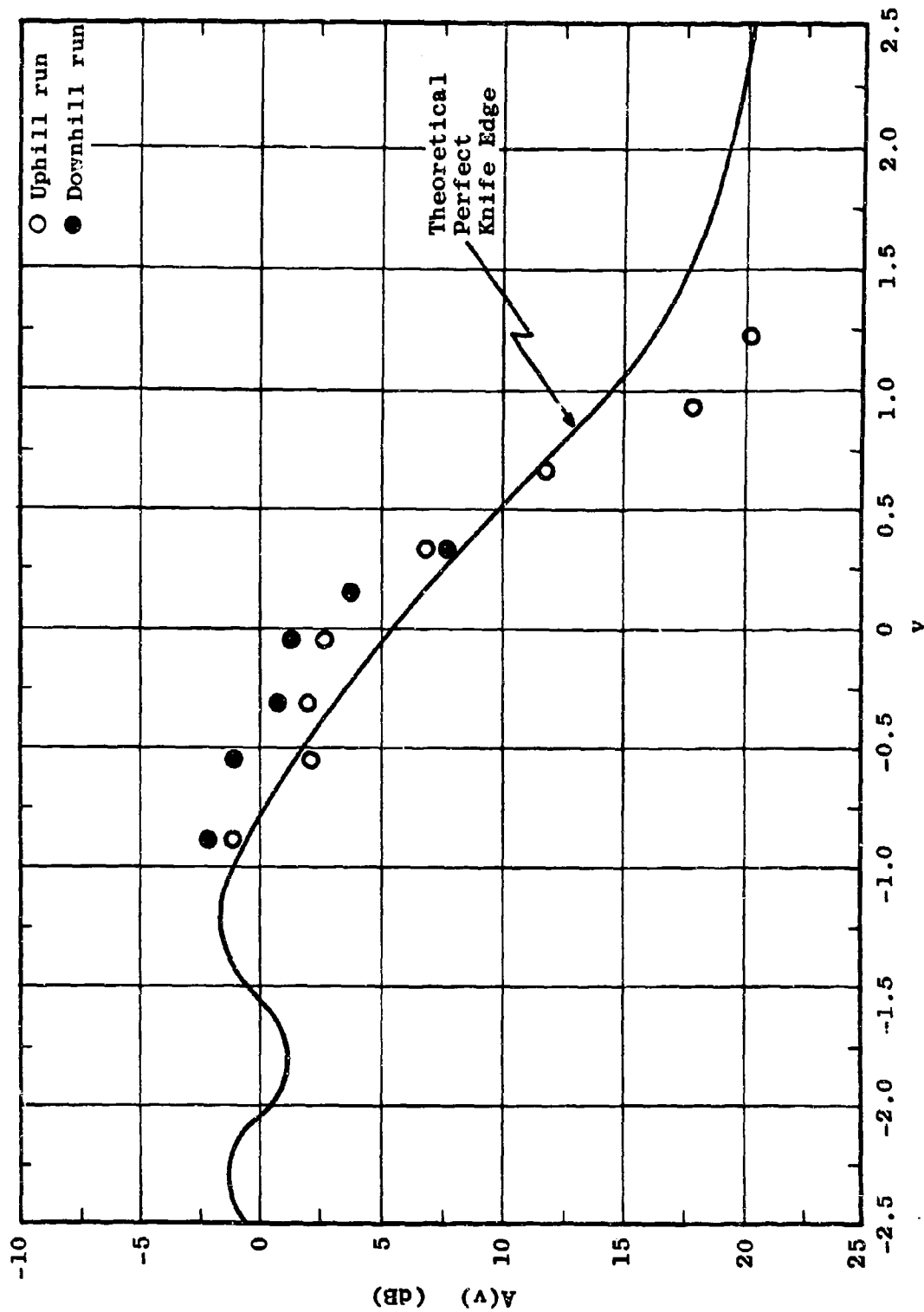


Figure 5.124 Measured Knife-Edge Loss at 1.0 Gc/s

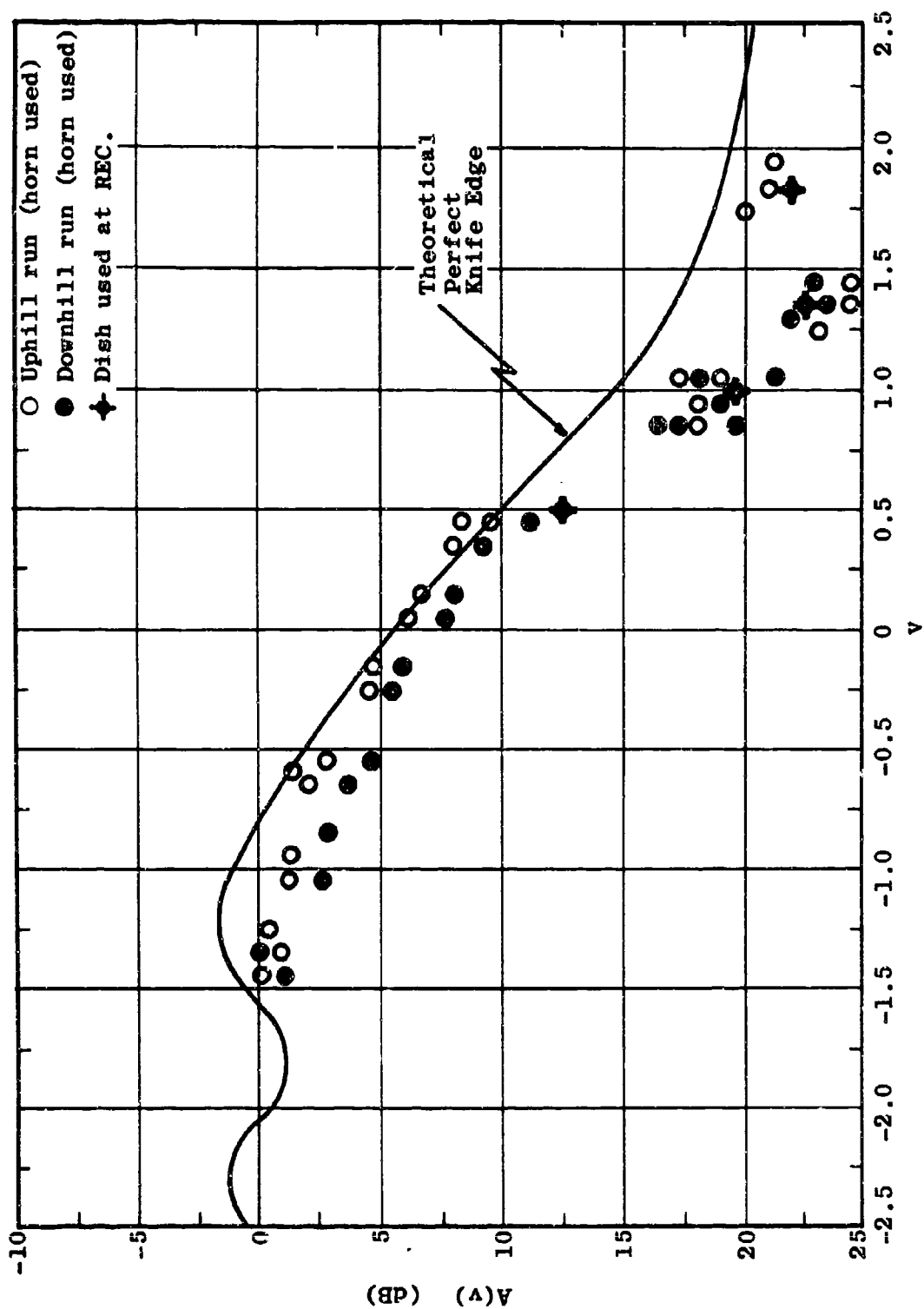


Figure 5.125 Measured Knife-Edge Loss at 2.5 Gc/s

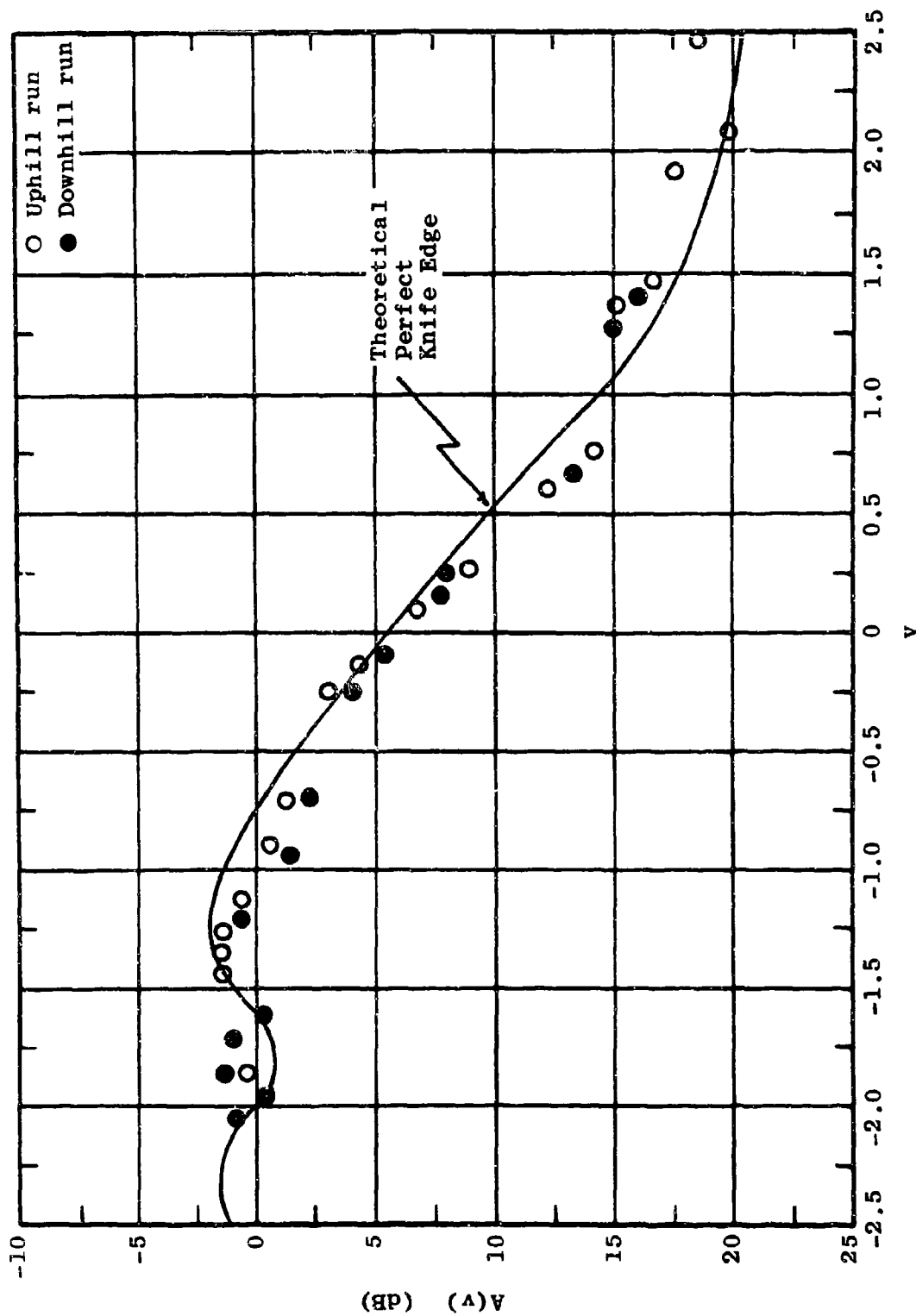


Figure 5.126 Measured Knife-Edge Loss at 5.0 Gc/s

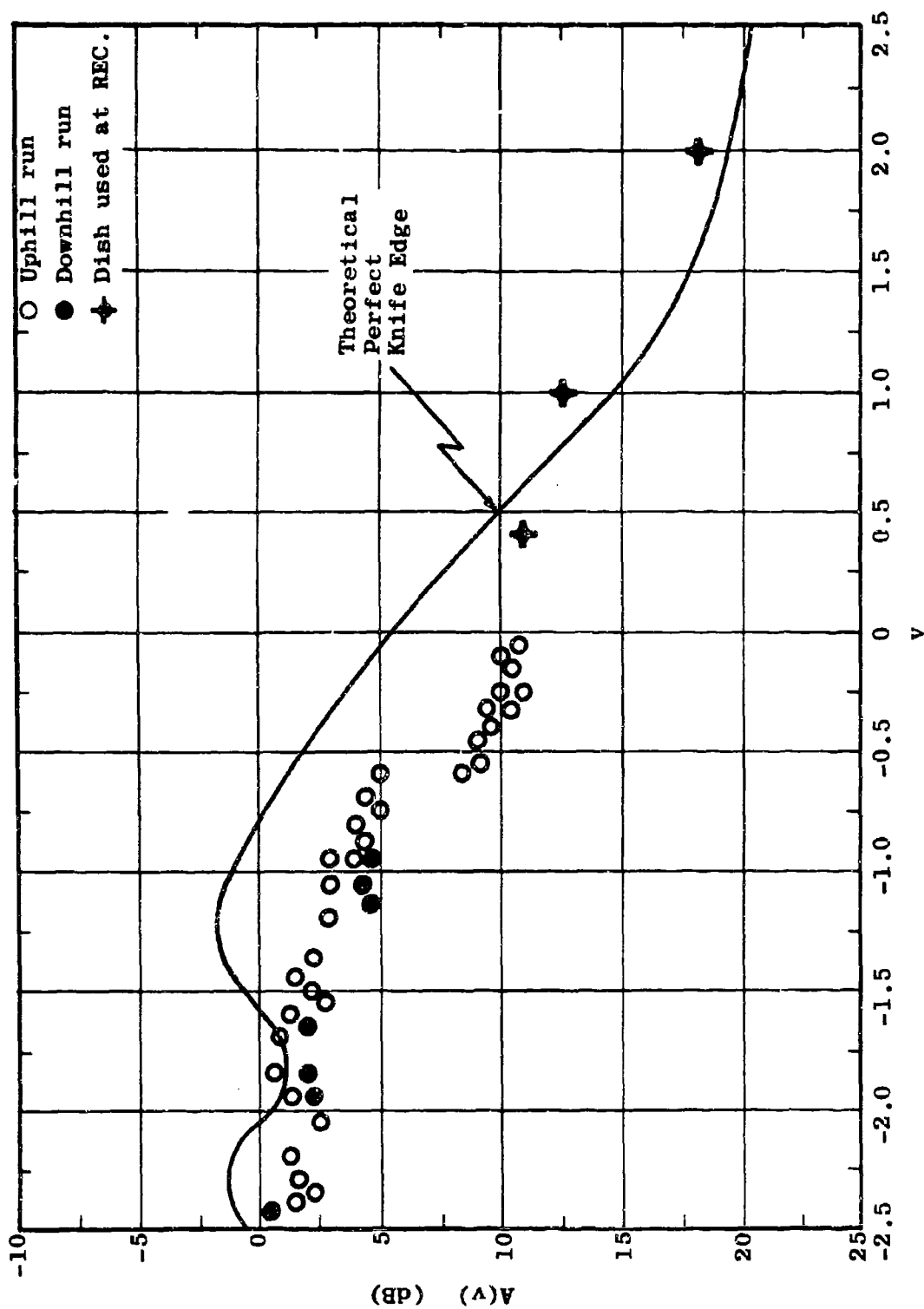


Figure 5.127 Measured Knife-Edge Loss at 10.0 Gc/s

been considered the diffracting surface. Due to the opaque nature of the trees at microwave frequencies, the height of the perfect knife edge must include the height of the foliage on the terrain obstacle. The actual loss experienced should be within about 5 dB of the theoretical loss. For more detailed information concerning the diffraction loss experiment, refer to Section 6 of Semiannual Report Number 7.

5.9.1.4 Diurnal Fading Tests

Diurnal fading, which is the variation of signal levels over a 24-hour period, is due primarily to changes in atmospheric conditions for line-of-sight paths. For long transmission paths, at microwave frequencies, significant amounts of fading may occur, affecting system reliability. A common design consideration for such paths is to utilize experimentally determined fading distribution functions. Since these functions may vary with the environment, it is desirable to use functions which correspond most closely to the environment of the path being considered. Thus, the primary purpose of the diurnal measurements in this program was to provide fading distribution functions applicable to tropical areas.

Due to numerous logistical problems, only relatively short line-of-sight paths could be employed for these tests. The path used was the same path employed for the diffraction measurements. Typical diurnal plots taken over this path are presented in Figures 5.128 through 5.130. Weather conditions varying from clear skies to heavy rain were encountered with no significant deviation of the received signal level.

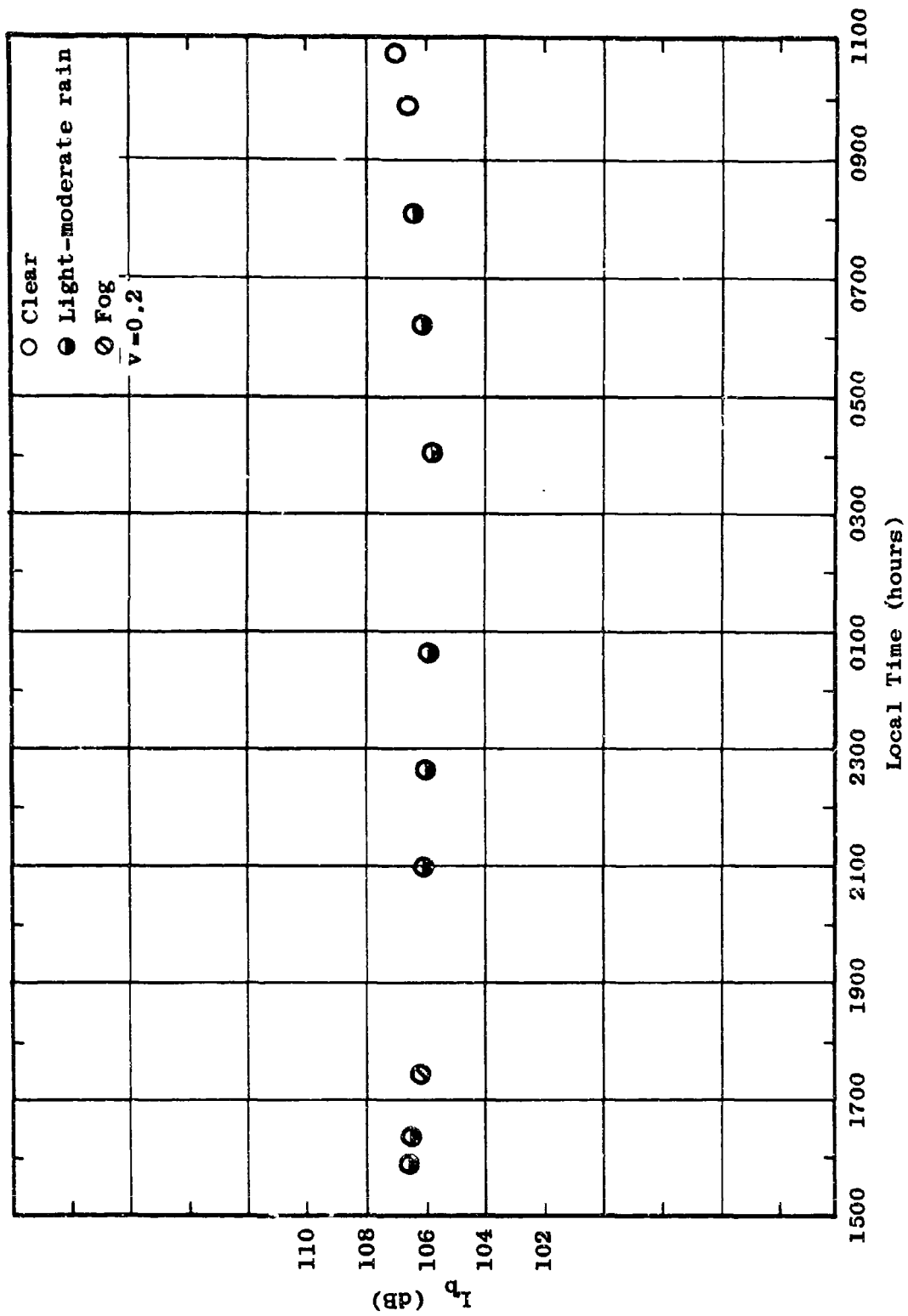
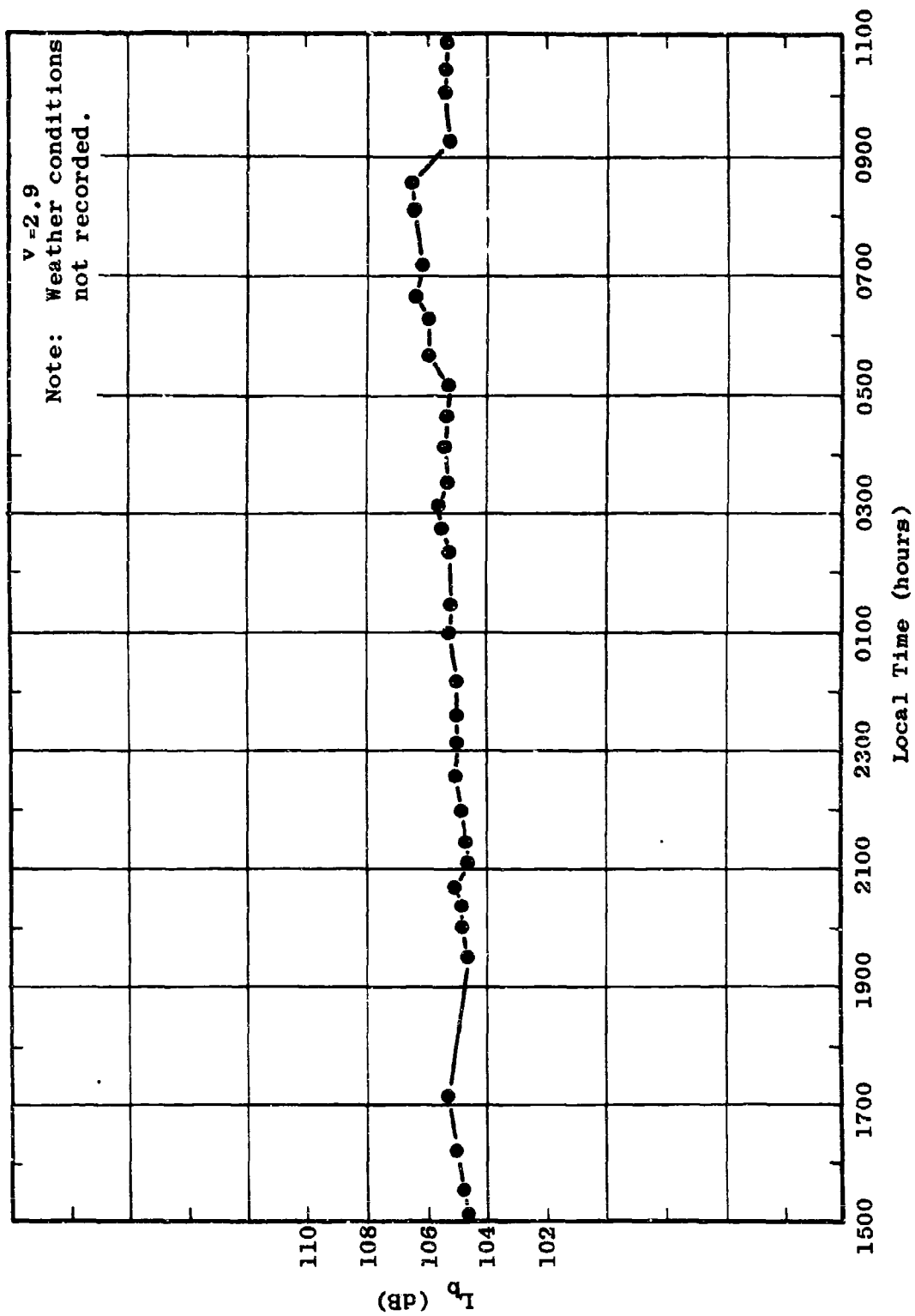


Figure 5.128 Diurnal Variation of L_p at 550 Mc/s



It can be concluded from these tests that fading due to refractivity profile changes or to actual weather changes need not be considered in the design of short, 3 to 5 mile paths.

5.9.2 In-Foliage Measurements

The propagation of electromagnetic energy at centimeter and decimeter wavelengths directly through foliage is a complex phenomena. In order to obtain quantitative measures of foliage effects at these frequencies, an in-foliage measurement program was carried out. The following basic experiments were performed: (1) measurement of foliage attenuation, (2) antenna pattern measurements, and (3) continuous 24-hour signal recordings. For each of these experiments, the measurement variables were frequency, polarization, antenna height, and antenna type.

In order to obtain a sufficiently large and representative data base, the measurement program was conducted in two extensively different foliated environments. The two environments, for sake of clarity, have been designated Area A and Area B. Within each area, the data base was further broadened by establishing a number of transmission paths.

This section includes a description of the environments, and the test setup and results for each series of measurements. Whenever possible, test results have been compared with those of similar tests performed by other investigators.

5.9.2.1 Test Area Environment

For an in-foliage transmission path of a given length, the characteristics of the incident field upon the receiving antenna are governed in a large part by the intervening foliage. When using low gain antennas, a certain volume of foliage around the direct line-of-sight ray is illuminated. When high-gain antennas are used, the volume of foliage involved in the transmission of energy is decreased. Thus, at microwave frequencies where it is easy to obtain high directivity, the foliage lying directly in the line-of-sight path is particularly important.

Due to the increasing dependency of transmission loss upon specific features of the foliage for high-gain antennas, it was important to specify in as much detail as possible the foliage parameters associated with each transmission path over which data was taken.

This section presents the results of a foliage study conducted by Jansky & Bailey personnel in Areas A and B. In addition, a general description of both test areas is given, including photographs showing typical patches of foliage. Additional information regarding the location and nature of foliage in the Pak Chong Area A can be found in a special report prepared by the Military Research and Development Center in Bangkok.¹ Similar information may also be found in Semiannual Report No. 6.

5.9.2.1.1 Area A Description

Area A, located at the main Pak Chong test site,

contains three transmission paths. The three in-foliage receivers on these paths share a common transmitter. The layout, to scale, is shown in Figure 5.131. The jungle in Area 1 is classified as a semi-evergreen forest. There are a large number of different tree types in this area, but about 35 percent are of two species. The botanical names for these two species are "Diospyras" and "Hydnocarpus Illicifolius."

Although the undergrowth is very dense, it can usually be penetrated on foot without cutting a path. Optical measurements made throughout the Pak Chong area show that the crown cover is such that the best angle for ground-to-air observation is vertical, which is not true in all types of forests. These measurements also indicate that at a vertical angle, 80 percent of the hemisphere is obscured and that obscuration generally increases as the angle from vertical increases.

Since the actual foliage along the three transmission paths in Area A was selected on the basis of its similarity to the general nature of foliage in the area, it is expected that the general measurements mentioned above also apply to specific vegetation through which in-foliage tests were made.

Photographs showing the typical nature of foliage directly in the transmission path are presented in Figure 5.132.

A rather detailed tree study has been conducted in Area A. For each transmission path, a region running

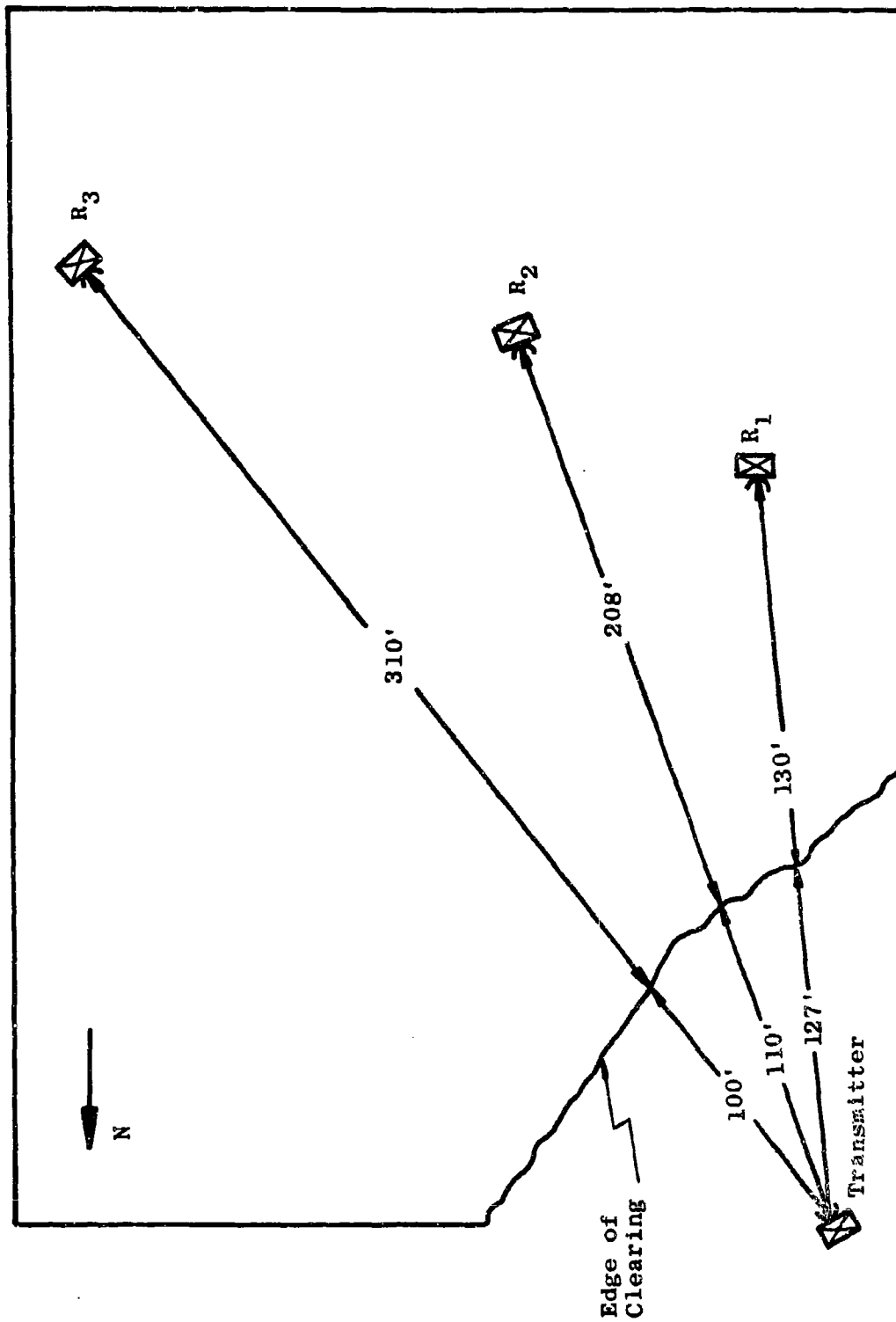
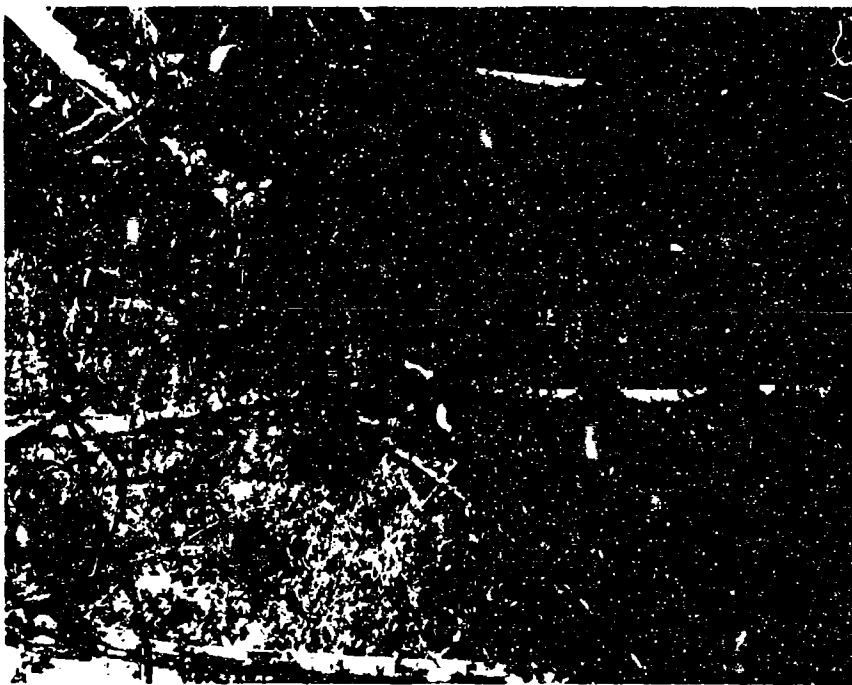


Figure 5.131 Transmission Path Layout for Area A



Antenna at Medium Height
Viewed from Transmitter



Antenna above Treetops
Viewed from Transmitter

Figure 5.132 Typical Foliage in Area A

from the transmitter to receiver and extending to about 30 or 40 feet on either side of the line-of-sight path was examined. Within each region, three parameters of the trees were measured or estimated. These were position, base diameter, and height. Other floral characteristics such as species, leaf size, leaf density, and height of canopy were not considered in this study. However, these characteristics are presented in the MRDC report for 18 sample plots in the Pak Chong area.¹

The treetops were seldom visible from the ground, and their height was probably estimated to within \pm 5 feet. Several of the taller treetops were estimated by sighting from the receiver tower. Only trees with diameters of 2 inches or greater were tabulated.

Plots showing the position of each tree for paths T-R₁, T-R₂, T-R₃ are shown in Figures 5.133 through 5.138. The approximate edge of the clearing and the distance from the clearing edge to the transmitter tower are also indicated in each plot. Each tree is represented by a circle, the circle diameter indicating in a rough fashion the relative size of the tree.

Cumulative distribution plots of tree diameter and tree height have been prepared for each of the paths. These graphs indicate the percent of trees whose diameter or height are less than or equal to any specified range of interest. Superimposed on the cumulative distribution plots are the corresponding frequency distribution plots. The bars give the number of trees that are within a given height interval.

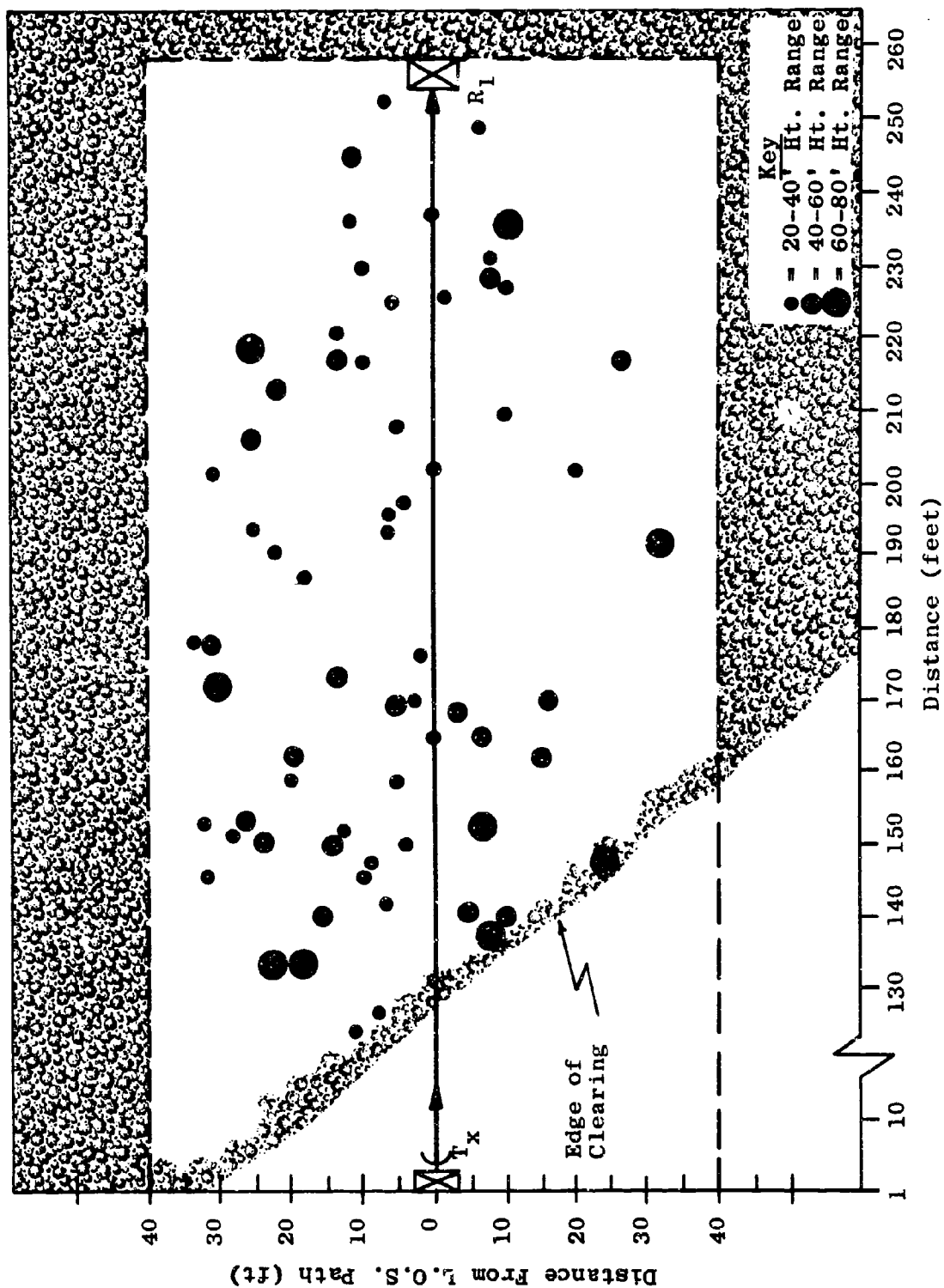


Figure 5.133 Tree Plot for T- R_1 Path, Area A

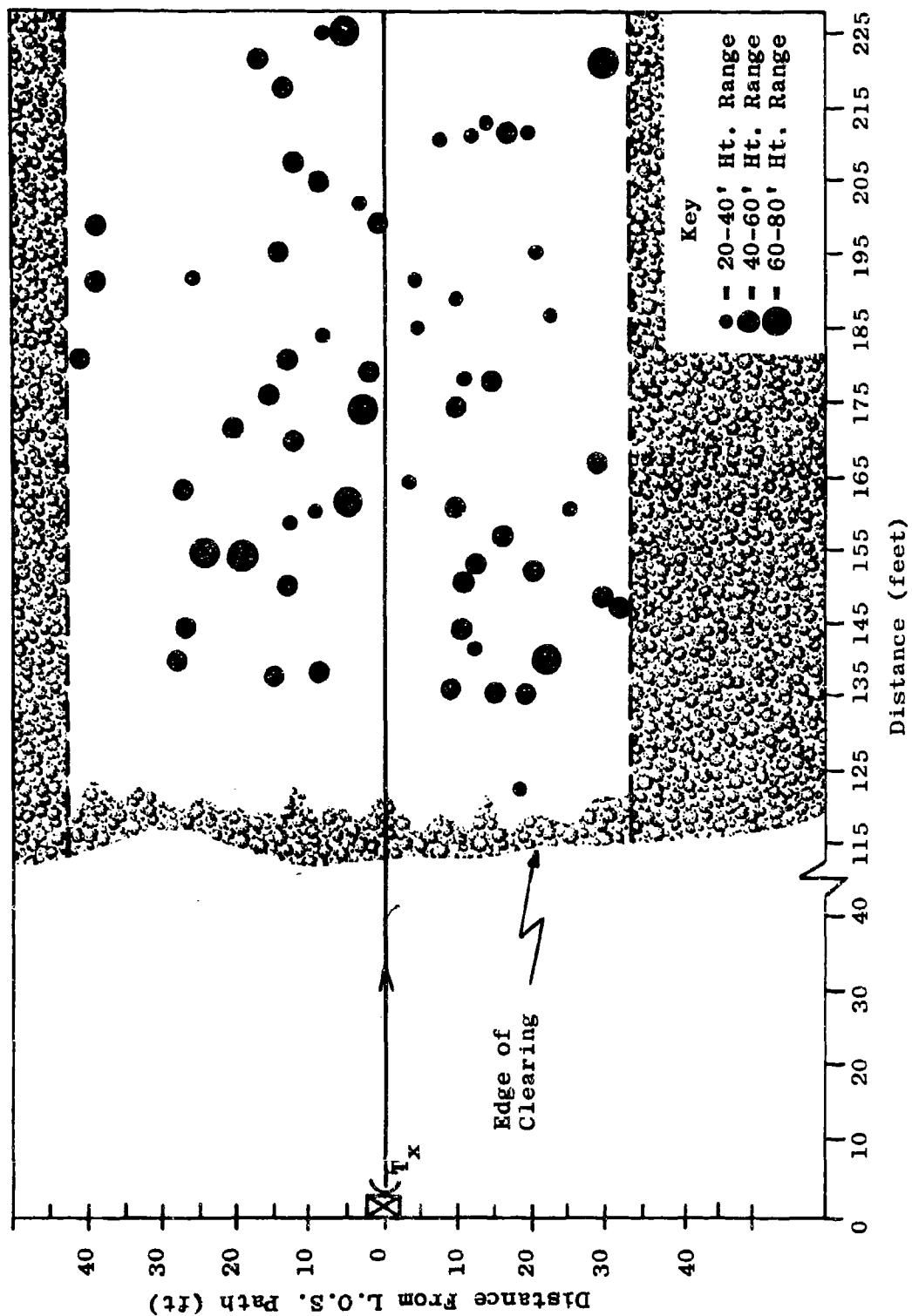
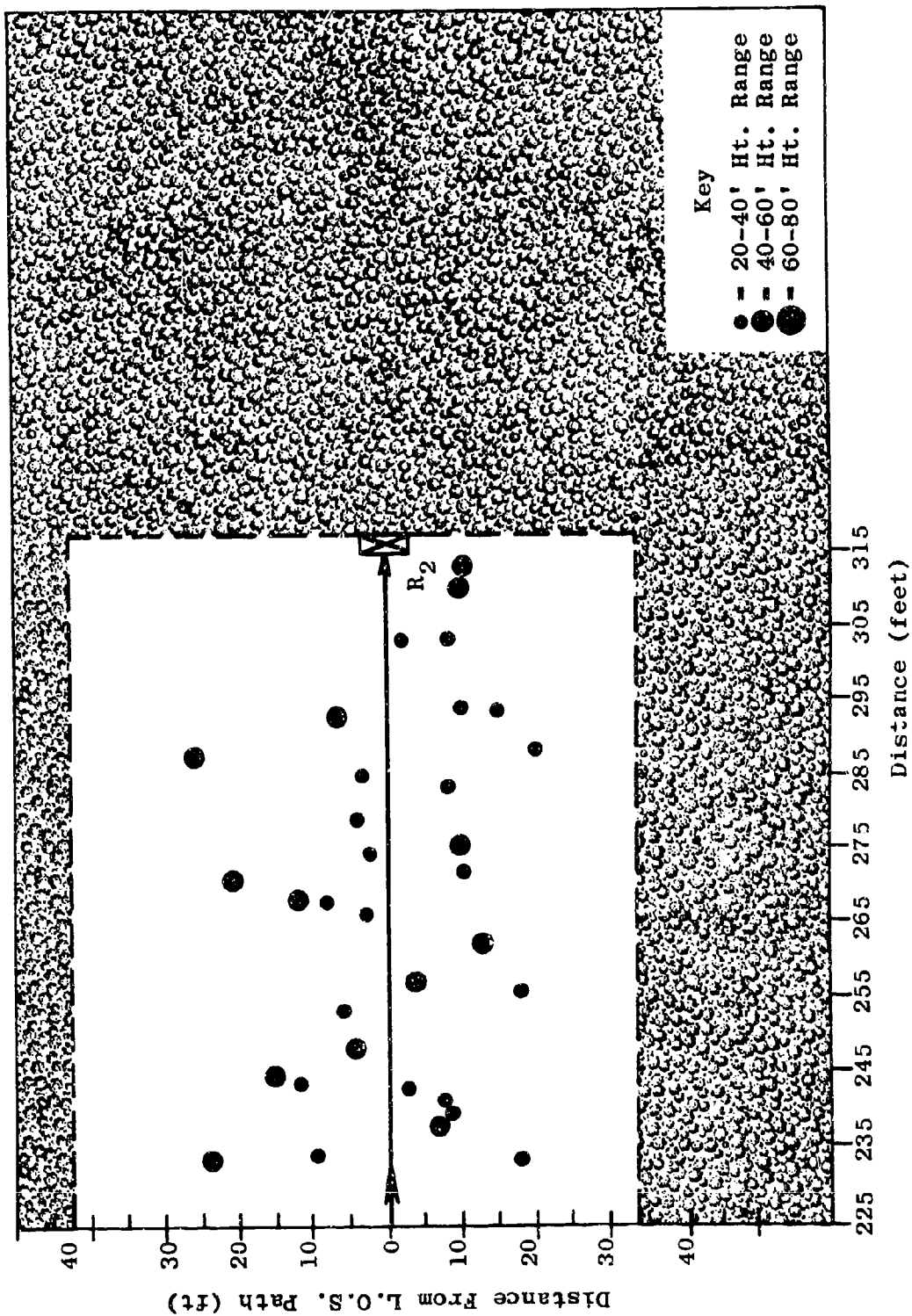


Figure 5.134 Tree Plot for T-R₂ Path, Area A

Figure 5.135 Tree plot for T-R₂ Path, Area A

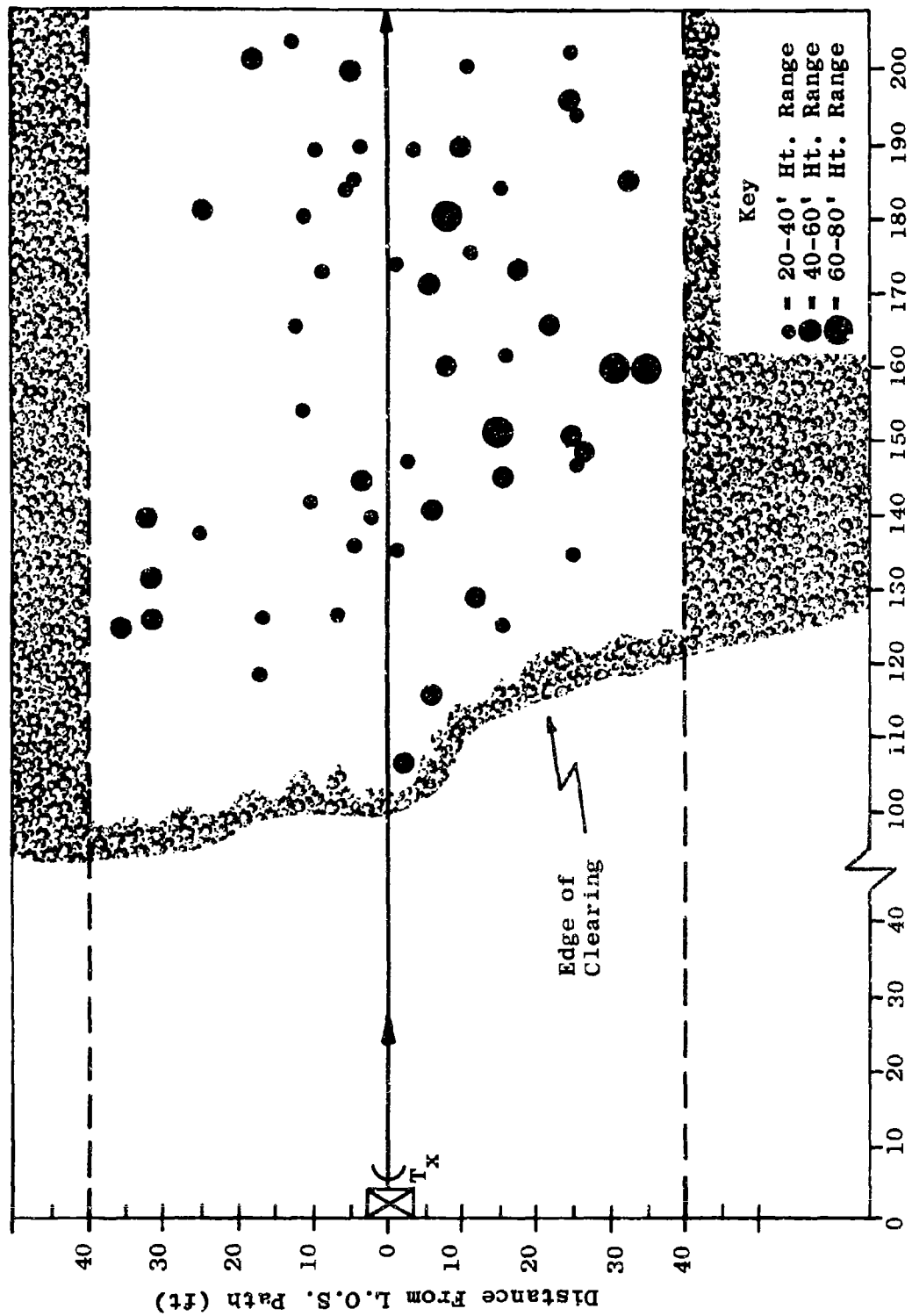


Figure 5.136 Tree Plot for T-R₃ Path, Area A

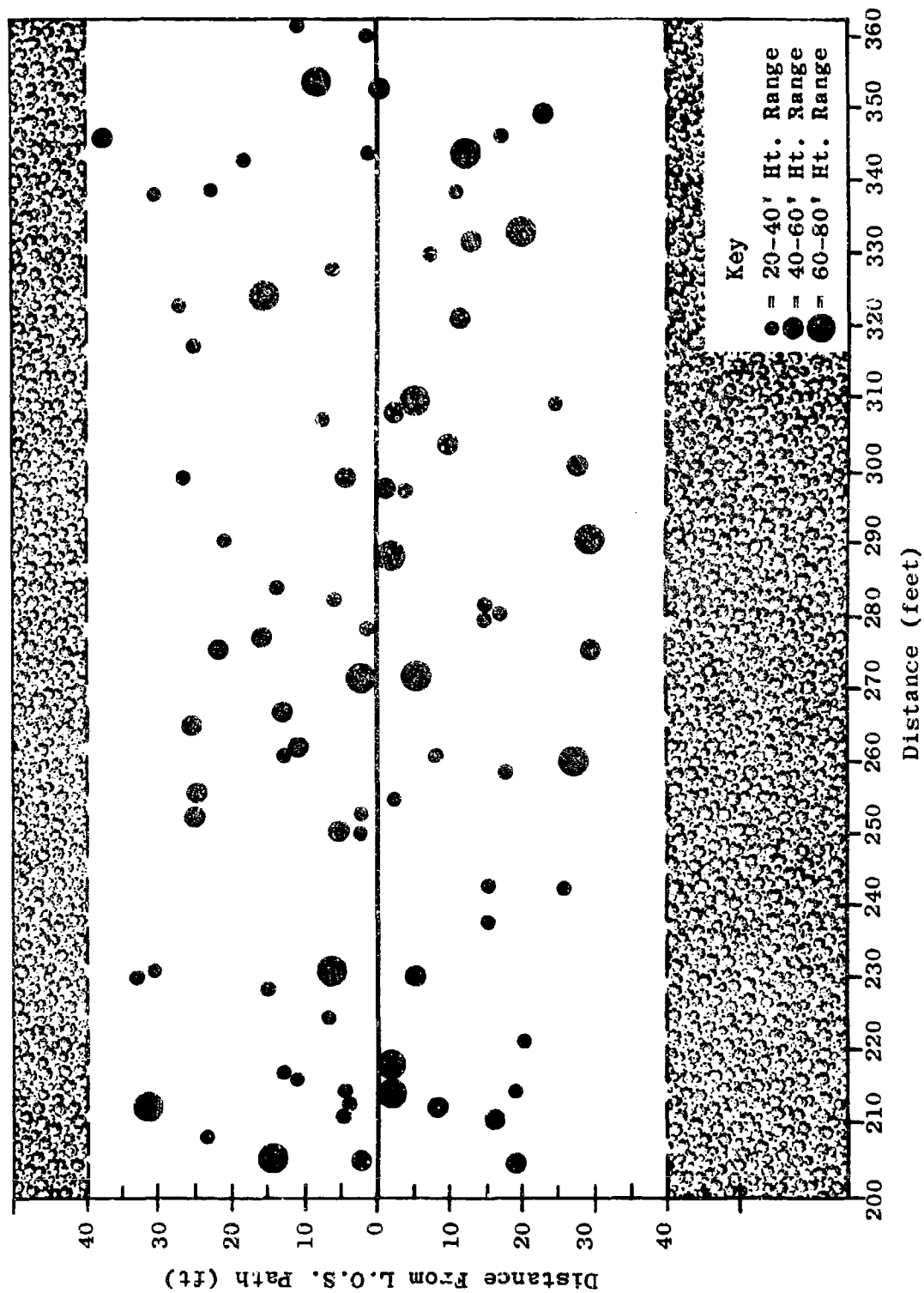


Figure 5.137 Tree Plot for T-R₃ Path, Area A

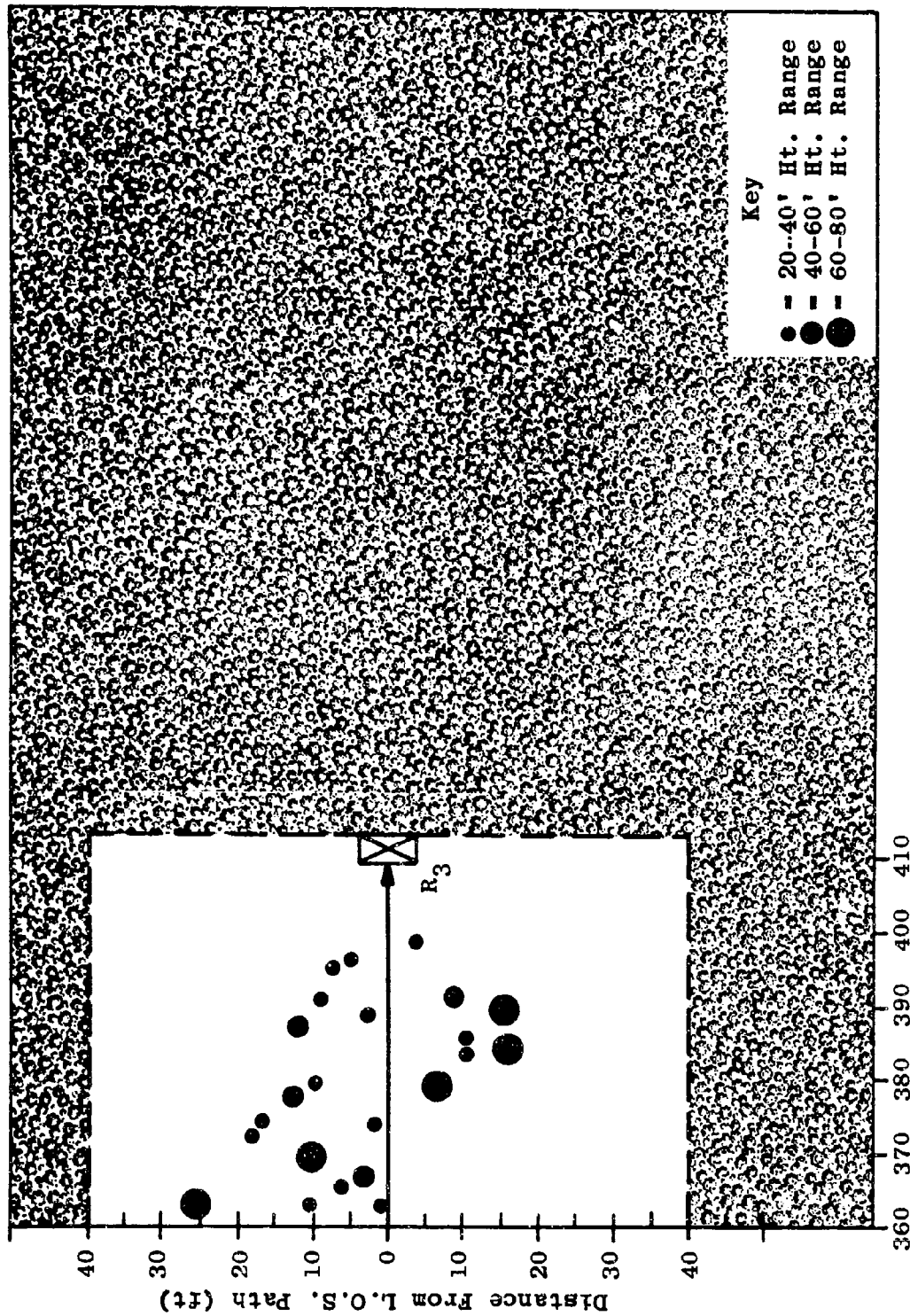


Figure 5.138 Tree Plot for T-R₃ Path, Area A

These graphs are presented in Figures 5.139 through 5.144.

For comparative purposes, the 10, 50 and 90 percent points from the cumulative distribution plots are listed in Table 5.25 for each transmission path.

Table 5.25

DISTRIBUTION OF TREE SIZE

<u>Path</u>	<u>Percent of Trees Below Listed Ht. and Diameter</u>	<u>Height (ft)</u>	<u>Diameter (in)</u>
T-R ₁	10	15	2
T-R ₁	50	35	4.5
T-R ₁	90	57	11
T-R ₂	10	19	3
T-R ₂	50	38	4.5
T-R ₂	90	55	9
T-R ₃	10	20	2.8
T-R ₃	50	35	4.5
T-R ₃	90	60	9.5

Table 5.25 shows that the distribution of tree heights and diameters for the three transmission paths are very similar. Reference to the cumulative distribution curves of tree heights indicates that in the 10 to 90 percent range, the distributions closely follow a straight line function. Since the grid construction of this graph paper is such that normal distributions plot as straight lines,

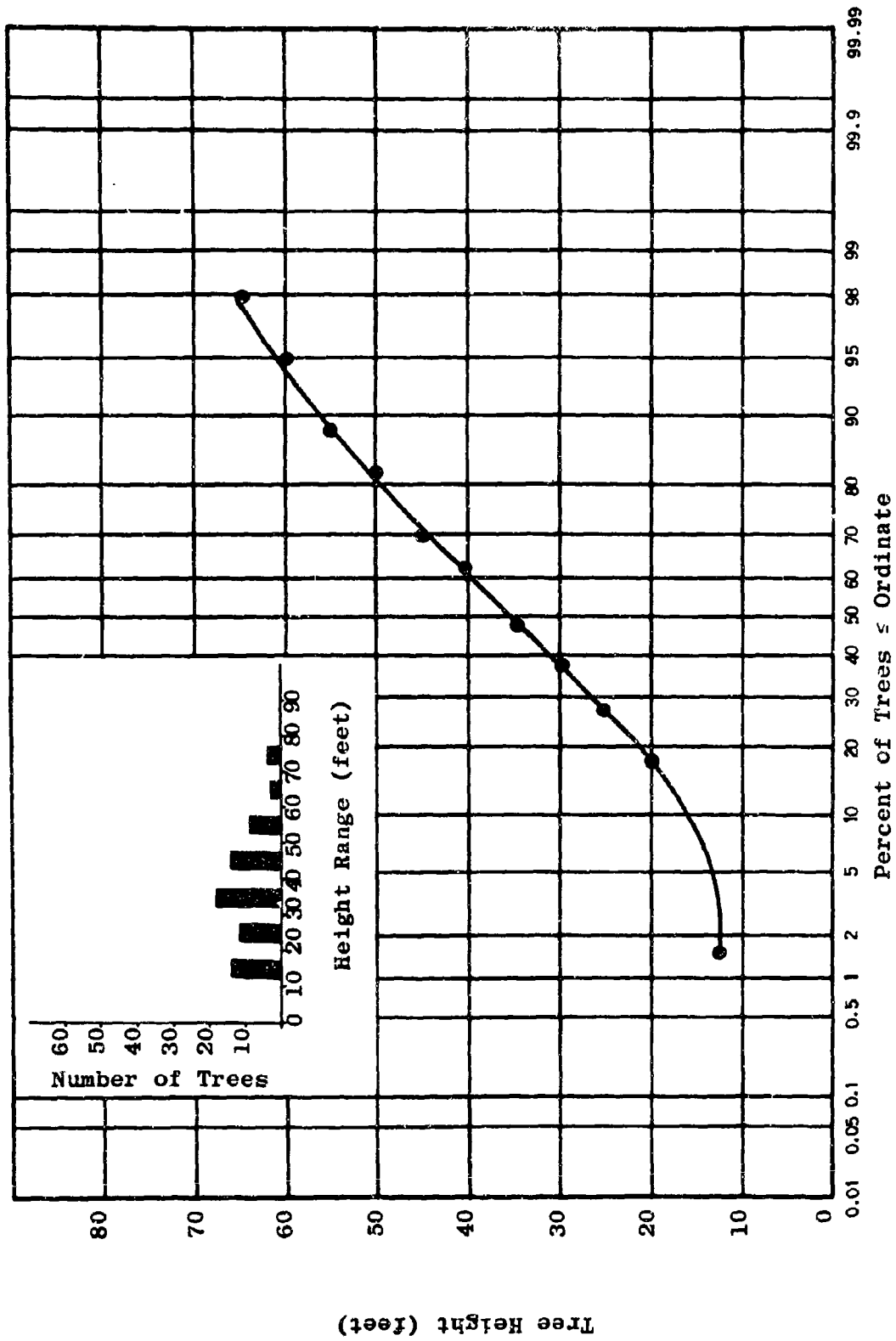


Figure 5.139 Cumulative Distribution of Tree Heights for T-R₁ Path
(Insert Graph Gives Frequency Distribution)

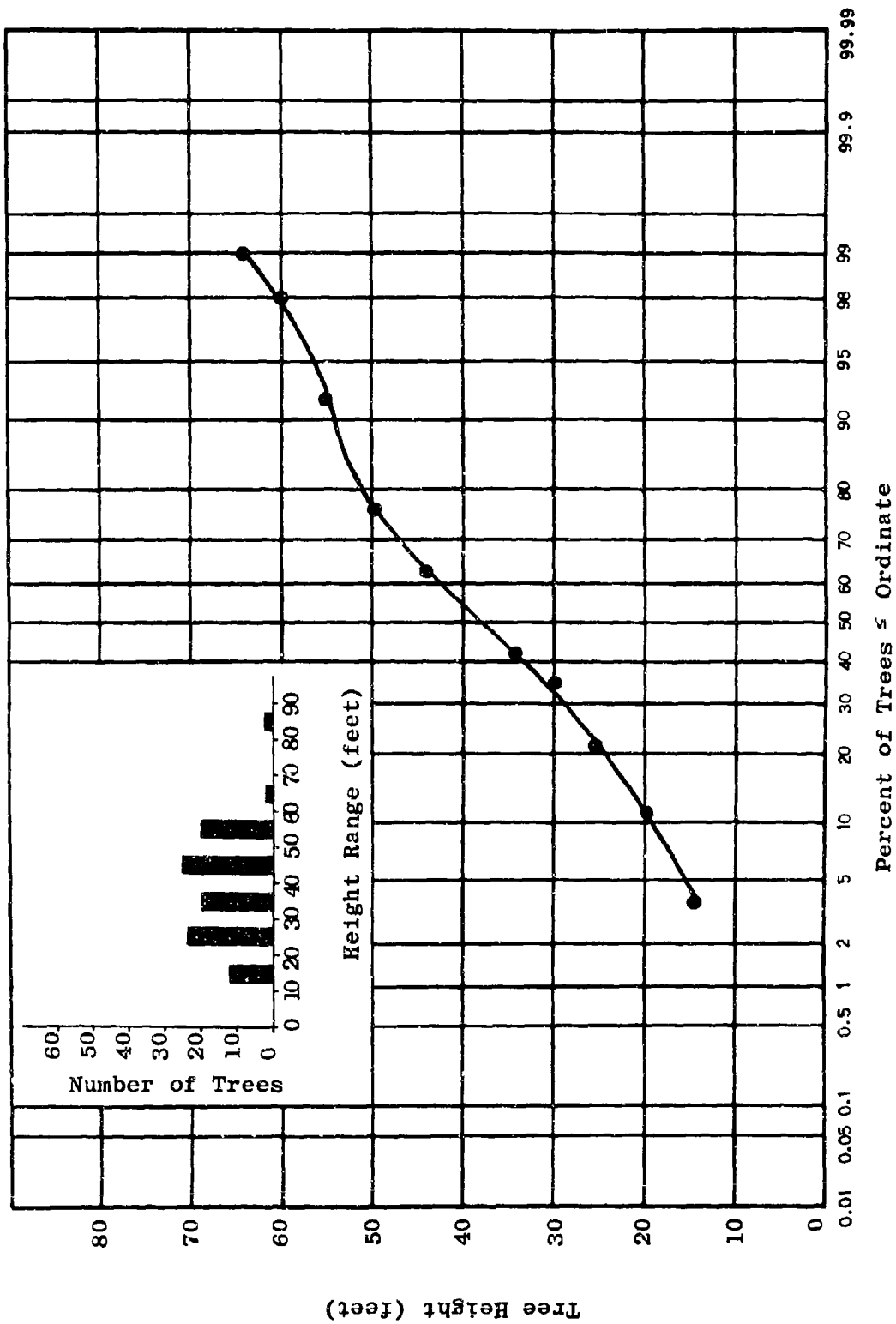


Figure 5.140 Cumulative Distribution of Tree Heights for T-R₂ Path
(Insert Graph Gives Frequency Distribution)

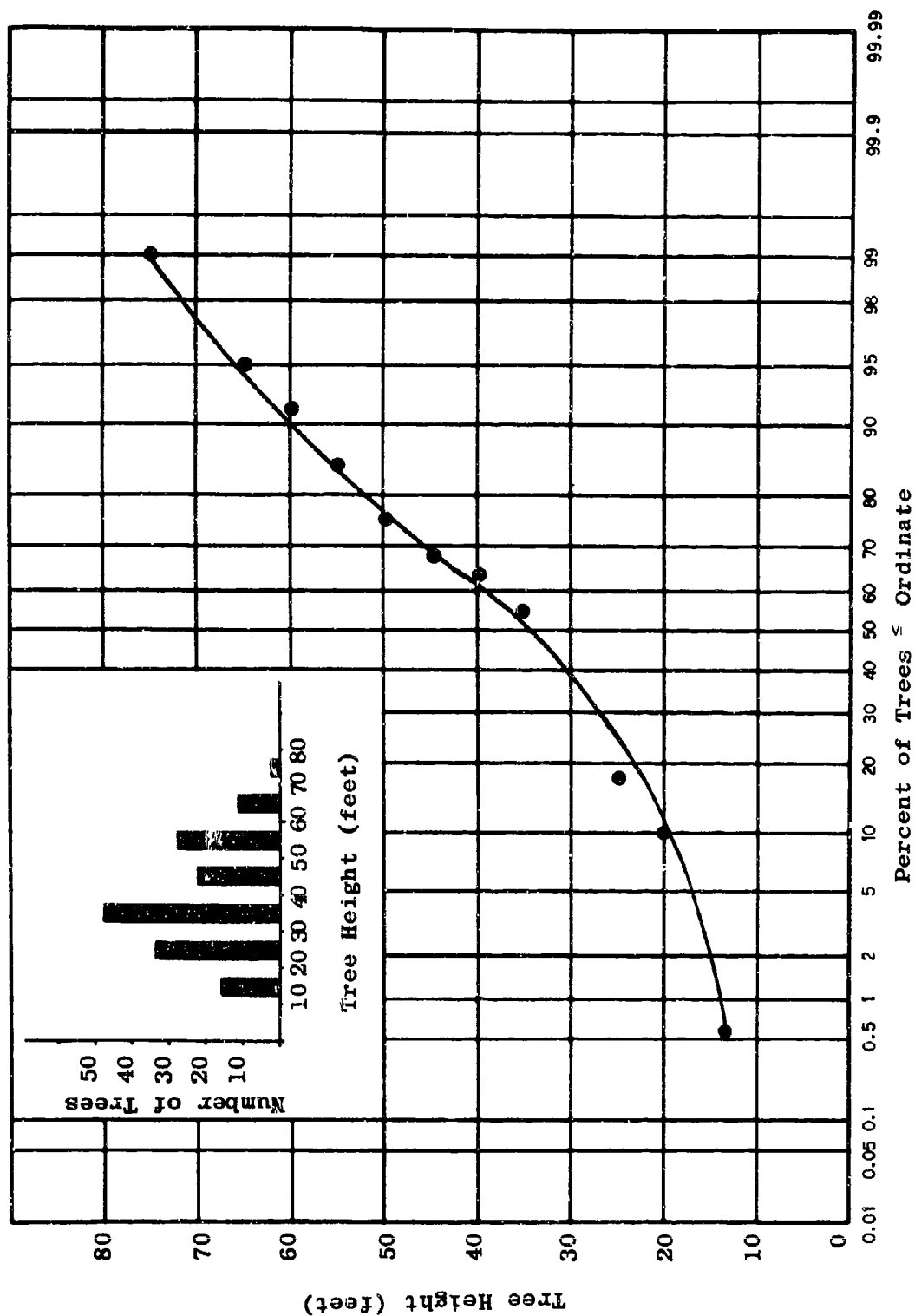


Figure 5.141 Cumulative Distribution of Tree Heights for T-R₃ Path
(Insert Graph Gives Frequency Distribution)

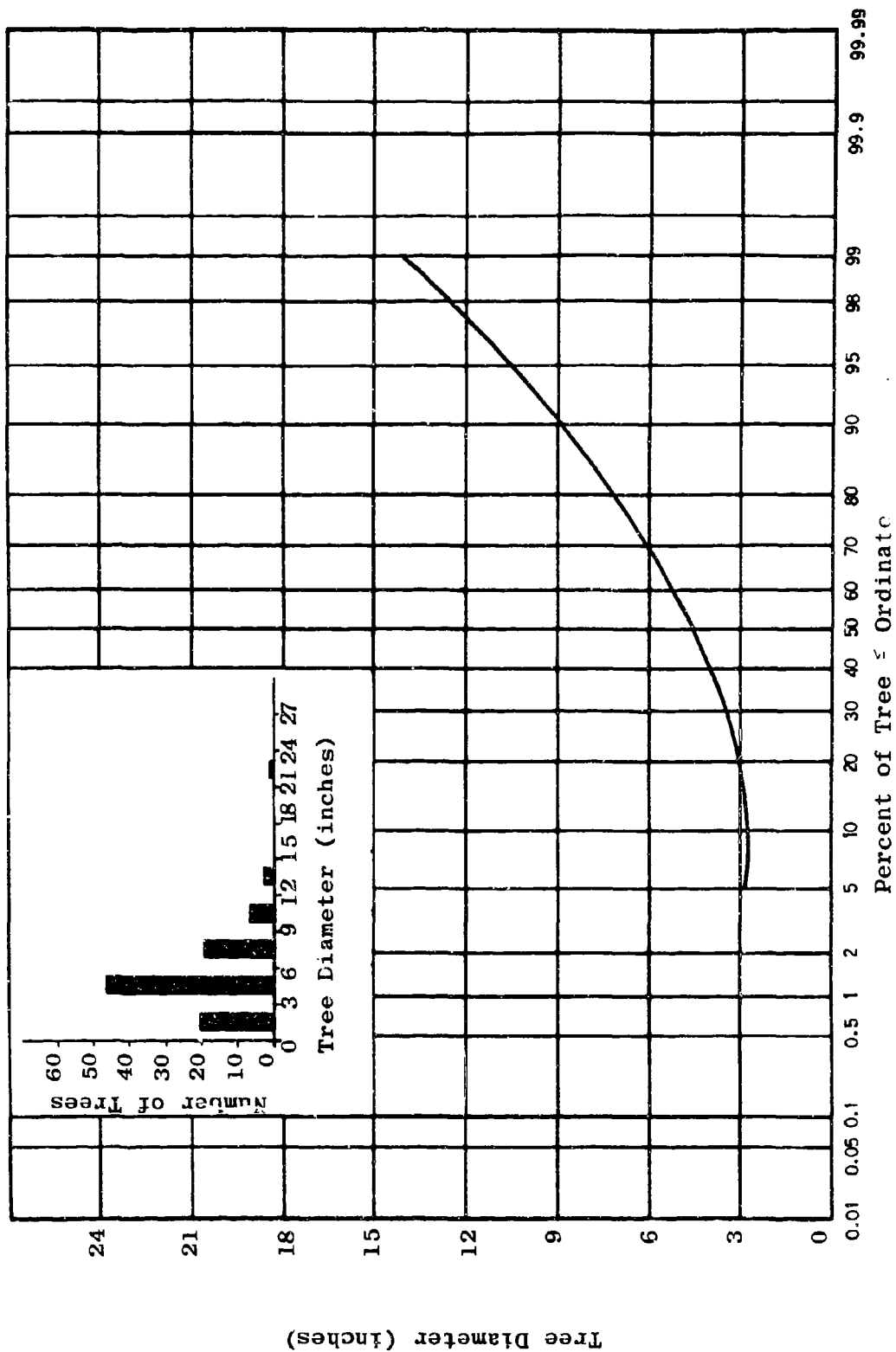


Figure 5.142 Cumulative Distribution of Tree Diameter for T-R₁ Path
(Insert Graph Gives Frequency Distribution)

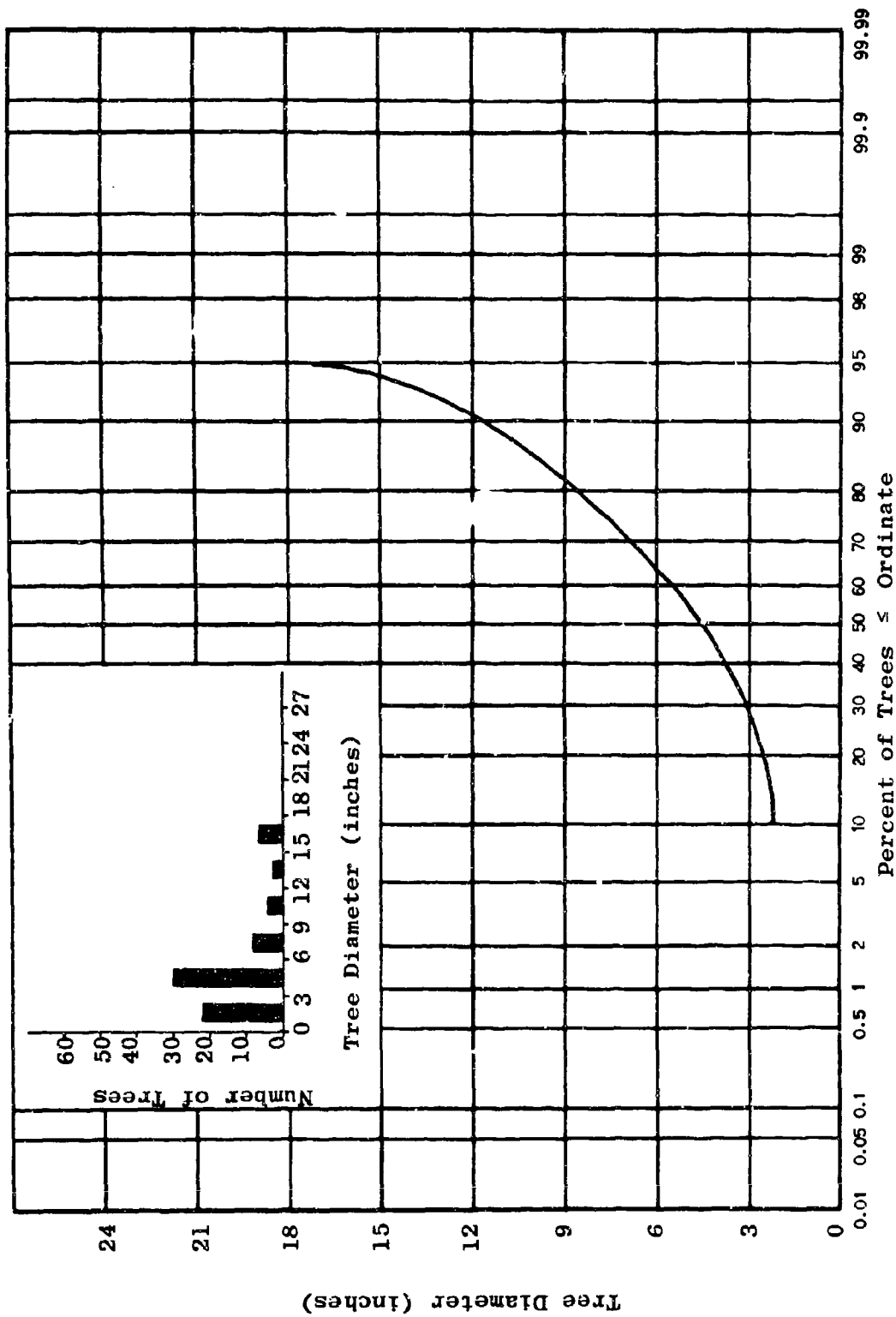


Figure 5.143 Cumulative Distribution of Tree Diameter for T-R₂ Path
(Insert Graph Gives Frequency Distribution)

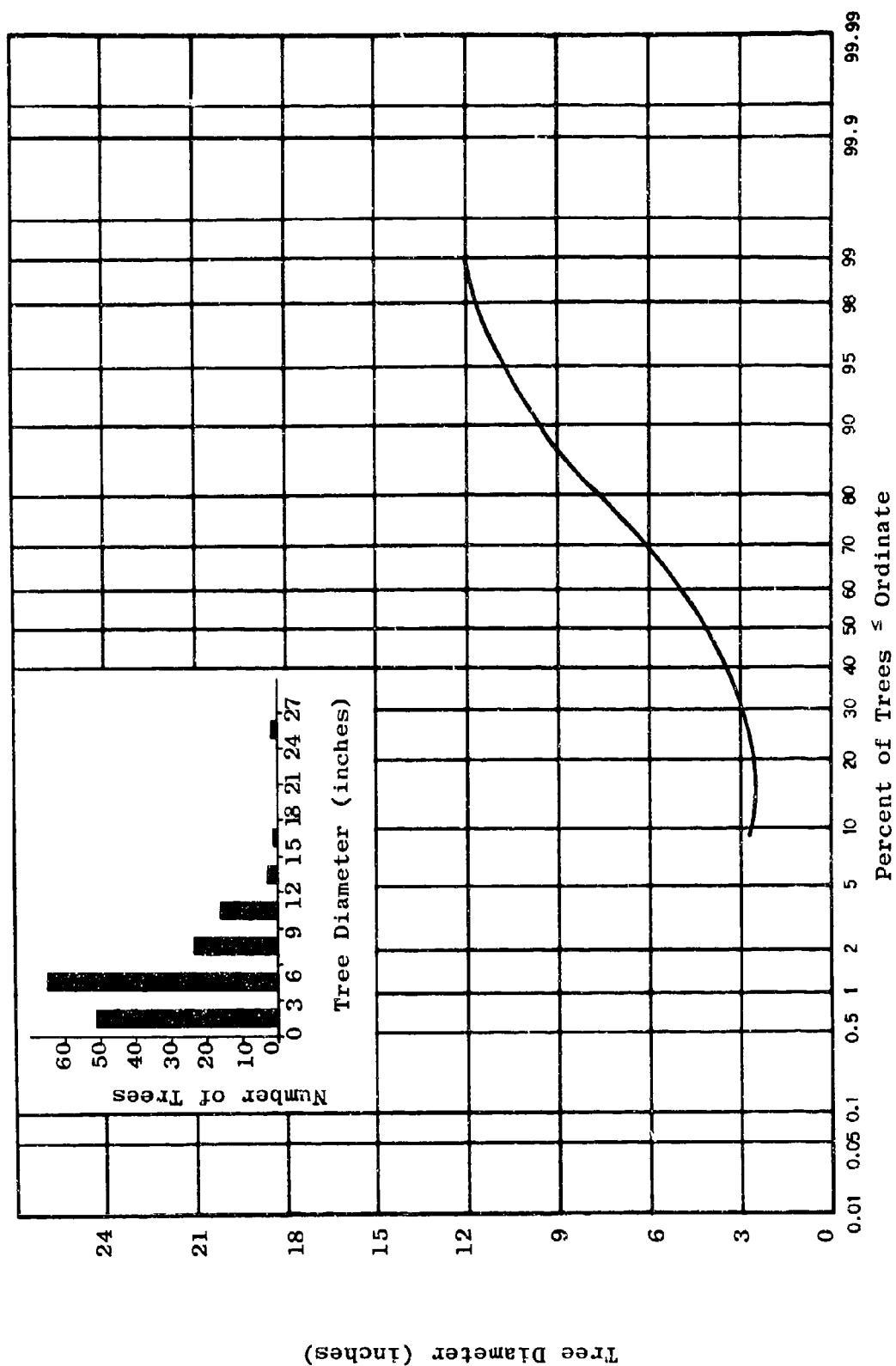


Figure 5.144 Cumulative Distribution of Tree Diameters for T-R₃ Path
(Insert Graph Gives Frequency Distribution)

trees in the 10 to 90 percent range appear to be almost normally distributed.

Additional information concerning tree characteristics in each test path is listed in Table 5.26.

Table 5.26

TREE CHARACTERISTICS IN AREA A TEST PATHS

	<u>T-R₁</u> <u>Path</u>	<u>T-R₂</u> <u>Path</u>	<u>T-R₃</u> <u>Path</u>
Area of plot (ft ²)	9100	16,240	24,400
Total Number of trees	66	95	160
Tree density (trees/acre)	316	255	287
Avg. tree height (ft)	38.9	40.3	40.5
Med. tree height (ft)	35	38	35
Avg. tree diameter (in)	6.2	5.7	5.6
Med. tree diameter (in)	5	5	4.5
Total basal area (ft ²)	20.8	20.9	37
Percent covered by basal area (%)	0.23	0.13	0.15

The following similarities are noted from the above table: (1) the tree density (trees/acre) is about the same for each plot, (2) the average and median tree height values are about the same in each case and, (3) the percent of basal area coverage in each case is roughly the same.

5.9.2.1.2 Area B Description

Area B is located approximately 100 miles south of Bangkok near the town of Sattahip. Four transmission paths were selected in this area for tests. Each of the four infoliage receivers, designated R_1 through R_4 , utilizes a common transmitter situated in a clearing. The path layout is shown in Figure 5.145.

The foliage in this area is much different from that in Area A, mainly because of the difference in tree type. While Area A contains mostly tall, deciduous hardwood, Area B is almost totally covered with bamboo. The growth of bamboo in the actual transmission paths is extremely dense. The canopy, or foliated portion, is sufficiently thick to keep out the light required to sustain an undergrowth. Thus, near ground level, transmission takes place almost totally through the wood trunk portion of the trees. In Area A, however, a heavy crop of undergrowth provides foliated conditions even near ground level.

Bamboo, rather than having a single stem trunk, tends to grow in "clumps," i.e., several trunks attach at a common point near the ground. From each of these individual trunks emerge the many bamboo "shoots" that grow vertically and contain the foliated portion of the tree. The close spacing of clumps on the ground causes the overlapping and intertwining of the vast number of vertical shoots. The result is a very dense canopy, and ground-to-air observation is almost totally impossible.

Although the spacing of clumps and the lack of undergrowth allows penetration on foot, treacherous condi-

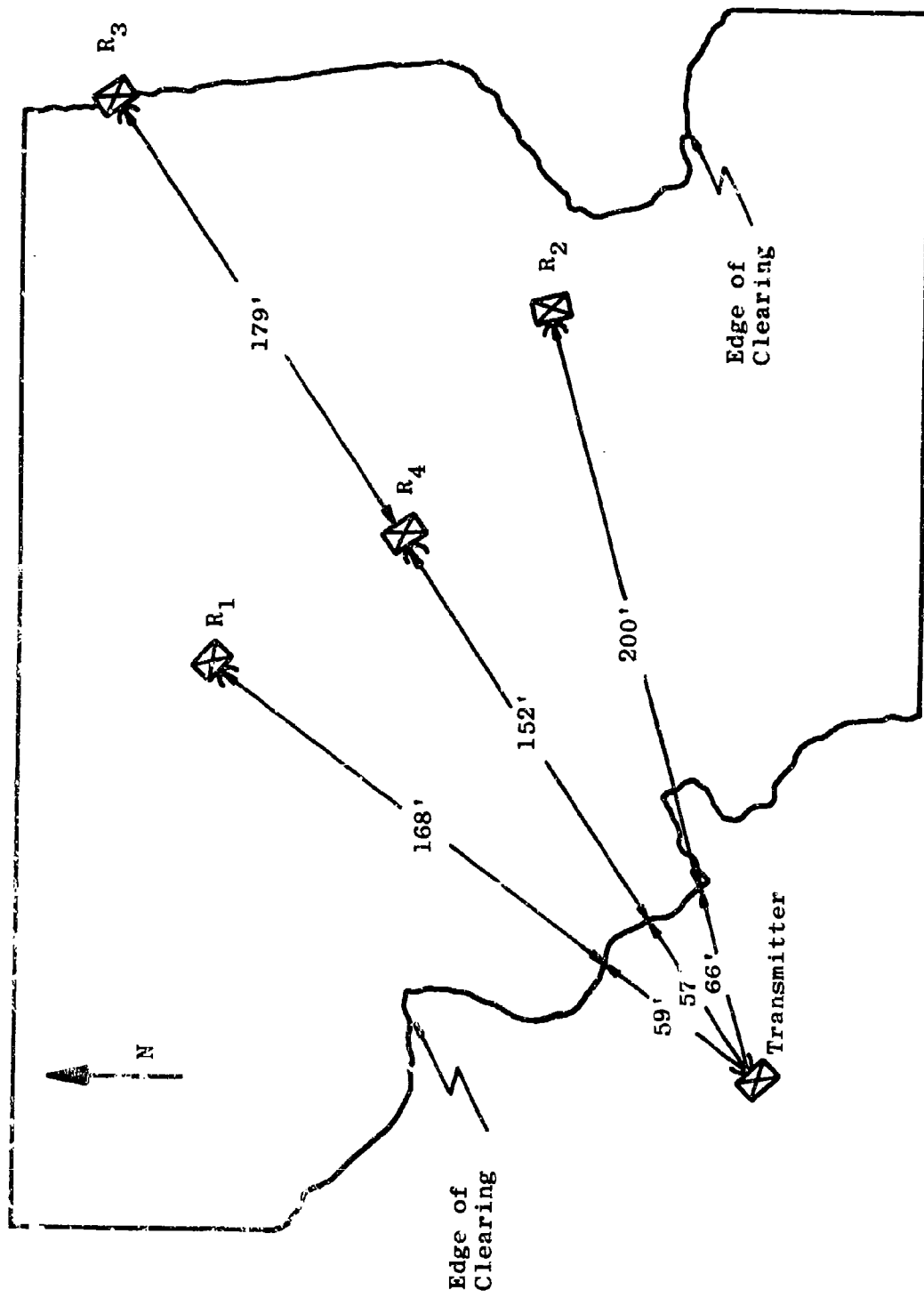


Figure 5.145 Transmission Path Layout for Area B

tions are imposed by large thorns which grow on the lower trunk portion of the trees.

Photographs showing the general nature of foliage in Area B are presented in Figures 5.146a and 5.146b.

The nature of the bamboo restricted the tree analysis to less detail than that performed in Area A. The analysis for this area consists of a single plot, Figure 5.147, which shows the position of each major tree between the transmitter and each of the four in-foliage receivers. Symbols are used to indicate whether the tree was bamboo or of some other species. Areas containing foliage less than about 10 to 15 feet high are marked on the plot, but tree positions within these areas are not indicated. Individual tree height was difficult and sometimes impossible to estimate due to the bending and overlapping of the individual bamboo shoots. Due to the clump arrangement, tree diameter was not recorded as was done for the single-stem trees in Area A. Tree size for bamboo is largely a function of the density of individual shoots per clump. Anywhere from 10 to 50 shoots per clump were noted in the area. A rough sketch of a single clump of bamboo is shown in the upper-right position of Figure 5.147.

5.9.2.2 Parameters Influencing Median Foliage Attenuation

When transmitting directly through foliage over short distances, the transmitted signal level is reduced by free-space attenuation and additional losses imposed by



Bamboo at 21 Feet Viewed from R₄

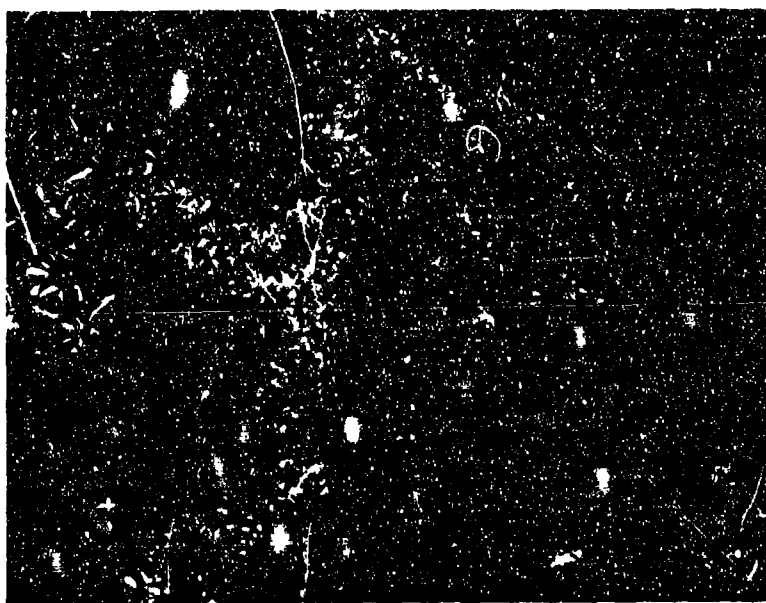


Above Treetops
(XMTR in Background)

Figure 5.146a Typical Views of Bamboo in Area B



Bamboo at 21 Feet Viewed from R_3



Matted Bamboo at 9 Feet Viewed from R_3

Figure 5.146b Typical Views of Bamboo in Area B

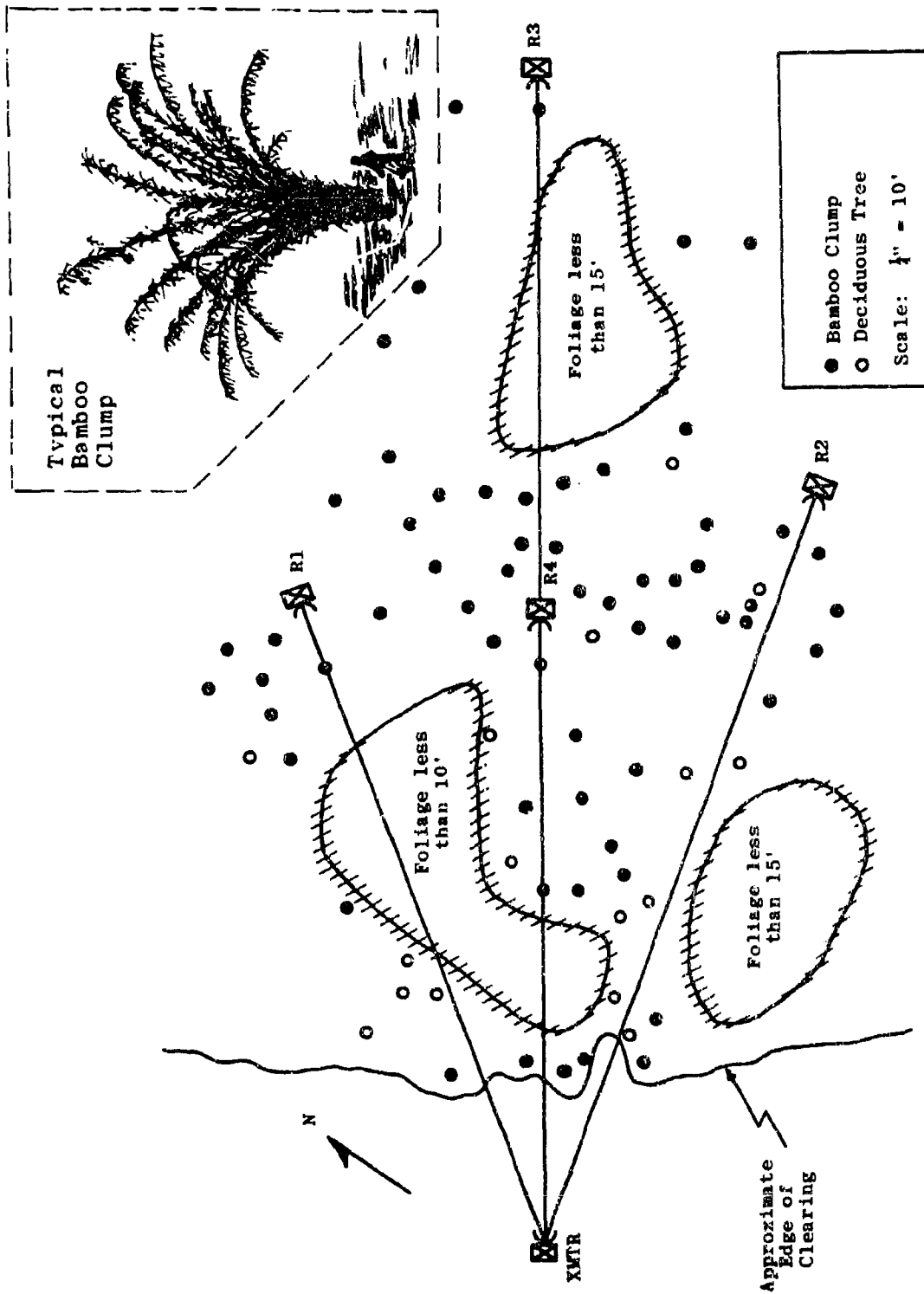


Figure 5.147 Tree Plot of Area B

the presence of the foliage. The magnitude of the foliage attenuation has been found to be highly variable and affected by a large number of parameters.

One of the parameters which can be expected to affect the magnitude of foliage attenuation is the type of foliage through which transmission is taking place. Of particular interest is a comparison of losses in tropical and non-tropical environments. A literature search was made to obtain measured data applicable to a non-tropical environment. Surprisingly little data could be found. Experimental data gathered by Saxton and Lane¹⁷ and empirically derived theoretical curves generated by LaGrone¹¹ appeared most suitable for comparison purposes. Their figures are presented later in Section 5.9.2.5.

The magnitude and variability of foliage attenuation increases with frequency, becoming of paramount concern at UHF and above. The frequency range covered in this study is from 550 Mc/s to 10 Gc/s.

The median path loss measured in foliage at microwave frequencies is a function of the following parameters: (1) frequency, (2) polarization, (3) separation distance, (4) density of foliage, (5) type of foliage, (6) antenna characteristics.

In addition to the influence of the above factors, a "fine grain" variation in the median foliage loss is imposed by time and spatial variation of the field over a small sector. In order to obtain meaningful median foliage attenua-

tion values the "fine grain" influence must be eliminated through the measurement technique.

The factors that affect the median foliage loss are discussed in detail in Sections 5.9.2.2.1 to 5.9.2.2.6. Section 5.9.2.3 covers the "fine grain" spatial and time variations. The measurement technique used to eliminate the "fine grain" influence is explained in the test descriptions, Section 5.9.2.4. Finally, the median foliage attenuation results are presented in Section 5.9.2.5.

5.9.2.2.1 Frequency

The rate of foliage attenuation, expressed as decibels per meter (dB/m), has been experimentally found to increase with frequency. The rate of attenuation for VHF and below is reported to be less than 0.1 dB/m for dense, deciduous woods in full leaf.¹⁸ For frequencies at UHF and above, the rate of attenuation can exceed 1.0 dB/m. A functional relationship between rate of foliage attenuation and frequency has been presented by LaGrone.¹¹ However, for the Thailand data, the measured attenuation increases at a slower rate with frequency than that given by the LaGrone expression.

Unfortunately, no published data above about 3 Gc/s could be found for comparison purposes. For a further discussion of attenuation versus frequency, see Section 5.9.2.5 and Figures 5.155 through 5.166.

5.9.2.2.2 Polarization

Horizontally and vertically polarized waves undergo essentially the same amount of attenuation for direct transmission through deciduous trees in full leaf with undergrowth. Trevor's measurements¹⁹ made at 500 Mc/s in the United States showed polarization independence for trees with or without leaves. Saxton and Lane's measurements¹⁸ made at 540 Mc/s and 1.24 Gc/s through similar types of trees with leaves also indicate no substantial difference due to polarization.

For certain situations, however, a polarization effect has been observed. Measurements made at 100 Mc/s by Saxton and Lane through dense pine woods with no undergrowth indicated attenuations of 0.06 and 0.03 dB/m respectively for vertically and horizontally polarized waves. Also, the spatial variation of the received field over a small sector was reported to be less for horizontal than for vertical polarization.

Tests made in Areas A and B partially support and partially oppose the above observations. Area A is composed of dense deciduous trees with a heavy crop of undergrowth. The measurements in this area generally displayed the polarization independence mentioned previously for similar types of environments.

On the other hand, Area B is characterized by very dense bamboo, so that not enough light penetrates to support any undergrowth. At low antenna heights, transmission takes place through clumps of vertical bamboo trunks without leaves. For low antenna heights, results similar to those reported by

Saxton and Lane for transmission through pine trees with no undergrowth, might be expected. However, the opposite trend was observed. Horizontal polarization in most cases provided more loss. However, the additional loss was not great, seldom exceeding 5 dB.

5.9.2.2.3 Path Length

When transmission takes place directly through foliage, the additional loss above free-space loss naturally increases with separation distance. However, the rate of foliage attenuation (dB/m) remains constant with distance for a completely homogeneous media, but since perfect homogeneity is never encountered in practice the rate of attenuation can also be expected to vary with separation distance.

In addition to the variation of attenuation rate due to foliage non-homogeneity, a further variation may be imposed by a secondary mode of transmission, such as treetop diffraction. The role that treetop diffraction plays depends to a large degree upon the location of the two antennas, the beamwidths of each antenna, and the separation distance. When a low-gain transmitting antenna is situated above treetop level, treetop diffraction can be the dominant mode of propagation when the receiver is low and is located near or in foliage. The reception of television signals is often via this type of diffraction.

If the separation distance is sufficiently short, if the antenna beamwidths are narrow, and if both antennas are located below treetop level, the treetop diffraction mode can be discriminated against to the point that direct

transmission through the foliage provides the total energy that is received. To obtain valid values of attenuation rates, the "treetop" mode should be minimized to the greatest possible extent. When the "treetop" mode begins to contribute an appreciable amount of energy to the receiver, there is a general tendency for the rate of attenuation to decrease. Thus, a test for "treetop" contamination is to plot the rate of attenuation as a function of path length. A persistent tendency for the attenuation rate to decrease with distance would then be a strong indication of treetop diffraction.

However, if the function increases and decreases in a more or less random fashion, then direct transmission is most likely to be the only mode present. A random variation of attenuation rate is produced by a change in foliage density with separation distance.

The data gathered in Areas A and B was tested for treetop diffraction by the above method. No consistent tendency toward a decreasing attenuation rate with distance was noted. Thus, the data is assumed to reflect the attenuation characteristics associated with direct transmission through foliage.

5.9.2.2.4 Foliage Density

The rate of foliage attenuation (dB/m) increases with an increase in foliage density. Foliage density can vary drastically as a function of azimuth angle and elevation above ground. Thus, measured values of attenuation

can in turn be expected to vary over a wide range of values for a number of transmission paths selected in any foliated area.

For a given separation distance, the volume of foliage illuminated by an antenna is governed by the antenna's beamwidth. As the illuminated volume is decreased, specific features of the foliage become more important. Hence, the variability of foliage density in a given area becomes more noticeable as the beamwidth is decreased.

In order to obtain adequate attenuation data for narrow beam transmission, it is advantageous to sample the variability of foliage density by selecting paths at different azimuth angles and obtaining a vertical attenuation profile for each such path. Average attenuation values as well as maximum and minimum values can then be obtained.

5.9.2.2.5 Type of Vegetation

The attenuating properties of trees depend not only upon density and other physical characteristics, but also upon tree type. Trees vary in type by their wood, bark, leaves and certain physical characteristics.

Forest trees are generally divided into two basic groups: (1) conifers or softwoods and (2) broadleaf or hardwoods. Although attenuation variation within a group is to be expected, a larger variation probably exists between groups. Most hardwood trees are deciduous; i.e., they shed their leaves in the fall. A substantial change in attenua-

tion properties has been reported for deciduous trees in full leaf as compared to their leafless state.

Pounds and LaGrone²⁰ of the University of Texas have performed perhaps the most detailed theoretical treatment of the electrical characteristics of trees. The approach taken was first to define the physical parameters associated with the dielectric constant. Next, a mathematical model to compute the dielectric constant was constructed; and, finally, the mathematical model was used in conjunction with empirical data taken at a few discrete frequencies to predict the attenuation at other frequencies.

The relationship thus obtained is shown plotted along with the Thailand data in Section 5.9.2.5, Figure 5.166.

5.9.2.2.6 Antenna Beamwidth

The in-foliage field incident upon a receiving antenna at microwave frequencies is strongly flavored by scatter components. The various components can arrive off-axis and have random magnitude, phase and polarization. Due to the directional characteristics of the incident energy, the beamwidth of the receiving antenna influences the quantity of power that is extracted from the field.

For a non-scatter field the received voltage varies directly with the gain of the antenna in the direction of the source. But, when the field is scattered, the received voltage does not necessarily vary directly with the antenna gain in the direction of the original source of

emission. Additional energy may arrive in phase from an off-axis direction adding to the total power extracted. The characteristics of the in-foliage field is such that as the main beam gain is made to decrease and the beam-width increase, the received voltage or power does not decrease by the amount of decrease in main beam gain, but by a lesser amount.

Thus, the foliage attenuation derived from measurements made in foliage is dependent upon the beamwidths utilized at the receiver. This necessitates specifying the beamwidths when reporting measured attenuation rates. Table 5.28, listing the beamwidths used in this program, is in Section 5.9.2.4.

5.9.2.3 "Fine Grain" Field Variations

Fine grain variations, as used here, refer to variations in the received field over very short time or spatial intervals. At microwave frequencies, small sector spatial variations exist all of the time and at all in-foliage locations. On the other hand, short time variations occur only during windy periods and are produced by movement of the foliage.

The effect of foliage movement with the receiver stationary is similar to the effects seen by moving the receiver over a small sector when the foliage is stationary. In this respect, the small spatial and short time variations are inter-related.

Both of the above factors are discussed in detail below. A correlation study relating wind velocity to signal deviation is presented.

5.9.2.3.1 Time Variability

The rapid field variation produced during windy periods are assumed to result from the alteration of the incident scatter field due to movement of tree leaves and branches. To obtain representative median foliage loss values, these wind effects have to be removed. This has been accomplished in the measurement setup by recording the signal for two or three minutes, then visually selecting the median value over this duration that represents the level expected under no-wind conditions. Under no-wind conditions, the signal level is steady as a function of time. As the wind begins to pick up, the received signal begins to oscillate about the no-wind level, and as the velocity of wind increases, the deviation about the median level increases.

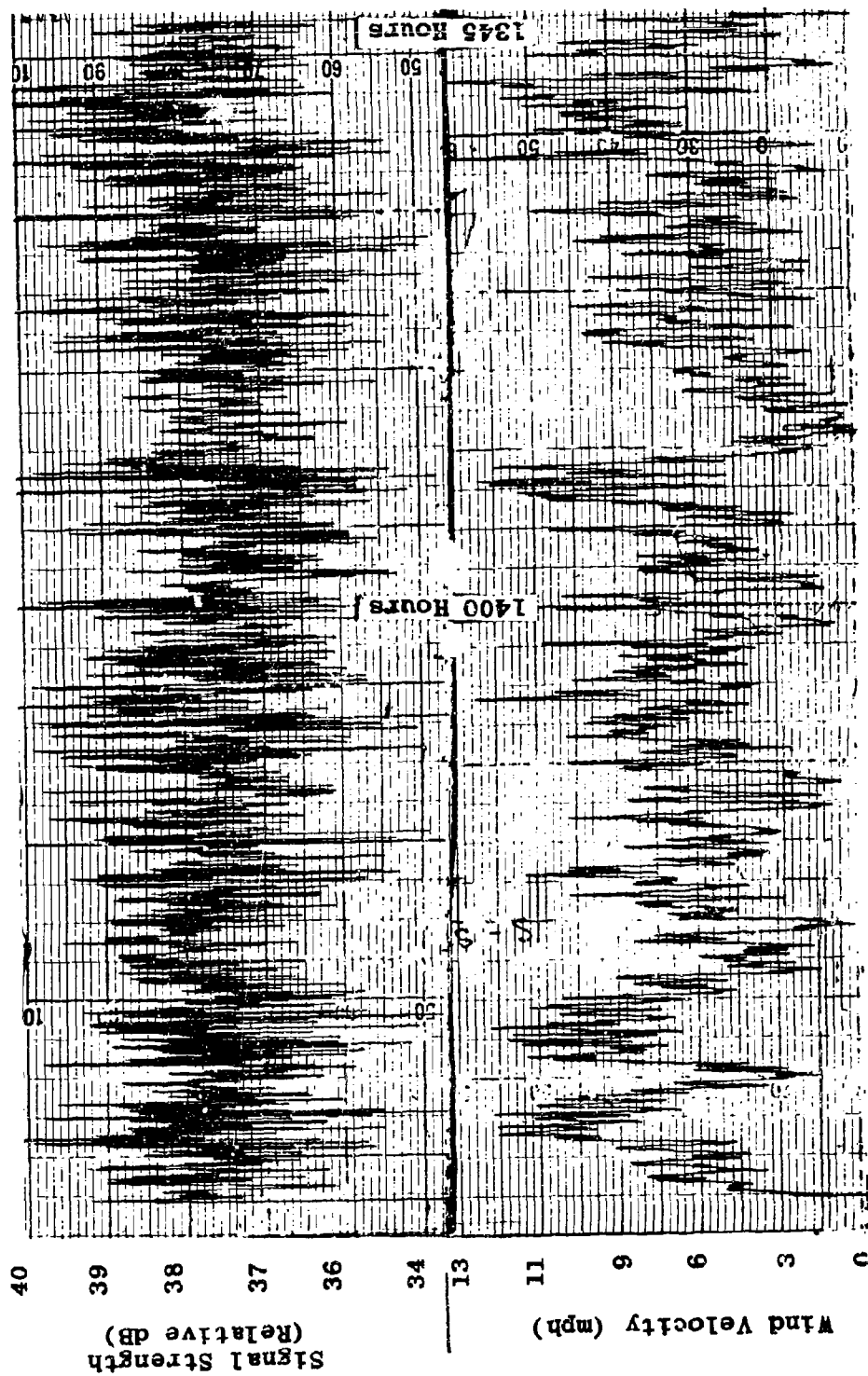
To obtain a correlation between wind velocity and signal variability, several simultaneous signal and wind recordings were made. Signal recordings were obtained as a function of time in the normal manner. The wind sensing device was a standard rotating cup indicator coupled mechanically to an AC generator. The output of the generator was then rectified and passed through a circuit with time constants compatible with the input circuit response of the Varian strip chart recorder. The strip chart was then calibrated to directly record the wind velocity in miles per hour.

The wind speed indicator was physically located at the same height as the transmitting and receiving antennas. The two recorders were synchronized and run at equal record rates.

Being partially comprised of a mechanical device, the response of the wind recorder mechanism was slower than that of the signal recorder. Thus, rapid changes in wind velocity were indicated on the signal trace before the same change was recorded by the wind sensing device.

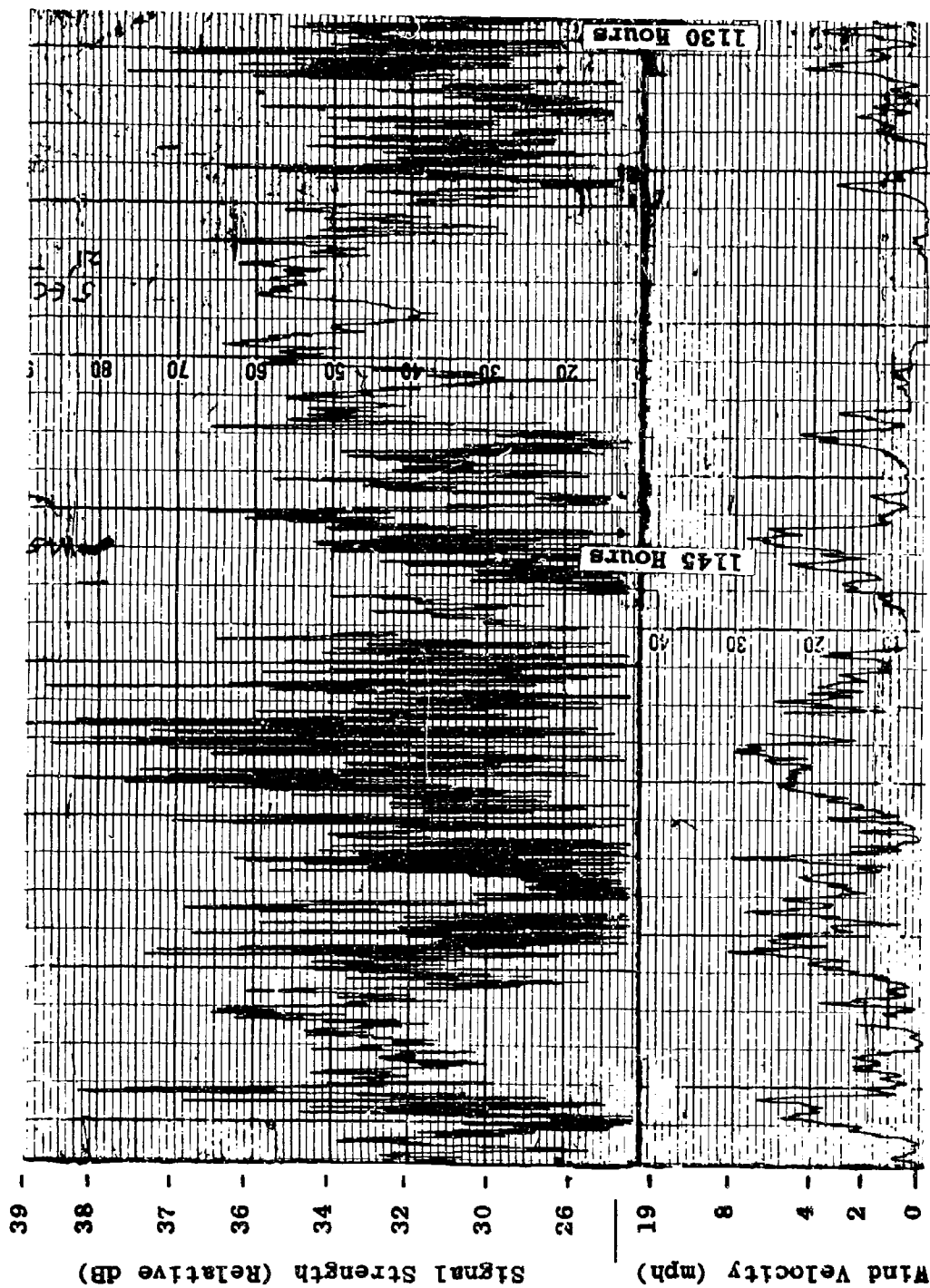
Typical wind and signal recordings are shown in Figures 5.148 through 5.151. The ordinate scale of the signal trace is calibrated in relative dB while the corresponding wind scale is calibrated in miles per hour. The abscissa in both cases represents elapsed time, increasing from right to left. The two traces are positioned so that the starting times are synchronized at the extreme right. As the traces progress from right to left, minute time differentials between the two usually occur due to slight differences in record rates.

By close observation of these recordings the predominant effect of wind, which is the deviation of the signal about its median value, can be noted. This effect can be more clearly seen by constructing an envelope about the signal and wind traces. Rough envelope sketches of Figures 5.148 and 5.149 are shown in Figures 5.152 and 5.153. Again, the wind and signal envelopes are synchronized at the extreme right side of the graph. Wind minima have been denoted by numbers. In all cases, it is noted that each



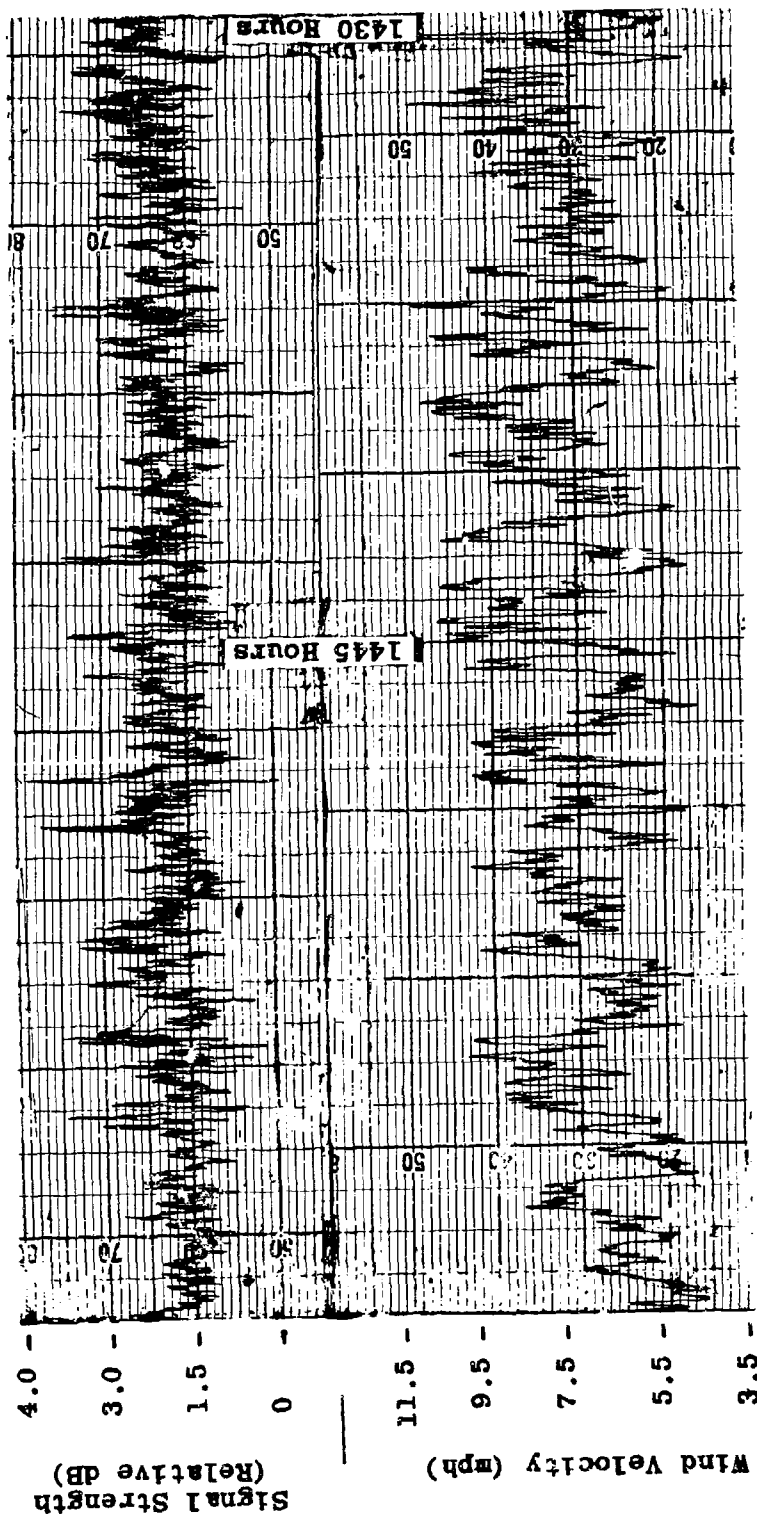
Frequency - 2.5 Gc/s $H_t = H_r = 21 \text{ ft.}$

Figure 5.148 Strip Chart Recording of Wind and Signal



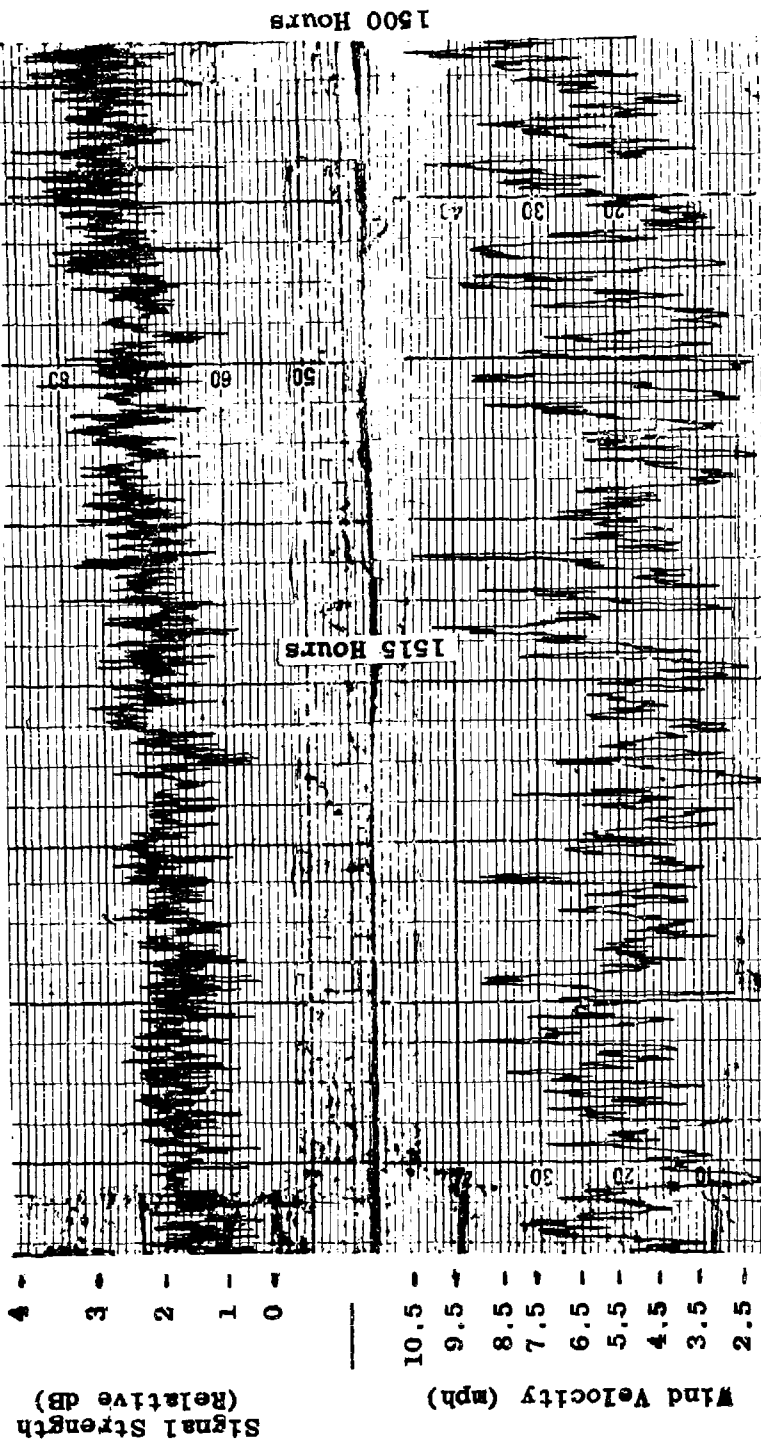
Frequency = 5 Gc/s $H_t = H_r = 21$ ft.

Figure 5.149 Strip Chart Recording of Wind and Signal



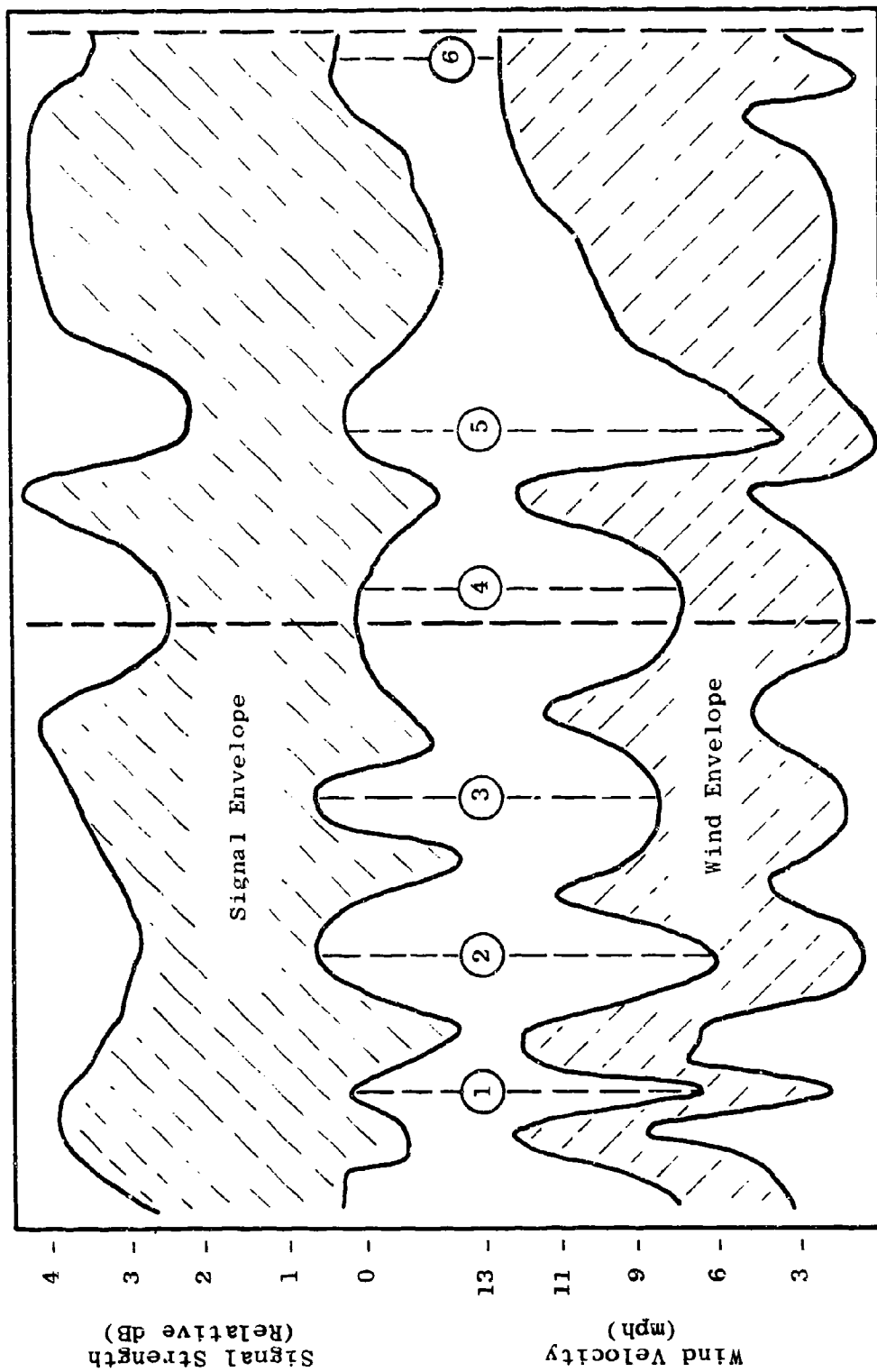
Frequency - 2.5 Gc/s $H_t = H_r = 9$ ft.

Figure 5.150 Strip Chart Recording of Wind and Signal



Frequency = 10 Gc/s $H_t = H_r = 33$ ft.

Figure 5.151 Strip Chart Recording of Wind and Signal

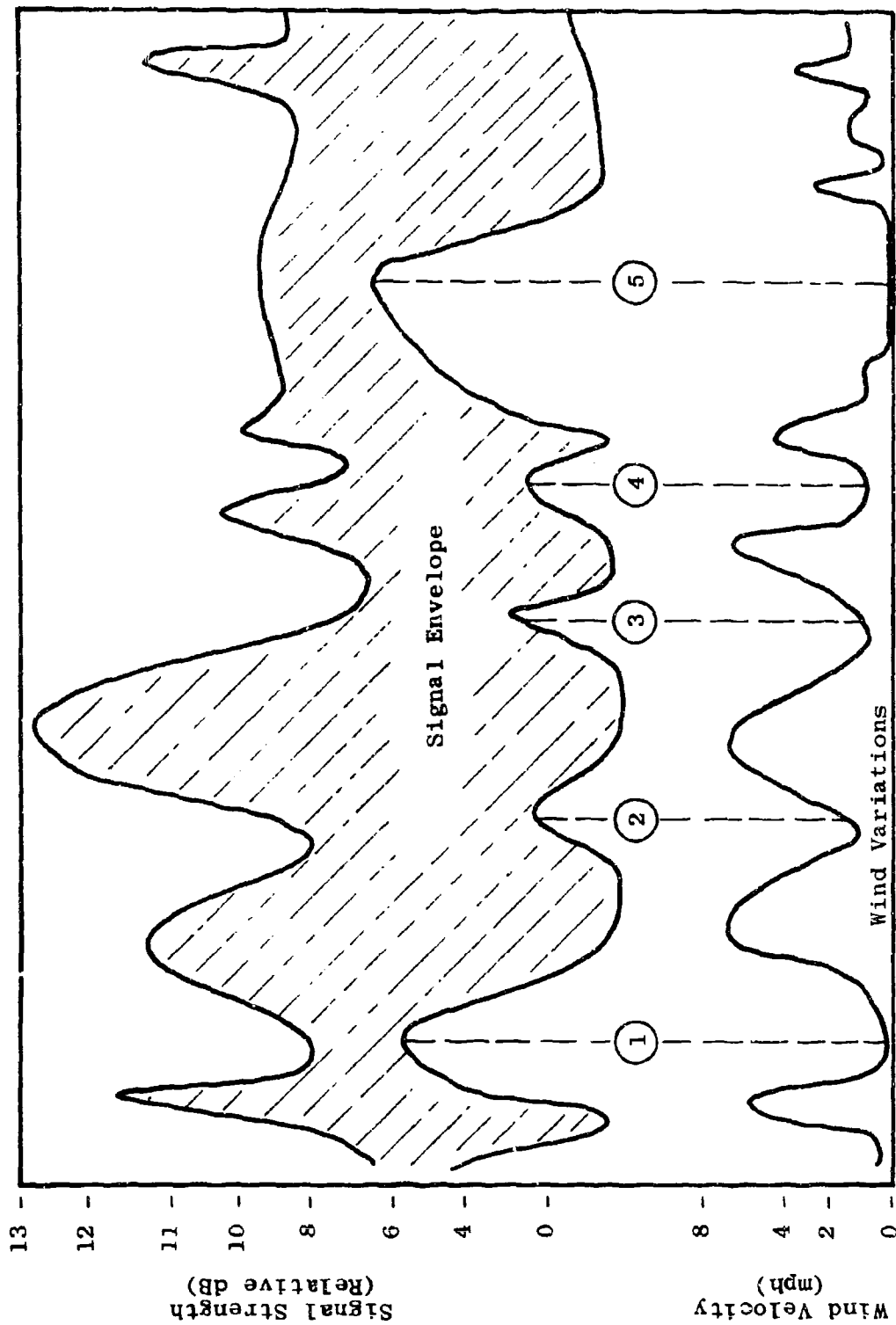


1345 Hrs.

1400 Hrs.

Frequency = 2.5 Gc/s $H_t = H_r = 21$ ft.

Figure 5.152 Typical Wind-Signal Correlation



Frequency - 5 Gc/s $H_t = H_r = 21 \text{ ft.}$

Figure 5.153 Typical Wind-Signal Correlation

wind envelope minimum is matched by a decrease in the width of the signal envelope, denoted by the same numbers.

At a given frequency and wind velocity, the magnitude of the signal variability decreases as the antennas are raised from within the foliage to above treetop level.

Figure 5.151 correlates wind and signal variation when both antennas were above treetop level. A smaller signal deviation is noted in this case as compared with Figure 5.149, which represents in-foliage transmission.

Numerical data relating signal deviation to wind velocity is presented in Table 5.27, which lists average wind velocities with the associated signal deviation. This table was constructed by visually approximating the average signal deviation and the corresponding average wind velocity for each of the simultaneous recordings.

Table 5.27 indicates that in some cases equal average wind velocities do not produce the same average signal deviation. A possible explanation for this is that wind direction and rate of change of wind velocity may also influence the magnitude of the signal deviation. At 5 and 10 Gc/s, using 33-foot antenna heights, a signal fluctuation of only 1 dB is observed.

From this study it can be stated that, in the case of through-foliage transmission, wind velocities up to 10 m.p.h. may produce up to 10 dB of signal variability depending upon possible factors such as wind direction, rate of change of velocity, antenna height, and frequency. A more

detailed study would be required to isolate all of the influencing variables and to assess the degree of importance of each.

It should be pointed out that for wind velocities exceeding 10 m.p.h. signal deviations in excess of 10 dB can be expected. During the course of the program, signal deviations up to 20 dB have been encountered. Unfortunately, the wind velocity responsible for this degree of variability is not known.

Table 5.27

AVERAGE WIND EFFECTS

<u>Frequency (Gc/s)</u>	<u>Polarization</u>	<u>H_t (ft)</u>	<u>Avg. Wind Velocity (mph)</u>	<u>Avg. Signal Deviation (dB)</u>
1.0	V	9	10	5
1.0	H	9	7.5	3
1.0	V	21	9	2
2.5	V	9	7.5	1
2.5	V	21	7	3.5
5.0	V	21	4	11
5.0	V	33	5.5	1
10.0	V	33	5.5	1

5.9.2.3.2 Small Sector Variability

As is characteristic of a scattered field, variations of the in-foliage field strength can be experienced by moving the receiving antenna over a distance of a few

wavelengths. At microwave frequencies, this variability can be seen with just slight vertical or horizontal displacements of the antenna. For a given displacement, greater variations are seen with small aperture antennas such as horns than with larger aperture dish-type antennas. This is assumed to be due to the integrating effect associated with a large capture area when the incident field is composed of a number of scattered components. A small capture area on the other hand "sees" fewer components so that it is more likely that it will encounter small areas of constructive and destructive interference.

It was considered important to sample the field over some small sector area in order both to determine the variability in foliage attenuation produced by fine adjustments of receiver position and to obtain an average representative value of foliage attenuation for a given transmission path.

When using a small aperture receiving antenna, field variations over a small sector of 5 to 10 dB are common. In extreme cases variations of up to 20 dB have been measured. Methods of taking into account this variability in determining median loss values are discussed in Section 5.9.2.4 which describes the test procedures.

5.9.2.4 Test Setup and Data Reduction Methods for Foliage Attenuation Measurements

As described in Section 5.9.2.1, attenuation tests were conducted in two foliated environments, Area A

and Area B. Area A is characterized by dense hardwood-type trees with thick undergrowth. Area B, on the other hand, is populated almost totally with thick bamboo having practically no undergrowth. In Area A, 90 percent of the tree heights are less than about 60 feet, while in Area B, the maximum tree height is about 40 feet.

In Area A, tests were conducted over three transmission paths, and in Area B four paths were selected for tests. The extra path in Area B was added to provide an adequate range of the foliage density in that area. In each area a common transmitter located in a clearing was used to transmit to the in-foliage receiver points. The foliage at the receiver end of the paths was not disturbed in any way. A photograph showing a receiver tower immersed in foliage is in Figure 5.154. Transmission path layouts of both areas giving azimuth and range information are shown in Figures 5.131 and 5.147.

Narrow beam dish antennas were used at the transmitter to illuminate the foliage while wide beam horns were used to receive. Narrow beam emission was used to discriminate against treetop diffraction and so assure direct, through-foliage propagation. Small aperture horns were used in foliage at the receiver to minimize possible antenna-to-foliage coupling losses and to allow a small sector to be easily probed for field strength variability.

As discussed previously, the amount of power extracted from an in-foliage field is a function of the receiving antenna's beamwidth. Hence, the calculated foliage attenuation will be a function of the beamwidth

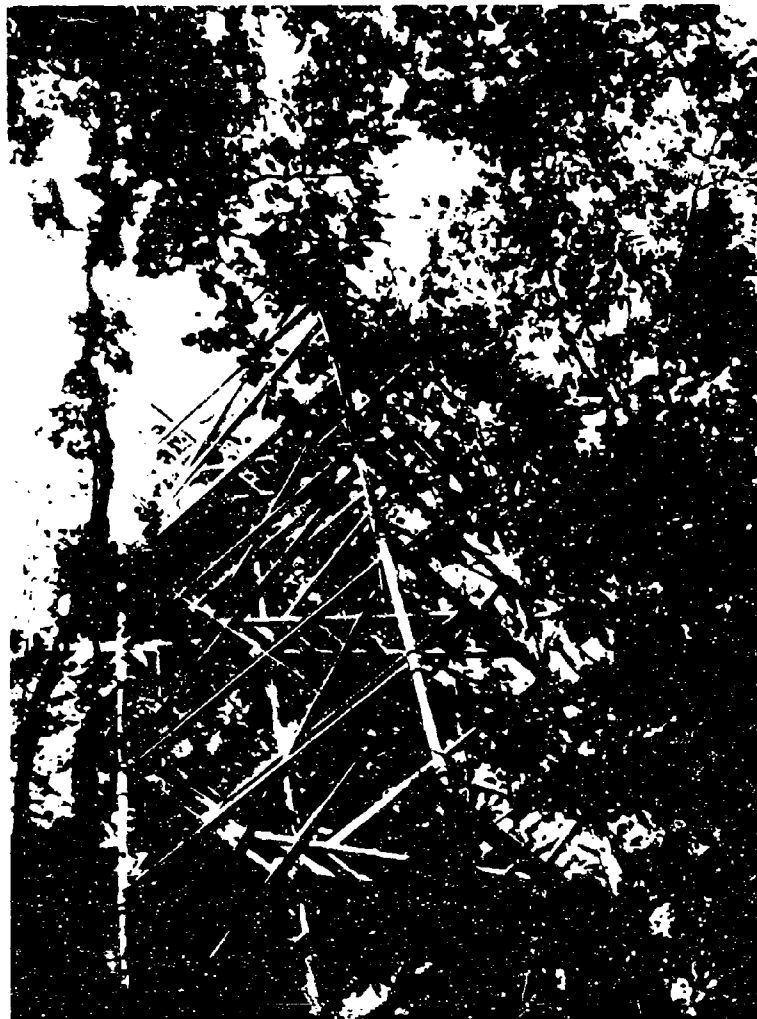


Figure 5.154 Typical View of Receiver Tower Located in Vegetation

employed. For this reason it is important to specify the beamwidths used in making attenuation tests. The following table gives this information for the various test frequencies.

Table 5.28
ANTENNA BEAMWIDTHS IN 10 GC/S PROGRAM

Frequency (Gc/s)	Test Area	Beamwidths (degrees)			
		Transmitting Antenna		Receiving Antenna	
		E-Plane	H-Plane	E-Plane	H-Plane
0.55	B	>60	>60	>60	>60
1.0	B	≈60	≈60	≈60	≈60
2.5	A & B	10	10	38	37
5.0	A	5	5	20	20
5.0	B	10	8	20	20
10.0	A	2	2	40	55
10.0	B	5	5	40	55

Prior to making an attenuation measurement, both the transmitting and receiving antennas were orientated for maximum power transfer when possible. Maximum power alignment seldom corresponded to optical line-of-sight alignment due to the scattering nature of the foliage. In Area B, the presence of an almost continual wind produced rapid fluctuations in the received field making it impossible to determine the exact alignment for maximum power transfer.

However, a good approximation was obtained by running each antenna to the same elevation above treetop level where they were aligned for maximum power transfer. Then, without disturbing either antenna position, both antennas were lowered to the desired in-foliage elevation. A steady field always existed above treetop level regardless of wind conditions. Spot measurements made in Area B during calm periods, utilizing true maximum power alignments, gave results very close to those obtained by this approximate alignment method.

In the majority of cases, the transmitting and receiving antennas were placed at the same height above ground so that transmission took place parallel to the terrain. In addition, some measurements were made at slant angles to the terrain. Slant angle measurements always showed more loss than did those parallel transmissions. A few cross polarization measurements were also made. This condition likewise always produced a greater loss than when polarizations were matched.

At all receiver heights within foliage, the field strength was found to vary drastically with slight displacements of the receiver horn. Due to this variability it was necessary to probe a small area around the nominal height of interest in order to adequately describe the field at a given antenna height. Values of field strength thus obtained were then averaged to provide a representative nominal height measurement. A description of the measuring apparatus and averaging technique is given below.

To determine the variability of the field over a small sector, a "slider" arrangement was used. The "slider"

mechanism consisted of a 5-foot long arm attached at the center to the antenna positioner mounting plate. A metal sliding bracket with the horn attached was moved along the length of the arm. Recordings could then be made with the horn in motion or at fixed positions. Normally, fixed position recordings were used.

A complete set of "slider" attenuation measurements for a given frequency, polarization, and antenna height consisted of ten recordings, each lasting 3 to 5 minutes. The ten samples were obtained in the following way. The "slider" arm was rotated to the horizontal plane, the slider bracket moved 2 feet left of center, and a 3 to 5 minute time recording made. Similar recordings were then made at the following positions: 1 foot left, center, 1 foot right and 2 feet right. The "slider" arm was then rotated to the vertical plane and recordings made at positions of 2 feet up, 1 foot up, center, 1 foot down and 2 feet down. For each of the ten positions the horns were orientated to maintain the desired polarization. The transmitting and receiving antennas were positioned for maximum power transfer with the receiver horn at the center position of the "slider" arm.

Attempts were made to remove wind effects from the measurements by taking the median level of each 3 to 5 minute recording to represent the expected field under no wind condition. The ten median samples were then averaged and the maximum and minimum values recorded.

The average foliage attenuation was then computed at a given antenna height from the average signal level

obtained. Maximum and minimum attenuation levels were likewise obtained from the corresponding signal levels.

For each path, tests were made at a number of elevations ranging from near-ground level to above-treetop level. In most cases heights of 6, 9, 15, 21, 33, 45 and 69 feet were selected for measurements. Data was obtained for both polarizations at test frequencies of 2.5, 5.0 and 10.0 Gc/s. In addition, data was also obtained at 0.55 and 1.0 Gc/s over two transmission paths in Area B.

Attenuation values were derived from "slider" measurements described above. The strip charts, on which the slider measurements are recorded, are calibrated to read directly the power available, P_a , to the receiver. By knowing the power transmitted, P_t , the available power, P_a , and the free-space antenna gains, G_t and G_r , the basic transmission loss for a given transmission path can be calculated. The following basic relationships are used. System loss is given by:

$$L_s = P_t - P_a \quad (21)$$

where

L_s = system loss (dB)

P_t = power radiated by transmitter (dBm)

P_a = power delivered to the receiver (dBm)

Basic transmission loss is related to system loss by:

$$L_b = L_s + G_t + G_r \quad (22)$$

where

L_b = basic transmission loss (dB)

G_t = free-space gain of transmitting antenna
referenced to an isotropic source

G_r = free-space gain of receiving antenna
referenced to an isotropic source

The free-space antenna gains have been previously determined through a measurement procedure described in Semiannual Report Number 7.

Having now determined the basic transmission loss by equation 2 for the in-foliage path, the loss in dB imposed by the foliage is simply the difference between the measured value of L_b and the L_b value corresponding to free space, i.e.,

$$\Delta(\text{foliage}) = L_b(\text{foliage}) - L_b(\text{fs}) \quad (23)$$

where

$\Delta(\text{foliage})$ = loss due to foliage (dB)

$L_b(\text{foliage})$ = basic transmission loss for
transmission path through foliage

$L_b(\text{fs})$ = calculated free-space basic
transmission loss

Free-space basic transmission loss, $L_b(fs)$, is given by equation 24.

$$L_b(fs) = 36.6 + 20 \log f + 20 \log d \quad (24)$$

where

f = frequency in megacycles per second

d = separation distance in miles

The rate of foliage attenuation, α , is obtained by dividing the foliage loss by the thickness of the slab of foliage through which transmission is taking place.

$$\alpha = \frac{\Delta(\text{foliage})}{d_1} \quad (25)$$

where

α = foliage attenuation rate (dB/m)

$\Delta(\text{foliage})$ = loss due to foliage (dB)

d_1 = slab width of foliage (m)

5.9.2.5 Results of Foliage Attenuation Tests

For each transmission path, curves have been generated giving the attenuation rate, α , as a function of height, frequency, polarization, and distance. The number of graphs involved far exceeds the quantity desirable for report purposes. Thus, to reduce the number of graphs to

a manageable amount, data from different test paths was combined when possible and average attenuation rates were calculated from the combined data.

The combined attenuation rates better represent the attenuating properties of each area than the rates derived from individual transmission paths. Figures 5.155 through 5.157 show combined attenuation rates plotted as a function of antenna height for three test frequencies. Both Area A and Area B data appear on these graphs. The individual curves utilize a coded identifier. For example, the identifier, A-V($R_2 + R_3$), represents Area A, vertical polarization, and combined data taken over R_2 and R_3 paths. As a second example, the identifier B-H($R_1 + R_2 + R_3$) represents horizontally polarized data taken in Area B over paths R_1 , R_2 and R_3 .

As can be noted in Figures 5.155 through 5.157 and in other figures of this section, two curves for a given area are often used to cover the range of abscissa values. This was necessary when combining test paths in order that identical data bases be used for each path involved in a particular combination. For example, in Figure 5.155 one Area A curve using R_2 and R_3 data extends from 6 to 21 feet, and another using R_1 , R_2 and R_3 data extends from 15 to 63 feet. No R_1 data exists at 6 and 9 feet. Thus, curve distortion would have resulted had one continuous curve been used to cover the complete range.

Observation of Figures 5.155 through 5.157 shows that on a combined path basis, horizontal polarization consistently experienced slightly greater attenuation rates

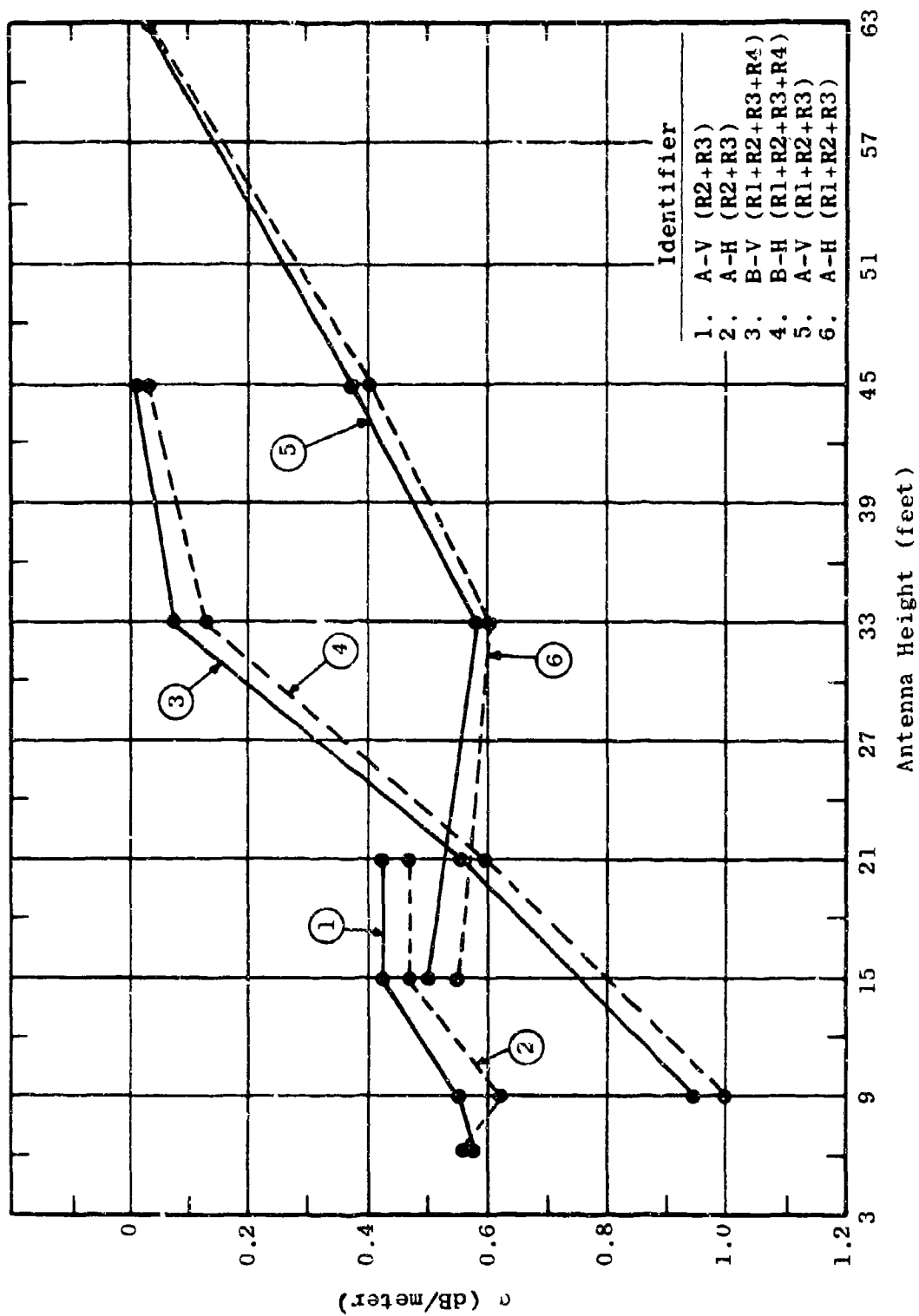


Figure 5.155 Rate of Attenuation, α , Vs. Antenna Height
Frequency = 2.5 Gc/s

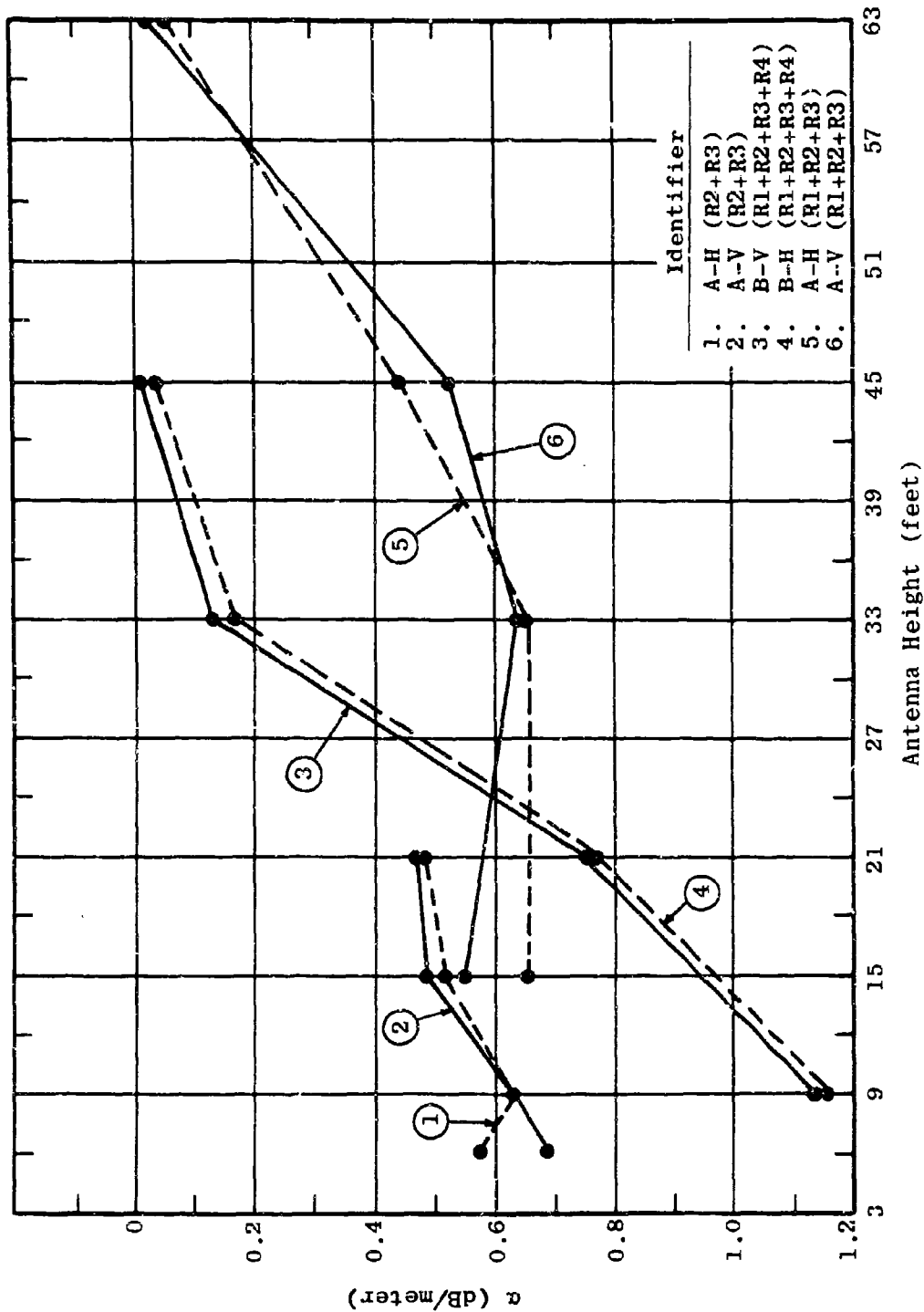


Figure 5.156 Rate of Attenuation, α , Vs. Antenna Height
Frequency = 5 Gc/s

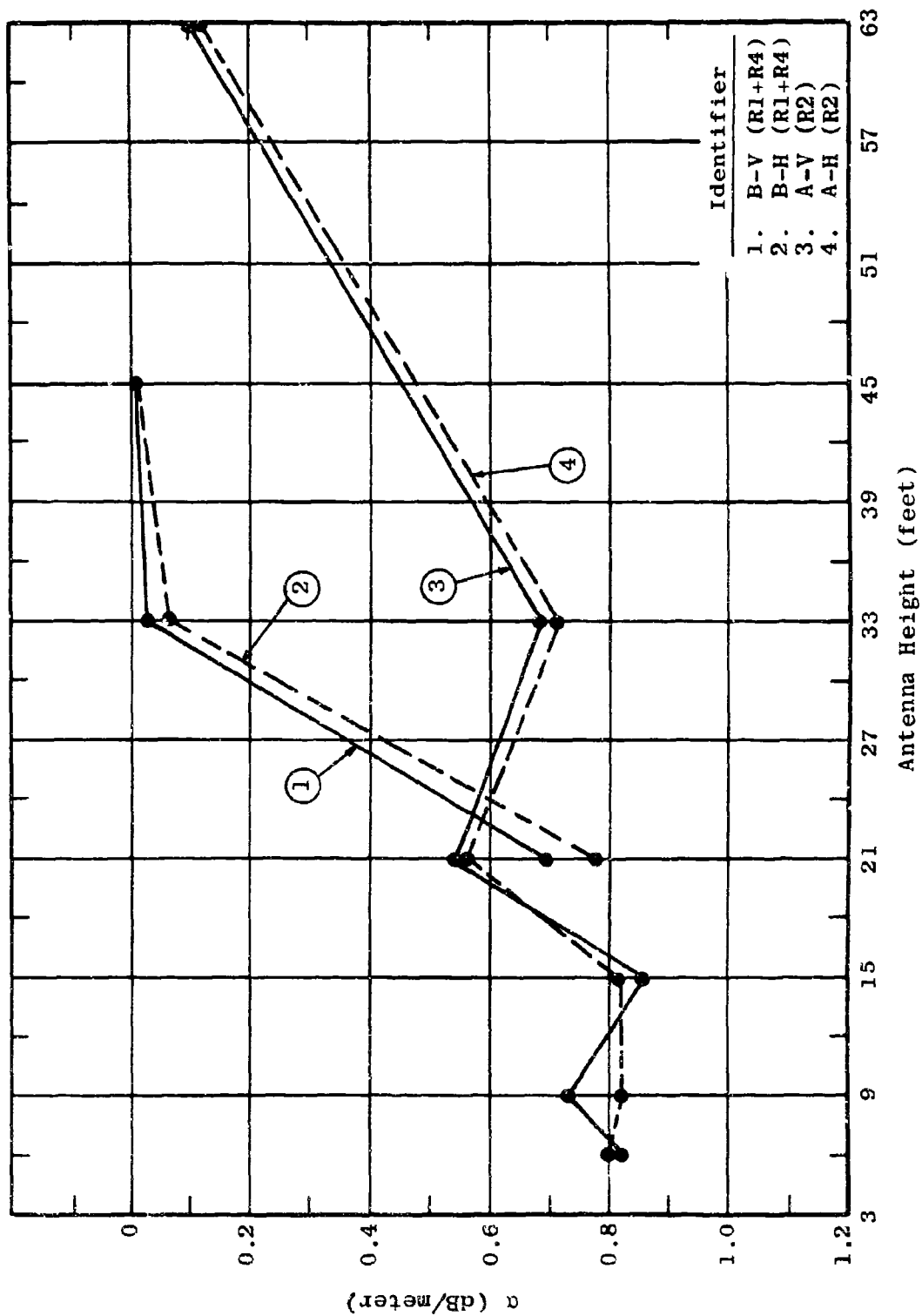


Figure 5.157 Rate of Attenuation, α , Vs Antenna Height
Frequency = 10 Gc/s

than vertical. This behavior is displayed in both Area A and Area B graphs.

The rate of decrease in α with antenna height is greater for Area B than Area A. The rate of attenuation for Area A tends to decrease in the height range of 6 to about 21 feet, but then increases from 21 to 33 feet. Above 33 feet, the attenuation rate continually decreases, approaching close to free space conditions at 63 feet. The increase of attenuation in the 21 to 33 foot range is probably due to transmission through the thick crown portion of the trees. Below 21 feet transmission takes place through the stem portion of the trees and undergrowth.

The difference in tree heights in the two areas can easily be seen in Figures 5.155 through 5.157. In Area B, free space conditions are met at about 33 feet as compared to 63 feet for Area A.

The frequency dependence of the attenuation rate, when antenna height is a parameter, is shown plotted in Figures 5.158 through 5.163. Again, Area A and Area B data appears on these graphs, and the same identification code discussed previously is utilized. In order to maintain a common data base for all combined data and to use frequency as the abscissa, it was sometimes necessary to use a different combination of paths than was used for plotting α vs height. In a few of these combinations, horizontal polarization showed slightly less loss than dH vertical polarization. As expected for all heights within the foliage, the rate of attenuation increases with frequency. When treetop height is approached, α approaches zero and becomes frequency independent.

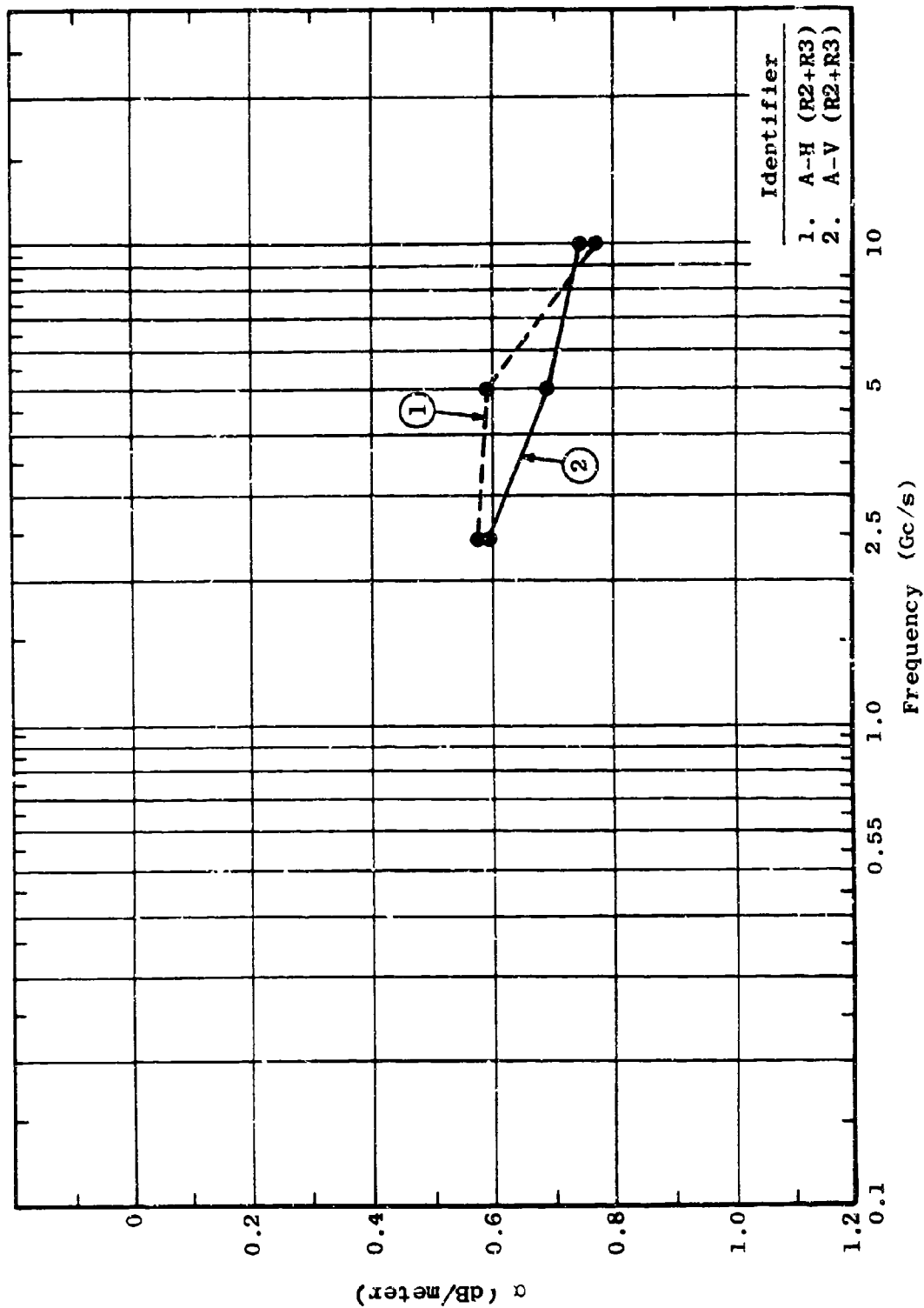


Figure 5.158 Rate of Attenuation, α , Vs. Frequency
 $H_t = 6$ feet

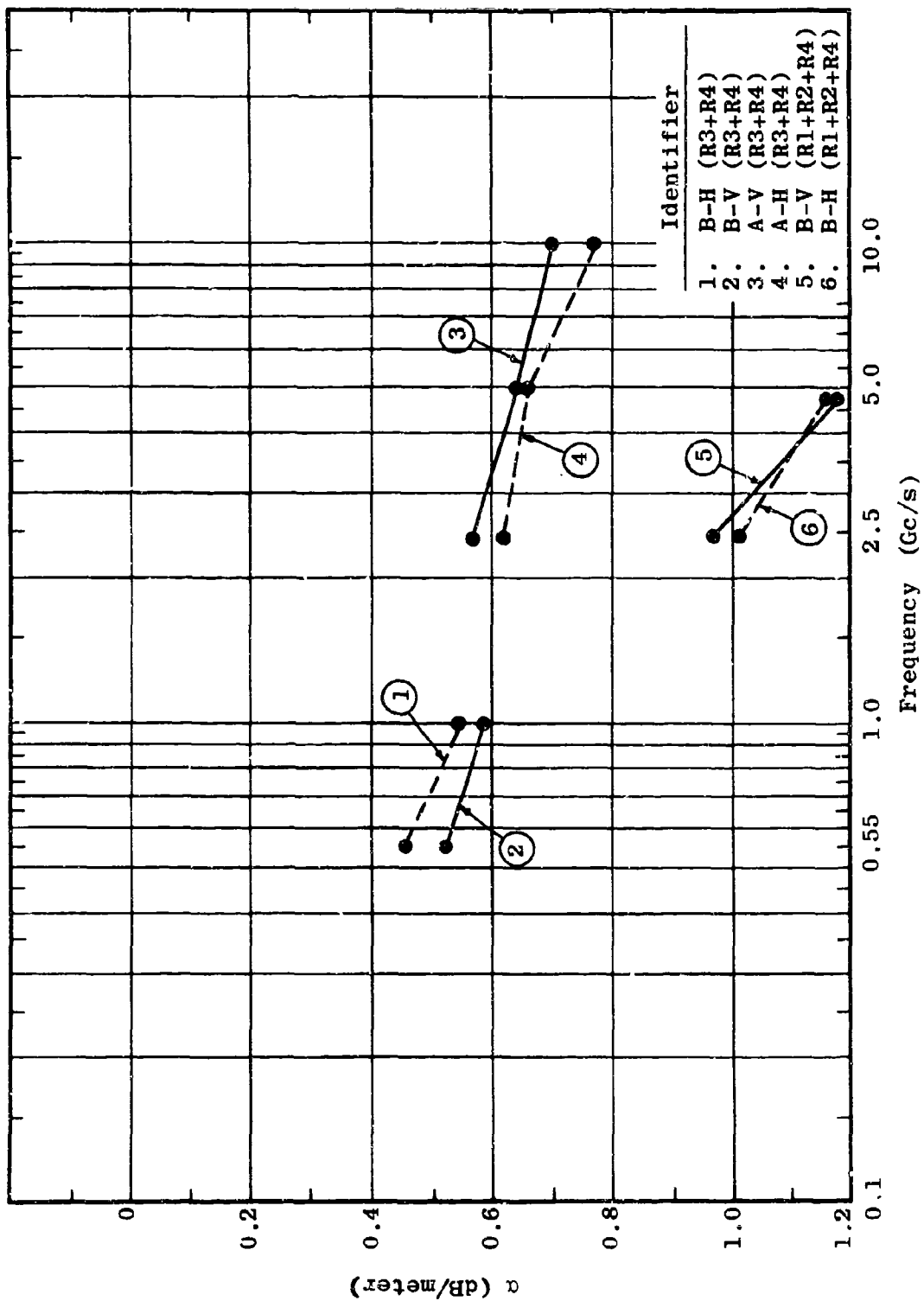


Figure 5.159 Rate of Attenuation, α , Vs. Frequency
 $H_t = 9$ feet

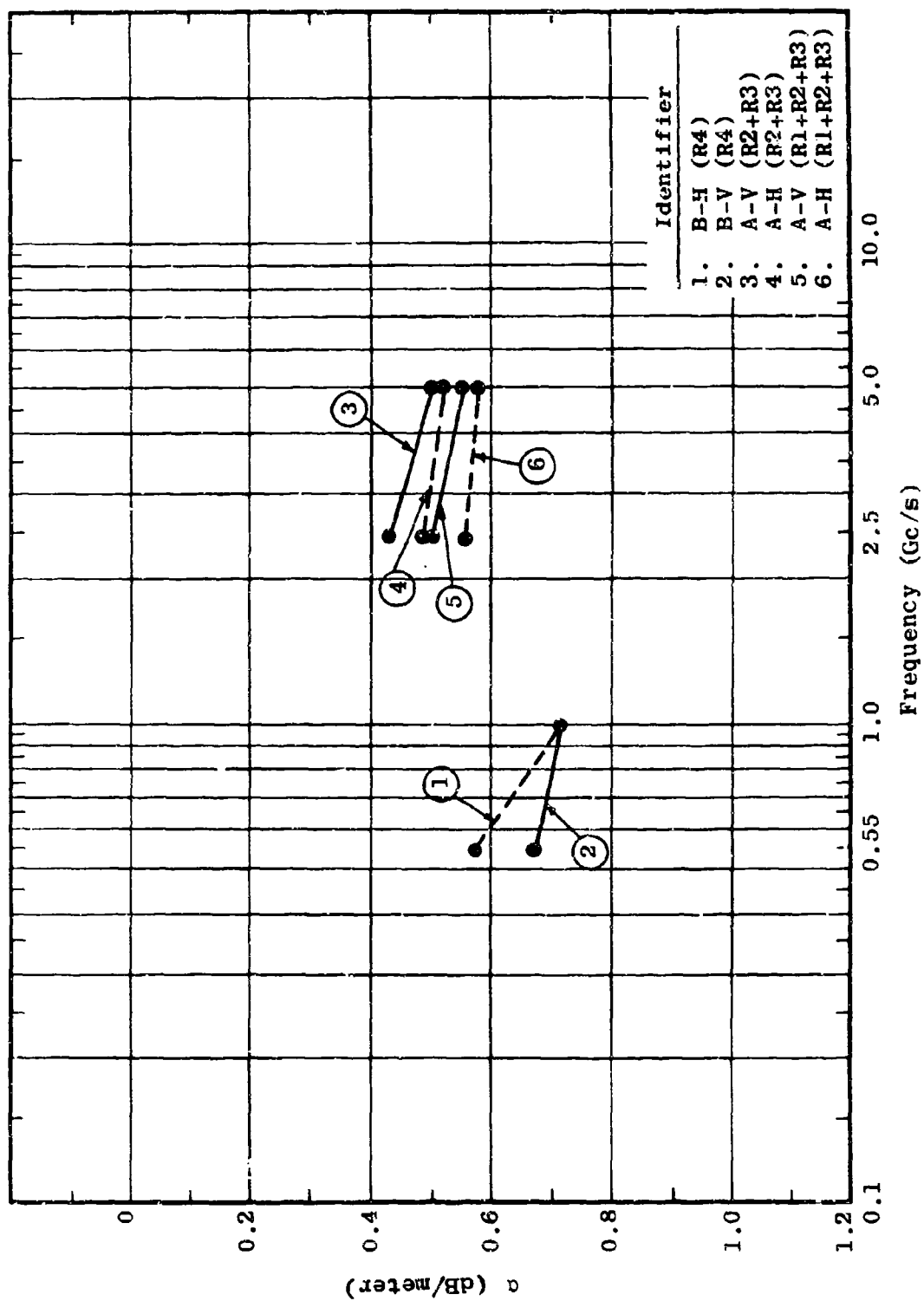


Figure 5.160 Rate of Attenuation, α , Vs. Frequency
 $H_t = 15$ feet

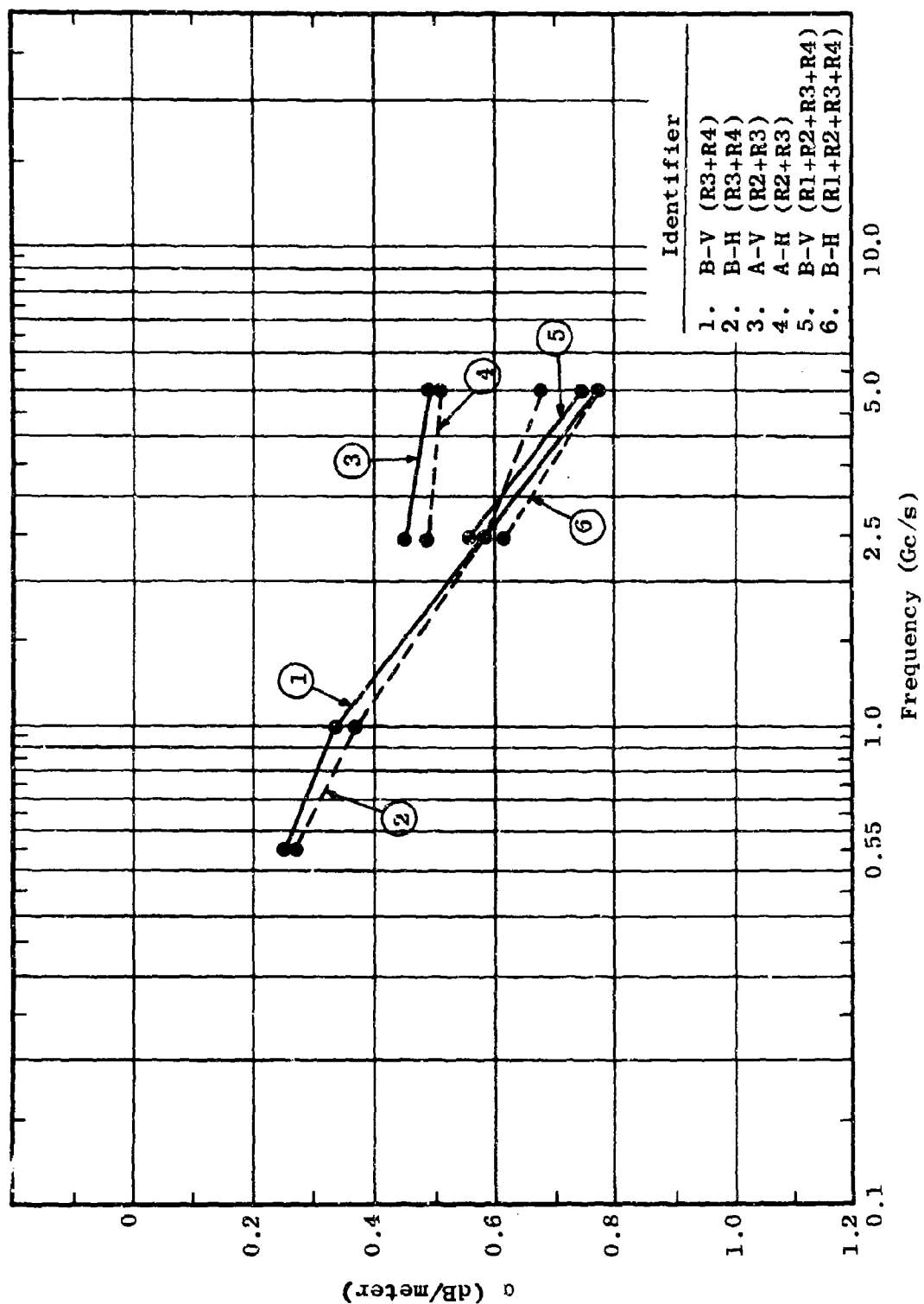


Figure 5.161 Rate of Attenuation, α , Vs. Frequency
 $H_t = 21$ feet

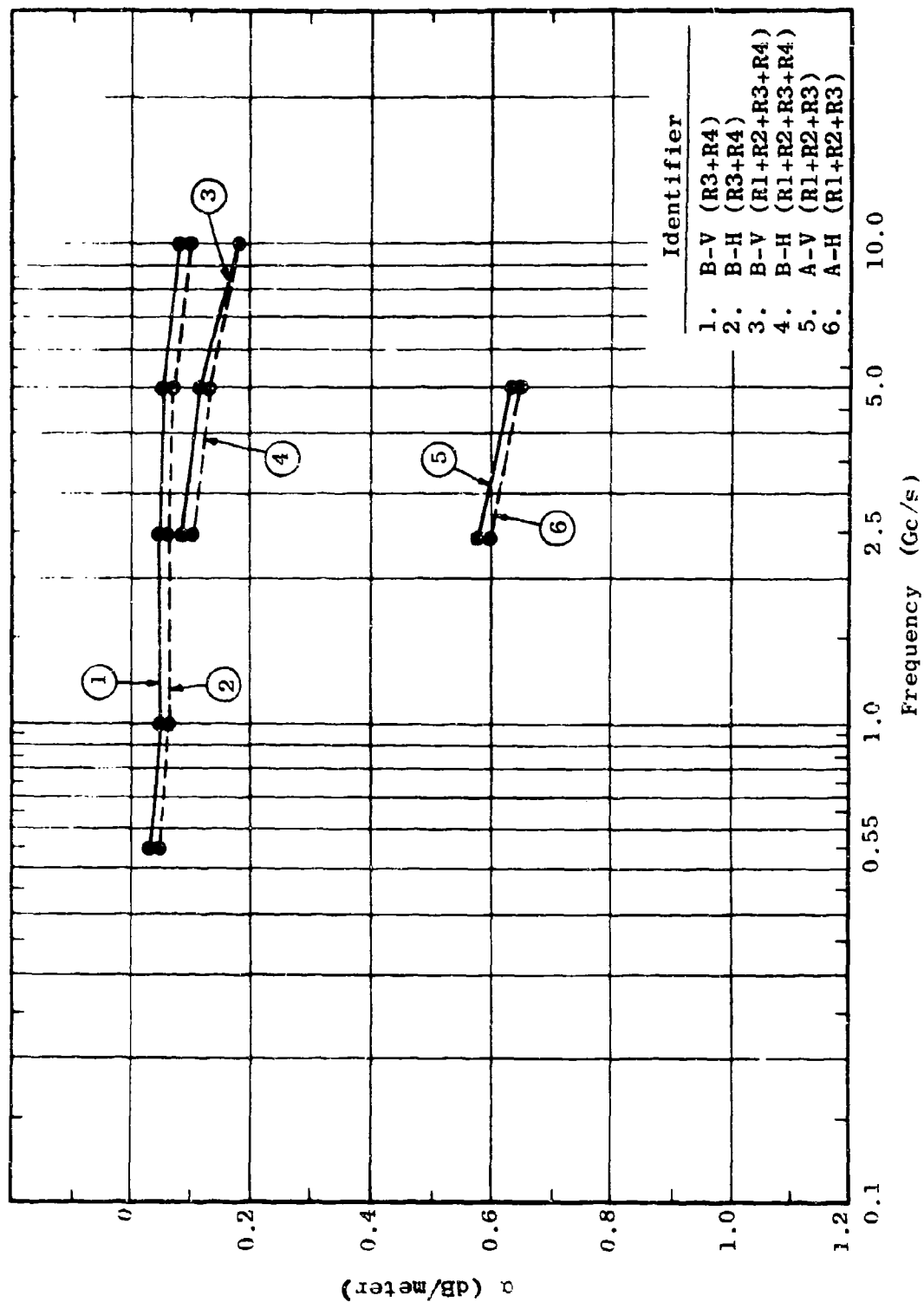


Figure 5.162 Rate of Attenuation, α , Vs. Frequency
 $H_t = 33$ feet

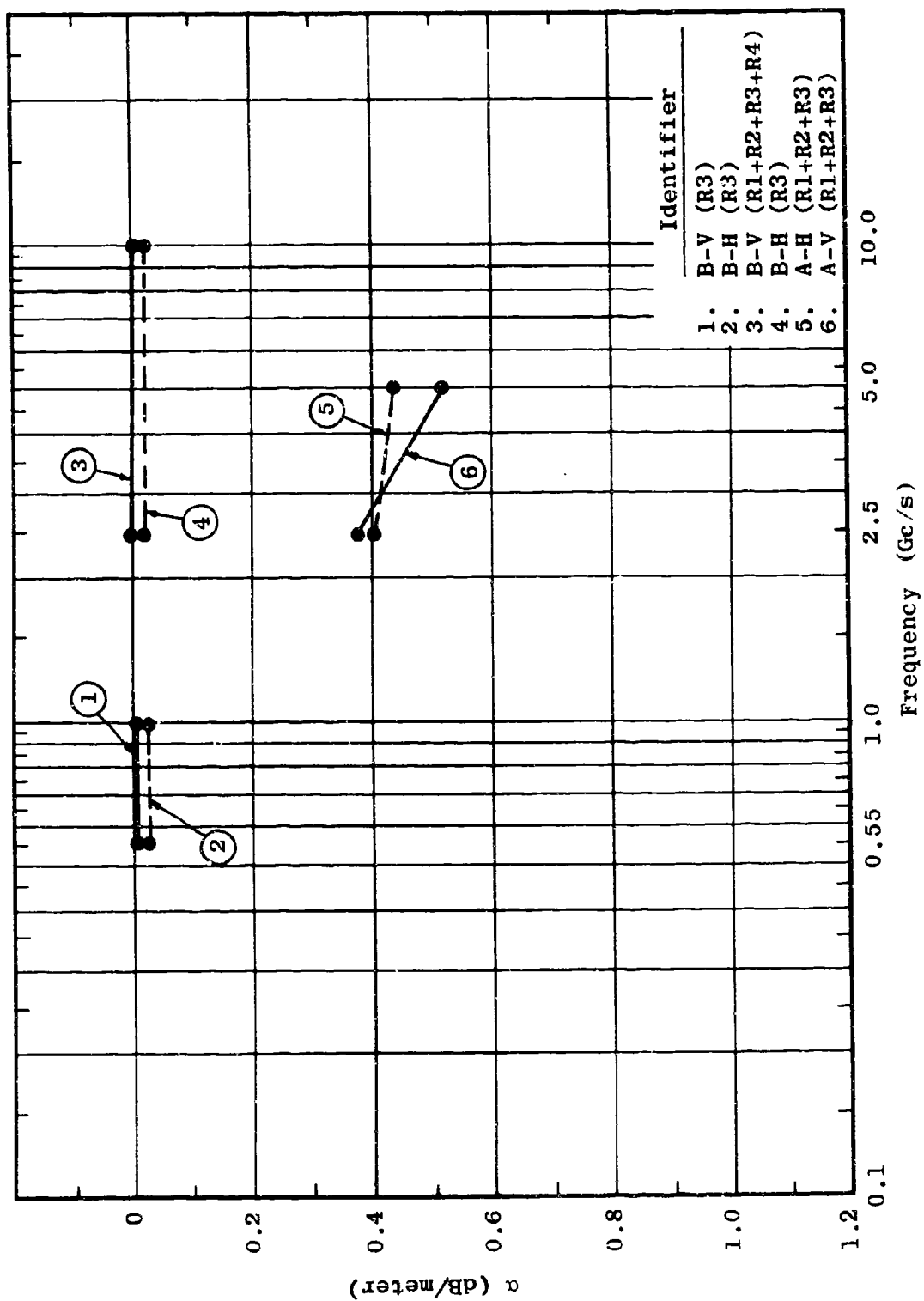


Figure 5.163 Rate of Attenuation, α , Vs. Frequency
 $H_t = 45$ feet

Since the rate of attenuation has been shown to vary over a wide range both in a vertical and horizontal direction, attempts were made to obtain a composite attenuation curve for each area to characterize the over-all attenuating properties of the two environments. To obtain these curves, data taken at different heights and over different paths was combined. Again, care was used to obtain a common data base at each frequency. Heights of 9 and 21 feet were common to both areas and provided the same data base at each frequency. The resulting curves are shown in Figure 5.164. Figure 5.165 gives the composite curves resulting from a smooth best-fit of Figure 5.164.

The composite curves in Figure 5.165 may be thought of as representing the typical attenuation rates in each area for an arbitrary low-level transmission through the foliage. The composite α for Area B is greater than that for Area A and increases at a steeper rate with frequency. It should be noted, however, that other composite curves of lower attenuation would result from the combination of data taken at higher elevations, especially for heights near the treetop level.

The composite attenuation curves in Figure 5.165 have been replotted in Figure 5.166 along with the measured data of Saxton and Lane.¹⁷ Also shown on this graph is the theoretical LaGrone expression which has been extended up to 10 Gc/s. The LaGrone expression was empirically derived from the Saxton and Lane measurements, which accounts for the excellent agreement between these two curves in Figure 5.166.

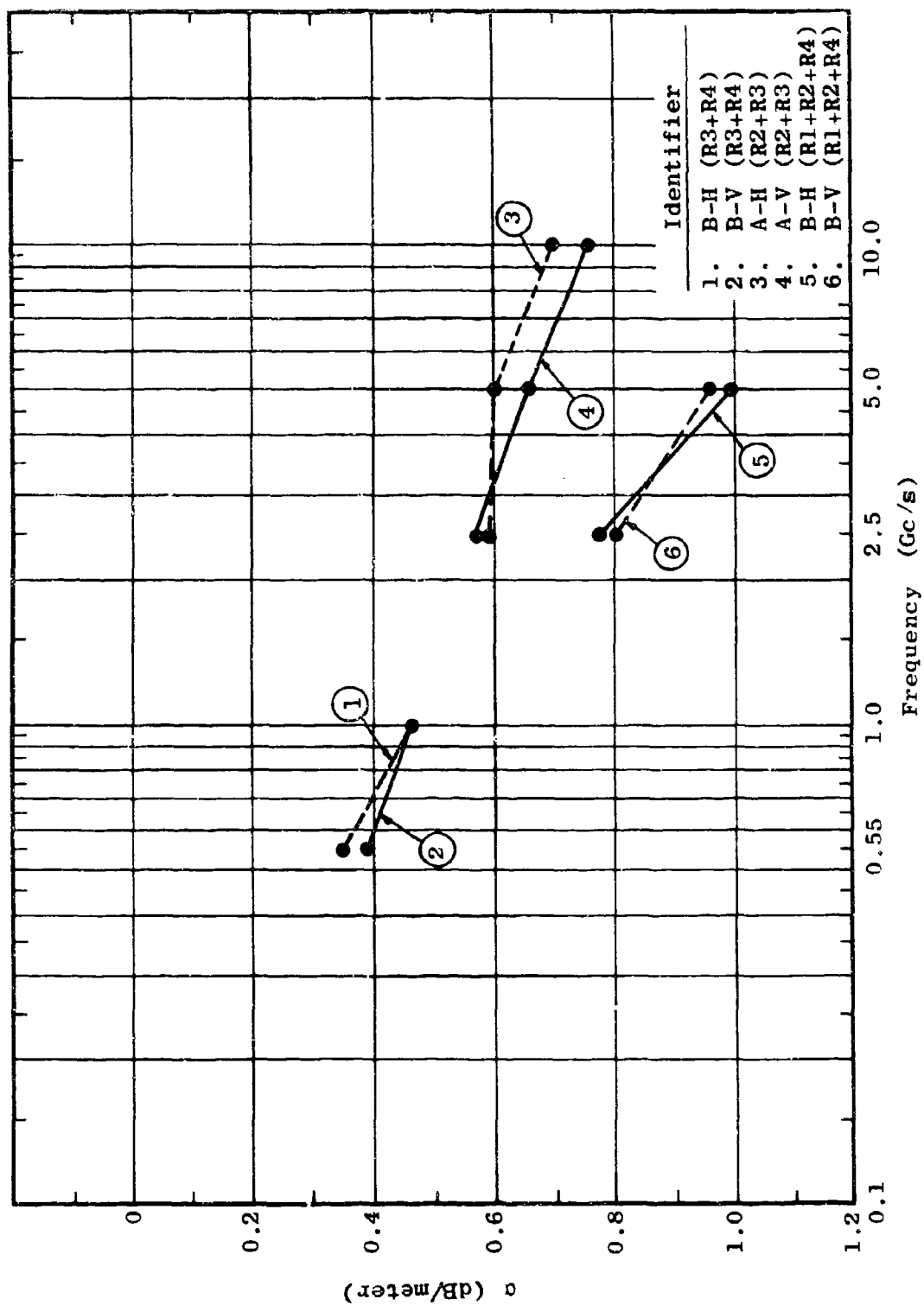


Figure 5.164 Rate of Attenuation, α , Vs. Frequency
 $H_t = 9$ and 21 feet

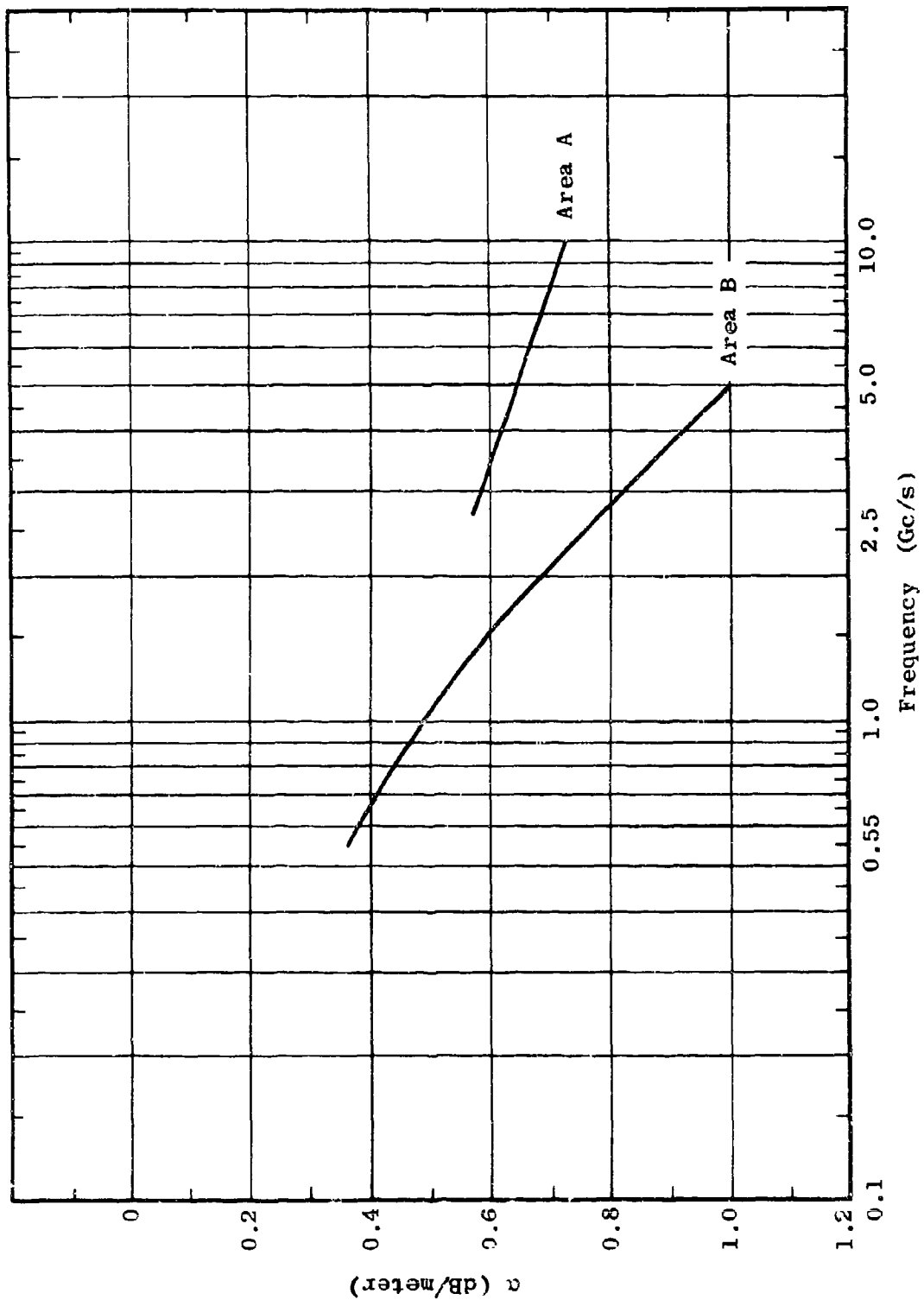


Figure 5.165 Composite Attenuation Curves for Areas A and B

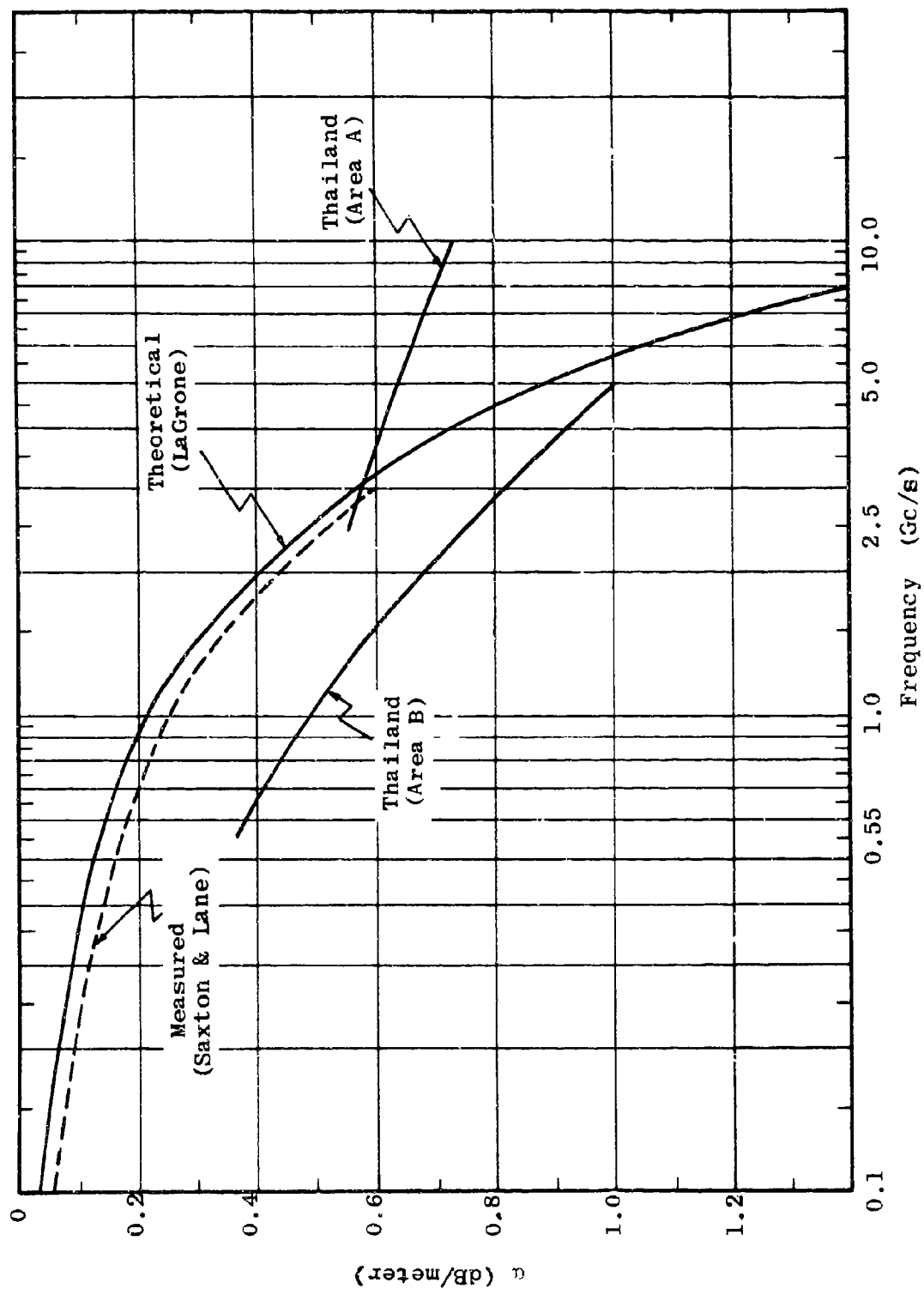


Figure 5.166 Comparison of Thailand Data with Other Measurements

The increase in attenuation rate, α , with frequency for direct transmission through foliage is of particular importance. As stated previously, at antenna heights near the treetop level, a significant amount of diffraction takes place around and over the trees resulting in attenuation rates which are essentially independent of frequency. However, for low level transmission, a frequency dependence is always observed. Unfortunately, many of the low level measurements made at 10 Gc/s were near the noise level of the receiver, making it necessary to apply a correction factor to arrive at the true signal level. The application of this correction factor to signals near the noise level may at times produce signal levels of questionable accuracy. For this reason, a large portion of the 10 Gc/s data was omitted in Figures 5.158 through 5.164.

To obtain a valid set of data for determining the increase in attenuation with frequency, short distance transmission paths were selected in each area and attenuation rates versus frequency were plotted for low antenna heights. The results are shown in Figures 5.167 through 5.169 for three selected paths. At each frequency, the signal level was well above the noise level, and no noise correction was required. On each of the above graphs, the theoretical relationship derived by LaGrone for frequencies up to about 3 Gc/s has been extended to 10 Gc/s. The median curves in Figures 5.167 through 5.169 have been replotted in Figure 5.170 where all attenuation levels have been normalized to zero at 2.5 Gc/s. Again, the LaGrone relationship is shown in this figure also normalized to zero at 2.5 Gc/s.

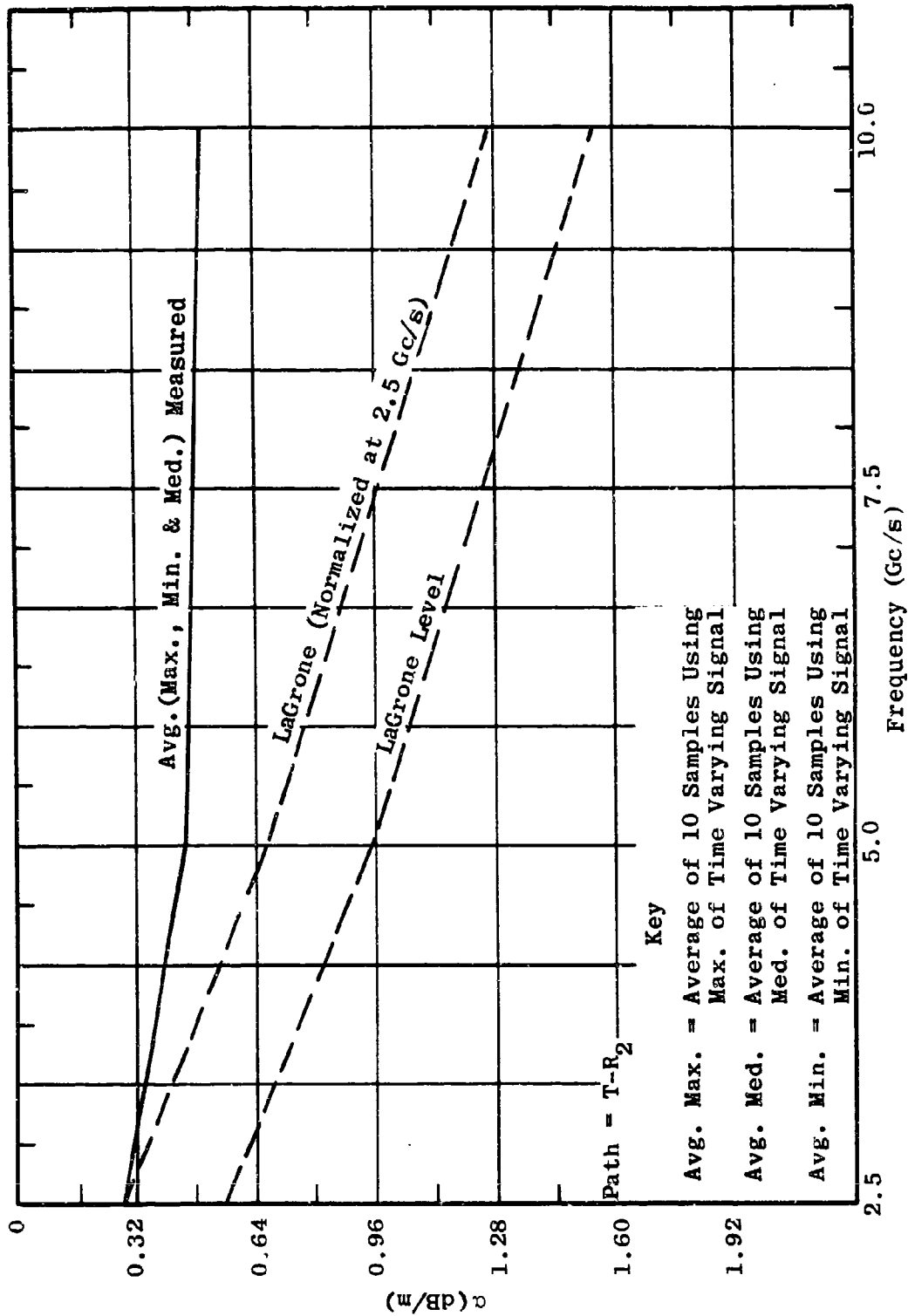


Figure 5.167 LaGrone Function and Measured α vs. Frequency

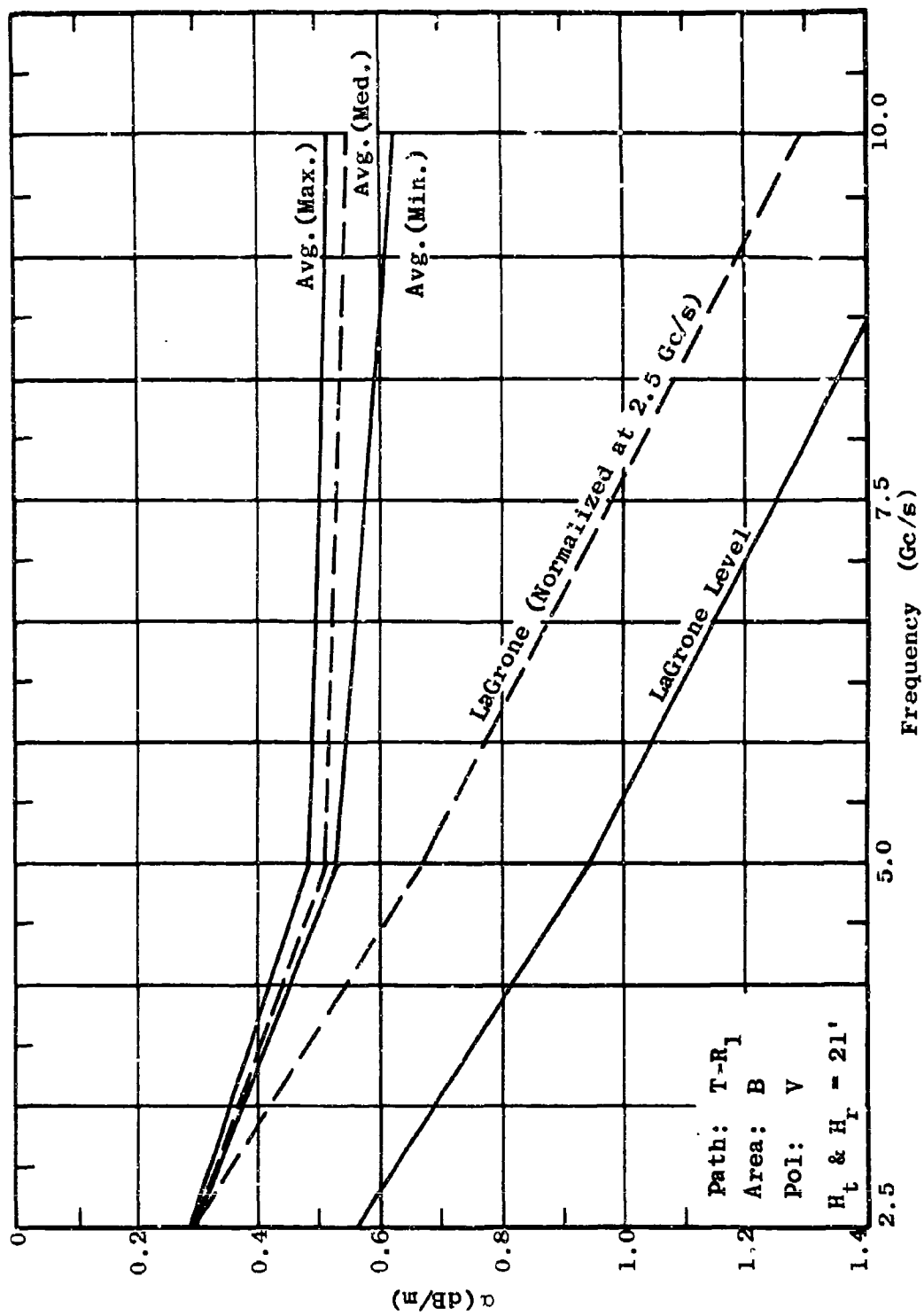


Figure 5.168 LaGrone Function and Measured α vs. Frequency

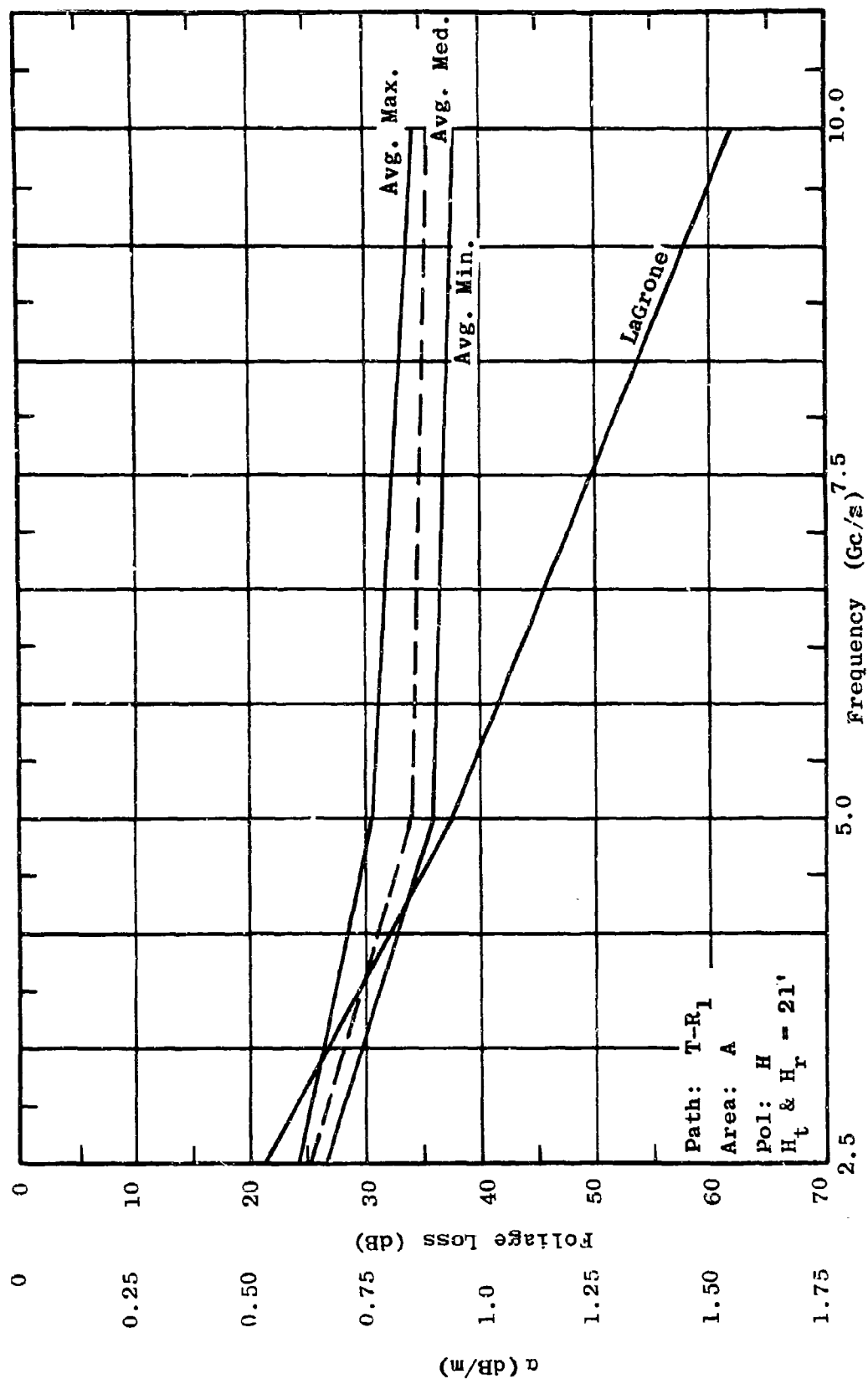


Figure 5.169 LaGrone Function and Measured α vs. Frequency

Figure 5.170 illustrates clearly that the measured increase in attenuation with frequency is much less than that given by the LaGrone expression. It is also interesting to note that the results are nearly the same for each transmission path and that the increase in attenuation from 5 to 10 Gc/s is small. This fact seems to imply that for operation above about 5 Gc/s, using conventional equipment, the rate of attenuation can almost be treated as a constant.

An important consideration which might, however, affect the validity of the above implications concerns the beamwidths employed at 5 and 10 Gc/s. The 10 Gc/s receiving antenna beamwidth was nearly twice that employed at 5 Gc/s. To definitely establish the functional relationship between frequency and attenuation, the beamwidth should be held fixed as the frequency varies.

Tests scheduled in another foliated environment in Southern Thailand during 1967 will provide additional data to refine and extend the results reported here.

5.9.2.6 24-Hour In-Foliage Measurements

The purpose of making 24-hour continuous recordings of signal level was to determine if there is a long term, or diurnal, time variation in the received signal. Significant weather changes were recorded throughout these tests for correlation with significant changes in the signal level. These tests were conducted in both Area A and Area B.

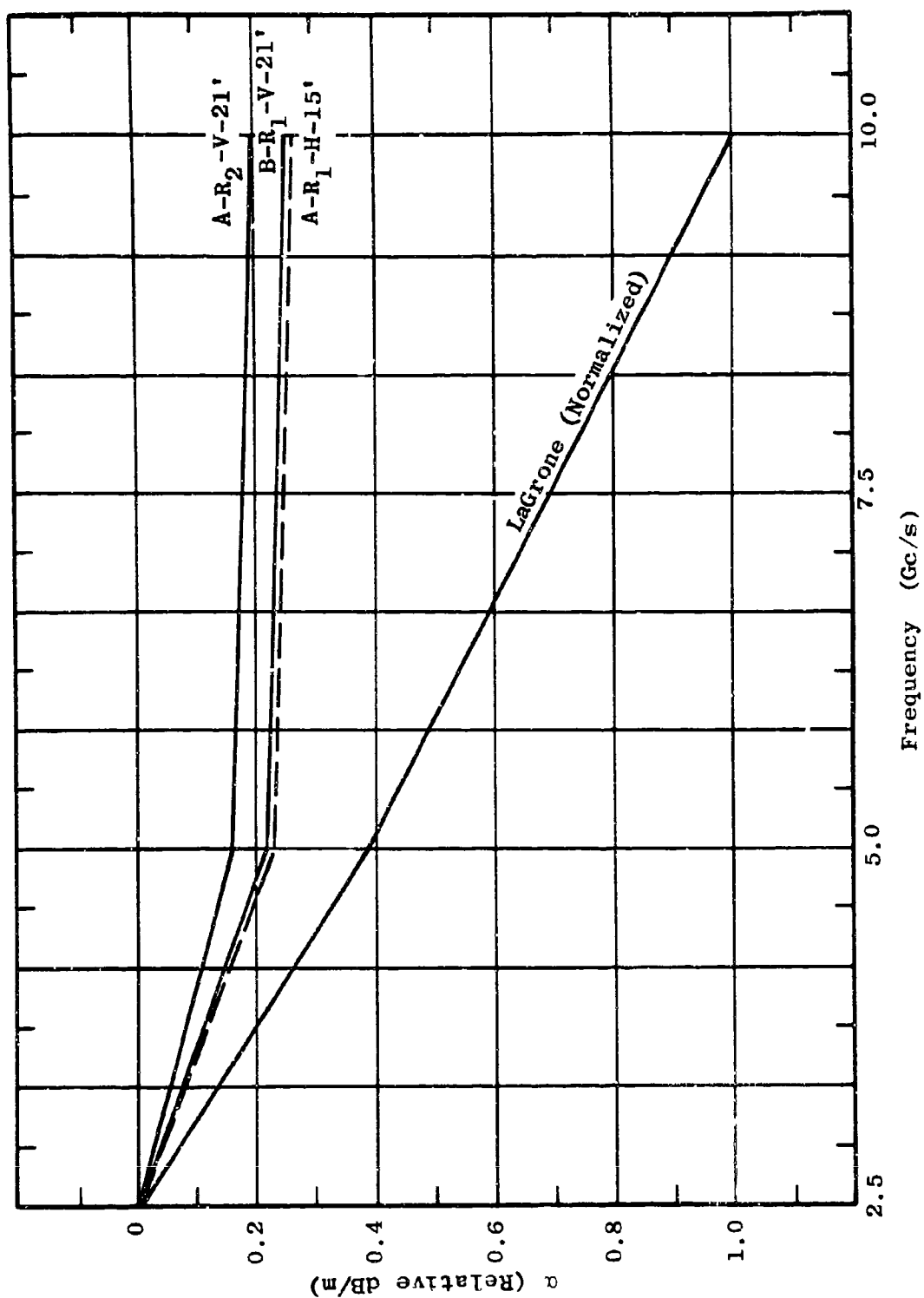


Figure 5.170 All Three Transmission Paths Normalized at 2.5 Gc/s
(i.e., $\alpha = 0$ at 2.5 Gc/s for all paths)

The test setup utilized was identical to that discussed in Section 5.9.2.4 for making the attenuation measurements. The transmitting and receiving antennas were at equal heights. The strip chart recording of receiver output was run continuously while all equipment parameters such as output power, receiver sensitivity, etc., were held constant. The receiver and recorder were calibrated initially and periodically throughout the 24-hour duration. Automatic frequency control was used to minimize frequency drifting. Prior to the beginning of a run, both antennas were aligned for maximum power transfer.

Over the range of environmental conditions encountered during all the test periods, no significant change in the median signal level was noted, even though rain and fog were experienced during certain periods as well as heavy dew in the early morning hours.

Extreme care had to be used to protect the antennas and connectors from moisture during rains and dew. If the dampness had penetrated, equipment degradation rather than path loss change would have been the most likely effect of changes in weather during extended in-foliage transmissions.

As discussed in Section 5.9.2.3, however, rapid field variations produced by wind were encountered practically all the time in Area B and most of the daytime hours in Area A. These variations simply represent oscillations about the median signal level and do not alter the median level itself.

5.9.2.7 Antenna Pattern Measurements

For free-space conditions, the radiation characteristics of an antenna in various directions can be accurately determined by rotating the test antenna while measuring the relative power transferred to an auxiliary antenna situated in the far-field. However, when either or both antennas are placed in an environment containing reflecting objects, the true radiation characteristics of the test antenna may not be represented by the pattern obtained by the above method. Instead, the pattern for this condition reflects the combined characteristics of the true radiation pattern plus environmental or "site" effects.

The purpose of this section is to investigate the environmentally caused changes in antenna patterns when either the test or auxiliary antenna is immersed in foliage. This effect of the foliage can be seen by comparing the in-foliage pattern with the pattern obtained in free space. To provide the free-space reference, a separate set of measurements was made with each antenna located in a clearing and elevated sufficiently to approximate closely free-space conditions. In addition to the absolute comparisons between the in-foliage and free-space patterns, relative comparisons between various types of in-foliage patterns are also important. For example, the change in pattern shape as a function of antenna height can be studied by directly comparing in-foliage patterns made with the same antenna at different heights.

Four types of antennas were used during the program: (1) small aperture horns, (2) large aperture horns, (3) small aperture dishes, (4) large aperture dishes. These

different antennas provided a sufficiently wide range of beamwidth to allow a study of pattern shape as a function of aperture capture area. Three test frequencies, 2.5, 5.0 and 10 Gc/s, and both polarizations were used. The antenna heights were usually 15, 33, 45 and 63 feet. For each measurement condition, a pattern in both the horizontal and vertical planes was made.

Since it is not practical to include all of the patterns in this section, selected patterns typical of the general case will be presented to represent the results of certain measurement conditions.

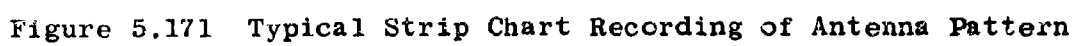
5.9.2.7.1 Test Setup and Procedure

The tower positions for each test path in both test areas are shown in Figures 5.131 and 5.145. In most cases, the transmitter was located in the clearing and the receiver in the foliage, but in a few cases the opposite arrangement was used to determine if a pattern change could be produced by reversing the direction of power flow through the foliage. At most of the heights where patterns were taken, the transmission took place directly through foliage. At the highest tower levels, however, few trees exist in the transmission path. For these cases, diffraction around and over the trees could possibly be taking place, so creating patterns different from the case of through foliage transmission.

Both the transmitter and receiver towers were equipped with antenna positioners capable of sweeping in

both the horizontal and vertical planes. The sweep arc was always large enough to allow the entire pattern structure to be recorded.

When sweeping the transmitting antenna, the receiver acts as the auxiliary antenna, and similarly when sweeping the receiver, the transmitting antenna serves as the auxiliary antenna. Regardless of which antenna was being rotated, the pattern recording apparatus was fed the signal at the receiver output. The general procedure of obtaining a pattern is outlined as follows: (1) the auxiliary antenna was positioned in both azimuth and elevation for maximum power transfer (2) the azimuth positioner of the test antenna was rotated to full counterclockwise position (3) the strip chart recorder at the receiver output was started and run at constant speed by an internal electric motor (4) the test antenna was then swept at a constant rate in the clockwise direction until the full sweep arc in the azimuth direction was reached. During the sweep at each twenty degree interval, indicated by a remote reading position indicator, a mark was placed on the strip chart by momentarily shorting the recorder input. Since both the recorder and the antenna were run at constant speed, the horizontal scale of the strip chart is linearly related to the angular displacement of the test antenna, and, therefore, the strip chart response represents the pattern. The above procedure was also used for determining the elevation pattern, except that the test antenna was swept vertically rather than horizontally. A typical pattern obtained by the above procedure is shown in Figure 5.171.



5.9.2.7.2 Test Results

Since it is not possible to present the results of each measurement condition, only patterns representing some of the more important situations will be presented.

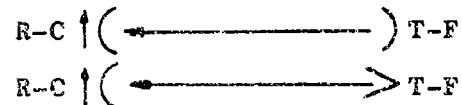
The cases selected for presentation are given in this section. Immediately following the results of each case, there is a brief description of the major implications of the patterns. It should be pointed out that tentative conclusions drawn from observation of these patterns are based not only on the patterns presented, but also on many similar patterns which have been studied but not shown here.

Since many combinations of antennas, sweeps and other parameters are involved, it is advantageous to represent the basic measurement setup to be described with a sketch using a consistent set of symbols. The following symbols will be used universally to describe the transmission setup.

- $\uparrow($ = dish antenna being rotated (test antenna)
- $($ = dish antenna stationary (auxiliary antenna)
- $\uparrow<$ = horn antenna being rotated (test antenna)
- $<$ = horn antenna stationary (auxiliary antenna)
- \longrightarrow = direction of power flow
- R-C = receiver located in clearing
- T-C = transmitter located in clearing
- R-F = receiver located in foliage
- T-F = transmitter located in foliage

Out of the vast number of antenna patterns taken in both test areas, the following cases illustrate the significant differences between in-foliage and free-space antenna patterns. Again it should be emphasized that many patterns have been observed to display the same characteristics seen in the representative cases presented below. The transmitting configuration used in the following cases is described by the code presented above. General conclusions are discussed in Section 5.9.2.7.3.

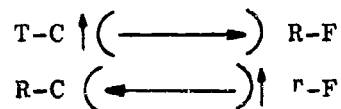
Case 1



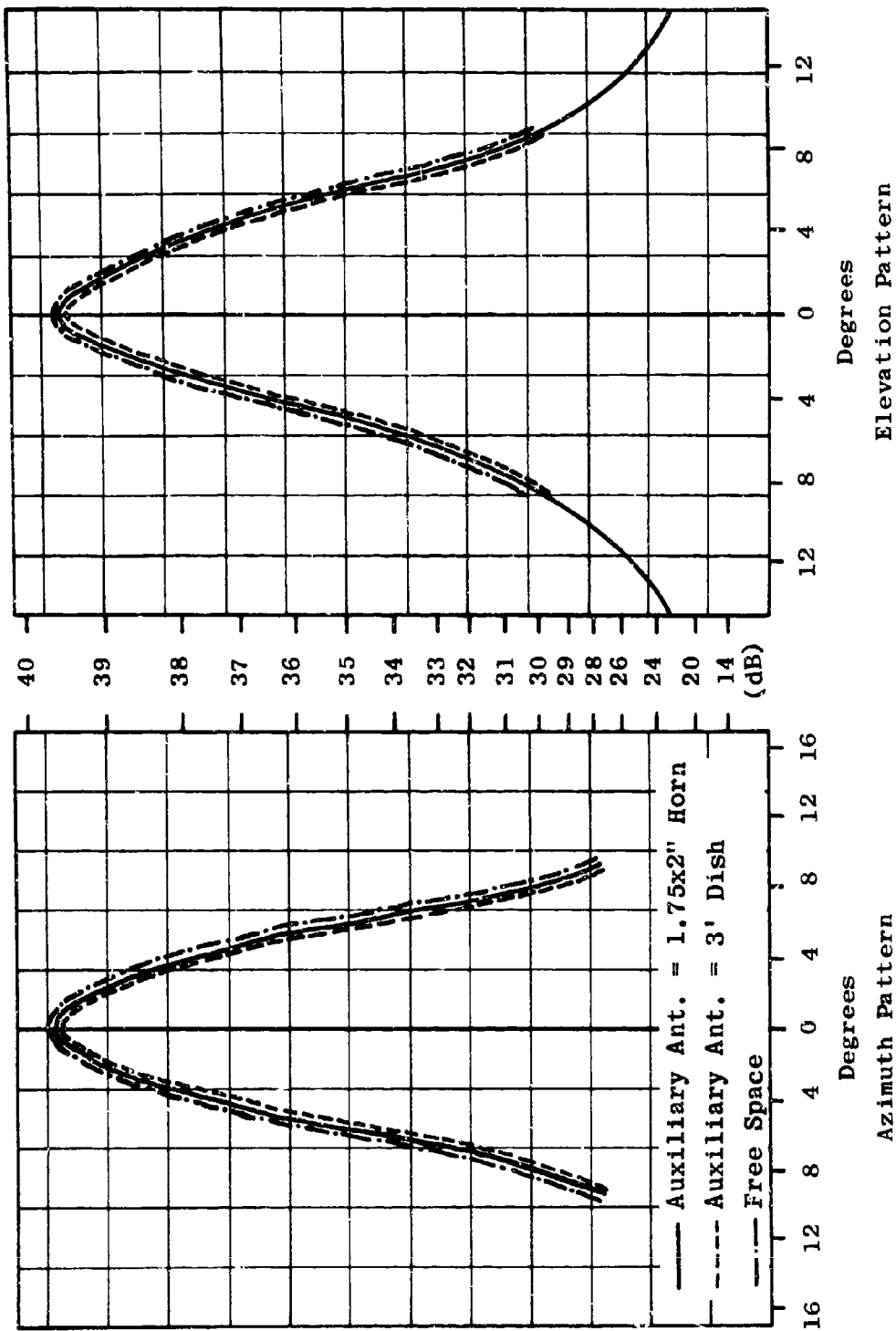
The purpose of Case 1 is to illustrate the effect of changing the beamwidth of an in-foliage auxiliary antenna. The test antenna in each case is a narrow beam dish.

The resulting patterns are shown in Figure 5.172 along with the free-space pattern. Notice that all three patterns are the same, indicating that the beamwidth of the auxiliary antennas has no effect and that the intervening foliage does not alter the free-space pattern of a narrow beam dish.

Case 2



The purpose of Case 2 is to compare the patterns of a large aperture dish when located in a clearing and when



Freq: 5 Gc/s Polarization: V Test Ant: 18" Dish
 Figure 5.172 Dish Patterns Showing Effect of Changing Beamwidth of Auxiliary Antenna

immersed directly in foliage.

The results are presented in Figure 5.173 with the free-space pattern. Again all patterns are identical, indicating that the antenna's performance is not degraded when placed in foliage and that the intervening foliage does not change the free-space pattern of the dish.

Case 3

T-C $\uparrow \longleftrightarrow$ R-F
R-C $\longleftrightarrow \uparrow$ T-F

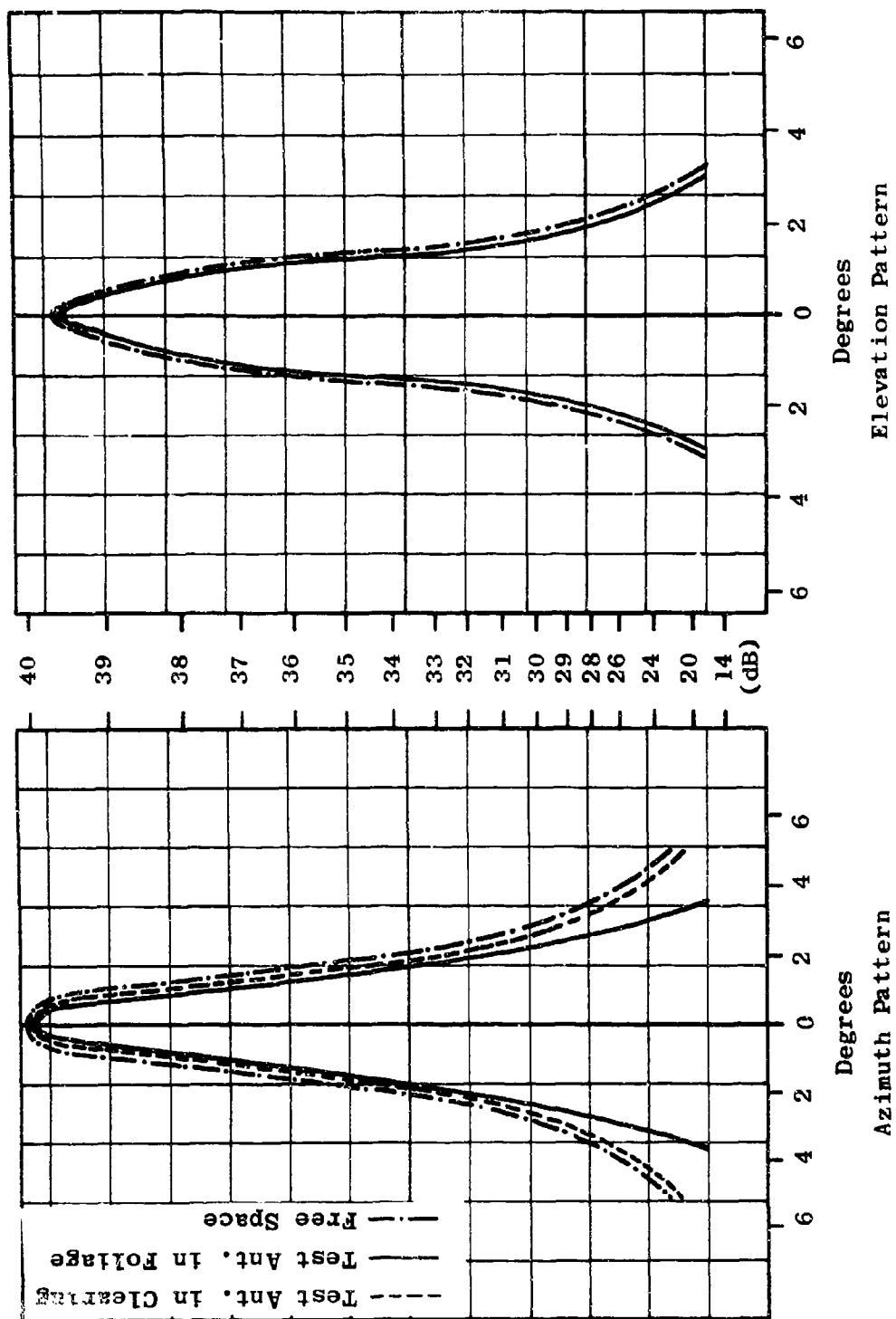
Case 3 is identical to Case 2 except wide beam horns have replaced the narrow beam dishes.

Results are presented in Figure 5.174. The azimuth patterns for the two cases are quite dissimilar, and neither resembles the free-space pattern. For this case, better agreement exists for the vertical pattern, but in other cases observed the degree of distortion appears about the same for both planes.

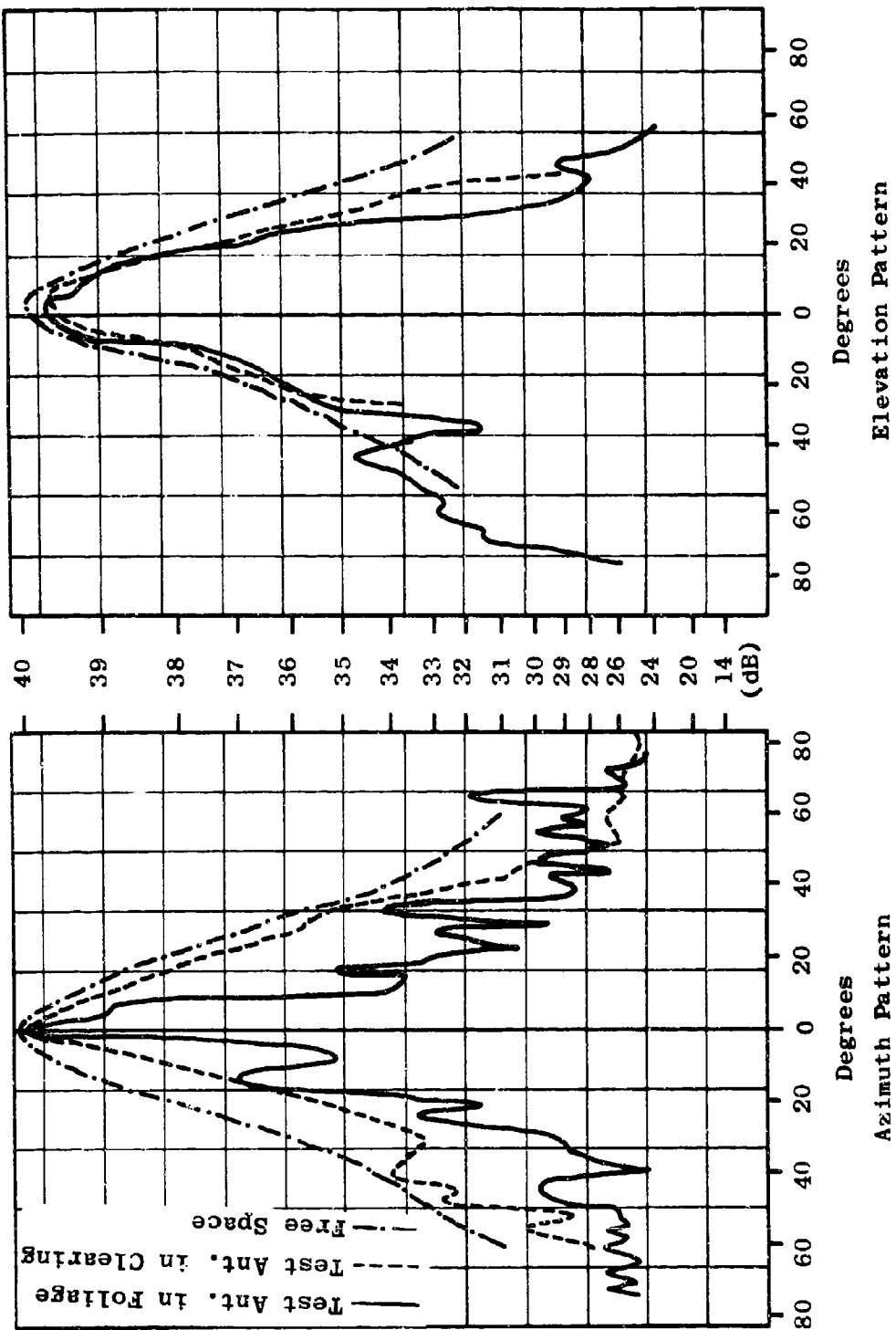
From the observation of many patterns, the degree of degradation in the in-foliage pattern appears to be a function of the antenna aperture or beamwidth. The next case presented illustrates this relationship.

Case 4

T-C $(\longrightarrow \rhd) \uparrow$ R-F (B.W. $\approx 50^\circ$)
T-C $(\longrightarrow \rhd) \uparrow$ R-F (B.W. $\approx 20^\circ$)
T-C $(\longrightarrow \rhd) \uparrow$ R-F (B.W. $\approx 10^\circ$)



Freq: 10 Gc/s Polarization: V Test Ant: 3' Dish
 Figure 5.173 Foliage Effect on Large Aperture Antenna



Freq: 5 Gc/s Polarization: V Test Ant: 1.75"x2" Horns

Figure 5.174 In-Foliage and In-Clearing Patterns of Horn Antenna

In this case, the same transmitting antenna was used for all three tests but the receiving antenna's beamwidth varied as indicated above. The results of these three tests are displayed in Figures 5.175, 5.176 and 5.177, respectively.

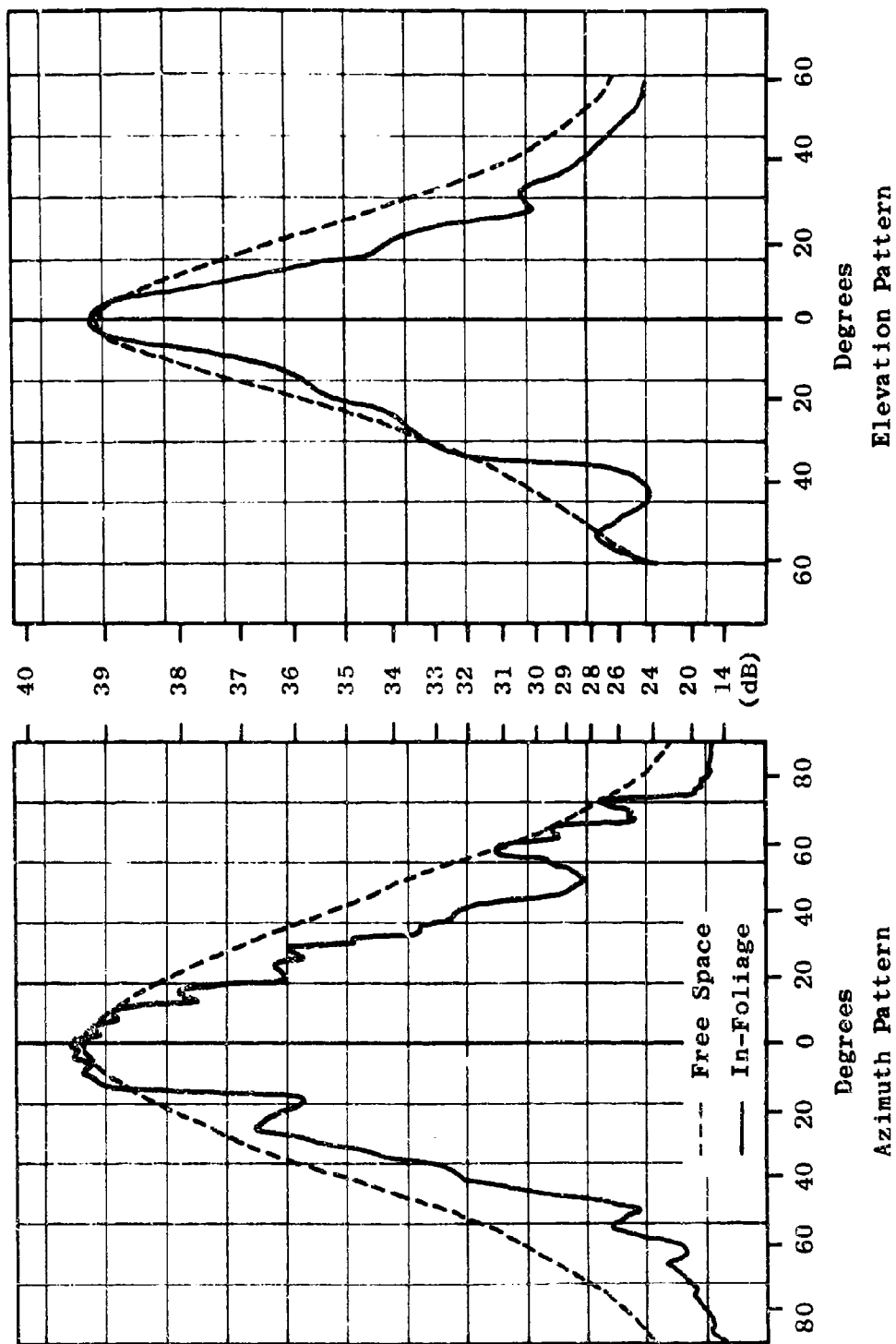
Observation of these patterns reveals that pattern break-up decreases as the beamwidth decreases. Well preserved patterns were always obtained for beamwidth of 10 degrees or less. For beamwidths in the neighborhood of 20 degrees, a certain amount of distortion is usually observed. For beamwidth in excess of 40 degrees, pattern breakup of varying severity always exists.

For a given beamwidth in excess of about 20 degrees, pattern breakup appears to increase with frequency. The next case shows the pattern breakup at 10 Gc/s.

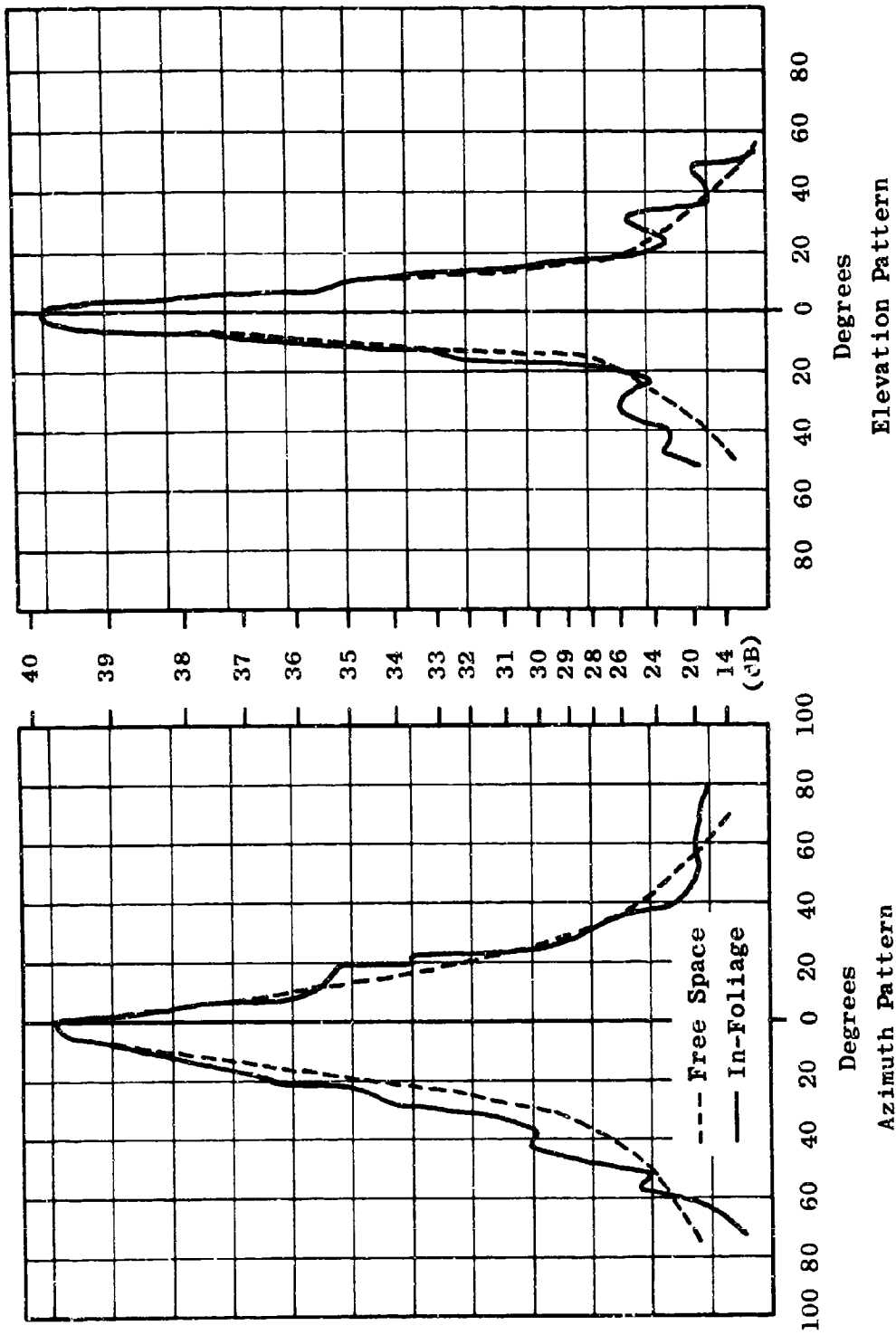
Case 5

T-C (—————>) R-F (B.W. \approx 50 degrees)

The test antenna was a widebeam horn located in foliage and the auxiliary antenna was a narrow beam dish situated in the clearing. The resulting patterns are given in Figure 5.178. Figure 5.178 may be compared with the 5 Gc/s, 50 degree beamwidth case presented in Figure 5.175. The azimuth pattern of Figure 5.178 appears to be more severely degraded than the elevation, but observation of other cases indicates about the same degradation for both planes. The elevation pattern of Figure 5.178, although being fairly smooth, is substantially different from the free-space pattern.

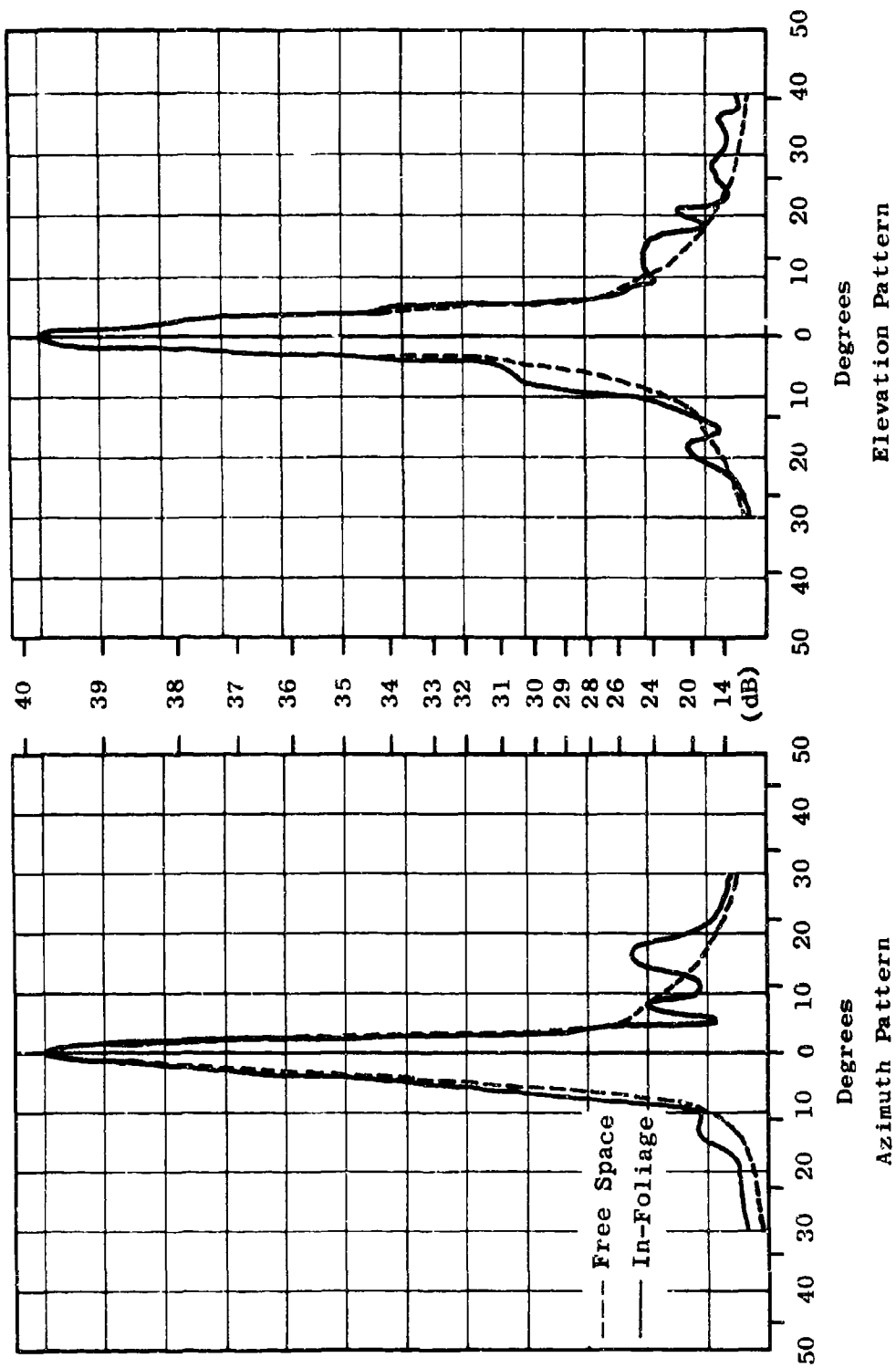


Freq: 5 Gc/s Polarization: H Test Ant: 1.75"x2" Horn (B.W. $\approx 50^\circ$)
 Figure 5.175 In-Foliage Pattern of Widebeam Horn



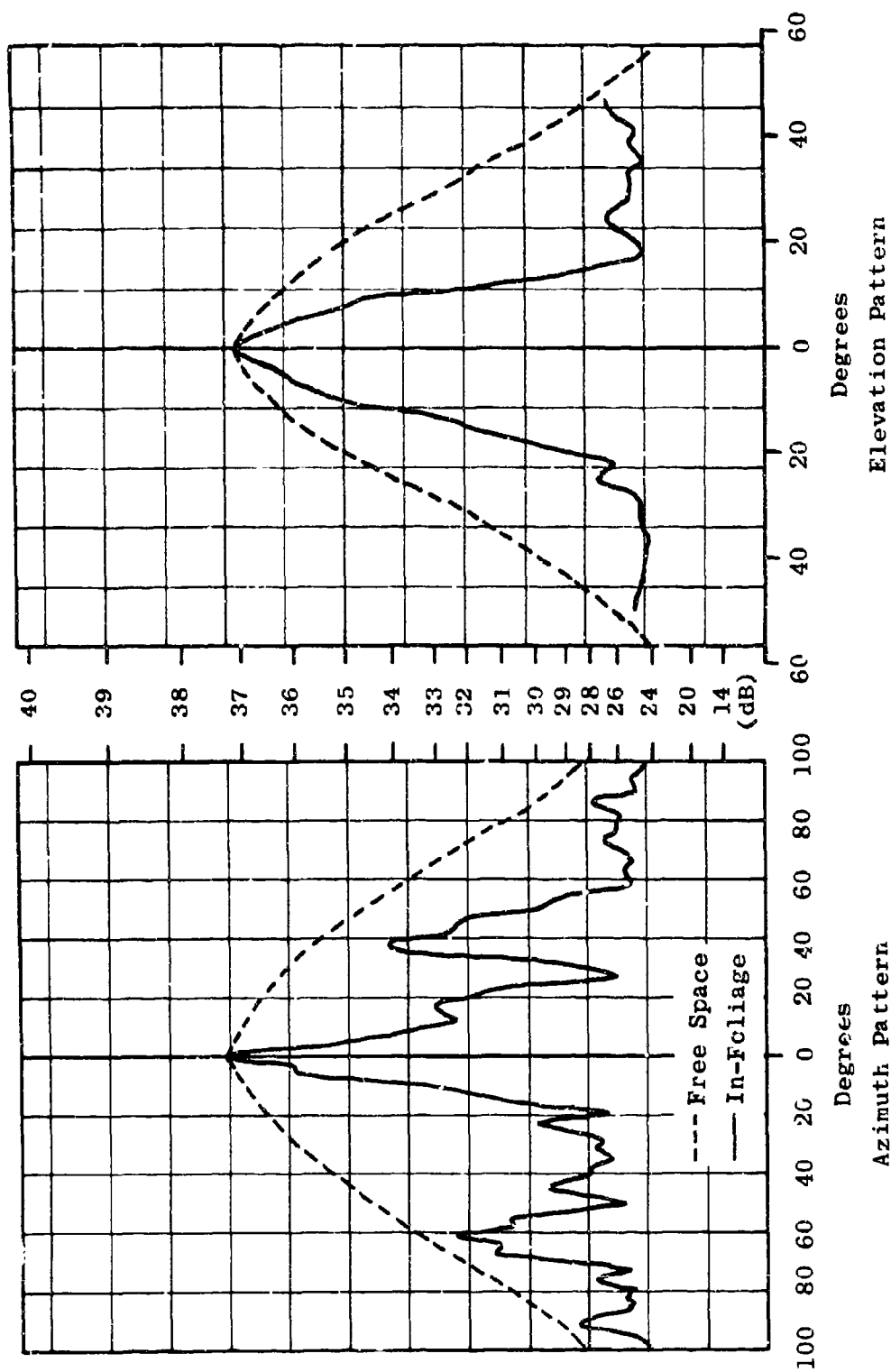
Freq: 5 Gc/s Polarization: H Test Ant: 5"x8" Horn (B.W. $\approx 20^\circ$)

Figure 5.176 In-Foliage Pattern of Narrow Beam Horn



Freq: 5 Gc/s Polarization: H Test Ant: 18" Dish
(B.W. $\approx 10^\circ$)

Figure 5.177 In-Foliage Pattern of Widebeam Dish



Freq: 1.0 Gc/s Polarization: H Test Ant: 1'x1' Horn
 (B.W. ≈ 50°)

Figure 5.178 In-Foliage Pattern of Widebeam Horn

5.9.2.7.3 General Conclusions

Based upon all the antenna patterns taken to date and those particular ones illustrated in the preceding cases, the following conclusions are suggested concerning in-foliage antenna patterns.

- (1) The beamwidth of the auxiliary antenna has no effect on the antenna pattern of a narrow beam dish.
- (2) The performance of a large aperture dish is not altered by placement directly in foliage.
- (3) The direction of power flow through foliage is unimportant.
- (4) The current distribution on a large aperture antenna in foliage is same as in free space.
- (5) The degree of pattern breakup decreases with a decrease in beamwidth of the test antenna.
- (6) For a given beamwidth, pattern breakup increases with increasing frequency.

5.9.2.8 Treetop Mode Study

To insure that radio waves transmit directly through foliage, certain conditions must be imposed. The

major conditions involve limits on antenna height, antenna directivity, and separation distance. Each of these parameters depends upon the other two for successful direct transmission. For example, at a given separation distance and antenna height, the antenna directivity must not fall below a certain value. Likewise, for a given directivity, excessive separation distances or antenna heights are not allowed. When any one of the above parameters exceeds its allowed limit, a treetop diffraction mode, in addition to the direct mode, usually transmits significant microwave energy to the receiving antenna.

During the in-foliage microwave measurement program, questions arose concerning the amount of power associated with the treetop component and specifically whether the treetop mode could be intentionally excited to provide a path with less loss under certain conditions than that for direct line-of-sight transmission. Special measurements were carried out to answer these questions. The measurement setup, test results and general conclusions are discussed below.

Several equipment configurations were set up to experimentally determine the combination yielding the strongest treetop component. For each configuration, antenna patterns and path loss measurements were performed with various transmitter and receiver antenna orientations. The setup which provided the most favorable results on an over-all basis is illustrated in Figure 5.179.

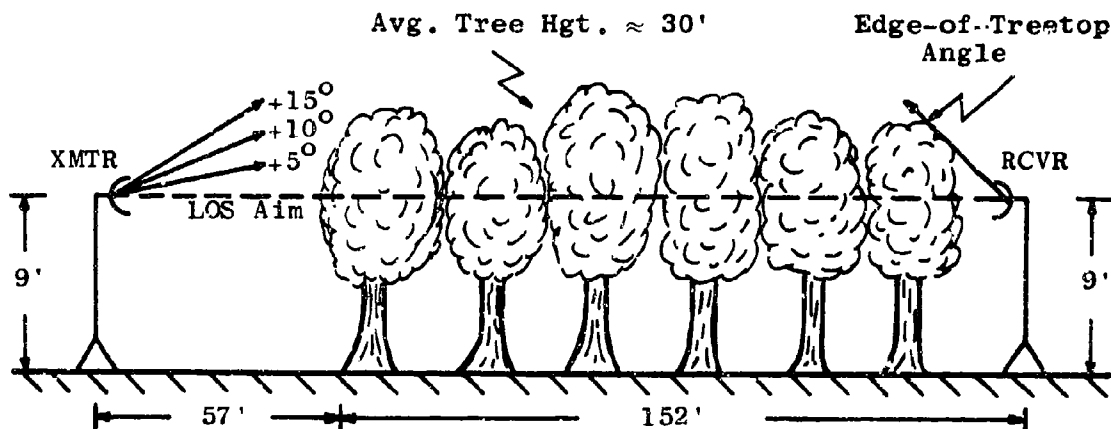


Figure 5.179 Test Setup for Treetop Mode Study

The transmitter, located in a clearing, was elevated to either 9 feet or 21 feet. The receiver, located in foliage, was always situated 9 feet above the ground.

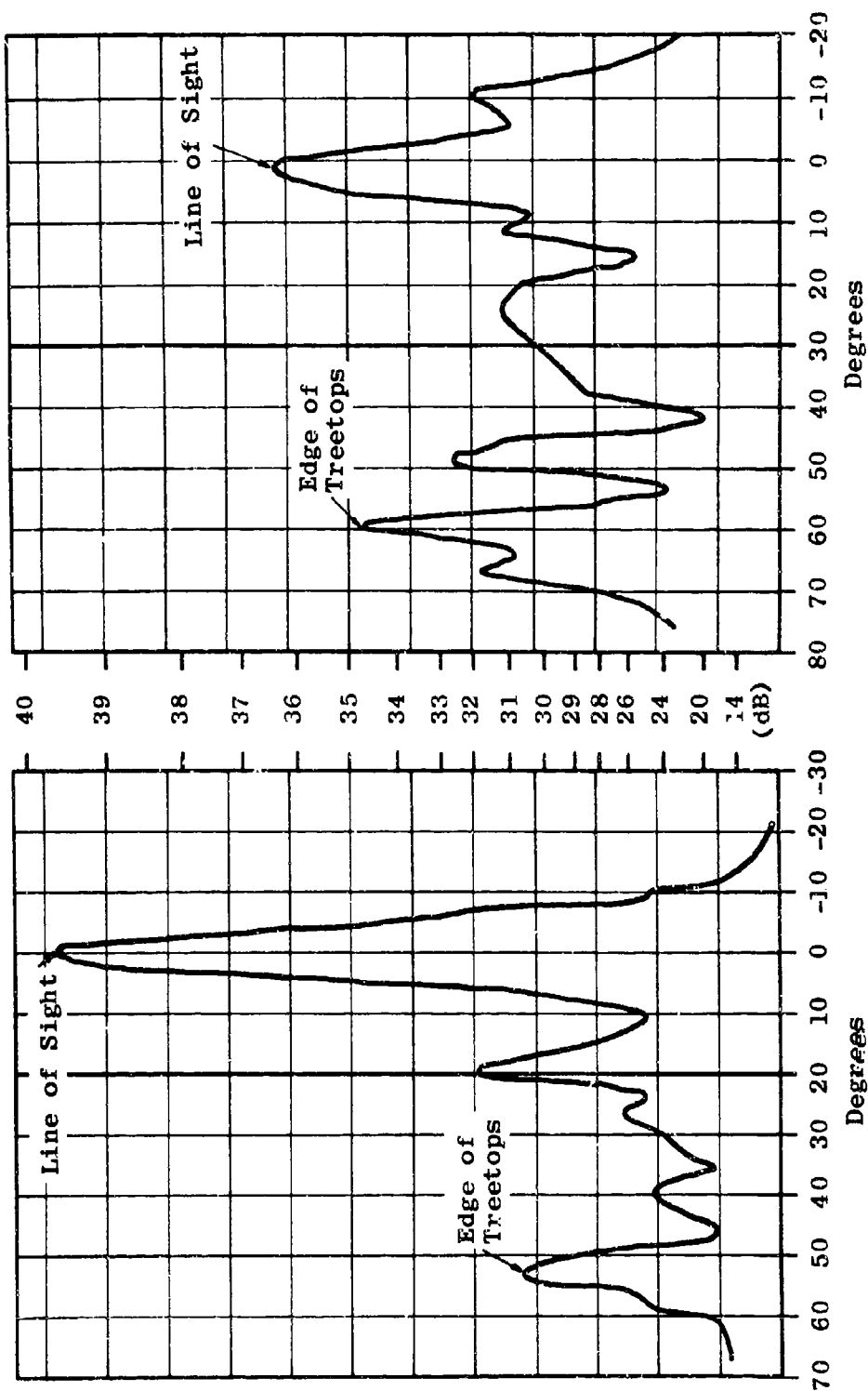
The test consisted of obtaining vertical antenna patterns for the receiver at various orientations of the transmitting antenna. The initial transmitter aim was directly at the receiver (line of sight for non-foliated conditions). Subsequently, the transmitter aim was moved above the line of sight by 5-degree increments. At each transmitter orientation, a complete vertical receiver pattern

was obtained. Sample patterns taken at 1.0 and 2.5 Gc/s are in Figures 5.180 through 5.184. These patterns have been slightly smoothed for illustrative purposes.

The two main points of interest about these patterns are the twin peaks occurring when treetop diffraction exists. One of the peaks corresponds to the receiver line-of-sight elevation angle and represents direct propagated energy. The other peak, when present, occurs when the receiver is "looking" upward at the tops of the trees directly in front of the receiver. This energy represents the treetop component and is received via diffraction over the treetops.

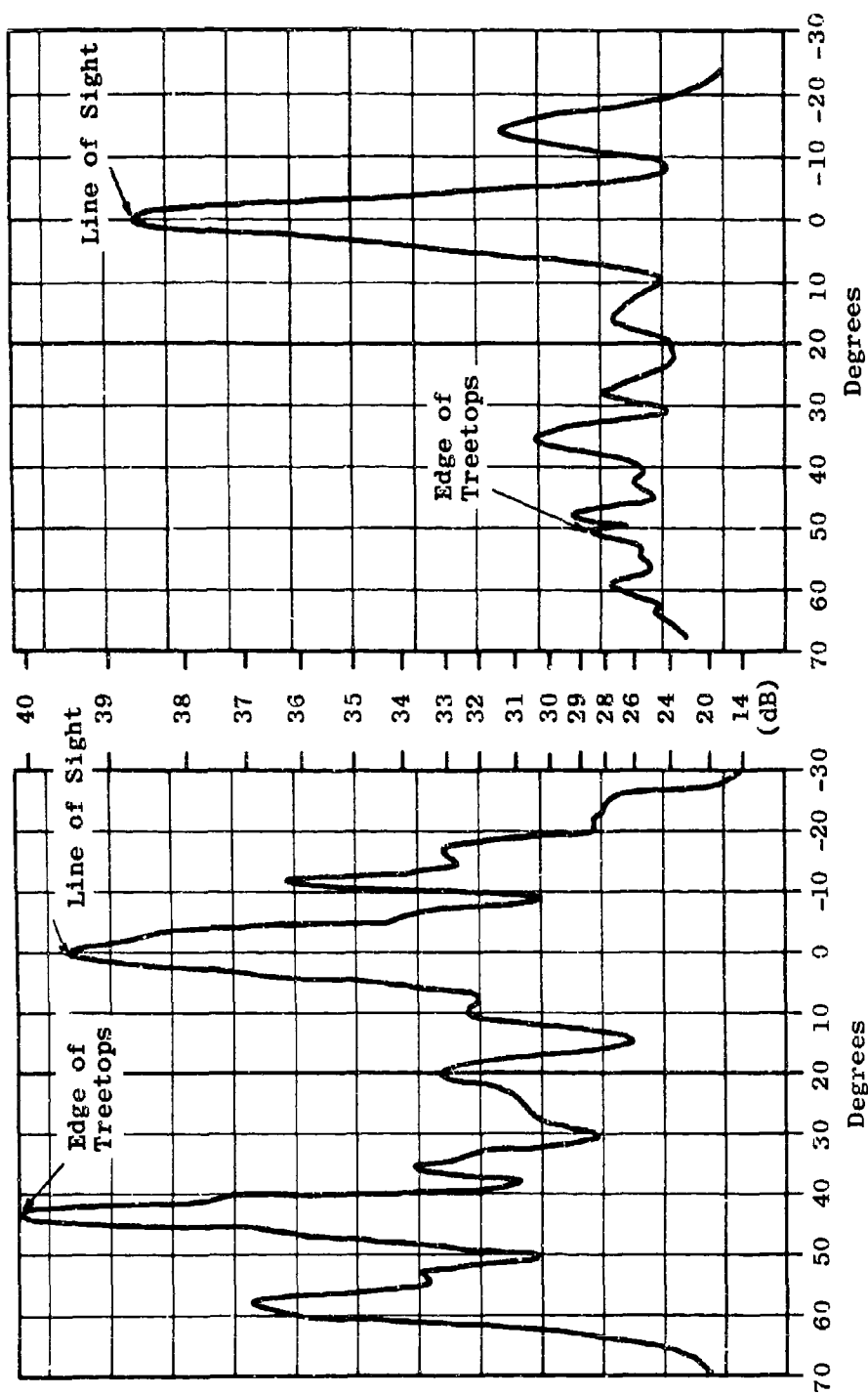
Figures 5.180 and 5.181 show the effect of raising the transmitter aim by 5 degrees. The first pattern presented was made with the transmitter aimed at the receiver (line-of-sight aim). The large peak in the pattern occurs when the receiver is "looking" back at the transmitter. As the receiver antenna is elevated further, the next peak of interest shows up about 55 degrees above the line of sight. This peak coincides with a visual sighting of the edge of the treetops in front of the receiver. In this case, however, the treetop peak is about 10 dB below the main line-of-sight peak. In the next pattern the transmitter was aimed 5 degrees above the line of sight. The treetop component increased by about 3 dB. The decrease in direct component is, of course, due to non-alignment of the antennas.

In the first pattern of Figure 5.182 (line-of-sight plus 10 degrees), the treetop component is slightly



RCVR Elevation Pattern, XMTR Aim = LOS RCVT Elevation Pattern, XMTR Aim = LOS+5°
 Freq: 2.5 Gc/s Polarization: V Ants: 3' Dishes

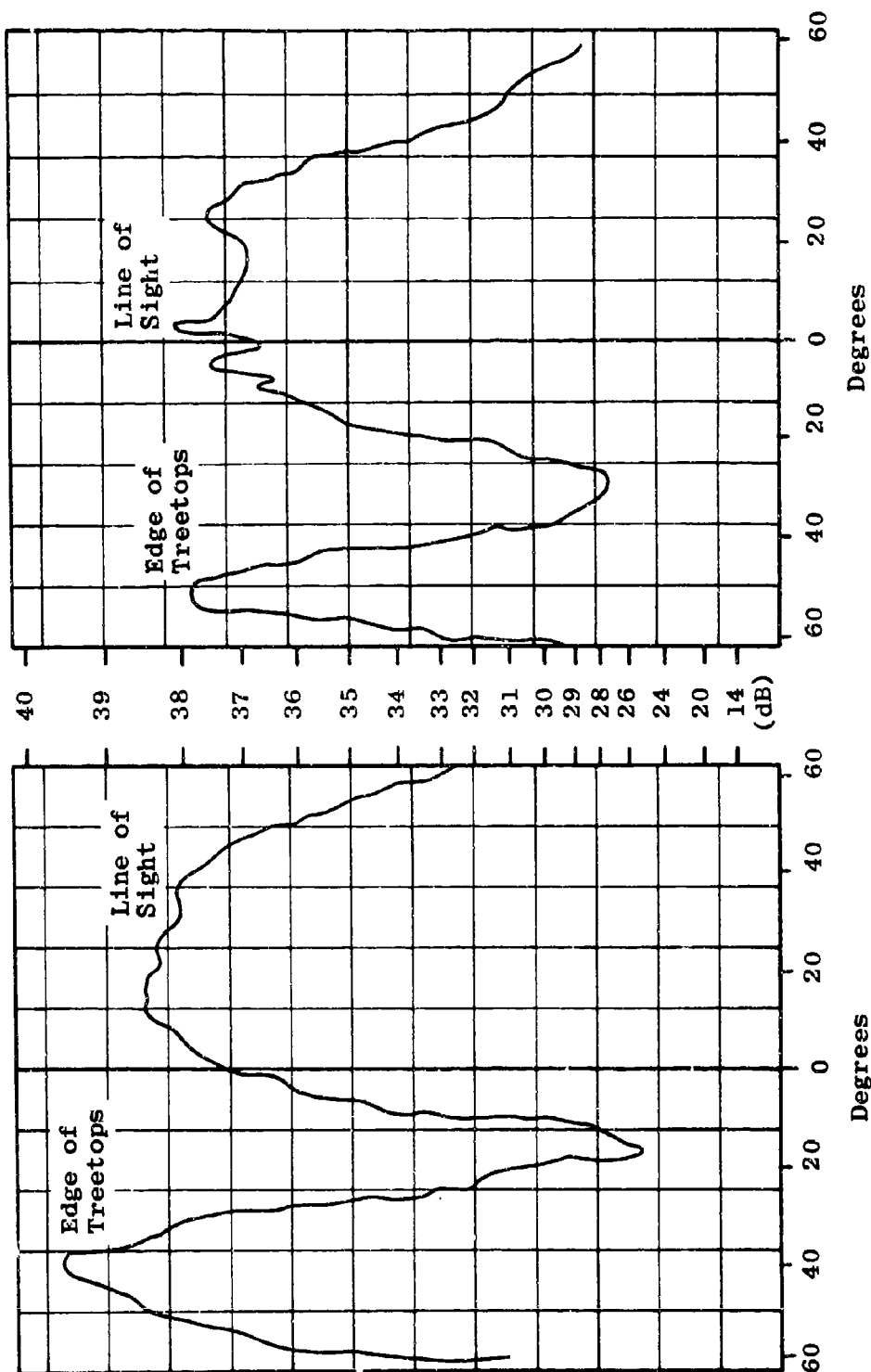
Figure 5.180 Antenna Patterns Showing Treetop Mode



RCVR Elevation Pattern, XMTR Aim = LOS+10° RCVR Elevation Pattern, XMTR Aim = LOS+15°

Freq: 2.5 Gc/s Polarization: V Ants: 3' Dishes

Figure 5.181 Antenna Patterns Showing Treetop Mode



RX Elevation Pattern, Tx Aim = LOS
 RX Elevation Pattern, Tx Aim = LOS + 5°

Freq: 1.0 Gc/s Polarization: H Ant: TACO

Figure 5.182 Antenna Patterns Showing Treetop Mode

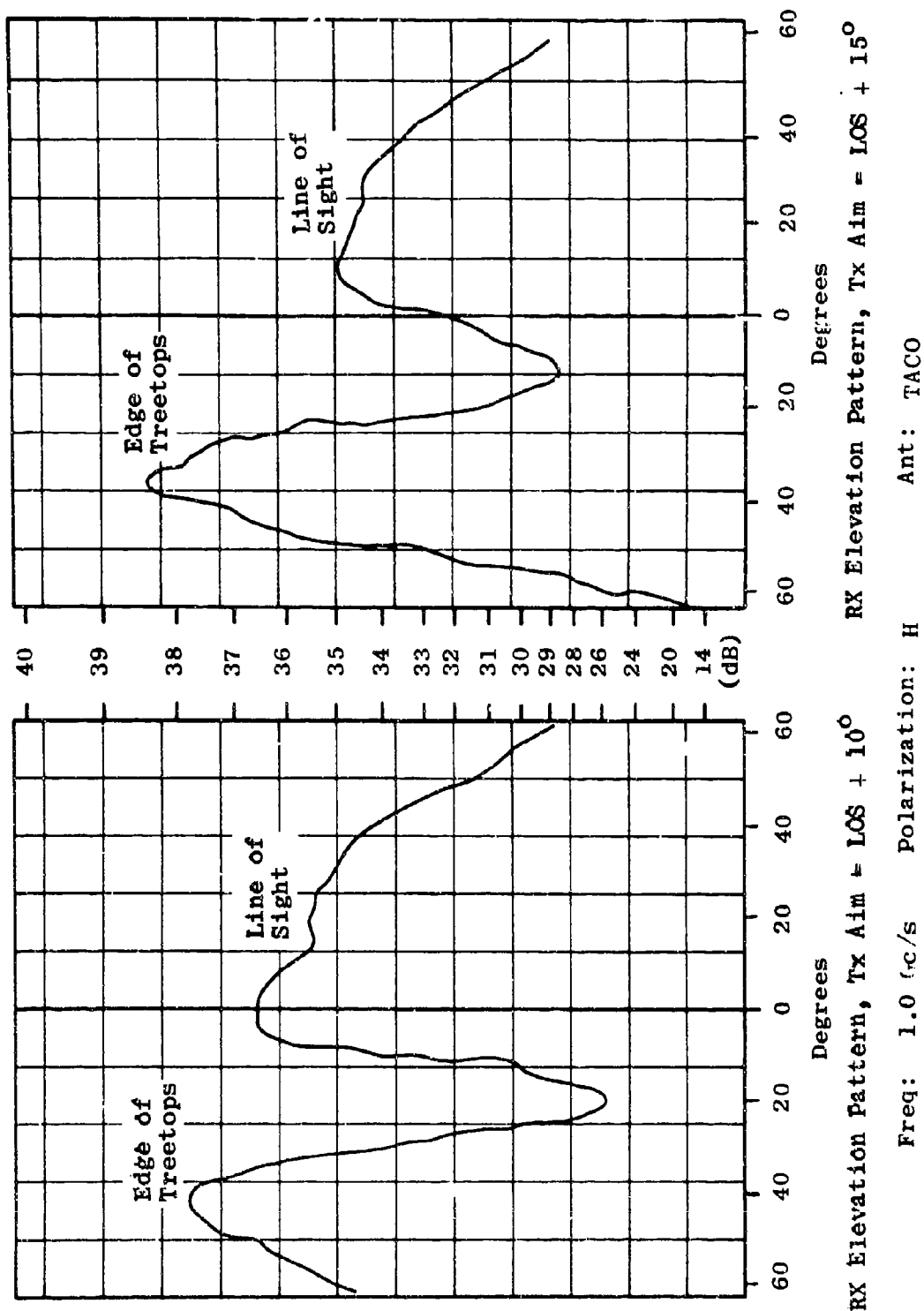
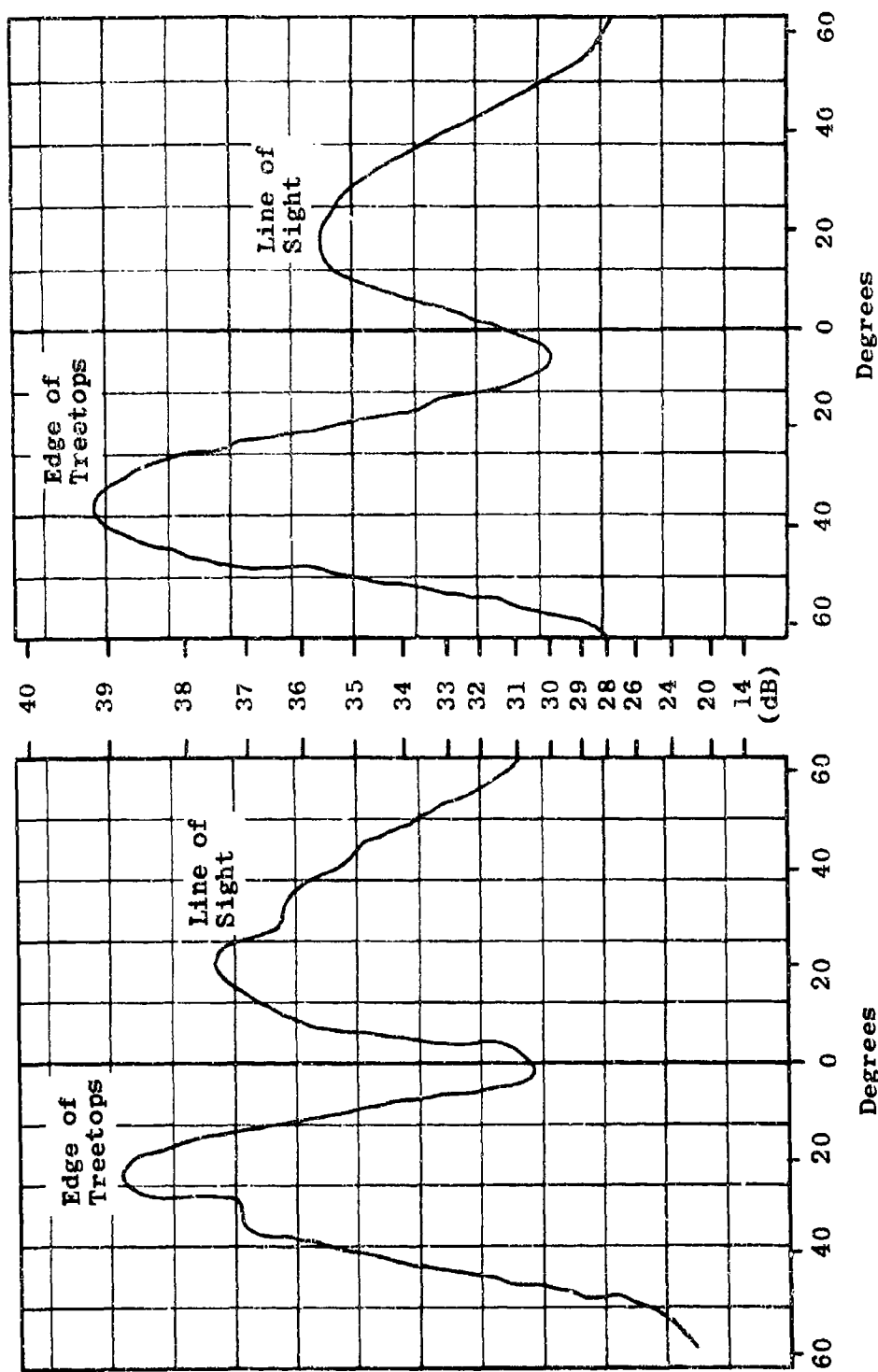


Figure 5.183 Antenna Patterns Showing Treetop Mode



RX Elevation Pattern, Tx Aim = LOS + 20° RX Elevation Pattern, Tx Aim = LOS + 25°

Freq: 1.0 Gc/s Polarization: H Ant: TACO

Figure 5.184 Antenna Patterns Showing Treetop Mode

larger than the direct component. However, when the transmitter antenna is raised an additional 5 degrees (line of sight plus 15 degrees), the treetop component completely disappears while the direct component remains. These patterns have shown that the treetop component is largest when the transmitting antenna is elevated to around 10 degrees above the line of sight and the receiver is elevated about 55 degrees above the line of sight. These elevation angles correspond roughly to the edge of the treetops in front of the respective antennas. In this case, a transmitter aim 15 degrees above the line of sight apparently does not result in sufficient treetop illumination to produce a measurable treetop component. Reference to Figures 5.182 through 5.184 shows, however, that the 1.0 Gc/s antennas registered a substantial treetop component even when the transmitter was aimed 25 degrees above the line of sight.

As the beamwidth of the transmitting antenna is broadened, less precision is required to obtain a sizeable treetop component. Also, to detect the treetop mode, a certain directivity is required at the receiver end to resolve the twin peak effect.

In some of the measurements, a treetop mode could not be detected with both antennas at 9 feet, but when the transmitter was raised to about 21 feet and aimed at the treetops a sizeable component was stimulated.

The antenna patterns in Figures 5.180 through 5.184 prove the existence of the treetop mode. It is interesting to compare the foliage losses associated with

the direct and treetop modes. This has been done by measuring the system loss for each mode, converting to basic transmission loss, and then subtracting the free-space basic transmission loss. Table 5.29 gives the resulting foliage losses for three sample cases. The 1.0 Gc/s case indicates that for optimum treetop alignments the treetop mode loss is roughly the same as the direct loss sustained when both antennas are orientated for optimum line-of-sight transmission. The other cases examined usually show slightly more loss for the treetop mode than for the direct mode, especially at low transmitting heights.

5.9.3 Refractivity Measurements

At microwave frequencies for long line-of-sight or beyond the horizon paths, propagation loss is strongly influenced by the vertical radio refractivity profile. Moreover, the signal strength fading often experienced over such paths is primarily due to fluctuations in the refractivity profile along the transmission path. The severity of this fading is a function of frequency, separation distance and the amount of change in the refractivity gradient. The refractivity gradient itself depends mostly on the climate and other environmental factors present at a given location. To obtain refractivity data applicable to a tropical region, extensive measurements have been carried out in the Pak Chong area.

This section presents measured profiles made both in and out of foliage. The in-foliage measurements extend

Table 5.29

COMPARISON OF TREETOP AND
LINE-OF-SIGHT LOSSES

Freq. (Gc/s)	Trans. Antenna Height (ft)	Rec. Antenna Height (ft)	Trans. Aim	Foliage Loss	
				Rx Aimed at Tx (dB)	Rx Aimed at Treetops (dB)
1.0	21	9	LOS	26	24
	21	9	LOS+5°	26	26
	21	9	LOS+10°	26	25
	21	9	LOS+15°	28	25
	21	9	LOS+20°	28	26
	21	9	LOS+25°	30	26
2.5	9	9	LOS	57	66
	9	9	LOS+5°	60	61
	9	9	LOS+10°	64	63
	9	9	LOS+15°	65	75
5.0	21	9	LOS	62	>75
	21	9	LOS+5°	65	68
	21	9	LOS+10°	80	70
	21	9	LOS+15°	>80	>80

from about 10 feet above ground level to about 80 feet (treetop height). Out-of-foliage profiles were taken from about 70 to 900 feet above the ground. The basic measurements have been reduced to show diurnal and monthly profile variations. The methods of measuring and reducing the data are explained.

5.9.3.1 Measurement Setup

In-foliage measurements were conducted at a location very close to the Pak Chong base camp. To obtain the 10 to 80 foot in-foliage profiles, sensing equipment was attached to a telescoping tower identical to the ones being used for the vertical field-strength profiles. Readings were taken every 10 feet as the tower was being raised and lowered. The approximate time taken to complete a profile in one direction was about 30 minutes. A reading was taken about once every 4 minutes.

The sensing equipment consisted of two thermistors, one for sensing dry-bulb temperature and the other for sensing wet-bulb temperature. The wet-bulb thermistor was mounted in a "wet-sock," and a battery-operated fan blew air over it. The dry-bulb thermistor was exposed to the ambient environment. The resistances of the two thermistors then varied in accordance with the temperatures of the two environments. A resistance bridge, set on the ground and connected to the thermistors by wires, was used to determine the thermistor resistances, and, by means of calibration curves, the wet and dry-bulb temperatures were calculated.

A waiting period was required at each successive elevation level to allow the wet-bulb resistance to stabilize.

Out-of-foliage profiles from about 70 to 1000 feet were made in a clearing near the Pak Chong base camp. The equipment used was an AN/UMC-4 wiresonde set. The vehicle for housing the sensing equipment was a lighter-than-air device with lift surfaces attached. Thus, when it is flown in a wind, there are two sources of lift.

The vehicle was connected by light cable to a play-out reel on the ground. The amount of cable play-out was monitored by an odometer. The height of the vehicle above ground was determined from the cable payout and the elevation angle, measured with a clinometer at the mooring point. Greater precision in height determination could possibly have been obtained by using two clinometers at different locations. However, the lack of cleared space in the area precluded this technique. Clinometer readings were obtained during darkness by installing a light source aboard the vehicle. Weather conditions, such as rain or lack of wind, sometimes prevented obtaining a complete profile.

Resistance bridge readings were obtained in a fashion identical to that used for the in-foliage measurements. Wires along the mooring cable, leading from the vehicle to ground, were used to connect the thermistors to the resistance bridge.

5.9.3.2 Measurement Accuracy

A radio wave refractometer which directly measures the dielectric constant of air is the most precise method of measuring the radio refractivity. This device, however, is expensive and not well suited to general field conditions. A second method and the one used in this experiment, is to measure certain climatological parameters which are then put in a mathematical expression to compute the refractive index, N .

The three quantities measured are dry-bulb temperature, wet-bulb temperature, and ambient pressure of the atmosphere. The accuracy to which N can be determined is then related to the precision of measuring these parameters. Of these, the wet-bulb temperature is the parameter which must be measured with by far the greatest precision. Unfortunately, it is also the most difficult parameter to measure precisely under field conditions. Fairly accurate results can be obtained with a sling psychrometer, if care is exercised in operation and readout. However, this device is limited to making surface observations.

The use of a thermistor placed in a "wet sock" environment to make refractive index measurements allowed several additional factors to affect accuracy. These factors consisted of uneven flow of air across the sensor from the battery operated fan, variations in elevation of the vehicle which would not allow temperature to stabilize, drift in thermistor characteristics, and bridge-reading errors. The accuracy of a given reading is not usually known.

A study was carried out to determine the uncertainty in N produced by inaccuracies in wet-bulb temperature. Results of this study indicate that, under very favorable conditions, the prediction uncertainty of N would be about four N units for a sling psychrometer. Under less favorable conditions, the uncertainty could rise to around 10 to 15 N-units. It is very likely that the thermistor sensing method at best would also create uncertainties on the order of 10 to 15 N units. This degree of variation in N can be produced by wet-bulb temperature variation of about ± 2 degrees.

A least square fit analysis, presented in the next section, was employed to enhance the usefulness of the data by taking into account the uncertainty in computed values of N.

5.9.3.3 Refractivity Analysis

The calculation of refractive index values from raw field data and the subsequent analysis of refractive index profiles were carried out by a digital computer. The field data consisting of (1) dry bulb temperature, (2) wet bulb temperature, (3) elevation and, (4) time of day was transferred from the original data sheets to punched cards. The punched card data was then read into a computer and the radio refractive index profiles computed using the following equation.²¹

$$N = \frac{103.5}{T} \left[P_a - \frac{(4810)(e)}{T} \right] \quad (26)$$

where

N = radio refractive index (units)

T = ambient dry bulb temperature (degrees Kelvin)

P_a = ambient atmospheric pressure (millimeters of mercury)

e = partial pressure of water vapor (millimeters of mercury)

The partial pressure of water vapor, e, was in turn evaluated through the following expression:

$$e = 4.579 \exp 19.667 \left[\frac{t}{T+273} \right] - 0.000660 P_a (T - t)(1 + 0.00115 t) \quad (27)$$

where

t = wet bulb temperature (degrees Centigrade)

T = dry bulb temperature (degrees Centigrade)

P_a = atmospheric pressure (millimeters of mercury)

A computer printout of all refractivity measurements was obtained for use in plotting of profiles. To test the general behavior of the data, several profiles were plotted for visual observation. In nearly every case, an apparent random variation in N from one measurement to the next was observed. The magnitude of this variation was on the order of 10 N-units. However, definite trends in the data could be noted, namely a general tendency for N

to decrease with elevation. The fluctuation of N is assumed to be due to the measurement accuracy of wet bulb temperature previously discussed. Due to the inherent fluctuation of individual data points, a linear curve fitting technique was used to represent all measured profiles, both in and out of foliage.

The curve fitting process used was the linear least-squares-fit. A linear fit was used because of the observed linear trend in the plotted profiles. Again, the computer was used to generate these best-fit lines from the original input data card deck. All straight line profiles presented in this section were computer generated from the actual data. In most of the profiles illustrated, the actual data points themselves are not shown.

One of the objectives of the measurement program was to obtain the diurnal variation of the refractivity profile for in-foliage and out-of-foliage conditions. This was accomplished by sampling a complete refractivity gradient several times throughout a 24-hour period. The number and duration of these samplings over a 24-hour period often varied due to weather and equipment limitations. The number of samplings for a particular diurnal period varied from 3 to 5. Generally a sampling lasted 2 to 3 hours.

Two sample cases showing diurnal profile variations for out-of-foliage conditions are presented in Figures 5.185 and 5.186. For these two cases the actual data points are shown, different symbols being used to identify different time blocks. Also shown on these two plots is a theoretical linear gradient proposed by NBS.²²

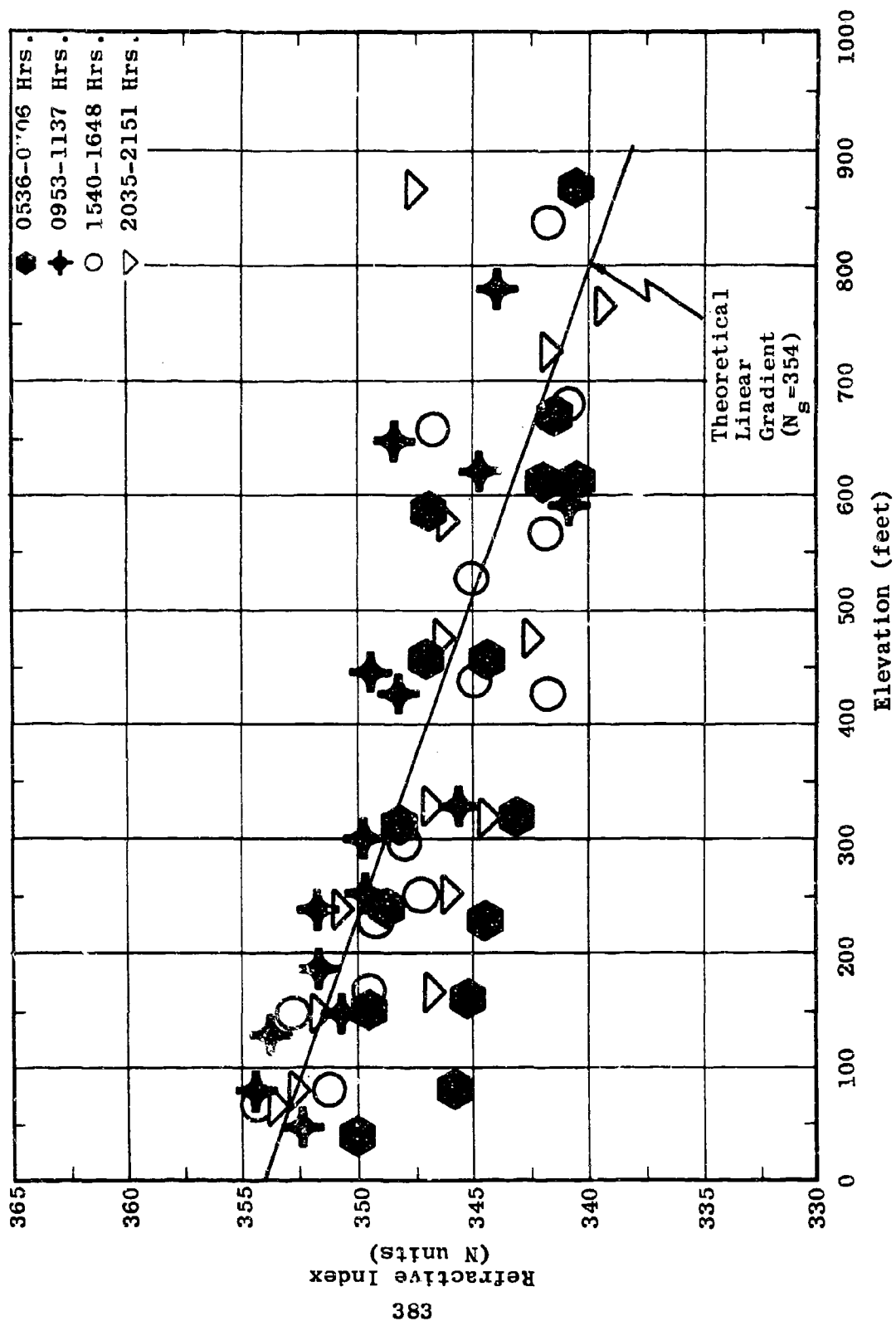


Figure 5.185 Diurnal Variation of Refractivity Profile (1-2 August 1965)

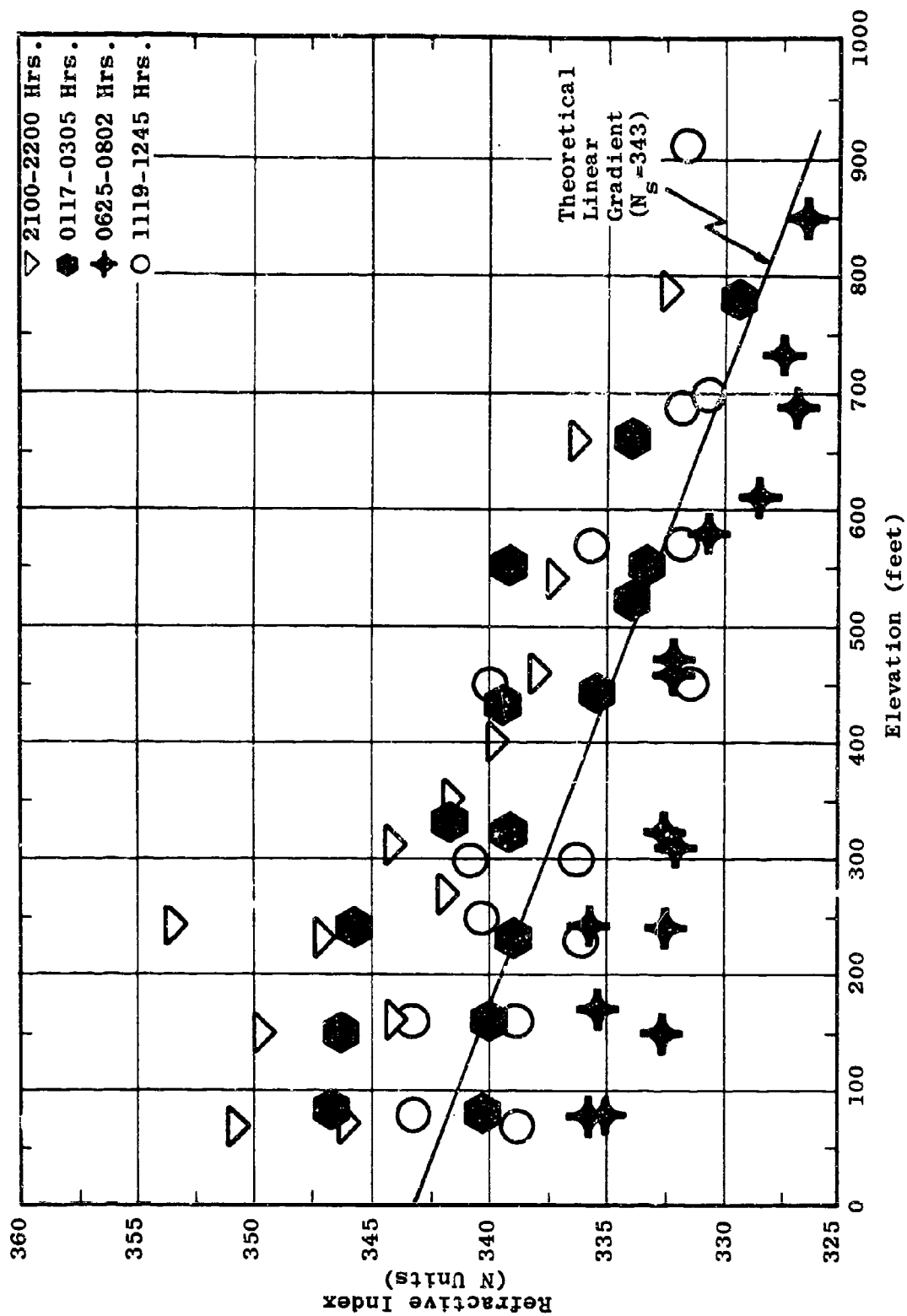


Figure 5.186 Diurnal Variation of Refractivity Profile (30-31 July 1965)

This gradient was positioned at zero elevation to a value of N which appeared to fit the data best. The slope of the line then was computed from the following equation.

$$\Delta N = -7.32 \exp (0.005577 N_s) \quad (28)$$

where

ΔN = slope of gradient (units/feet)

N_s = surface refractivity (N units)

Two in-foliage diurnal plots are presented in Figures 5.187 and 5.188. The actual data in these cases has been replaced by least-squares-fit gradients. All data within the time blocks indicated was used to obtain the individual gradients. Representative out-of-foliage diurnal plots for August, September and October 1965 are presented in Figures 5.189, 5.190 and 5.191. Again, the actual data is not shown, and the least squares procedure was used.

To study the profile variation over a longer period of time, Figures 5.192 through 5.195 were generated. Each line on these graphs represents the best fit to data taken over a 24-hour period rather than a time block as before. The series of lines represents different days for the same month indicated on the graphs.

By combining all of the daily gradients for a given month, the monthly least squares gradient for the out-of-foliage cases was obtained for the months of August, September and October. These are shown in Figure 5.196, along with the NBS model. Finally, by combining all the

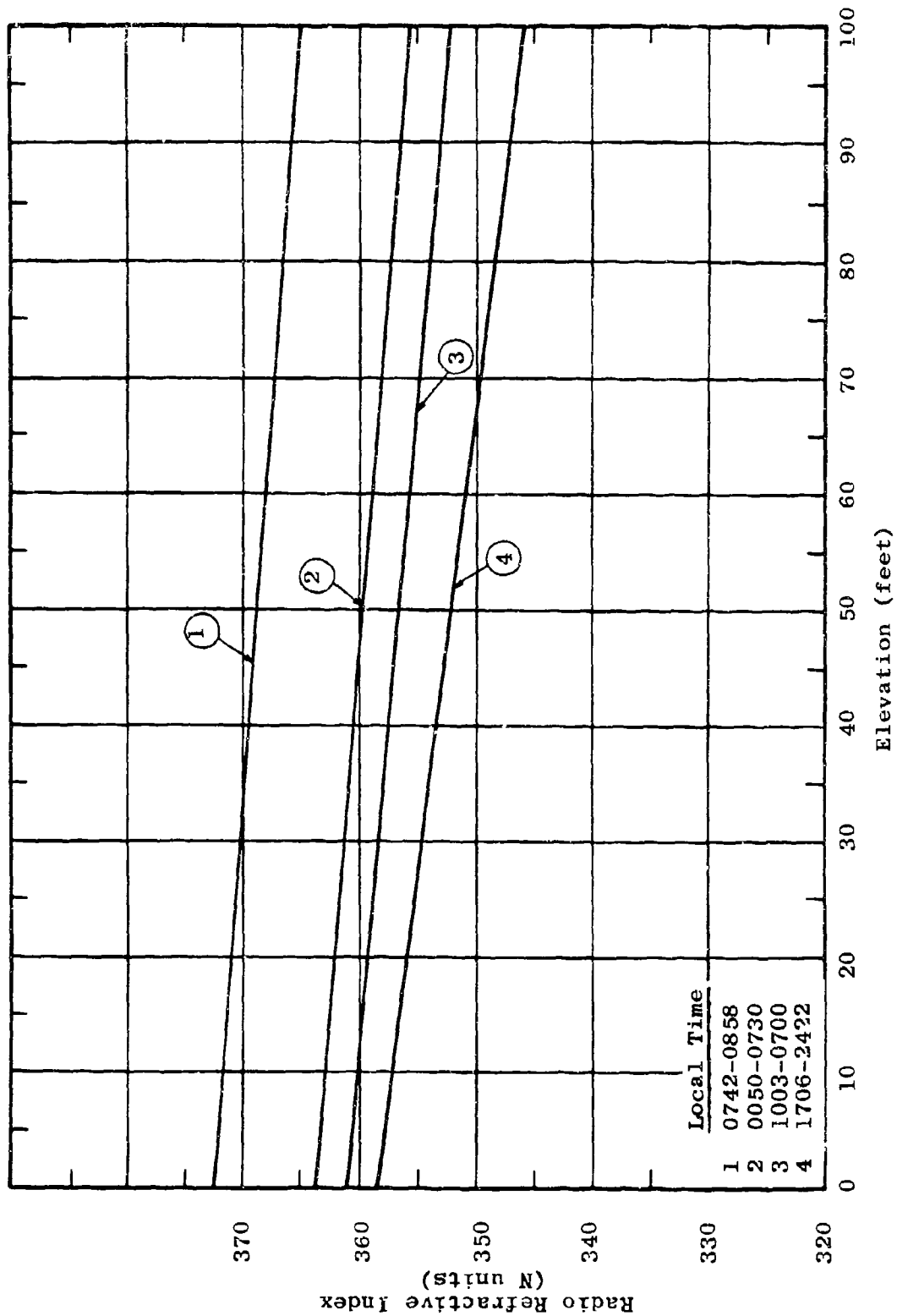


Figure 5.187 Diurnal Variation of In-Foliage Refractivity
for July 25-26, 1965

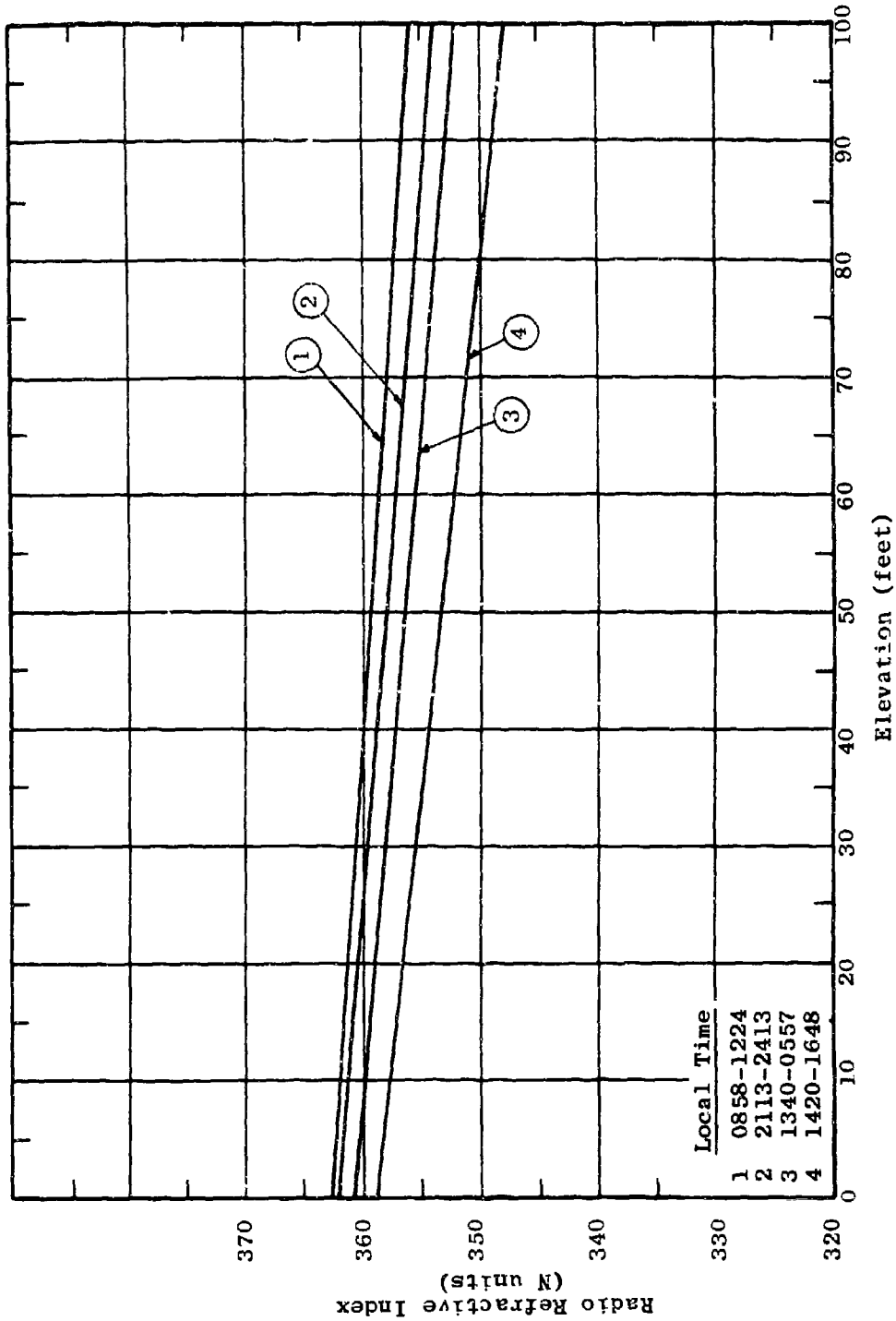


Figure 5.188 Diurnal Variation of In-Foliage Refractivity
for July 26-27, 1965

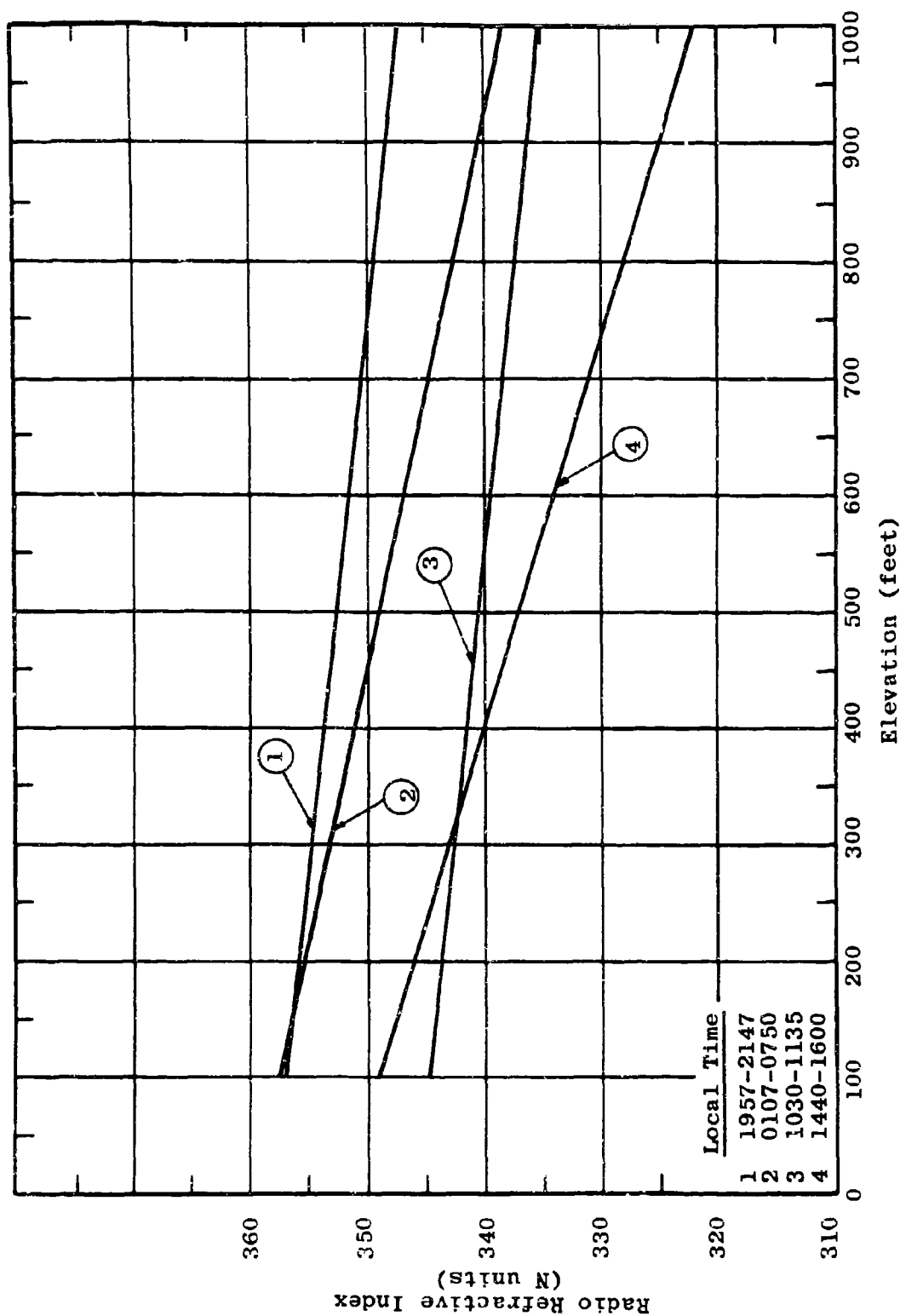


Figure 5.189 Diurnal Variation of Out-of-Foliage Refractivity for August 21-22, 1965

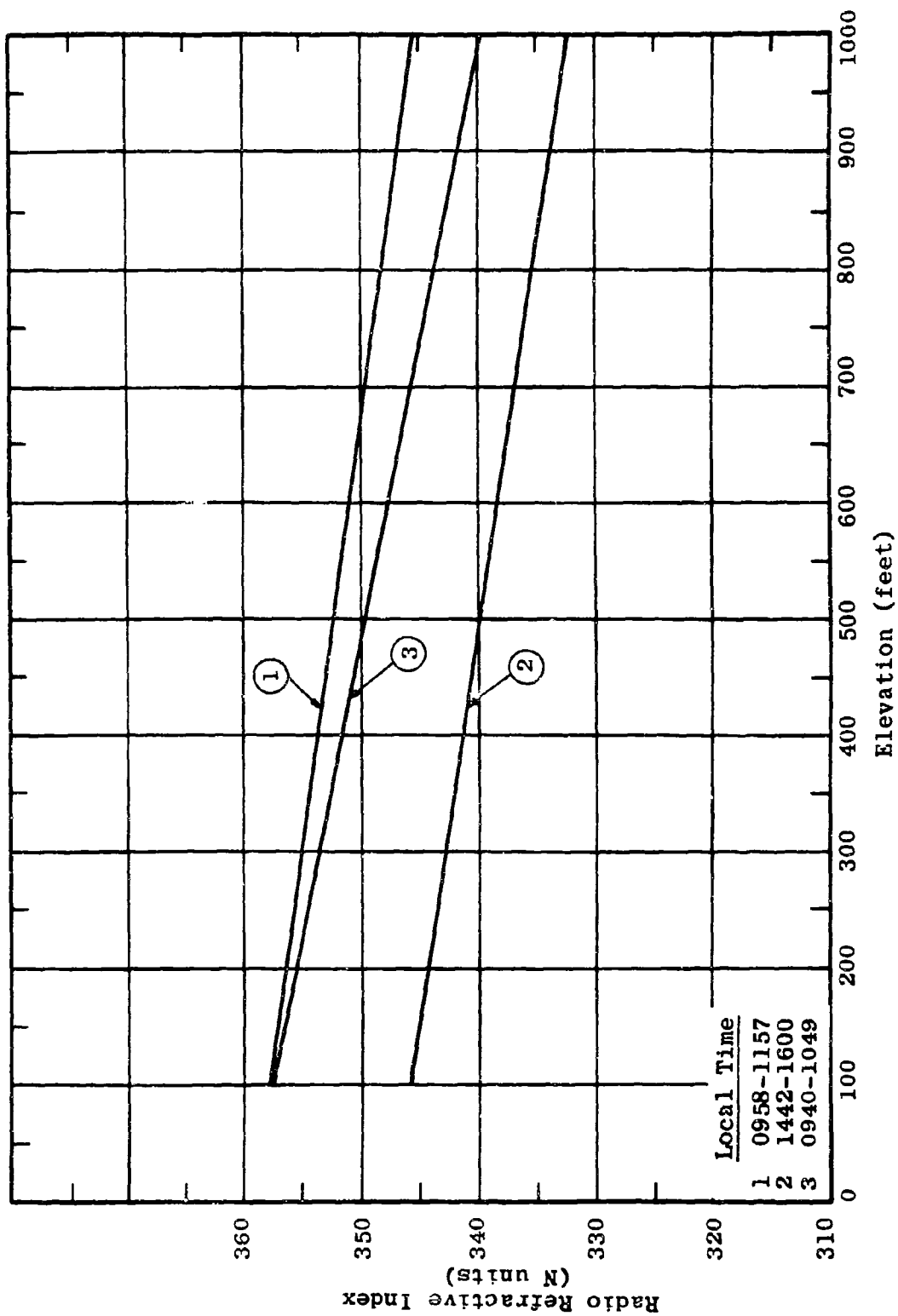


Figure 5.190 Diurnal Variation of Out-of-Foliage Refractivity
for October 7-8, 1965

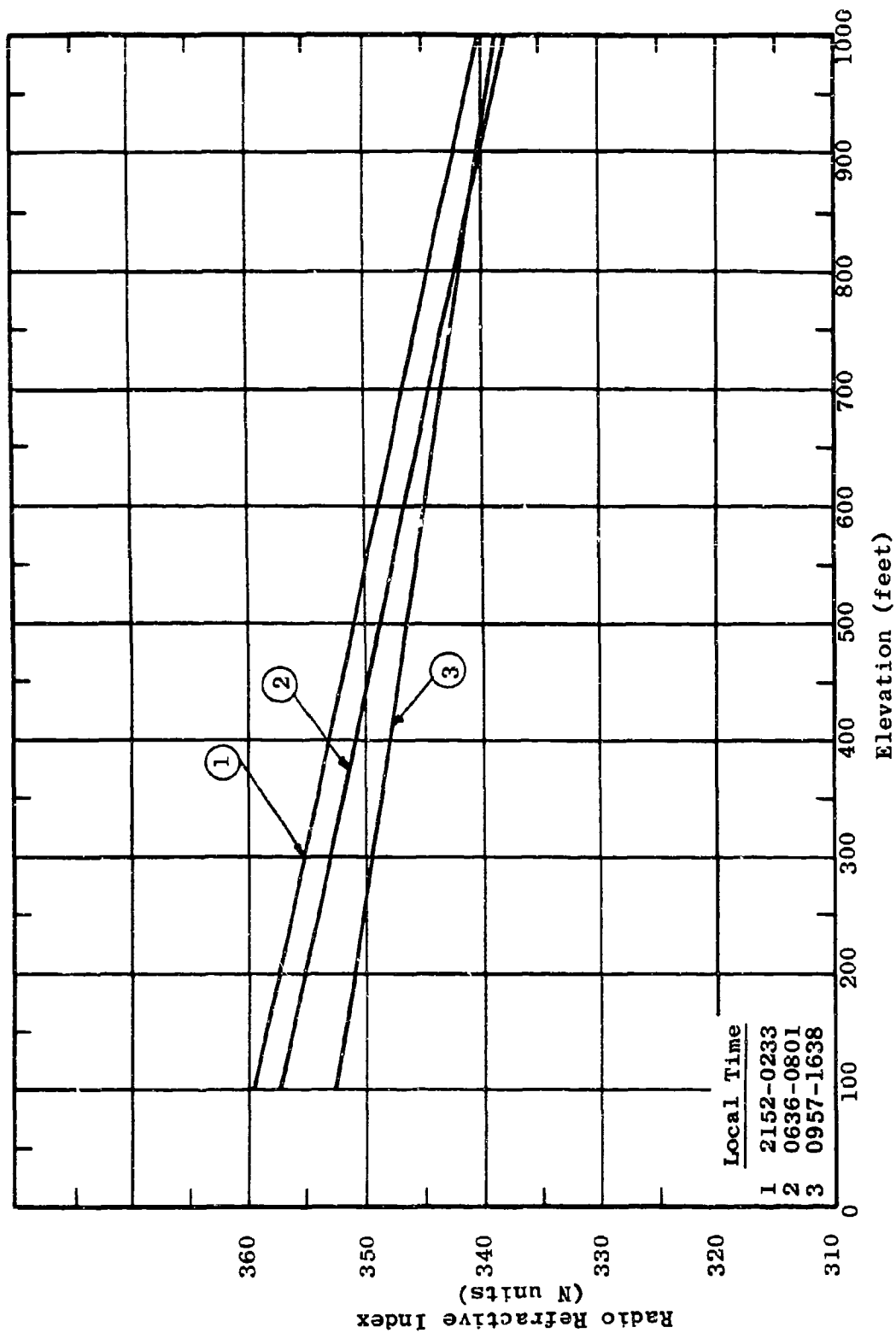


Figure 5.191 Diurnal Variation of Out-of-Foliage Refractivity for September 21-22, 1965

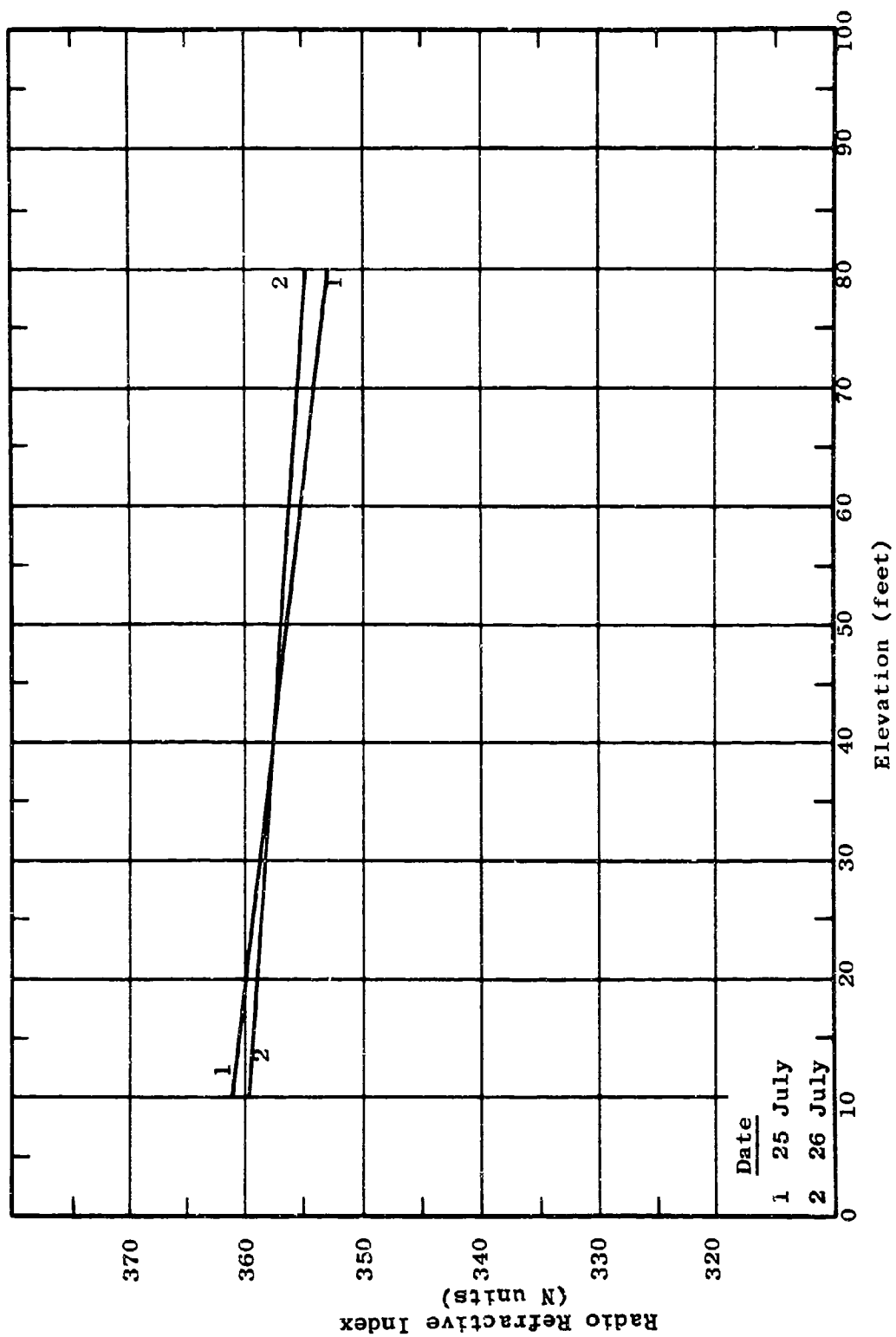


Figure 5.192 24-Hour Refractivity Gradients Taken In-Foliage During July 1965

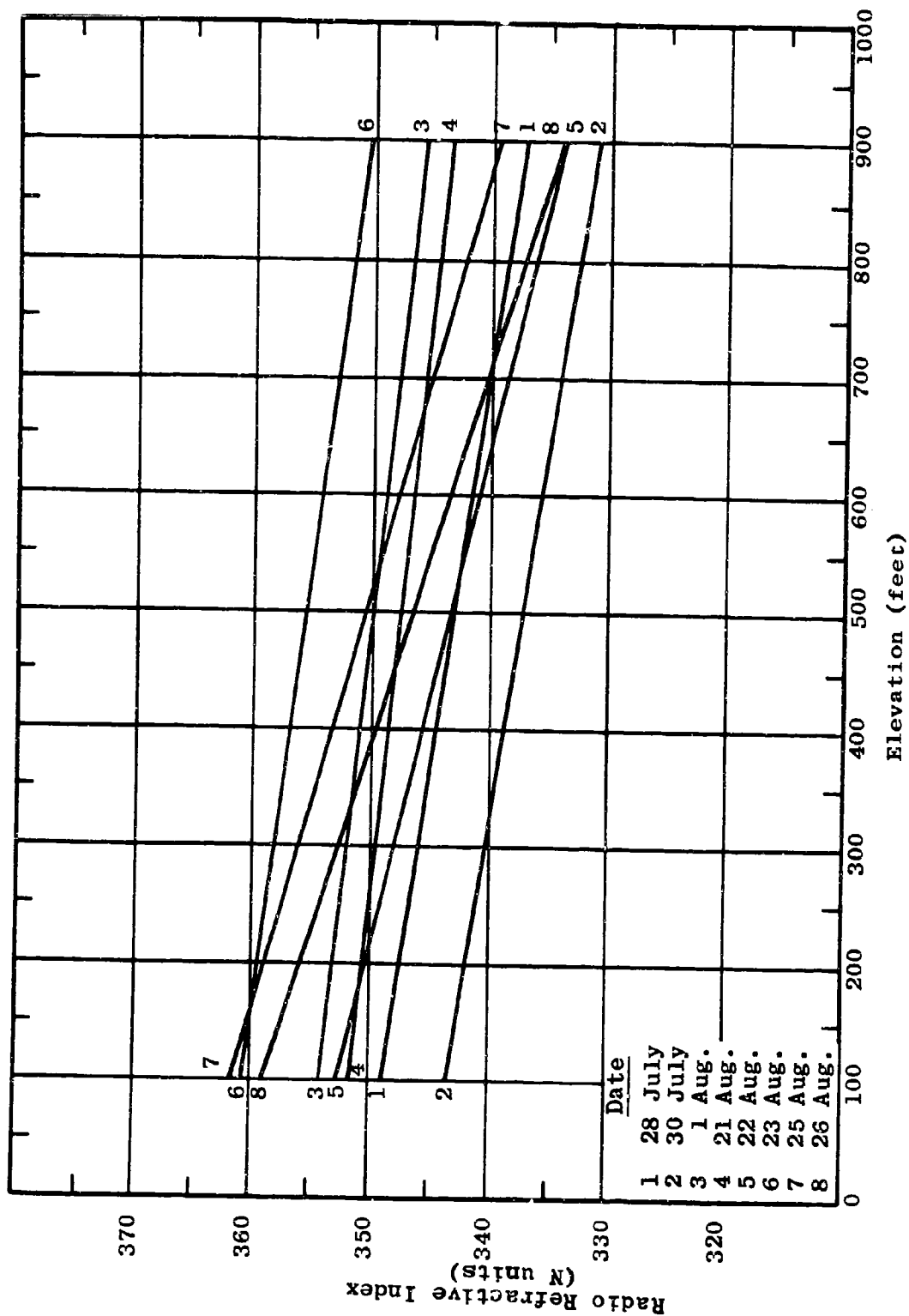


Figure 5.193 24-Hour Refractivity Gradients Taken Out-of-Foliage During Latter July and August, 1965

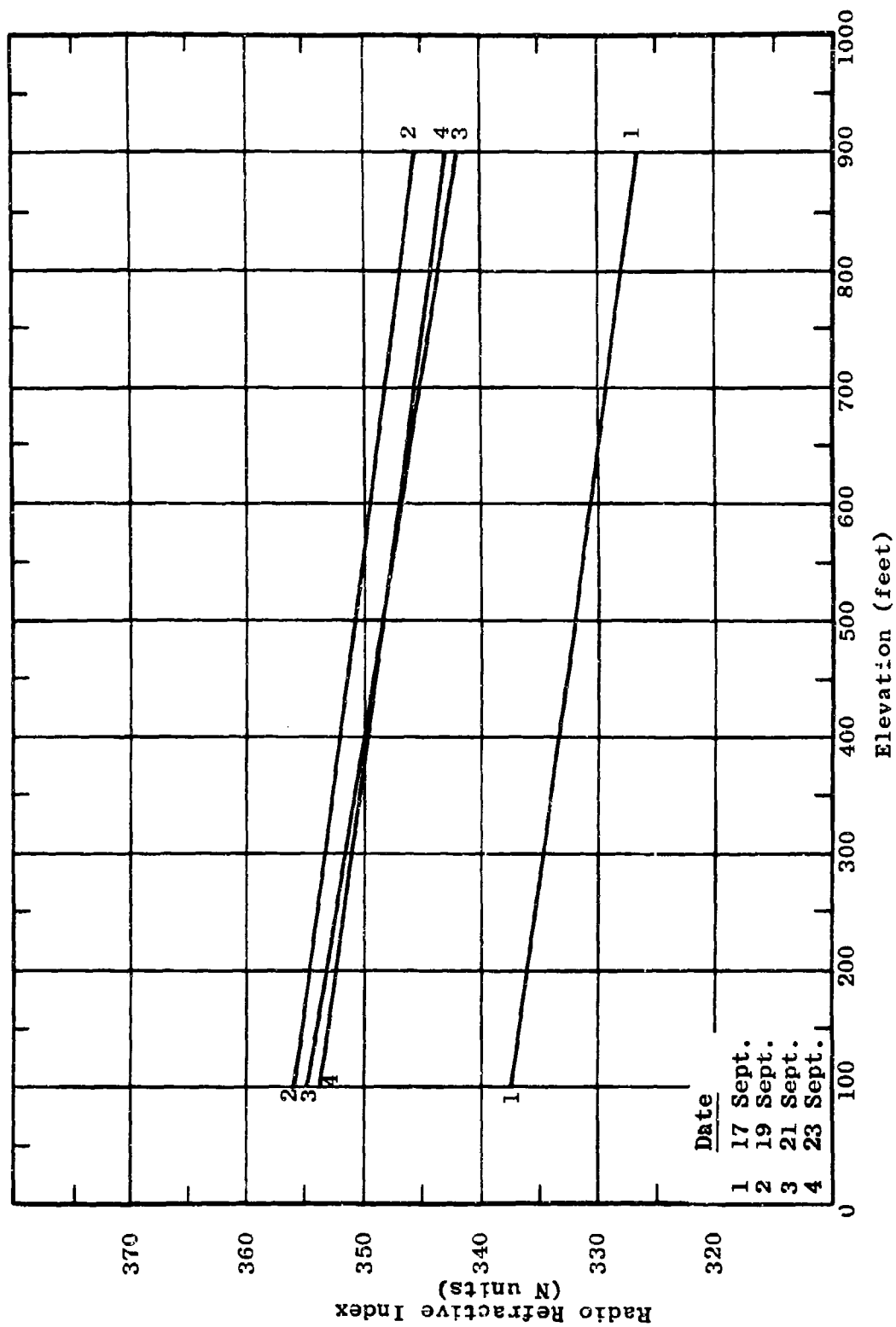


Figure 5.194 24-Hour Refractivity Gradients Taken Out-of-Foliage During September, 1965

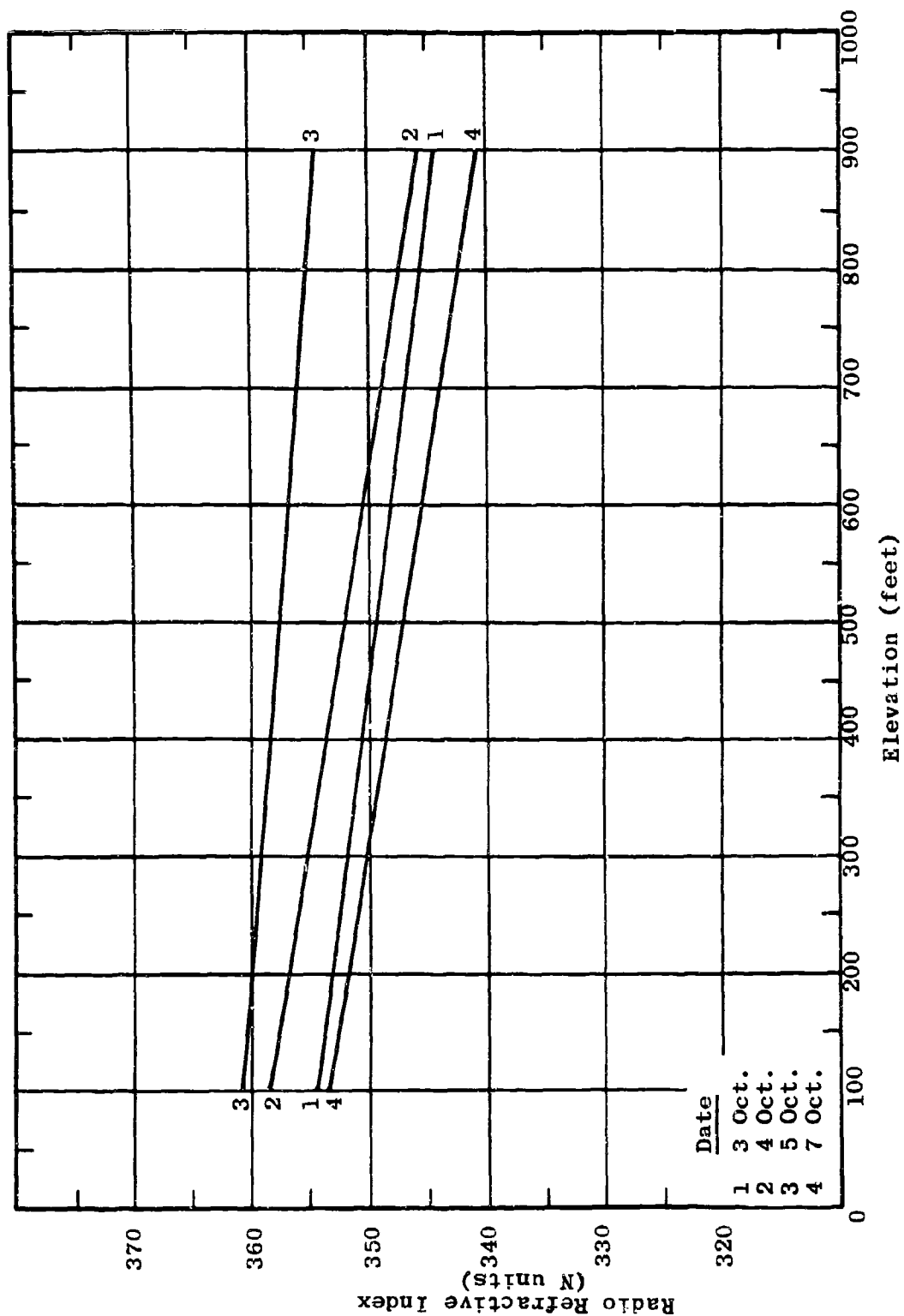


Figure 5.195 24-Hour Refractivity Gradients Taken Out-of-Foliage During October, 1965

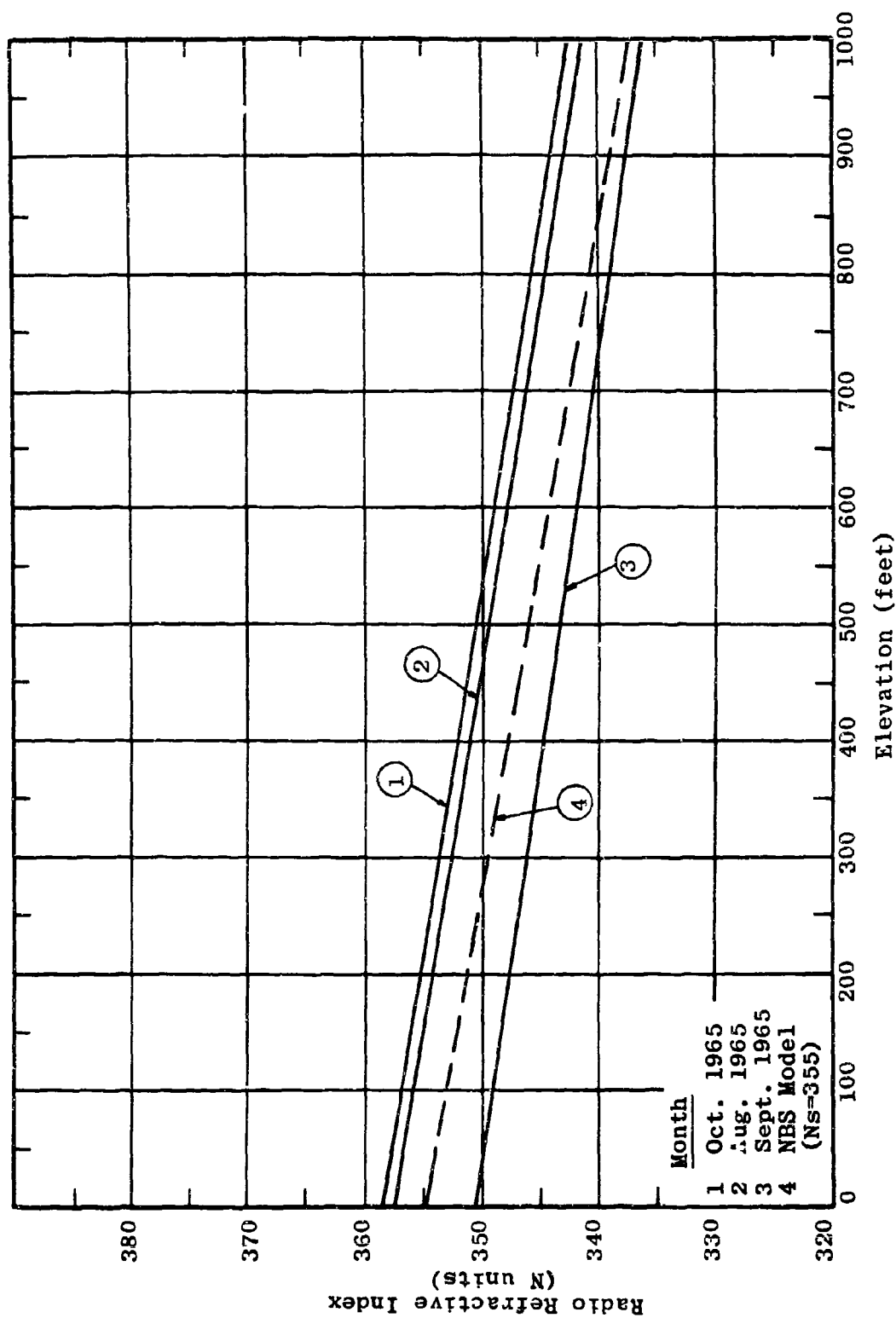


Figure 5.196 Monthly Refractivity Gradients Taken Out-of-Foliage

monthly data, a representative gradient for the three-month period is obtained. This gradient is shown in Figure 5.197. Again the NBS model is presented for comparison with the tri-monthly average.

Certain patterns, not apparent in the original data, have become noticeable through the use of the least-squares curve fitting method. Some of the important implications are listed below.

In Figures 5.187 and 5.188 it can be seen that the diurnal variation of the in-foliage refractivity at a particular height appears to be between 5 and 10 N units. The in-foliage refractivity gradient does not appear to undergo a significant diurnal variation. Based on data from all in-foliage profiles, the average gradient was -9.0 N units/100 feet, the maximum -13.6 N units/100 feet, and the minimum -6.0 N units/100 feet.

In referring to Figures 5.189, 5.190 and 5.191, it can be seen that the out-of-foliage diurnal gradient variation is significant in some cases and not in others. In the largest diurnal variation shown in these figures, the refractivity gradient changed from -10 N units/1000 feet to about -30 N units/1000 feet. Considering all out-of-foliage profiles, the average gradient was found to be -1.8 N units/100 feet, the minimum -0.3 N units/100 feet and the maximum -5.7 N units/100 feet.

Figures 5.193 through 5.195 show that the variation of the out-of-foliage gradients for a monthly period was about the same as that observed in a diurnal period.

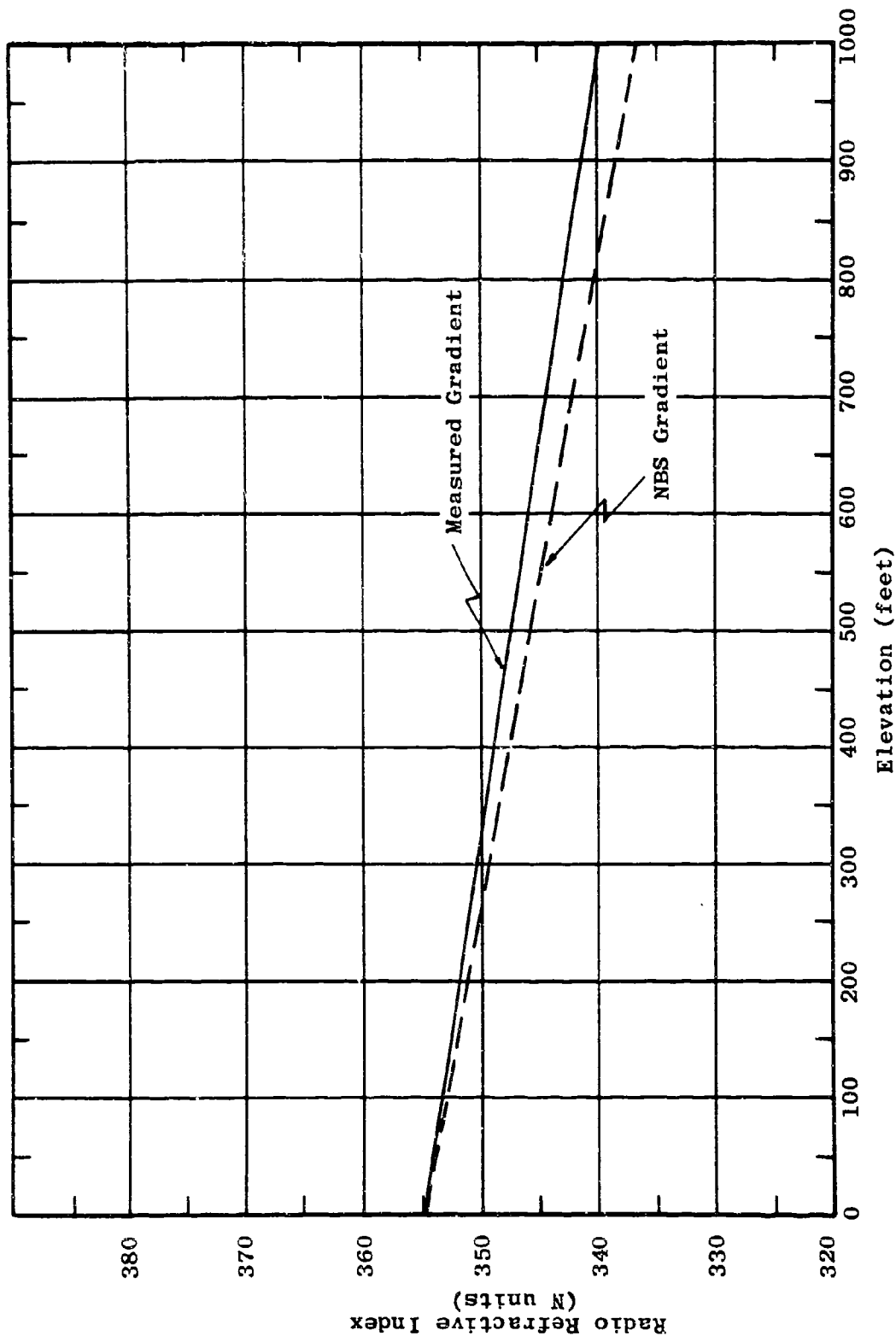


Figure 5.197 Comparison of Tri-Monthly Measured Gradient with NBS Model

However, the bias level of the refractive index varied by as much as 20 N units in some cases.

Figure 5.196 shows that the over-all monthly gradients have strikingly similar slopes for the three-month period shown and that the absolute refractive index levels are less than 10 N units apart for the three cases. These measured monthly gradients are almost identical to the NBS model for an N_s (surface refractivity) value of 355.

Finally, referring to Figure 5.197, the over-all tri-monthly gradient is compared with the NBS model for the same N_s value. Again, excellent agreement is noted.

5.9.3.4 Conclusions of the Refractivity Analysis

As stated previously, there were large fluctuations in N , presumably due to measurement accuracy of wet bulb temperature. Because of this and because of the observed linear trend in the plotted profiles, only a linear curve fitting technique was used.

It should be noted that this does not rule out the possibility of an inversion in the refractive index above the treetops. However, more refined measurements will be needed to definitely establish the existence or non-existence of such an inversion.

It is well known that, when the refractive index decreases with height, radio rays will tend to be bent back toward the earth. Based on a linear variation, Bean²² has shown that when the gradient of the refractive index exceeds

4.8 N units per 100 feet, the curvature of the rays is greater than the curvature of the earth. Therefore, the rays will be trapped if their grazing angles are low. Although practically none of the out-of-foliage gradients were as large as 4.8 N units per 100 feet, all of the observed in-foliage gradients exceeded this value. However, any energy trapped within such a duct in the foliage is highly attenuated.

THIS PAGE INTENTIONALLY BLANK

6. INSTRUMENTATION, EQUIPMENT, AND TECHNIQUES

The contents of this section fall into three main categories. They begin with a listing and description of the major pieces of test equipment. This is followed by a review of the fundamental calibration and measurement procedures that were applied to the propagation tests at Pak Chong and Sattahip. Finally, there is a review of the important field equipment. This section, along with the Test Area Description, Section 4, should give the reader a complete picture and comprehensive understanding of how the propagation data was obtained.

Although most of the material in this section and in Section 4 has been covered more fully in previous semi-annual reports, it is presented again here not only for the purposes of combining and summarizing what has been scattered through a number of volumes, but also to serve the reader in a different and broader way. In the preliminary stages of this program, when many of the existing technical reports on radio propagation were being reviewed, it was noted that practically none of the reports contained even a rudimentary description of the instrumentation and techniques used to obtain the data. The omission of this information often made it difficult to interpret and analyze the data, and occasionally put the validity of the data into question. Thus, it is hoped that the descriptive sections of this report will make the data contained herein more understandable and concrete.

With the exception of the ionospheric path loss measurements, all of the propagation test data came from a conventional, two-terminal type of measurement system. The two terminals were comprised of a calibrated transmitting system and a calibrated receiving system. The transmission system included a signal source, or transmitter, calibrated power measuring equipment, and calibrated transmitting antennas. The receiving terminal included calibrated receiving antennas, a calibrated field strength meter, and associated signal recording equipment. To assure measurement accuracy under field conditions throughout the program, calibrating equipment was reserved strictly for calibrations. The calibrations were conducted on a regularly scheduled basis throughout the field measurement program. The results of the program to date strongly bear out the fact that good calibration equipments and techniques are absolutely essential to a field program of this nature in order to obtain reliable and repeatable data.

6.1 Transmitters

The measurements in the 100 kc/s to 400 Mc/s range have been referred to as the "basic measurement program." During the planning phase of the basic measurement program, a survey was made of military transmitting equipment. The selection criteria included frequency coverage and power output plus the logistical factors of size, weight, power consumption and availability. Modulation characteristics were of secondary importance since the tests primarily used CW transmission, although AM modulation did prove to be useful for identification purposes during the tests. The selected transmitters were installed in air conditioned

S-141-G shelters and shipped from Alexandria, Virginia, to the main base camp at Pak Chong, Thailand. The transmitting equipment is listed in Section 6.1.1.

The propagation tests in the frequency band of 400 Mc/s to 10 Gc/s were planned to be conducted at three different geographic locations. Consequently, the test equipment had to be more portable than that for the basic program. This imposed rather stringent limitations on the equipment size, weight, and power characteristics. The basic approach in selecting this equipment was to get signal sources of relatively low power level and use high-gain antennas to obtain the system gain required for the propagation tests. Commercially available signal sources were used throughout, and a list of this equipment is given in Section 6.1.2.

6.1.1 100 kc/s to 400 Mc/s Test Transmitters

The following table lists the transmitting equipment used in the 100 kc/s to 400 Mc/s measurements.

Table 6.1
BASIC PROGRAM TRANSMITTERS

<u>Quantity</u>	<u>Type</u>	<u>Frequency (Mc/s)</u>	<u>Power (watts)</u>
1	OA-232/GR	0.1 to 2	500
2	T-368/URT	1.5 to 20	500
1	AN/FRC-15	25 to 50	45
1	AN/GRC-75	50 to 100	50 to 120
1	AN/GRC-78	100 to 225	50 to 120
1	AN/GRC-81	225 to 400	50 to 120

6.1.2 400 Mc/s to 10 Gc/s Test Transmitters

The following table lists the signal sources used in the 400 Mc/s to 10 Gc/s measurements.

Table 6.2
10 GC/S PROGRAM TRANSMITTERS

<u>Quan.</u>	<u>Description</u>	<u>Frequency (Gc/s)</u>	<u>Power (watts)</u>
1	Singer Metrics ED1241 UHF Power Oscillator	0.25 to 2.5	5 to 40
1	Polarad Model 1206 Modular Microwave Signal Source	1.95 to 4.2	.050
2	Polarad Model 1207 Modular Microwave Signal Source	3.8 to 8.2	.050
2	Polarad Model 1208 Modular Microwave Signal Source	6.95 to 11	.025
2	American Electronics Lab Model T601 TWT Amplifier	2 to 16	1.0

6.2 Transmitter Calibration

The most important part of the transmitter calibration is the accurate measurement of the output power or, more specifically, the power supplied to the input terminals of the test transmitting antennas. In general, RF ammeters were used to measure at the test frequencies up to 12 Mc/s. Above 12 Mc/s, calibrated power meters, with associated directional couplers, were used. In all cases the power

measurements were made at points in the transmission system where the impedance was known.

The measurement of the transmitter operating frequency was of secondary importance. In general, the operating frequency of the test transmitters was controlled by variable frequency oscillators, and the actual output frequency was monitored with an AN/URM-2 frequency meter. The bandwidth of the transmitting antennas was more than enough to make extreme frequency precision unnecessary in this respect.

Power measuring equipment and methods for the various frequency ranges are described below, as are the measuring equipment calibration procedures periodically used throughout the test period.

6.2.1 RF Power Measurements (0.1 to 25 Mc/s)

In this frequency range, antenna power input was measured with Weston Type 308 RF ammeters having full scale values of 1 to 10 amperes and accuracies of ± 2 per cent. The meters were placed in the antenna circuits at points of measured impedance and were selected so that needle deflections were in the upper half of the current scale.

Within this frequency range, current was measured at the base of the vertical whip antennas. That is, the ammeter was installed in the feed line between the antenna matching network and the base of the vertical antenna. In the case of the horizontal dipoles, the current was measured

by an ammeter located in the output of the balun used to transform the transmission line to the dipole balanced feed.

6.2.2 Power Meters (25 to 400 Mc/s)

Power meters and directional couplers were used to measure antenna input power in this frequency range. Typical equipments are shown below:

Sierra Electronic Corporation

Bi-directional Power Monitor
Model 164 with plug-in heads

<u>Head No.</u>	<u>Freq. Range (Mc/s)</u>	<u>Power Measurement Range (watts)</u>
270-30	2 - 30	50, 100, 500, 1000
181-250	25 - 250	10, 50, 100, 500
181-1000	200 - 1000	10, 50, 100, 500

Accuracy ± 5 per cent full scale.

Microwave Devices, Inc.

Directional Coupler
Model 576N5 with remote indicator
25-1000 Mc/s, 120 watts

Feedthrough Wattmeter
8-1000 Mc/s; 30, 75, 300 watts
Accuracy ± 5 per cent.

During tests, the power level was monitored at the output of the transmitter and at points as close to the transmitting antenna as practical. The selection of either the Sierra bi-directional power monitor or the Microwave

Devices feedthrough wattmeter to measure transmitter power output depended on the operating frequency and the output power level of the test. The Model 576N5 directional coupler was installed in the transmission feed line to the antenna. When vertical dipole antennas were used, the installation point was in the coaxial line close to the lower element. In the case of the horizontal dipoles, the installation point for the directional couplers was in the coaxial line near the input to the balun impedance transformer. Since these points were as high as 80 feet above ground, the directional coupler dc output was returned to a remote indicator located at the base of the supporting mast. Power measured at the directional coupler was corrected to account for measured losses of the baluns and transmission lines between the antenna terminals and the directional coupler, and these corrected values were used as the values of antenna input power in the data reduction computations. The wattmeters at the transmitter were useful as continuous power monitors to detect any possible changes in the transmission line between the transmitter and the directional coupler.

6.2.3 Power Measurements (0.4 to 10 Gc/s)

Essentially the same techniques were used for measuring power in this frequency range as for the range of 25 to 400 Mc/s. However, due to the difference in frequency, different types of equipment were required. Typical equipments used in this frequency range are listed below.

Hewlett-Packard

Power Meter

Model 431B, 10 Mc/s to 10 Gc/s, 10 μ w to 10 mw
Accuracy ± 3 per cent full scale.

Thermistor Mount

Model 478A, 10 Mc/s to 10 Gc/s

Narda Microwave Corporation

Dual Coaxial Directional Coupler

Model 3020, 0.25 to 1 Gc/s

Model 3022, 1 to 4 Gc/s

Model 3004-20, 4 to 10 Gc/s

In addition, various models and values of Weinschel fixed coaxial attenuators along with low pass filters manufactured by Microlab were used as required to obtain power readings within the range of the wattmeter and to eliminate the effects of any spurious outputs generated by the signal sources.

During the calibration of the microwave antennas, the established procedure was to include any necessary transmission line as part of an antenna thus including the losses in those lines in the measured gain of the antennas. For example, practical considerations made it necessary to permanently connect a 6-foot length of coaxial transmission line to the feed of the AEL Model APN-110B antenna, which has a 3-foot parabolic reflector. The calibrated gain of the antenna included the loss in this 6-foot coaxial feed line. Thus, during the tests, antenna power input was measured by connecting the directional coupler to the 6-foot coaxial feed line.

6.2.4 Equipment Calibration

The technique used to maintain measurement accuracy throughout the test program was to establish routine calibration procedures and regular intervals for each piece of test equipment. Basic calibration equipment was obtained and used only as reference standards. Calibrations were then performed using these standards so that all equipment accuracies could be compared to these standards. In general, the calibration procedures were divided into monthly and tri-monthly intervals. Monthly calibrations were performed on equipment exposed to weather and vibration environments, while tri-monthly calibrations were performed on equipment largely kept in a protected environment. When required by equipment repair, additional calibrations were conducted on an unscheduled basis.

The basic instrument against which all test equipment was calibrated, either directly or indirectly, was the Hewlett-Packard 434A calorimetric power meter which has a frequency range of dc to 12.4 Gc/s, and full scale power ranges from 10 mw to 10 watts. The instrument rated accuracy is ± 5 per cent of full scale, with estimated attainable accuracy of ± 1 per cent up to 1 Gc/s and ± 3 per cent from 1 to 10 Gc/s. In addition to the power meter, various Weinschel precision fixed coaxial attenuators were reserved for use only as calibration standards. Calibration data of attenuation versus frequency and VSWR are supplied with the attenuators, and the accuracy of the calibration is within ± 0.1 dB up to 10 dB values and ± 0.2 dB up to 20 dB. As part of the calibration procedures, these standards were cross checked to assure continuing accuracy.

The Weston Type 308 RF ammeter is a thermocouple-type ammeter which is essentially frequency insensitive throughout the range from 60 cps to 25 Mc/s. Therefore, for convenience and practical operation reasons, it was decided to calibrate these meters at 6 Mc/s and at 60 cps. The group of meters having a 3-ampere movement was calibrated at 6 Mc/s using the output of the T-368/URT loaded into a 50-ohm RF load. Comparisons were made against the Sierra 164 bi-directional power monitor which had previously been calibrated against the Hewlett-Packard 434A calorimetric power meter. The output waveform was monitored with an oscilloscope to assure that there was no distortion which could cause errors in the Sierra power meter readings.

The remaining ammeters, having full scale values up to 10 amperes, were calibrated at 60 cps. The meter to be calibrated was placed in series with a parallel combination of the 3-ampere meters. The sums of the currents as measured by the parallel combination were corrected in accordance with the original calibration results at 6 Mc/s and used as the reference values for the meter being calibrated. All meters were calibrated over the current ranges used in the measurement system where they were installed.

Power meters and directional couplers were used for power measurements above 25 Mc/s. Generally, these instruments are frequency sensitive; and, consequently, their operation was restricted to particular frequency bands. Because of this, it was necessary to calibrate these instruments over small frequency ranges around the test frequency at which they were used. The power levels selected for calibration were those covering the range used during testing.

To obtain the required power levels, the test transmitters were used as signal sources during calibration. Directional couplers and fixed coaxial attenuators were used to reduce the calibration power levels to values which could be measured by the Hewlett-Packard 434A calorimetric power meter. Coupling factors of the directional couplers and the fixed coaxial attenuators were calibrated against precision coaxial attenuators which were reserved for this purpose.

Transmission line losses were measured at the frequency and power level normally used during the tests. The method used was to measure transmitter power output when loaded into a 50-ohm RF load with and without the transmission line. This measurement was repeated a number of times and the averages used to calculate the transmission line losses. Since this was a comparative-type measurement, the errors in the power meter did not affect the accuracy of the loss measurements.

6.3 Transmitting Antennas

This section briefly describes the mechanical and electrical characteristics of the transmitting antennas employed in the test program at the Pak Chong field site.

The selection of the types of transmitting antennas to be used for the measurements in the frequency range of 100 kc/s to 400 Mc/s was governed by two main considerations. First, because the field strength measurements had to be made in several different radial directions from the transmitting site, it was necessary to select transmitting antennas which provided a fairly broad beam in

the horizontal plane. The choice was therefore restricted to antennas having relatively low directive gain. The next important consideration involved the selection of antennas having radiation pattern characteristics that could be easily calibrated in the field. Thus, in the frequency range of 100 kc/s to 400 Mc/s, two basic classical antenna configurations were selected; the horizontal and vertical dipole, and the vertical monopole. With these types of antennas, the calculation of theoretical values of field strength at unit distance from the antennas could be confirmed very closely by simple field strength measurements. Table 6.3 lists the various transmitting antennas that were used for each of the test frequencies. The antenna heights for the dipoles in this table are the heights from the ground to the center of the dipole.

The positions of the various transmitting antenna locations, with respect to the foliage, transmitters, and buildings at the test site, are shown in Figure 6.1.

6.3.1 Transmitting Antennas (0.1 to 2.0 Mc/s)

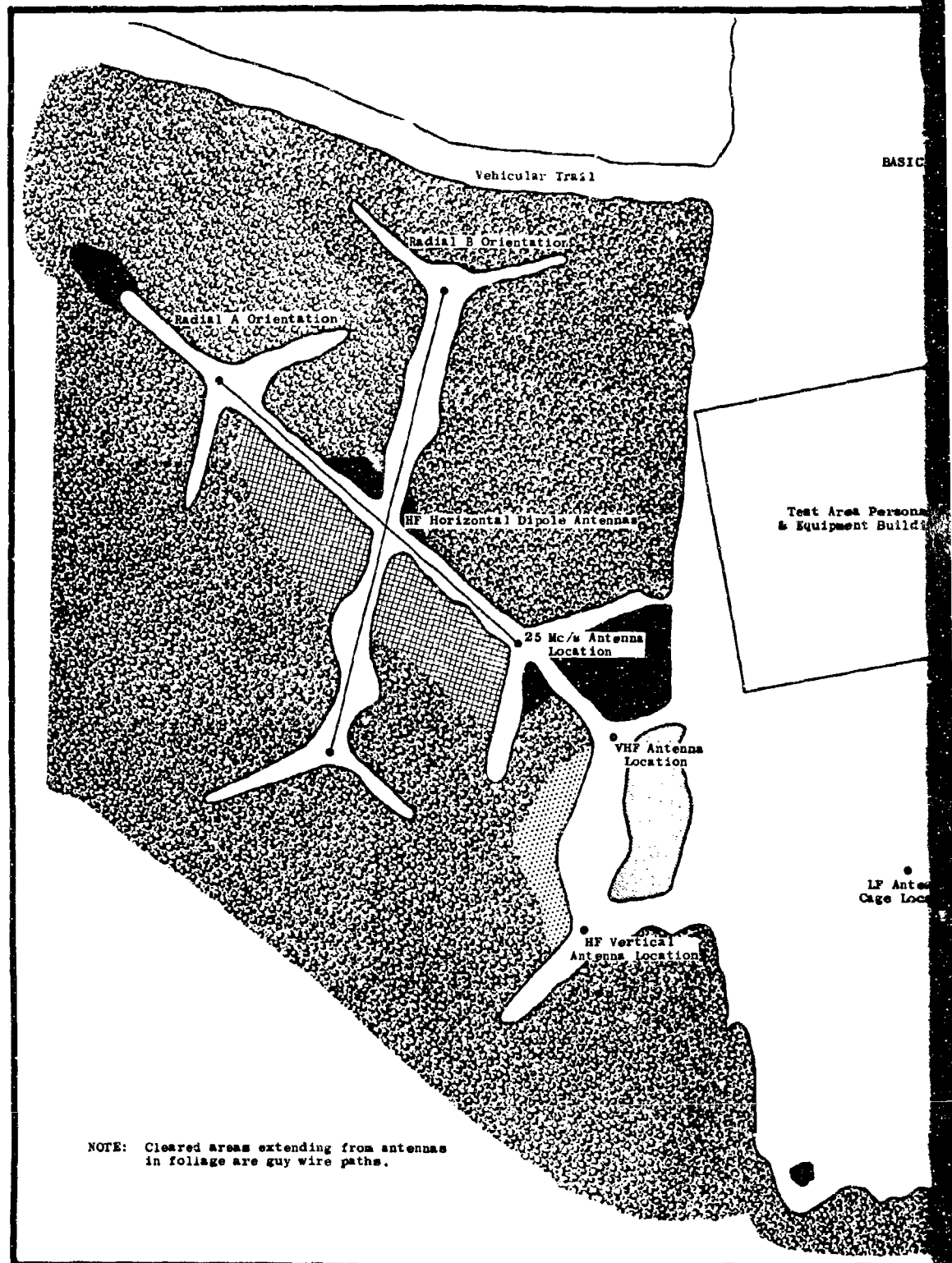
At 0.100 Mc/s, 0.300 Mc/s, and 0.880 Mc/s, the test frequencies within this range, it was impractical to construct a horizontally polarized antenna large enough to provide efficient radiation. Consequently, all of the tests at these particular frequencies were conducted with vertically polarized transmissions. At 2.0 Mc/s and above, all the tests were conducted with both horizontally and vertically polarized transmissions. Table 6.3 lists the antennas used for all the different frequencies.

Table 6.3

TRANSMITTING ANTENNAS FOR BASIC AND 10-GC/S PROGRAMS

<u>Frequency (Mc/s)</u>	<u>Description</u>	<u>Polarization</u>	<u>Transmitting Height</u>
0.10	Top Loaded 80' Tower	Vertical	Ground
0.30	Top Loaded 80' Tower	Vertical	Ground
0.88	Top Loaded 80' Tower	Vertical	Ground
2.	80' Tower	Vertical	Ground
	$\lambda/2$ Dipole	Horizontal	40', 80'
6.	40' Tower	Vertical	Ground
	$\lambda/2$ Dipole	Horizontal	40', 80'
12.	$\lambda/4$ Monopole	Vertical	Ground
	$\lambda/2$ Dipole	Horizontal	40', 80'
25.	$\lambda/4$ Monopole	Vertical	Ground
	$\lambda/2$ Skirt Dipole	Vertical	40', 80'
	$\lambda/2$ Dipole	Horizontal	13', 40', 80'
50.	$\lambda/2$ Skirt Dipole	Vertical	13', 40', 80'
	$\lambda/2$ Dipole	Horizontal	13', 40', 80'
100.	$\lambda/2$ Skirt Dipole	Vertical	13', 40', 80'
	$\lambda/2$ Dipole	Horizontal	13', 40', 80'
250.	$\lambda/2$ Skirt Dipole	Vertical	13', 40', 80'
	$\lambda/2$ Dipole	Horizontal	13', 40', 80'
400.	$\lambda/2$ Skirt Dipole	Vertical	13', 40', 80'
	$\lambda/2$ Dipole	Horizontal	13', 40', 80'
550.	6" x 11" Corner Reflector	Vert. & Hor.	9' - 63'
1,000.	6" x 11" Corner Reflector	Vert. & Hor.	9' - 63'
	3' Dish	Vert. & Hor.	9' - 63'
2,500.	3' Dish	Vert. & Hor.	9' - 63'
	8.25" x 6.19" Horn	Vert. & Hor.	9' - 63'
5,000.	3' Dish	Horizontal	9' - 63'
	18" Dish	Vert. & Hor.	9' - 63'
	8.25" x 6.19" Horn	Horizontal	9' - 63'
	2.25" x 2.25" Horn	Vert. & Hor.	9' - 63'
10,000.	3' Dish	Vert. & Hor.	9' - 63'
	18" Dish	Vert. & Hor.	9' - 63'
	2.5" x 1.5" Horn	Vert. & Hor.	9' - 63'

THIS PAGE INTENTIONALLY BLANK



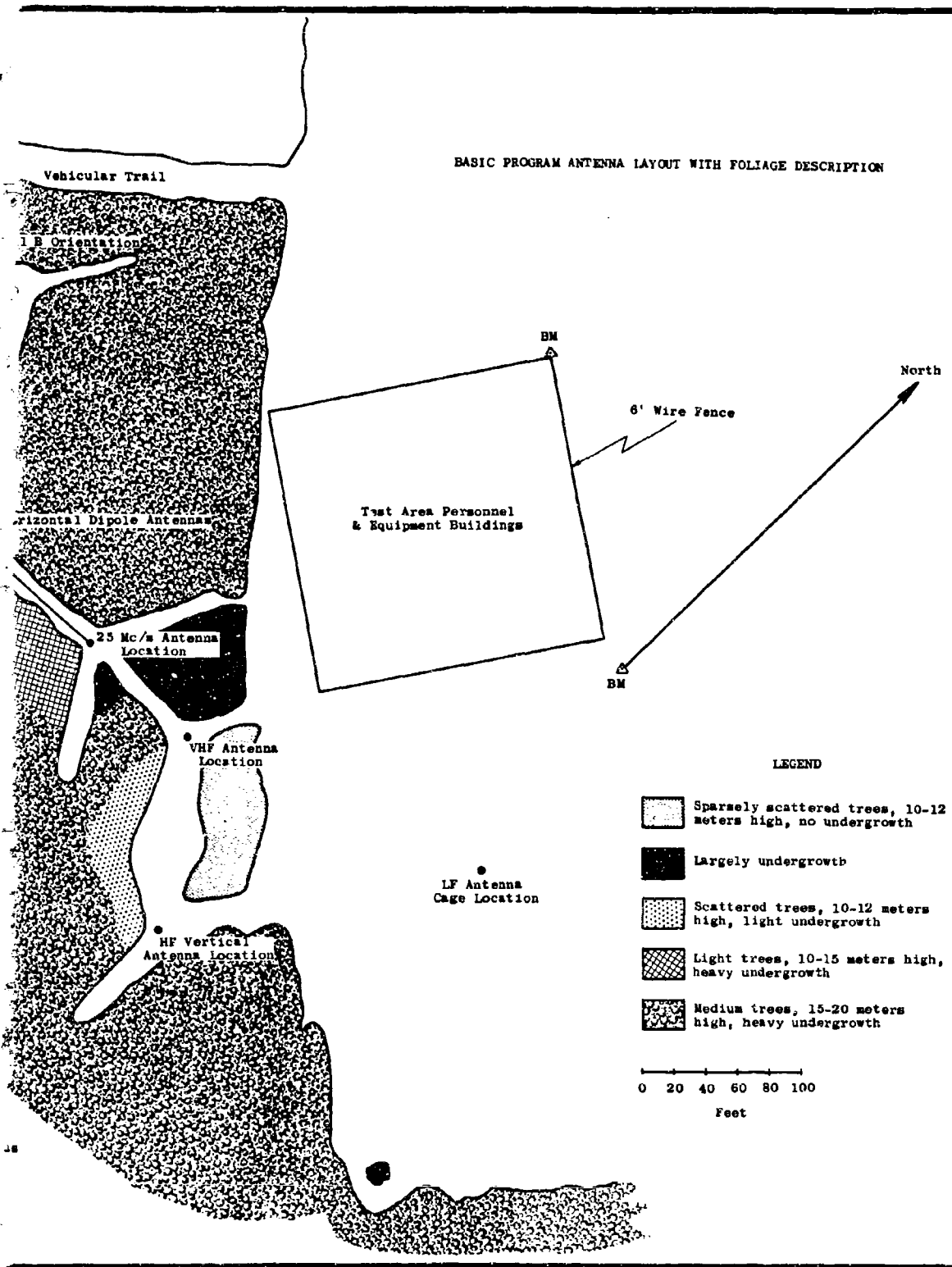


Figure 6.1 Antenna Locations for
0.100-400 Mc/s Measurements

The transmitting antenna used below 2.0 Mc/s was a short monopole with top loading, a drawing of which is shown in Figure 6.2. Its mast, described in Section 6.6.1, was 80 feet high and had a mean diameter of 3 inches. It was of stepped, tapered construction and was insulated from the ground by a Premax insulator. The top loading consisted of four 80-foot-long wire cage assemblies. Each cage assembly consisted of four copper wires fastened to copper loops 17 inches in diameter. These assemblies were electrically connected to the top of the monopole and were supported in a downward slanting direction by insulated guys connected to earth anchors. This type of top loading is often referred to as an "umbrella." The electrical effects of having the top loading directed downward from the mast instead of horizontally were checked and found to be negligible.

At each test frequency in this band, the antenna's impedance was matched to the characteristic impedance of the transmission line by means of an L or an LC matching network, shown in Figures 6.3(a) and 6.3(b). The power radiated by the antenna was monitored by placing an RF ammeter at the base of the antenna to measure the line current.

The ground system consisted of twelve 100-foot-long radials emanating from the antenna base at 30-degree intervals. At the extreme ends of six of the radial wires, five additional 50-foot-long wires radiated out at 60-degree intervals. Figure 6.4 is a layout of the ground system. All ground wires were mechanically joined and soldered where they intersected.

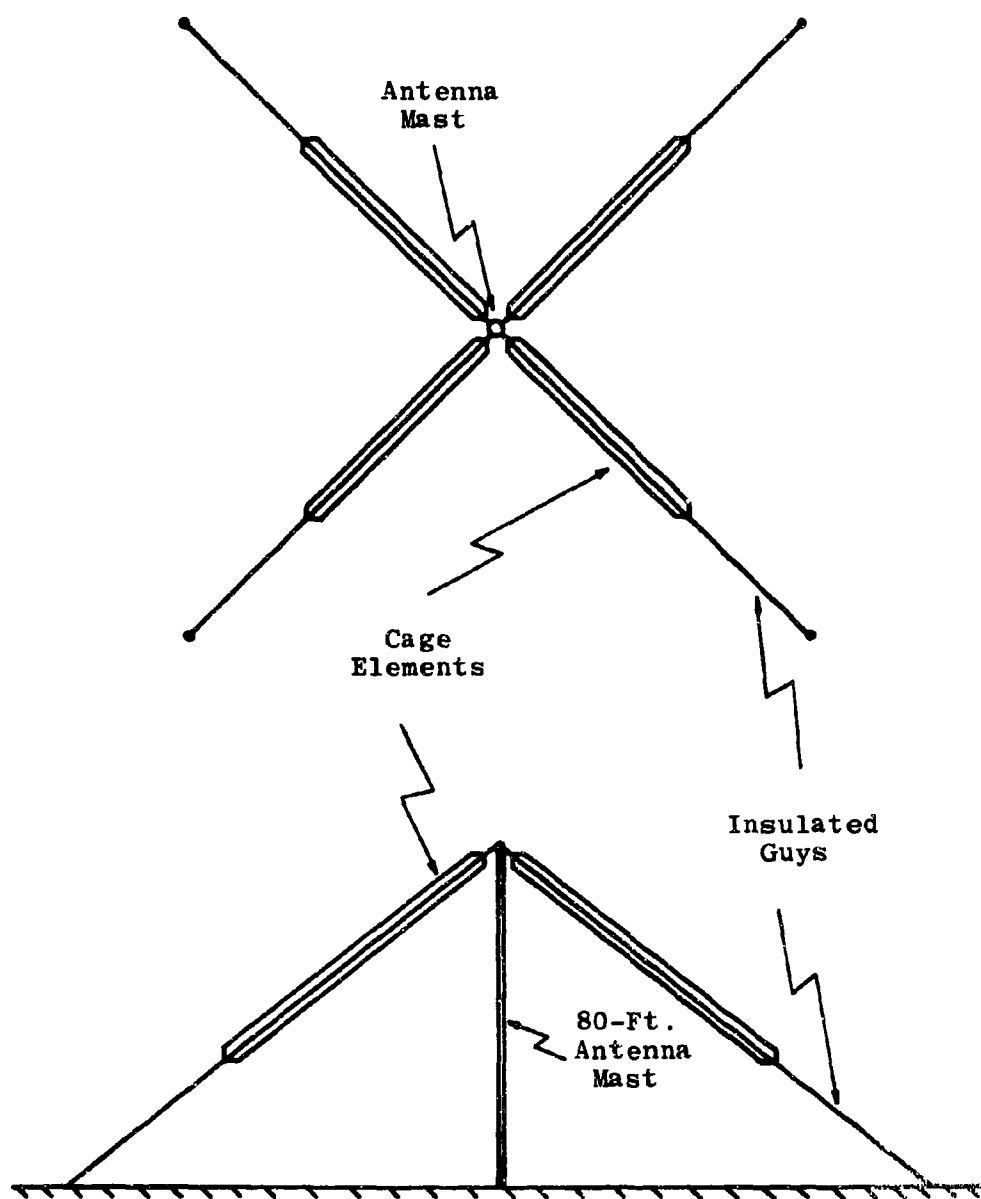


Figure 6.2 Cage Antenna (0.1 to 2.0 Mc/s)

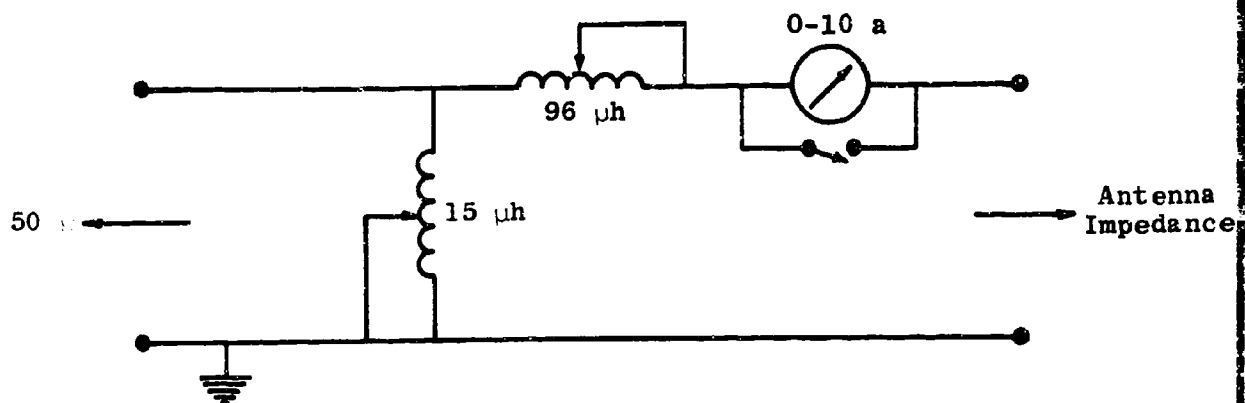


Figure 6.3(a) 0.880 Mc/s Matching Network

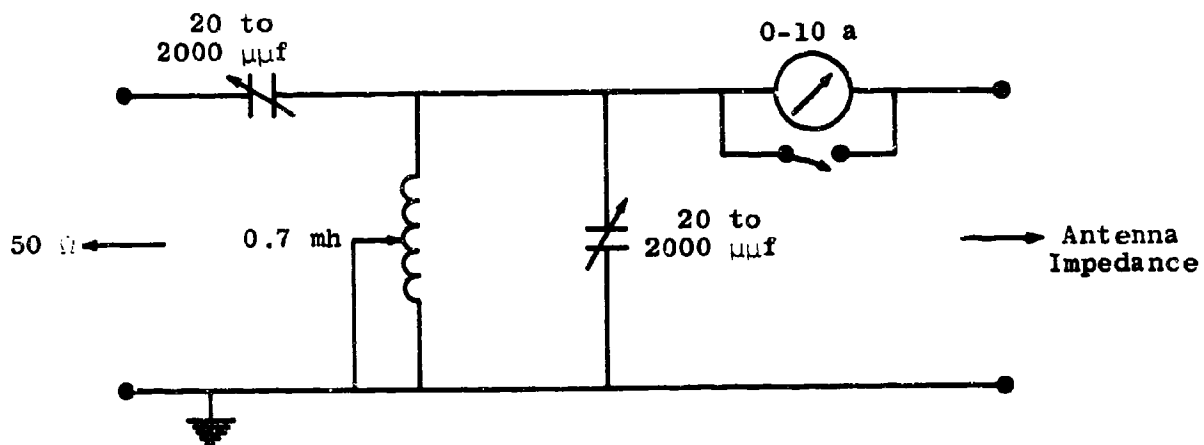


Figure 6.3(b) 0.100 and 0.300 Mc/s Matching Network

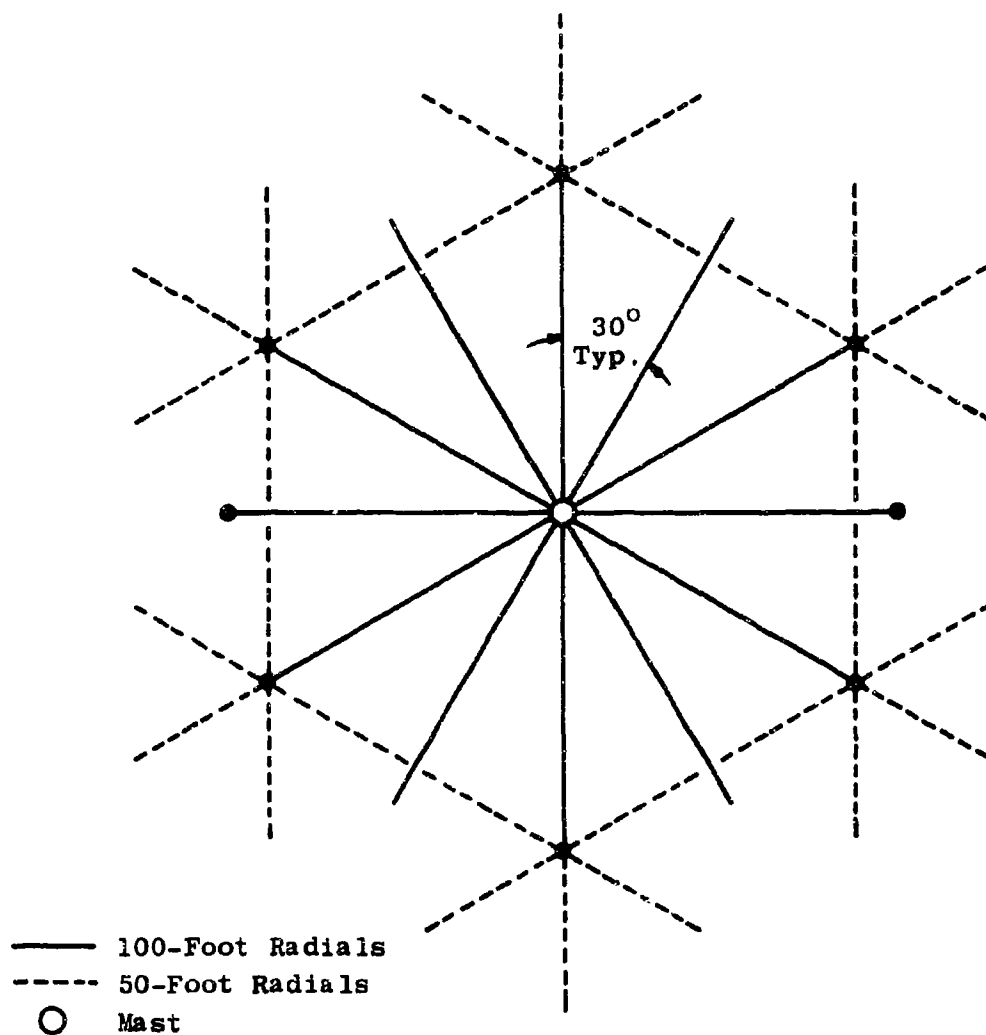


Figure 6.4 Cage Antenna Ground Radial Layout

6.3.2 Transmitting Antennas (2.0 - 12.0 Mc/s)

In this range the test frequencies included 2.0, 6.0, and 12.0 Mc/s, with both horizontal and vertical polarizations.

The vertically polarized 2.0 Mc/s antenna was a vertical monopole consisting of the same 80-foot mast that was employed as the vertical radiator in the 0.1 Mc/s to 2.0 Mc/s frequency band. At this frequency, however, the top loading elements were removed and nylon rope guys substituted.

The vertical antenna for the 6.0 Mc/s tests was a quarter-wavelength monopole. This monopole mast consisted of only the top seven sections of the 2.0 Mc/s monopole. It rested on a standard Premax insulator and was 39 feet 3 inches high.

The 12.0 Mc/s antenna was also a quarter-wavelength monopole, consisting of a standard commercial Premax telescoping monopole adjusted to resonant length. It mounted on a Premax insulator base and had a section connector which permitted height adjustments. This antenna is pictured in Figure 6.5.

At 2.0 Mc/s and 6.0 Mc/s, the monopole antenna impedance was matched to the transmission line by means of a modified BC-939 antenna matching unit, a schematic of which is shown in Figure 6.6. At 12.0 Mc/s, the antenna impedance was close enough to the transmission line impedance to eliminate the need for additional matching networks. An RF ammeter at the base of the antenna monitored the output power of the monopole by measuring the line current.

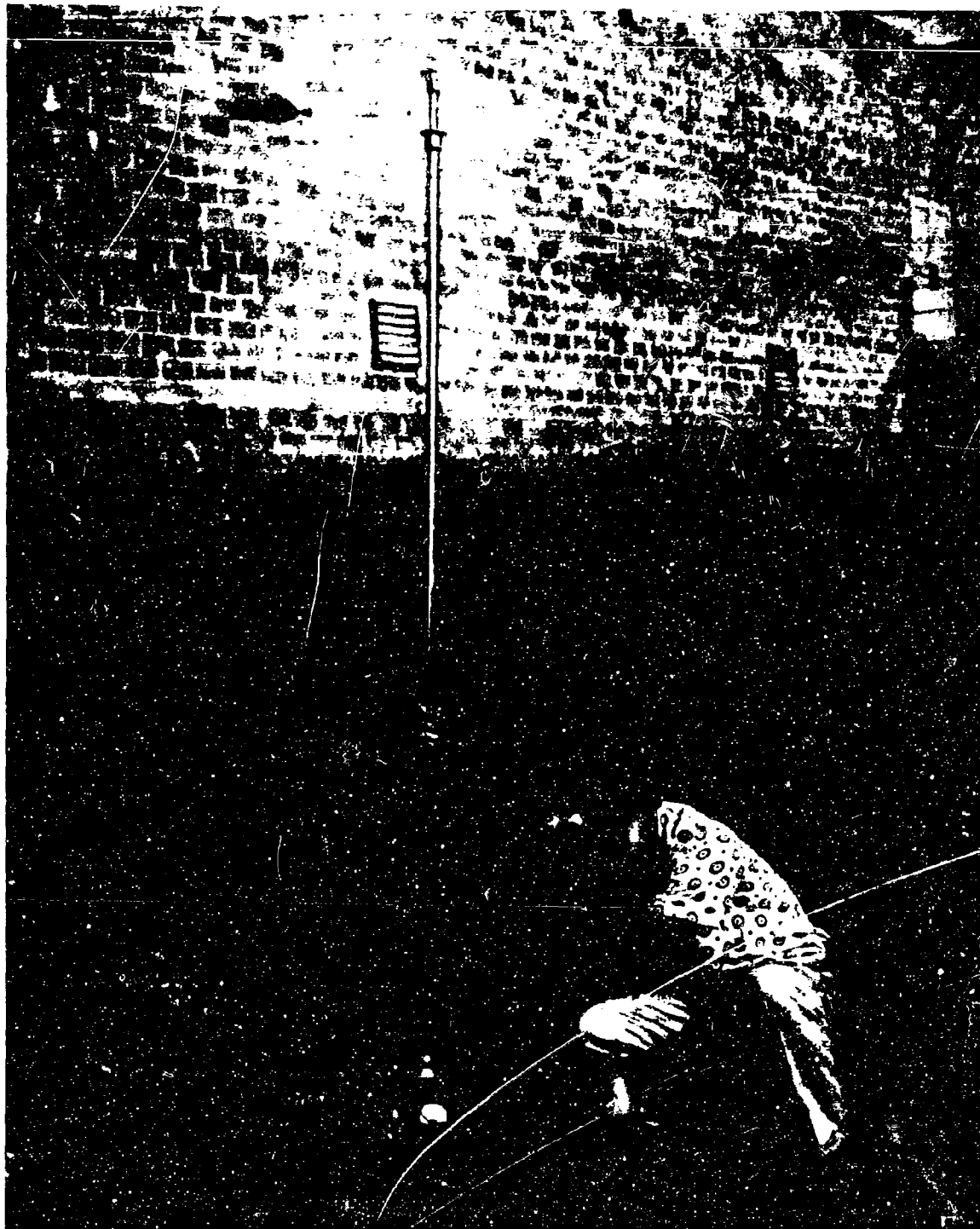


Figure 6.5 Whip Antenna for 12-Mc/s Operation

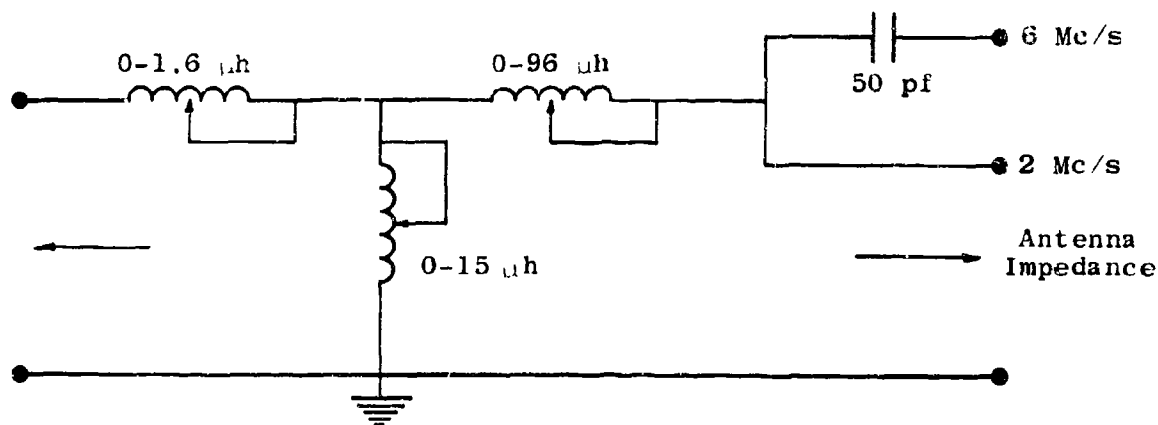


Figure 6.6 Modified BC-939 Antenna Matching Unit for 2 and 6-Mc/s Monopoles

The ground system for all three antennas consisted of 60 radial wires each 100 feet long and spaced 6 degrees apart. All radials were mechanically bonded and soldered to the base of the antennas. This ground plane layout is shown in Figure 6.7.

Resonant half-wavelength dipole antennas were used for all horizontally polarized transmissions between 2.0 and 12.0 Mc/s. These dipoles were constructed so that the different antenna sizes and heights required could be obtained without changing the position or location of the support towers. To permit efficient radiation at the different frequencies from this one structure, the 12.0 Mc/s or shortest dipole, after it was adjusted to resonant length had insulators fastened to its ends. To the other sides of these insulators were attached wire extensions of a length that would make the dipole resonant at 6.0 Mc/s. This same process was repeated to obtain a 2.0 Mc/s resonant length. By bridging one or both sets of insulators, the antenna would

30856

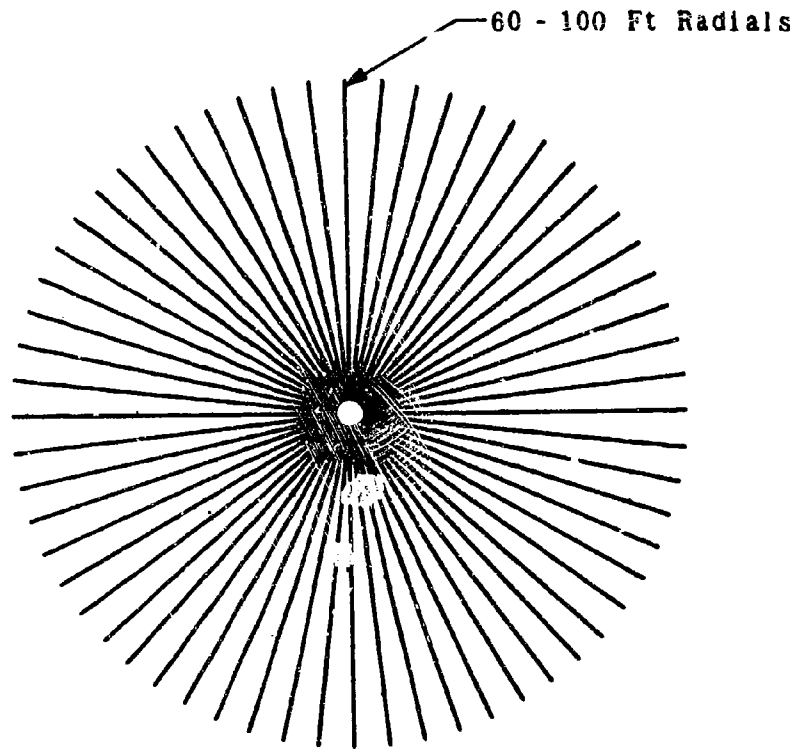


Figure 6.7 Ground Plane for 2, 6, 12, and 25-Mc/s Monopoles

be resonant at 6.0 or 2.0 Mc/s, respectively. A sketch of the final arrangement is shown in Figure 6.8. The supporting towers were two of the special 80-foot aluminum masts referred to previously. The height of the dipole was adjusted by means of two pulleys mounted on each mast, one at the 80-foot level and the other at the 40-foot level. The matching networks and balun were mounted at ground level to allow feed system changes and to prevent strain on the radiating elements.

The dipoles were fed by a length of 70-ohm twin lead from a balun transformer, which in turn was connected to a modified BC-939 antenna matching unit through a length of RG9/U coaxial cable. A schematic of the feed system is shown in Figure 6.9. A separate balun transformer was constructed for each frequency of operation. The transformer consisted of a primary and center-tapped secondary, each of No. 10 enamel wire wound on a $2\frac{1}{2}$ -inch diameter porcelain coil form. The primary was separated from the secondary by a thin sheet of mylar and an electrostatic shield. The capacitor in the primary circuit was used to tune out the inductive reactance of the transformer.

An RF ammeter measured the antenna current. As shown in Figure 6.9 this meter was used in conjunction with Sierra bi-directional power meter to monitor the antenna input power.

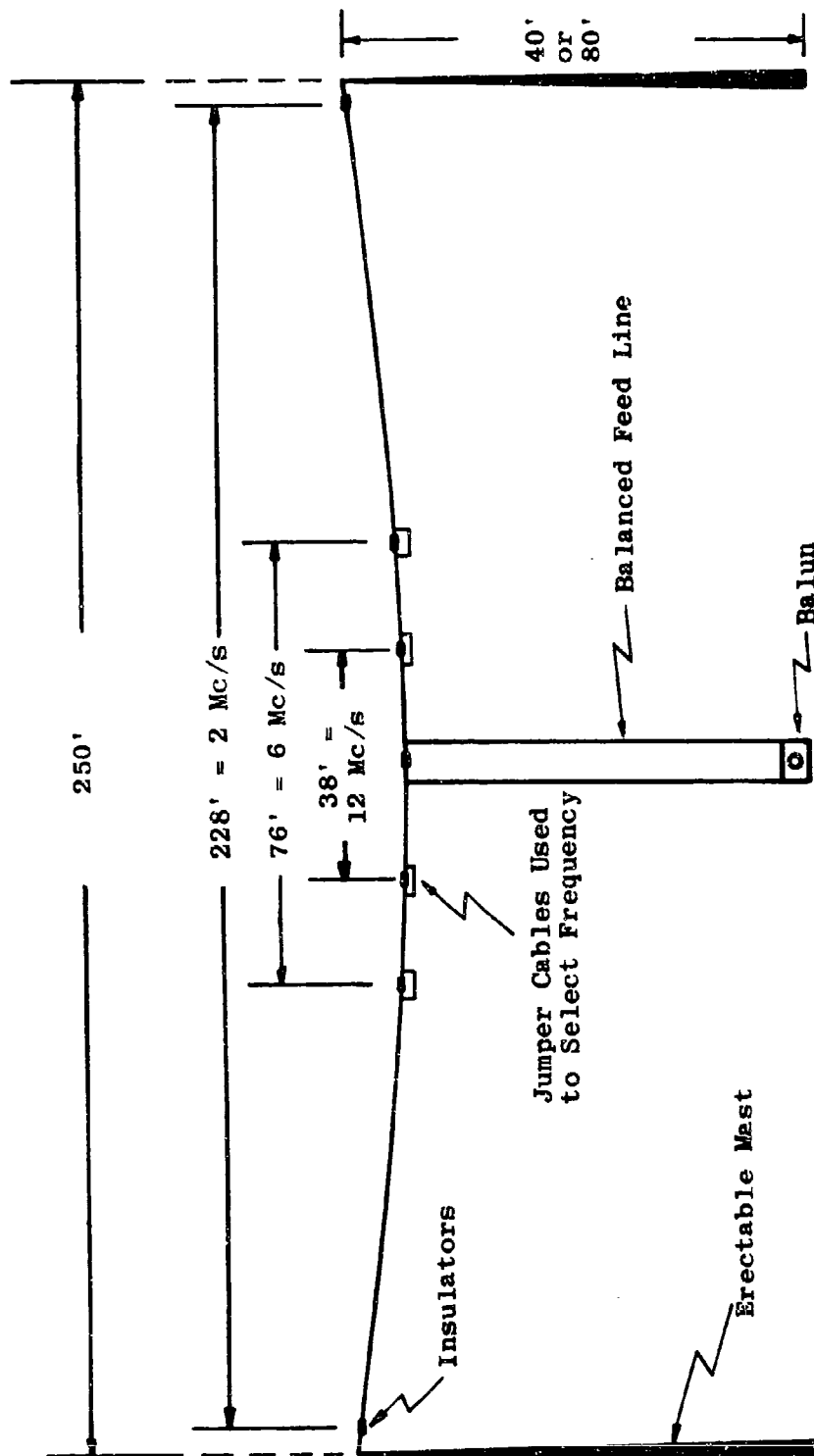


Figure 6.8 Horizontal Dipole Antenna for 2, 6, and 12 Mc/s

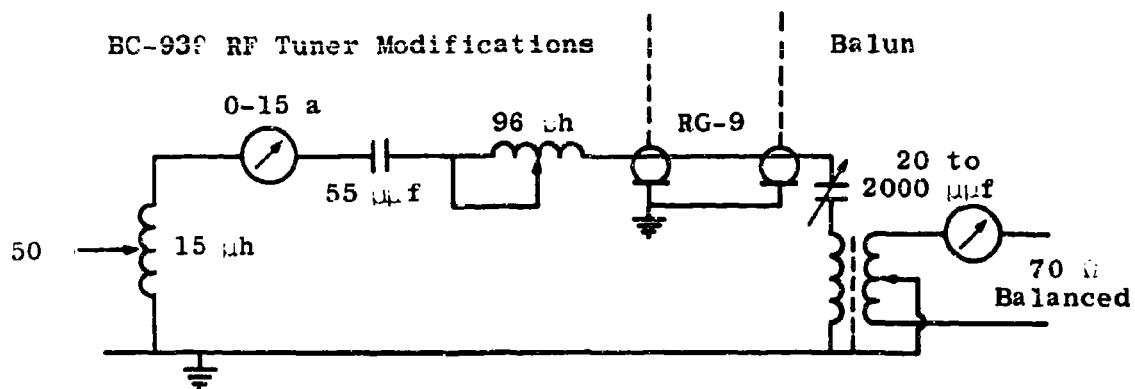


Figure 6.9 2, 6, and 12-Mc/s Tuner and Balun

6.3.3 Transmitting Antennas (12 to 400 Mc/s)

In this frequency band the test frequencies included vertical and horizontal polarizations at 25, 50, 100, 250, and 400 Mc/s.

For vertically polarized transmissions at 25 Mc/s a quarter-wavelength monopole and a half-wavelength skirt dipole were used. The 25-Mc/s monopole radiating element was obtained by adjusting the 12-Mc/s telescoping monopole for quarterwave resonance.

The skirt dipole used for the vertically polarized transmissions in this frequency range was specially constructed for these tests. It consisted of two aluminum tube sections each approximately 10 feet long. The dipole was insulated from the aluminum supporting mast by a Fiberglas tube on which the lower dipole element was mounted. A block of dielectric material was used to provide mechanical support at the feed point. This antenna is pictured in Figure 6.10.

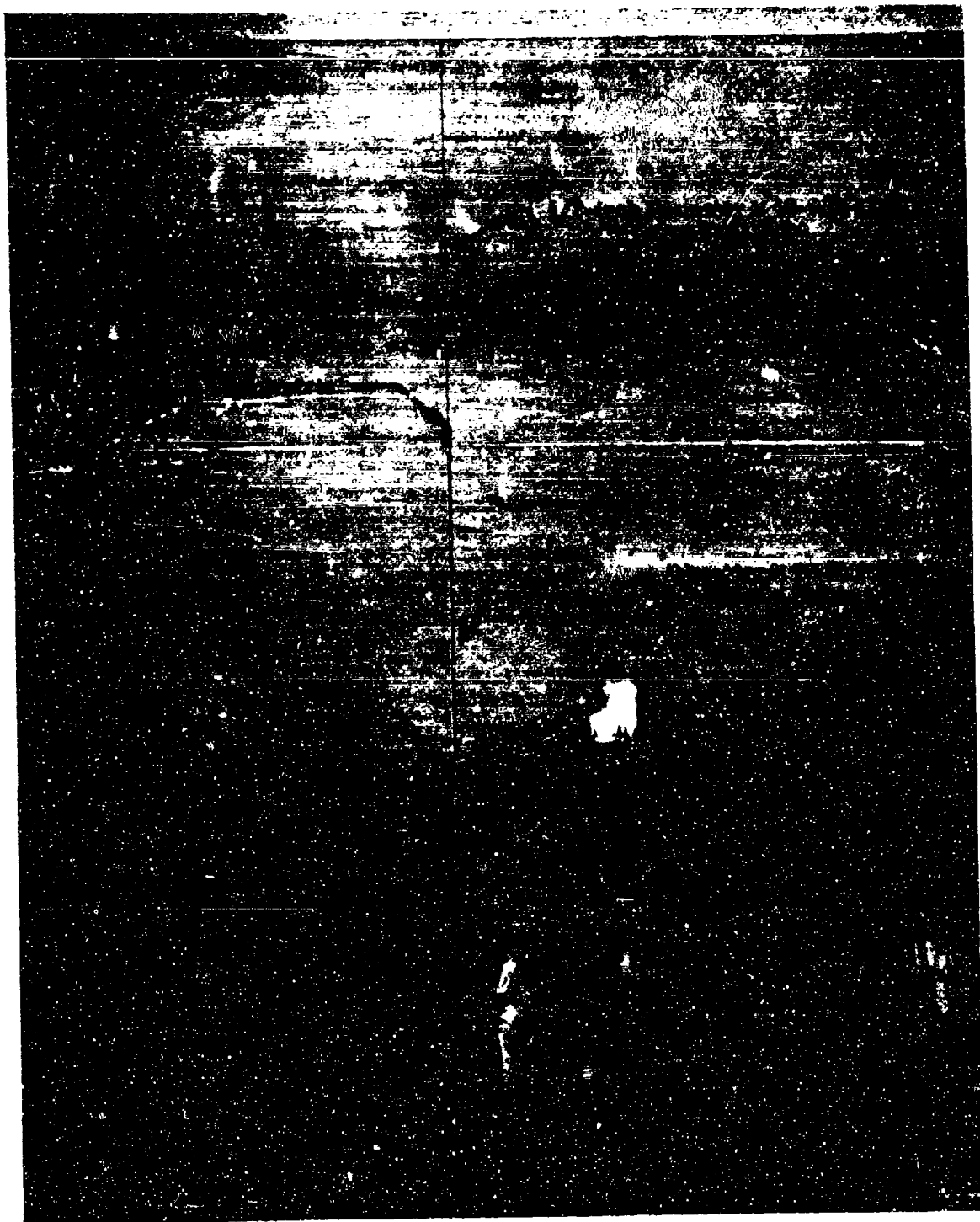


Figure 6.10 25-Mc/s Vertical Dipole Transmitting Antenna

For the tests at 50, 100, 250 and 400 Mc/s, a similar type of skirt dipole configuration was used. These antennas are pictured in Figures 6.11 and 6.12.

The input impedance of the 25-Mc/s quarter-wavelength monopole was close enough to the transmission line impedance that matching networks were not needed in this instance. The 25-Mc/s skirt dipole antenna, however, was matched with a balun transformer of the same type as those used in the 2 to 12-Mc/s frequency range. All of the other skirt dipoles described above were fed unbalanced. The coaxial feed line for these antennas passed up through the insides of the tube sections of the support and insulating towers and the lower antenna element. At the dipole feed point, the shield of the feed cable was connected to the bottom half of the element, and the inner conductor of the feed cable was connected to the top half. In this configuration, the skirt acted as a balun transformer, and the coaxial feed line was stub-matched to the transmission line.

Of the vertically polarized antennas in this frequency range, only the 25-Mc/s monopole required a ground plane, and it used the same one provided for vertically polarized transmissions in the 2 to 12-Mc/s frequency range.

All of the horizontally polarized antennas in between 12 Mc/s and 400 Mc/s were balance-fed, half-wavelength resonant dipoles. The 25-Mc/s dipole, fabricated at the Principal Laboratories, uses 3/4-inch diameter thin-walled aluminum tubing for half elements. A phenolic insulating block supports the two half elements and provides a convenient feed point. The phenolic insulator is bolted to a

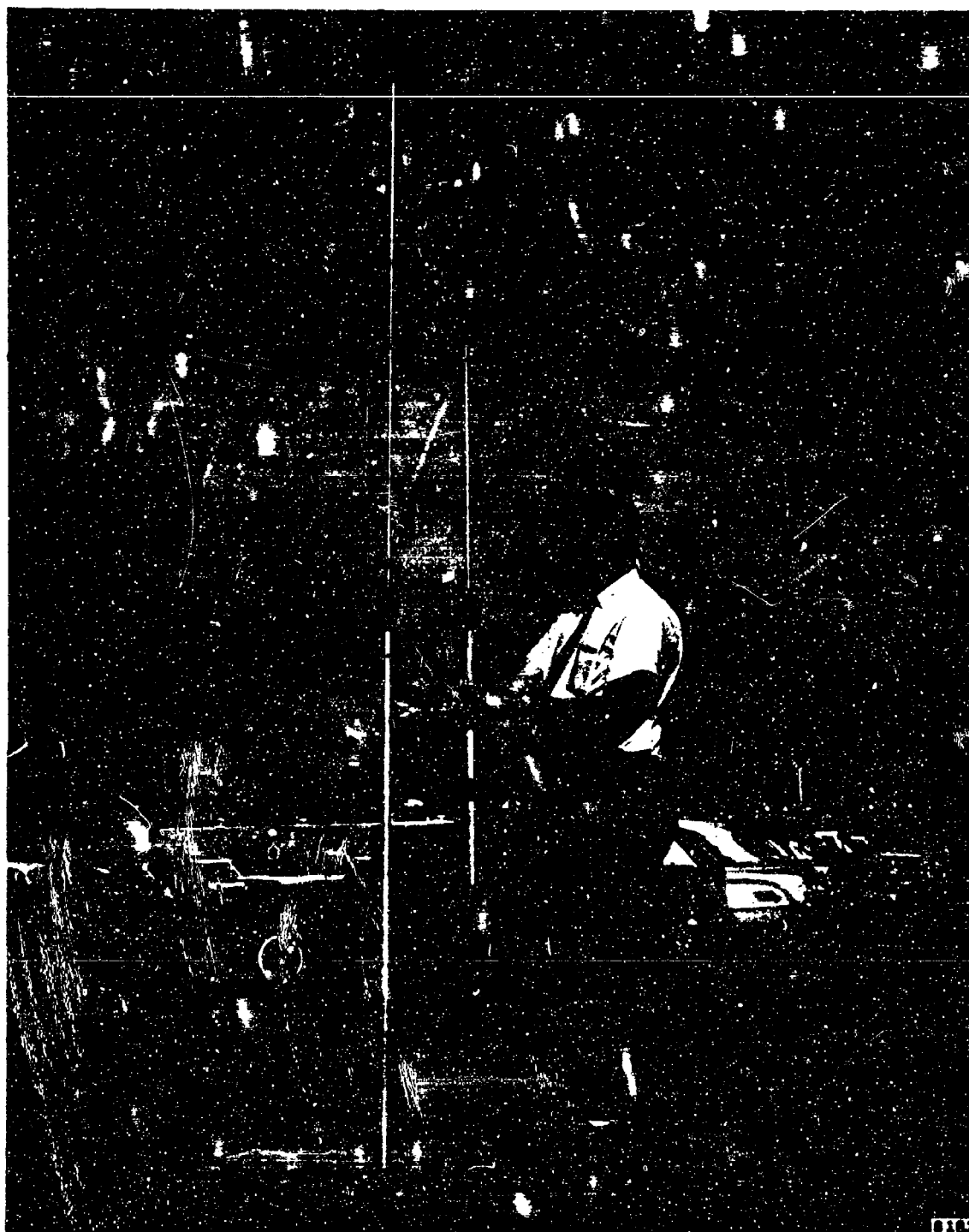


Figure 6.11 Vertical Dipole Antenna 50 to 100-Mc/s Range



Figure 6.12 Vertical Dipole Antenna 225 to 400-Mc/s Range

short Fiberglas rod that mounts on the aluminum support tower. This antenna is shown in Figure 6.13.

At 50 Mc/s and 100 Mc/s a single antenna was used. It is the driven element of a three-element beam used in conjunction with the TRC-24 transmitting system. The nomenclature for the antenna set is: "A" band AS-756/GRC. This antenna, which is shown in Figure 6.14, has half elements, which are adjustable for resonance at the desired frequency.

The 250-Mc/s and 400-Mc/s tests also used one antenna. Like the 50 and 100-Mc/s antenna, it is one of an array of dipoles for the TRC-24 transmitting system. This antenna is used in conjunction with a reflector. The nomenclature for the dipole is: Signal Corps U. S. Army antenna dipole AT-413/TRC, Philco Corporation. The antenna half elements can be adjusted for resonance at the desired frequency. The antenna is shown in Figure 6.15.

The balun feed for the 25-Mc/s dipole was specially constructed at the Principal Laboratories and is of the same type as those employed on the horizontal dipoles in the 2 to 12-Mc/s frequency range. The two TRC-24 system dipoles were supplied with their own baluns. All that was required was the stub matching of the baluns' input impedances to that of the transmission line. This stub matching was performed at each frequency above 25 Mc/s.

The radiated power of all the horizontal and vertical antennas in the 12 to 400-Mc/s range was monitored by means of the Model 164 Sierra bi-directional power meter.



Figure 6.13 25-Mc/s Horizontal Dipole Transmitting Antenna

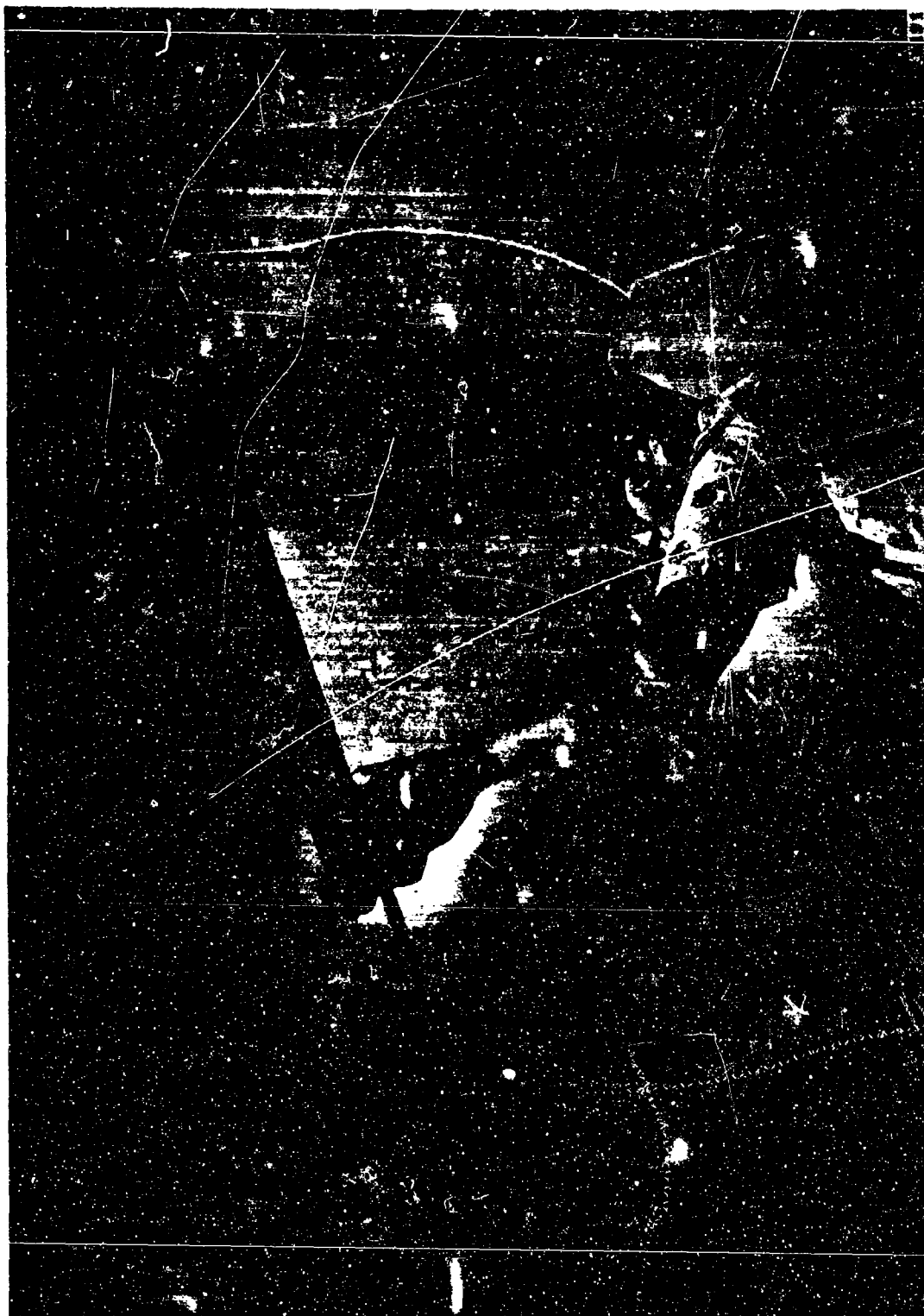


Figure 6.14 Adjustable Horizontal Dipole Antenna 50 to 100-Mc/s Range

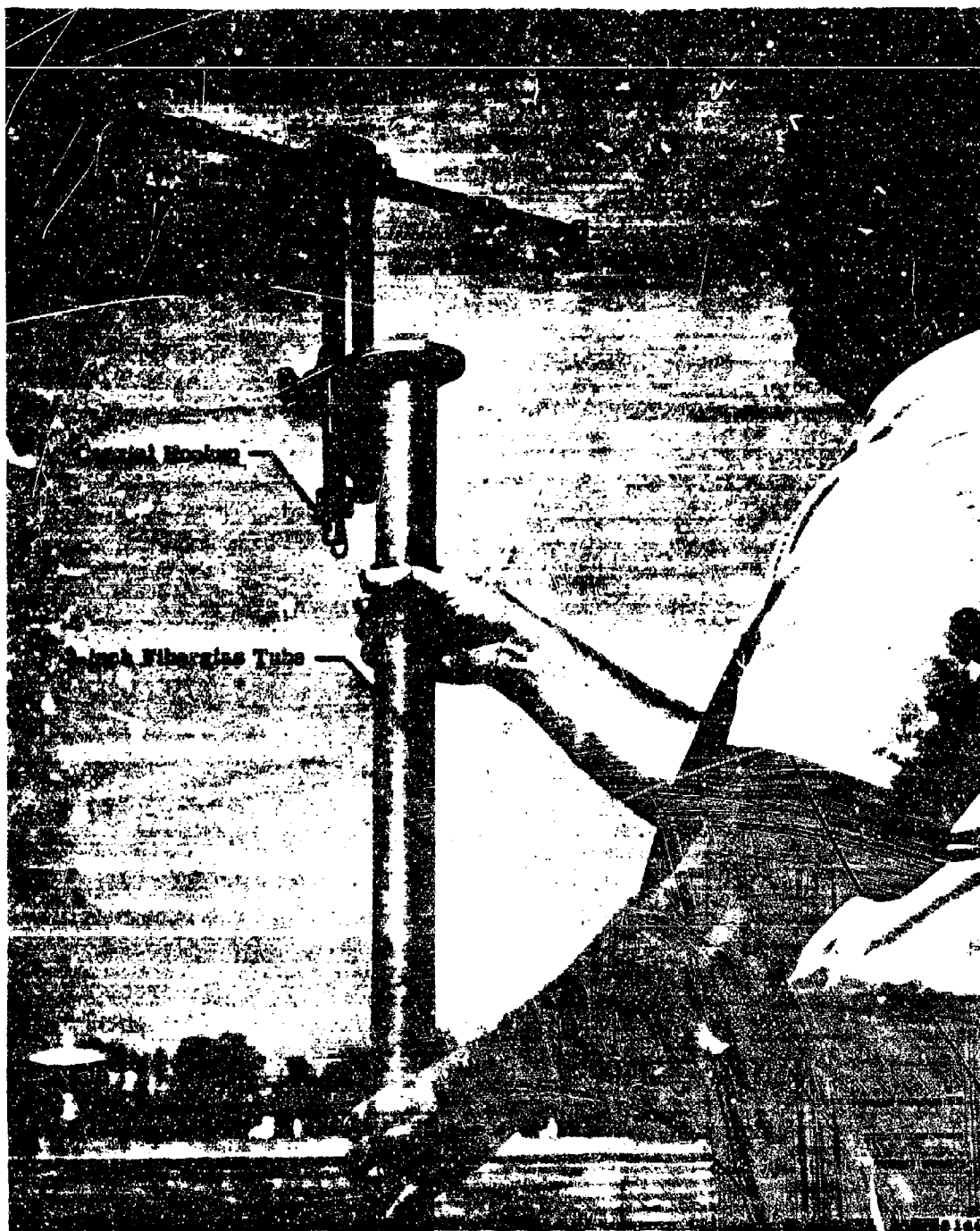


Figure 6.15 Military Antenna 225 to 400-Mc/s Range

6.3.4 Transmitting and Receiving Antennas (0.4 to 10 Gc/s)

Within this frequency range, transmission tests were conducted at 0.55, 1.0, 2.5, 5.0, and 10.0 Gc/s. For a given test at these frequencies, the same antenna was generally used for horizontal and vertical polarizations. Also, because the antennas had a large bandwidth, they were often used at more than one test frequency. For some of the tests, identical antennas were employed at both transmitting and receiving points; in other tests, dissimilar antennas were used. The actual antenna associated with each test is specified in the test descriptions of Section 5.9. Table 6.4 lists these antennas with the manufacturer's name and specifications. The modifications to these antennas during the measurements involved only their mountings, not the electrical specifications.

In the tests which were conducted with these antennas, the most important antenna characteristics were the E-plane and H-plane beamwidths. These characteristics, along with the antenna input VSWR, are listed in Table 6.5. The power transmitted by each antenna configuration was monitored with a Narda directional coupler and a Hewlett-Packard power meter, Model 431B.

Table 6.4
10 GC/S PROGRAM ANTENNA SPECIFICATIONS

Type	Manufacturer	Model	Frequency (Gc/s)	Dimensions
Corner Reflector w/Discone Feed	Technical Appliance Corporation (TACO)	AS-544/U	0.45 - 1.2	6" x 11" x 3.5"
Horn	American Electronic Laboratories, Inc.	H5101	2.0 - 5.0	8 $\frac{1}{4}$ " x 6 $\frac{3}{16}$ " x 8 $\frac{7}{8}$ "
Horn	Polarad Electronics Corporation	CA-M	4.19 - 7.74	2 $\frac{1}{4}$ " x 2 $\frac{1}{2}$ " x 2 $\frac{7}{16}$ "
Horn	Polarad Electronics Corporation	CA-X	7.36 - 10.0	2 $\frac{1}{2}$ " x 1 $\frac{1}{2}$ " x 3 $\frac{3}{8}$ "
Parabolic Reflector	American Electronic Laboratories, Inc.	APN110B	1.0 - 11.0	3' Effective Diameter
Parabolic Reflector	Polarad Electronics Corporation	CA-R	4.19 - 21.0	18" Effective Diameter

Table 6.5

ANTENNA CHARACTERISTICS, 10-GC/S PROGRAM

Manufacturer	Model	Frequency (Gc/s)	VSWR	Beamwidths	
				E Plane	H Plane
American Electronic Laboratories, Inc.	H5101	2.5	1.4:1	38°	37°
		5.0	1.4:1	20°	20°
Polarad Electronics Corporation	CA-M	5.0	3:1	45°	45°
Polarad Electronics Corporation	CA-X	10.0	3:1	40°	40°
American Electronic Laboratories, Inc.	APN110B	2.5	2.5:1	10°	10°
		5.0	2.5:1	5°	5°
		10.0	2.5:1	2°	2°
Polarad Electronics Corporation	18" Para. Ref. with CA-M Feed	5.0	3:1	10°	8°
	18" Para. Ref. with CA-X Feed	10.0	3:1	5°	5°

6.4 Transmitting Antenna Calibration

The propagation path loss measurements performed in Thailand during this program have been presented and analyzed in Section 5, Data Analysis. Among the various ways of expressing propagation loss, it appeared desirable for this program to consistently use the concept of basic transmission loss as defined by Norton.⁵ Here, transmission loss is defined as the ratio of the power radiated from a transmitting antenna to the power available from the receiving antenna. It normally is expressed in decibels. For several reasons it is also convenient to express measured and theoretical results in terms of the basic transmission loss; that is, the loss expected, if isotropic transmitting and receiving antennas are used.

However, the data obtained directly from the measurement systems was generally in terms of electromagnetic field strength, and in units such as volts per meter. This section therefore describes the equations employed in calculating path loss from the measured data in the basic program, (0.1 Mc/s to 400 Mc/s), and in the 10-Gc/s program, (0.4 Gc/s to 10 Gc/s). It also explains the antenna calibration techniques used to obtain the reference parameters required in the equations for reduction to units of basic transmission loss.

6.4.1 Transmission Path Loss and Antenna Calibration Equations (0.1 to 400 Mc/s)

The transmission loss, L , is defined as the ratio, expressed in decibels, of the power, p_r , radiated from a

transmitting antenna to the power, p_a , available from the receiving antenna.

$$L = 10 \log_{10} (p_r/p_a) \quad (1)$$

Since it is desirable to express the results of propagation measurements and theoretical calculations in terms of the "basic transmission loss," it is necessary to account for the path antenna gain inherently involved in the measurement system. This is done by adding the path antenna gain, G_p , to the measured loss, L , to obtain basic transmission loss, L_b . That is,

$$L_b = L + G_p \quad (2)$$

Note that equation 2 is true from the practical point of view only when the maximum antenna directivity gain is achieved. When G_p is not known by calibration, an estimate of L_b may be made for short paths by assuming that the free-space gains of the transmitting and receiving antennas are realized; that is,

$$G_p = G_t + G_r \quad (3)$$

Since the data measured at the receiving antennas is indicated in field strength rather than power, the transmission path loss equation was modified to give path loss as the ratio of the received and transmitted field strengths.

This meant that a reference value of the field strength of the transmitting antenna had to be determined. Under free-space conditions, the following equation gives the field strength at a distance, d , of a transmitting antenna when it is radiating a power, p_r .

$$p_r = \frac{4\pi(1609 d)^2 (E_o \times 10^{-6})^2}{G_t \eta_o} \quad (4)$$

where

- E_o = free-space field in $\mu\text{V/m}$
- η_o = impedance of free space in ohms
- G_t = gain of the antenna above an isotrope
- d = distance from the antenna in miles

The power available from a receiving antenna in free space is given by

$$p_a = \frac{E^2 \lambda^2 G_r \times 10^{-12}}{4\pi \eta_o} \quad (5)$$

where

- G_r = gain of the antenna above an isotrope
- E = field strength at the receiver in $\mu\text{V/m}$
- λ = free-space wavelength in meters

The expression for the transmission loss, L , is then obtained by substituting equations 4 and 5 into equation 1.

$$L = 36.57 + 20 \log f_{\text{Mc/s}} + 20 \log d_{\text{mi}} + 20 \log E_o - 20 \log E_{\text{meas}} - G_t - G_r \text{ (dB)} \quad (6)$$

where

E_o = transmitted free-space field strength in $\mu\text{v/m}$

Substituting equations 3 and 6 into equation 2 yields the expression for the basic transmission loss, L_b .

$$L_b = 36.57 + 20 \log f_{\text{Mc/s}} + 20 \log d_{\text{mi}} + 20 \log E_o - 20 \log E_{\text{meas}} \text{ (dB)} \quad (7)$$

In order to simplify data reduction, it is convenient to choose a value of E_o which corresponds to the free-space field at 1 mile. In this case, the term $20 \log d_{\text{mi}}$ is zero, and equation 7 becomes

$$L_b = 36.57 + 20 \log f_{\text{Mc/s}} + 20 \log E_{o_1} - 20 \log E_{\text{meas}} \text{ (dB)} \quad (8)$$

Equation 8 has been used to convert measured values of field strength to values of basic transmission loss.

In deriving the expression to obtain basic transmission loss from measured data, the use of a free-space field at 1 mile, E_{o1} , was introduced. The inclusion of this term in the expression for L_b requires calibrating the transmitting antennas employed in the measurements in terms of this reference field strength. This calibration can be accomplished by using what is known as the standard-field field method.

In this method of calibration, the field strength, E , is measured at a finite distance from the transmitting antenna. Next, a signal generator and its antenna are substituted for the transmitting source, and its field strength, E' , is measured. The free-space field strength, E_o , at the transmitting antenna is then determined by comparing the field strength, E , from the antenna under measurement with E' , the standard field. Then,

$$E_o = E_o' \times \frac{E}{E'} \text{ v/m} \quad (9)$$

where

- E' = radiation field at distance "d" on the Earth's surface from standard field antenna
- E_o' = free-space electric field strength due to the standard transmitting antenna
- E = radiation field at distance "d" on the Earth's surface from the unknown antenna
- E_o = unknown free-space field strength

Distance "d" can be arbitrary; however, in most cases, it should be at least a wavelength at the measured frequency.

The general equation used to obtain the reference fields for the vertically polarized antennas in the 0.1 to 2.0-Mc/s frequency band is

$$E_o = \frac{60\pi}{d} \frac{h}{\lambda} I_a \quad \text{v/m} \quad (10)$$

In particular, the two equations used to determine the reference fields for the antennas used in the 2 to 12-Mc/s frequency band are, for vertical monopoles,

$$E_o = \frac{60 I_a \times 10^3}{1609 \sin \phi h} (1 - \cos \phi h) \quad \mu\text{v/m} \quad (11)$$

and, for horizontal dipoles,

$$E_o = \frac{60 I_a \times 10^3}{1609} \left[\frac{\cos \left(\frac{\pi}{2} \sin \theta \right)}{\sin \theta} \right] \mu\text{v/m} \quad (12)$$

The equations used to determine the reference fields for the antennas used in the 25 to 400-Mc/s frequency band are, for vertical dipoles,

$$E_o = 4.359 \times 10^3 \sqrt{P} \text{ } \mu\text{v/m} \quad (13)$$

and, for horizontal dipoles,

$$E_o = \frac{60 I_a \times 10^3}{1609} \left[\frac{\cos \left(\frac{\pi}{2} \cos \theta \right)}{\sin \theta} \right] \text{ } \mu\text{v/m} \quad (14)$$

where

I_a = antenna base current in amperes

d = distance in meters

λ = wavelength in meters

h = height of antenna in meters

$\beta = 2\pi/\lambda$

θ = angle between the dipole axis and the ray to the receiving point

P = power delivered to the antenna in watts

6.4.2 Transmission Loss Equation (0.4 to 10 Gc/s)

In this frequency range, system loss was defined, as previously stated, as the ratio of the power delivered to the transmitting antenna, p_t , to the power available from the receiving antenna, p_a , expressed in decibels.

$$L_s = 10 \log_{10} (p_t/p_a) \quad (15)$$

However, at microwave frequencies, it is generally a valid assumption that the power delivered to the transmitting antenna is the same as the power radiated by the antenna. Using this assumption it is seen that system loss is the same as the transmission loss used in Section 3.4.1. Since basic transmission loss is determined from the measured transmission loss, L , by adding the path gain, G_p , then

$$L_b = L + G_p \quad (\text{dB}) \quad (16)$$

When G_p is equal to the sum of the gains of lossless transmitting and receiving antennas, equation 16 can be written as

$$L_b = L + G_t + G_r \quad (\text{dB}) \quad (17)$$

or

$$L_b = p_t - p_a + G_t + G_r \quad (\text{dB}) \quad (18)$$

where

- G_t - gain of transmitting antenna above an isotrope in dB
- G_r - gain of receiving antenna above an isotrope in dB
- p_t - power delivered to the transmitting antenna in dBm
- p_a - power available from the receiving antenna in dBm

Equation 18 is the expression which has been used to convert measured data to basic transmission loss. Equation 18 rather than equation 8 is used in the 10-Gc/s test program because at microwave frequencies it is a relatively simple task to measure the antenna gain by using the technique of two identical antennas described below.

The calibration required for the 10-Gc/s program consists of measuring the gain of each of the antennas. This allows basic transmission loss for this frequency band to be determined directly once the transmitted and received powers are known. In this calibration procedure one antenna is connected to a transmitter and the other to a receiver. After both antennas have been impedance matched to their respective loads, they are separated a distance R, greater than the Fraunhofer distance, and aligned for maximum power transfer. For all the calibrations involved here, the distance R was chosen at 180 feet. The maximum power gain is given by

$$G_t = G_r = \frac{4\pi R}{\lambda} \sqrt{\frac{p_r}{p_t}} \quad (19)$$

where

R = separation distance

λ = wavelength at frequency of measurement in same units as R

p_r = received power

p_t = transmitted power

As is usual in all calibrations, many factors influence the resulting accuracy, and care must be taken to either minimize their influence or include them in the gain computations. One major source of error lies in the effects introduced by the test site. To eliminate these effects in the 10-Gc/s program calibrations, the antennas were mounted at a height that provided a minimum of first Fresnel zone clearance at all points along the path between the antennas. Also, the path chosen was flat and free of any irregularities which would cause undesirable reflections. Additionally, the calibrations must include the effects of any impedance mismatch between each antenna and its load. In each of the measurements these mismatch errors were eliminated by the use of additional matching networks.

6.5 Field Strength Meters

The preceding sections have discussed the basic features of the two-terminal measurement system and how the measurement of field strength is related to the measurement of transmission loss from which values of basic transmission loss are obtained by computation. This section particularly describes the receiving portion of the system, which includes the precision field strength meters together with their calibrated receiving antennas. Also covered in this section are the schedules and procedures for calibrating this instrumentation.

6.5.1 Meters

The field strength meters used in the 0.1 to 400 Mc/s range of the basic program included the Model 120-E, manufactured by Vitro Electronics, the SM-2S and the SM-1M, manufactured by Smith Electronics, Inc., and the NF-105, manufactured by the Singer Company, Metrics Division.

The Model 120-E field strength meter is continuously tunable over the frequency range 0.540 to 1.60 Mc/s. It is a portable, lightweight, self-contained radio receiver with a metered output and calibration oscillator. Its maximum sensitivity is 10 μ v throughout the frequency range. This meter is supplied with its own loop antenna, and is calibrated by means of an internal sine wave oscillator. The output of the calibrating oscillator is fed directly into the loop antenna to permit direct calibration in μ v/m. The meter is powered by five 1.5-volt and two 67.5-volt batteries, and it can also use an external power supply when conditions require continual operation.

The SM-2S field strength meter is continuously tunable over the frequency range 25 to 80 Mc/s. Like the 120-E meter, it is a portable, lightweight, self-contained solid-state radio receiver with a metered output and calibrating oscillator. The maximum input sensitivity is 10 μ v throughout its operating range. Internal calibration is provided by a sine wave oscillator. The meter is powered by a 12-volt rechargeable nickel-cadmium battery.

The SM-1M meter covers the frequency ranges of 60 to 250 Mc/s and 400 to 850 Mc/s with continuous tuning. This meter is basically an SM-1 field strength meter which

was specially modified for this project. It is a portable, lightweight, self-contained solid-state radio receiver with a metered output. The maximum input sensitivity for both frequency ranges is 50 μ v. The external calibration required by this meter is provided by a tunnel diode calibrating oscillator, also manufactured by Smith Electronics, Inc. For calibrations in the VHF range the oscillator operates on a fundamental frequency continuously variable from 52 to 225 Mc/s. The fourth harmonic of the fundamental is used for UHF calibrations. The instrument is powered by a 12-volt rechargeable nickel-cadmium battery.

The NF-105, consisting of one basic unit with four plug-in tuning units, measures over the frequency range of 14 kc/s to 1000 Mc/s. Basically, the NF-105 contains a receiver, calibrating circuits, meter indicators, and calibrated antennas. Maximum full scale sensitivity is 1 μ v from 14 kc/s to 30 Mc/s, and 10 μ v from 20 to 1000 Mc/s. Internal calibration is provided by an impulse generator and a sine wave calibrator. It requires a 115-volt, 40 to 400-cps, exterior power source.

For the frequencies between 1.0 and 10 Gc/s, the NF-112 field strength meter, also manufactured by Singer-Metrics, was employed. This field strength meter measures over the frequency range of 1 to 10 Gc/s with the use of four plug-in tuning units. Maximum full scale sensitivity is 10 μ v. In respect to design, construction, calibration, and power requirements, it is identical to the NF-105 described above.

6.5.2 Measuring Antennas

The antennas used with the NF-105 field strength meter for the majority of measurements taken in the frequency range of 15 kc/s to 20 Mc/s were the LG-105 and LP-105 loops. These calibrated loops were provided by Singer-Metrics for use with the NF-105 field strength meter. All calibration information was supplied with the equipment. For the frequencies of 20 Mc/s to 400 Mc/s, dipole elements were used. These dipoles were calibrated by the manufacturer and were supplied with their own balun matching networks.

The Singer-Metrics NF-105 antennas were also used with the SM-2S and the SM-1M field strength meters. For use with these meters, antenna calibration was achieved by direct comparison with the appropriate NF-105 tuning head and calibrated antenna.

The antennas used with the NF-112 field strength meter for the 10-Gc/s measurements were the same microwave transmitting antennas which were discussed in Section 6.3.4. Identification of each combination that was used in the measurements has been done in the appropriate test descriptions contained in Section 5.9.

The antennas used for the vehicular measurements were of the whip type for vertical polarization and of the loop type for horizontal polarization. All antennas were mounted on the roof of a Land Rover, and the ground plane consisted of the roof and hood structure. In actual operation on the trails, the antennas were protected by a conical Fiberglas radome.

For vertical polarization tests in the frequency band 100 kc/s to 50 Mc/s the Singer-Metrics VA-105 antenna was used. This antenna is a monopole with its own auto-transformer matching network which is band switched for various frequency ranges. The frequency range of this antenna and its matching network is 150 kc/s to 30 Mc/s. For use at 100 kc/s, a series capacitor was inserted in the line to properly match it to the input impedance of the matching network. At 50 Mc/s the transformer input impedance was stub matched to the line. For 100, 250 and 400 Mc/s quarter-wavelength monopoles were employed. Each antenna was supplied with a stub matching network.

For horizontal polarization tests in the frequency range 2 to 50 Mc/s, the LP-105 loop antenna was employed. This antenna, mounted on a wooden stand approximately $2\frac{1}{2}$ feet above the truck roof, is a single turn, shielded, one terminal grounded loop. It is supplied with an auto-transformer matching network which can be band switched for various frequency ranges. The frequency range for this antenna is 150 kc/s to 30 Mc/s. At 50 Mc/s, which is outside this range, the matching network was stub matched to the transmission line.

For 100, 250 and 400 Mc/s, special antennas were constructed. At 100 Mc/s the antenna was a half wavelength folded dipole made to conform with the circular cross section of the radome. The dipole element was made of 72-ohm twin lead. It was matched by means of a half-wavelength coaxial balun which, in turn, was stub matched to the transmission line. A similar antenna was employed at 250 and 400 Mc/s. This antenna, shown in Figure 6.16, is a folded

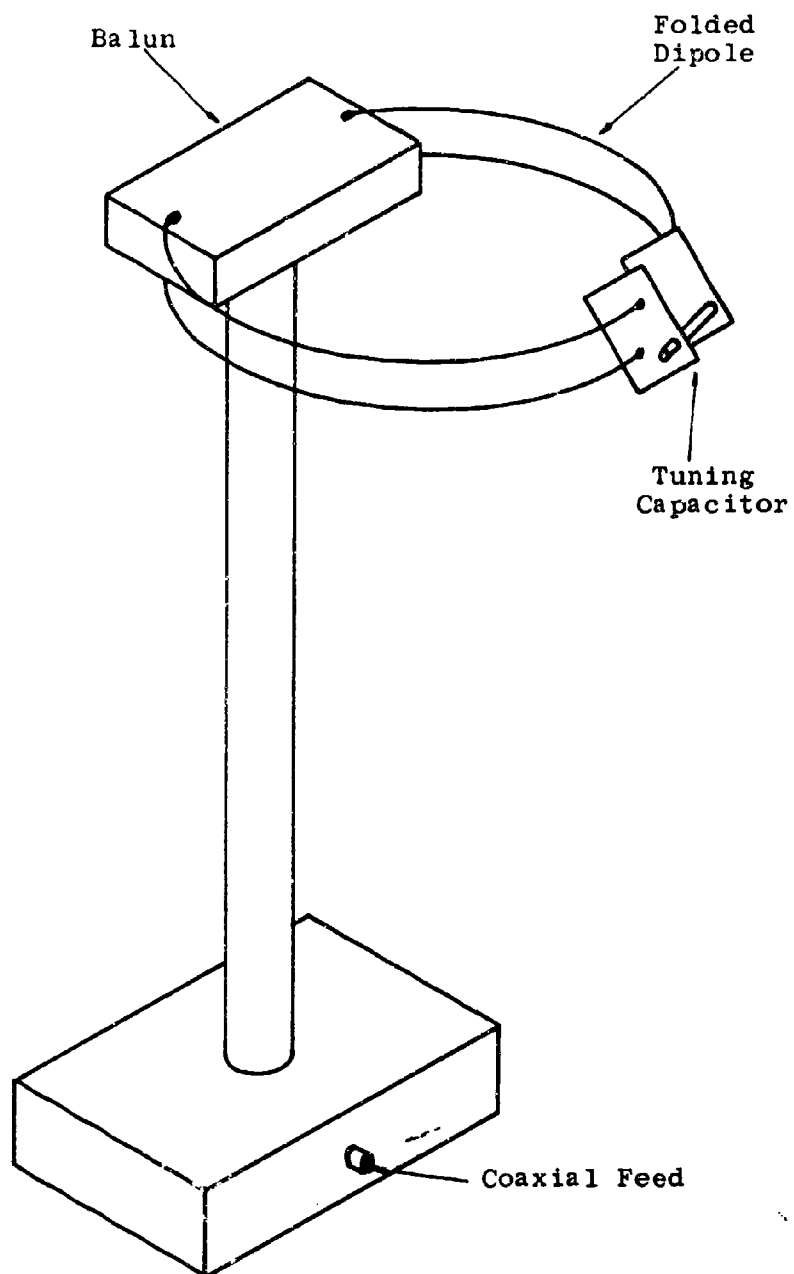


Figure 6.16 Vehicular Antenna for Horizontal Polarization Tests at 250 and 400 Mc/s

dipole shaped into a circle. At the end of each arm of the dipole a diamond shaped copper plate was secured. These two plates form a capacitor which facilitates tuning the element. The tuning consisted of varying the separation of the plates by means of a threaded nylon screw which joined the two plates. The antenna was matched by means of the T-2 broadband balun, one part of the equipment complement of the Singer-Metrics NF-105 field strength meter. At each of the two frequencies the input impedance of the balun was stub matched to the transmission line.

6.5.3 Calibration

Since the NF-105 field strength meter was used in the field under adverse conditions of humidity and vibration, it was necessary to keep it in constant calibration by reference to the same standards used to calibrate the instruments for measuring transmitting power and current. The calibrating procedure for the meter was broken down into monthly and tri-monthly tasks. The monthly task consisted of calibrating the RF tuning heads by providing the correct impulse generator settings at the frequencies to be used in the next month. The tri-monthly task consisted of checking the impulse generator and the meter's step attenuator for malfunctions.

To obtain the correct impulse generator settings for 12 Mc/s and above, a Hewlett-Packard 606 or Hewlett-Packard 608 signal generator, a Hewlett-Packard 431B calorimetric power meter and the AN/URM-32 frequency meter were used. The output of the signal generator, after being calibrated at 100 μ v into a 50-ohm load, was fed into the proper

RF tuning head. The meter was peaked on frequency; and then, with the field strength meter step attenuator set at 20 dB, the IF gain was adjusted for maximum meter deflection. When the impulse generator was set up for a clean 1 kc/s tone, the signal was removed, and the output of the impulse generator was adjusted to give the same meter indication. The output of the impulse generator was recorded for each frequency, thereby completing the calibration. For frequencies below 12 Mc/s a Hewlett-Packard 606 signal generator in conjunction with a Hewlett-Packard 434A calorimetric power meter provided the calibrated signal source, though the calibrating procedures remain unchanged. On the tri-monthly schedule the impulse generator was checked for 1 kc/s tone distortion at varying output levels. The output level was checked against the main meter movement, and the step attenuators were cross checked against Weinschel precision coaxial attenuators.

The NF-112 field strength meter, because it was used in the same adverse environment, was calibrated in a similar manner, the only changes being in the equipment required to cover the frequency range of the 10-Gc/s program.

The vehicular antennas were calibrated by measuring the radiation patterns of the antennas mounted on the vehicle, and then comparing their received signals to those of the antennas that were employed in the fixed point measurements. The comparison antennas were mounted at the same height as those mounted on the vehicle. Thus, by direct comparison with previously calibrated antennas, the antenna factor for each direction from the vehicle was obtained.

The radiation patterns were measured by a fixed transmitting antenna and by rotating the vehicle over a fixed point to provide different orientations with respect to the signal source. In general, the pattern of each antenna was omnidirectional.

All calibration and pattern measurements for 6 Mc/s and above were performed in the test site area. Below 2 Mc/s the measurements were performed at convenient locations on the trail away from the test site. The antenna factors for different combinations of vehicles and antennas were checked and found to be within 1 dB for all combinations with exception of 100 Mc/s. At this frequency the antenna was calibrated for each vehicle and antenna combination.

6.6 Special Equipment

In addition to the basic measuring equipment previously described, field equipment of a specialized nature was required for this field project. This included such items as antenna supporting masts, antenna positioners, recorders and recorder chart drive mechanisms, all of which are described in this section. When this program was started, most of these items could not be obtained from commercial sources and therefore had to be designed and fabricated at the Principal Laboratories.

6.6.1 Portable Mast

The vast bulk of the field measurements in this program, being conducted in the tropical vegetation of

Thailand, placed specialized demands upon the masts that would support the transmitting and receiving antennas. In particular, there were four primary capabilities which were required of these antenna masts.

First, because they were continually transported down the vehicular trails and occasionally even hand carried into the small jungle clearings used for field points, the antenna masts had to be extremely portable. Second, because it was intended to get a large number of detailed recordings of antenna height gain, it was necessary to be able to quickly and easily adjust the antenna height up to 80 feet, which was above tree height. Third, because there were about 40 field points where the masts had to be transported and set up, there had to be the means of rapidly erecting and disassembling the masts. And fourth, because the normal procedure of cutting down vegetation to permit guying an antenna mast was incompatible with the intention that the antennas should be closely surrounded by vegetation, it was also necessary for the mast to be self-supporting, even when erected to its full height of 80 feet.

Efforts to locate an antenna mast with these characteristics were unsuccessful. Although there were available masts that satisfied some requirements, there was none that satisfied all. Therefore, a special mast for this project had to be designed and built by the Company. Since the mast has been covered in detail in Semiannual Report Number 3, only its main features will be reviewed in the following paragraphs.

Despite the fact that the mast and tripod were designed only to meet the previously mentioned requirements,

they eventually came to serve a number of additional purposes in the field measurement program. From an operational point of view, it is interesting to follow the manner in which these extra functions of the mast evolved from the original conception. There is the possibility that some of the operational principles learned in the creation of this mast can be usefully applied to operations differing from those involved in this program.

The antenna mast specifications which have already been mentioned pertained only to the needs of the receiving antennas which were to be moved to the different field points where they would measure transmission loss. For this purpose, it was originally anticipated that only four or five masts would be needed. For the entire program, however, there were also needed other towers which could support the test transmitting and control communications antennas, and even serve as the radiating element of low-frequency, vertically polarized antennas. Altogether, about 25 masts, or towers, were required for various applications in the project.

At first, it was planned to procure the additional towers from established sources; and, therefore, the initial design attempts were only addressed to the program of meeting the particular needs of the receiving antennas. The result was a mast constructed of 6-foot-long tubular sections with stepped diameters and a supporting tripod assembly. The tripod assembly allowed the mast to be erected in 6-foot increments and could hold the mast vertically without guys. At this point it became obvious that, if the tripod assembly were designed so that it could easily

be removed from around the mast, and if the mast could be guyed, then both devices could be used in more ways than originally intended. For example, by putting an insulator at the base of the mast and by insulating the guys, the mast itself could function as an excellent vertical radiator after the tripod was removed.

Thus, the tripod assembly was designed so that, with the removal of a few bolts, it could be disengaged from the mast after the latter had been erected and guyed. The tripod could then be used to raise another mast. This feature permitted the original receiving antenna mast to be used for almost all the tower requirements in the entire field program.

The mast, shown packaged in Figure 6.17, consists of 15 thin-wall aluminum tube sections, 6 feet long and varying in diameter from 2 to 6 inches. The specially designed sleeves, which are shown in Figure 6.18 with their container, are used to connect the different tube sections and to distribute any bending forces that might distort the tubes.

The launching tripod, shown in Figure 6.19, is about 15 feet high, depending on the leg adjustment. It is equipped with a clutching type of brake mechanism which can hold any section of the mast vertically in place while another section is being attached or detached.

When erecting the mast in the guyed configuration, the guy rings are stacked on top of the launcher tube. Since each of the five guy rings has a different inside

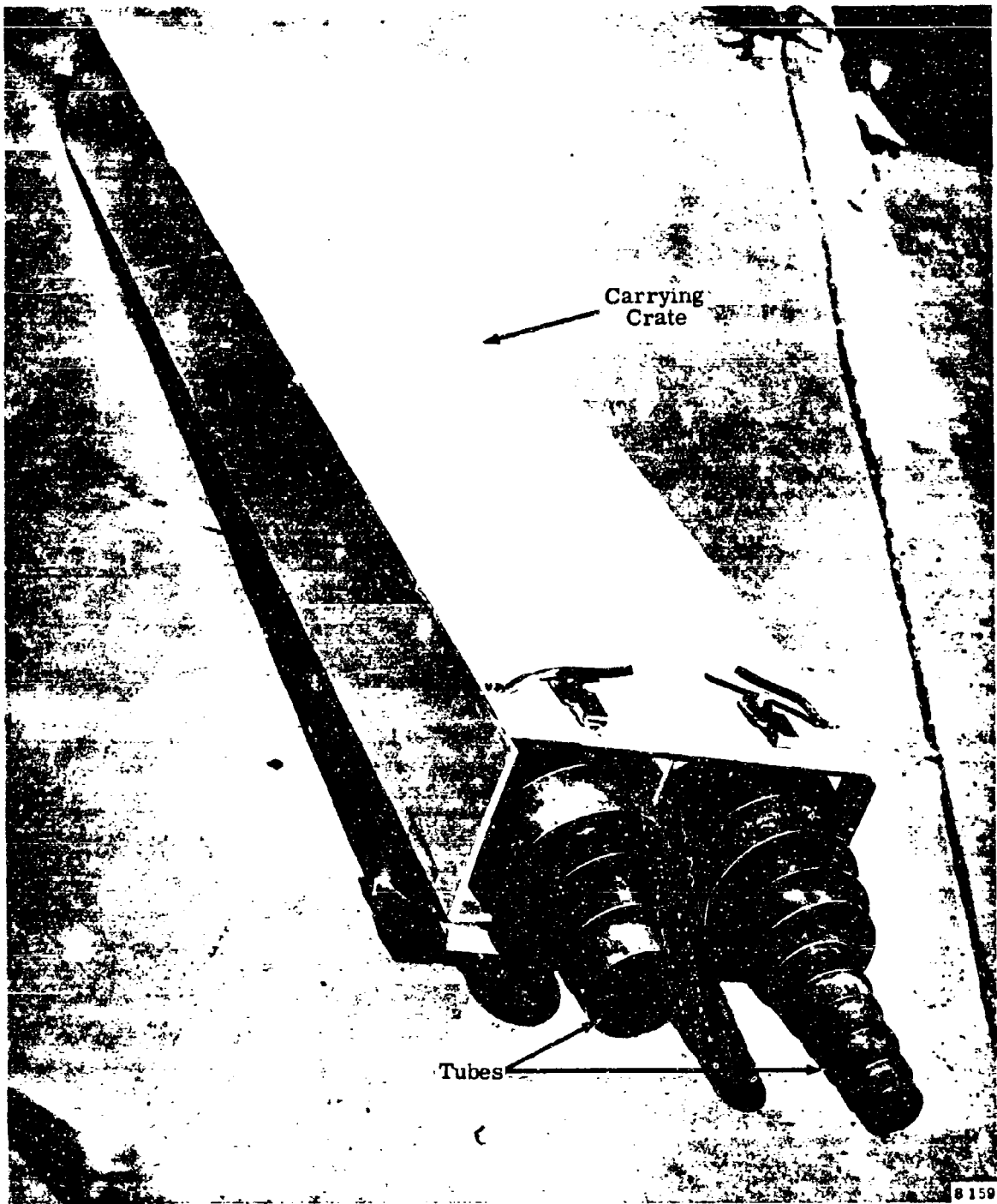


Figure 6.17 Mast Tubes in Their Carrying Case



R31652

Figure 6.18 Mast-Joining Sleeves

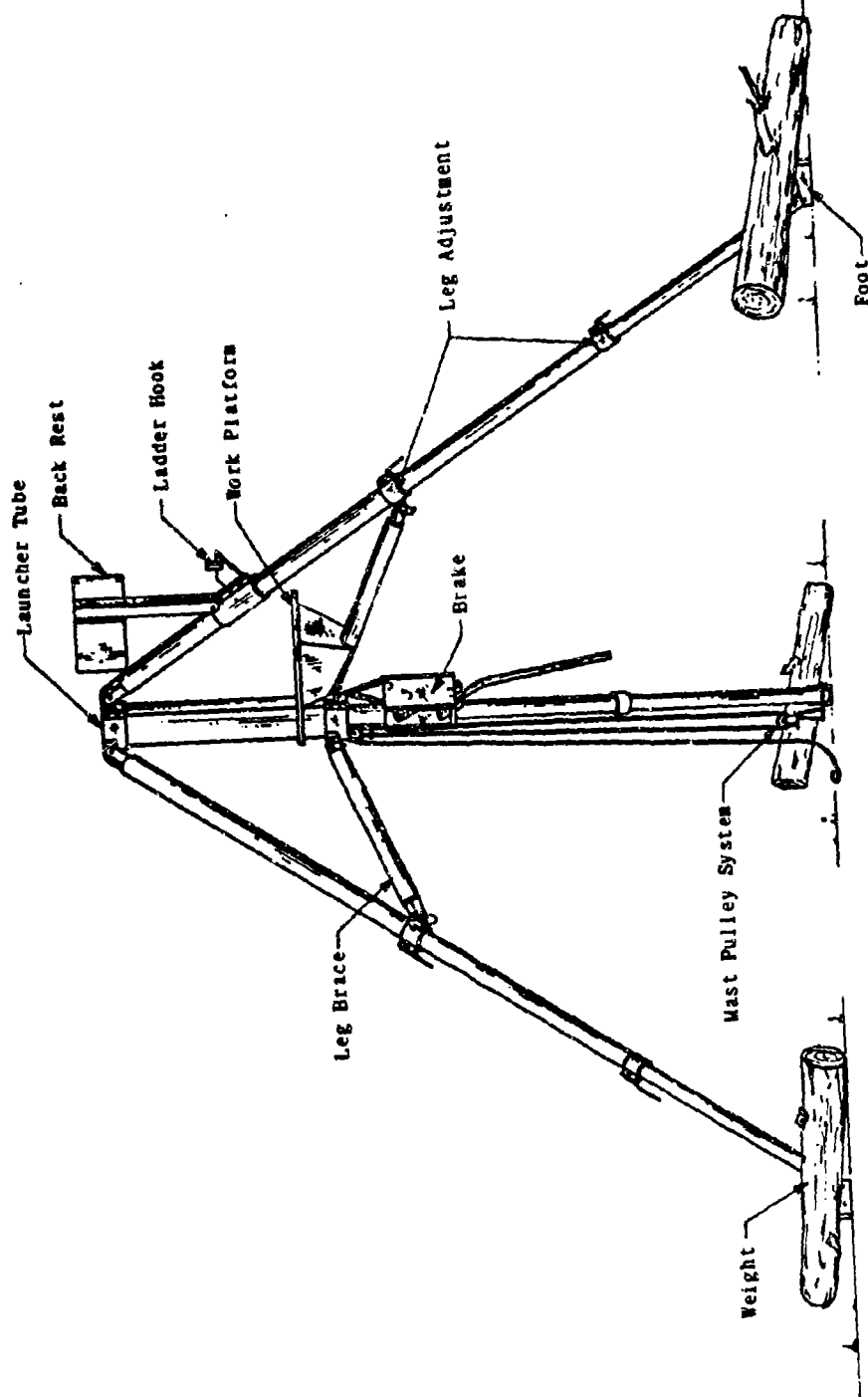


Figure 6.19 Tripod and All Working Accessories

diameter, it will be picked up by the appropriate section of the mast passing through the launcher tube.

Figure 6.20 shows the fully extended mast, the guying ropes, and the tripod erecting mechanism. In this position the erecting mechanism can be removed and used to erect another mast by removing the bolts that hold together the two sides of the launch tube. The whole mechanism may then be carried away to another location.

The portable mast was used as a radiating antenna for vertical polarization propagation tests at 100, 300, and 880 kc/s and at 2 and 6 Mc/s. For this use the mast was erected in the normal manner using the mast tripod as a support during erection. After the mast had been raised to the appropriate height, a base insulator was installed, as shown in Figure 6.21, and the mast was guyed using the Dacron guy ropes. The launcher tube was then unbolted, and the tripod removed. For the frequencies below 2 Mc/s, top loading elements were attached to the mast during erection, and the portable mast served as the radiating element and support for the top loading. The physical characteristics of this "umbrella" antenna are discussed earlier in Section 6.

The portable masts were also used as supporting structures for transmitting and receiving antennas. For the horizontal transmitting antennas at 2, 6, and 12 Mc/s, two masts were erected and guyed after placing them on the mast base plate. The horizontal dipole antenna was then strung between the towers and raised and lowered using Dacron rope halyards.



7695

31155

Figure 6.20 Guyed Mast

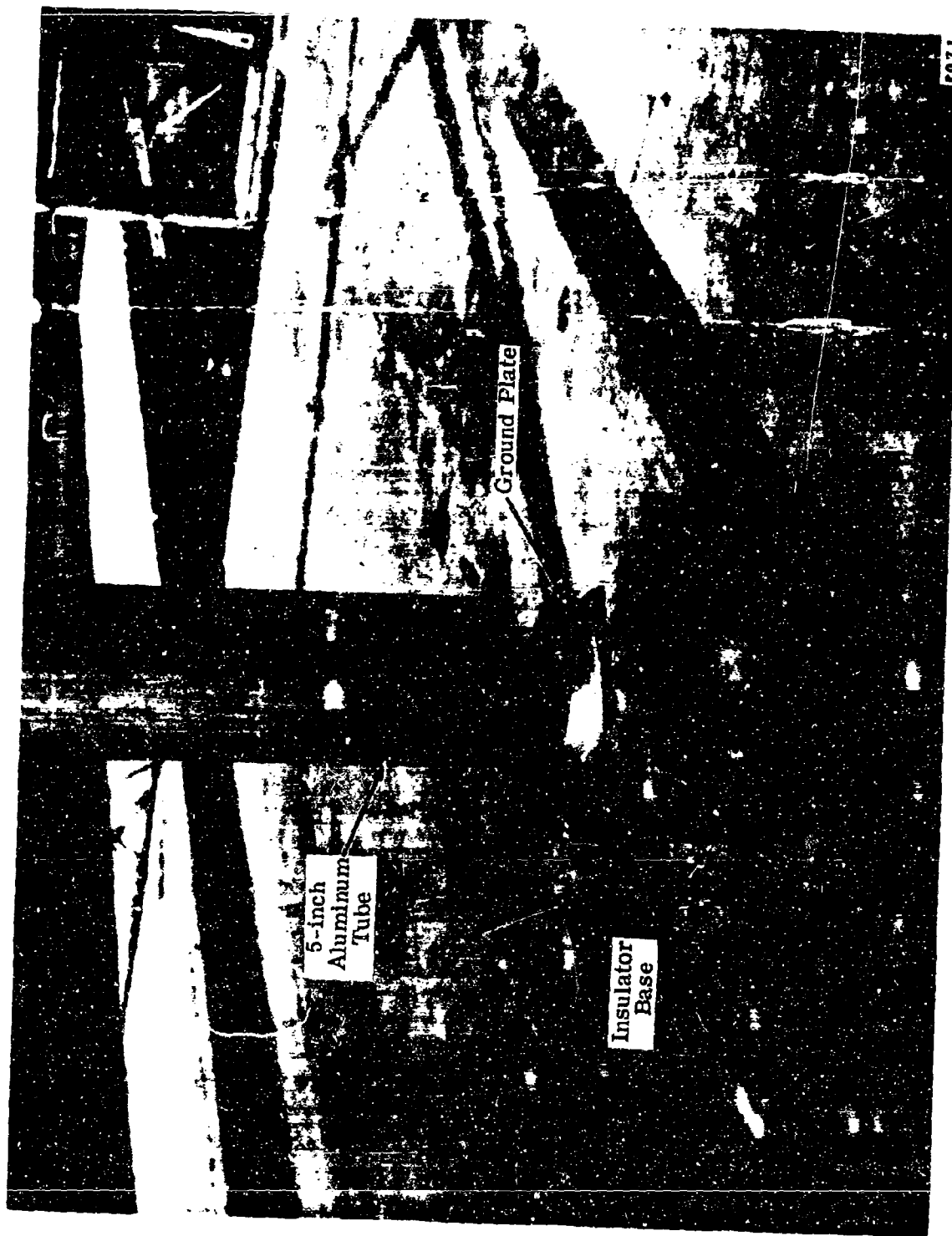


Figure 6.21 Insulated Mast Base Plate

31624

At frequencies from 12 to 400 Mc/s, a single mast was used to support the transmitting antennas. For these applications the tripod remained at the base of the mast because test frequencies and heights were changed frequently. The appropriate transmitting antenna was installed on the top mast section using insulating sections as required. The transmission line was connected and secured to the mast at intervals during erection. After the transmitting antenna was raised to the desired height, the mast was seated on a base plate and lightly guyed.

At fixed points along the measuring radials, referred to as "field points," field strength measurements were made from near-ground level to treetop heights. The receiving antennas were mounted on the mast and raised using the normal mast erection procedures. Making these measurements, for which guying could not be used, was the original purpose which the mast was designed to serve. In general, measurements were made at one location, or field point, for a number of test parameters, including frequency, polarization and transmitting antenna height. This procedure minimized the equipment movement time and took advantage of the short time required for raising and lowering an antenna. Once the tripod was installed and the mast parts laid out, the tower could be raised by two men in approximately five minutes.

6.6.2 10-Gc/s Antenna Towers and Positioners

The 10-Gc/s test program used high gain directional antennas in most receiving and transmitting configurations. To correctly use these antennas a tower was needed that

could provide a rigid mounting at different heights. These towers also had to be large enough to allow personnel to work on the antennas, and strong enough to support the weight of the antenna positioners and other instrumentation which had to be near the antennas.

To most satisfactorily meet the above requirements, a military tower, AB-216/U, was selected. Figure 6.22 shows such a tower, partially assembled. This tower is a sectionalized, guyed tower which consists of interlocking sections mounted on base plates and supported by guys and ground anchors. The towers employed on this program reached a maximum height of 120 feet. Each sectionalized element is 6 feet high and has a cross section of 4 feet by 6 feet. These sections are stored in a folded position. To erect the sections, they are unfolded and snap-locked into their extended configuration. Each section incorporates a stairway and a level walking-working platform. After preparing a mounting surface for the base plates, the tower is erected by stacking and interlocking the opened sections first on the base plates and then on each other. This process is continued until the desired height is reached. At every fourth or fifth section a set of supporting guys is installed. The resulting structure is very stable and capable of supporting the necessary antennas, positioners, instrumentation and operating personnel. The enclosed stairways make it simple and safe for personnel to climb the towers, and the use of hoists facilitated moving the equipment.

The antenna positioning equipment for the 10-Gc/s program had to meet a number of different requirements. The transmission tests demanded that the antennas be accurately aligned and that there be accurate indication of the

antenna's angular displacement. Also needed was the ability to align the antennas in both the azimuth and elevation planes, and to axially rotate the antennas so that horizontal and vertical polarizations could be provided. To expedite all these adjustments, it was necessary to have a means of controlling and reading the positioners from a remote position.

In this instance, it was impossible to find a single piece of commercially available equipment that would have all the required functions. Instead, a number of items were assembled which collectively met the requirements. An Antlab Model 3733 azimuth-over-elevation antenna positioner plus its associated position indicator and control box formed the basic elements of the antenna positioners. This unit was mounted on a heavy-duty gear-driven turntable. An appropriate drive and position indicator were mounted on the turntable and the entire assembly installed on a structural aluminum frame, as shown in Figure 6.23.

With the 3-foot dish antenna shown mounted on the positioner in Figure 6.23 a change in azimuth of ± 90 degrees and elevation of ± 60 degrees was possible. The antenna can also be rotated 90 degrees to change polarization.

During the tests identical positioners were used for transmitting and receiving. They were hoisted to the desired height on the supporting tower. During measurements they were aligned for maximum power transfer when making path loss measurements. When making antenna pattern measurements one positioner was held fixed and the other swept.

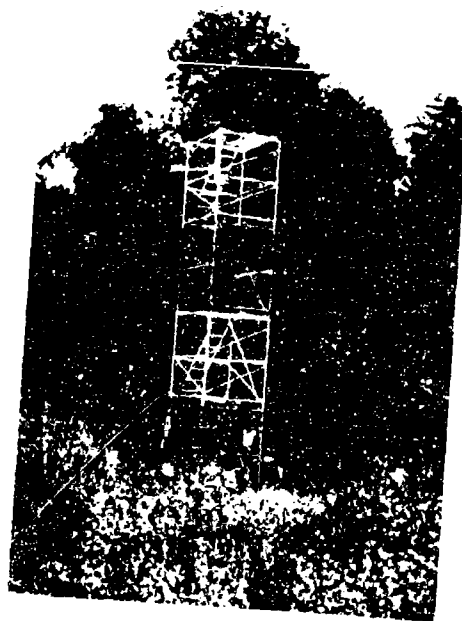


Figure 6.22 Transmitter Tower

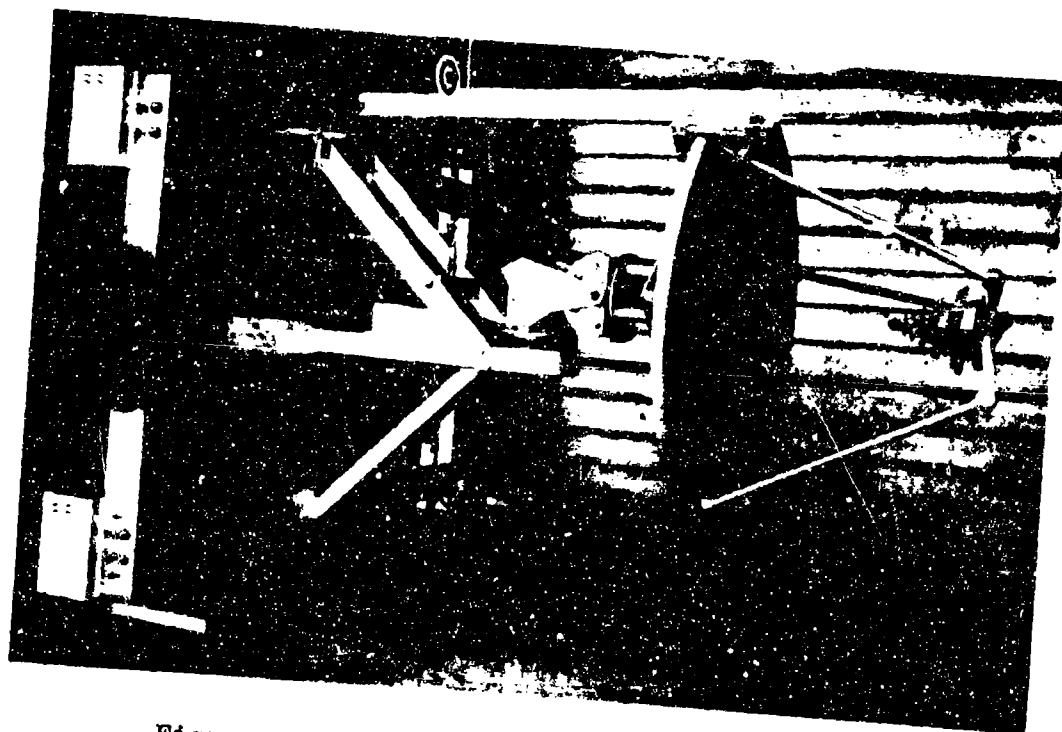


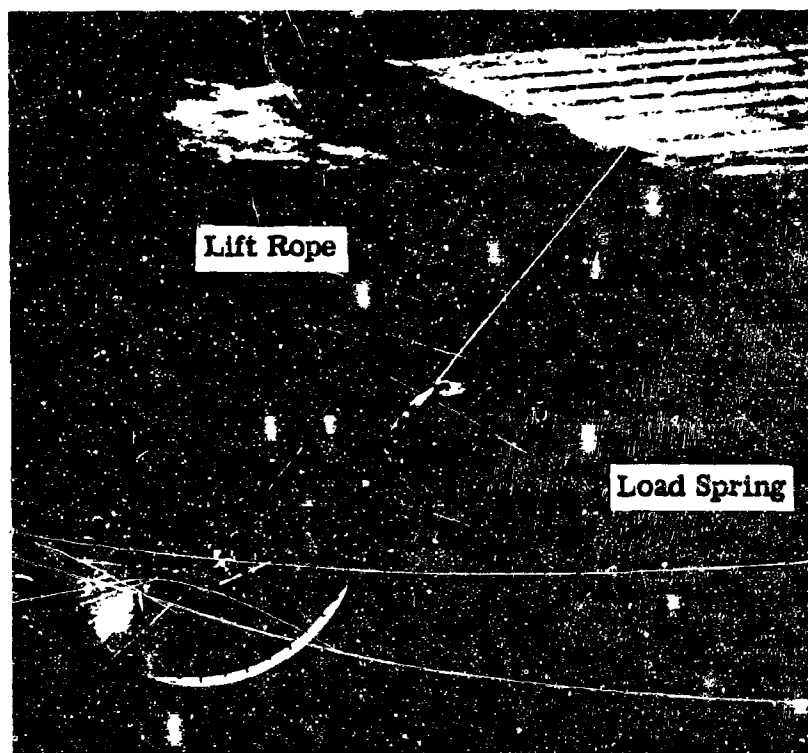
Figure 6.23 Antenna Positioner System

6.6.3 Recorder Chart Drives

The primary objective of the propagation program was to investigate the horizontal and vertical spatial distributions of field strength. To accomplish this, a chart recorder was used to record received field strength as the receiving antenna was moved. For the horizontal distribution measurements a "fifth wheel" was used to drive the chart; and for vertical distribution measurements a movement pickup mechanism, mounted on the portable mast, was used.

To measure field strength versus horizontal distance, the measuring equipment was mounted in a vehicle. Some means was needed to drive the chart recorder in the manner of an odometer. After considering and rejecting, for reasons of inaccuracy and complexity, several mechanisms which would connect directly to the wheels of the vehicles, it was decided to use a fifth wheel device to drive the chart recorder. When an investigation of commercially available fifth wheels showed that none would be likely to stand up under the rough and muddy trail conditions, a more rugged one was designed.

The configuration of the fifth wheel, shown in Figure 6.24, was such that it could follow the very rough terrain and withstand the heavy pounding it would encounter in being pulled by the vehicles. A horizontal/vertical pivot, attached to the rear bumper of a vehicle, allowed the wheel to move approximately 70 degrees in any direction. Spring loading, combined with large tires and low inflation pressures, was used to improve the tracking ability of the tire. To increase the durability of the units that were



31675

Figure 6.24 Fifth Wheel Assembly

sent to Thailand, the wheels, tires, bearings and forks utilized were of heavy duty construction.

Initially, a worm gear and long flexible shaft were used to translate the rotation of the fifth wheel to the driving gears of the chart recorder. But, after muddy trail conditions caused repeated clogging of the flexible shaft and the consequent shearing of the rotation pickup component, this system was changed and replaced with a set of bicycle sprockets connected by a chain. One sprocket was attached to the fifth wheel; the other was mounted on the vehicle where it would not collect mud. The flexible shaft was then connected to this protected sprocket. Different gearing ratios were incorporated to allow various distance scales on the chart ordinate.

Besides plotting field strength against distance, the chart recorder was also used to record variations in field strength as the receiving antennas were adjusted to different heights. This was accomplished by coupling the chart recorder drive to the portable antenna mast through a friction roller. The components of this recorder drive can be seen in Figure 6.25 which shows the pivoted and spring loaded arm that presses a roller against the antenna mast. The roller is driven as the mast is raised and lowered. To ensure accuracy, the roller was wrapped with foam neoprene to increase its adhesion to the mast. In order to drive the chart recorder forward regardless of whether the mast is going up or down, the roller was connected to the flexible cable through two ratchet drives, one normal, the other reverse. Their arrangement was such that the flexible cable was always turned in the same direction. Here, too,

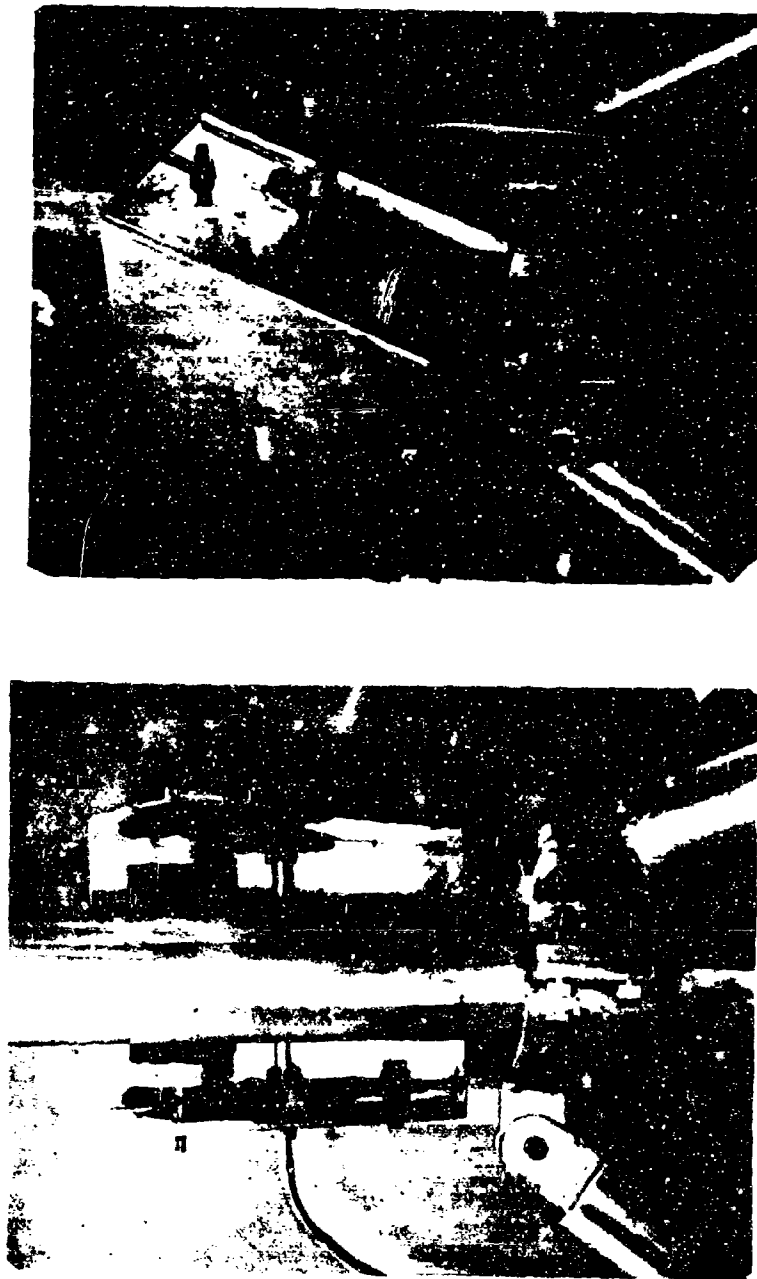


Figure 6.25 Internal and External Views of Drive Take-Off Mounted Above the Tower Tripod

changeable gearing ratios were provided to allow a selection of height versus chart spacing.

The mast movement chart drive was protected by an aluminum cover which could be quickly removed from the antenna mast's supporting tripod by taking out a single pin.

6.6.4 Recorders

The primary factors considered in the selection of the recorder for the propagation tests were accuracy and response time plus reliability, continuous contact of the marking stylus with the chart, and a dry marking method. The high ambient temperature of the environment was also a strong factor to be considered. Commercial recorders of the null balancing type using pressure sensitive chart material were reviewed for use on the program.

The first type obtained and used in the field measurements incorporated the desired operational features but was found to be unreliable when subjected to field conditions in Thailand. The major problem was a reduction in sensitivity at high temperatures. A change was made to the Varian Associates Model G-11A strip chart recorder which has proved to be very reliable.

The Varian G-11A recorder employs the automatic null-balance potentiometer principle. It utilizes a high-gain servo amplifier, a null-balance measuring circuit sensitive to small dc voltage signals, a balancing motor and precision slidewire coupled to a mechanical stylus positioning system. The stylus traces a continuous and

permanent record on a chart moved by a synchronous motor. Modifications were made to allow the selection of either the chart drive mechanisms or the synchronous motor drive. Varian Type 5F chart paper was used, which is a plastic-coated pressure-sensitive type paper.

An input circuit for the recorder was selected which had a continuously adjustable input span of 9 to 100 millivolts dc with a rated accuracy of 1 per cent. In operation the circuit output was adjusted and calibrated against the field strength meter output prior to each set of recordings. Thus, the chart values were related to the field strength meter output on all recordings.

THIS PAGE INTENTIONALLY BLANK

REFERENCES

1. Kelley Christensen, Anan Nalampoon, and Sommart Sukhawong, Environmental Description I of the Jansky & Bailey Test Site at Khao Yai, Thailand, 66-015 Joint Thai - U.S. Military Research and Development Center; January 1966.
2. K. Christensen and D. Neal, Environmental Description II of Jansky & Bailey Test Site at Khao Yai, Thailand, 66-026 Joint Thai - U.S. Military Research and Development Center; July 1966.
3. J. W. Herbstreit and W. Q. Crichlow, "Measurement of Factors Affecting Jungle Radio Communications," Office of Chief Signal Officer, Operational Research Branch, ORB-2-3; November 1943.
4. H. C. T. Whale, "Ground Aerials," M. Sc. Thesis; 1945.
5. K. A. Norton, "Transmission Loss in Radio Propagation - II," NBS Technical Note 12; 1959.
6. John J. Egli, "Radio Propagation Above 40 Mc Over Irregular Terrain," Proc. IRE: October 1957.
7. Leonard E. Wood, "The Measurement of Biomass," Internal Memorandum, ARPA/RDFU-T, MRDC, Thailand.
8. Tropical Propagation Research, Atlantic Research Corporation, Alexandria, Virginia, Primary Field Test Plan, Signal Corps Contract DA 36-039 SC-90889; January 1963.
9. Tropical Propagation Research, Atlantic Research Corporation, Alexandria, Virginia, Primary Field Test Plan, Signal Corps Contract DA 36-039 SC-90889; September 1964.
10. P. L. Rice, A. G. Longley, K. A. Norton, and A. P. Barsis, "Transmission Loss Predictions for Tropospheric Communication Circuits," NBS Technical Note 101, Vol. I; May 7, 1965.
11. A. H. LaGrone, "Forecasting Television Service Fields," Proc. IRE, p. 1011; June 1960.

12. Federal Register, Federal Communications Commission, Chapter 1, Graph No. 10 Facing p. 28, December 1955.
13. K. A. Norton, "The Calculation of Ground Wave Field Intensity Over a Finitely Conducting Spherical Earth," Proc. IRE, vol. 29, pp. 623-639; December 1941.
14. K. A. Norton, et al., "The Use of Angular Distance in Estimating Transmission Loss and Fading Range for Propagation Through a Turbulent Atmosphere Over Irregular Terrain," Proc. IRE; October 1955.
15. K. Bullington, "Radio Propagation at Frequencies Above 30 Megacycles," Proc. IRE, vol. 35, p. 1122; 1947.
16. Documents of the VIIIth Plenary Assembly, Vol. I, International Radio Consultive Committee, Warsaw, p. 352; 1956.
17. Transmission Loss Predictions for Tropospheric Communication Circuits, C.C.I.R. Study Groups Doc. V/2a, Question 185(V), Study Programs 188, 190, 192 (V), Geneva, Switzerland; January 13, 1965.
18. J. A. Saxton and J. A. Lane, "VHF and UHF Reception," Wireless World, pp. 229-231; May 1955.
19. B. Trevor, "Ultra High Frequency Propagation Through Woods and Underbrush," RCA Review, Vol. 5, pp. 97-100; July 1940.
20. D. J. Pounds and A. H. LaGrone, "Considering Forest Vegetation as an Imperfect Dielectric Slab," Electrical Engineering Research Laboratory, University of Texas, Report 6-53; May 31, 1963.
21. B. R. Bean, "The Radio Refractivity Index of Air," Proc. IRE, Vol. 50, pp. 260-273.
22. B. R. Bean and G. D. Thayer, "A Model Radio Refractivity Atmosphere," NBS Report 5576; July 1958.

UNCLASSIFIED
Security Classification

DOCUMENT CONTROL DATA - R&D		
(Security classification of title, body of abstract and indexing annotation must be entered when the overall report is classified)		
1. ORIGINATING ACTIVITY (Corporate author) Atlantic Research Corp. Jansky & Bailey Engineering Department Shirley Highway at Edsall Road Alexandria, Virginia 22314		2a. REPORT SECURITY CLASSIFICATION Unclassified 2b. GROUP
3. REPORT TITLE Tropical Propagation Research (U)		
4. DESCRIPTIVE NOTES (Type of report and inclusive dates) Final Report Volume I, 1 January 1966 - 30 June 1966		
5. AUTHOR(S) (Last name, first name, initial) Sturgill, Lester G., and Staff		
6. REPORT DATE 31 June 1966	7a. TOTAL NO. OF PAGES 502	7b. NO. OF REFS 22
8a. CONTRACT OR GRANT NO. DA 36-039 SC-90889 b. PROJECT NO. AMC Code #5621-11-919-01-13 c. AMC Sub Task #1P620501 A 4480113 d. pertaining to ARPA Order #371		9a. ORIGINATOR'S REPORT NUMBER(S) 9b. OTHER REPORT NO(S) (Any other numbers that may be assigned this report)
10. AVAILABILITY/LIMITATION NOTICES DISTRIBUTION OF THIS DOCUMENT IS UNLIMITED.		
11. SUPPLEMENTARY NOTES Report on experimental studies of RF propagation in tropically vegetated environments.		12. SPONSORING MILITARY ACTIVITY Advanced Research Projects Agency Washington, D. C.
13. ABSTRACT This Final Report, Volume I, presents the results obtained from the first phase of an extensive experimental and theoretical research program on radio wave propagation in the environment of a tropical, thickly vegetated jungle. Although aimed primarily at the problems encountered by ground based, tactical radio communications systems, the measured data and the results derived therefrom are general enough to have applications in the field of electromagnetic surveillance and intrusion detection. The experimental work during this first phase has been carried out in Thailand in a geographical area classified as a wet-dry, or monsoon, tropical region. The vegetation in the main test area has a density of about 130 tons per acre and is considered to be typical of many jungle regions throughout Southeast Asia. The propagation tests and analyses contained in this report cover the frequency range of 100 kc/s to 10 Gc/s for propagation distances extending from 25 feet to 30 miles and antenna heights from about 7 to 80 feet above ground. Except at the lowest frequencies, all tests were conducted at both horizontal and vertical polarizations. Most of the data is presented in graphs of basic transmission loss plotted against horizontal distance, terrain characteristic, antenna height, transmission polarization or frequency. Also covered are the results of special measurements in the 1 to 10-Gc/s frequency range, the data from which is applicable to problems with line-of-sight systems operating over vegetated terrain and with short range radar systems propagating horizontally through vegetation. The large quantity of measured data demonstrates the complex effects upon path loss of irregular topography combined with dense tropical vegetation. The findings of the program to date, which have been drawn from the data analysis, are summarized into a number of tentative conclusions which may be applied to many types of problems involving radio propagation in tropically vegetated regions.		

DD FORM 1 JAN 64 1473

UNCLASSIFIED
Security Classification

UNCLASSIFIED
Security Classification

14 KEY WORDS	LINK A		LINK B		LINK C	
	ROLE	WT	ROLE	WT	ROLE	WT
Propagation Techniques Tropical Environment SFA - Southeast Asia Thailand - SEA Path Loss Climatology - Rainfall, Temperature, Barometric Pressure Antenna Height Transmission Distance Refractivity						

INSTRUCTIONS

1. **ORIGINATING ACTIVITY:** Enter the name and address of the contractor, subcontractor, grantee, Department of Defense activity or of an organization (corporate author) issuing the report.
- 2a. **REPORT SECURITY CLASSIFICATION:** Enter the overall security classification of the report. Indicate whether "Restricted Data" is included. Marking is to be in accordance with appropriate security regulations.
- 2b. **GROUP:** Automatic downgrading is specified in DoD Directive 5200.10 and Armed Forces Industrial Manual. Enter the group number. Also, when applicable, show that optional markings have been used for Group 3 and Group 4 as authorized.
3. **REPORT TITLE:** Enter the complete report title in all capital letters. Titles in all cases should be unclassified. If a meaningful title cannot be selected without classification, show title classification in all capitals in parenthesis immediately following the title.
4. **DESCRIPTIVE NOTES:** If appropriate, enter the type of report, e.g., interim, progress, summary, annual, or final. Give the inclusive dates when a specific reporting period is covered.
5. **AUTHOR(S):** Enter the name(s) of author(s) as shown on or in the report. Enter last name, first name, middle initial. If military, show rank and branch of service. The name of the principal author is an absolute minimum requirement.
6. **REPORT DATE:** Enter the date of the report as day, month, year; or month, year. If more than one date appears on the report, use date of publication.
- 7a. **TOTAL NUMBER OF PAGES:** The total page count should follow normal pagination procedures, i.e., enter the number of pages containing information.
- 7b. **NUMBER OF REFERENCES:** Enter the total number of references cited in the report.
- 8a. **CONTRACT OR GRANT NUMBER:** If appropriate, enter the applicable number of the contract or grant under which the report was written.
- 8b, &, & 8d. **PROJECT NUMBER:** Enter the appropriate military department identification, such as project number, subproject number, system numbers, task number, etc.
- 9a. **ORIGINATOR'S REPORT NUMBER(S):** Enter the official report number by which the document will be identified and controlled by the originating activity. This number must be unique to this report.
- 9b. **OTHER REPORT NUMBER(S):** If the report has been assigned any other report numbers (either by the originator or by the sponsor), also enter this number(s).
10. **AVAILABILITY/LIMITATION NOTICES:** Enter any limitations on further dissemination of the report, other than those

imposed by security classification, using standard statements such as:

- (1) "Qualified requesters may obtain copies of this report from DDC."
- (2) "Foreign announcement and dissemination of this report by DDC is not authorized."
- (3) "U. S. Government agencies may obtain copies of this report directly from DDC. Other qualified DDC users shall request through _____."
- (4) "U. S. military agencies may obtain copies of this report directly from DDC. Other qualified users shall request through _____."
- (5) "All distribution of this report is controlled. Qualified DDC users shall request through _____."

If the report has been furnished to the Office of Technical Services, Department of Commerce, for sale to the public, indicate this fact and enter the price, if known.

11. **SUPPLEMENTARY NOTES:** Use for additional explanatory notes.

12. **SPONSORING MILITARY ACTIVITY:** Enter the name of the departmental project office or laboratory sponsoring (paying for) the research and development. Include address.

13. **ABSTRACT:** Enter an abstract giving a brief and factual summary of the document indicative of the report, even though it may also appear elsewhere in the body of the technical report. If additional space is required, a continuation sheet shall be attached.

It is highly desirable that the abstract of classified reports be unclassified. Each paragraph of the abstract shall end with an indication of the military security classification of the information in the paragraph, represented as (TS) (S) (C) or (U).

There is no limitation on the length of the abstract. However, the suggested length is from 150 to 225 words.

14. **KEY WORDS:** Key words are technically meaningful terms or short phrases that characterize a report and may be used as index entries for cataloging the report. Key words must be selected so that no security classification is required. Identifiers, such as equipment model designation, trade name, military project code name, geographic location, may be used as key words but will be followed by an indication of technical context. The assignment of links, rules, and weights is optional.

UNCLASSIFIED
Security Classification